รายงานวิจัยฉบับสมบูรณ์

โครงการ ความเกี่ยวข้องของวิถี ADAM9/EGFR/Akt ในมะเร็งเยื่อบุผิวช่องปากชนิดสความัสเซลล์

Involvement of the ADAM9/EGFR/Akt Pathway in Oral Squamous Cell Carcinoma

จัดทำโดย

ศาสตราจารย์ ทันตแพทย์ ดร. สุทธิชัย กฤษณะประกรกิจ และคณะ

ภาควิชาชีววิทยาช่องปากและวิทยาการวินิจฉัยโรคช่องปาก

คณะทันตแพทยศาสตร์ มหาวิทยาลัยเชียงใหม่

เมษายน 2563

บทคัดย่อ

มะเร็งเยื่อบุผิวช่องปากชนิดสความัสเซลล์ (OSCC) เป็นโรคที่ร้ายแรงซึ่งพบได้ในช่องปากและคอหอยส่วนปาก มีอัตราการตายและทุพพลภาพสูง พบการแสดงออกที่เพิ่มขึ้นของเอดิสอินเทกรินแอนด์เมทัลโลโปรทีเนสไนน์หรือ ADAM9 ซึ่งเป็นไกลโคโปรตีนบนเยื่อหุ้มเซลล์ชนิดที่ 1 ในโรคมะเร็งหลากหลายชนิดรวมถึง OSCC และในเซลล์ไลน์บางชนิดที่สกัดแยกได้จาก OSCC แต่ก็ยังไม่มีข้อสรุปที่ชัดเจนเกี่ยวกับความผิดปกติของโครโมโซมตรงตำแหน่งที่พบยีนสำหรับ ADAM9 หรือยังมีการศึกษาเฉพาะการแสดงออกของอาร์เอ็นเอนำรหัสของ ADAM9 ในมะเร็งช่องปากเท่านั้น นอกจากนั้นยังไม่พบว่ามีการศึกษาใดศึกษาถึงความเกี่ยวข้องของ ADAM9 ต่อพยาธิกำเนิดของ OSCC โดยเฉพาะอย่างยิ่งการกระตุ้นวิถีให้สัญญาณของเอพิเดอร์มัลโกรธแฟกเตอร์รีเซ็พเตอร์ (EGFR) และเอเคที (Akt) และต่อการที่เซลล์มะเร็งมีความก้าวร้าวเพิ่มมากขึ้น **วัตถุประสงค์:** ดังนั้นการศึกษานี้มีวัตถุประสงค์ที่จะศึกษาถึงระดับการแสดงออกของโปรตีน ADAM9 ในเนื้อเยื่อมะเร็งช่องปากเปรียบเทียบกับเยื่อบุผิวช่องปากปกติและในเซลล์มะเร็งเปรียบเทียบกับเซลล์เยื่อบุผิวช่องปากปกติซึ่งถูกเพาะเลี้ยงในห้องปฏิบัติการ นอกจากนั้น ยังศึกษาบทบาทหน้าที่ของ ADAM9 ในการกระตุ้นกระบวนการเติมหมู่ฟอสเฟตของ EGFR และ Akt และความก้าวร้าวของเซลล์มะเร็งช่องปากนอกกาย **วัสดุและวิธีการทดลอง:** ศึกษาการแสดงออกของโปรตีน ADAM9 โดยวิธีอิมมูโนฮิสโตเคมิสตรีในเนื้อเยื่อมะเร็งช่องปากชนิด OSCC 34 ชิ้น และเยื่อบุผิวช่องปากปกติ 10 ชิ้น คำนวณคะแนนอิมมูโนฮิสโตเคมิสตรีโดยการนำคะแนนของร้อยละของเซลล์ที่ให้ผลบวกรวมกับคะแนนของความเข้มของการติดสี ทำการเพาะเลี้ยงเซลล์มะเร็งช่องปากที่แตกต่างกัน 4 ชนิด ได้แก่ HN5, HN6, HN15 และ HN008 และเซลล์เยื่อบุผิวปฐมภูมิจากเนื้อเยื่อช่องปากปกติที่ไม่อักเสบซึ่งปกคลุมฟันกรามคุดซี่ที่สามของผู้บริจาคที่แตกต่างกันจำนวน 8 ราย ซึ่งมีสุขภาพแข็งแรงและไม่มีประวัติสูบบุหรี่ที่ให้ความยินยอมเข้าร่วมโครงการวิจัย ทำการเพาะเลี้ยงเซลล์ทุกชนิดในอาหารเลี้ยงเซลล์ keratinocyte growth medium ซึ่งไม่มีซีรัมที่อุณหภูมิ 37 องศาเซลเซียส ปริมาณคาร์บอนไดออกไซด์ร้อยละ 5 ทำการเปลี่ยนอาหารเลี้ยงเซลล์ทุกวันเว้นวันจนเซลล์มีความหนาแน่นร้อยละ 80 จากนั้นตรวจหาการแสดงออกของโปรตีน ADAM9 ที่เยื่อหุ้มเซลล์ด้วยวิธีโฟลไซโทเมตรี และเปรียบเทียบระดับการแสดงออกของโปรตีน ADAM9 ขนาดที่ทำงานได้ที่ 84 กิโลดาลตัน ในเซลล์มะเร็งช่องปากกับเซลล์เยื่อบุผิวช่องปากปกติด้วยวิธีเวสเทิร์นบลอทไฮบริไดเซชัน นอกจากนั้นดำเนินการถ่าย siRNA ที่จำเพาะต่อ ADAM9 เพื่อยับยั้งการแสดงออกของ ADAM9 ในเซลล์มะเร็งช่องปากบางชนิดด้วยวิธี cell transfection และศึกษาการแสดงออกของ EGFR ที่ถูกเติมหมู่ฟอสเฟตที่ tyrosine1173 และ Akt ที่ถูกเติมหมู่ฟอสเฟตที่ serine473 ในเซลล์ที่ถูกยับยั้งการแสดงออกของ ADAM9 พร้อมกับนำเซลล์ดังกล่าวไปใช้ศึกษาการแบ่งตัวเพิ่มจำนวนเซลล์และการรุกรานของเซลล์ **ผลการทดลอง:** ค่ามัธยฐานของการแสดงออกของ ADAM9 ในเนื้อเยื่อมะเร็งช่องปากมากกว่าในเนื้อเยื่อปกติอย่างมีนัยสำคัญทางสถิติ ($p<0.001$) และพบว่าการแสดงออกของ ADAM9 สัมพันธ์กับลักษณะทางจุลพยาธิวิทยาของมะเร็งโดยมีการแสดงออกของ ADAM9 โปรตีนใน OSCC ชนิดที่เซลล์มะเร็งเปลี่ยนสภาพเป็นอย่างดีและใน OSCC ชนิดที่เซลล์มะเร็งเปลี่ยนสภาพอย่างปานกลางมากกว่าใน OSCC ชนิดที่เซลล์มะเร็งเปลี่ยนสภาพอย่างไม่ดีอย่างมีนัยสำคัญทางสถิติ ($r=0.557$; $p=0.001$) ผลการทดลองจาก

โฟลไซโทเมตรีพบว่าเซลล์มะเร็งช่องปาก 3 ใน 4 ชนิดได้แก่ HN6, HN15 และ HN008 มีการแสดงออก ของ ADAM9 โปรตีนบนเยื่อหุ้มเซลล์ และพบว่ามีการแสดงออกของ ADAM9 โปรตีนที่ทำงานได้ แตกต่างกันไปในแต่ละเซลล์ แต่พบว่ามีการแสดงออกของ ADAM9 โปรตีนเพิ่มสูงขึ้นใน HN6 และ HN15 อย่างมีนัยสำคัญทางสถิติเมื่อเปรียบเทียบกับเซลล์เยื่อบุผิวช่องปากปกติ ($p<0.05$) นอกจากการ แสดงออกที่เพิ่มขึ้นของ ADAM9 ในเซลล์มะเร็ง HN6 และ HN15 แล้วยังพบการแสดงออกที่เพิ่มขึ้นของ EGFR และ Akt ที่ถูกเติมหมู่ฟอสเฟตมากกว่าเซลล์ชนิดอื่นๆ อีกด้วย ซึ่งการแสดงออกที่เพิ่มขึ้นของ ADAM9 ดังกล่าวนี้สามารถถูกยับยั้งด้วย siRNA ที่จำเพาะต่อ ADAM9 อย่างมีนัยสำคัญทางสถิติเมื่อ เปรียบเทียบกับตัวอย่างที่ใช้ siRNA ซึ่งมีลำดับนิวคลีโอไทด์ที่ไม่เกี่ยวข้อง ($p<0.05$) พบว่าการ แสดงออกของ Akt ที่ถูกเติมหมู่ฟอสเฟตเท่านั้น แต่ไม่ใช่การแสดงออกของ EGFR ที่ถูกเติมหมู่ ฟอสเฟต ที่สามารถถูกยับยั้งอย่างมีนัยสำคัญทางสถิติด้วย siRNA ที่จำเพาะต่อ ADAM9 ในเซลล์ HN6 และ HN15 ($p<0.05$) ถึงแม้ว่าอัตราการแบ่งเซลล์มะเร็ง HN6 และ HN15 ที่ถูกยับยั้งการแสดงออกของ ADAM9 ด้วย siRNA ไม่แตกต่างไปจากกลุ่มควบคุม แต่พบว่าอัตราการรุกรานของเซลล์มะเร็งช่องปาก ทั้งสองชนิดลดลงอย่างมีนัยสำคัญทางสถิติ เมื่อเซลล์มะเร็งช่องปากทั้งสองชนิดถูกยับยั้งการแสดงออก ของ ADAM9 ด้วย siRNA ที่จำเพาะต่อ ADAM9 ($p<0.05$) **สรุปผลการทดลองและข้อเสนอแนะ สำหรับการศึกษาในอนาคต:** การแสดงออกของ ADAM9 เพิ่มขึ้นในเนื้อเยื่อมะเร็ง OSCC และใน เซลล์มะเร็งช่องปากบางชนิด แสดงให้เห็นถึงบทบาทของ ADAM9 ต่อพยาธิกำเนิดของโรคมะเร็งช่อง ปาก รวมไปถึงการแสดงออกที่เพิ่มขึ้นของ ADAM9 นี้ยังสัมพันธ์กับการเปลี่ยนสภาพของเซลล์มะเร็ง OSCC ชนิดที่เปลี่ยนสภาพเป็นอย่างดีซึ่งสอดคล้องกับมะเร็งของต่อมลูกหมาก ผลการศึกษานี้แสดงให้ เห็นถึงบทบาทหน้าที่ของวิถีให้สัญญาณ ADAM9 และ Akt ต่อการรุกรานของเซลล์มะเร็งช่องปากซึ่ง อาจจะเป็นประโยชน์ต่อการรักษามะเร็งช่องปากแบบมุ่งเป้า

คำสำคัญ: 5-โบรโม-2'-ดีออกซียูริดีน; เอดิสอินเทกรินแอนด์เมทัลโลโปรทีเนสไนน์; เอเคที; เอพิเดอร์มัล โกรธแฟกเตอร์รีเซ็พเตอร์; มะเร็งเยื่อบุผิวช่องปากชนิดสความัสเซลล์; สมอลอินเทอร์เฟียริงอาร์เอ็นเอ

ABSTRACT

Oral squamous cell carcinoma (OSCC), a devastating disease with high morbidity and mortality rates, is commonly found in the oral cavity and the oropharynx. A Disintegrin and Metalloproteinase 9 (ADAM9), a type I transmembrane glycoprotein, is overexpressed in various types of cancer, including OSCC tissues and certain oral cancer cell lines, but some studies have reported inconclusive findings regarding chromosomal aberrations in the ADAM9-containing region or only ADAM9 mRNA expression has been reported in oral cancer. Moreover, ADAM9 involvement in the pathogenesis of OSCC, especially for the activation of the epidermal growth factor receptor (EGFR)/Akt signaling pathway and cancer cell aggressiveness, has not yet been addressed. **Objectives:** Therefore, this study aimed to determine and compare ADAM9 protein expression in OSCC and normal oral tissues *in vivo* and in cultured oral cancer cell lines and human oral keratinocytes (HOKs) and to examine the functional role of ADAM9 in phosphorylation of EGFR and Akt and in oral cancer cell aggressiveness *in vitro*. **Materials and Methods:** Thirty-four OSCC and ten healthy paraffin-embedded sections were probed with the anti-ADAM9 antibody, and the immunohistochemical score was determined by combining the score of the percentage of positively-stained cells with the intensity score. Four oral cancer cell lines, including HN5, HN6, HN15 and HN008, and primary HOKs that were isolated from non-inflamed oral tissues overlying the impacted third molars of healthy and non-smoking donors (n=8) with their informed consent were cultured in serum-free keratinocyte growth medium at 37°C in a humidified chamber with 5% CO_2. The culture medium was replenished every other day until 80% cell confluence. Expression of membrane ADAM9 and active ADAM9 at 84 kDa in these cell lines was assayed by flow cytometry and western blot hybridization, respectively. Cell transfection with small interfering RNA (siRNA) was performed to inhibit ADAM9 expression in some oral cancer cells. ADAM9-knockdown cells were examined for expressions of phosphorylated-EGFR^{tyrosine1173} (p-EGFR^{tyr1173}) and phosphorylated-Akt^{serine473} (p-Akt^{ser473}) and used in cell proliferation and invasion assays. **Results:** The median immunohistochemical score of ADAM9 expression in OSCC tissues was significantly greater than that in normal tissues (p<0.001). Moreover, among OSCC cases, intense staining of ADAM9 expression was detected in well-differentiated and moderately-differentiated OSCC, and ADAM9 expression was correlated with an increasing degree of cell differentiation (r=0.557; p=0.001). Expression of membrane ADAM9 was found in three of four cancer cell lines, including HN6, HN15 and HN008. Expression of active ADAM9 varied among all tested cell lines, but significantly higher ADAM9 expression was found in HN6 and HN15 than that in HOKs (p<0.05). Enhanced expressions of p-EGFR^{tyr1173} and p-Akt^{ser473}

were also found in HN6 and HN15. ADAM9 expressions in both cells were significantly inhibited by ADAM9 siRNA compared to scramble ($p<0.05$). Expression of p-Akt^{ser473}, but not that of p-EGFR^{tyr1173}, was significantly blocked by ADAM9 siRNA in HN6 and HN15 ($p<0.05$). Although the cell proliferation rate of ADAM9-knockdown cells did not differ from that of scramble, a significant decrease in cell invasion was found in ADAM9-knockdown HN6 and HN15 ($p<0.05$). **Conclusions and suggestions for future studies:** ADAM9 is overexpressed in OSCC and certain oral cancer cell lines, suggesting its role in the pathogenesis of oral cancer. Similar to the overexpression of ADAM9 in well-differentiated prostate cancer, high degrees of ADAM9 expression are also observed in the well-differentiated OSCC. Moreover, the findings from the functional studies suggest the involvement of the ADAM9/Akt signaling pathway in oral cancer cell invasion, which may be beneficial for a therapeutic target of oral cancer.

KEYWORDS: 5-Bromo-2'-Deoxyuridine; A Disintegrin and Metalloproteinase 9; Akt; Epidermal Growth Factor Receptor; Oral Squamous Cell Carcinoma; Small Interfering RNA

รายงานวิจัยฉบับสมบูรณ์

ทุนองค์ความรู้ใหม่ที่เป็นพื้นฐานต่อการพัฒนา

โครงการ ความเกี่ยวข้องของวิถี ADAM9/EGFR/Akt ในมะเร็งเยื่อบุผิวช่องปากชนิดสความัสเซลล์

Involvement of the ADAM9/EGFR/Akt Pathway in Oral Squamous Cell Carcinoma

คณะผู้วิจัย	**สังกัด**
1. ศาสตราจารย์ ทพ. ดร. สุทธิชัย กฤษณะประกรกิจ	คณะทันตแพทยศาสตร์ มหาวิทยาลัยเชียงใหม่
2. ผศ. ทพ. ดร. ชยารพ สุพรรณชาติ	คณะทันตแพทยศาสตร์ มหาวิทยาลัยเชียงใหม่
3. อ. ทพญ. ดร. วรกัญญา บูรณพัฒนา	คณะทันตแพทยศาสตร์ มหาวิทยาลัยเชียงใหม่
4. ดร. อนุพงศ์ เมฆอุดม	คณะทันตแพทยศาสตร์ มหาวิทยาลัยเชียงใหม่

บทคัดย่อ

มะเร็งเยื่อบุผิวช่องปากชนิดสความัสเซลล์ (OSCC) เป็นโรคที่ร้ายแรงซึ่งพบได้ในช่องปากและคอหอยส่วนปาก มีอัตราการตายและทุพพลภาพสูง พบการแสดงออกที่เพิ่มขึ้นของเอดิสอินเทกรินแอนด์เมทัลโลโปรทีเนสไนน์หรือ ADAM9 ซึ่งเป็นไกลโคโปรตีนบนเยื่อหุ้มเซลล์ชนิดที่ 1 ในโรคมะเร็งหลากหลายชนิดรวมถึง OSCC และในเซลล์ไลน์บางชนิดที่สกัดแยกได้จาก OSCC แต่ก็ยังไม่มีข้อสรุปที่ชัดเจนเกี่ยวกับความผิดปกติของโครโมโซมตรงตำแหน่งที่พบยีนสำหรับ ADAM9 หรือยังมีการศึกษาเฉพาะการแสดงออกของอาร์เอ็นเอนำรหัสของ ADAM9 ในมะเร็งช่องปากเท่านั้น นอกจากนั้นยังไม่พบว่ามีการศึกษาใดศึกษาถึงความเกี่ยวข้องของ ADAM9 ต่อพยาธิกำเนิดของ OSCC โดยเฉพาะอย่างยิ่งการกระตุ้นวิถีให้สัญญาณของเอพิเดอร์มัลโกรธแฟกเตอร์รีเซ็พเตอร์ (EGFR) และเอเคที (Akt) และต่อการที่เซลล์มะเร็งมีความก้าวร้าวเพิ่มมากขึ้น **วัตถุประสงค์:** ดังนั้นการศึกษานี้มีวัตถุประสงค์ที่จะศึกษาถึงระดับการแสดงออกของโปรตีน ADAM9 ในเนื้อเยื่อมะเร็งช่องปากเปรียบเทียบกับเยื่อบุผิวช่องปากปกติและในเซลล์มะเร็งเปรียบเทียบกับเซลล์เยื่อบุผิวช่องปากปกติซึ่งถูกเพาะเลี้ยงในห้องปฏิบัติการ นอกจากนั้น ยังศึกษาบทบาทหน้าที่ของ ADAM9 ในการกระตุ้นกระบวนการเติมหมู่ฟอสเฟตของ EGFR และ Akt และความก้าวร้าวของเซลล์มะเร็งช่องปากนอกกาย **วัสดุและวิธีการทดลอง:** ศึกษาการแสดงออกของโปรตีน ADAM9 โดยวิธีอิมมูโนฮิสโตเคมิสตรีในเนื้อเยื่อมะเร็งช่องปากชนิด OSCC 34 ชิ้น และเยื่อบุผิวช่องปากปกติ 10 ชิ้น คำนวณคะแนนอิมมูโนฮิสโตเคมิสตรีโดยการนำคะแนนของร้อยละของเซลล์ที่ให้ผลบวกรวมกับคะแนนของความเข้มของการติดสี ทำการเพาะเลี้ยงเซลล์มะเร็งช่องปากที่แตกต่างกัน 4 ชนิด ได้แก่ HN5, HN6, HN15 และ HN008 และเซลล์เยื่อบุผิวปฐมภูมิจากเนื้อเยื่อช่องปากปกติที่ไม่อักเสบซึ่งปกคลุมฟันกรามคุดซี่ที่สามของผู้บริจาคที่แตกต่างกันจำนวน 8 ราย ซึ่งมีสุขภาพแข็งแรงและไม่มีประวัติสูบบุหรี่ที่ให้ความยินยอมเข้าร่วมโครงการวิจัย ทำการเพาะเลี้ยงเซลล์ทุกชนิดในอาหารเลี้ยงเซลล์ keratinocyte growth medium ซึ่งไม่มีซีรัมที่อุณหภูมิ 37 องศาเซลเซียสปริมาณคาร์บอนไดออกไซด์ร้อยละ 5 ทำการเปลี่ยนอาหารเลี้ยงเซลล์ทุกวันเว้นวันจนเซลล์มีความหนาแน่นร้อยละ 80 จากนั้นตรวจหาการแสดงออกของโปรตีน ADAM9 ที่เยื่อหุ้มเซลล์ด้วยวิธีโฟลไซโทเมตรี และเปรียบเทียบระดับการแสดงออกของโปรตีน ADAM9 ขนาดที่ทำงานได้ที่ 84 กิโลดาลตัน ในเซลล์มะเร็งช่องปากกับเซลล์เยื่อบุผิวช่องปากปกติด้วยวิธีเวสเทิร์นบลอทไฮบริไดเซชัน นอกจากนั้นดำเนินการถ่าย siRNA ที่จำเพาะต่อ ADAM9 เพื่อยับยั้งการแสดงออกของ ADAM9 ในเซลล์มะเร็งช่องปากบางชนิดด้วยวิธี cell transfection และศึกษาการแสดงออกของ EGFR ที่ถูกเติมหมู่ฟอสเฟตที่ tyrosine1173 และ Akt ที่ถูกเติมหมู่ฟอสเฟตที่ serine473 ในเซลล์ที่ถูกยับยั้งการแสดงออกของ ADAM9 พร้อมกับนำเซลล์ดังกล่าวไปใช้ศึกษาการแบ่งตัวเพิ่มจำนวนเซลล์และการรุกรานของเซลล์ **ผลการทดลอง:** ค่ามัธยฐานของการแสดงออกของ ADAM9 ในเนื้อเยื่อมะเร็งช่องปากมากกว่าในเนื้อเยื่อปกติอย่างมีนัยสำคัญทางสถิติ ($p<0.001$) และพบว่าการแสดงออกของ ADAM9 สัมพันธ์กับลักษณะทางจุลพยาธิวิทยาของมะเร็งโดยมีการแสดงออกของ ADAM9 โปรตีนใน OSCC ชนิดที่เซลล์มะเร็งเปลี่ยนสภาพเป็นอย่างดีและใน OSCC ชนิดที่เซลล์มะเร็งเปลี่ยนสภาพอย่างปานกลางมากกว่าใน OSCC ชนิดที่เซลล์มะเร็งเปลี่ยนสภาพอย่างไม่ดีอย่างมีนัยสำคัญทางสถิติ (r=0.557; $p=0.001$) ผลการทดลองจาก

โฟลไซโทเมตรีพบว่าเซลล์มะเร็งช่องปาก 3 ใน 4 ชนิดได้แก่ HN6, HN15 และ HN008 มีการแสดงออกของ ADAM9 โปรตีนบนเยื่อหุ้มเซลล์ และพบว่ามีการแสดงออกของ ADAM9 โปรตีนที่ทำงานได้แตกต่างกันไปในแต่ละเซลล์ แต่พบว่ามีการแสดงออกของ ADAM9 โปรตีนเพิ่มสูงขึ้นใน HN6 และ HN15 อย่างมีนัยสำคัญทางสถิติเมื่อเปรียบเทียบกับเซลล์เยื่อบุผิวช่องปากปกติ ($p<0.05$) นอกจากการแสดงออกที่เพิ่มขึ้นของ ADAM9 ในเซลล์มะเร็ง HN6 และ HN15 แล้วยังพบการแสดงออกที่เพิ่มขึ้นของ EGFR และ Akt ที่ถูกเติมหมู่ฟอสเฟตมากกว่าเซลล์ชนิดอื่นๆ อีกด้วย ซึ่งการแสดงออกที่เพิ่มขึ้นของ ADAM9 ดังกล่าวนี้สามารถถูกยับยั้งด้วย siRNA ที่จำเพาะต่อ ADAM9 อย่างมีนัยสำคัญทางสถิติเมื่อเปรียบเทียบกับตัวอย่างที่ใช้ siRNA ซึ่งมีลำดับนิวคลีโอไทด์ที่ไม่เกี่ยวข้อง ($p<0.05$) พบว่าการแสดงออกของ Akt ที่ถูกเติมหมู่ฟอสเฟตเท่านั้น แต่ไม่ใช่การแสดงออกของ EGFR ที่ถูกเติมหมู่ฟอสเฟต ที่สามารถถูกยับยั้งอย่างมีนัยสำคัญทางสถิติด้วย siRNA ที่จำเพาะต่อ ADAM9 ในเซลล์ HN6 และ HN15 ($p<0.05$) ถึงแม้ว่าอัตราการแบ่งเซลล์มะเร็ง HN6 และ HN15 ที่ถูกยับยั้งการแสดงออกของ ADAM9 ด้วย siRNA ไม่แตกต่างไปจากกลุ่มควบคุม แต่พบว่าอัตราการรุกรานของเซลล์มะเร็งช่องปากทั้งสองชนิดลดลงอย่างมีนัยสำคัญทางสถิติ เมื่อเซลล์มะเร็งช่องปากทั้งสองชนิดถูกยับยั้งการแสดงออกของ ADAM9 ด้วย siRNA ที่จำเพาะต่อ ADAM9 ($p<0.05$) **สรุปผลการทดลองและข้อเสนอแนะสำหรับการศึกษาในอนาคต:** การแสดงออกของ ADAM9 เพิ่มขึ้นในเนื้อเยื่อมะเร็ง OSCC และในเซลล์มะเร็งช่องปากบางชนิด แสดงให้เห็นถึงบทบาทของ ADAM9 ต่อพยาธิกำเนิดของโรคมะเร็งช่องปาก รวมไปถึงการแสดงออกที่เพิ่มขึ้นของ ADAM9 นี้ยังสัมพันธ์กับการเปลี่ยนสภาพของเซลล์มะเร็ง OSCC ชนิดที่เปลี่ยนสภาพเป็นอย่างดีซึ่งสอดคล้องกับมะเร็งของต่อมลูกหมาก ผลการศึกษานี้แสดงให้เห็นถึงบทบาทหน้าที่ของวิถีให้สัญญาณ ADAM9 และ Akt ต่อการรุกรานของเซลล์มะเร็งช่องปากซึ่งอาจจะเป็นประโยชน์ต่อการรักษามะเร็งช่องปากแบบมุ่งเป้า

คำสำคัญ: 5-โบรโม-2'-ดีออกซียูริดีน; เอดิสอินเทกรินแอนด์เมทัลโลโปรทีเนสไนน์; เอเคที; เอพิเดอร์มัลโกรธแฟกเตอร์รีเซ็พเตอร์; มะเร็งเยื่อบุผิวช่องปากชนิดสความัสเซลล์; สมอลอินเทอร์เฟียริงอาร์เอ็นเอ

ABSTRACT

Oral squamous cell carcinoma (OSCC), a devastating disease with high morbidity and mortality rates, is commonly found in the oral cavity and the oropharynx. A Disintegrin and Metalloproteinase 9 (ADAM9), a type I transmembrane glycoprotein, is overexpressed in various types of cancer, including OSCC tissues and certain oral cancer cell lines, but some studies have reported inconclusive findings regarding chromosomal aberrations in the ADAM9-containing region or only ADAM9 mRNA expression has been reported in oral cancer. Moreover, ADAM9 involvement in the pathogenesis of OSCC, especially for the activation of the epidermal growth factor receptor (EGFR)/Akt signaling pathway and cancer cell aggressiveness, has not yet been addressed. **Objectives:** Therefore, this study aimed to determine and compare ADAM9 protein expression in OSCC and normal oral tissues *in vivo* and in cultured oral cancer cell lines and human oral keratinocytes (HOKs) and to examine the functional role of ADAM9 in phosphorylation of EGFR and Akt and in oral cancer cell aggressiveness *in vitro*. **Materials and Methods:** Thirty-four OSCC and ten healthy paraffin-embedded sections were probed with the anti-ADAM9 antibody, and the immunohistochemical score was determined by combining the score of the percentage of positively-stained cells with the intensity score. Four oral cancer cell lines, including HN5, HN6, HN15 and HN008, and primary HOKs that were isolated from non-inflamed oral tissues overlying the impacted third molars of healthy and non-smoking donors (*n*=8) with their informed consent were cultured in serum-free keratinocyte growth medium at 37°C in a humidified chamber with 5% CO_2. The culture medium was replenished every other day until 80% cell confluence. Expression of membrane ADAM9 and active ADAM9 at 84 kDa in these cell lines was assayed by flow cytometry and western blot hybridization, respectively. Cell transfection with small interfering RNA (siRNA) was performed to inhibit ADAM9 expression in some oral cancer cells. ADAM9-knockdown cells were examined for expressions of phosphorylated-EGFR^{tyrosine1173} (p-EGFR^{tyr1173}) and phosphorylated-Akt^{serine473} (p-Akt^{ser473}) and used in cell proliferation and invasion assays. **Results:** The median immunohistochemical score of ADAM9 expression in OSCC tissues was significantly greater than that in normal tissues (*p*<0.001). Moreover, among OSCC cases, intense staining of ADAM9 expression was detected in well-differentiated and moderately-differentiated OSCC, and ADAM9 expression was correlated with an increasing degree of cell differentiation (r=0.557; *p*=0.001). Expression of membrane ADAM9 was found in three of four cancer cell lines, including HN6, HN15 and HN008. Expression of active ADAM9 varied among all tested cell lines, but significantly higher ADAM9 expression was found in HN6 and HN15 than that in HOKs (*p*<0.05). Enhanced expressions of p-EGFR^{tyr1173} and p-Akt^{ser473}

were also found in HN6 and HN15. ADAM9 expressions in both cells were significantly inhibited by ADAM9 siRNA compared to scramble ($p<0.05$). Expression of p-Akt^{ser473}, but not that of p-EGFR^{tyr1173}, was significantly blocked by ADAM9 siRNA in HN6 and HN15 ($p<0.05$). Although the cell proliferation rate of ADAM9-knockdown cells did not differ from that of scramble, a significant decrease in cell invasion was found in ADAM9-knockdown HN6 and HN15 ($p<0.05$). **Conclusions and suggestions for future studies:** ADAM9 is overexpressed in OSCC and certain oral cancer cell lines, suggesting its role in the pathogenesis of oral cancer. Similar to the overexpression of ADAM9 in well-differentiated prostate cancer, high degrees of ADAM9 expression are also observed in the well-differentiated OSCC. Moreover, the findings from the functional studies suggest the involvement of the ADAM9/Akt signaling pathway in oral cancer cell invasion, which may be beneficial for a therapeutic target of oral cancer.

KEYWORDS: 5-Bromo-2'-Deoxyuridine; A Disintegrin and Metalloproteinase 9; Akt; Epidermal Growth Factor Receptor; Oral Squamous Cell Carcinoma; Small Interfering RNA

EXECUTIVE SUMMARY

For the past three years, I have conducted several *in vivo* and *in vitro* experiments as follows.

1) To determine ADAM9, p-EGFR^{tyr1173} and p-Akt^{ser473} protein expression by immunohistochemistry using their specific antibodies in formalin-fixed and paraffin-embedded tissue sections of oral squamous cell carcinoma (OSCC) and normal oral tissues; 2) To compare the expression of ADAM9, p-EGFR^{tyr1173} and p-Akt^{ser473} between OSCC and normal oral tissues; and 3) To find the correlations for the expression of ADAM9, p-EGFR^{tyr1173} and p-Akt^{ser473} with different histopathological grading of OSCC, including well, moderately and poorly differentiated, and those for the expression of these three molecules in the same OSCC and normal tissues.

The results demonstrated significant increases in the median immunohistochemical (IHC) scores of all three biomolecules in OSCC compared to those in normal tissues ($p<0.01$). Only expressions of p-EGFR^{tyr1173} and p-Akt^{ser47}, but **not** ADAM9, were significantly correlated with increased disease severity, stratified according to histological grading ($r=0.429$ and $r=0.351$, respectively). Expressions of all three biomolecules were significantly and positively correlated between each other ($p<0.01$), suggesting their interconnections. Therefore, these proposed three aims have already been achieved.

4) To examine ADAM9, p-EGFR^{tyr1173} and p-Akt^{ser473} expression *in vitro* by investigating their protein expression in OSCC cell lines and compare with that in normal oral epithelial cells by immunoblotting.

A significant increase in the median ratios for protein expressions of ADAM9, p-EGFR^{tyr1173} and p-Akt^{ser473}, relative to β-actin, total EGFR and total Akt, respectively, was found in two OSCC cell lines, HN6 and HN15 ($p<0.05$), but **not** in the other two OSCC cell lines, HN5 or HN008, compared to expressions of the respective proteins in 8 normal human oral keratinocyte cell lines from 8 different donors. Interestingly, the significantly increased expressions of these three biomolecules were simultaneously found in HN6 and HN15 as well, suggesting that the ADAM9-EGFR-Akt pathway exists in some OSCC cells, consistent with a concept of "personalized" medicine. So, this aim is accomplished.

5) To investigate membrane ADAM9 expression in OSCC cell lines by flow cytometry.

Expression of membrane ADAM9 was found in HN6, HN15 and HN008, but **not** in HN5. Membrane ADAM9 expression was also detected in HepG2 as a positive control. So, this aim is accomplished.

6) To determine the inhibitory effect of cell transfection with small interfering RNA (siRNA) specific for ADAM9 in OSCC cell lines on phosphorylation of EGFR at the tyrosine 1173 residue and of Akt at the serine 473 residue by immunoblotting analysis.

Expressions of both ADAM9 mRNA and protein in HN6 and HN15 were significantly inhibited by cell transfection with 5 and 10 nM of siRNA against ADAM9 compared to no inhibition by a scrambled sequence ($p<0.05$). Interestingly, only expression of p-Akt^{ser473}, but **not** that of p-EGFR^{tyr1173}, was significantly blocked by transfection with siRNA against ADAM9 in HN6 and HN15 ($p<0.05$), indicating different behaviors between OSCC and esophageal SCC cell lines (Liu et al., 2015). No inhibitory effect of transfection with siRNA against ADAM9 on p-EGFR^{tyr1173} expression was corroborated with the absence of inhibitory effect on the cell proliferation rate of HN6 and HN15, as determined by the BrdU assay. So, this aim is accomplished.

7) To investigate the blocking effect on cancer cell aggressiveness in ADAM9-siRNA-transfected-OSCC cell lines using the migration and the invasion assays. By the cell invasion assay, a significant decrease in oral cancer cell invasion through ECM matrix was found in HN6 and HN15 cells that were transfected with siRNA against ADAM9 ($p<0.05$) as compared to a scrambled sequence. So, this aim is accomplished.

8) To determine the function of ADAM9 *in vivo*. This aim has **not** been addressed due to the **absence** of inhibitory effect on the cancer cell proliferation *in vitro* in ADAM9-knockdown HN6 and HN15, mentioned in aim 6. For more details regarding all of these findings, please see the following pages. Finally, I have been successful in publishing **18** international articles using the budget from this grant (see Outputs).

เนื้องานวิจัยที่ทำทั้งหมดประกอบด้วย วัตถุประสงค์ และผลงานวิจัยที่ได้รับ

1. To determine ADAM9, p-EGFR^{tyr1173} and p-Akt^{ser473} protein expression by immunohistochemistry using their specific antibodies in formalin-fixed and paraffin-embedded tissue sections of OSCC and normal oral tissues.

2. To compare the expression of ADAM9, p-EGFR^{tyr1173} and p-Akt^{ser473} between OSCC and normal oral tissues.

3. To find the correlations for the expression of ADAM9, p-EGFR^{tyr1173} and p-Akt^{ser473} with different histopathological grading of OSCC, including well, moderately and poorly differentiated, and those for the expression of these three molecules in the same OSCC and normal tissues.

Thirty-four OSCC cases from 2002 to 2012 and 10 normal tissues were included in this study. The clinicopathologic characteristics of all 34 OSCC cases (17 males and 17 females; average age = 66.38 years; range = 43-85 years) are summarized in Table 1. The severity of OSCC was histologically categorized as well differentiated, moderately differentiated and poorly differentiated (Table 1), based on the histopathological diagnosis by an oral pathologist, Faculty of Dentistry, Chiang Mai University. Moreover, four clinical diagnostic criteria according to Sobin et al., 2009 were used to group 34 OSCC cases (Table 1). Subsequently, immunohistochemistry was conducted to determine ADAM9, p-EGFR^{tyr1173} and p-Akt^{ser473} protein expression in these tissue blocks according to the modified method of Iamaroon and Krisanaprakornkit, 2009, using specific primary antibodies for ADAM9 (cat no. sc-23290, Santa Cruz Biotechnology, Inc.), p-EGFR^{tyr1173} (cat no. sc-101668, Santa Cruz Biotechnology, Inc.) and p-Akt^{ser473} (cat no. 4051, Cell Signaling Technology). Then, digitized images were captured and the ImageJ program version 1.48 (National Institutes of Health, Bethesda, MD, USA) was used to quantitatively determine the percentage of positively stained cells and the staining intensity of digitized images. The mean percentage of positive cells was determined from the percentage of positive cells (the number of brown stained cells against that of total cells in each image) in each of the three representative images and scored using the modified Fromowitz standard (Fromowitz et al., 1987) as follows; 0, <10%; 1, ≥10 to <25% ; 2, ≥25 to <50%; 3, ≥50 to <75%; and 4, ≥75%. For the intensity score, the color of counterstaining was first removed and the brown intensity was analyzed by mean RGB (0-255). The average mean RGB was determined from the mean RGB in each of the three representative images and scored as follows; 0, no staining (mean RGB>245.75); 1, weak (227.25<mean RGB≤245.75);

2, moderate (208.75<mean RGB≤227.25); and 3, intense (mean RGB≤208.75). The lower and upper limits of mean RGB were derived from a linear equation as $y=13.77-0.054x$, where y=intensity score and x=mean RGB. To formulate this equation, the intensity of each section was semi-quantitatively scored (Table 2) as 0 (none), 1 (weak), 2 (moderate), or 3 (intense) based on the criteria of Pirker et al., 2012 by two independent observers with an inter-calibration value equal to 0.881. The intensity score and its mean RGB value were plotted on a y axis and an x axis of the scatter diagram, respectively, and a linear regression line was drawn and used for the equation (Kongkaew et al., 2018). The immunohistochemical (IHC) score (0-7) was then determined by combining the average percentage score of positive cells (0-4) with the average intensity score (0-3). The intensity scores of ADAM9 immunostaining of all 34 OSCC cases are summarized in Table 2 according to their histological grading.

By immunohistochemistry, intense ADAM9 staining was observed in both the cytoplasm and the membrane of most cancer cell nests, which were localized in the connective tissue layer of OSCC specimens (arrowheads in Fig. 1), compared to weak and diffuse ADAM9 staining in the cytoplasm of normal epithelial cells, especially in the suprabasal cell layers (Fig. 1). Note that the intensity of ADAM9 staining in the overlying epithelium of OSCC tissue was weak (bracket in Fig. 1). Similarly to ADAM9 overexpression in OSCC, the immunostaining were strikingly more intense in OSCC than in normal tissues, reacted with the anti-p-EGFR^{tyr1173}and anti-p-Akt^{ser473} antibodies (Fig. 2). Note that no immunostaining was seen in the absence of primary antibodies in OSCC or normal tissues as a negative control (not shown).
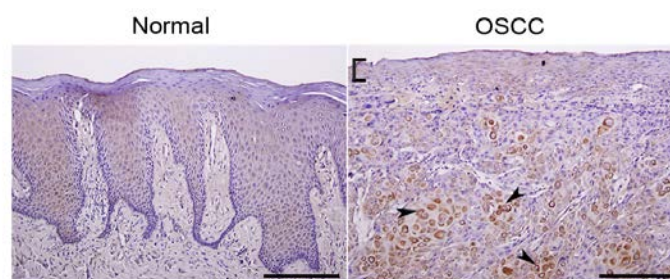

Figure 1. ADAM9 overexpression in OSCC. Representative images of ADAM9 expression in normal and OSCC tissues. Weak ADAM9 staining is present in the suprabasal layers of normal epithelium and in the overlying epithelium of OSCC (bracket); intense cytoplasmic staining of ADAM9 is in tumor cell nests within the connective tissue layer of OSCC (arrowheads). Bar = 200 μm.
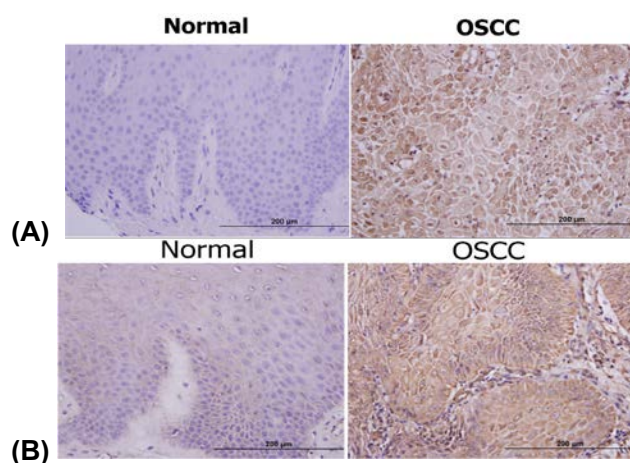
Figure 2. Overexpression of p-EGFR^{tyr1173} (A) and p-Akt^{ser473} (B) in OSCC tissues. Some representative images show intense immunostaining in cancer cell nests within the connective tissue layer of OSCC compared to weak staining in the normal epithelium.

Table 1. Clinicopathologic characteristics of OSCC cases.

Variables		Number of cases
Clinical diagnostic staging [a]	I	6
	II	6
	III	5
	IV	17
Histological grading	Well differentiated	14
	Moderately differentiated	12
	Poorly differentiated	8
Location	Buccal mucosa	10
	Lateral tongue	5
	Gingiva/alveolar mucosa	13
	Labial mucosa	1
	Retromolar pad	1
	Lip vermillion	2
	Mandible	2

Criteria described in (Sobin et al., 2009) as follows:

I   = Tumor size ≤2 cm without regional lymph node spreading.

II = Tumor size >2-4 cm without regional lymph node spreading.

III = Tumor size >4 cm or of any size with spread to a single ipsilateral lymph node (≤3 cm).

IV = Tumor of any size with spread to at least a single ipsilateral lymph node (>3 cm) or with spread to at least a single contralateral lymph node, or tumor invasion to adjacent organs or spreading to other parts of the body, regardless of lymph node involvement.

Table 2. A semi-quantitative analysis of the intensities of ADAM9 expression in 34 OSCC cases, as categorized by their histological grading.

Intensity score [a]	Well differentiated N (%)	Moderately differentiated N (%)	Poorly differentiated N (%)
0	0 (0)	0 (0)	0 (0)
1	2 (14.3)	1 (8.3)	3 (37.5)
2	3 (21.4)	**8 (66.7)**	**5 (62.5)**
3	**9 (64.3)**	3 (25)	0 (0)
Total	14 (100)	12 (100)	8 (100)

[a] 0 = no staining; 1 = weak (light brown staining, visible only with high magnification); 2 = moderate (between 1 and 3); 3 = intense (dark brown staining, visible with low magnification) (Pirker et al., 2012).

Using the Mann Whitney U test, the median IHC scores were significantly higher in OSCC than in normal tissues for ADAM9 ($p<0.001$; Fig. 3A), for p-EGFR[tyr1173] ($p<0.001$; Fig. 3B) and for p-Akt[ser473] ($p<0.01$; Fig. 3C) expressions.
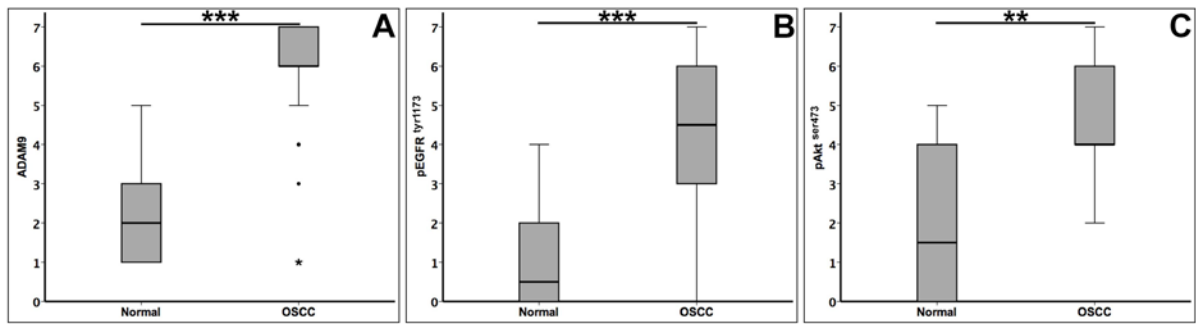
Figure 3. Significantly higher immunohistochemical (IHC) score (0-7) in OSCC than in normal tissues for ADAM9 (A), p-EGFR^{tyr1173} (B), and p-Akt^{ser473} (C). **, $p<0.01$; ***, $p<0.001$. Two small black circles and an asterisk in A represent outliers and an extreme value, respectively.

Next, all 34 OSCC cases were grouped into four clinical diagnostic stages (Table 1) according to tumor size and nodal status (Sobin et al., 2009), based on the histopathological reports. By the Spearman correlation test, the IHC scores, representing ADAM9 expression, were not found to correlate with these four clinical diagnostic stages (r=-0.082, p=0.661). However, when all OSCC cases were categorized according to their histological grading, including 14 well differentiated, 12 moderately differentiated and 8 poorly differentiated cases (Table 1), it was found that the intensity of ADAM9 staining was greatest in the well differentiated OSCC, followed by the moderately and the poorly differentiated OSCC, respectively (Fig. 4A). A semi-quantitative analysis of the staining intensity in all OSCC specimens is summarized in Table 2. In general, the intense staining score (=3) was found in more than 60% of the well differentiated OSCC cases, whereas it was found in only 25% and 0% of the moderately and the poorly differentiated OSCC cases, respectively (Table 2). On the contrary, more than 60% of the moderately and the poorly differentiated OSCC cases were scored as moderate staining (=2). As with the staining intensity score results, the average percentage of positively stained cells, irrespective of staining intensity, was greater in the well and in the moderately differentiated OSCC than in the poorly differentiated OSCC (data not shown). By the Spearman correlation test, the IHC scores for ADAM9 were positively correlated with an increased degree of cell differentiation (r=0.557, p=0.001; Fig. 4B). In other words, the median IHC scores in both moderately and well differentiated OSCC were significantly higher than that in the poorly differentiated OSCC ($p<0.01$; Fig. 4B). However, there was no difference in the median IHC score between the well and the moderately differentiated OSCC (Fig. 4B).

In contrast to no significant correlation (p=0.101; Fig. 5A) between increased ADAM9 expression and OSCC severity, histologically stratified as well, moderately and poorly differentiated, expressions of p-EGFR^{tyr1173} and of p-Akt^{ser473} were significantly correlated with OSCC severity as their expressions were increased in moderately and poorly differentiated OSCC (p=0.005 in Fig. 5B and p=0.022 in Fig. 5C, respectively). Note that a significant correlation was only found between up-regulated ADAM9 expression and increased cell differentiation (Fig. 4B). Representative images for the expressions of ADAM9, p-EGFR^{tyr1173} and p-Akt^{ser473} according to the histopathological grading are shown in Figure 6.
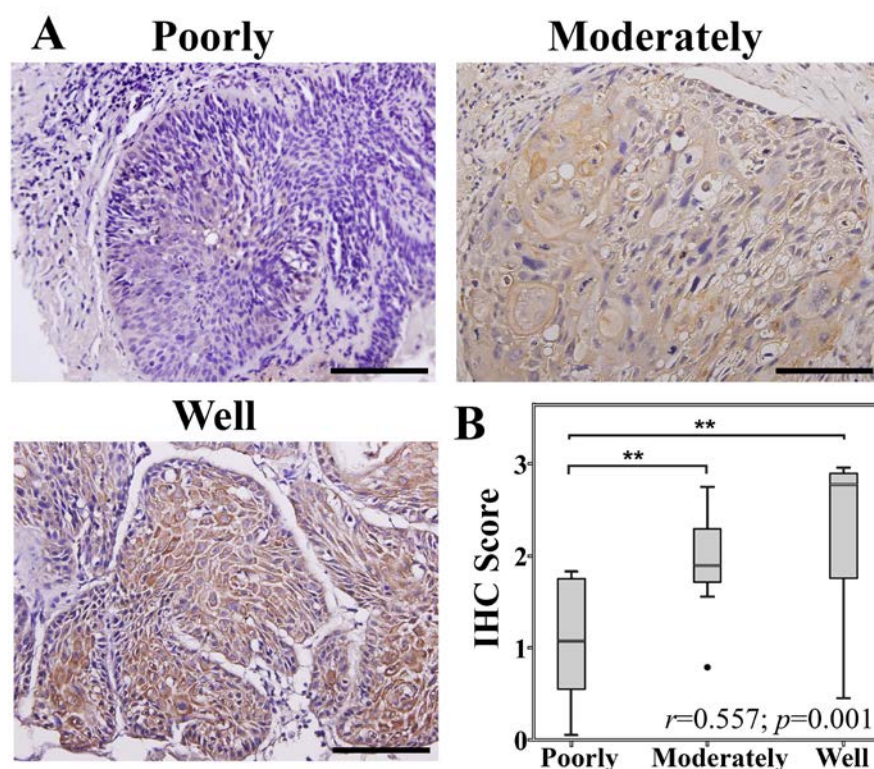

Figure 4. A positive correlation between ADAM9 expression and cell differentiation in OSCC. (A) A representative image of ADAM9 expression in each histological grading. Note the strongest intensity of ADAM9 staining in the well differentiated OSCC, followed by the moderately differentiated and the poorly differentiated OSCC. Bar = 100 μm. (B) A box plot diagram showing the positive correlation between increased immunohistochemical (IHC) scores (0-3) for ADAM9 expression and enhanced levels of cell differentiation. ** = p<0.01. A small black circle represents an outlier in the moderately differentiated OSCC.
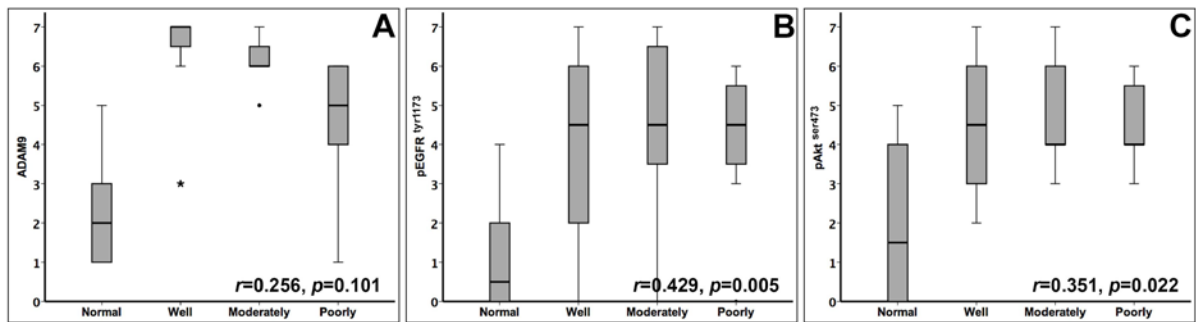
Figure 5. The significant and positive correlations between OSCC severity, histologically stratified as well, moderately and poorly differentiated, and expressions of p-EGFR^{tyr1173} (B) and of p-Akt^{ser473} (C), but not that of ADAM9 (A). An asterisk and a small black circle in A represent an extreme and an outlier value, respectively.
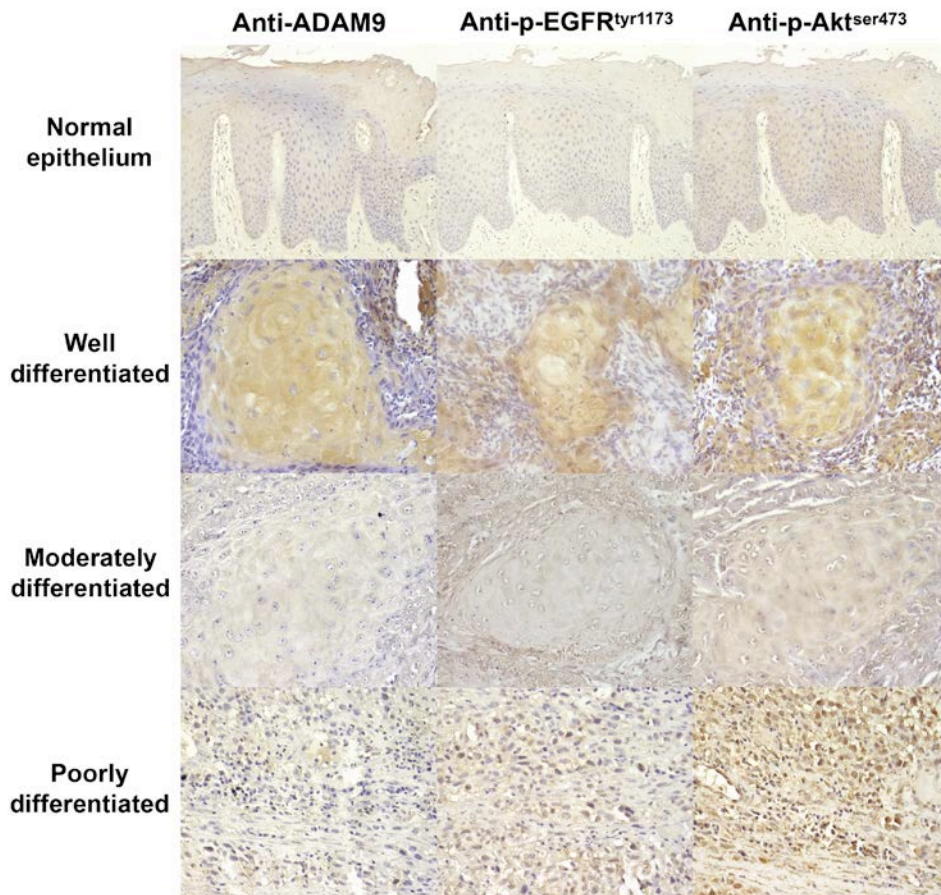

Figure 6. Representative images of ADAM9, p-EGFR^{tyr1173} and p-Akt^{ser473} expressions in normal epithelium and OSCC, histologically stratified as well, moderately and poorly differentiated. Note intense immunostaining for p-EGFR^{tyr1173} and p-Akt^{ser473} expressions were still found in poorly differentiated OSCC, whereas ADAM9 immunostaining was weak.

Interestingly, when the correlations were determined for the IHC scores between each pair of the three biomolecules, including ADAM9, p-EGFR^{tyr1173} and p-Akt^{ser473}, in both OSCC and normal tissues, it was demonstrated that the IHC scores of ADAM9 expression were positively correlated with those of p-EGFR^{tyr1173} expression (r=0.456; p=0.002; Fig. 7A) and with those of p-Akt^{ser473} expression (r=0.515; p<0.001; Fig. 7B), suggesting the interrelationships among these three biomolecules that possibly involves in oral carcinogenesis. As expected, the IHC scores of p-EGFR^{tyr1173} expression were positively correlated with those of p-Akt^{ser473} expression (r=0.581; p<0.001; Fig. 7C), since it is well known that phosphorylated EGFR (p-EGFR) is an upstream signaling molecule to activate Akt by phosphorylation (p-Akt).
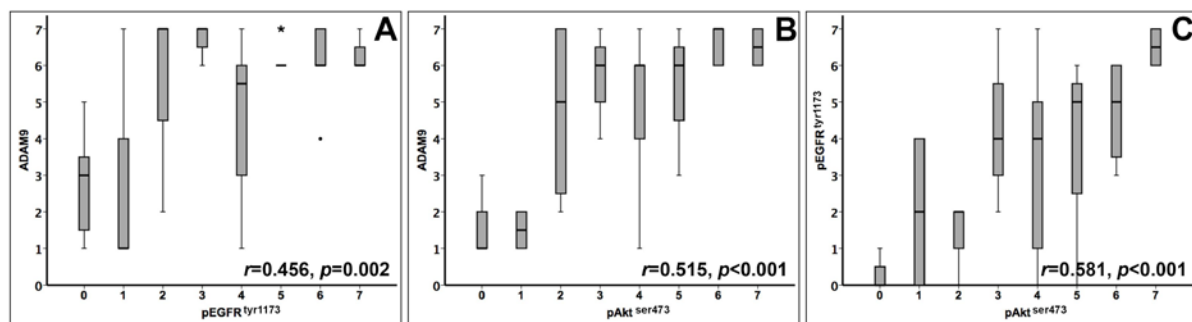

Figure 7. Significantly positive correlations among three biomolecules, including ADAM9, p-EGFR^{tyr1173} and p-Akt^{ser473} in all 34 OSCC and 10 normal tissues. An asterisk and a small black circle in A represent an extreme and an outlier value, respectively.

4. To examine ADAM9, p-EGFR^{tyr1173} and p-Akt^{ser473} expressions *in vitro* by investigating their protein expression in OSCC cell lines and compare with that in normal oral epithelial cells by immunoblotting.

5. To investigate membrane-bound expression of ADAM9 in OSCC cell lines and compare with that in normal oral epithelial cells by flow cytometry.

The expression of membrane ADAM9 in four different oral cancer cell lines, including HN5, HN6, HN15 and HN008, by flow cytometry in aim 5 was first determined. These four oral cancer cell lines have been previously studied for overexpression and activation of Akt2 (Iamaroon and Krisanaprakornkit, 2009). As a positive control cell line for membrane ADAM9 expression, a hepatoblastoma cell line, HepG2, was obtained from Professor Dr. Prachya Kongtawelert, Excellence Center of Tissue Engineering and Stem Cells, Department of Biochemistry, Faculty of Medicine, Chiang Mai University. These cancer cell lines were cultured

in Dulbecco's Modified Eagle Medium (Invitrogen[TM]), supplemented with 10% fetal bovine serum and 1% penicillin/streptomycin (Invitrogen[TM]). All cells were maintained at 37°C in a humidified chamber with 5% CO_2. Culture medium was changed every two days until cell growth reached 80% confluence prior to flow cytometry. It was found that membrane ADAM9 was expressed in three of the four tested oral cancer cell lines, HN6, HN15 and HN008, whereas membrane ADAM9 was not expressed in HN5 (Fig. 8). As expected, membrane ADAM9 was expressed in the HepG2 cell line (Fig. 8). No expression signal was detected in all tested cell lines, incubated with the purified rabbit immunoglobulins (dark gray area) as an isotype antibody control or without the anti-ADAM9 antibody (light gray area) as a conjugate control (Fig. 8).
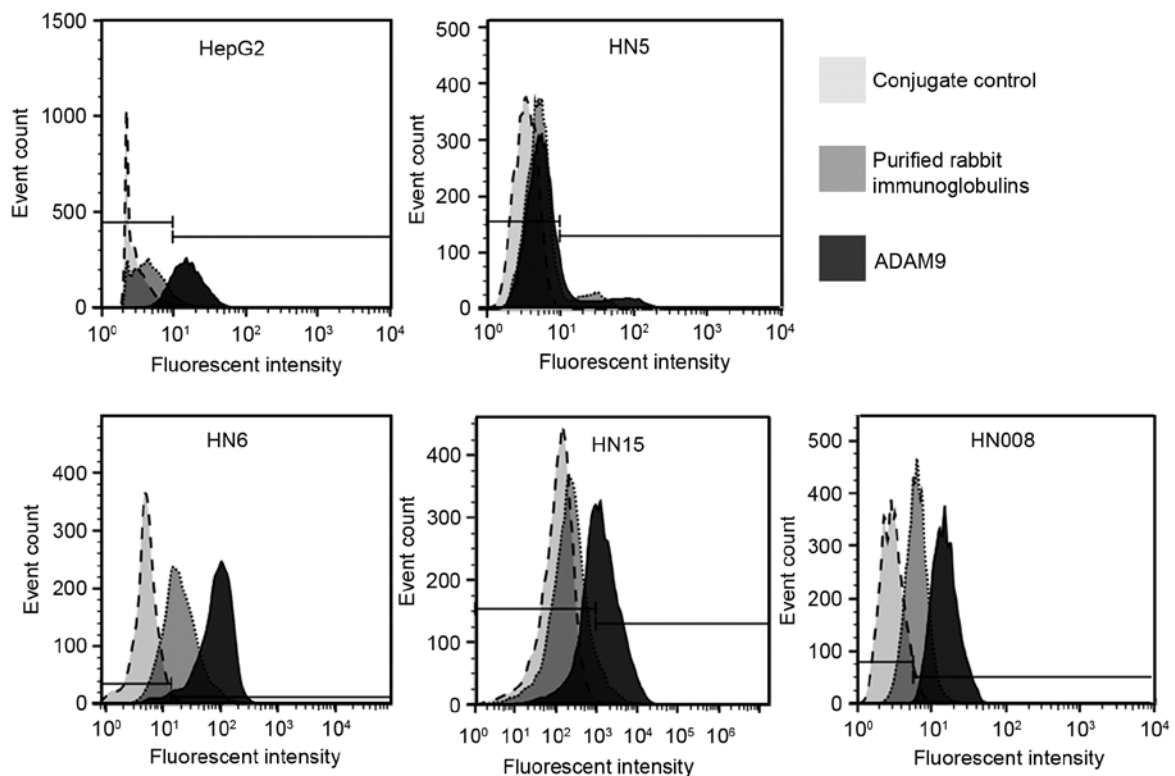

Figure 8. Expression of membrane ADAM9 in oral cancer cell lines. Representative histograms for expression of membrane ADAM9 in four oral cancer cell lines, including HN5, HN6, HN15 and HN008, from three separate experiments. Note expression of membrane ADAM9 (black area) in HN6, HN15 and HN008, whereas membrane ADAM9 expression was not detected in HN5. Membrane ADAM9 was expressed in the HepG2 cell line as a positive control, while there was no membrane ADAM9 expression in a conjugate control (light gray area) or in purified rabbit immunoglobulins (dark gray area) as two negative controls.

Next, the expressions of ADAM9, p-EGFR^{tyr1173} and p-Akt^{ser473} proteins *in vitro* in OSCC cell lines in comparison with that in normal human oral epithelial cells, or called normal human oral keratinocytes (HOKs), were examined by immunoblotting in aim 4. Primary HOKs were isolated from normal non-inflamed oral tissues overlying impacted third molars of eight healthy and non-smoking donors (*n*=8) with their informed consent, as previously described (Iamaroon and Krisanaprakornkit, 2009). HOKs were cultured in serum-free keratinocyte growth medium (Lonza, Walkersville, MD, USA) and maintained at 37ºC in a humidified chamber with 5% CO_2. Culture medium was changed every two days until cell growth reached 80% confluence prior to Western blot hybridization. It was demonstrated that varying degrees of ADAM9, p-EGFR^{tyr1173}, EGFR and p-Akt^{ser473} protein expressions were detected in the whole cell lysates of HN5, HN6, HN15, HN008, and eight independent HOK cell lines (Fig. 9). In general, the expressions of ADAM9 as well as of p-EGFR^{tyr1173}, EGFR and p-Akt^{ser473} proteins in HN6 and HN15 were greater than those in HN5, HN008 and HOKs (Fig. 9). It is interesting to note that HN6 and HN15, in which ADAM9 was overexpressed, also greatly expressed p-EGFR^{tyr1173}, EGFR and p-Akt^{ser473} proteins (Fig. 9). Expression of β-actin was equivalent among different samples, which confirms equivalent loadings among different samples (Fig. 9).

By densitometry, the median ratios of ADAM9, p-EGFR^{tyr1173} and p-Akt^{ser473} protein expression relative to those of β-actin, as a housekeeping gene, EGFR and Akt expression, respectively, in the corresponding samples, in HN6 and HN15 were significantly higher than those in HN5, HN008 and all eight cell lines of HOKs (Fig. 10). Furthermore, the median ratios of ADAM9, p-EGFR^{tyr1173} and p-Akt^{ser473} expression in HN6 and HN15 adjusted in relation to those in HN008, whose ratio was set to 1.0, were significantly higher than those in HN5, HN008 and all eight cell lines of HOKs (Fig. 10). As with the *in vivo* results in the previous sections, all of these *in vitro* findings suggest the existence of interconnections among the three biomolecules, including ADAM9, p-EGFR^{tyr1173} and p-Akt^{ser473}, in both OSCC tissues and a few oral cancer cell lines, particularly in the two high-expressing ADAM9 cell lines, HN6 and HN15. These *in vitro* findings are also essential for the experiments in aims 6, 7 and 8 to determine the effects of ADAM9 silencing by suppressing expression of ADAM9 in these high-expressing ADAM9 cell lines on expression of p-EGFR^{tyr1173} and p-Akt^{ser473}, on aggressive behaviors of cancer cells, and on tumorigenesis in mice, respectively.
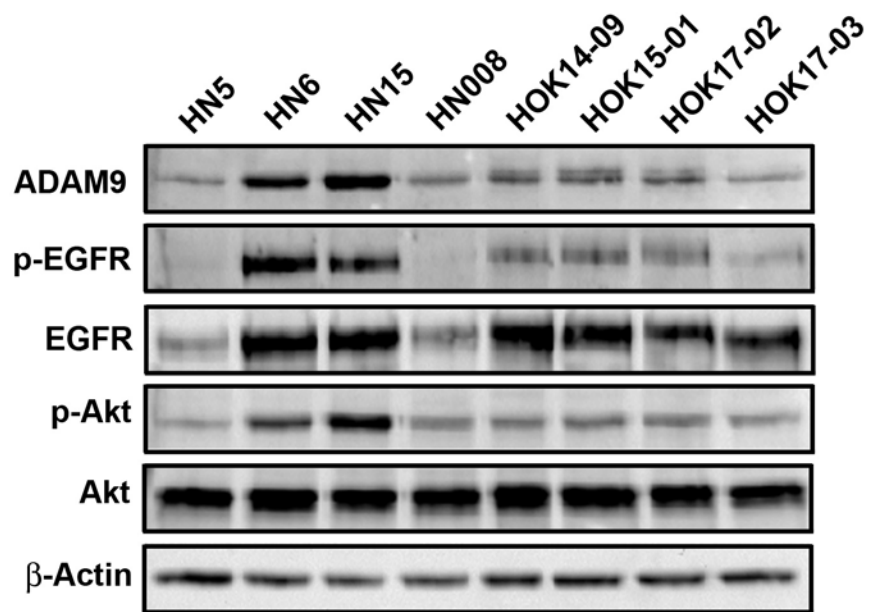
Figure 9. An up-regulation of the protein expressions of ADAM9, p-EGFR^{tyr1173}, EGFR, and p-Akt^{ser473} in HN6 and HN15. Representative blots demonstrate varying expressions of ADAM9, p-EGFR^{tyr1173}, EGFR and p-Akt^{ser473} in four different oral cancer cell lines, including HN5, HN6, HN15, and HN008, and in four normal human oral keratinocytes (HOK14-09, 15-01, 17-02 and 17-03). Expression of β-actin was equal among all different samples.
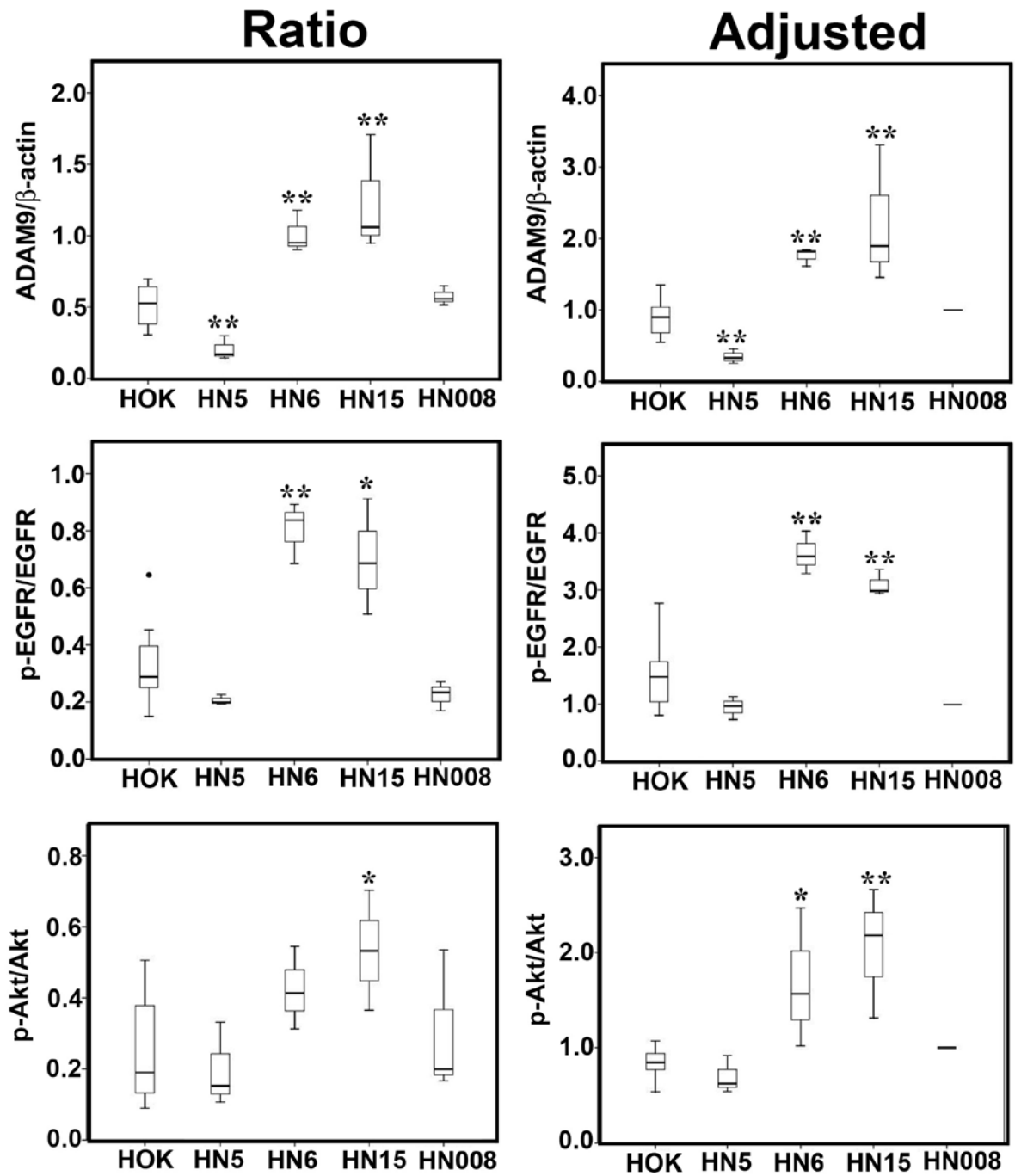
Figure 10. The box plot graphs demonstrate the significantly higher median ratios of ADAM9, p-EGFR[tyr1173] and p-Akt[ser473] expressions in HN6 and HN15 than those in HN5, HN008 from three separate experiments (n=3) and those in eight independent HOK cell lines (n=8). The relative ratios of ADAM9/β-actin, p-EGFR[tyr1173]/EGFR and p-Akt[ser473]/Akt expressions in each oral cancer and HOK cell line were adjusted by comparison with the ratios in HN008, set to 1.0. * = $p<0.05$; ** = $p<0.01$.

6. To determine the inhibitory effect of cell transfection with small interfering RNA (siRNA) specific for ADAM9 in OSCC cell lines on phosphorylation of EGFR at the tyrosine 1173 residue and of Akt at the serine 473 residue by immunoblotting analysis.

From the cell transfection study with siRNA against ADAM9 in HN6 and HN15, two high ADAM9-expressing OSCC cell lines (Fig. 9), it was shown by quantitative RT-PCR that the median ratios of ADAM9 mRNA expression normalized by glyceraldehyde 3-phosphate dehydrogenase (GAPDH) mRNA expression was significantly and almost completely inhibited by cell transfection with both 5 and 10 nM of siRNA against ADAM9 for 48 hours, but not by a scrambled sequence at the same doses, in HN6 and HN15 ($p<0.05$; Fig. 11A and B, respectively).
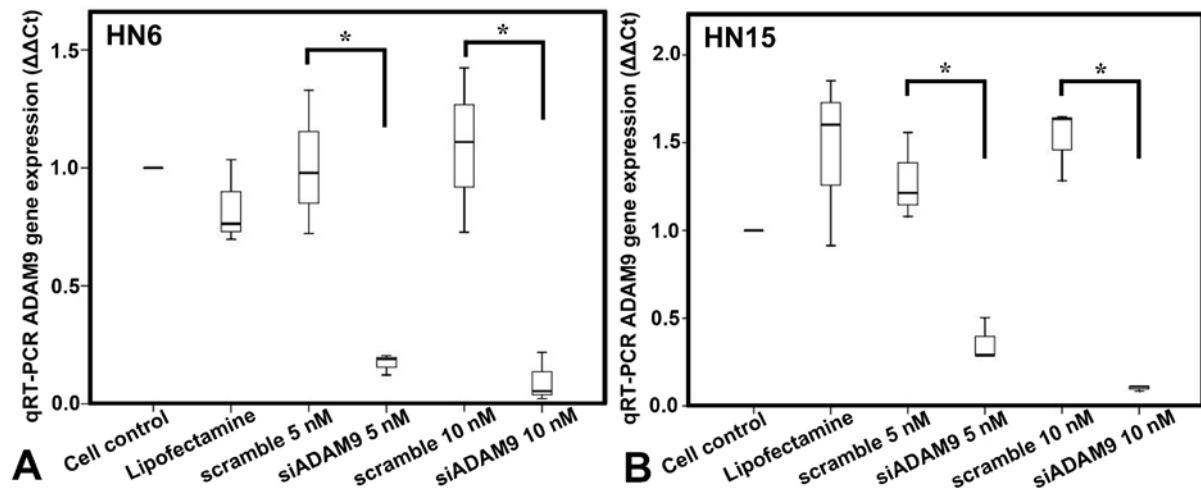

Figure 11. Significant inhibition of the median ratios (horizontal lines in the boxes) for ADAM9 mRNA expression, normalized by GAPDH mRNA expression, in HN6 (A) and HN15 (B) by transfection with siRNA against ADAM9 at 5 and 10 nm in comparison to a scrambled sequence at the same doses, as analyzed by quantitative RT-PCR. Cell control = no treatment; Lipofectamine = OSCC cell lines treated with only transfection reagent. * = $p<0.05$.

Expression of ADAM9 protein was also consistently blocked by transfection with both 5 and 10 nM of siRNA against ADAM9, but not with a scrambled sequence at the same doses, in HN6 and HN15 (Fig. 12A and B, respectively), and these inhibitions reached the significance level at $p<0.05$ in both HN6 and HN15 (Fig. 13A and B, respectively). Interestingly, inhibition of ADAM9 expression by transfection with siRNA against ADAM9 at 5 or 10 nM only resulted in a partial blockade of p-Akt^{ser473} expression, but **not** p-EGFR^{tyr1173} expression, in HN6 and HN15

compared to transfection with a scrambled sequence at the same doses (Fig. 12A and B, respectively). Moreover, the statistical analyses from three separate and repeated transfection experiments demonstrated that significant inhibitions of the median ratios of p-Akt[ser473] relative to total Akt expression was found by transfection with siRNA against ADAM9 at 10 nM in HN6 and at 5 or 10 nM in HN15 ($p<0.05$; Fig. 13E and F, respectively) compared to transfection with the equivalent doses of a scrambled sequence. However, transfection with siRNA against ADAM9 at any of the two doses failed to suppress the median ratios of p-EGFR[tyr1173] relative to total EGFR expression in HN6 and HN15 (Fig. 13C and D, respectively), compared to transfection with the equivalent doses of a scrambled sequence.
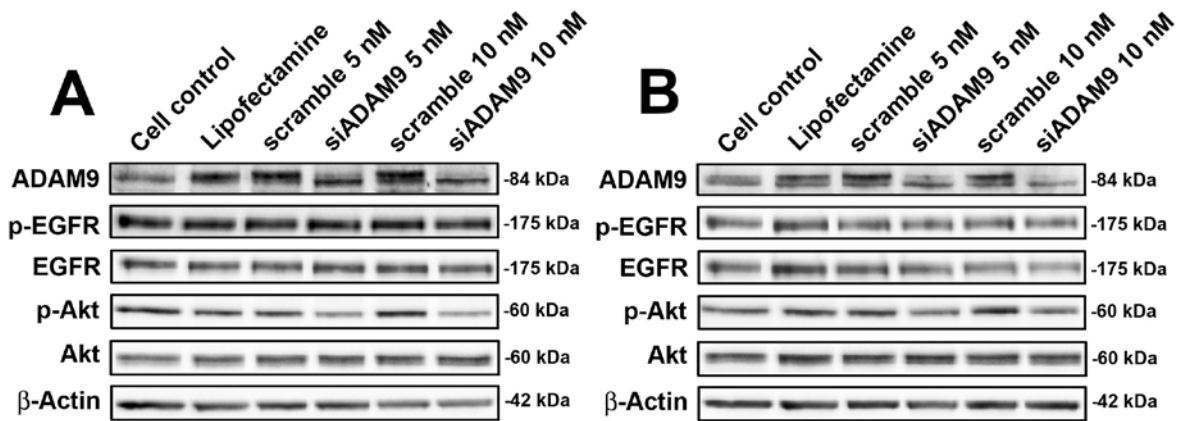

Figure 12. Representative blots from three independent transfection experiments showed partial inhibitions of ADAM9 and p-Akt[ser473] protein expressions by transfection with siRNA against ADAM9 at 5 or 10 nM in HN6 (A) and HN15 (B), but not by a scrambled sequence at the same doses. However, p-EGFR[tyr1173] expression was not blocked by transfection with siRNA against ADAM9 at any doses. Expressions of total EGFR, total Akt, and β-actin, as a housekeeping gene, were equivalent among different samples.

Consistent with no inhibitory effect of transfection with siRNA against ADAM9 on p-EGFR[tyr1173] expression in HN6 or HN15 (Figs. 12 and 13), it was found that transfection with siRNA against ADAM9 at 5 or 10 nM also failed to inhibit cell proliferation of HN6 or HN15 as analyzed by the BrdU assay (Fig. 14A or B, respectively). Taken together, all of these results suggest different characteristics between OSCC cell lines used in this study and esophageal squamous cell carcinoma cell lines (Liu et al., 2015). Moreover, other targets besides EGFR for ADAM9 enzymatic activity are needed to be elucidated. However, it is still probable that ADAM9

plays a pivotal role in other aspects of carcinogenesis, such as cancer cell invasion, since inhibition of ADAM9 expression can in fact result in a partial blockade of p-Akt[ser473] expression.
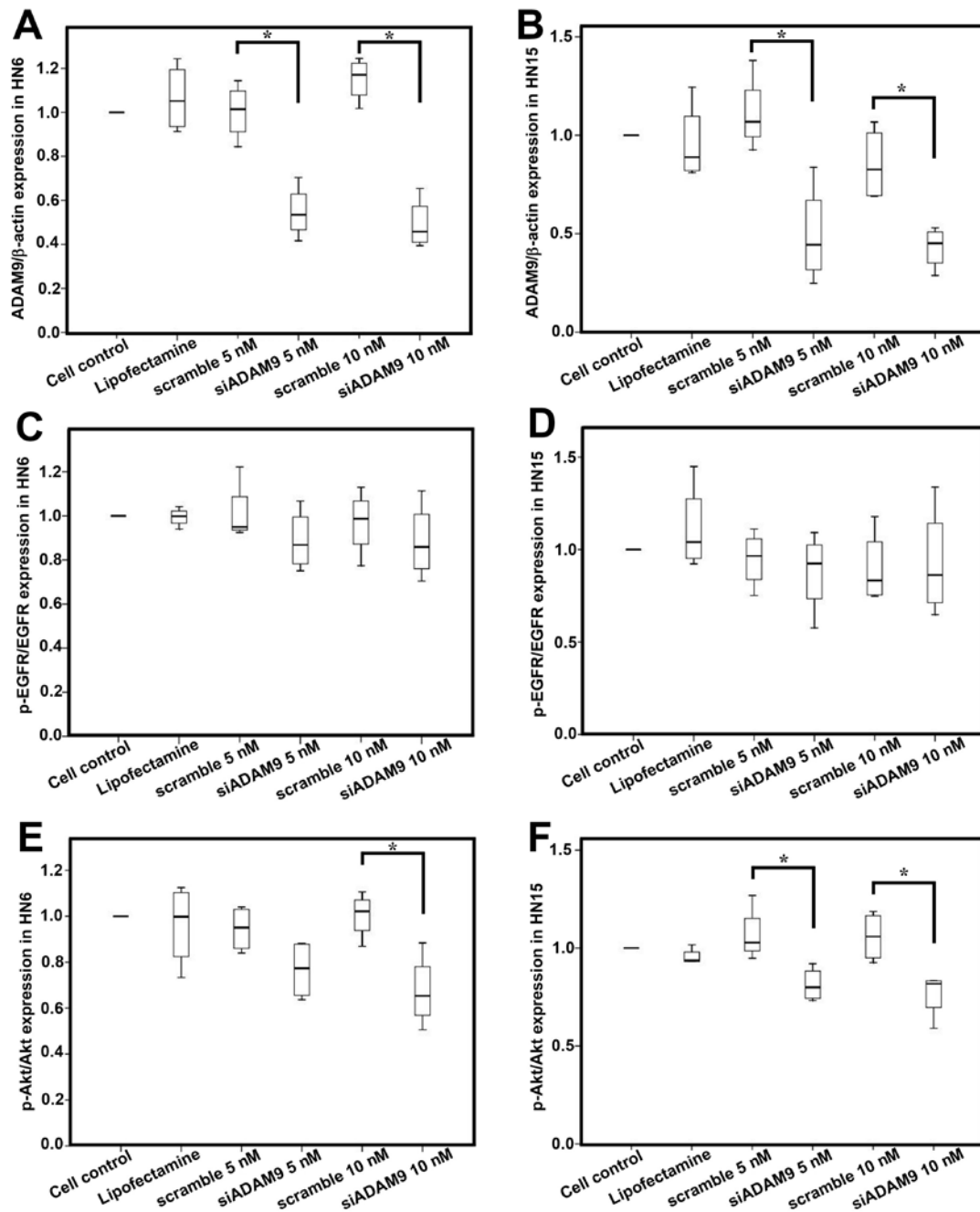

Figure 13. Significant inhibitions of the median ratios (horizontal lines in the boxes) of ADAM9 relative to β-actin expression in HN6 (A) and HN15 (B) and of the median ratios of p-Akt[ser473] relative to total Akt expression in HN6 (E) and HN15 (F) by transfection with siRNA against ADAM9 (siADAM9) compared to transfection with a scrambled sequence at the equivalent doses (5 or 10 nM). However, these inhibitions were not found to be different for the median ratios of p-EGFR[tyr1173] relative to total EGFR expression in HN6 (C) or HN15 (D). This experiment was separately performed three times with the same result. * = $p < 0.05$.
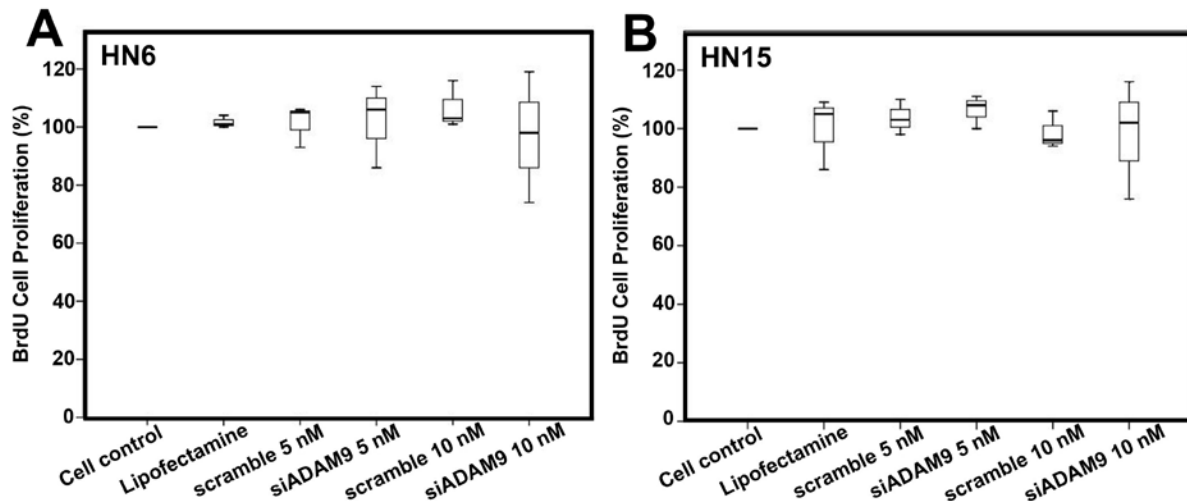
Figure 14. No difference in terms of the median percentages (horizontal lines in the boxes) of cell proliferation as analyzed by the BrdU assay upon transfection with siRNA against ADAM9 at 5 or 10 nM compared to transfection with a scrambled sequence at the equivalent doses in HN6 (A) or HN15 (B).

For a control of enhanced cell proliferation as detected by the BrdU assay, HN6 oral cancer cells that were treated with phorbol 12-myristate 13-acetate (PMA) at 10 ng/ml for 24 or 48 h showed a significant increase in cell proliferation ($p < 0.05$; Fig. 15), whereas silencing ADAM9 expression by siRNA at 5 or 10 nM did not result in a change in the percentage of cell proliferation rate as compared to that of the control untreated cells, set to 100%.

Figure 15. Significant increases in percentage of cell proliferation in HN6 after treatment with PMA at 10 ng per ml for 24 or 48 h. Note no change in the percentage of cell proliferation by treatment with siRNA against ADAM9 or a scrambled sequence at 5 or 10 nM. Error bars = standard deviation; * = $p < 0.05$.
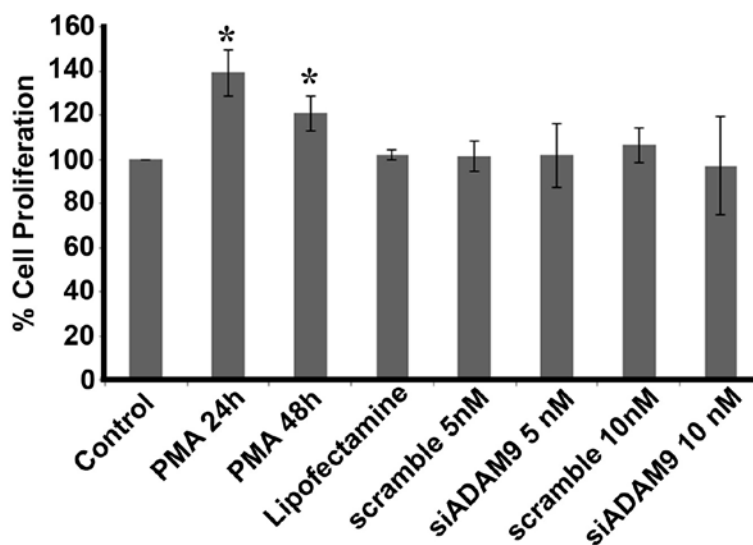
Moreover, HN6 and HN15 cell lines were treated with 2% (v/v) DMSO for 24 h for a suppressive control of cell proliferation. It was found that treatment with 2% DMSO for 24 h significantly inhibited the rate of cell proliferation in HN6 and HN15 ($p<0.05$; Fig. 16A and B, respectively), whereas treatment with PMA at 10 ng/ml for 24 h significantly enhanced cell proliferation in HN6 and HN15 similar to the findings in Figure 15 ($p<0.05$; Fig. 16A and B, respectively).
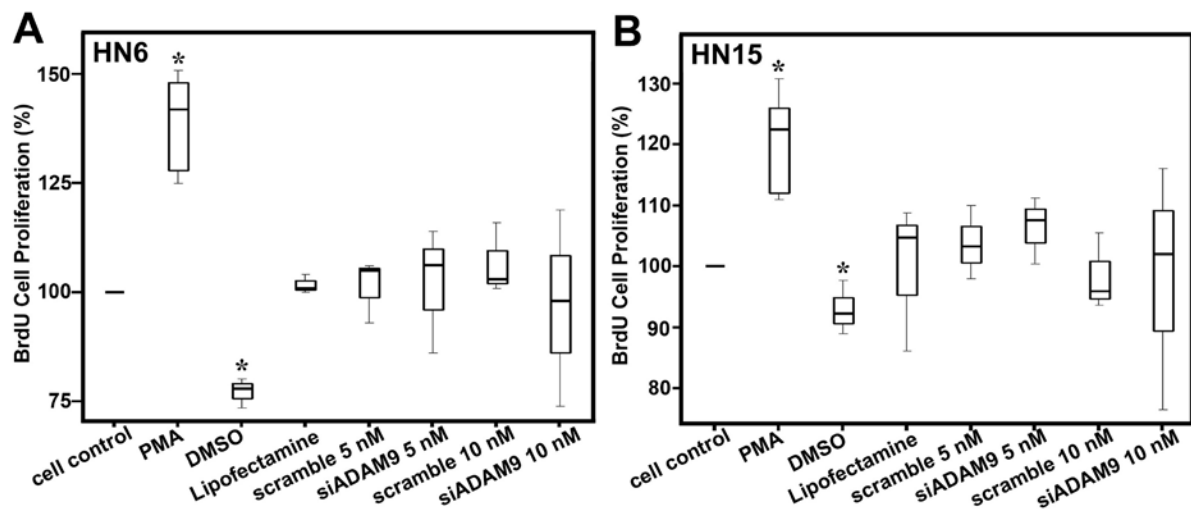
Figure 16. Significant decreases in the percentage of cell proliferation in HN6 (A) and HN15 (B) after treatment with 2% (v/v) DMSO for 24 h, as detected by the BrdU assay, while significant increases in the percentage of cell proliferation in HN6 (A) and HN15 (B) were found after treatment with PMA at 10 ng per ml for 24 h. Note no change in the percentage of cell proliferation by treatment with siRNA against ADAM9 or a scrambled sequence at 5 or 10 nM. A horizontal line within each box represents the median percentage of cell proliferation; * = $p<0.05$.

7. To investigate the blocking effect on cancer cell aggressiveness in ADAM9-siRNA-transfected-OSCC cell lines using the invasion assay.

Next, the effect of ADAM9 silencing by siRNA on cancer cell invasion *in vitro*, as one of the aggressive hallmarks of oral cancer, was determined in HN6 and HN15. It was demonstrated that transiently silenced ADAM9 expression by siRNA against ADAM9 at 10 nM dramatically decreased cancer cell invasion of HN16 through the ECM matrix *in vitro* (Fig. 17), whereas transfection with lipofectamine, as a reagent control, or with a scrambled sequence at 10 nM showed no suppression of oral cancer cell invasion as compared to that of the control untreated cells (Fig. 17). This experiment was independently carried out for four times in both HN6 and HN15 with a representative figure of each condition for HN6 shown below in Figure 17. Note the red arrows indicate HN6 oral cancer cells stained with crystal violet that have invaded through the ECM matrix in a Transwell chamber (Fig. 17).

Figure 17. A decrease in HN6 oral cancer cell invasion through the ECM matrix in a Transwell chamber by transient transfection with siRNA against ADAM9 (siADAM9) at 10 nM. Note the red arrows indicate HN6 oral cancer cells stained with crystal violet that have invaded through the ECM matrix in a Transwell chamber.
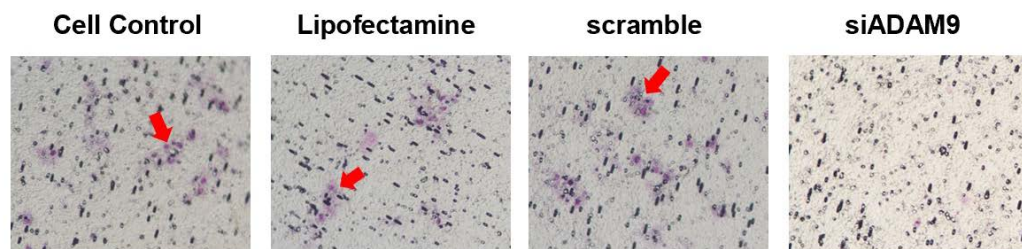
By manually counting the number of invasive oral cancer cells (both HN6 and HN15), it was found that transiently silenced ADAM9 expression by siRNA against ADAM9 at 10 nM significantly decreased the number of invasive oral cancer cells in both HN16 and HN15 through the ECM matrix *in vitro* ($p<0.05$; Fig. 18), whereas transfection with lipofectamine, as a reagent control, or with a scrambled sequence at 10 nM showed no suppression on the number of invasive oral cancer cells as compared to that of the control untreated cells (Fig. 18).
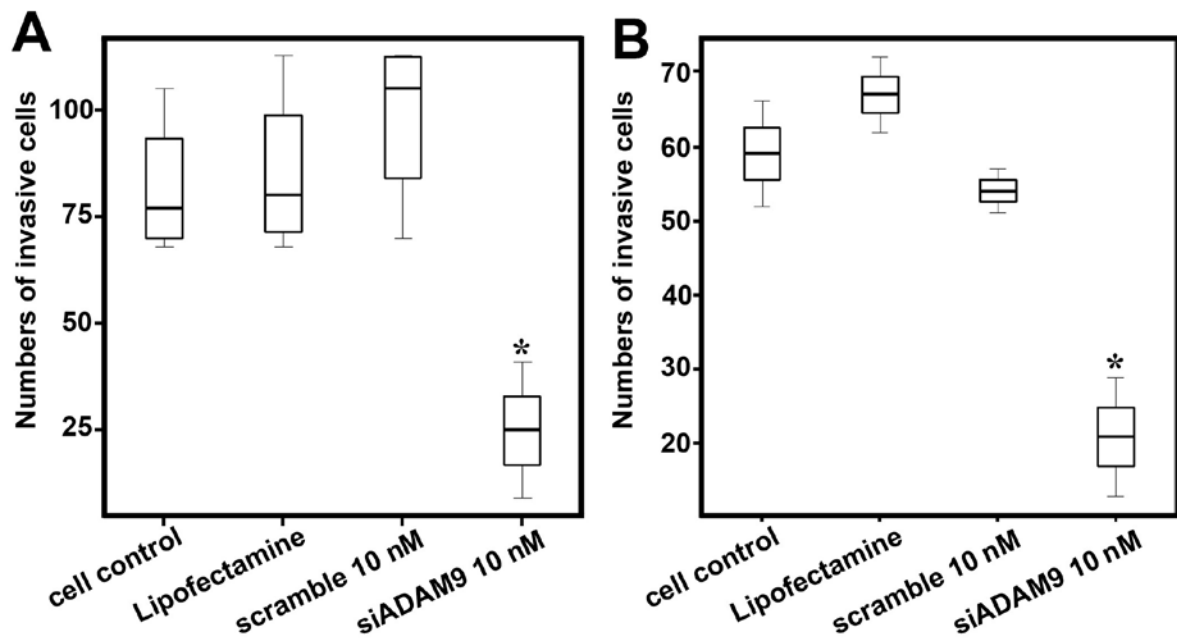
Figure 18. Significant decreases in the number of invasive oral cancer cells in both HN6 (A) and HN15 (B) through the ECM matrix. A horizontal line within each box represents the median number of invasive cells. * = $p<0.05$.

8. To determine the function of ADAM9 *in vivo*.

This aim has **not** been addressed due to the **absence** of inhibitory effect on the cancer cell proliferation *in vitro* in ADAM9-knockdown HN6 and HN15 cell lines, mentioned in aim 6. Therefore, I do not think that it is necessary to perform this *in vivo* experiment in order to save animals' lives.

References

Fromowitz FB, Viola MV, Chao S, Oravez S, Mishriki Y, Finkel G, Grimson R, Lundy J (1987). ras p21 expression in the progression of breast cancer. Hum Pathol 18(12):1268-1275.

Iamaroon A and Krisanaprakornkit S (2009). Overexpression and activation of Akt2 protein in oral squamous cell carcinoma. Oral Oncol 45:e175-179.

Kongkaew T, Aung WPP, Supanchart C, Makeudom A, Langsa-Ard S, Sastraruji T, Chaiyarit P, Krisanaprakornkit S (2018). O-GlcNAcylation in oral squamous cell carcinoma. J Oral Pathol Med 47(3):260-267.

Liu R, Gu J, Jiang P, Zheng Y, Liu X, Jiang X, Huang E, Xiong S, Xu F, Liu G, Ge D, Chu Y (2015). DNMT1-microRNA126 epigenetic circuit contributes to esophageal squamous cell carcinoma growth via ADAM9-EGFR-AKT signaling. Clin Cancer Res 21(4):854-863.

Pirker R, Pereira JR, von Pawel J, Krzakowski M, Ramlau R, Park K, de Marinis F, Eberhardt WE, Paz-Ares L, Storkel S, *et al*. (2012). EGFR expression as a predictor of survival for first-line chemotherapy plus cetuximab in patients with advanced non-small-cell lung cancer: analysis of data from the phase 3 FLEX study. Lancet Oncol 13:33-42.

Sobin LH, Gospodarowicz MK, Wittekind C (2009). TNM classification of malignant tumours. Blackwell Publishing Ltd, United Kingdom, pp. 5-29.

OUTPUTS

1. Pattamapun K, Handagoon S, Sastraruji T, Gutmann JL, Pavasant P, **Krisanaprakornkit S** (2017). Decreased levels of matrix metalloproteinase-2 in root-canal exudates during root canal treatment. *Archives of Oral Biology* 82:27-32. [Impact Factor 1.663 ISI Journal Citation Reports[©] Ranking 2018 (Dentistry Oral Surgery & Medicine)]

2. Makeudom A, Supanchart C, Montreekachon P, Khongkhunthian S, Sastraruji T, Krisanaprakornkit J, **Krisanaprakornkit S** (2017). The antimicrobial peptide, human β-defensin-1, potentiates *in vitro* osteoclastogenesis via activation of the p44/42 mitogen-activated protein kinases. *Peptides* 95:33-39. [Impact Factor 2.659 ISI Journal Citation Reports[©] Ranking 2018]

3. Truntipakorn A, Makeudom A, Sastraruji T, Pavasant P, Pattamapun K, **Krisanaprakornkit S** (2017). Effects of prostaglandin E_2 on clonogenicity, proliferation and expression of pluripotent markers in human periodontal ligament cells. *Archives of Oral Biology* 83:130-135. [Impact Factor 1.663 ISI Journal Citation Reports[©] Ranking 2018 (Dentistry Oral Surgery & Medicine)]

4. Pahumunto N, Chotjumlong P, Makeudom A, **Krisanaprakornkit S**, Dahlen G, Teanpaisan R (2017). Pro-inflammatory cytokine responses in human gingival epithelial cells after stimulation with cell wall extract of *Aggregatibacter actinomycetemcomitans* subtypes. *Anaerobe* 48:103-109. [Impact Factor 2.704 ISI Journal Citation Reports[©] Ranking 2018]

5. Tanasubsinn P, Aung WPP, Pata S, Laopajon W, Makeudom A, Sastraruji T, Kasinrerk W, **Krisanaprakornkit S** (2018). Overexpression of ADAM9 in oral squamous cell carcinoma. *Oncology Letters* 15(1):495-502. [Impact Factor 1.871 ISI Journal Citation Reports[©] Ranking: 2018: 196/321 (Oncology)]

6. Tupyota P, Chailertvanitkul P, Laopaiboon M, Ngamjarus C, Abbott PV, **Krisanaprakornkit S** (2018). Supplementary techniques for pain control during root canal treatment of lower posterior teeth with irreversible pulpitis: A systematic review and meta-analysis. *Australian Endodontic Journal* 44(1):14-25. [Impact Factor 1.714 ISI Journal Citation Reports[©] Ranking: 2018: 42/91 (Dentistry Oral Surgery & Medicine)]

7. Kongkaew T, Aung WPP, Supanchart C, Makeudom A, Langsa-Ard S, Sastraruji T, Chaiyarit P, **Krisanaprakornkit S** (2018). O-GlcNAcylation in oral squamous cell carcinoma. *Journal of Oral Pathology and Medicine* 47(3):260-267. [Impact Factor 2.03 ISI Journal Citation Reports[©] Ranking: 2018: 28/91 (Dentistry Oral Surgery & Medicine)]

8. Wimolsantirungsri N, Makeudom A, Louwakul P, Sastraruji T, Chailertvanitkul P, Supanchart C, **Krisanaprakornkit S** (2018). Inhibitory effect of Thai propolis on human osteoclastogenesis. *Dental Traumatology* 34(4):237-244. [Impact Factor 1.494 ISI Journal Citation Reports$^©$ Ranking: 2018: 52/91 (Dentistry Oral Surgery & Medicine)]

9. Likitpongpipat N, Sangmaneedeth S, Klanrit P, Noisombut R, **Krisanaprakornkt S**, Chailertvanitkul P (2019). Promotion of dental pulp wound healing in New Zealand White rabbits' teeth by Thai propolis. *Journal of Veterinary Dentistry* Mar;36(1):17-24. doi: 10.1177/0898756418818891. Epub 2018 Dec 26. [Impact Factor 0.349 ISI Journal Citation Reports$^©$ Ranking 2018]

10. Nimcharoen T, Aung WPP, Makeudom A, Sastraruji T, Khongkhunthian S, Sirinirund B, **Krisanaprakornkit S**, Montreekachon P (2019). Reduced ADAM8 levels upon non-surgical periodontal therapy in patients with chronic periodontitis. *Archives of Oral Biology* 97:137-143. doi: 10.1016/j.archoralbio.2018.10.021. Epub 2018 Oct 23. [Impact Factor 1.663 ISI Journal Citation Reports$^©$ Ranking 2018 (Dentistry Oral Surgery & Medicine)]

11. Manmontri C, Nirunsittirat A, Piwat S, Wattanarat O, Pahumunto N, Makeudom A, Sastraruji T, **Krisanaprakornkit S**, Teanpaisan R (2019). Reduction of Streptococcus mutans by probiotic milk: A multicenter randomized controlled trial. *Clinical Oral Investigations* Dec 14. doi: 10.1007/s00784-019-03095-5. [Epub ahead of print] [Impact Factor 2.453 ISI Journal Citation Reports$^©$ Ranking 2018 (Dentistry Oral Surgery & Medicine)]

12. Wongpang D, Makeudom A, Sastraruji T, Khongkhunthian S, **Krisanaprakornkit S**, Supanchart C (2020). Anesthetic efficacies of intrapapillary injection in comparison to inferior alveolar nerve block for mandibular premolar extraction: A randomized clinical trial. *Clinical Oral Investigations* Feb;24(2):619-629. doi: 10.1007/s00784-019-02954-5. Epub 2019 May 21. [Impact Factor 2.453 ISI Journal Citation Reports$^©$ Ranking 2018 (Dentistry Oral Surgery & Medicine)]

13. Pathomburi J, Nalampang S, Makeudom A, Klangjorhor J, Supanchart C, **Krisanaprakornkit S** (2020). Effects of low-dose irradiation on human osteoblasts and periodontal ligament cells. *Archives of Oral Biology* Jan;109:104557. doi: 10.1016/j.archoralbio.2019.104557. Epub 2019 Sep 17. [Impact Factor 1.663 ISI Journal Citation Reports$^©$ Ranking 2018 (Dentistry Oral Surgery & Medicine)]

14. Nakdilok K, Langsa-ard S, **Krisanaprakornkit S**, Suzuki EY, Suzuki B (2020). Enhancement of human periodontal ligament by pre-application of orthodontic loading. *American Journal of Orthodontics and Dentofacial Orthopedics* Feb;157(2):186-193. doi: 10.1016/j.ajodo.2019.03.019. [Impact Factor 1.911 ISI Journal Citation Reports[©] Ranking 2018 (Dentistry Oral Surgery & Medicine)]

15. Rattanakuntee S, Chaiyawat P, Pruksakorn D, **Krisanaprakornkit S**, Makeudom A, Supanchart C (2020). Associations between expression levels of O-GlcNAc transferase (OGT) and chemo-response in osteosarcoma. *Journal of the Medical Association of Thailand* 103:1-6.

16. Kantaputra PK, Dejkhamron P, Intachai W, Ngamphiw C, Kawasaki K, Ohazama A, **Krisanaprakornkit S**, Olsen B, Tongsima S, Ketudat Cairns JR (2020). Juberg-Hayward syndrome is a cohesinopathy, caused by mutation in ESCO2. *European Journal of Orthodontics* 1–6. doi:10.1093/ejo/cjaa023 [Impact Factor 1.841 ISI Journal Citation Reports[©] Ranking 2018 (Dentistry Oral Surgery & Medicine)]

17. Promchaiwattana P, Suzuki B, **Krisanaprakornkit S**, Suzuki EY (2020). Periodontal ligament enhancement in mesio-angulated impaction of third molars following orthodontic tooth movement: A prospective cohort study. *American Journal of Orthodontics and Dentofacial Orthopedics* (accepted). [Impact Factor 1.911 ISI Journal Citation Reports[©] Ranking 2018 (Dentistry Oral Surgery & Medicine)]

18. Phutinart S, Suzuki B, **Krisanaprakornkit S**, Makeudom A, Suzuki EY (2020). Periodontal ligament proliferation and expressions of bone biomolecules upon orthodontic preloading: Clinical implication for tooth autotransplantation. *Korean Journal of Orthodontics* (accepted). [Impact Factor 1.476 ISI Journal Citation Reports[©] Ranking 2018 (Dentistry Oral Surgery & Medicine)]

Note that only **six** interesting and relevant articles (#5, #7, #11, #12, #14 and #16) are printed and included in the following Appendix in order to indicate a total of **at least five** papers published in Quartile 1 or 2 journals with impact factor, according to the Science Citation Index and the ISI Journal Citation Reports[©] Ranking 2018, as the output of this proposal as promised; however, the remaining 12 papers can be found in the "Outputs" folder saved in a CD.

OTHER OUTPUTS

1. ผลงานอื่นๆ เช่น การตีพิมพ์ผลงานวิชาการในวารสารภายในประเทศไทย การไปนำเสนอผลงาน การได้รับเชิญเป็นวิทยากรและการได้รับรางวัล

- A total of three national papers and one proceeding (see the "Other Outputs" folder saved in a CD) have been published in the Thai journals upon the financial support of the Thailand Research Fund as follows.

1) Pattamapun K, Jiamjit N, Saelo A, Krisanaprakornkit J, **Krisanaprakornkit S** (2017). Root canal therapy and intentional replantation of the maxillary central incisor with a combined periodontic and endodontic lesion from a palatogingival groove: a case report. *Journal of the Dental Association of Thailand* 67(3):197-211.

2) Pengchum S, Chailertvanitkul P, Laopaiboon M, Thaweesit P, Abbott PV, **Krisanaprakornkit S** (2018). Thai propolis extract as root canal medication against *Enterococcus faecalis* infection. *Khon Kaen University Dental Journal* 21(1):30-38.

3) Kundacha P, Makeudom A, Sastraruji T, Wanachantararak P, Charumanee S, Pattamapun K, **Krisanaprakornkit S** (2019). Efficacy of double antibiotics in hydroxypropyl methylcellulose gel against *Enterococcus faecalis* in root canals: An *in vitro* study. *Journal of the Dental Association of Thailand* 69(Suppl.):2-12.

4) Sonjaitum W, Makeudom A, Sastraruji T, Louwakul P, Supanchart C, **Krisanaprakornkit S** (2019). Long-term treatment with LL-37 promotes proliferation, odontoblastic differentiation, and mineralization of human dental pulp cells. Emerging Trends in Dentistry, The 17th International Scientific Conference of the Dental Faculty Consortium of Thailand, July 8-10, 2019, Pullman Khon Kaen Raja Orchid, Khon Kaen, Thailand.

- Several abstracts for both oral and poster presentations were prepared and presented at the Scientific Conferences of the Dental Faculty Consortium of Thailand from 2017 to 2019.

- An invited judging committee member for abstract selection at the 7th Federation of Immunological Societies of Asia-Oceania (FIMSA) in Bangkok, Thailand, November 10-13, 2018.

- An invited speaker in the topic of "Dental Research in Bone Cells" School of Dentistry, Mae Fah Laung University, Chiang Rai, Thailand, May 3, 2018.

- Distinguished Alumni Award, Faculty of Dentistry, Mahidol University, Bangkok, Thailand, December 18, 2019.

- A number of postgraduate students have achieved their Master and Ph.D. degrees in various dental disciplines by the sponsorship of the Thailand Research Fund.

2. กิจกรรมที่เกี่ยวข้องกับการนำผลจากโครงการไปใช้ประโยชน์

- I have now set up an Oral Biology research group in the Faculty of Dentistry, Chiang Mai University, to promote the academic atmosphere in this school by organizing a routine journal club. My research group is also financially sponsored by Chiang Mai University as the Center of Excellence in Oral and Maxillofacial Biology.

3. การเชื่อมโยงทางวิชาการกับนักวิชาการอื่นๆ ทั้งในและต่างประเทศ

- I am currently collaborating with Assistant Professor Dr. Jan GM Bolscher, Academic Centre for Amsterdam (ACTA), the Netherlands, in the project that involves with the role of cathelicidin antimicrobial peptides in bone biology. He generously continues to provide me LL-37 and CRAMP peptides.

- I am also working with Professor Dr. Rawee Teanpisan, Faculty of Dentistry, Prince of Songkla University, on two different research projects. The first project is a field trial phase II, involving with the reduction of *Streptococcus mutans*, dental caries prevention, and enhancement of salivary human neutrophil peptide 1-3 levels by probiotic milk powder in preschool children. Some of these works have recently been published in Clinical Oral Investigations and been majorly revised in Caries Research. The second is a study of *Enterococcus faecalis* in root canal exudates. This project is part of an M.S. thesis of Professor Rawee's students.

- I continue to work with Professor Dr. Watchara Kasinarerk, Faculty of Associate Medical Sciences, Chiang Mai University, and our laboratories now become part of the Center of Excellence in Medical Biotechnology, sponsored by the Thai government. Professor Watchara generously introduced me to a talented PhD student, who is now working on the antimicrobial peptide and bone project. He also provides me valuable technical assistance in flow cytometry as needed.

Appendix

OXFORD

Original article

Juberg-Hayward syndrome is a cohesinopathy, caused by mutation in *ESCO2*

Piranit Nik Kantaputra[1,2], Prapai Dejkhamron[3], Worrachet Intachai[1], Chumpol Ngamphiw[4], Katsushige Kawasaki[5], Atsushi Ohazama[5], Suttichai Krisanaprakornkit[6,7], Bjorn Olsen[8], Sissades Tongsima[4] and Jame R. Ketudat Cairns[9]

[1]Division of Pediatric Dentistry, Department of Orthodontics and Pediatric Dentistry, Faculty of Dentistry, Chiang Mai University, Chiang Mai, Thailand [2]Dentaland Clinic, Chiang Mai, Thailand [3]Department of Pediatrics, Faculty of Medicine, Chiang Mai University, Chiang Mai, Thailand [4]National Biobank of Thailand, National Center for Genetic Engineering and Biotechnology, National Science and Technology Development Agency, Pathum Thani, Thailand [5]Division of Oral Anatomy, Department of Oral Biological Science, Niigata University Graduate School of Medical and Dental Sciences, Niigata, Japan [6]Center of Excellence in Oral Biology, Chiang Mai University, Chiang Mai, Thailand [7]Department of Oral Biology and Diagnostic Sciences, Faculty of Dentistry, Chiang Mai University, Chiang Mai, Thailand [8]Department of Developmental Biology, Harvard School of Dental Medicine, Boston, MA, USA [9]School of Chemistry, Institute of Science, and Center for Biomolecular Structure, Function and Application, Suranaree University of Technology, Nakhon Ratchasima, Thailand

Correspondence to: Piranit Nik Kantaputra, Division of Pediatric Dentistry; Faculty of Dentistry, Chiang Mai University, Chiang Mai 50200, Thailand. E-mail: dentaland17@gmail.com

Summary

Background: Juberg-Hayward syndrome (JHS; MIM 216100) is a rare autosomal recessive malformation syndrome, characterized by cleft lip/palate, microcephaly, ptosis, short stature, hypoplasia or aplasia of thumbs, and dislocation of radial head and fusion of humerus and radius leading to elbow restriction.
Objective: To report for the first time the molecular aetiology of JHS.
Patient and methods: Clinical and radiographic examination, whole exome sequencing, Sanger sequencing, mutant protein model construction, and *in situ* hybridization of *Esco2* expression in mouse embryos were performed.
Results: Clinical findings of the patient consisted of repaired cleft lip/palate, microcephaly, ptosis, short stature, delayed bone age, hypoplastic fingers and thumbs, clinodactyly of the fifth fingers, and humeroradial synostosis leading to elbow restriction. Intelligence is normal. Whole exome sequencing of the whole family showed a novel homozygous base substitution c.1654C>T in *ESCO2* of the proband. The sister was homozygous for the wildtype variant. Parents were heterozygous for the mutation. The mutation is predicted to cause premature stop codon p.Arg552Ter. Mutations in *ESCO2*, a gene involved in cohesin complex formation, are known to cause Roberts/SC phocomelia syndrome. Roberts/SC phocomelia syndrome and JHS share similar clinical findings, including autosomal recessive inheritance, short stature, cleft lip/palate, severe upper limb anomalies, and hypoplastic digits. *Esco2* expression during the early development of lip, palate, eyelid, digits, upper limb, and lower limb and truncated protein model are consistent with the defect.
Conclusions: Our study showed that Roberts/SC phocomelia syndrome and JHS are allelic and distinct entities. This is the first report demonstrating that mutation in *ESCO2* causes JHS, a cohesinopathy.

1

Introduction

Juberg-Hayward syndrome (JHS; MIM 216100) is a rare autosomal recessive malformation syndrome, characterized by cleft lip/palate, microcephaly, ptosis, short stature, hypoplasia or aplasia of thumbs, and dislocation of radial head and fusion of humerus and radius leading to elbow restriction (1–5).

Here we report for the first time that a novel homozygous base substitution in *Establishment of cohesion 1 homologue 2* (*ESCO2*; MIM 609353), which leads to a nonsense mutation, is the cause of JHS.

Patient and methods

The study was conducted in accordance with the Declaration of Helsinki and national guidelines. Informed consent was obtained from the parents in accordance with the regulations of the Human Experimentation Committee of the Faculty of Dentistry, Chiang Mai University (No. 51/2016, 29 September 2016).

A 28-month-old Lisu tribe girl came to the Center of Excellence in Medical Genetics Research, Chiang Mai University for genetic evaluation. She and her unaffected younger sister were children of healthy consanguineous parents (Figure 1A–1C). Her birth weight was 2920 g (10th percentile). At the age of 28 months, weight, height, and occipitofrontal circumference were 8.4 kg (<third percentile), 80.5 cm (<third percentile), and 45.5 cm (<third percentile), respectively. Proportionate short stature, microcephaly, ptosis, hanging nasal columella, and repaired cleft lip and palate were observed (Figure 1B and 1C). Fingers were slightly short but the second and fifth fingers were more severely shortened. Clinodactyly of the fifth fingers was observed (Figure 1D). Her elbow joint movement was limited since birth, leading to marked restriction of pronation and supination (Figure 1B). Bilateral soft tissue syndactyly between fingers 2–3 and 4–5 was observed. Her fingernails were unremarkable (Figure 1D). Her toes appeared normal.

Radiographic examination showed bilateral humeroradial synostosis (Figure 1E). Tibiae, fibulae, and knee joints were unremarkable. The metacarpals and phalanges of the thumbs were short and narrow. Regarding carpal bones, delayed bone age was noted. Only capitate and hamate were observed. The proximal and middle phalanges of the second and the fifth fingers were short bilaterally (Figure 1G).

Whole exome sequencing and Sanger direct sequencing

The extracted DNA of each family member was exome sequenced with the SureSelect V6+UTR exome capture library. Genome Analysis Toolkit (GATK) germline mutation workflow version 3.8.1 (6) was used to identify variants (variant calling process). Particularly, sequencing reads from each sample were aligned using the Burrows-Wheeler Aligner tool version 0.7.17 (7), against the reference sequence hg19. To avoid read-duplications during NGS read amplification, the output BAM files (*.bam) were cleaned of duplicates using the Picard tools version 2.9 (Picard Toolkit. 2019, Broad Institute, GitHub Repository; http://broadinstitute.github.io/picard/). Base-recalibration was performed by re-aligning reads belonging to known INDEL region on hg19 to reduce potential false-positive variants. After receiving cleaned BAM files, HaplotypeCaller was used to call variants resulting in individual genomic variant call format (GVCF) files which represent high-quality potential variants as well as those regions with no variants. GVCF from all samples in this study was genotyped using GenotypeGVCFs. At this point, the combined-VCF file containing all predicted genotypes from each individual was created. We deployed variant quality score recalibration from GATK to recalculate more accurately the variant quality score so that we could use these quality scores to annotate if a predicted mutation was valid.

To predict causative mutations, we annotated the aforementioned variants using the Ensembl variant effect predictor (VEP) version 95 tool (8). VEP provided predicted consequences of each variant which were used to compare against known mutation databases, including in-house variant database, 1000G, and gnomAD. We tested our hypothesis that the causative variants were in coding regions. Those predicted variants distributed over coding regions were chosen. Then those variants that were present more than 0.01 per cent in those public variant databases were filtered out, resulting in 4275 variants to be investigated. Different genetic segregation models were tested, including autosomal recessive, *de novo* autosomal dominant, compound heterozygous, and X-linked recessive.

In situ hybridization of *Esco2*

In situ hybridization was carried out as described previously (9). Briefly, for radioactive *in situ* hybridization, embryonic mouse heads were sectioned at 8 mm. The slides were pre-treated with 5 mg/ml
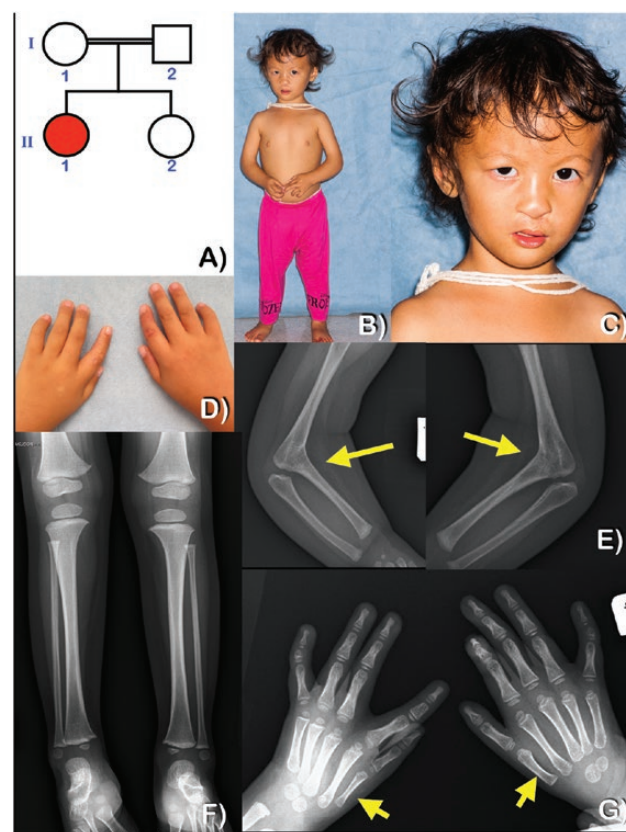

Figure 1. Proband and family members. (A) Pedigree of the consanguineous Lisu tribe family. (B and C) Patient at age 28 months: proportionate short stature, repaired cleft lip and palate, hanging nasal columella, arched eyebrows, ptosis, and thin upper lip. Note the restricted extension of the forearms. (D) Hypoplastic thumbs. (E) Radiographs of forearms; bilateral humeroradial synostosis (arrows). (F) Radiographs of lower limbs; tibiae, fibulae, and knee joints are unremarkable. (G) Antero-posterior radiograph of hands. The metacarpals and phalanges of the thumbs were short and narrow (arrows). Only capitate and hamate are observed. The proximal and middle phalanges of the second and the fifth fingers are short bilaterally.
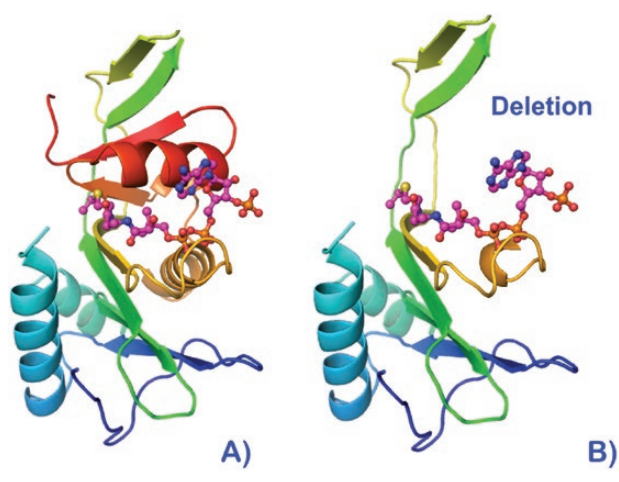
Figure 2. Model of human ESCO2 and its deletion. (A) Model of human ESCO2 acetyltransferase domain with the acetyl-CoA superimposed according to the X-ray crystal structure of the human ESCO1 acetyltransferase domain complexed with acetyl-CoA (11). The acetyl-CoA is shown in ball and stick with carbons in magenta, oxygen red, nitrogen blue, and sulfur yellow. (B) Model as in D with the region C-terminal to Arg552 deleted to show the loss of the acetyl-CoA binding helix. The homology model was created with the Phyre2 homology modelling server (10) and visualized in PyMOL (Schrödinger LLC).

proteinase K. Hybridization was carried out overnight at 55°C. The slides were then washed at high stringency at 65°C for 20 minutes and treated with 40 mg/ml RNAse A for 30 minutes at 37°C to remove any non-specifically bound probe. The sections were then washed at room temperature and dehydrated through ethanol. The slides were air-dried and dipped in Ilford K.5 photographic emulsion. Autoradiography was performed by exposing the sections in a light-tight box at 4°C for 10–14 days. Slides were developed using Kodak D19, fixed in Kodak UNIFIX, counterstained with haematoxylin.

For whole-mount *in situ* hybridization, explants were pretreated with proteinase K at 37°C, refixed in 4 per cent PFA, and then prehybridized for 5 hours at 60°C in a hybridization buffer. The probe was added at a concentration of approximately 1 mg/ml of the hybridization mix. After hybridization, tissues were washed in high-stringency conditions and pre-blocked in antibody blocking solution, then incubated with a preabsorbed antibody. DIG-labelled antisense and sense riboprobes were detected with alkaline phosphatase-coupled anti-DIG antibodies using NBT and BCIP as the colour substrates in NMT solution. Following visualization of the stain, the tissues were postfixed and cleared in 50 per cent glycerol before photography. The radioactive or DIG antisense probes or fluorescent antisense probes were generated from mouse complementary DNA clones.

Mutant protein model

A homology model of the acyltransferase domain of ESCO2 was created with the Phyre2 homology modelling server (10) with default parameters and visualized in PyMOL (Schrödinger LLC).

Results

Mutation analysis

The autosomal recessive model revealed 37 potential pathogenic variants, and these variants were ranked according to their predicted consequential impacts. We observed those with HIGH and MODERATE impacts proposed by the Ensembl Variant Predictor and found that the proband carried the highly probable homozygous stop-gain resulting in the premature termination on codon 552 of ESCO2, namely NM_001017420.2:c.1654C>T (NP_001017420.1:p. Arg552Ter). This c.1654C>T variant was cross-checked against our in-house 168 Exome database and found that no one carried this variant. This variant is extremely rare with only one heterozygous case among the 15 308 Southeast Asians and none in other populations reported in gnomAD. Thus, it has never been found in the homozygous state. In gnomAD, the allele frequency of this variant was 0.000004. The sister was homozygous for the wildtype variant and the parents heterozygous for the mutation. The mutation is predicted to truncate the C-terminus by 50 amino acids. This variant was highly likely to cause the phenotype in the proband, because truncating mutations in ESCO2 have been found in a Roberts syndrome/ SC phocomelia (OMIM 268300, 269000). The mutation was predicted to be disease-causing by MutationTaster (prob = 1.0).

Sanger direct sequencing was performed in order to validate the mutation (Supplementary Figure 1). The primer sequences used were TCGTAATGCTATGGGACACACT for forward primer; TAGCTCAGAAGCCGAGAGGT for reverse primer.

In situ hybridization

In situ hybridization at E14.5 the expression of Esco2 was detected in the developing murine lip (Figure 3A), eyelid (Figure 3B and 3I), palate (Figure 3C and 3H), digit (Figure 3D and 3K), tongue (Figure 3J), and hair follicles (Figure 3G). Its expression was also observed in the long bones of the developing forelimb (Figure 3E and 3L) but not the hindlimb (Figure 3F and 3M).

Mutant protein model

Based on its similarity to the corresponding region in ESCO1 (11), the protein segment deleted as the result of the Arg552Ter mutation contains the C-terminal of part of the acetyltransferase domain critical for the acetyl-CoA binding (Figure 1D and 3E).

Discussion

We report a novel homozygous base substitution mutation (c.1654C>T) in *ESCO2*, leading to protein truncation of 50 amino acids in a patient affected with JHS. This is the first report of the aetiology of JHS. The mutation was identified in *ESCO2*, an important gene for cohesin complex formation. Mutations in *ESCO2*, a homolog to yeast *Eco1* acetyltransferase, are known to lead to a loss of acetyltransferase activity and subsequent Roberts/SC phocomelia syndrome (MIM 268300). Protein truncations are the most common type of mutations found in *ESCO2* (12–13).

ESCO2 encodes a 601-amino acid protein belonging to the Eco1 family of acetyltransferases, which comprises two conserved regions, a Zn finger-like motif and a C-terminal acetyltransferase domain. This protein has an important role in the establishment of sister chromatid cohesion during S phase until their separation in anaphase. It also plays an important role in post-replicative sister chromatid cohesion induced by double-strand breaks. Chromosomes from the patients with *ESCO2* mutations show a characteristic lack of cohesion at the heterochromatic regions around centromeres and in the long arm of the Y chromosomes (precocious sister chromatid separation) (12).

Esco2-depleted zebrafish recapitulate a number of phenotypes observed in patients with Roberts/SC phocomelia syndrome, including craniofacial abnormalities and fin truncations, similar to phocomelia
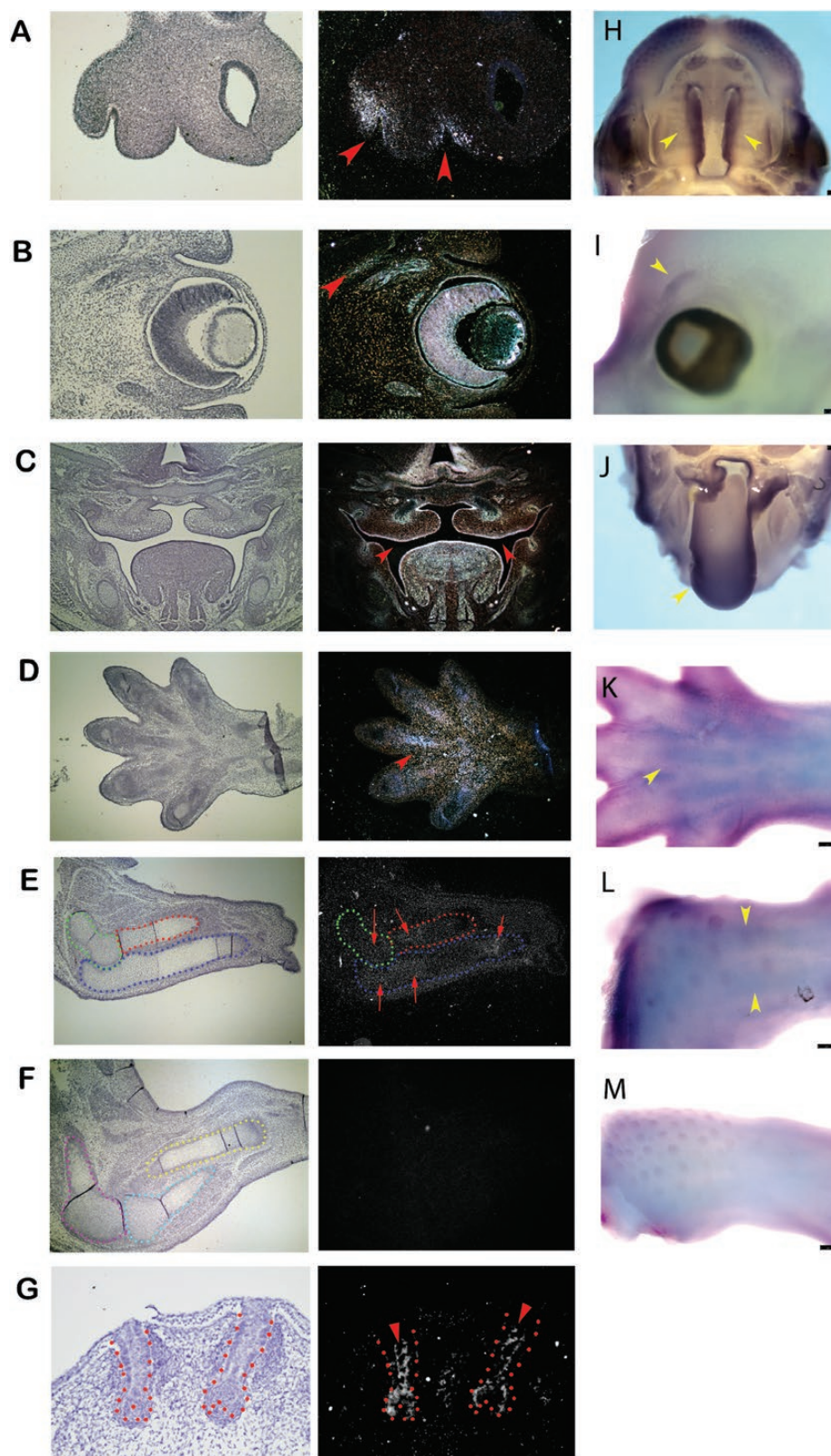
Figure 3. Esco2 expression in various tissues. Frontal (A–C and G) and sagittal (D–F) sections showing *in situ* hybridization of *Esco2* expression in developing murine lip (A), eyelid (B), palate (C), digit (D), forelimb (E) hindlimb (F), and hair follicles (G) at E11.5 (A) and E14.5 (B–G). (A–G) Bright-field (left) and dark-field (right) images. Red arrows and arrowheads indicate *Esco2* expression. The radius (red), humerus (green), ulna (blue), tibia (yellow), femur (purple), and fibula (light blue) are outlined with dotted lines (E and F). Hair follicles are outlined with red dotted lines (G). No apparent expression in F. (H–M) Whole-mount *in situ* hybridization of *Esco2* expression in maxilla (H), eyelid (I), mandible (J), digit (K), forelimb (L), and hindlimb (M) at E14.5. Yellow arrowheads indicate *Esco2* expression (H–L). No apparent expression in M.

in some patients with *ESCO2* mutations (14). The p.Arg552Ter mutation found in our patient is located near the C-terminal and would be predicted to result in truncation of the C-terminal 50 amino acid residues of the protein affecting the acetyltransferase domain critical for the acetyl-CoA binding. This was likely to cause a severe loss of the acetyltransferase activity (15), since the amino acid residues comprising two alpha-helices that form the centre of the domain structure and interact with the acetyl-CoA substrate are lost (Figure 2A and 2B). Acetyltransferase activity is required for cell proliferation, viability, and apoptosis (13). It is hypothesized that the acetyltransferase activity in our patient may not have been completely lost, therefore our patient had milder phenotype than those with Roberts syndrome who had completely lost the acetyltransferase activity, the activity crucial for the building of cohesin complex. Cleft lip and palate, syndactyly of fingers, and humeroradial synostosis seen in our patient might have been caused by abnormal cell proliferation and apoptosis, because *Esco2*-depleted zebrafish embryos have a high level of cell death (14).

Our findings demonstrate that JHS is allelic to Roberts/SC phocomelia syndrome which is scientifically and genetically sensible because JHS shares a number of phenotypes with Roberts/SC phocomelia syndrome, including autosomal recessive inheritance, short stature, cleft lip/palate, microcephaly, limb truncation, hypoplastic digits, clinodactyly, and elbow flexion contracture (1–5). This is in line with our findings of *Esco2* expression in developing murine lip, palate, and digits. The expression in the eyelid explains ptosis in our patient and the previously reported one (5). Even though JHS and Roberts/SC phocomelia syndromes are caused by mutations of the same gene, the phenotypes of patients with JHS are milder than those of Roberts/SC phocomelia syndrome (16). According to OMIM and to the best of our knowledge the disorders are distinct entities, because they have not been reported within the same families. Both syndromes may have cleft lip with or without cleft palate. The characteristic features of JHS are a fusion of humerus and radius or dislocation of the radial head and the normal lower limbs (1–5). Patients with Roberts/SC phocomelia syndrome are more severe with intrafamilial and interfamilial variability of the phenotypes (13). Some patients with JHS might have probably been misdiagnosed as Roberts/SC phocomelia syndrome (e.g. patient 2 in Ref. (17)). However, there may be a genotype–phenotype correlation between the two syndromes, which is similar to TP63-associated syndromes including Ectrodactyly-Ectodermal dysplasia-Clefting syndrome, Ankyloblepharon-Ectodermal dysplasia-Cleft lip/palate syndrome, and Rapp-Hodgkin syndrome (18). Although the deletion is expected to eliminate the acetyltransferase function of ESCO2, the phenotype of JHS is mild relative to Roberts/SC phocomelia syndrome. The sequence at the mutation-derived stop codon is UGACUG, which was found to be the fourth most frequently read through 6-nucleotide stop sequence in a mammalian cell culture assay (19). Therefore, the mild phenotype in the current case is consistent with spontaneous read through, which was reported to occur at the R943X nonsense mutation of LAMA3 and prevent stop-codon mediated decay and severe symptoms (20). In addition, variation in other genes or genetic background probably also affect the severity of the symptoms.

It is interesting to note that JHS, Roberts/SC phocomelia syndrome, and Cornelia de Lange syndrome (MIM 122470) are caused by mutations in the genes that are involved in the formation of cohesin complex, and the upper limbs in these patients are more severely affected than the lower limbs. The presence of *Esco2* expression in the developing murine forelimb and its apparent absence in the hindlimb (Figure 3E and 3F) are in line with the severity of limb malformations found in patients with mutations involving the cohesin complex formation.

Some syndromes are caused by mutations in genes that encode proteins that can be affected by teratogens. It is noteworthy that the similarity between phenotypes of patients with *ESCO2* mutations and those with thalidomide embryopathy suggests that *ESCO2* is a thalidomide target (21).

Conclusions

Here we report for the first time that protein truncation of ESCO2, which is expected to lead to abnormal acetyltransferase activity, causes JHS and suggests that this syndrome belongs to cohesinopathies.

Supplementary material

Supplementary material is available at *European Journal of Orthodontics* online.

Acknowledgements

We thank our patient and her family for their kind cooperation.

Conflicts of interest

All authors declare no conflict of interest.

References

1. Juberg, R.C. and Hayward, J.R. (1969) A new familial syndrome of oral, cranial, and digital anomalies. *The Journal of Pediatrics,* 74, 755–762.
2. Nevin, N.C., Henry, P. and Thomas, P.T. (1981) A case of the orocraniodigital (Juberg-Hayward) syndrome. *Journal of Medical Genetics,* 18, 478–480.
3. Kingston, H.M., Hughes, I.A. and Harper, P.S. (1982) Orocraniodigital (Juberg-Hayward) syndrome with growth hormone deficiency. *Archives of Disease in Childhood,* 57, 790–792.
4. Verloes, A., Le Merrer, M., Davin, J.C., Wittamer, P., Abrassart, C., Bricteux, G. and Briard, M.L. (1992) The orocraniodigital syndrome of Juberg and Hayward. *Journal of Medical Genetics,* 29, 262–265.
5. Kantaputra, P.N. and Mongkolchaisup, S. (1999) Juberg-Hayward syndrome: a new case report and clinical delineation of the syndrome. *Clinical Dysmorphology,* 8, 123–127.
6. McKenna, A., et al. (2010) The genome analysis toolkit: a MapReduce framework for analyzing next-generation DNA sequencing data. *Genome Research,* 20, 1297–1303.
7. Li, H. and Durbin, R. (2009) Fast and accurate short read alignment with Burrows-Wheeler transform. *Bioinformatics (Oxford, England),* 25, 1754–1760.
8. McLaren, W., Gil, L., Hunt, S.E., Riat, H.S., Ritchie, G.R., Thormann, A., Flicek, P. and Cunningham, F. (2016) The Ensembl variant effect predictor. *Genome Biology,* 17, 122.
9. Ohazama, A., et al. (2008) Lrp4 modulates extracellular integration of cell signaling pathways in development. *PLoS One,* 3, e4092.
10. Kelley, L.A., Mezulis, S., Yates, C.M., Wass, M.N. and Sternberg, M.J. (2015) The Phyre2 web portal for protein modeling, prediction and analysis. *Nature Protocols,* 10, 845–858.
11. Rivera-Colón, Y., Maguire, A., Liszczak, G.P., Olia, A.S. and Marmorstein, R. (2016) Molecular basis for cohesin acetylation by establishment

of sister chromatid cohesion *N*-Acetyltransferase ESCO1. *The Journal of Biological Chemistry,* 291, 26468–26477.

12. Vega, H., et al. (2005) Roberts syndrome is caused by mutations in *ESCO2*, a human homolog of yeast ECO1 that is essential for the establishment of sister chromatid cohesion. *Nature Genetics,* 37, 468–470.

13. Vega, H., et al. (2010) Phenotypic variability in 49 cases of *ESCO2* mutations, including novel missense and codon deletion in the acetyltransferase domain, correlates with *ESCO2* expression and establishes the clinical criteria for Roberts syndrome. *Journal of Medical Genetics,* 47, 30–37.

14. Mönnich, M., Kuriger, Z., Print, C.G. and Horsfield, J.A. (2011) A zebrafish model of Roberts syndrome reveals that *Esco2* depletion interferes with development by disrupting the cell cycle. *PLoS One,* 6, e20051.

15. Dyle, M.C., Kolakada, D., Cortazar, M.A. and Jagannathan, S. (2020) How to get away with nonsense: mechanisms and consequences of escape from nonsense-mediated RNA decay. *Wiley Interdisciplinary Reviews. RNA,* 11, e1560.

16. Van Den Berg, D.J. and Francke, U. (1993) Roberts syndrome: a review of 100 cases and a new rating system for severity. *American Journal of Medical Genetics,* 47, 1104–1123.

17. Afifi, H.H., Abdel-Salam, G.M., Eid, M.M., Tosson, A.M., Shousha, W.G., Abdel Azeem, A.A., Farag, M.K., Mehrez, M.I. and Gaber, K.R. (2016) Expanding the mutation and clinical spectrum of Roberts syndrome. *Congenital Anomalies,* 56, 154–162.

18. Kantaputra, P.N., Malaivijitnond, S., Vieira, A.R., Heering, J., Dötsch, V., Khankasikum, T. and Sripathomsawat, W. (2011) Mutation in SAM domain of TP63 is associated with nonsyndromic cleft lip and palate and cleft palate. *American Journal of Medical Genetics. Part A,* 155A, 1432–1436.

19. Cridge, A.G., Crowe-McAuliffe, C., Mathew, S.F. and Tate, W.P. (2018) Eukaryotic translational termination efficiency is influenced by the 3′ nucleotides within the ribosomal mRNA channel. *Nucleic Acids Research,* 46, 1927–1944.

20. Pacho, F., Zambruno, G., Calabresi, V., Kiritsi, D. and Schneider, H. (2011) Efficiency of translation termination in humans is highly dependent upon nucleotides in the neighbourhood of a (premature) termination codon. *Journal of Medical Genetics,* 48, 640–644.

21. Gomes, J.D.A., Kowalski, T.W., Fraga, L.R., Macedo, G.S., Sanseverino, M.T.V., Schuler-Faccini, L. and Vianna, F.S.L. (2019) The role of *ESCO2*, *SALL4* and *TBX5* genes in the susceptibility to thalidomide teratogenesis. *Scientific Reports,* 9, 11413.

ORIGINAL ARTICLE

WILEY | Journal of Oral Pathology & Medicine

O-GlcNAcylation in oral squamous cell carcinoma

Tassaporn Kongkaew[1] | Win Pa Pa Aung[2] | Chayarop Supanchart[1,2] |
Anupong Makeudom[2] | Sarawat Langsa-ard[2] | Thanapat Sastraruji[2] |
Ponlatham Chaiyarit[3,4] | Suttichai Krisanaprakornkit[2,5] (iD)

[1]Department of Oral and Maxillofacial Surgery, Faculty of Dentistry, Chiang Mai University, Chiang Mai, Thailand

[2]Center of Excellence in Oral and Maxillofacial Biology, Faculty of Dentistry, Chiang Mai University, Chiang Mai, Thailand

[3]Department of Oral Diagnosis, Faculty of Dentistry, Khon Kaen University, Khon Kaen, Thailand

[4]Research Group of Chronic Inflammatory Oral Diseases and Systemic Diseases Associated with Oral Health, Khon Kaen University, Khon Kaen, Thailand

[5]Department of Oral Biology and Diagnostic Sciences, Faculty of Dentistry, Chiang Mai University, Chiang Mai, Thailand

Correspondence
Suttichai Krisanaprakornkit, Center of Excellence in Oral and Maxillofacial Biology, Department of Oral Biology and Diagnostic Sciences, Faculty of Dentistry, Chiang Mai University, Chiang Mai, Thailand.
Email: suttichai.k@cmu.ac.th

Background: Two post-translational mechanisms commonly demonstrated in various cancers are protein phosphorylation and glycosylation by O-linked β-N-acetylglucosamine (O-GlcNAc). However, only phosphorylation of the epidermal growth factor receptor (EGFR)/Akt pathway has been reported in oral squamous cell carcinoma (OSCC). Therefore, we aimed to determine both post-translational modifications in OSCC tissues and in oral cancer cells compared to normal tissues and oral keratinocytes and to find correlations of these modifications with histological grading.

Methods: Thirty-two OSCC and ten normal formalin-fixed and paraffin-embedded sections were probed with the anti-O-GlcNAc, anti-O-GlcNAc transferase (OGT), anti-phosphorylated-EGFR^{tyr1173}, and anti-phosphorylated-Akt^{ser473} antibodies following standard immunohistochemistry. The immunohistochemical (IHC) score was determined using the Fromowitz standard. Whole cell lysates of oral cancer cells and normal oral keratinocytes were immunoblotted with the anti-O-GlcNAc antibody.

Results: The median IHC scores of O-GlcNAc or OGT between OSCC and normal tissues were not different, whereas those of phosphorylated-EGFR^{tyr1173} and phosphorylated-Akt^{ser473} were significantly higher in OSCC than normal tissues ($P < .001$ and $P < .01$, respectively). Similarly, expression of O-GlcNAcylated proteins in oral cancer cells and normal oral keratinocytes did not differ. In the OSCC group, the median IHC scores of O-GlcNAc and OGT were significantly lower than those of phosphorylated-EGFR^{tyr1173} and phosphorylated-Akt^{ser473} ($P < .01$ and $P < .001$, respectively). The IHC scores of O-GlcNAc or OGT were not determined to correlate with histological grading.

Conclusion: Unlike other types of cancers, our findings demonstrate that the levels of O-GlcNAcylation are not significantly increased in OSCC tissues or in oral cancer cells and are not associated with the histological grading of OSCC.

KEYWORDS
Akt, epidermal growth factor receptor, O-GlcNAc transferase, O-GlcNAcylation, oral squamous cell carcinoma

1 | INTRODUCTION

Oral squamous cell carcinoma (OSCC) accounts ~90% of oral cancer cases.[1] In 2012, an incidence of oral cancer was reported ~2.1% of all cancers worldwide.[2] In Thailand, 3733 new oral cancer cases

(~3.3% of all cancers) were reported between 2010 and 2012 with an estimated incidence rate of 5.1 and 3.6 per 100 000 population in males and females, respectively.[3] Major extrinsic risk factors include smoking, alcohol consumption, smokeless tobacco use, and human papillomavirus infection,[2] whereas intrinsic factors that alter

normal cells to cancer cells comprise a series of genetic and epigenetic changes[4] and several protein post-translational modifications (PTMs), such as phosphorylation, glycosylation, and ubiquitination.[5]

Among the phosphorylated proteins that are well documented for the pathogenesis of OSCC is epidermal growth factor receptor (EGFR), a member of the protein tyrosine kinase receptor family. The binding of its cognate ligands to EGFR activates intrinsic tyrosine kinase activity, resulting in phosphorylation of specific tyrosine residues. The phosphorylated tyrosine residues lead to activation of the phosphatidylinositol 3′-kinase/Akt pathway that causes tumor-promoting activities.[6,7] Two previous studies have reported overexpression of phosphorylated EGFR at tyrosine 1173 (p-EGFR^{tyr1173}) from 40% to 65% of OSCC cases,[7,8] while our previous study has shown overexpression of phosphorylated-Akt at serine 473 (p-Akt^{ser473}) in 14 of 15 OSCC cases.[9]

Besides phosphorylation, addition of *N*-acetylglucosamine (GlcNAc) at the hydroxyl groups of serine and/or threonine residues, known as *O*-linked β-*N*-acetylglucosamine (*O*-GlcNAc) or *O*-GlcNAcylation, of cytosolic and nuclear proteins functioning in various intracellular processes, such as transcription, cell cycle regulation, epigenetic control of gene expression in response to nutrients and stress,[10-12] is involved with cancer cell biology.[11,13] Increased *O*-GlcNAcylation levels are reported in several solid mass tumors, such as breast cancer,[14,15] prostate cancer,[16-18] cholangiocarcinoma,[19] laryngeal[20] and esophageal squamous cell carcinoma,[21] and skin cancer,[22] and are associated with tumor progression, metastasis, recurrence, and poor survival rates.[14,16,18,19] Both EGFR[23] and Akt[24,25] can be modified by *O*-GlcNAcylation in addition to phosphorylation. Overexpression of *O*-GlcNAc transferase (OGT), an enzyme that adds *O*-GlcNAc to modify proteins,[26] is shown in certain types of cancers.[15,18,19,21] However, to the best of our knowledge, involvement of *O*-GlcNAcylation and OGT in OSCC has not yet been investigated. Therefore, it was hypothesized that the *O*-linked glycosylation was elevated in OSCC tissues and oral cancer cells. The objectives were (i) to determine *O*-GlcNAc levels and OGT, p-EGFR^{tyr1173}, and p-Akt^{ser473} expressions in OSCC and then compare with normal tissues; (ii) to compare the *O*-GlcNAc levels and the OGT expression with the p-EGFR^{tyr1173} and p-Akt^{ser473} expressions in OSCC; (iii) to find correlations between the *O*-GlcNAc levels or the OGT, p-EGFR^{tyr1173}, or p-Akt^{ser473} expression and histological grading; and (iv) to examine *O*-GlcNAcylated and phosphorylated protein expressions in oral cancer cells and normal human oral keratinocytes (HOKs).

2 | MATERIALS AND METHODS

2.1 | Antibodies

For immunohistochemistry, the mouse monoclonal anti-*O*-GlcNAc (clone RL2; cat no. sc-59624), the mouse monoclonal anti-OGT (clone F12; cat no. sc-74546), and the rabbit polyclonal anti-p-EGFR^{tyr1173} (cat no. sc-101668) antibodies were purchased from Santa Cruz Biotechnology (Dallas, TX, USA). The mouse monoclonal anti-p-

Akt^{ser473} (clone 587F11; cat no. 4051) antibody was from Cell Signaling Technology (Danvers, MA, USA). For immunoblotting, the mouse monoclonal anti-phosphoserine/threonine/tyrosine (p-ser/thr/tyr) (clone SPM101; cat no. ab15556) antibody was bought from Abcam (Cambridge, MA, USA). The mouse monoclonal anti-*O*-GlcNAc and the mouse anti-beta-actin (cat no. sc-47778) antibodies were from Santa Cruz Biotechnology.

2.2 | Formalin-fixed and paraffin-embedded tissues

Thirty-two formalin-fixed and paraffin-embedded OSCC blocks were retrieved from the tissue archive of the Dental Hospital, Faculty of Dentistry, Chiang Mai University, between 2002 and 2012. The clinicopathologic data of OSCC cases are summarized in Table 1; the mean age was 66.38 years (43-85 years old). The histological grading of OSCC specimens was given by an oral pathologist (Faculty of Dentistry, Chiang Mai University). Ten normal oral tissue blocks, previously used in the Akt study,[9] were from the non-inflamed tissues overlying bony impaction of third molars from 5 males and 5 females, who underwent a surgical procedure at the Oral and Maxillofacial Surgery Clinic, Faculty of Dentistry, Chiang Mai University. The blocks were serially sectioned at 5-μm thickness and placed on silanized glass slides (Dako, Agilent Technologies, Santa Clara, CA, USA). The study protocol (no. 21/2017) was approved by the Human Experimentation Committee, Chiang Mai University. The cholangiocarcinoma sections, generously obtained from Professor Dr. Sopit Wongkham, Department of Biochemistry, Liver Fluke and Cholangiocarcinoma Research Center, Faculty of Medicine, Khon Kaen University, were used as a control for the immunohistochemical (IHC) protocol.

TABLE 1 Clinicopathologic characteristics of OSCC cases

Variables		Number of cases
Histological grading	Well differentiated	12
	Moderately differentiated	12
	Poorly differentiated	8
Age (years)	41-50	2
	51-60	9
	61-70	6
	71-80	11
	81-90	4
Gender	Male	17
	Female	15
Location	Buccal mucosa	9
	Lateral tongue	5
	Gingiva/alveolar mucosa	12
	Labial mucosa	1
	Retromolar pad	1
	Lip vermillion	2
	Mandible	2

2.3 | Immunohistochemistry

The standard IHC protocol was performed as previously described.[9] The sections were deparaffinized in xylene and rehydrated through graded alcohol and distilled water. Endogenous peroxidase was blocked by incubation with 3% hydrogen peroxide for 10 minutes at room temperature and washed with Tris-buffered saline (TBS). The antigen unmasking was performed at 100°C for 15 minutes in 0.05% Tween in 10 mM sodium citrate buffer, pH 6.0, for the anti-O-GlcNAc and anti-OGT antibodies[19] and the anti-p-EGFR^{tyr1173} antibody[7] or in 1 mM EDTA, pH 8.0, for the anti-p-Akt^{ser473} antibody.[9] The sections were cooled down for 20 minutes, blocked with 2.5% normal blocking serum (Vectastain Elite ABC-HRP kit R.T.U., Vector Laboratories, Burlingame, CA, USA) for 20 minutes, and incubated at 4°C overnight with the anti-O-GlcNAc, anti-OGT, anti-p-EGFR^{tyr1173} or anti-p-Akt^{ser473} antibody at 1:50. For a negative control, normal blocking serum was added onto the sections.

The sections were washed with TBS and reacted with secondary antibody and R.T.U. Elite ABC reagent (Vectastain Elite ABC-HRP kit R.T.U.) for 20 minutes each. The color was developed by 3,3′-diaminobenzidine (DAB Peroxidase [HRP] substrate kit, Vector Laboratories), and the sections were counterstained with hematoxylin for 30 seconds. The sections were first observed under ×100 magnification power using a bright field microscope (Axio Imager.Z2 m, Carl Zeiss Microscopy GmbH, Göttingen, Germany) for tissue orientation. Three representative fields of vision were selected from each section by 2 independent observers (T.K. and W.P.P.A.). The interexaminer calibration value was 0.881. The digitized images were captured in the epithelial layer of normal tissues and in the epithelial cell nest in the connective tissue layer of OSCC using a charge-coupled device (CCD) camera (Axiocam ICc5, Carl Zeiss Microscopy GmbH) attached to the microscope under x400 magnification power together with the ZEN 2 (blue edition) software (Carl Zeiss Microscopy GmbH).

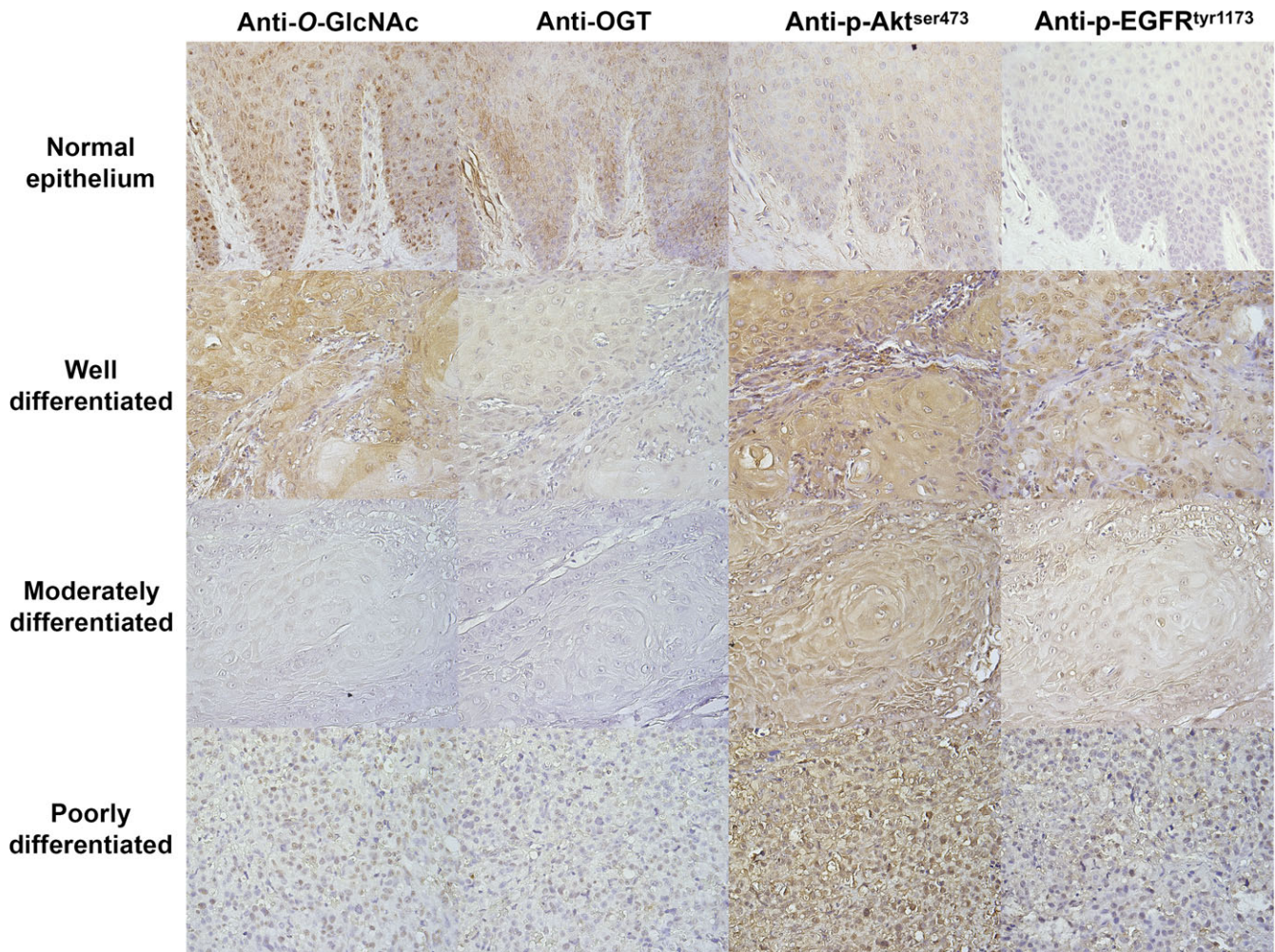**FIGURE 1** Representative images under ×400 magnification power for O-GlcNAc levels and expressions of OGT, p-Akt^{ser473}, and p-EGFR^{tyr1173} in the consecutive sections of normal oral epithelial and OSCC tissues, stratified by histological grading as well, moderately, and poorly differentiated. In general, immunostaining of p-Akt^{ser473} and p-EGFR^{tyr1173} was stronger in OSCC than normal tissues, whereas weak staining of O-GlcNAc and OGT was observed in the moderately and poorly differentiated OSCC

2.4 | Determination of IHC scores

The ImageJ program version 1.48 (National Institutes of Health, Bethesda, MD, USA) was used to quantitatively determine the percentage of positively stained cells and the staining intensity of digitized images. The mean percentage of positive cells was determined from the percentage of positive cells (the number of brown-stained cells against that of total cells in each image) in each of the 3 representative images and scored using the modified Fromowitz standard[27] as follows: 0, <10%; 1, ≥10 to <25%; 2, ≥25 to <50%; 3, ≥50 to <75%; and 4, ≥75%. For the intensity score, the color of counterstaining was first removed and the brown intensity was analyzed by mean RGB (0-255). The average mean RGB was determined from the mean RGB in each of the 3 representative images and scored as follows: 0, no staining (mean RGB>245.75); 1, weak (227.25 < mean RGB≤245.75); 2, moderate (208.75 < mean RGB≤227.25); and 3, intense (mean RGB≤208.75). The lower and upper limits of mean RGB were derived from a linear equation as $y = 13.77 - 0.054x$, where y = intensity score and x = mean RGB. To formulate this equation, the intensity of each section was semiquantitatively scored as 0, 1, 2, or 3 by 2 observers as aforementioned. The intensity score and its mean RGB value were plotted on a y-axis and an x-axis of the scatter diagram, respectively, and a linear regression line was drawn and used for the equation. The IHC score (0-7) was determined by combining the average percentage score of positive cells (0-4) with the average intensity score (0-3).

2.5 | Immunoblotting

Four oral cancer cell lines, HN5, HN6, HN15, and HN008, and 8 normal HOK cell lines were obtained from our recent study.[28] Primary HOKs were isolated from normal non-inflamed gingival biopsies overlying bony impaction of third molars of 8 healthy donors. All cell lines were cultured in serum-free keratinocyte growth medium (Lonza, Walkersville, MD, USA) at 37°C in a humidified chamber with 5% CO_2 until 80% cell confluence. A 20-μg quantity of whole cell lysates extracted in radio-immunoprecipitation assay buffer[28] was boiled at 100°C for 5 minutes, resolved on 7.5% SDS-PAGE, and blotted onto nitrocellulose membranes (Bio-Rad Laboratories, Hercules, CA, USA). The membranes were blocked with 5% non-fat dry milk (Santa Cruz Biotechnology) in 0.1% Tween-TBS for 1 hour and incubated with the antibody against O-GlcNAc (1:1000), p-ser/thr/tyr (1:500), or beta-actin (1:1000) at 4°C overnight. The rabbit anti-mouse HRP-conjugated immunoglobulins (cat no. P0260; 1:2000; Dako, Agilent Technologies) were added onto the membranes for 1 hour. The membranes were reacted with LumiGLO Reserve® chemiluminescent reagent (KPL, Gaithersburg, MD, USA), and the signals were captured by a CCD camera attached to the ChemiDoc XRS gel documentation system (Bio-Rad Laboratories). The ImageJ program version 1.48 was used to quantify the intensities of all O-GlcNAcylated and phosphorylated protein bands from 30 to 200 kDa in each cell line, normalized by the intensity of beta-actin band at 42 kDa within the same sample as a loading control. The relative ratio for the expression of O-GlcNAcylated or phosphorylated proteins in each cell line was adjusted by comparison with that in HN15 that showed the highest value of band intensities, set to 1.0.

2.6 | Statistical analysis

The Mann-Whitney U test was used to compare median IHC scores between OSCC and normal tissues and those between each pair of the 4 antibodies in the OSCC group. The Spearman's correlation
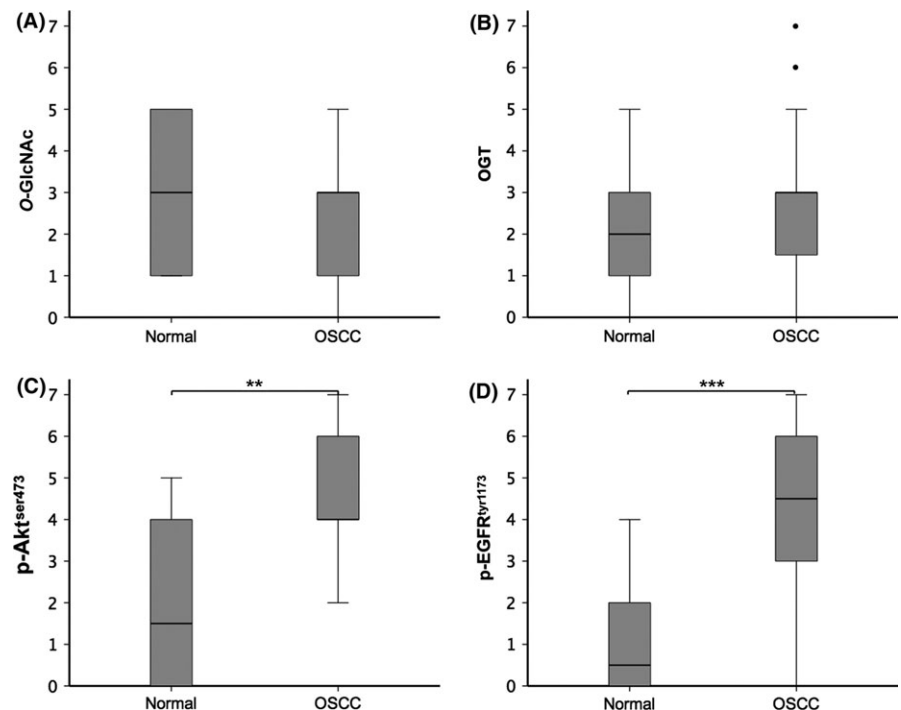

FIGURE 2 Significantly higher expressions of p-Akt[ser473] and p-EGFR[tyr1173] in OSCC than normal tissues. The box plot graphs demonstrate the immunohistochemical score (0-7) on a y-axis for O-GlcNAc levels (A) and expressions of OGT (B), p-Akt[ser473] (C), and p-EGFR[tyr1173] (D) in normal oral and OSCC tissues. The horizontal lines within each box represent the median and interquartile range. Two small black circles in B represent outliers that were included in statistical analysis. **P < .01; ***P < .001

coefficient was used to determine correlations between IHC scores and histological grading and those between each pair of the 4 antibodies. The independent t test was used to compare mean relative ratios of O-GlcNAcylated proteins or those of phosphorylated proteins between 4 HN and 8 HOK cell lines. $P < .05$ was considered to indicate a statistically significant difference. All statistical analyses were performed using SPSS version 17.0 (IBM, Armonk, NY, USA).

3 | RESULTS

3.1 | No difference in O-GlcNAc levels or OGT expression between OSCC and normal tissues

To optimize the IHC protocol for anti-O-GlcNAc and anti-OGT antibodies, each antibody was tested for immunostaining in the cholangiocarcinoma sections. The result showed brown immunostaining in the ductal epithelial cells with both antibodies at 1:50 (arrowheads in supplemental data), consistent with the previous finding.[19] The optimization was only performed for anti-O-GlcNAc and anti-OGT antibodies because our study[9] and the others[7] have already demonstrated positive immunostaining of p-Akt[ser473] and p-EGFR[tyr1173] in OSCC tissues using the same antibodies and conditions. Varying intensities were generally observed in OSCC tissues reacted with the anti-O-GlcNAc and anti-OGT antibodies, which appeared not to differ from those in normal tissues, whereas the immunostaining was strikingly more intense in OSCC than normal tissues, reacted with the anti-p-Akt[ser473] and anti-p-EGFR[tyr1173] antibodies (Figure 1). Note weaker intensities of p-Akt[ser473] and p-EGFR[tyr1173] than those of O-GlcNAc and OGT in normal epithelium (Figure 1) and no immunostaining in OSCC or normal tissues in a negative control (data not presented). There was no difference in median IHC scores between OSCC and normal tissues for O-GlcNAc levels (Figure 2A) or OGT expression (Figure 2B), whereas median IHC scores were significantly higher in OSCC than normal tissues for p-Akt[ser473] ($P < .01$; Figure 2C) and p-EGFR[tyr1173] expressions ($P < .001$; Figure 2D).

3.2 | Lower O-GlcNAc levels and OGT expression than p-Akt[ser473] and p-EGFR[tyr1173] expressions

The distributions of IHC scores among 32 OSCC cases are illustrated in a clustered-bar chart (Figure 3A). Over 24 cases were scored between 0 and 3 for the immunostaining with anti-O-GlcNAc and anti-OGT antibodies, while ≥22 were scored between 4 and 7 for that with anti-p-Akt[ser473] and anti-p-EGFR[tyr1173] antibodies. Correspondingly, median IHC scores of O-GlcNAc levels and OGT expression were significantly lower than those of p-Akt[ser473] and p-EGFR[tyr1173] expressions ($P < .001$ and $P < .01$, respectively; Figure 3B).

3.3 | No correlation between O-GlcNAc levels or OGT expression and histological grading

When correlations between IHC scores and histological grading, including 12 well, 12 moderately, and 8 poorly differentiated OSCC
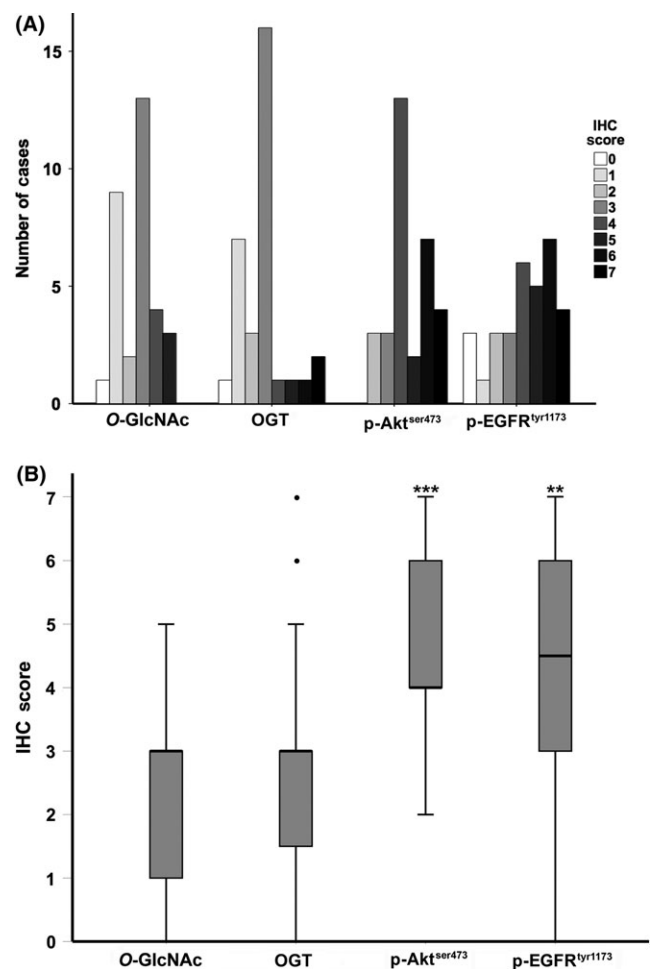

FIGURE 3 (A) Distributions of immunohistochemical (IHC) scores (0-7) among 32 OSCC cases from using 4 antibodies, including anti-O-GlcNAc, anti-OGT, anti-p-Akt[ser473], and anti-p-EGFR[tyr1173], illustrated in a clustered-bar chart and the number of cases was plotted on a y-axis. (B) Significantly higher expressions of p-Akt[ser473] and p-EGFR[tyr1173] than O-GlcNAc levels and OGT expression in OSCC tissues. The box plot graph demonstrates the IHC scores (0-7) on a y-axis for the O-GlcNAc levels and the expressions of OGT, p-Akt[ser473], and p-EGFR[tyr1173] in OSCC tissues. The horizontal lines within each box represent the median and interquartile range. Two small black circles represent outliers that were included in statistical analysis. **$P < .01$; ***$P < .001$

cases (Table 1), together with ten normal tissues were determined, O-GlcNAc levels (Figure 4A) or OGT expression (Figure 4B) did not correlate with histological grading, whereas p-Akt[ser473] (Figure 4C) and p-EGFR[tyr1173] (Figure 4D) expressions were positively correlated with histological grading ($r = .351$; $P = .022$ and $r = .429$; $P = .005$, respectively). Note that the IHC scores of O-GlcNAc tended to decrease in the moderately and poorly differentiated OSCC (Figure 4A). Although the O-GlcNAc levels or the OGT expression was not determined to correlate with histological grading, their IHC scores were positively correlated between each other ($r = .537$; $P < .001$; Figure 4E), implying a true result of no correlation. As expected, the IHC scores of p-EGFR[tyr1173] expression were positively correlated with those of p-Akt[ser473] expression ($r = .581$; $P < .001$; Figure 4F).
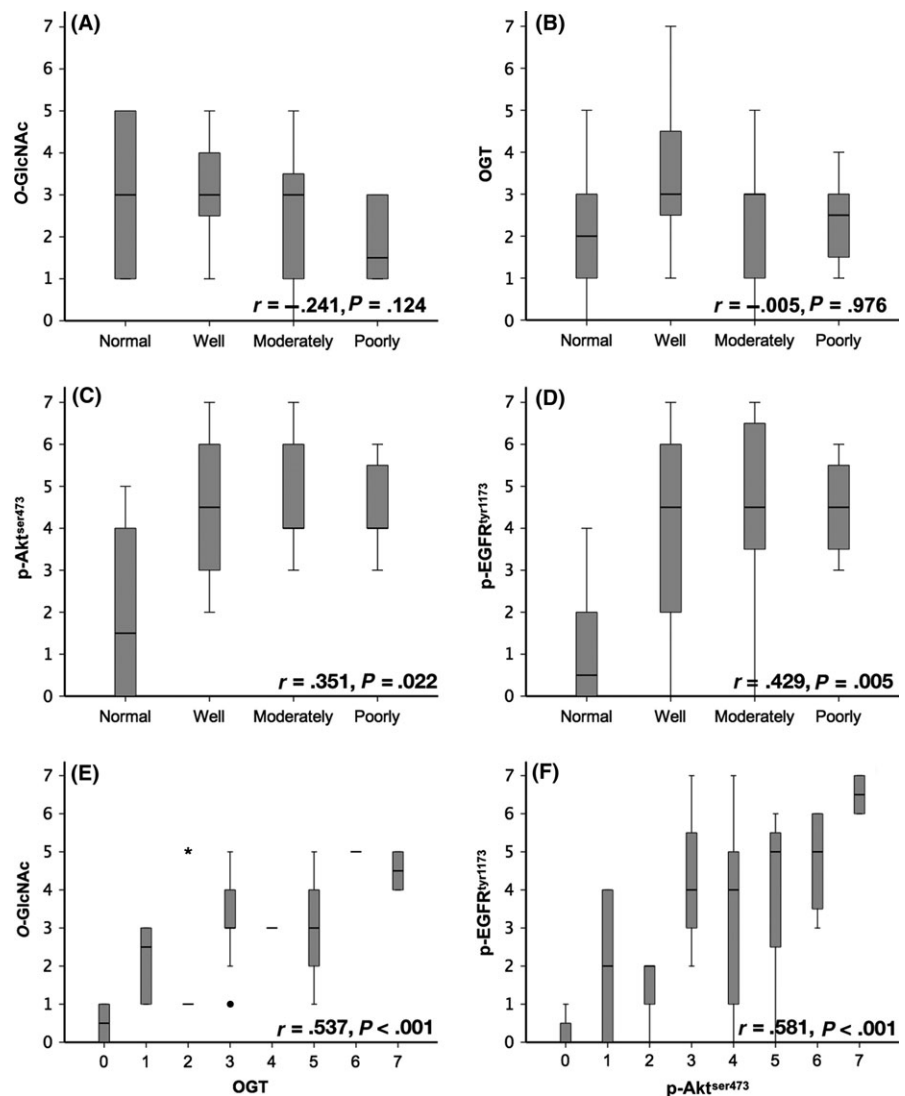
FIGURE 4 Significantly positive correlations between immunohistochemical (IHC) scores of p-Akt^{ser473} or p-EGFR^{tyr1173} and histological grading and those between O-GlcNAc and OGT or between p-EGFR ^{tyr1173} and p-Akt^{ser473}. A-D, The box plot graphs demonstrate the IHC scores (0-7) on a y-axis for O-GlcNAc levels (A) and expressions of OGT (B), p-Akt^{ser473} (C), and p-EGFR^{tyr1173} (D) in normal oral tissues and different histological grades of OSCC, including well, moderately, and poorly differentiated. E and F, The box plot graphs demonstrate a correlation between the IHC scores of O-GlcNAc levels and those of OGT expression and that between the IHC scores of p-EGFR ^{tyr1173} expression and those of p-Akt^{ser473} expression, respectively. The horizontal lines within each box represent the median and interquartile range. A small black circle and an asterisk in E indicate an outlier and an extreme value, respectively, which were included in statistical analysis

3.4 | No difference in O-GlcNAcylated protein expression between oral cancer cells and HOKs

Representative immunoblots, probed with anti-O-GlcNAc, anti-p-ser/thr/tyr, or anti-beta-actin antibody, are shown in Figure 5A. Generally, varying expressions of O-GlcNAcylated proteins in 4 oral cancer cell lines (HNs) did not differ from those in 4 HOK cell lines, while those of phosphorylated proteins seemed to be greater in HN than HOK cell lines. Beta-actin expression was equal among different samples. The mean relative ratio of O-GlcNAcylated proteins in 4 HN cell lines was not different from that in 8 HOK cell lines, whereas the mean relative ratio of phosphorylated proteins was significantly higher in HN than HOK cell lines ($P < .01$; Figure 5B).

4 | DISCUSSION

By immunohistochemistry, the median IHC scores of O-GlcNAc or OGT between OSCC and normal tissues were not different, whereas those of p-Akt^{ser473} and p-EGFR^{tyr1173} were significantly higher in

OSCC than normal tissues. Accordingly, the median IHC scores of p-Akt^{ser473} and p-EGFR^{tyr1173} were significantly greater than those of O-GlcNAc and OGT in the OSCC group. Consistent with these immunohistochemical findings, O-GlcNAcylated protein expression in oral cancer cells or HOKs, assayed by immunoblotting, was not different (Figure 5), while phosphorylated protein expression was significantly increased in oral cancer cells. A lack of enhanced O-GlcNAc levels or OGT overexpression in OSCC or oral cancer cells suggests that PTM by O-GlcNAcylation may not be involved in oral carcinogenesis. These results were inconsistent with hyper-O-GlcNAcylation and OGT overexpression in squamous cell carcinoma of the larynx,[20] the esophagus,[21] and the skin,[22] suggesting distinct tissue-specific PTMs. However, our findings are still similar to no differences in O-GlcNAc immunostaining intensities between liver or pancreatic cancer and their adjacent normal tissues.[17] Moreover, O-GlcNAc levels in >60% of prostate cancer cases were lower than those in the adjacent normal tissues.[16]

The IHC scores of p-Akt^{ser473} and p-EGFR^{tyr1173} were significantly higher in OSCC than normal tissues and positively correlated with histological grading, indicating that PTM via phosphorylation of
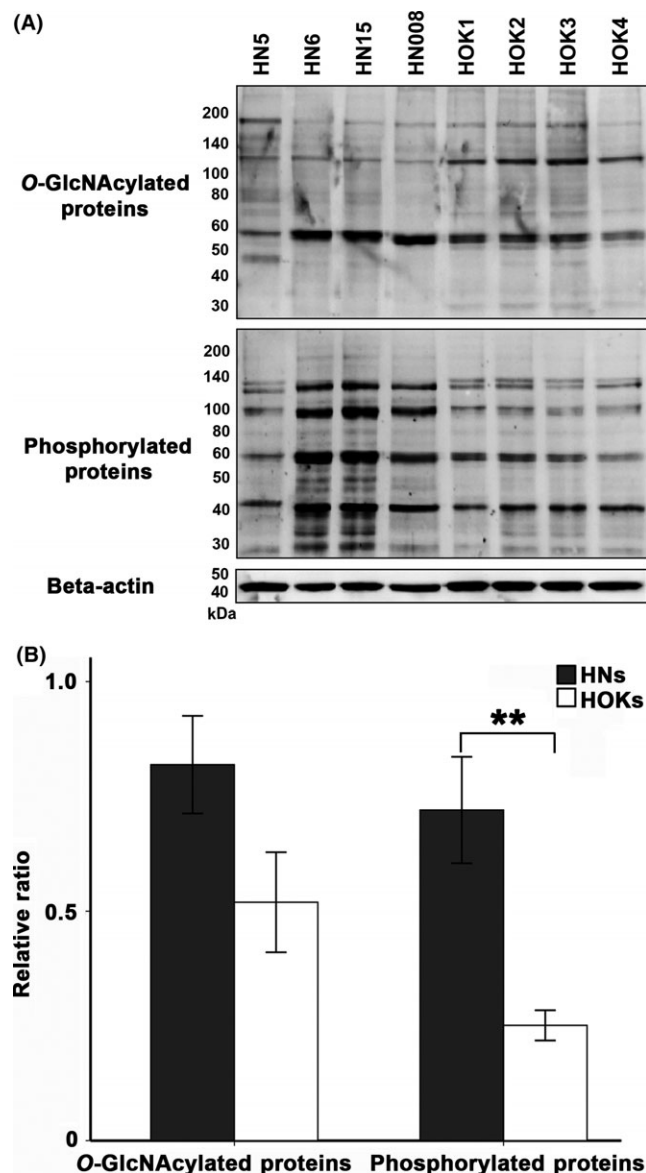
(A)

(B)

FIGURE 5 (A) Representative immunoblots showing expressions of O-GlcNAcylated proteins (upper panel; 30-200 kDa), phosphorylated proteins (middle panel; 30-200 kDa), and beta-actin (lower panel; at 42 kDa) in 4 oral cancer cell lines (HN5, HN6, HN15, HN008) and 4 normal human oral keratinocyte cell lines (HOK1-4). (B) Significantly greater expression of the phosphorylated proteins in HNs than HOKs. A bar chart demonstrating the mean relative ratio of the O-GlcNAcylated proteins/beta-actin expression and that of the phosphorylated proteins/beta-actin expression in 4 HNs (gray bar) and 8 HOKs (empty bar) derived from 8 different donors. The normalized ratio of O-GlcNAcylated proteins or of phosphorylated proteins in each cell line was adjusted by comparison with the corresponding ratio in HN15, set to 1.0. Error bars = standard deviations. **$P < .01$

Akt and EGFR is associated with enhanced OSCC severity. These findings were concordant with those showing p-Akt[ser473] overexpression in OSCC tissues and significantly increased p-Akt[ser473] expression in poorly differentiated OSCC[9] and a significant correlation between p-EGFR[tyr1173] overexpression and poor prognosis of OSCC.[7] By contrast, the IHC scores of O-GlcNAc or OGT failed to correlate with the histological grading of OSCC. These results differ from the relationship between hyper-O-GlcNAcylation and the presence of lymph node metastasis in different types of cancer.[14,21] However, to the best of our knowledge, this study is the first to determine the association of O-GlcNAcylation with the severity of squamous cell carcinoma, as stratified by histological features. The notable limitation of this study is the absence of clinical data for patients with OSCC, such as primary tumor size and its invasion into adjacent tissues, lymph node involvement, metastasis at distant organs, recurrence, and survival rates. Therefore, it is still required to further determine the relationship of O-GlcNAc levels and OGT expression with all clinicopathologic characteristics.

As IHC scores from each pair of the 4 antibodies were determined for a correlation, significantly positive correlations were found between O-GlcNAc and OGT and between p-Akt[ser473] and p-EGFR[tyr1173]. These 2 positive correlations are anticipated because of the known OGT function as an enzyme for O-GlcNAcylation[26] and the Akt function as a downstream signaling molecule upon EGFR activation.[6] Such these 2 correlations can verify our immunostaining results with the 4 antibodies and their IHC protocol. The quality of OSCC specimens was also controlled by intense immunostaining of p-Akt[ser473] or p-EGFR[tyr1173] demonstrated in certain consecutive OSCC sections that were not or weakly stained with anti-O-GlcNAc or anti-OGT antibody (Figure 1).

Up to the present, over 4000 O-GlcNAcylated proteins have been reported;[29] however, almost all O-GlcNAcylated proteins, particularly Akt, can also be modified by phosphorylation.[30] In cancer biology, O-GlcNAcylation is described as an alternative PTM to phosphorylation for activation of cellular signaling and tumor-promoting activity.[11,13,30] Moreover, these 2 PTMs can occur at the same, adjacent, and/or distant serine/threonine within the same protein, so they usually have an interplay between each other.[10,12] Relevant to this study, the reciprocal interaction is exemplified by an interference of phosphorylation by O-GlcNAcylation in both normal and cancer cells. For example, Akt at serine 473 could be competitively modified by phosphorylation or O-GlcNAcylation in normal pancreatic cells; hence, enhanced O-GlcNAc modification resulted in decreased phosphorylated-Akt and its function, which led to increased cell apoptosis.[24] Furthermore, O-GlcNAcylation of Akt at threonine 305 and 312 inhibited phosphorylation at threonine 308 in breast cancer cells, leading to diminished cancer cell proliferation and migration.[25] By analogy, it is logical to assume that if O-GlcNAc levels are raised at serine or threonine of Akt in oral cancer cells, phosphorylation of Akt would be blocked, resulting in increased oral cancer cell death, while cancer cell growth and migration are deterred. This concept warrants further investigations and may be developed as a future targeted therapy for OSCC. Besides Akt, O-GlcNAcylation of EGFR in human carcinoma epidermoid cells and human lung carcinoma cells has been reported.[23] Therefore, it is interesting to further investigate the O-GlcNAcylation status of EGFR in comparison with its phosphorylation status in different stages of OSCC tissues or in oral cancer cells by

immunoprecipitation. In summary, unlike several types of cancer, PTM by *O*-linked glycosylation may not be implicated in oral carcinogenesis as compared to phosphorylation of certain proteins, such as EGFR and Akt, and *O*-GlcNAcylation is not associated with OSCC severity, as stratified by the histological features.

ACKNOWLEDGEMENTS

CONFLICT OF INTEREST

All authors report no conflict of interests relating to this study.

ORCID

Suttichai Krisanaprakornkit [ID] http://orcid.org/0000-0001-9189-0333

REFERENCES

1. Neville B, Damm D, Allen C, Chi A. *Oral and Maxillofacial Pathology*, 4th edn. St. Louis, MO: Elsevier; 2016:374 p.
2. Torre LA, Bray F, Siegel RL, Ferlay J, Lortet-Tieulent J, Jemal A. Global cancer statistics, 2012. *CA Cancer J Clin*. 2015;65:87-108.
3. Imsamran W, Chaiwerawattana A, Wiangnon S, Sangrajrang S, Buasom R. *Cancer in Thailand Vol. VIII, 2010–2012*. Bangkok: National Cancer Institute Thailand; 2015. 13 p.
4. Singh JP, Zhang K, Wu J, Yang X. *O*-GlcNAc signaling in cancer metabolism and epigenetics. *Cancer Lett*. 2015;356:244-250.
5. Krueger KE, Srivastava S. Posttranslational protein modifications: current implications for cancer detection, prevention, and therapeutics. *Mol Cell Proteomics*. 2006;5:1799-1810.
6. Schlessinger J. Common and distinct elements in cellular signaling via EGF and FGF receptors. *Science*. 2004;306:1506-1507.
7. Monteiro L, Ricardo S, Delgado M, Garcez F, do Amaral B, Lopes C. Phosphorylated EGFR at tyrosine 1173 correlates with poor prognosis in oral squamous cell carcinomas. *Oral Dis*. 2014;20:178-185.
8. Theocharis S, Giaginis C, Dana E, et al. Phosphorylated epidermal growth factor receptor expression is associated with clinicopathologic parameters and patient survival in mobile tongue squamous cell carcinoma. *J Oral Maxillofac Surg*. 2017;75:632-640.
9. Iamaroon A, Krisanaprakornkit S. Overexpression and activation of Akt2 protein in oral squamous cell carcinoma. *Oral Oncol*. 2009;45:e175-e179.
10. Hart GW, Slawson C, Ramirez-Correa G, Lagerlof O. Cross talk between *O*-GlcNAcylation and phosphorylation: roles in signaling, transcription, and chronic disease. *Annu Rev Biochem*. 2011;80:825-858.
11. Ma Z, Vosseller K. *O*-GlcNAc in cancer biology. *Amino Acids*. 2013;45:719-733.
12. Butkinaree C, Park K, Hart GW. *O*-linked beta-*N*-acetylglucosamine (*O*-GlcNAc): extensive crosstalk with phosphorylation to regulate signaling and transcription in response to nutrients and stress. *Biochim Biophys Acta*. 2010;1800:96-106.
13. Ferrer CM, Sodi VL, Reginato MJ. *O*-GlcNAcylation in cancer biology: linking metabolism and signaling. *J Mol Biol*. 2016;428:3282-3294.
14. Gu Y, Mi W, Ge Y, et al. GlcNAcylation plays an essential role in breast cancer metastasis. *Cancer Res*. 2010;70:6344-6351.
15. Krzeslak A, Forma E, Bernaciak M, Romanowicz H, Brys M. Gene expression of *O*-GlcNAc cycling enzymes in human breast cancers. *Clin Exp Med*. 2012;12:61-65.
16. Kamigaito T, Okaneya T, Kawakubo M, Shimojo H, Nishizawa O, Nakayama J. Overexpression of *O*-GlcNAc by prostate cancer cells is significantly associated with poor prognosis of patients. *Prostate Cancer Prostatic Dis*. 2014;17:18-22.
17. Gu Y, Gao J, Han C, et al. *O*-GlcNAcylation is increased in prostate cancer tissues and enhances malignancy of prostate cancer cells. *Mol Med Rep*. 2014;10:897-904.
18. Lynch TP, Ferrer CM, Jackson SR, Shahriari KS, Vosseller K, Reginato MJ. Critical role of *O*-linked beta-*N*-acetylglucosamine transferase in prostate cancer invasion, angiogenesis, and metastasis. *J Biol Chem*. 2012;287:11070-11081.
19. Phoomak C, Silsirivanit A, Wongkham C, Sripa B, Puapairoj A, Wongkham S. Overexpression of *O*-GlcNAc-transferase associates with aggressiveness of mass-forming cholangiocarcinoma. *Asian Pac J Cancer Prev*. 2012;13(Suppl):101-105.
20. Starska K, Forma E, Brzezińska-Błaszczyk E, et al. Gene and protein expression of *O*-GlcNAc-cycling enzymes in human laryngeal cancer. *Int J Clin Exp Med*. 2015;15:455-468.
21. Qiao Z, Dang C, Zhou B, et al. *O*-linked *N*-acetylglucosamine transferase (OGT) is overexpressed and promotes *O*-linked protein glycosylation in esophageal squamous cell carcinoma. *J Biomed Res*. 2012;26:268-273.
22. Lee Y, Hong DK, Choi DK, et al. Immunohistochemical study of *O*-GlcNAcylation in human skin tumors. *Korean J Phys Anthropol*. 2014;27:71-77.
23. Stateva SR, Villalobo A. *O*-GlcNAcylation of the human epidermal growth factor receptor. *Org Biomol Chem*. 2015;13:8196-8204.
24. Kang ES, Han D, Park J, et al. *O*-GlcNAc modulation at Akt1 Ser473 correlates with apoptosis of murine pancreatic beta cells. *Exp Cell Res*. 2008;314:2238-2248.
25. Wang S, Huang X, Sun D, et al. Extensive crosstalk between *O*-GlcNAcylation and phosphorylation regulates Akt signaling. *PLoS One*. 2012;7:e37427.
26. Haltiwanger RS, Holt GD, Hart GW. Enzymatic addition of *O*-GlcNAc to nuclear and cytoplasmic proteins. Identification of a uridine diphospho-*N*-acetylglucosamine:peptide beta-*N*-acetylglucosaminyltransferase. *J Biol Chem*. 1990;265:2563-2568.
27. Fromowitz FB, Viola MV, Chao S, et al. Ras p21 expression in the progression of breast cancer. *Hum Pathol*. 1987;18:1268-1275.
28. Tanasubsinn P, Aung WP, Pata S, et al. Overexpression of ADAM9 in oral squamous cell carcinoma. *Oncol Lett*. 2018;15:495-502.
29. Ma J, Hart GW. *O*-GlcNAc profiling: from proteins to proteomes. *Clin Proteomics*. 2014;11:8.
30. Bond MR, Hanover JA. A little sugar goes a long way: the cell biology of *O*-GlcNAc. *J Cell Biol*. 2015;208:869-880.

SUPPORTING INFORMATION

Additional Supporting Information may be found online in the supporting information tab for this article.

Promotion of Dental Pulp Wound Healing in New Zealand White Rabbits' Teeth by Thai Propolis Product

Nattriya Likitpongpipat, DDS, MS[1], Somboon Sangmaneedet, DVM, MS, PhD[2], Poramaporn Klanrit, DDS, PhD[3], Rajda Noisombut, DDS, PhD[4], Suttichai Krisanaprakornkit, DDS, PhD[5], and Pattama Chailertvanitkul, DDS, PhD[1]

Abstract

This study examined and compared wound healing between Thai propolis product and calcium hydroxide paste as pulp-capping agents after partial pulpotomy in New Zealand white rabbits. Forty incisor teeth from 10 rabbits were treated. Thirty-six teeth received class V cavity preparations with partial pulpotomy and application of either propolis or calcium hydroxide paste. Similar cavity preparations were performed in 2 teeth without any capping material as a positive control, whereas 2 teeth without the cavity preparation served as a negative control. Histological evaluation showed that both groups had dentin bridge formation. Dentinal tubules in the dentin bridge were more orderly arranged in the Thai propolis group than in the calcium hydroxide group. Wound healing and the median number of hyperemic blood vessels were not statistically significant different between the 2 groups. Thai propolis product may be used as a pulp-capping agent.

Keywords

calcium hydroxide, direct pulp capping, propolis, pulpotomy, reparative dentin, rabbit

Introduction

Vital pulp therapy, including indirect and direct pulp capping with partial pulpotomy, is an alternative to root canal therapy for maintaining vital pulp tissue.[1] However, case selection for vital pulp therapy depends upon clinicians' judgment on symptoms, progression, or severity of dental caries and trauma; duration and extent of pulp exposure; immature root apices; and radiographic findings.[2] Calcium hydroxide paste has been commonly used as a pulp-capping material for years due to its antibacterial activity after being dissociated into hydroxyl ions[3] and its promotion of reparative dentin formation, particularly in young permanent molars.[4] A previous systematic review of success rates of vital pulp therapy using calcium hydroxide and mineral trioxide aggregate (MTA) by clinical and radiographic evaluations of 199 teeth has revealed a treatment success over 97% after follow-up periods ranging from 6 months to 3 years, especially in immature teeth with open root apices.[5] A randomized controlled trial[6] showed that partial pulpotomy in teeth of young human patients with reversible pulpitis, either using MTA or calcium hydroxide paste,[a] resulted in favorable treatment outcomes for up to 2 years. The incidence of unfavorable outcomes tended to be higher in teeth with pulp exposure areas larger than 5 mm. However, a major drawback for a long-term use of calcium hydroxide as a pulp-capping agent is bacterial leakage into the pulp from poor sealing ability and solubility of calcium hydroxide, lack of adhesion, and tunnel defects from porous dentin bridges.[7]

With knowledge of disadvantages of calcium hydroxide, MTA has been developed and tested for its chemical, physical, and antibacterial properties; biocompatibility; sealability; and regenerative capacity for dentin bridge formation.[8,9] However, tooth staining and long setting times may affect decisions for its use as a pulp-capping agent.[10] An alternative to MTA, propolis, or bee glue, is a natural hive product collected by honeybees and used as a home remedy in folk medicine, which has been introduced and tested for its potential use as a pulp-capping

[1] Department of Restorative Dentistry, Faculty of Dentistry, Khon Kaen University, Khon Kaen, Thailand
[2] Department of Pathobiology, Faculty of Veterinary Medicine, Khon Kaen University, Khon Kaen, Thailand
[3] Department of Oral Diagnosis, Research Group of Chronic Inflammatory Oral Diseases and Systemic Diseases Associated With Oral Health, Faculty of Dentistry, Khon Kaen University, Khon Kaen, Thailand
[4] Department of Community Dentistry, Faculty of Dentistry, Khon Kaen University, Khon Kaen, Thailand
[5] Department of Oral Biology and Diagnostic Sciences, Faculty of Dentistry, Center of Excellence in Oral and Maxillofacial Biology, Chiang Mai University, Chiang Mai, Thailand

Corresponding Author:
Pattama Chailertvanitkul, Department of Restorative Dentistry, Faculty of Dentistry, Khon Kaen University, 123 Mittraparp Highway, Muang District, Khon Kaen 40002, Thailand.
Email: patchai@kku.ac.th

material in rats, humans, guinea pigs, and pigs.[11-14] By histologic assessments, the propolis extracts from these studies can generally decrease inflammation within the exposed pulp tissue and induce collagen synthesis resulting in reparative dentin formation with an organized tubular structure. The anti-inflammatory property is likely due to various organic constituents within the extract, such as phenols, esters, and flavonoids.[15,16] Recently, the Thai propolis extract has been developed as a storage medium for avulsed teeth and has been demonstrated to preserve the viability of human periodontal ligament cells from extracted premolars for up to 3 hours,[17] indicating the biocompatibility of Thai propolis extract when in contact with human cells.

Because chemical composition and biological properties of propolis extracts from different geographical areas vary, we sought to histologically determine and compare the efficacy of Thai propolis extract on promotion of dental pulp wound healing with that of calcium hydroxide in New Zealand white rabbits' teeth. The Thai propolis extract was formulated as a pulp-capping agent and has recently been shown to inhibit *Streptococcus mutans* and *Lactobacillus casei* but is not toxic to human dental pulp cells in vitro.[18] It was hypothesized that enhancement of dental pulp wound healing between Thai propolis and calcium hydroxide would be similar when assessed histologically.

Methods

Preparation of Thai Propolis Product

Extract of raw propolis, collected from *Apis mellifera* beehives in Nong Khai Province, Thailand, was prepared as previously described.[17] One gram of propolis was chopped into small pieces and extracted using 5 mL of 95% ethanol. The mixture was stirred at 25°C in an orbital shaker[b] at 200 rpm for 5 days protected from light. The extract was filtered through No. 1 filter paper,[c] stored at $-20°C$ for 48 hours, and then filtered again. Ethanol in the filtrate was evaporated using a rotary evaporator[d] at 40°C and the concentrated filtrate was dried using a freeze dryer.[e] To prepare a ready-to-use propolis product packed in a sterilized amber bottle (Figure 1A) for a one-time use, the semisolid brownish propolis extract (Figure 1B) at the final concentration of 78.26 mg/mL, which is 2 times higher than the minimal bactericidal concentration against *S mutans* and *L casei*,[18] was mixed with 0.87 g of Carbomer 934P,[f] 13.04 mL of triethanolamine, and 76.09 mL of distilled water. The bottles were sterilized by γ irradiation at 21.6 kGy, controlled by dosimeters,[g] and their sterilization was confirmed by bacterial and fungal cultures in soybean casein digest media[h] for 14 days at 35°C. This Thai propolis product was patented (#10572) by the Department of Intellectual Property, Ministry of Commerce, Thailand.

Animals

Ten New Zealand white rabbits (3 males and 7 females, mean age = 16.9 ± 3.2 weeks, mean weight = 2.8 ± 0.4 kg) were
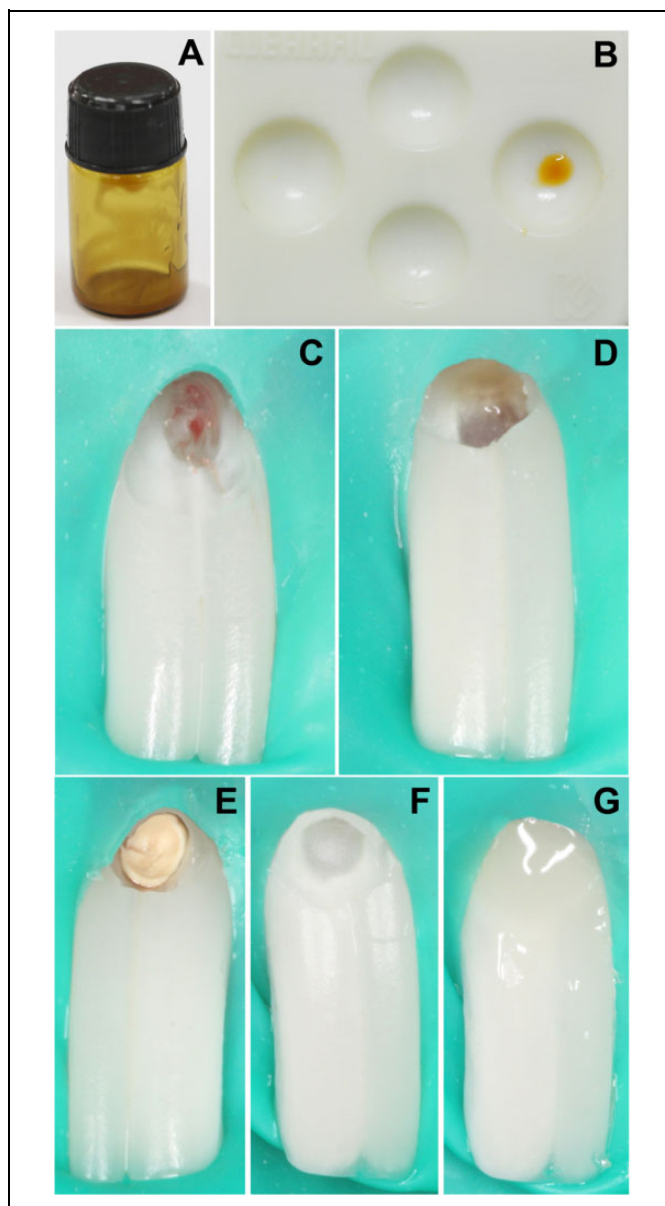

Figure 1. Photographs of Thai propolis product, tooth preparation, and restorative procedures. (A) Propolis product in an amber bottle. (B) Propolis extract—note the brown color. (C) Tooth preparation on the labial surface of an anterior tooth with mechanically exposed pulp. (D) Site of pulp exposure capped with the propolis product. (E) Capped with calcium hydroxide paste. (F) Lined with resin-modified glass ionomer cement. (G) Filled with flowable composite resin.

individually caged at the Northeast Laboratory Animal Center, Khon Kaen University, Khon Kaen, Thailand, in a sterile room with 23°C ± 2°C, 30% to 60% relative humidity, 350 to 400 Lux, less than 85 dB, and a 12-hour day and night period in accordance with current care and use guidelines for laboratory animals.[19] They were kept for 5 days before cavity preparation and fed with commercial pellets (SmartHeart; Perfect Companion Group, Co, Ltd, Bangkok, Thailand), steamed rice straw and Timothy grass, and potable water containing 3 to 4 ppm of

chlorine. The research protocol was approved by the ethics committee in Standard Animal Care and Use for Scientific Research, Khon Kaen University. A total of 40 incisor teeth from 10 rabbits were randomly categorized into 4 groups:

- Negative control group: teeth received no treatment (n = 2).
- Positive control group: teeth were mechanically exposed pulp and partial pulpotomy without any capping material (n = 2).
- Thai propolis group: teeth were mechanically exposed pulp and partial pulpotomy capped with the Thai propolis product (n = 18).
- Calcium hydroxide group: teeth were mechanically exposed pulp and partial pulpotomy capped with calcium hydroxide paste[a] (n = 18).

After randomization, 12 of 18 teeth in 2 experimental groups were from female rabbits, while the remaining 6 were from male rabbits. Two teeth in the negative control group and positive control group were from female rabbits. The sample size calculation for 2 experimental groups was computed using software,[i] based on the differences in the proportions between 2 dependent groups with type I error and power of test equal to 0.05 and 0.80, respectively. In a sterile operating room, intramuscular injection with xylazine (3 mg/kg)[j] and ketamine (20 mg/kg)[k] was administered to anesthetize all rabbits under intravenous fluid via an auricular marginal vein. The levels of consciousness were assessed and the vital signs were intermittently monitored throughout tooth preparation, partial pulpotomy, and restorative procedures.

Tooth Preparation and Partial Pulpotomy

The tooth was cleaned with pumice in a rubber prophy angle and isolated by a rubber dam. The operative area was disinfected with 2.5% tincture of iodine and 70% isopropyl alcohol. A class V cavity with the dimension of 1.5 mm × 2 mm was prepared on the labial surface of each tooth using a sterile pear-shaped diamond bur (0.10 ISO standards).[l] After cavity preparation, the pulp horn was mechanically exposed approximately 1 mm in diameter (Figure 1C) by drilling with a sterile high-speed diamond bur (0.10 ISO standards)[l] under copious sterile water irrigation. After bleeding was controlled by applying sterile cotton pellets with 0.9% normal saline to the exposed pulp, Thai propolis (Figure 1D) or calcium hydroxide paste (Figure 1E) was applied to each exposure site in the experimental groups, respectively. The cavity was subsequently lined with resin-modified glass ionomer cement[m] (Figure 1F) and filled with flowable composite resin[n] (Figure 1G). After the restorative procedure, patients were monitored for any symptoms and the operative sites were monitored daily. To alleviate pain, subcutaneous injection with a nonsteroidal anti-inflammatory drug[o] at 2 to 4 mg/kg was administered daily for 3 consecutive days.

Histologic Assessments

All rabbits were euthanized after 14 days by intravenous injection with a lethal dose (100 mg/kg) of pentobarbital sodium.[p] Jaws were removed and processed by decalcification and routine hematoxylin and eosin staining for histologic evaluations. Jaws were fixed in 10% neutral buffered formalin, decalcified in 10% nitric acid for 3 days, sequentially dehydrated in graded alcohols, 70%, 80%, 90%, and 100%, immersed in xylene, and finally embedded in paraffin blocks. The blocks were serially cut with an average thickness of 5 mm along the labiolingual direction passing through the center of pulp exposure site. The sections were stained with hematoxylin and eosin for histologic observations under light microscopy[q] and the images were captured using software.[r] Five selected images of each specimen with the best view of pulp exposure were evaluated and scored by a board-certified oral pathologist (P.K.), who was blinded to the experimental groups of samples, each of which was given a code to avoid a possible bias. The scoring was repeated by the same examiner 7 days after the first evaluation and the reliability of assessment was determined by the measure of agreement with κ values between 0.935 and 1.000.

Statistical Analysis

For descriptive statistics, the continuity and morphology of hard tissue formation at the interface with the capping material, pulp inflammation, including type and extent, and other histologic features of the pulp tissue, including calcification and necrosis, were graded from I to III according to the criteria modified from Aeinehchi et al[20] and Asgary et al[21] (Table 1) using UTHSCSA Image Tool 3.0 program[s] and reported as numbers and percentages. For inferential statistics, the proportions of pulp wound healing between the experimental groups were compared using the McNemar test. Since the data were not normally distributed, the Wilcoxon signed rank test was used to compare the median numbers of hyperemic blood vessels between the experimental groups. Statistical significance was considered if P values were less than .05.

Results

Formation of dentin bridge was assessed in every specimen of the Thai propolis group and of the calcium hydroxide group (Table 2) with 5 different patterns according to the continuity and morphology of dentin bridge as follows, (1) no dentin bridge, (2) incomplete and disorganized tubules, (3) incomplete but orderly arranged tubules, (4) complete but disorganized tubules, and (5) complete and orderly arranged tubules (Figure 2A-E, respectively). The numbers and percentages of these 5 patterns among 4 groups are summarized in Table 2. Complete dentin bridge formation was found in 12 of 18 teeth of the Thai propolis group and in 15 of 18 teeth of the calcium hydroxide group. Interestingly, teeth with orderly arranged dentinal tubules (a combination of patterns C and E) were found more in the Thai propolis group than in

Table 1. Criteria for Histologic Evaluations.[a]

	Grades		
	No Wound Healing	Signs of Wound Healing	
Interpretation	I (Poor)	II (Moderate)	III (Good)
Dentine bridge formation (Asgary et al[21])			
Continuity	None detected	The exposure site incompletely covered	The exposure site completely covered
Morphology of dentinal tubules	None detected	Disorganized arrangement	Orderly arranged
Pulp inflammation (Asgary et al[21])			
Type	Acute and chronic inflammation (macrophages, lymphocytes, plasma cells, and neutrophils)	Chronic inflammation (macrophages, lymphocytes, and plasma cells)	None detected
Extent	Occupy the whole pulp chamber	Restricted to the areas beneath the exposure site/dentine bridge or within some parts of the pulp chamber	None detected
Other histologic features (Asgary et al[21])			
Calcification	Diffuse calcification	Stone in the pulp chamber	None detected
Necrosis	Occupy the whole pulp chamber	Some parts of the pulp chamber	None detected

[a]Modified From Aeinehchi et al[20] and Asgary et al.[21] An increase in hyperemia (Aeinehchi et al[20]) as determined from the tissue section that contained the maximal number of hyperemic blood vessels compared to that in the negative control.

Table 2. A summary of Dentin Bridge Formation Among 4 Groups.

Pattern of Dentin Bridge (Continuity and Morphology)	Negative Control, n (%)	Positive Control, n (%)	Thai Propolis, n (%)	Calcium Hydroxide, n (%)
(A) None	0 (0)	1 (2.5)	0 (0)	0 (0)
(B) Incomplete and disorganized tubules	0 (0)	1 (2.5)	4 (10)	3 (7.5)
(C) Incomplete but orderly arranged tubules	0 (0)	0 (0)	2 (5)	0 (0)
(D) Complete but disorganized tubules	0 (0)	0 (0)	2 (5)	6 (15)
(E) Complete and orderly arranged tubules	2 (5)	0 (0)	10 (25)	9 (22.5)

the calcium hydroxide group (12 vs 9 of 18 teeth, respectively). Secondary dentin with orderly arranged dentinal tubules was found in both teeth of the negative control group, whereas no dentin bridge formation was found in one tooth and incomplete dentin bridge with disorganized tubules was found in the other tooth of the positive control group (Table 2).

With respect to the type and extent of pulp inflammation, most specimens in the Thai propolis group (15 of 17 teeth; Figure 3A) and in the calcium hydroxide group (16 of 18 teeth; Figure 3B) exhibited no pulp inflammation with a slight increase in hyperemic blood vessels. However, chronic inflammation restricted to the area next to the newly formed dentin bridge was still observed in 2 teeth of the Thai propolis group and in 2 teeth of the calcium hydroxide group. There was no pulp tissue present in the paraffin block in one tooth of the Thai propolis group and that specimen was excluded from histologic evaluations for the type and extent of pulp inflammation, necrosis, and calcification, but its dentin bridge formation could still be examined. As anticipated, chronic inflammation with an infiltration of macrophages, lymphocytes, and plasma cells (Figure 3C) was detected in both teeth of the positive

control group, whereas there was no pulp inflammation in the negative control group. The percentage of teeth with an increase in the number of hyperemic blood vessels ($\geq$4), when compared to that found in the negative control group (0-3 blood vessels), was lower in the Thai propolis group than in the calcium hydroxide group (2.56 vs 7.69, respectively). Nonetheless, by the Wilcoxon signed rank test, the median numbers of hyperemic blood vessels between the Thai propolis group and the calcium hydroxide group were not significantly different ($P = .056$; Figure 4). As expected, both teeth in the positive control group exhibited an obvious increase in hyperemia (5-6 hyperemic blood vessels).

With regard to other histologic features of the pulp, dental pulp stone was detected in 1 of 18 teeth in the calcium hydroxide group (Figure 5A), whereas no mineralization was observed in the pulp of the Thai propolis group and the negative control group. Note that diffuse mineralization was detected in 1 of 2 teeth in the positive control group (Figure 5B). Partial pulp necrosis beneath the pulp capping materials was found in one tooth of either the Thai propolis group (Figure 5C) or the calcium hydroxide group (Figure 5D), whereas partial to total necrosis was found in both teeth of the
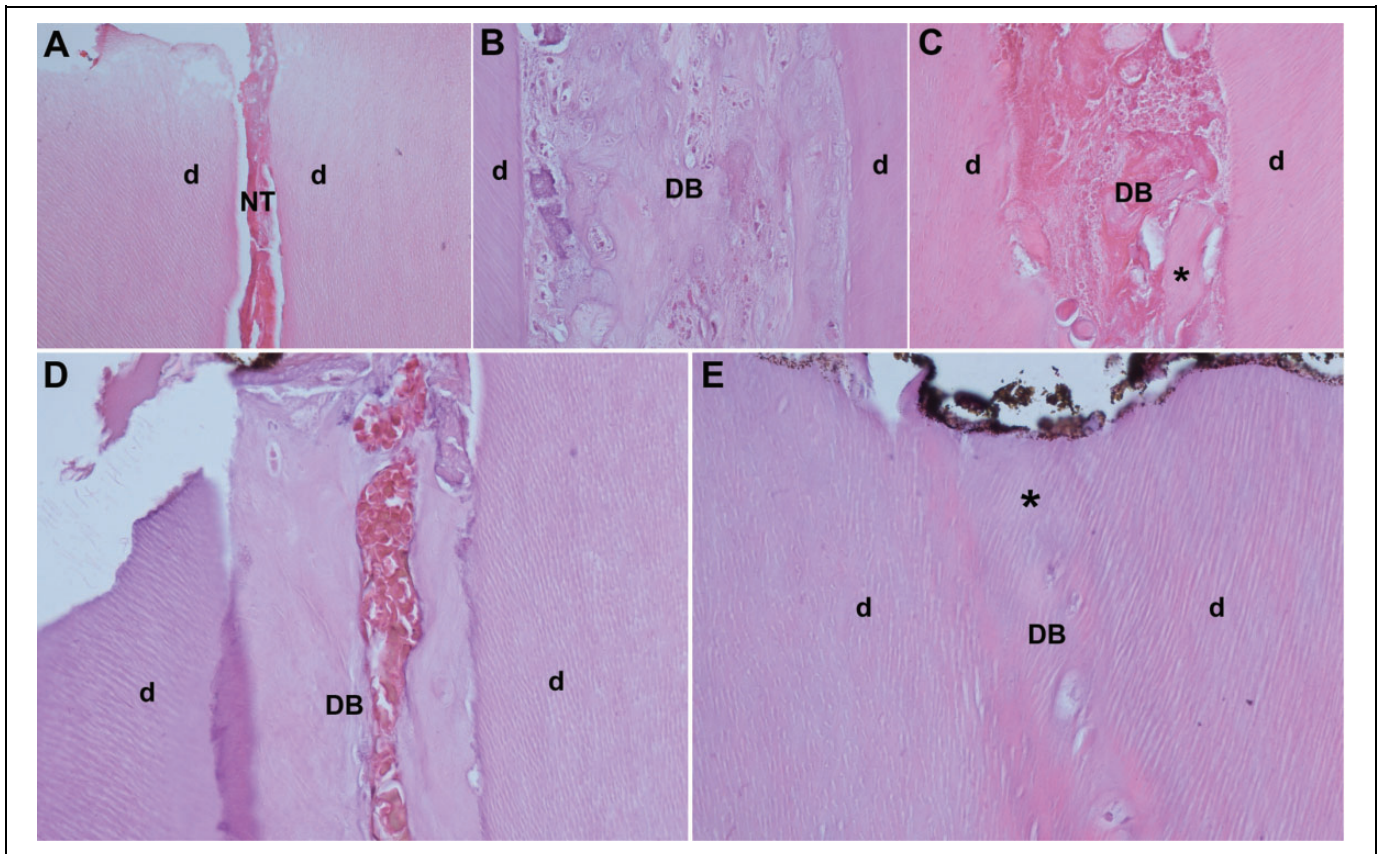
Figure 2. Five patterns of reparative dentin according to the continuity and morphology of dentinal tubules under ×400 magnification power. (A) No dentin bridge. (B) Incomplete and disorganized tubules. (C) Incomplete but orderly arranged tubules. (D) Complete but disorganized tubules. (E) Complete and orderly arranged tubules. DB indicates dentin bridge; d, dentin; NT, necrotic tissue; *, orderly arranged dentinal tubules.
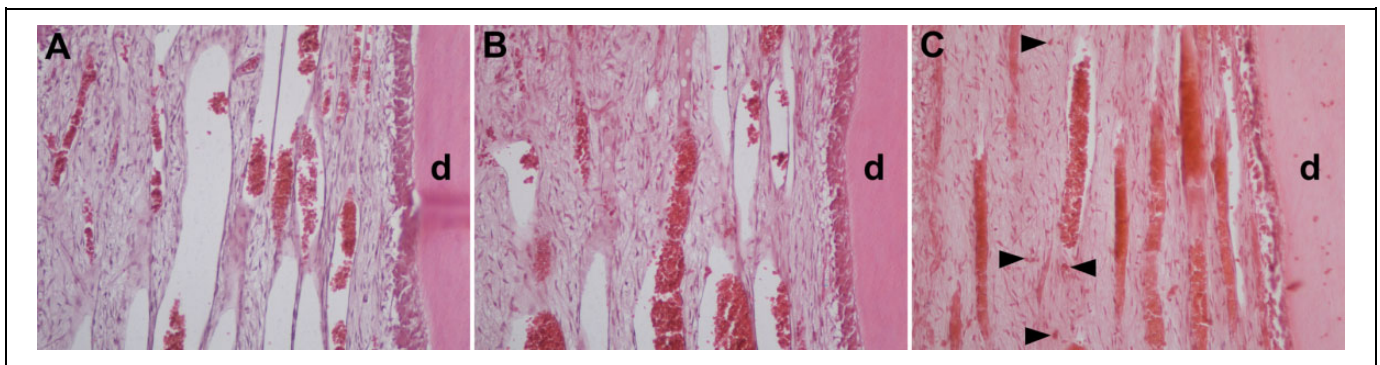

Figure 3. Representative hematoxylin and eosin staining sections of pulp tissues in the Thai propolis group (A), the calcium hydroxide group (B), and the positive control group (C) under ×200 magnification power. Note no chronic inflammation with a slight increase in hyperemic blood vessels was found in (A) and (B), while an infiltration of macrophages, lymphocytes, and plasma cells was observed in C (arrowheads). d indicates dentin.

positive control group (Figure 2A). No pulp necrosis was found in the negative control group.

Next, the proportions of pulpal wound healing were compared between the Thai propolis group and the calcium hydroxide group, based on moderate (grade II) and good (grade III) criteria that show signs of pulpal wound healing in all histologic features (Table 1). By the McNemar test, it was demonstrated that the proportions of the continuity and morphology of dentin bridge formation, the type and extent of pulp inflammation, and pulp necrosis between the 2 groups were not significantly different, while the P value for mineralization in pulp could not be computed due to identical proportions between the 2 groups (Table 3).
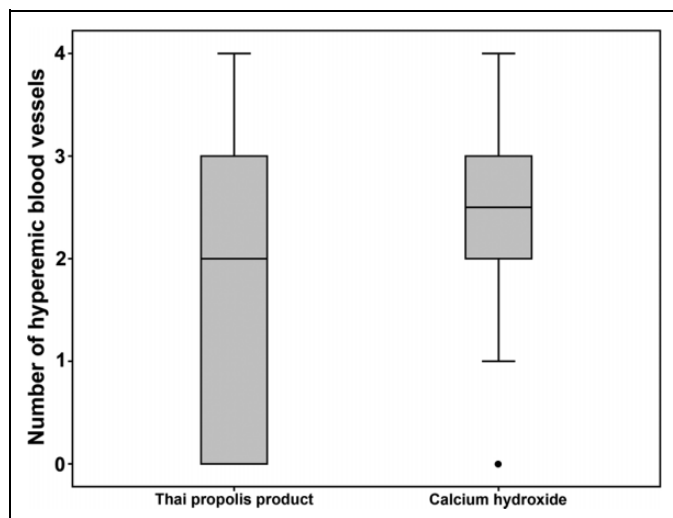
Figure 4. A box plot graph shows the distribution of the number of hyperemic blood vessels and compares their quantities between the Thai propolis group and the calcium hydroxide group. No significant difference was found between the 2 groups. The horizontal lines in each box plot represent values at the 25th, 50th, and 75th percentiles and a black circle indicates an outlier.
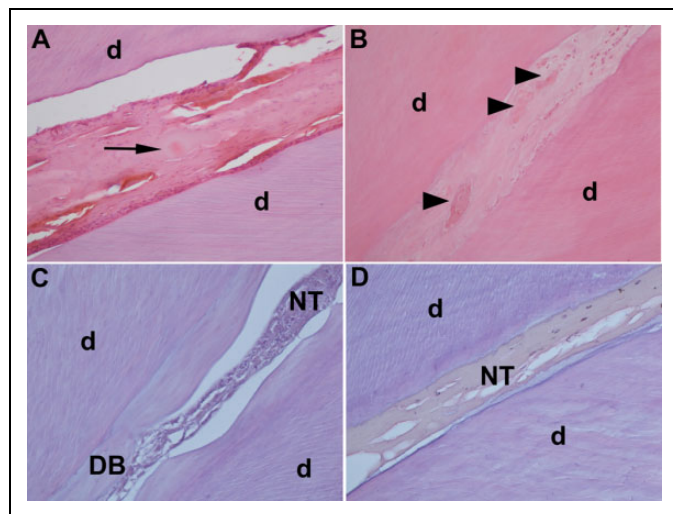

Figure 5. Hematoxylin and eosin staining sections of pulp tissues from the calcium hydroxide group (A and D), the positive control group (B), and the Thai propolis group (C) under $\times 200$ (for A and B) and $\times 400$ magnification (for C and D). An arrow in (A) indicates a dental pulp stone. Arrowheads in (B) show diffuse mineralization. d indicates dentin; DB, dentin bridge; NT, necrotic tissue.

Discussion

In this study, formation of reparative dentin with distinct patterns was found in all specimens from New Zealand white rabbits' teeth that were capped with the Thai propolis product and calcium hydroxide. Dentinal tubules of the dentin bridge were more orderly arranged in the propolis group than in the calcium hydroxide group, consistent with a previous finding in human premolars.[12] Furthermore, the propolis product was

Table 3. The Proportions of Pulpal Wound Healing in the Thai Propolis Group Compared to Those in the Calcium Hydroxide Group.

| | | Thai Propolis Group | | | |
| | | Grade (%) | | | |
		Moderate	Good	Total	P Value
Continuity					
Grade (%)	Moderate	1 (33.3)	2 (66.7)	3 (100)	.453
	Good	5 (33.3)	10 (66.7)	15 (100)	
Morphology					
Grade (%)	Moderate	3 (33.3)	6 (66.7)	9 (100)	.508
	Good	3 (33.3)	6 (66.7)	9 (100)	
Type[a]					
Grade (%)	Moderate	1 (50)	1 (50)	2 (100)	1.000
	Good	1 (6.7)	14 (93.3)	15 (100)	
Extent[a]					
Grade (%)	Moderate	1 (50)	1 (50)	2 (100)	1.000
	Good	1 (6.7)	14 (93.3)	15 (100)	
Calcification[a]					
Grade (%)	Moderate	0 (0)	1 (100)	1 (100)	-
	Good	0 (0)	16 (100)	16 (100)	
Necrosis[a]					
Grade (%)	Moderate	1 (100)	0 (0)	1 (100)	1.000
	Good	0 (0)	16 (100)	16 (100)	

[a]The pulp tissue in one specimen of the Thai propolis group accidentally dislodged from the paraffin block, so the type and extent of pulp inflammation, pulp necrosis, and calcification could not be evaluated. However, the continuity and morphology of dentin bridge formation could still be evaluated in that specimen.

shown to promote dental pulp wound healing comparable to that of calcium hydroxide, as determined by several aspects of histologic evaluations, including the type and extent of pulp inflammation and other histologic features, including mineralization and necrosis. The numbers of hyperemic blood vessels between the propolis and the calcium hydroxide groups were not statistically significantly different ($P = .056$). Several histologic features found in the calcium hydroxide group, such as incomplete dentin bridge, partial pulp necrosis, dental pulp stone, and mild chronic inflammation with a slight increase in the number of hyperemic blood vessels,[1-3] are in line with those reported in 2 previous studies.[20,21] All of these histologic findings have suggested that the Thai propolis product possesses biological properties involving reparative dentin formation, dental pulp regeneration, and anti-inflammatory activity similar to those of propolis extracts from other regions,[11-14] and it can thus have a potential to be commercially developed. In addition, these in vivo results correspond with our in vitro study[22] demonstrated mild pulp inflammation and fiber formation beneath an exposure site of the whole human tooth culture model after an application of the Thai propolis product.

The concentration of Thai propolis extract at 90 mg/mL (2-fold of minimum bactericidal concentration which planned for pharmaceutical preparation) was found not to be toxic to cultured human dental pulp cells in vitro.[18] Consequently, partial pulp necrosis was observed in only 1 of 17 teeth in the Thai propolis group. Mild pulp inflammation with an infiltration of

macrophages, lymphocytes, and plasma cells, observed in a few teeth of the Thai propolis and calcium hydroxide groups similar to that in the negative control, is consistent with minimal pulp inflammation in pigs' anterior teeth capped with propolis extract.[14] This low degree of inflammation may be due to anti-inflammatory constituents present in the propolis extract, such as flavonoids, caffeic acid, and caffeic phenethyl ester, which can inhibit local immune responses.[23] Besides dentin bridge formation and pulp inflammation, other pulpal reactions to external injuries from drilling, mechanical pulp exposure, and pulp capping materials can be displayed by dense fibrous encapsulation and diffuse mineralization seen in the positive control (Figure 5B) and dental pulp stone in the calcium hydroxide group (Figure 5A).

The reasons that rabbits, particularly a New Zealand white species, were used in this study are because of their short life span,[24] their larger tooth size than that of other rodents' teeth, which is suitable for restorative procedures, and their similar tooth structure and jaw to human teeth.[25] In addition, several teeth can be selected for any experiment in one rabbit so the number of animals used in one study is reduced. Rabbits have been used in dental research, especially for some studies testing effects of different pulp capping materials on wound healing promotion of the pulp.[26-27] In those studies, several types of lining or pulp capping materials were tested for their promotion of dental pulp wound healing; however, to the best of our knowledge, none of these studies have ever tested the enhancing effect of propolis on pulp wound healing. A 2-week period for testing the efficacy of pulp capping materials in this study was chosen because of rapid formation of secondary and tertiary dentin in rabbits, possibly due to open-apex tooth roots and continuous tooth eruption throughout their life.[26]

In this study, demineralization using 10% nitric acid for 3 days was performed based on a protocol derived from 2 previous studies,[28,29] whose results demonstrate quick and efficient demineralization of calcified tissues, while preserving the integrity of pulp tissue. Since this animal experiment was designed to histologically test only the biological property of Thai propolis product in promotion of pulp wound healing, future studies are required to further investigate the sealing ability, solubility of the product, porosity of newly formed dentin bridge, and the quantities of released active chemicals from the product. Moreover, it is necessary to test this product in human teeth because differences in pulp tissue to repair itself between an open-apex root in the rabbit's tooth and a closed-apex root in the human tooth are likely to occur.

Conclusions

Thai propolis product may be used as a pulp-capping agent since it can promote wound healing responses in dental pulp comparable to those of calcium hydroxide paste.

Authors' Note

All authors have read, edited, and approved this manuscript.

## Materials

a. Dycal; L. D. Caulk, Dentsply Int. Inc, Milford, Delaware.
b. MRC, Ltd, Holon, Israel.
c. Sigma-Aldrich, St Louis, Missouri.
d. Eyela; Tokyo Rikakikai, Tokyo, Japan.
e. Alpha 2-4 LD plus; Martin Christ Gefriertrocknungsanlagen GmbH, Osterode am Harz, Germany.
f. Carbopol 934P, Lot No. 0101362222; Lubrizol Advanced Materials, The Lubrizol Corporation, Wickliffe, Ohio.
g. Harwell Dosimeters, Ltd, Oxfordshire, United Kingdom.
h. HiMedia Laboratories, Ltd, Mumbai, India.
i. The PS: Power and Sample Size Calculation version 3.1.2, 2014, licensed under the Creative Commons Attribution-Noncommercial-No Derivative 3.0, United States License, by William D. Dupont and Walter D. Plummer Jr, Department of Biostatistics, Vanderbilt University, Nashville, Tennessee.
j. Bezter Xylazine, L.B.S. Laboratory, Ltd, Bangkok, Thailand.
k. Ketamine-Hameln; Hameln Pharmaceuticals GmbH, Langes Feld, Hameln, Germany.
l. Meisinger; Hager & Meisinger GmbH, Neuss, Germany.
m. Vitrebond; 3M ESPE, St Paul, Minnesota.
n. Filtex Z350XT; 3M ESPE, St Paul, Minnesota.
o. Carprofen; Zoetis, Parsippany-Troy Hills, New Jersey.
p. Nembutal; Ceva Sante Animale, Z.I. La Ballastiere, Libourne, France.
q. Microscope; Eclipse E200, Nikon, Tokyo, Japan.
r. NIS Elements F3.2 software.
s. University of Texas Health Science Center, San Antonio, Texas.

References

1. Hilton TJ. Keys to clinical success with pulp capping: a review of the literature. *Oper Dent*. 2009;34(5):615-625.
2. Ward J. Vital pulp therapy in cariously exposed permanent teeth and its limitations. *Aus Endod J*. 2002;28(1):29-37.
3. Foreman PC, Barnes IE. Review of calcium hydroxide. *Int Endod J*. 1990;23(6):283-297.
4. Mass E, Zilberman U. Long-term radiologic pulp evaluation after partial pulpotomy in young permanent molars. *Quintessence Int*. 2011;42(7):547-554.
5. Aguilar P, Linsuwanont P. Vital pulp therapy in vital permanent teeth with cariously exposed pulp: a systematic review. *J Endod*. 2011;37(5):581-587.

6. Chailertvanitkul P, Paphangkorakit J, Sooksantisakoonchai N, et al. Randomized control trial comparing calcium hydroxide and mineral trioxide aggregate for partial pulpotomies in cariously exposed pulps of permanent molars. *Int Endod J*. 2014;47(9):835-842.

7. Cox CF, Sübay RK, Ostro E, Suzuki S, Suzuki SH. Tunnel defects in dentine bridges: their formation following direct pulp capping. *Oper Dent*. 1996;21(1):4-11.

8. Parirokh M, Torabinejad M. Mineral trioxide aggregate: a comprehensive literature review—part I: chemical, physical, and antibacterial properties. *J Endod*. 2010;36(1):16-27.

9. Torabinejad M, Parirokh M. Mineral trioxide aggregate: a comprehensive literature review—part II: leakage and biocompatibility investigations. *J Endod*. 2010;36(2):190-202.

10. Parirokh M, Torabinejad M. Mineral trioxide aggregate: a comprehensive literature review—part III: clinical applications, drawbacks, and mechanism of action. *J Endod*. 2010; 36(3):400-413.

11. Sabir A, Tabbu CR, Agustiono P, Sosroseno W. Histologic analysis of rat dental pulp tissue capped with propolis. *J Oral Sci*. 2005;47(3):135-138.

12. Parolia A, Kundabala M, Rao NN, et al. A comparative histological analysis of human pulp following direct pulp capping with Propolis, mineral trioxide aggregate and Dycal. *Aus Dent J*. 2010; 55(1):59-64.

13. Ahangari Z, Naseri M, Jalili M, Mansouri Y, Mashhadiabbas F, Torkaman A. Effect of propolis on dentine regeneration and the potential role of dental pulp stem cell in Guinea pigs. *Cell J*. 2012; 13(4):223-228.

14. Ozório JE, Carvalho LF, de Oliveira DA, de Sousa-Neto MD, Perez DE. Standardized propolis extract and calcium hydroxide as pulpotomy agents in primary pig teeth. *J Dent Child*. 2012; 79(2):53-58.

15. Marcucci MC. Propolis: chemical composition, biological properties and therapeutic activity. *Apidologie*. 1995;26(2): 83-99.

16. Banskota AH, Tezuka Y, Kadota S. Recent progress in pharmacological research of propolis. *Phytother Res*. 2001;15(7): 561-571.

17. Prueksakorn A, Puasiri S, Ruangsri S, et al. The preservative effect of Thai propolis extract on the viability of human periodontal ligament cells. *Dent Traumatol*. 2016;32(6):495-501.

18. Chailertvanitkul P, Namsirikul T, Damrongrungruang T, Peerapattana J. Phenolic and flavonoids contents and antibacterial activity of ethanolic extract of propolis. *lsan J Pharm Sci*. 2017; 13(3):59-67.

19. Institute of Laboratory Animal Research, Division on Earth and Life Science, eighth edition, National Research Council of the National Academies. *National Academy of Science*. Washington, DC: The National Academies Press; 2011.

20. Aeinehchi M, Eslami B, Ghanbariha M, Saffar AS. Mineral trioxide aggregate (MTA) and calcium hydroxide as pulp-capping agents in human teeth: a preliminary report. *Int Endod J*. 2003; 36(3):225-231.

21. Asgary S, Eghbal MJ, Parirokh M, Ghanavati F, Rahimi H. A comparative study of histologic response to different pulp capping materials and a novel endodontic cement. *Oral Surg Oral Med Oral Pathol Oral Radiol Endod*. 2008;106(4):609-614.

22. Rungcharassaeng N, Klanrit P, Chailertvanitkul P. Wound healing between Thai propolis product and calcium hydroxide in direct pulp capping using a whole tooth culture model. *Khon Kaen Dent J*. Accepted for Publication.

23. Parolia A, Thomas MS, Kundabala M, Mohan M. Propolis and its potential uses in oral health. *Int J Med Sci*. 2010;2(7):210-215.

24. Stübinger S, Dard M. The rabbit as experimental model for research in implant dentistry and related tissue regeneration. *J Invest Surg*. 2013;26(5):266-282.

25. Mapara M, Thomas BS, Bhat KM. Rabbit as an animal model for experimental research. *Dent Res J*. 2012;9(1):111-118.

26. Aljandan B, AlHassan H, Saghah A, Rasheed M, Ali AA. The effectiveness of using different pulp-capping agents on the healing response of the pulp. *Indian J Dent Res*. 2012;23(5): 633-637.

27. Davidović L, Ćuk M, Sandić MŽ, Grga D, Živković S. The influence of liners on the pulp inflammation. *Srp Arh Celok Lek*. 2015; 143(5-6):261-266.

28. Prasad P, Donoghue M. A comparative study of various decalcification techniques. *Indian J Dent Res*. 2013;24(3):302-308.

29. Gupta S, Jawanda MK, Sm M, Bharti A. Qualitative histological evaluation of hard and soft tissue components of human permanent teeth using various decalcifying agents—a comparative study. *J Clin Diag Res*. 2014;8(9):ZC69-ZC72.
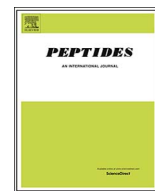
The antimicrobial peptide, human β-defensin-1, potentiates *in vitro* osteoclastogenesis via activation of the p44/42 mitogen-activated protein kinases

Anupong Makeudom[a,b], Chayarop Supanchart[c], Pattanin Montreekachon[d], Sakornrat Khongkhunthian[d], Thanapat Sastraruji[a], Julaporn Krisanaprakornkit[a], Suttichai Krisanaprakornkit[a,*]

[a] *Center of Excellence in Oral and Maxillofacial Biology, Faculty of Dentistry, Chiang Mai University, Chiang Mai, Thailand*
[b] *Department of Medical Technology, Faculty of Associated Medical Sciences, Chiang Mai University, Chiang Mai, Thailand*
[c] *Department of Oral and Maxillofacial Surgery, Faculty of Dentistry, Chiang Mai University, Chiang Mai, Thailand*
[d] *Department of Restorative Dentistry and Periodontology, Faculty of Dentistry, Chiang Mai University, Chiang Mai, Thailand*

ARTICLE INFO

ABSTRACT

Previous studies have demonstrated increased expression and raised levels of human β-defensin (hBD)-1 in gingival tissue and crevicular fluid of patients with chronic periodontitis and peri-implantitis, oral bone-resorbing diseases caused by enhanced osteoclastogenesis. Therefore, we aimed to investigate the effect of hBD-1 on osteoclast formation and function and to elucidate the involved signaling pathway *in vitro*. Human peripheral blood mononuclear cells (PBMCs) were first incubated with various doses of hBD-1 and cell viability was assayed by MTT. PBMCs were treated with macrophage-colony stimulating factor and receptor activator of nuclear factor kappa-B ligand (RANKL) in the presence or absence of non-toxic doses of hBD-1. *In vitro* osteoclastogenesis was analyzed by tartrate-resistant acid phosphatase (TRAP) staining, osteoclast-specific gene expression, and a resorption pit assay. Involvement of mitogen-activated protein kinases (MAPKs) was studied by immunoblotting and specific MAPK inhibitors. HBD-1 potentiated induction of *in vitro* osteoclastogenesis by RANKL, as shown by significantly increased number of TRAP-positive multinuclear cells and resorption areas on the dentin slices, and further up-regulated expressions of osteoclast-specific genes compared to those by RANKL treatment ($p < 0.05$). However, hBD-1 treatment without RANKL failed to induce formation of osteoclast-like cells. A significant and further increase in transient phosphorylation of the p44/42 MAPKs was demonstrated by hBD-1 co-treatment ($p < 0.05$), consistent with the inhibitory effect by pretreatment with U0126 or PD98059 on hBD-1-enhanced osteoclastogenesis. Collectively, hBD-1 potentiates the induction of *in vitro* osteoclastogenesis by RANKL via enhanced phosphorylation of the p44/42 MAPKs.

1. Introduction

The family of human defensins, small β-sheet cationic antimicrobial peptides that contain an amphipathic structure and three characteristic disulfide bonds, consists of α- and β-defensins [1]. β-defensins can exert various biological effects, including antimicrobial and pro-inflammatory activities, immune modulation, angiogenesis, wound healing, and chemotactic movement [2]. In the oral cavity, three β-defensin peptides, including human β-defensin (hBD)-1, hBD-2 and hBD-3, are expressed in oral epithelial cells [3] with distinct patterns of expression within stratified squamous gingival epithelium [4,5]. In

chronic periodontitis, hBD-1 mRNA and protein expression was increased in inflamed gingival biopsies compared to those from normal non-inflamed tissues [6,7], consistent with the finding from an *in vitro* study that demonstrated up-regulated expression of hBD-1 in gingival epithelial cells upon challenges with some specific periodontal pathogens [8]. Similarly, hBD-1 levels were significantly elevated in gingival crevicular fluid (GCF), serum exudate from blood vessels within gingival tissue, of patients with chronic periodontitis with or without type 2 diabetes mellitus [9], in peri-implant crevicular fluid of patients with peri-implantitis [10] and in serum of patients with systemic lupus erythematosus [11] and with liver cirrhosis [12]. Taken together, all of

these findings have suggested that enhanced hBD-1 expression and levels are likely to involve with inflammation-related soft and hard tissue destruction, especially alveolar bone loss in periodontitis and peri-implantitis resulting from enhanced formation and function of osteoclasts.

Osteoclasts are multinucleated giant cells derived from hematopoietic cells of the monocyte/macrophage lineage upon stimulation with macrophage-colony stimulating factor (M-CSF) and receptor activator of nuclear factor kappa-B ligand (RANKL) [13]. The characteristics of mature osteoclasts include degradation capability of mineralized tissues and expression of osteoclast-specific genes, such as tartrate-resistant acid phosphatase (TRAP), cathepsin K (CTSK), chloride voltage-gated channel 7 (CLCN7), calcitonin receptor (C-ALCR). Several cell signaling molecules and pathways, such as TNF receptor associated factor 6 (TRAF6), mitogen-activated protein kinases (MAPKs), calcium, and transcription factors, such as nuclear factor-kappa B (NF-κB) and nuclear factor of activated T cell 2 (NFAT2), play a major role in osteoclastogenesis [14]. In particular, activation of three MAPKs by phosphorylation has been demonstrated during osteoclast formation upon M-CSF and RANKL stimulation in bone marrow-derived murine mononuclear cells [15]. Moreover, activation of the MAPKs was shown by treatment with hBDs to induce interleukin-18 and interleukin-31 secretion from human keratinocytes and mast cells, respectively [16,17]. Therefore, it was hypothesized in this study that hBD-1 might promote *in vitro* osteoclastogenesis via activation of these MAPKs. The objectives of this study were to examine effect of hBD-1 on osteoclastogenesis and to determine involvement of MAPKs in mediating this effect on osteoclast-like cell formation *in vitro*.

2. Materials and Methods

2.1. Reagents and antibodies

Chemically-synthesized hBD-1 peptide was purchased from Peptide Institute, Inc. (Osaka, Japan). Recombinant human M-CSF and RANKL were bought from R & D Systems, Inc. (Minneapolis, MN, USA). U0126, a highly selective inhibitor of both MAPK/ERK kinase (MEK) 1 and MEK2, and its inactive analog (U0124) were bought from Calbiochem® Inhibitors (Merck Millipore, Temecula, CA, USA), and PD98059, a potent and selective cell-permeable MEK inhibitor, was from InvivoGen (San Diego, CA, USA). The inhibitors and the inactive analog were dissolved in dimethyl sulfoxide (DMSO; Sigma-Aldrich, Co., St. Louis, MO, USA), whose concentration was finally equated to 0.1% v/v. Primary antibodies against NFAT2, MAPKs and the phosphorylated MAPKs were obtained from Abcam (Cambridge, UK) and Cells Signaling Technology, Inc. (Danvers, MA, USA), respectively.

2.2. Cell isolation

A 20-ml quantity of heparinized whole blood samples was obtained from healthy donors with informed consent. The research protocol was approved by the Human Experimentation Committee, Chiang Mai University (#3/2559). Peripheral blood mononuclear cells (PBMCs) as osteoclast progenitors were obtained from the buffy coat by density gradient centrifugation using Ficoll-Paque™ (GE Healthcare Bio-Sciences, Uppsala, Sweden). To obtain enriched monocytes in a resorption pit assay, whole blood was incubated with antibody cocktails (RosetteSep™, STEMCELL Technologies, Vancouver, BC, Canada), which crosslink the unwanted cells and red blood cells before density gradient centrifugation. PBMCs and enriched monocytes were cultured in complete medium, containing αMEM (Lonza Walkersville, Inc., Walkersville, MD, USA), supplemented with 10% fetal bovine serum (GIBCO®, Thermo Fisher Scientific, Waltham, MA, USA), 2 mM L-glutamine (GIBCO®) and 1% penicillin/streptomycin (Invitrogen, Thermo Fisher Scientific). Cells at the density of 5×10^5 cells per cm^2 were seeded in 96- or 6-well plates (Nunc™, Thermo Fisher Scientific), or Nunc™ Lab-Tek™ II Chamber Slide™ (Thermo Fisher Scientific) in

complete medium with 25 ng/ml of M-CSF overnight and non-adherent cells were discarded on the following day. Thereafter, complete medium with M-CSF in the presence or absence of 30 ng/ml of RANKL or various doses of hBD-1 was added and replaced every other day.

2.3. MTT assay

Toxicity of hBD-1 on PBMCs was measured by an MTT assay. Cells seeded in 96-well plates were treated with 25 ng/ml of M-CSF and various doses (1–12 μM) of hBD-1 for 48 h. Subsequently, a 20-μl quantity of MTT dye solution (5 mg/ml in PBS; Sigma-Aldrich) was added for 4 h, followed by 200 μl of DMSO to solubilize formazan crystals. Absorbance values at the 540-nm wavelength were measured by a microplate reader (Sunrise, Tecan, Grödlg, Austria) and subtracted with those of the reference wavelength at 690 nm. The values of hBD-1-treated samples were adjusted for relative ratios of cell viability to a control untreated sample, set to 1.

2.4. In vitro osteoclastogenesis and quantification

Effect of hBD-1 on osteoclastogenesis was determined by incubating PBMCs in 96-well culture plates in the presence or absence of three non-toxic doses (0.2, 1, 5 μM) of hBD-1 during osteoclast induction by 25 ng/ml of M-CSF and 30 ng/ml of RANKL. PBMCs incubated with M-CSF alone were a negative control. On day 7, after cell fixation by 4% paraformaldehyde (Sigma-Aldrich) in PBS, cells were stained with 1.5 mM Fast Red Violet LB salt (Sigma-Aldrich). TRAP-positive multinuclear cells, containing at least three nuclei, were manually counted using Image-J software (National Institutes of Health, Bethesda, MD, USA).

To determine MAPK involvement in mediating hBD-1 effect, PBMCs in 96-well culture plates were pretreated with 20 μM of U0126 or U0124, 100 μM of PD98059 or 0.1% (v/v) DMSO as a solvent control for 30 min. After that, cells were washed with sterile PBS twice and complete medium containing M-CSF and RANKL with or without 5 μM of hBD-1 was added. Both pretreatment and medium replacement steps were repeated every other day. On day 7, TRAP staining was performed as aforementioned to assay *in vitro* osteoclastogenesis.

To determine F-actin ring formation in multinuclear cells, PBMCs seeded in Chamber Slide™ and induced by M-CSF and RANKL were treated with 5 μM of hBD-1 or left untreated for 7 days and were then stained with 20 nM Alexa Fluor® 488-conjugated phalloidin (Invitrogen) and 1 μM DAPI (Biotium, Inc., Hayward, CA, USA). Subsequently, the slides were mounted in fluorescence mounting medium (Fluoromount G, Electron Microscopy Sciences, Hatfield, PA, USA), and fluorescence images were visualized and captured by a fluorescence microscope (Zeiss AxioImager II, Göttingen, Germany).

2.5. RNA extraction and real-time RT-PCR

Total RNA was extracted from PBMCs cultured in 6-well plates in the presence of M-CSF and RANKL with or without 1 and 5 μM of hBD-1 co-treatment for 5 days using the RNAspin Mini RNA isolation kit (GE Healthcare Bio-Sciences). Three hundred nanograms of total RNA were converted into cDNA by using the Revert Aid H Minus First-Strand cDNA synthesis kit (Thermo Fisher Scientific). A real-time PCR was conducted with the SensiFAST™ SYBR® No-ROX reagent (Bioline, Taunton, MA, USA) in the LightCycler® 480 instrument II (Roche Molecular Biochemicals, Rotkreuz, Switzerland) with specific primer pairs for osteoclast genes, including *NFAT2*, *CTSK*, *receptor activator of nuclear factor kappa-B* (*RANK*), *CALCR* [18], and *CLCN7*: sense 5′-AC-TGTCCTTCTCCCTGTTGC-3′ and antisense 5′-TGAGGAAGCACTTGAT-CTGG-3′. Expression of these genes was normalized by that of *glyceraldehyde 3-phosphate dehydrogenase* (*GAPDH*), a housekeeping gene control [18], as relative C_t (ΔC_t) with aid of a calculation algorithm (LightCycler® 480 Software version 1.5, Roche Molecular
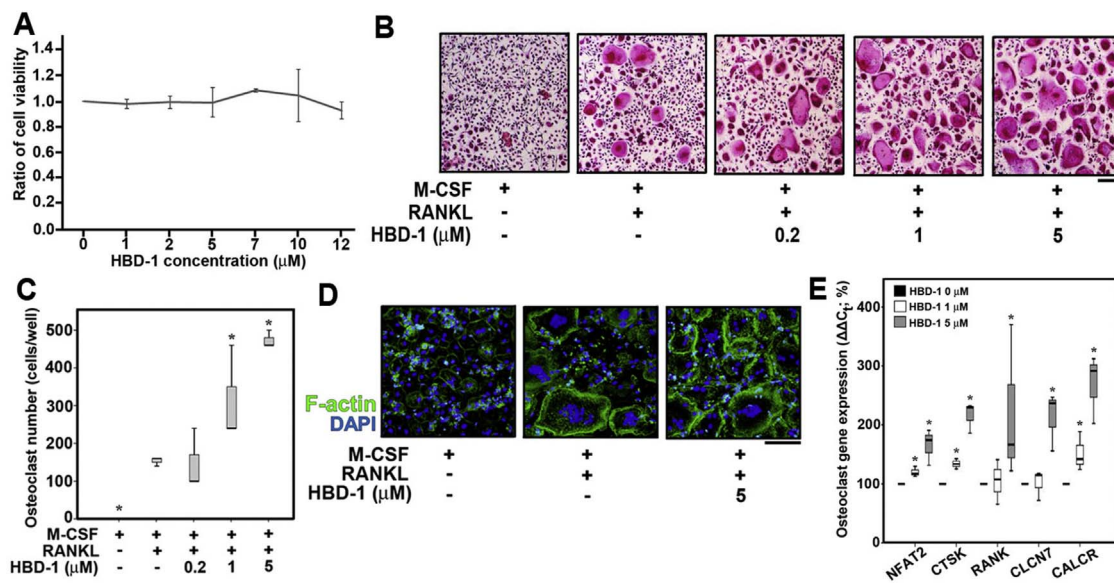
Fig. 1. HBD-1 enhances *in vitro* formation of osteoclast-like cells. (A) Cytotoxicity of hBD-1 was tested by an MTT assay. Peripheral blood mononuclear cells (PBMCs) were incubated with M-CSF and indicated doses of hBD-1 for 48 h. A linear graph demonstrates the ratios of cell viability in hBD-1-treated samples relative to the untreated sample, whose ratio was set to 1. (B) *In vitro* generation of human osteoclast-like TRAP-positive multinuclear cells from viable PBMCs induced by M-CSF and RANKL with (+) or without (−) indicated doses of hBD-1 for 7 days. Bar = 100 μm. (C) A box plot demonstrates the number of TRAP-positive multinuclear cells in the samples treated with M-CSF alone, M-CSF and RANKL, or M-CSF and RANKL in the presence of indicated doses of hBD-1 from blood of four different donors ($n = 4$). * = significant differences at $p < 0.05$ compared to the M-CSF- and RANKL-treatment sample. (D) Immunofluorescence images of F-actin rings (green) in PBMCs cultured with M-CSF and with (+) or without (−) RANKL and 5 μM of hBD-1 for 7 days. Nuclei were localized by DAPI staining (blue). Bar = 100 μm. (E) A box plot shows the percentages of osteoclast gene expression, including *NFAT2*, *CTSK*, *RANK*, *CLCN7* and *CALCR*, in hBD-1-treated samples (white and gray boxes for 1 and 5 μM of hBD-1, respectively) relative to those of the samples treated with RANKL alone (black box), set to 100% (*, $p < 0.05$).These data were derived from four separate experiments using blood of four different donors ($n = 4$).

Biochemicals). The relative gene expression ($\Delta\Delta C_t$) was obtained by comparing ΔC_t of hBD-1-treated samples with that of the untreated sample set to 100%.

2.6. Resorption pit assay

A resorption pit assay was performed to determine function of osteoclast-like cells by incubating enriched monocytes on dentin slices placed in 96-well culture plates in the presence of M-CSF and RANKL with or without 5 μM of hBD-1 for 14 days as previously described [18]. Indian ink was used to stain the resorption pits and grooves for 30 sec and excessive dye was wiped out. The resorption areas were captured under bright field microscopy and calculated as the percentages of stained areas against the total area of dentin slices by Image-J software.

2.7. Nuclear protein extraction and Western blot hybridization

To study involvement of NFAT2, PBMCs cultured in 6-well plates were treated with M-CSF with or without RANKL in the presence or absence of 5 μM of hBD-1 for four days. Thereafter, their nuclear and cytosolic proteins were extracted using an NE-PER® nuclear and cytoplasmic extraction kit (Pierce, Rockford, IL, USA) following the manufacturer's protocol. Briefly, PBMCs were lifted off by enzymatic digestion with trypsin-EDTA (Invitrogen), washed twice with PBS and lysed. The cytosolic and nuclear protein supernatants were sequentially collected by centrifugation at 19,000 g for 10 min at 4 °C. To study involvement of MAPKs, PBMCs were cultured as mentioned above for 5, 10, and 20 min. Total proteins were extracted from the cells using RIPA buffer [19] with Halt protease inhibitors (Thermo Fisher Scientific), 1 mM sodium orthovanadate and 50 mM sodium fluoride, as phosphatase inhibitors. A 10-μg quantity of nuclear protein and a 20-μg quantity of cytosolic or total protein were separated by 10% SDS-PAGE and transferred to nitrocellulose membranes. The membrane was blocked with 5% non-fat dry milk in 0.1% Tween-20 (Bio-Rad Laboratories, Hercules, CA, USA) in TBS, and incubated with anti-NFAT2, anti-JNK, anti-p38 MAPK, anti-p44/42 MAPK, anti-phospho-JNK, anti-

phospho-p38 MAPK (1:1000), or anti-phospho-p44/42 MAPK (1:2000) antibody at 4 °C overnight. The membrane was incubated with horseradish peroxidase-conjugated secondary antibody (1:2000) and reacted with LumiGLO Reserve® Chemiluminescent substrate (SeraCare Life Sciences, Gaithersburg, MD, USA). Immunoreactivity signals were captured by the ChemiDoc XRS instrument (Bio-Rad Laboratories). Band intensities of nuclear NFAT2 and phosphorylated MAPK were measured by Scion Image program (Scion Corporation, Frederick, MD, USA), normalized by those of cytosolic NFAT2 and total MAPK, respectively, in each sample, and reported as ratios against the ratio of sample treated with M-CSF alone set to 1.

2.8. Statistical analysis

Since all data were not normally distributed according to the test of normality by Shapiro-Wilk, box plots were used to quantitatively illustrate medians, 25th and 75th percentiles. The Kruskal–Wallis test was used to compare the medians among different groups, and the Mann–Whitney U test was used to compare the medians between each pair of groups with statistical significance levels at $p < 0.05$ by SPSS 17.0 software (SPSS, Inc., Chicago, IL, USA).

3. Results

3.1. HBD-1 potentiates induction of in vitro osteoclastogenesis by RANKL

Before examining effect of hBD-1 on osteoclast formation and function, toxicity of hBD-1 on PBMCs was investigated by an MTT assay. No significant difference in the ratios of cell viability was found between untreated cells and cells treated with any doses of hBD-1 from 1 to 12 μM for 48 h (Fig. 1A), indicating that the doses of hBD-1 up to 12 μM are not toxic to PBMCs. Subsequently, PBMCs were treated with three different non-toxic doses (0.2, 1, 5 μM) of hBD-1 during osteoclast induction by RANKL treatment for 7 days. HBD-1 treatment in the presence of RANKL further increased the number of TRAP-positive multinuclear cells in a dose-dependent manner when compared to

treatment with RANKL alone (Fig. 1B). Treatment with M-CSF alone as a negative control showed no TRAP-positive multinuclear cells (Fig. 1B). Note a number of large TRAP-positive cells by combined treatment between RANKL and 5 μM of hBD-1 in comparison with fewer TRAP-positive cells by treatment with RANKL alone (Fig. 1B). Quantitatively, the median number of osteoclast-like cells was significantly higher by combined treatment between RANKL and hBD-1 at 1 or 5 μM than that by RANKL treatment around 2–3 fold ($p < 0.05$; Fig. 1C). Consistently, the number of cells with an F-actin ring at their periphery was found more in the sample treated with both RANKL and hBD-1 than with RANKL alone (Fig. 1D). As expected, there was no F-actin ring formation in the sample treated with M-CSF alone (Fig. 1D). Moreover, the median percentages for expression of osteoclast genes, including *NFAT2, CTSK, RANK, CLCN7, CALCR*, were significantly higher in the samples treated with both RANKL and hBD-1 in a dose-dependent fashion than with RANKL alone ($p < 0.05$; Fig. 1E). Taken together, hBD-1 treatment potentiates induction of *in vitro* osteoclast formation by RANKL.

3.2. HBD-1 further enhances formation of resorption pits and grooves by RANKL in vitro

To determine effect of hBD-1 on osteoclast function, a resorption pit assay on dentin slices was performed in enriched monocytes cultured for 14 days. It was demonstrated that the stained areas, representing resorption pits and grooves, on the dentin slice were increased by combined treatment between RANKL and 5 μM of hBD-1 when compared to those by RANKL treatment (Fig. 2A). As anticipated, no stained area was found on the dentin slice by treatment with M-CSF alone (Fig. 2A). Quantitatively, the median percentage of resorption areas in the sample treated with both RANKL and hBD-1 was significantly higher than that with RANKL alone ($p < 0.05$; Fig. 2B), confirming that hBD-1 enhances osteoclast formation and function by RANKL *in vitro*.

3.3. No inductive effect on in vitro osteoclastogenesis by treatment with hBD-1 alone

To address a question whether or not treatment with hBD-1 alone was able to induce *in vitro* osteoclast formation, PBMCs were treated with hBD-1 at indicated doses in the presence or absence of RANKL for 7 days. Treatment with any indicated doses of hBD-1 in the absence of RANKL failed to induce the number of TRAP-positive multinuclear cells (Fig. 3A and B), whereas combined treatment between any doses of hBD-1 and RANKL significantly increased the number of TRAP-positive multinuclear cells compared to treatment with M-CSF alone ($p < 0.05$; Fig. 3B). As with the results in Fig. 1C, combined treatment between RANKL and hBD-1 at 1 or 5 μM further enhanced osteoclast formation by significantly increasing the number of TRAP-positive multinuclear cells in a dose-dependent fashion compared to treatment with RANKL alone ($p < 0.05$; Fig. 3B). All of these results suggest the potentiation effect rather than the additive or synergistic effect of hBD-1 on induction of *in vitro* osteoclast formation by RANKL.
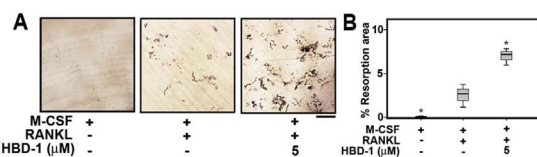

Fig. 2. HBD-1 increases *in vitro* function of osteoclast-like cells. (A) Representative images of dentin slices show resorption pits and grooves stained with Indian ink, formed by *in vitro* generated osteoclast-like cells for 14 days with (+) or without (−) 5 μM of hBD-1. Bar = 450 μm. (B) A box plot from four separate experiments using blood of four different donors ($n = 4$) shows the amounts of resorption areas as percentages of the stained areas against the total area of dentin slices from the conditions described in A. * = significant differences at $p < 0.05$ when compared to the M-CSF- and RANKL-treatment sample.
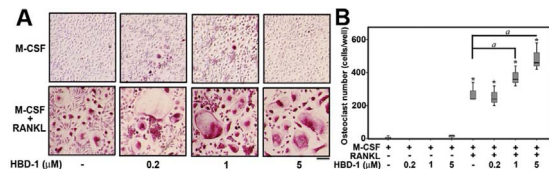

Fig. 3. HBD-1 has no inductive effect on *in vitro* osteoclastogenesis. (A) Representative TRAP-staining images from PBMCs cultured with or without RANKL in the presence or absence of indicated doses of hBD-1 for 7 days. Bar = 100 μm. (B) A box plot shows the number of TRAP-positive multinuclear cells from four independent experiments using blood of four different donors ($n = 4$) of the conditions described in A. * = significant differences at $p < 0.05$ when compared to the sample treated with M-CSF alone; a = significant differences at $p < 0.05$ when compared to the sample treated with M-CSF and RANKL.

3.4. The potentiation effect of hBD-1 on osteoclastogenesis is via phosphorylation of the p44/42 MAPKs

Because it has been previously shown that LL-37, a human antimicrobial peptide of the cathelicidin family, inhibited human osteoclastogenesis *in vitro* by blocking nuclear translocation of NFAT2 [18], the enhancing effect of hBD-1 on nuclear translocation of NFAT2 was first examined. Treatment with RANKL with or without hBD-1 significantly increased the ratio of nuclear/cytosolic NFAT2 ($p < 0.05$; Fig. 4A and B) compared to that of treatment with M-CSF alone, indicating RANKL treatment induces NFAT2 nuclear translocation. However, there was no difference in the ratio of nuclear/cytosolic NFAT2 between RANKL treatment and combination of RANKL and hBD-1 treatment, implying that the potentiation effect of hBD-1 on *in vitro* osteoclastogenesis is mediated by other signaling molecules.

Since activation of MAPKs by phosphorylation is implicated in osteoclastogenesis in bone marrow-derived mouse mononuclear cells and a mouse embryonic cell line [15,20], involvement of these MAPKs in mediating the potentiation effect of hBD-1 on *in vitro* human osteoclast formation was investigated. In general, a significant increase in transient phosphorylation at both 5-min and 10-min treatment periods of the p44/42 and the p54/46 MAPKs was shown by RANKL treatment with or without hBD-1 co-treatment compared to PBMCs treated with M-CSF alone ($p < 0.05$; Fig. 4C and D), whereas RANKL treatment in the presence or absence of hBD-1 co-treatment failed to significantly activate the p38 MAPK (Fig. 4C and D). Interestingly, a significant further increase in transient phosphorylation at a 5-min treatment period of only the p44/42 MAPKs was observed by combined treatment between RANKL and 5 μM of hBD-1 compared to treatment with RANKL alone ($p < 0.05$; Fig. 4C and D). These findings suggest that the potentiation effect of hBD-1 on *in vitro* human osteoclast formation is possibly mediated by activation of the p44/42 MAPKs.

To further verify involvement of the p44/42 MAPKs in mediating the potentiation effect of hBD-1 on human osteoclast formation, PBMCs were pretreated for 30 min with U0126 or PD98059, two specific MEK1/2 inhibitors that are upstream molecules of the p44/42 MAPKs, before treatment with M-CSF and RANKL in the presence or absence of co-treatment with hBD-1 at 5 μM. Pretreatment with either U0126 or PD98059 could completely and significantly inhibit the number of TRAP-positive multinuclear cells by RANKL treatment, regardless of the presence or absence of hBD-1 co-treatment ($p < 0.05$; Fig. 5A and B). In contrast, pretreatment with U0124 or DMSO could not inhibit the number of TRAP-positive multinuclear cells induced by RANKL treatment in the presence or absence of hBD-1 co-treatment (Fig. 5A and B), indicating the specificity of two MEK1/2 inhibitors used in this study and involvement of the p44/42 MAPKs in mediating both the inductive and the potentiation effects on *in vitro* osteoclastogenesis by RANKL and hBD-1, respectively.
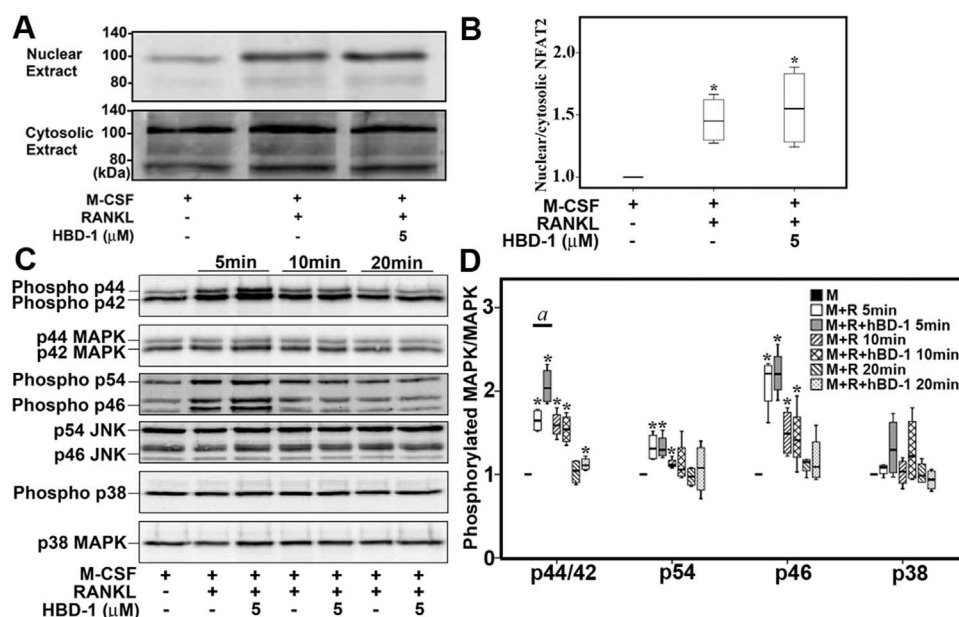
Fig. 4. HBD-1 potentiates *in vitro* osteoclastogenesis via transient phosphorylation of the p44/42 MAPKs. (A) PBMCs were treated with M-CSF and/or RANKL with (+) or without (−) 5 µM of hBD-1 for four days. Ten and 20 µg of nuclear and cytosolic proteins, respectively, were subject to immunoblotting analysis with antibody specific for NFAT2. Two clear bands at around 80–100 kilodalton (kDa) were consistent with those previously shown in [18]. (B) A box plot shows the ratio of nuclear to cytosolic NFAT2 expression (nuclear/cytosolic NFAT2) in each sample relative to the sample treated with M-CSF alone, whose ratio was set to 1, from four separate experiments using blood of four different donors (n = 4). * = significant differences at p < 0.05 when compared to the sample treated with M-CSF alone. (C) PBMCs were cultured as described above for 5, 10 and 20 min. Twenty µg of total proteins were subject to immunoblotting analysis with antibodies specific for MAPKs and their phosphorylated form. (D) A box plot shows the relative ratio of each phosphorylated MAPK to its total MAPK in each sample relative to the sample treated with M-CSF alone, whose ratio was set to 1, from four independent experiments using blood of four different donors (n = 4). * = significant differences at p < 0.05 when compared to the sample treated with M-CSF (M) alone; *a* = significant differences at p < 0.05 when compared to the sample treated with M-CSF (M) and RANKL (R).
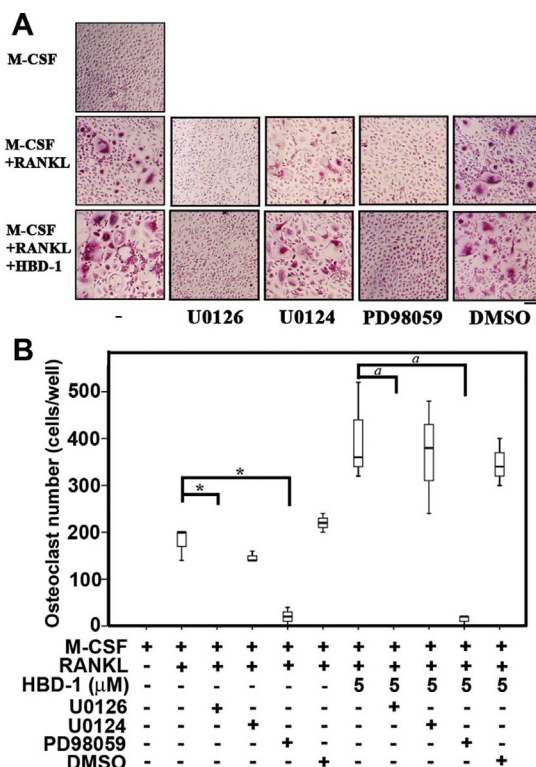

Fig. 5. The inductive and the potentiation effects on human osteoclastogenesis *in vitro* by RANKL and hBD-1, respectively, are blocked by pretreatment with two inhibitors against the p44/42 MAPKs. (A) Representative TRAP-staining images from PBMCs pretreated for 30 min with U0126 or PD98095, two specific inhibitors against MEK1/2 that function as upstream molecules of the p44/42 MAPKs, an inactive analog U0124, or 0.1% (v/v) DMSO prior to treatment with M-CSF and RANKL in the presence or absence of 5 µM of hBD-1 for 7 days. Bar = 100 µm. (B) A box plot shows the number of TRAP-positive multinuclear cells from four independent experiments using blood of four different donors (n = 4) of the conditions described in A. * = significant differences at p < 0.05 when compared to the sample treated with M-CSF and RANKL. *a* = significant differences at p < 0.05 when compared to the sample treated with M-CSF, RANKL, and 5 µM of hBD-1.

4. Discussion

In this study, the promoting effect of hBD-1 at varying non-toxic doses on human osteoclastogenesis was investigated during *in vitro* induction of osteoclast-like cells by RANKL treatment. Moreover, the signaling pathway mediating this effect was elucidated by using specific pharmacological inhibitors. The selected non-toxic doses of hBD-1 potentiated the induction of osteoclastogenesis by RANKL, as demonstrated by statistically significant increases in the number of TRAP-positive multinucleated giant cells with F-actin ring formation around the cell membrane, in mRNA expression of osteoclast-specific genes, and in the percentages of resorption pits and grooves on dentin slices. To the best of our knowledge, there has been one study demonstrating effects of hBDs on osteoblastic differentiation [21]; however, this study is the first to show the promoting effect of hBD-1 on human osteoclastogenesis *in vitro*. However, hBD-1 treatment without RANKL failed to induce formation of osteoclast-like cells, indicating only the potentiation effect of hBD-1 on human osteoclastogenesis, which is similar to the potentiation effect of dexamethasone on RANKL-induced expression of osteoclast-specific genes in mouse bone marrow macrophages [22]. As with no inductive effect of hBD-1 on formation of osteoclast-like cells, treatment with dexamethasone alone does not induce expression of osteoclast-specific genes. It is noteworthy that three essential characteristics of osteoclast-like cells *in vitro*, including TRAP-positive multinuclear cells, expression of osteoclast-specific genes and formation of resorption pits and grooves, were consistently enhanced by approximately 2–3 fold upon hBD-1 co-treatment (Figs. 1C, 1E, and 2B).

In addition, combined treatment between RANKL and hBD-1 significantly further enhanced phosphorylation of the p44/42 MAPKs compared to that by treatment with RANKL alone, suggesting possible involvement of the p44/42 MAPK in the potentiation effect of hBD-1 on RANKL-induced osteoclast differentiation *in vitro*. Interestingly, both the inductive effect by RANKL and the potentiation effect by hBD-1 on formation of TRAP-positive multinuclear cells *in vitro* were completely abrogated by pretreatment with either of the two specific p44/42 MAPK inhibitors, including U0126 and PD98059, suggesting the significance of the p44/42 MAPKs in generation of osteoclast-like cells *in vitro* from primary osteoclast precursor cells obtained from human peripheral blood, which is different from the significance of all three MAPKs in osteoclastogenesis of mouse bone marrow-derived

macrophages and a mouse macrophage cell line RAW264.7 [15,23,24]. This discrepancy reflects differences in cell types and species. Indeed, the importance of p44/42 MAPK activation has been recently shown in human osteoclast differentiation from PBMCs by macrophage inhibitory cytokine-1 [25]. Furthermore, in contrast to humans and mice, the p38 MAPK instead plays an essential role in lipopolysaccharide-induced osteoclastogenesis in a rat periodontitis model [26]. With regard to the candidate receptor for hBD-1, it has been recently shown that the molecular structure of hBDs is similar to that of epidermal growth factor (EGF), particularly a disulfide bond pairing the second and the fourth cysteine [27]. Therefore, it is probable that hBD-1 can bind to the EGF receptor that leads to further activation of the p44/42 MAPK observed in this study. Indeed, an interaction between hBDs and EGF receptor resulted in the regulation of ERK1/2 phosphorylation in an oral cancer cell line [27].

With respect to periodontitis and peri-implantitis, two common bone-resorbing disorders found in the oral cavity, mRNA [6] and protein [7] of hBD-1 are overexpressed in surrounding inflamed gingival tissues. Correspondingly, hBD-1 levels are also elevated in GCF of patients with chronic periodontitis with or without type 2 diabetes mellitus [9] and patients with peri-implantitis [10]. Therefore, it is likely that increased hBD-1 expression and levels are associated with alveolar bone resorption resulting from enhanced osteoclast formation. In addition, it has recently been shown that different single nucleotide polymorphisms at various loci on the hBD-1 gene, *DEFB1*, are associated with increased susceptibility to chronic periodontitis in German, Dutch, Chinese, Japanese, and Northeastern Italian populations [28–31]. Consequently, our *in vitro* results that demonstrated the potentiation effect of hBD-1 on osteoclastogenesis are in agreement with the findings obtained from all aforementioned studies relevant to periodontitis. Furthermore, higher frequencies of two single nucleotide polymorphisms of the *DEFB1* gene were found in Italian patients with oral lichen planus than in healthy subjects [32], implying an implication of hBD-1 in pathogenesis of oral inflammation-related diseases.

Low μM concentrations of hBD-1 have previously been used to treat human gingival fibroblasts [33] and human keratinocytes [16,34] with the maximal non-toxic dose of hBD-1 reported up to 40 μg/ml (∼10 μM). Therefore, all doses of hBD-1 used to treat human PBMCs in this study (0.2–5 μM), which were not cytotoxic (Fig. 1A), were within a range of peptide concentrations commonly used in those studies. Note that the lowest dose of hBD-1, *i.e.* 1 μM or 4 ng/μl, shown to significantly promote *in vitro* osteoclastogenesis (Figs. 1C, 1E, 2B, and 3B), is still somewhat higher than hBD-1 amounts in GCF collected from patients with chronic periodontitis with or without diabetes mellitus that were reported to be 300–400 pg per 30 sec [9]. Nevertheless, the concentrations of hBD-1 could possibly reach as high as low ng levels if periodontal tissue and GCF samplings are done deeply at the bottom of periodontal pockets where active alveolar bone destruction occurs by osteoclasts and accumulation of numerous host defense and immune cells, such as lymphocytes, macrophages, monocytes, dendritic cells that were demonstrated to express hBD-1 mRNA and protein [35–37], is expected. Therefore, it is likely that these immune cells play a major role as hBD-1-producing cells in addition to epithelial cells lining the pocket. Moreover, it is probable that the actual amounts of hBD-1 in GCF would have been higher than those reported by Ertugrul and coworkers [9] because some hBD-1 might still retain in periopaper strips due to incomplete elution of hBD-1 from the strips.

We have previously reported the inhibitory effect of LL-37 on human osteoclastogenesis *in vitro* [18]. It is reasonable to assume that differential effects on osteoclastogenesis between hBD-1 and LL-37 are simply due to their distinct molecular structures, *i.e.* anti-parallel β-sheet versus α-helical structure, respectively, although both peptides contain net positive charges at the physiological pH. In conclusion, the antimicrobial peptide hBD-1 potentiates human osteoclastogenesis *in vitro* by RANKL induction via phosphorylation of the p44/42 MAPKs. Involvement of other signaling molecules besides NFAT2 and the p44/

42 MAPKs as well as a candidate receptor in enhancement of osteoclast differentiation upon hBD-1 co-treatment and the effect of hBD-1 on *in vivo* osteoclast formation and function warrant further investigations.

Conflict of interest

All authors deny any conflict of interest relating to this study.

Acknowledgments

References

[1] B.A. Dale, L.P. Fredericks, Antimicrobial peptides in the oral environment: expression and function in health and disease, Curr. Issues Mol. Biol. 7 (2005) 119–133.

[2] F. Niyonsaba, C. Kiatsurayanon, H. Ogawa, The role of human β-defensins in allergic diseases, Clin. Exp. Allergy 46 (2016) 1522–1530.

[3] Y. Abiko, M. Saitoh, M. Nishimura, M. Yamazaki, D. Sawamura, T. Kaku, Role of beta-defensins in oral epithelial health and disease, Med. Mol. Morphol. 40 (2007) 179–184.

[4] B.A. Dale, J.R. Kimball, S. Krisanaprakornkit, F. Roberts, M. Robinovitch, R. O'Neal, E.V. Valore, T. Ganz, G.M. Anderson, A. Weinberg, Localized antimicrobial peptide expression in human gingival tissue, J.Periodontal Res. 36 (2001) 285–294.

[5] Q. Lu, L.P. Samaranayake, R.P. Darveau, L. Jin, Expression of human beta-defensin-3 in gingival epithelia, J.Periodontal Res. 40 (2005) 474–481.

[6] S. Vardar-Sengul, T. Demirci, B.H. Sen, V. Erkizan, E. Kurulgan, H. Baylas, Human beta defensin-1 and -2 expression in the gingiva of patients with specific periodontal diseases, J. Periodontal Res. 42 (2007) 429–437.

[7] H. Kuula, T. Salo, E. Pirilä, J. Hagström, M. Luomanen, A. Gutierrez-Fernandez, G.E. Romanos, T. Sorsa, Human beta-defensin-1 and −2 and matrix metalloproteinase-25 and −26 expression in chronic and aggressive periodontitis and in peri-implantitis, Arch. Oral Biol. 53 (2008) 175–186.

[8] A. Vankeerberghen, H. Nuytten, K. Dierickx, M. Quirynen, J.J. Cassiman, H. Cuppens, Differential induction of human beta-defensin expression by periodontal commensals and pathogens in periodontal pocket epithelial cells, J. Periodontol. 76 (2005) 1293–1303.

[9] A.S. Ertugrul, A. Dikilitas, H. Sahin, N. Alpaslan, A. Bozoglan, Y. Tekin, Gingival crevicular fluid levels of human beta-defensins 1 and 3 in subjects with periodontitis and/or type 2 diabetes mellitus: a cross-sectional study, J.Periodontal Res. 48 (2013) 475–482.

[10] A.S. Ertugrul, Y. Tekin, N.Z. Alpaslan, A. Bozoglan, H. Sahin, A. Dikilitas, Comparison of peri-implant crevicular fluid levels of adrenomedullin and human beta defensins 1 and 2 from mandibular implants with different implant stability quotient levels in nonsmoker patients, J. Periodontal Res. 49 (2014) 480–488.

[11] S. Vordenbäumen, M. Schneider, Defensins Potential effectors in autoimmune rheumatic disorders, Polymers 3 (2011) 1268–1281.

[12] G. Kaltsa, G. Bamias, S.I. Siakavellas, D. Goukos, D. Karagiannakis, E. Zampeli, J. Vlachogiannakos, S. Michopoulos, I. Vafiadi, G.L. Daikos, S.D. Ladas, Systemic levels of human β-defensin 1 are elevated in patients with cirrhosis, Ann Gastroenterol. 29 (2016) 63–70.

[13] I.E. Adamopoulos, E.D. Mellins, Alternative pathways of osteoclastogenesis in inflammatory arthritis, Nat. Rev. Rheumatol. 11 (2015) 189–194.

[14] T. Nakashima, H. Takayanagi, New regulation mechanisms of osteoclast differentiation, Ann. N. Y. Acad. Sci. 1240 (2011) E13–E18.

[15] K. Lee, Y.H. Chung, H. Ahn, H. Kim, J. Rho, D. Jeong, Selective regulation of MAPK signaling mediates RANKL-dependent osteoclast differentiation, Int. J. Biol. Sci. 12 (2016) 235–245.

[16] F. Niyonsaba, H. Ushio, I. Nagaoka, K. Okumura, H. Ogawa, The human beta-defensins (-1 −2, −3, −4) and cathelicidin LL-37 induce IL-18 secretion through p38 and ERK MAPK activation in primary human keratinocytes, J. Immunol. 175 (2005) 1776–1784.

[17] F. Niyonsaba, H. Ushio, M. Hara, H. Yokoi, M. Tominaga, K. Takamori, N. Kajiwara, H. Saito, I. Nagaoka, H. Ogawa, K. Okumura, Antimicrobial peptides human beta-defensins and cathelicidin LL-37 induce the secretion of a pruritogenic cytokine IL-31 by human mast cells, J.Immunol. 184 (2010) 3526–3534.

[18] C. Supanchart, S. Thawanaphong, A. Makeudom, J.G. Bolscher, K. Nazmi, U. Kornak, S. Krisanaprakornkit, The antimicrobial peptide LL-37, inhibits *in vitro* osteoclastogenesis, J. Dent. Res. 91 (2012) 1071–1077.

[19] S. Krisanaprakornkit, J.R. Kimball, B.A. Dale, Regulation of human beta-defensin-2 in gingival epithelial cells: the involvement of mitogen-activated protein kinase

pathways but not the NF-kappaB transcription factor family, J. Immunol. 168 (2002) 316–324.

[20] N. Kobayashi, Y. Kadono, A. Naito, K. Matsumoto, T. Yamamoto, S. Tanaka, J. Inoue, Segregation of TRAF6-mediated signaling pathways clarifies its role in osteoclastogenesis, EMBO. J. 20 (2001) 1271–1280.

[21] D. Kraus, J. Deschner, A. Jäger, M. Wenghoefer, S. Bayer, S. Jepsen, J.P. Allam, N. Novak, R. Meyer, J. Winter, Human β-defensins differently affect proliferation, differentiation, and mineralization of osteoblast-like MG63 cells, J. Cell Physiol. 227 (2012) 994–1003.

[22] H.H. Conaway, P. Henning, A. Lie, J. Tuckermann, U.H. Lerner, Activation of dimeric glucocorticoid receptors in osteoclast progenitors potentiates RANKL induced mature osteoclast bone resorbing activity, Bone 93 (2016) 43–54.

[23] S.E. Lee, K.M. Woo, S.Y. Kim, H.M. Kim, K. Kwack, Z.H. Lee, H.H. Kim, The phosphatidylinositol 3-kinase, p38, and extracellular signal-regulated kinase pathways are involved in osteoclast differentiation, Bone 30 (2002) 71–77.

[24] D. Thummuri, M.K. Jeengar, S. Shrivastava, H. Nemani, R.N. Ramavat, P. Chaudhari, V.G. Naidu, Thymoquinone prevents RANKL-induced osteoclastogenesis activation and osteolysis in an in vivo model of inflammation by suppressing NF-κB and MAPK Signalling, Pharmacol. Res. 99 (2015) 63–73.

[25] M. Yuan, J. Chen, Z. Zeng, Knockdown of macrophage inhibitory cytokine-1 in RPMI-8226 human multiple myeloma cells inhibits osteoclastic differentiation through inhibiting the RANKL-Erk1/2 signaling pathway, Mol. Med. Rep. 14 (2016) 5199–5204.

[26] G. Intini, Y. Katsuragi, K.L. Kirkwood, S. Yang, Alveolar bone loss: mechanisms, potential therapeutic targets, and interventions, Adv. Dent. Res. 26 (2014) 38–46.

[27] T. Hoppe, D. Kraus, N. Novak, R. Probstmeier, M. Frentzen, M. Wenghoefer, S. Jepsen, J. Winter, Oral pathogens change proliferation properties of oral tumor cells by affecting gene expression of human defensins, Tumor Biol. 37 (2016) 13789–13798.

[28] A.S. Schaefer, G.M. Richter, M. Nothnagel, M.L. Laine, A. Rühling, C. Schäfer, N. Cordes, B. Noack, M. Folwaczny, J. Glas, C. Dörfer, H. Dommisch, B. Groessner-Schreiber, S. Jepsen, B.G. Loos, S. Schreiber, A 3' UTR transition within DEFB1 is associated with chronic and aggressive periodontitis, Genes Immun. 11 (2010) 45–54.

[29] W.T. Loo, L.J. Bai, C.B. Fan, Y. Yue, Y.D. Dou, M. Wang, H. Liang, M.N. Cheung, L. Chow, J.L. Li, Y. Tian, L. Qing, Clinical application of human β-defensin and CD14 gene polymorphism in evaluating the status of chronic inflammation, J. Transl. Med. 10 (Suppl. 1) (2012) S9.

[30] T. Ikuta, Y. Inagaki, K. Tanaka, T. Saito, N. Nakajima, M. Bando, J. Kido, T. Nagata, Gene polymorphism of β-defensin-1 is associated with susceptibility to periodontitis in Japanese, Odontology 103 (2015) 66–74.

[31] L. Zupin, A. Robino, C.O. Navarra, N. Pirastu, R. Di Lenarda, P. Gasparini, S. Crovella, L. Bevilacqua, LTF and DEFB1 polymorphisms are associated with susceptibility towards chronic periodontitis development, Oral Dis. (2017), http://dx.doi.org/10.1111/odi.12689.

[32] V. Polesello, L. Zupin, R. Di Lenarda, M. Biasotto, G. Pozzato, G. Ottaviani, M. Gobbo, S. Crovella, L. Segat, DEFB1 polymorphisms and salivary hBD-1 concentration in oral lichen planus patients and healthy subjects, Arch. Oral Biol. 73 (2017) 161–165.

[33] P. Chotjumlong, S. Khongkhunthian, S. Ongchai, V. Reutrakul, S. Krisanaprakornkit, Human β-defensin-3 up-regulates cyclooxygenase-2 expression and prostaglandin E2 synthesis in human gingival fibroblasts, J. Periodontal Res. 45 (2010) 464–470.

[34] F. Niyonsaba, H. Ushio, N. Nakano, W. Ng, K. Sayama, K. Hashimoto, I. Nagaoka, K. Okumura, H. Ogawa, Antimicrobial peptides human β-defensins stimulate epidermal keratinocyte migration, proliferation and production of proinflammatory cytokines and chemokines, J. Invest. Dermatol. 127 (2007) 594–604.

[35] J. Wah, A. Wellek, M. Frankenberger, P. Unterberger, U. Welsch, R. Bals, Antimicrobial peptides are present in immune and host defense cells of the human respiratory and gastrointestinal tracts, Cell Tissue Res. 324 (2006) 449–456.

[36] L.K. Ryan, J. Dai, Z. Yin, N. Megjugorac, V. Uhlhorn, S. Yim, K.D. Schwartz, J.M. Abrahams, G. Diamond, P. Fitzgerald-Bocarsly, Modulation of human beta-defensin-1 (hBD-1) in plasmacytoid dendritic cells (PDC) monocytes, and epithelial cells by influenza virus, Herpes simplex virus, and Sendai virus and its possible role in innate immunity, J. Leukoc. Biol. 90 (2011) 343–356.

[37] J.I. Castañeda-Sánchez, D.A. Domínguez-Martínez, N. Olivar-Espinosa, B.E. García-Pérez, M.A. Loroño-Pino, J. Luna-Herrera, M.I. Salazar, Expression of antimicrobial peptides in human monocytic cells and neutrophils in response to dengue virus type 2, Intervirology 59 (2016) 8–19.

ORIGINAL ARTICLE

Reduction of *Streptococcus mutans* by probiotic milk: a multicenter randomized controlled trial

Chanika Manmontri[1,2] · Areerat Nirunsittirat[2,3] · Supatcharin Piwat[4,5] · Onnida Wattanarat[1,2] · Nuntiya Pahumunto[4,6] · Anupong Makeudom[2] · Thanapat Sastraruji[2] · Suttichai Krisanaprakornkit[2,7] · Rawee Teanpaisan[4,6]

Abstract

Objective To investigate the effects of probiotics, *Lactobacillus paracasei* SD1, on the quantities of *Streptococcus mutans* in saliva and plaque samples of preschool children.

Design This randomized trial recruited 487 preschool children from eight childcare centers. Participants were assigned to receive a 6-month course of placebo milk daily (group I), probiotic milk either daily (group II) or three days a week (triweekly, group III). The absolute quantities of *S. mutans* and total lactobacilli in the saliva and plaque samples at baseline (T0), after intervention (T6), and 6 months after discontinuation (T12) were assessed by qPCR.

Results Of 487 children, 354 completed all follow-up periods. However, only 268 children (3.2 ± 0.8 years old; groups I = 86, II = 89, and III = 93) provided adequate saliva for qPCR. Whereas the quantities of *S. mutans* were significantly decreased in groups II and III compared to group I in the saliva and plaque samples at T6 and T12, those of total lactobacilli were significantly increased ($p < 0.0167$). There was no difference in the quantities of *S. mutans* or total lactobacilli between groups II and III at any period. Significant changes in the quantities of *S. mutans* and total lactobacilli lasted until T12 compared to T0 ($p < 0.0167$).

Conclusions Probiotic administration daily or triweekly reduces *S. mutans* quantities, whereas it increases total lactobacilli quantities that persists at least 6 months after discontinuation in the saliva and plaque samples of preschool children.

Clinical relevance Daily or triweekly consumption of *L. paracasei* SD1 supplemented in milk may help prevent dental caries in preschool children.

Keywords *Lactobacillus paracasei* SD1 · Plaque · Preschool children · Probiotics · Saliva · *Streptococcus mutans*

✉ Rawee Teanpaisan
   rawee.t@psu.ac.th

1   Division of Pediatric Dentistry, Department of Orthodontics and Pediatric Dentistry, Faculty of Dentistry, Chiang Mai University, Chiang Mai 50200, Thailand

2   Center of Excellence in Oral and Maxillofacial Biology, Faculty of Dentistry, Chiang Mai University, Chiang Mai 50200, Thailand

3   Division of Community Dentistry, Department of Family and Community Dentistry, Faculty of Dentistry, Chiang Mai University, Chiang Mai 50200, Thailand

4   Common Oral Diseases and Epidemiology Research Center, Faculty of Dentistry, Prince of Songkla University, Hat Yai, Songkhla 90112, Thailand

5   Department of Preventive Dentistry, Faculty of Dentistry, Prince of Songkla University, Hat Yai, Songkhla 90112, Thailand

6   Department of Stomatology, Faculty of Dentistry, Prince of Songkla University, Hat Yai, Songkhla 90112, Thailand

7   Department of Oral Biology and Diagnostic Sciences, Faculty of Dentistry, Chiang Mai University, Chiang Mai 50200, Thailand

Introduction

Probiotics were originally used in medicine and have been a topic of extensive research in the fields of cariology, periodontology, mucositis, and halitosis in the past two decades [1]. Dental caries, a common preventable and multifactorial oral disease affecting all age groups worldwide [2], is caused by a shift of microbial compositions from physiologic to pathogenic bacteria. *Streptococcus mutans* plays an important role as an early colonizer in the dental biofilm, in which it produces acids and resists an acidic condition, resulting in demineralization of the tooth structure [3]. Dental caries is considered a non-communicable disease similar to hypertension, diabetes mellitus, and cardiovascular diseases; modifications of human lifestyles would, therefore, help prevent these diseases [1]. Early childhood caries adversely affects the general health of children and influences socioeconomic burdens of countries [4]. Consequently, caries prevention as early as the first 1,000

days of life by introducing probiotics in routine diets would be beneficial to modulate the ecology of oral microorganisms in the biofilm, leading to a reduction of cariogenic bacteria [1].

For caries prevention, *Lactobacilli* are commonly used as probiotic strains [5]. Previous studies have shown that *L. paracasei* SD1, isolated from caries-free Thai preschool children [6], exerts various effects in the oral cavity, including inhibition of mutans streptococci, production of less acids than other lactobacilli, bacterial adherence to oral epithelial cells [7], synthesis of bacteriocin [8], production of antioxidants [9], and immunomodulation by enhancing salivary human neutrophil peptide 1-3 levels [10]. Five previous clinical trials, using *L. paracasei* SD1 as probiotic supplementation in Thai adults, adolescents, children, and patients with clefts, have demonstrated bacterial changes in saliva and a favorable microbial symbiosis [10–14]. Whereas mutans streptococci were significantly decreased, the probiotic strain was significantly increased and persisted after discontinuation in conjunction with caries reduction. However, these five trials were conducted in a small cohort within southern Thailand and all participants obtained probiotics daily during the trial period. Accordingly, conducting a multicenter randomized controlled trial in a larger population of young children for an early exposure is necessary to verify the beneficial effects of *L. paracasei* SD1. Although it is generally recommended that probiotics be consumed daily for continuing benefits [1], daily consumption may not be practical for everyone. Moreover, concerns are raised whether children who miss some doses of probiotics would still receive benefits. This study designed with different dose intervals and conducted in different regions should lead to a more practical implementation of public health policy.

It was hypothesized that (1) the effect of early exposure to probiotics on the reduction of cariogenic bacteria in the saliva and the plaque is sustained after discontinuation, and (2) the frequency of probiotic administration either daily or 3 days in a week (triweekly) has similar impacts on the control of cariogenic microorganisms. The aim of this study was, thus, to determine the quantities of *S. mutans*, total lactobacilli, and total bacteria in saliva and plaque samples of healthy preschool children, who consumed milk supplemented with probiotics once daily or triweekly or without probiotics as a placebo, at baseline (T0), immediately after 6 months of probiotic intervention (T6), and 6 months after probiotic discontinuation (T12).

Material and methods

Participants

Eligible participants included healthy preschool children (aged 1-5 years) who had normal height and weight for their ages within 1.5 standard deviation of the Thai children growth chart and with a minimum weight of 10 kg. Exclusion criteria were 1) medically compromised children, who were at risk of episodic infections or prone to frequent uses of antibiotics, 2) allergy to cow milk or lactose intolerance, 3) receiving antibiotics within two weeks prior to the study in order to allow reestablishment of normal oral microflora [15], 4) having more than four cavitated teeth [12], and 5) refusal to participate by parents or legal guardians. Written informed consent was obtained before enrolling each child into the trial. This multicenter, stratified-randomized, double-blind, and placebo-controlled trial with three randomization arms (1:1:1), lasting for one year, was registered with the Thai Clinical Trial Registry (TCTR20170511002; http://www.clinicaltrials.in.th), being part of the WHO's Registry Network, Clinical Trials identifier (registration on May 10, 2017, first enrollment on May 22, 2017).

Probiotic and placebo milk powder

The probiotic milk powder was prepared by a spray drying technique, containing viable 1.8×10^7 CFU/ml of *L. paracasei* SD1 in 20% skimmed milk and < 4% humidity according to Teanpaisan et al., 2015 [11]. The placebo was the exact same milk powder devoid of *L. paracasei* SD1. Both probiotic and placebo milk were identical in appearance, scent, weight, and packaging. A single dose of 3 g of the milk powder was packaged for daily intake and sealed in plastic bags labeled specifically for each participant. The packages were stored at 4 °C until delivery to the childcare center monthly. The viability of *L. paracasei* SD1 in milk powder has been shown to last 6 months when being stored at 4 °C [16]. The powder was dissolved in 50 ml of child's milk at room temperature by caregivers or parents, who monitored the child intake on weekdays or weekends/holidays, respectively, and recorded the days that each child had consumed milk in the child's logbook. In addition, the caregivers recorded occurrence of any specific clinical symptoms, including fever, respiratory infection, allergy, diarrhea, constipation, school absence due to illnesses, and health care utilization in the logbook. The participants were allowed to withdraw from the study if they were suspected to be allergic to the milk or experienced any abnormal symptoms, including fever, nausea, vomiting, abdominal pain, or diarrhea. After each month, both the empty and full plastic bags of each child were collected to confirm the percentage of compliance, which was calculated by the number of days that participants had consumed milk divided by the total number of days for 6 months (Table 1).

Randomization, allocation, concealment, and blinding

After enrollment, participants were randomly assigned to one of the three study arms (placebo, daily probiotics, and triweekly probiotics), by stratified randomization using block of six in each childcare center. Children who consumed the placebo milk powder were classified in the placebo (group I), while

Table 1 Baseline characteristics for the children who completed the two follow-up periods (T6 and T12) and provided adequate saliva volume (at least 500 μl) at all three periods (T0, T6, and T12) for qPCR analysis

Characteristic	Group				p value
	Total $N = 268$	I (placebo) $N = 86$	II (daily probiotic) $N = 89$	III (triweekly probiotic) $N = 93$	
Age (year) mean ± SD	3.19 ± 0.77	3.25 ± 0.74	3.15 ± 0.78	3.16 ± 0.80	0.67[a]
Sex					0.36[b]
Female n (%)	137 (51.12)	41 (47.67)	51 (57.30)	45 (48.39)	
Male n (%)	131 (48.88)	45 (52.33)	38 (42.70)	48 (51.61)	
Unerupted and partially erupted (teeth) mean ± SD	0.76 ± 1.56	0.58 ± 1.29	0.73 ± 1.37	1.95 ± 1.92	0.29[a]
Dental caries (teeth) mean ± SD					
Caries free	14.77 ± 4.08	15.44 ± 3.71	14.37 ± 4.34	14.53 ± 4.11	0.17[a]
Non-cavitated	3.26 ± 3.27	2.77 ± 2.90	3.63 ± 3.48	3.37 ± 3.38	0.20[a]
Cavitated	1.19 ± 1.40	1.20 ± 1.53	1.25 ± 1.40	1.12 ± 1.28	0.82[a]
Visible plaque index					0.08[c]
Score 1 n (%)	16 (5.97)	6 (6.98)	2 (2.25)	8 (8.60)	
Score 2 n (%)	130 (48.51)	48 (55.81)	45 (50.56)	37 (39.78)	
Score 3 n (%)	90 (33.58)	26 (30.23)	27 (30.34)	37 (39.78)	
Score 4 n (%)	32 (11.94)	6 (6.98)	15 (16.85)	11 (11.83)	
Compliance rate % average	89.55	90.70	88.76	89.25	0.19[b]

The significant differences were tested by [a] ANOVA, [b] Chi-square, or [c] Fisher exact test

those who consumed the probiotic milk powder once daily for 6 months were grouped in the daily probiotics (group II). The triweekly probiotics (group III) included children who consumed the probiotic milk powder in any 3 days of a week and the placebo milk powder for the remaining 4 days. Participants, caregivers, parents, clinical examiners, investigators, laboratory staff, and research assistants who entered data to a database were blinded to the assigned groups until the codes were opened after statistical analysis.

Saliva collection

Saliva samples were collected from each child during the same time, i.e., mid-morning, at T0, T6, and T12. The unstimulated whole saliva was collected as much as possible by spitting into a small cup, while children who could not spit or were uncooperative, sterile 1.0-ml droppers were used to collect their saliva. The saliva samples were transferred to 1.5-ml sterile microcentrifuge tubes and stored on ice for a few hours while being transported to the research laboratories. The saliva samples were immediately stored at − 80 °C until being used for DNA extraction.

Oral examination and plaque sample collection

Oral examination by trained and calibrated pediatric dentists, with inter- and intra-examiner reliability greater than 0.8, was performed using light sources, mouth mirrors, and ball-ended periodontal probes (probe WHO-621). The visible dental biofilm index was recorded at T0, T6, and T12 using the overall index modified by Santos and Soviero (2006) [17, 18] as follows: 1 = absence of visible biofilm; 2 = thin biofilm, easily removed; 3 = thick biofilm, firmly adhered to either anterior or posterior teeth; 4 = thick biofilm, firmly adhered to both anterior and posterior teeth. Afterwards, the pooled plaque samples were collected using sterile toothpicks to scrape plaque from the mesial, distal, buccal, and lingual surfaces of all erupted teeth, placed into pre-weighed 1.5-ml sterile microcentrifuge tubes, and stored dry for a few hours while being transported to the laboratories. Each plaque sample was weighed, mixed with 200 μl of Tris-EDTA buffer, and stored at − 80 °C until being used for DNA extraction.

Dental caries status was recorded at T0, T6, and T12 according to the modified Nyvad criteria for caries assessment [19–21]; code 0, sound surface; code 1, active non-cavitated lesion; code 2, active cavitated lesion; code 3, inactive non-cavitated lesions; code 4, inactive cavitated lesions; code 5, filling; code 6, filling associated with active caries; code 7 missing due to caries. The overall status for each tooth was determined by the greatest severity among all tooth surfaces of each tooth and presented as follows; caries free, non-cavitated, and cavitated. The number of unerupted or partially erupted teeth was also recorded.

DNA extraction

DNA isolation from the saliva and plaque samples in the three intervention groups at T0, T6, and T12 was performed in only

the samples whose saliva volume was at least 500 µl. A 500-µl and a 200-µl volume of saliva and reconstituted plaque samples, respectively, were thawed, vortexed, and centrifuged at 10,000 rpm for 5 min. The resultant pellet was resuspended in 200 µl of 20 mg/ml freshly prepared lysozyme (Amresco Inc., Solon, OH, USA) and incubated at 37 °C for 30 min to lyze the bacterial cell wall. Bacterial DNA was then extracted, purified, and eluted in 40 µl of Tris-EDTA buffer, using the PureDirex Genomic DNA Isolation kit (Bio-Helix Co., LTD., Keelung City, Taiwan) according to the manufacturer's instructions.

Absolute quantification of bacterial DNA

To establish a standard curve for each microorganism, *S. mutans* ATCC25175 for *S. mutans*, *Escherichia coli* ATCC25922 for total bacteria and *S. sobrinus* ATCC33478 as a negative control, were cultured on 5% blood agar (Difco^{TM}, Sparks, MD, USA), while *L. fermentum* ATCC14931 for total lactobacilli was cultured on de Man Rogosa and Sharpe (MRS) agar (Difco^{TM}) anaerobically at 37 °C for 24–48 h. A single colony of *E. coli* ATCC25922, *S. mutans* ATCC25175, or *S. sobrinus* ATCC33478 was inoculated in Brain Heart Infusion broth (Difco^{TM}), and a single colony of *L. fermentum* ATCC14931 was inoculated in MRS broth (Difco^{TM}), overnight at 37 °C anaerobically. The bacterial pellets were collected after centrifugation at 5,000 rpm for 10 min, washed twice with phosphate-buffered saline (PBS), pH 7.0, and adjusted to an optical density of 2.0 at 600 nm using a UV/VIS spectrophotometer (Biochrom Ltd., Cambridge, UK). The bacterial cell suspensions were twofold diluted until 1:4096 and divided into two aliquots. Whereas the first aliquot was streaked on agar plates for bacterial count as CFU/ml using the aforementioned cultivation method, the second was used for DNA isolation as aforementioned to determine the cycle threshold (C_t) of qPCR using the CFX96 Touch^{TM} Real-Time PCR detection system (Bio-Rad Laboratories, Inc., Hercules, CA, USA). A linear standard curve was plotted for each bacterial species from log$_{10}$ CFU/ml against the corresponding C_t and showed a high correlation coefficient ($R^2 > 0.99$).

A 20-µl aliquot of qPCR master mix, comprising 5 µl of purified DNA template from saliva or plaque sample, 2 µl of a specific primer pair, 3 µl of nuclease-free water, and 10 µl of 2x SensiFAST SYBR® No-ROX mix (Bioline Reagent Ltd., Foster City, CA, USA), was amplified using the CFX96 Touch^{TM} Real-Time PCR detection system (Bio-Rad Laboratories, Inc). The primer sequences for detecting each bacterial species are presented in Table 2 [22–24]. The qPCR conditions for both unknown samples and bacterial genomic DNA were as follows; 1 cycle at 95 °C for 10 min and 1 cycle at 50 °C for 2 min, followed by 40 cycles at 95 °C for 20 s; at 60 °C, 58 °C, or 60 °C for *S. mutans*, total lactobacilli, or total

bacteria, respectively, for 20 s; and at 72 °C for 25 s. The melting curve analysis for targeted bacterial species demonstrated a sharp peak at the expected melting temperature, indicating that qPCR products were homogeneous without primer-dimers, and the chosen primers specifically amplified the target DNA. Additionally, DNA isolated from *S. sobrinus* ATCC33478 was used as a negative control for qPCR analysis of *S. mutans* and total lactobacilli, and the findings showed no amplified products (data not presented). The absolute quantities of *S. mutans*, total lactobacilli, and total bacteria in the saliva and plaque samples were extrapolated by comparing the C_t value of each unknown sample with the standard curve for *S. mutans* ATCC25175, *L. fermentum* ATCC14931, and *Escherichia coli* ATCC25922, respectively. The quantities of bacteria in the saliva samples were reported as log$_{10}$ CFU/ml, whereas those in the plaque samples were normalized by the plaque weight and expressed as log$_{10}$ CFU/mg. All qPCR reactions for saliva and plaque samples were performed in duplicate, and their averages were used in statistical analysis.

Statistical analysis

Descriptive analysis was used to describe mean age, sex, the number of non- or partially erupted teeth, caries status, including caries-free, non-cavitated and cavitated teeth, and visible plaque index at baseline. ANOVA was used to compare continuous variables and the Chi-square or Fisher exact test was used to compare categorical variables among the three groups. Statistical significance was accepted at $p < 0.05$. To compare bacterial quantities, non-parametric statistical tests were used due to the non-normal distribution of the data. For intergroup comparisons, the Kruskal-Wallis H test was used to determine the differences in bacterial quantities at each period, followed by multiple comparisons using the Mann-Whitney U test with Bonferroni adjustment. For intragroup comparisons, the Friedman test was used to determine the differences in bacterial quantities among the three periods (T0, T6, and T12), followed by multiple comparisons using the Wilcoxon signed rank test with Bonferroni adjustment. Statistical significance for both intergroup and intragroup comparisons was accepted at $p < 0.0167$. The Pearson's correlation was used to evaluate the correlations of bacterial quantities between the saliva and plaque samples. All analyses were performed using SPSS® software version 17.0 for Windows (IBM, Armonk, NY, USA).

Results

Of 1050 children assessed for eligibility, 487 children from eight childcare centers of two provinces, Satun ($n = 250$) and Chiang Mai ($n = 237$) in the southern and northern regions of Thailand, respectively, were registered in this trial (Fig. 1). Of

Table 2 Oligonucleotide primer sequences for qPCR analysis

Bacterial species	Primer sequence	Reference
Streptococcus mutans (S. mutans ATCC25175)	Forward: 5′-ACTACACTTTCGGGTGGCTTGG-3′	[22]
	Reverse: 5′-CAGTATAAGCGCCAGTTTCATC-3′	
Total lactobacilli (L. fermentum ATCC14931)	Forward: 5′-CATTTGGAAACAGATGCTAATACC-3′	[24]
	Reverse: 5′-GTCCATTGTGGAAGATTCCC-3′	
Total bacteria (E. coli ATCC25922)	Forward: 5′-TCCTACGGGAGGCAGCAGT-3′	[23]
	Reverse: 5′-GGACTACCAGGGTATCTAATCCTGTT-3′	
Streptococcus sobrinus (S. sobrinus ATCC33478)*	Forward: 5′-GATAACTACCTGACAGCTGACT-3′	[22]
	Reverse: 5′-AAGCTGCCTTAAGGTAATCACT-3′	

*Used as a negative control

487 registered participants, 354 (72.69%) completed all follow-up periods (T6 and T12; Fig. 1). The reasons for dropout included failure to comply with the research protocol, withdrawal due to allergy, and relocation, as summarized in Fig. 1. However, only 268 of 354 children (75.70%), comprising 86 in group I, 89 in group II, and 93 in group III, provided adequate saliva volume (at least 500 μl) at T0, T6, and T12 for qPCR analysis (Fig. 1). The baseline variables for participants, including mean age, sex, the number of unerupted or partially erupted teeth, that of carious teeth, the visible plaque index, or the average percentage of compliance, were not found to be different among the three groups (Table 1).

Reduction of S. mutans by the probiotic strain

At T6 and T12, there were significant decreases in the median quantities of S. mutans, expressed as $\log_{10}$ CFU/ml and $\log_{10}$ CFU/mg for saliva and plaque samples, respectively, in the children receiving daily probiotics (group II) and the children receiving triweekly probiotics (group III) compared to the children receiving the placebo (group I) ($p < 0.0033$; Fig. 2a, b). As anticipated, the median quantities of total lactobacilli were significantly increased in both the saliva and plaque samples in groups II and III compared to those in group I ($p < 0.0167$; Fig. 2c, d, respectively). In contrast to significant changes in the median quantities of S. mutans or total lactobacilli by probiotic administration, those of total bacteria in the saliva or plaque samples were not found to be different among the three groups at any periods (Fig. 2e or f, respectively), indicating true reduction in the quantities of S. mutans by probiotic consumption. Moreover, the median quantities of S. mutans or of total lactobacilli in the saliva or plaque samples were not found to be different between the two probiotic groups at T0, T6, or T12 (Fig. 2a–d). Note that the median quantity of S. mutans in the saliva samples at T0 was significantly lower in group I than in groups II and III ($p < 0.00033$; Fig. 2a), whereas that of total lactobacilli in the saliva samples at T0 was significantly greater in group I than in groups II and III ($p < 0.00033$; Fig. 2c).

Sustained decreases in S. mutans and increases in total lactobacilli quantities after probiotic discontinuation

At T6 and T12, similar trends of changes in the median quantities of S. mutans and total lactobacilli in both the saliva and plaque samples were found both in the children receiving daily (group II) and triweekly probiotics (group III; Fig. 3a, b, respectively). Particularly for the median quantities of total lactobacilli in both the saliva and plaque samples from groups II and III, there were significant increases at T6 and T12 compared to T0 ($p < 0.0033$). On the contrary, there were significant decreases in the median quantities of S. mutans found only in the saliva samples from groups II and III at T6 and T12 compared to T0 ($p < 0.0033$; Fig. 3a), whereas a significant decrease was found in the plaque samples of group II at T6 ($p < 0.0033$; Fig. 3b). Taken together, these findings suggest sustained effects on microbial shifts after probiotic discontinuation for at least 6 months and saliva samples as a better surrogate for microbial quantification than plaque samples. Without probiotic consumption in the placebo group, there were significant increases in the median quantities of S. mutans, and significant decreases in those of total lactobacilli were found in both the saliva and plaque samples at T6 and T12 compared to T0 ($p < 0.0167$; Fig. 3a, b, respectively). With respect to the median quantities of total bacteria, significant increases were found at T6 and T12 compared to T0 in the saliva samples of all three groups ($p < 0.0167$; Fig. 3a), but not in the plaque samples (Fig. 3b), confirming saliva samples as a better surrogate for detection of changes in microbial quantities. Details of the medians together with the interquartile ranges of S. mutans, total lactobacilli, and total bacteria quantities in saliva and plaque samples at T0, T6, and T12 are summarized in Table 3.

Weak correlations for the quantities of S. mutans and total lactobacilli between saliva and plaque samples

When all data from the three periods and the three intervention groups were pooled and compared between the saliva ($\log_{10}$
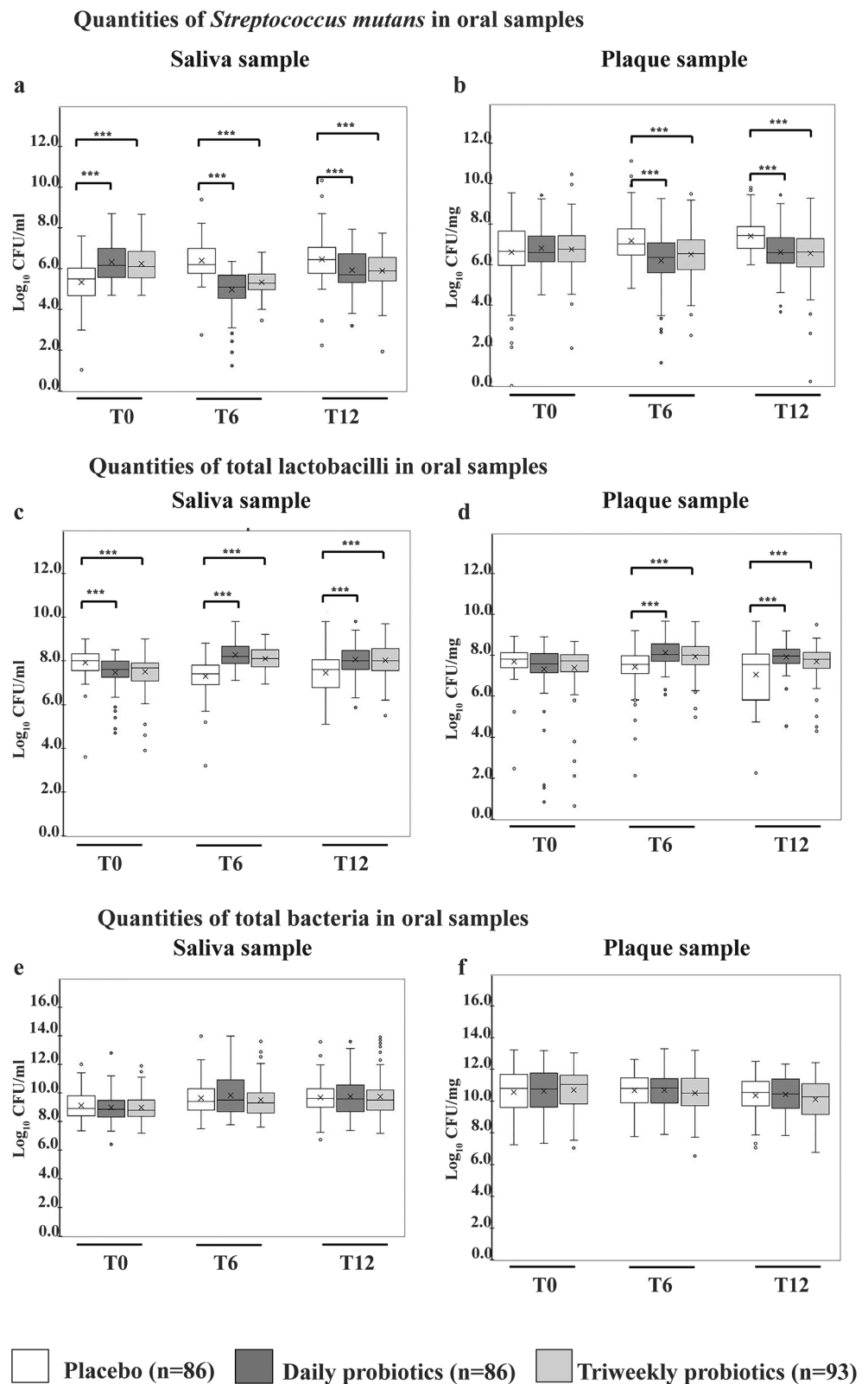
Fig. 1 Consort flow of the participants
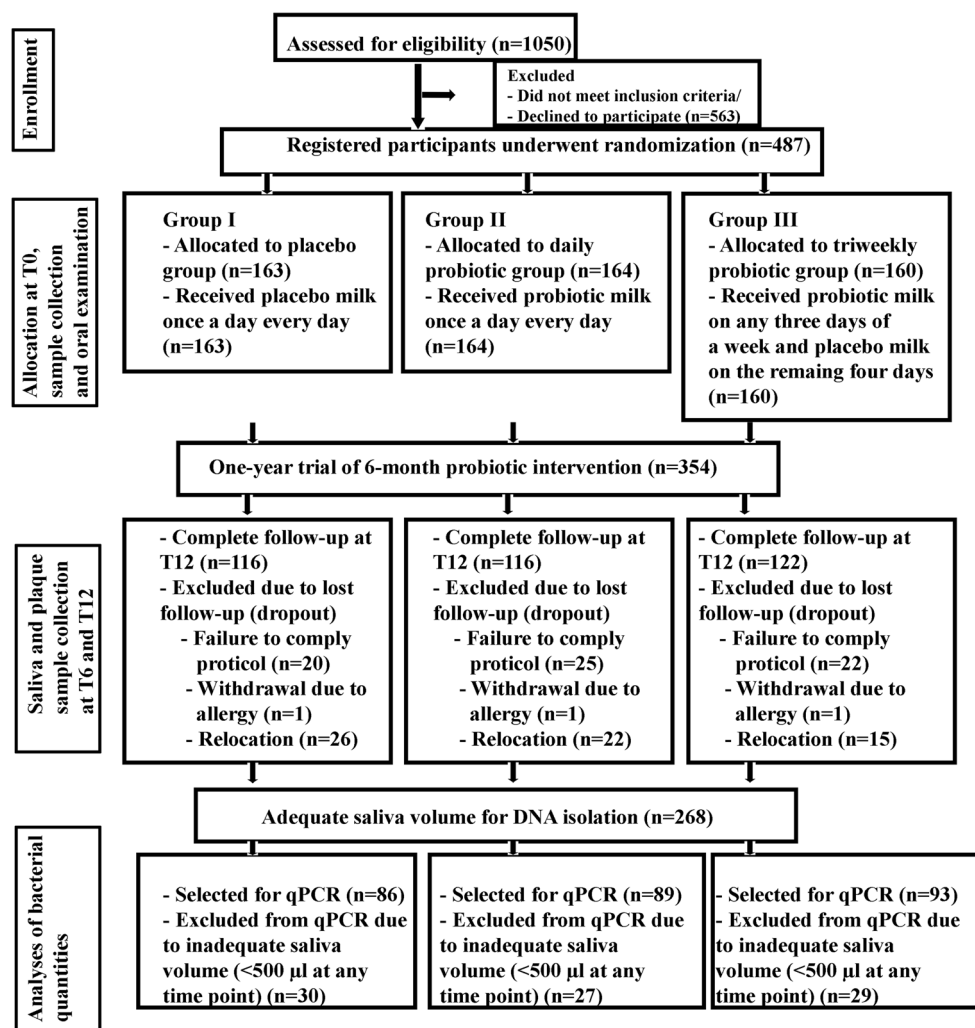
CFU/ml) and plaque ($\log_{10}$ CFU/mg) samples, significantly, but weakly, positive correlations were found in the quantities of *S. mutans* ($r = 0.206$, $p < 0.001$; Fig. 4a) and in those of total lactobacilli ($r = 0.036$, $p < 0.001$; Fig. 4b).

Discussion

This large-scale multicenter trial, in which several hundreds of preschool children were registered, demonstrates the beneficial effect of probiotic supplementation with *L. paracasei* SD1 on a significant reduction in cariogenic bacteria, *S. mutans*, which is in agreement with our previous studies using standard cultivation to quantify salivary mutans streptococci [11–14]. The reduction of *S. mutans* by probiotic consumption is also supported by a number of studies analyzed in three systematic reviews, showing that various probiotic strains could significantly reduce cariogenic mutans streptococci [25–27]. Furthermore, some studies in a review by Zaura and Twetman, 2019 [28], showed that probiotics could even reduce

caries incidence, but the authors suggested that further long-term clinical studies are needed. In this study, we also found that our probiotic strain could decrease caries progression while increase caries regression at T6 and T12, suggesting that reduction of *S. mutans* by probiotic consumption would ultimately lead to impede demineralization while facilitate remineralization processes. The details of these findings will be published in a separate article. The possible mechanism of action for the probiotic *L. paracasei* SD1 may be due to the production of bacteriocin, named "paracasin SD1," which possesses potent antimicrobial activities against cariogenic bacteria (*S. mutans*, *Streptococcus. sobrinus*) and periodontopathogens (*Aggregatibacter actinomycetemcomitans* and *Porphyromonas gingivalis*) as well as *Candida albicans* [7, 8]. Moreover, the inhibitory effect of paracasin SD1 was shown to work in a broad pH range from 3.0 to 8.0 [8]. Our finding is also in line with another proposed inhibitory action of *L. paracasei* by co-aggregation with *S. mutans* to prevent *S. mutans* adherence to the tooth surfaces [29]. The bacterial co-aggregation in saliva results in elimination of *S. mutans* from the oral cavity by swallowing, which corresponds to more significant decreases

Fig. 2 Box plot graphs presenting median quantities along with interquartile ranges (25th to 75th percentiles) of **a** *Streptococcus mutans* in saliva, **b** *Streptococcus mutans* in plaque, **c** total lactobacilli in saliva, **d** total lactobacilli in plaque, **e** total bacteria in saliva and **f** total bacteria in plaque. The measurement units for saliva and plaque samples are $\log_{10}$ CFU/ml and $\log_{10}$ CFU/mg, respectively. Empty, gray, and hatched boxes represent the placebo, daily probiotic, and triweekly probiotic groups, respectively. The horizontal line in each box represents the median of the data, and X within each box represents the mean. Empty circles are outliers. T0, T6, and T12 are the time points at baseline, after 6 months of probiotic intervention, and 6 months after probiotic discontinuation, respectively. *p < 0.0167, **p < 0.0033, ***p < 0.00033

Quantities of *Streptococcus mutans* in oral samples

Quantities of total lactobacilli in oral samples

Quantities of total bacteria in oral samples

Placebo (n=86)   Daily probiotics (n=86)   Triweekly probiotics (n=93)

in the quantities of *S. mutans* observed in the saliva than in the plaque samples (Fig. 3).

This field trial showed that the efficacy of probiotic consumption on *S. mutans* reduction in several childcare centers meets the criteria of a phase 2 trial, defined by a Joint FAO/WHO Working Group on Drafting Guidelines for the Evaluation of Probiotics in Food [30]. In such guidelines, it is recommended that "human trials be repeated by more than
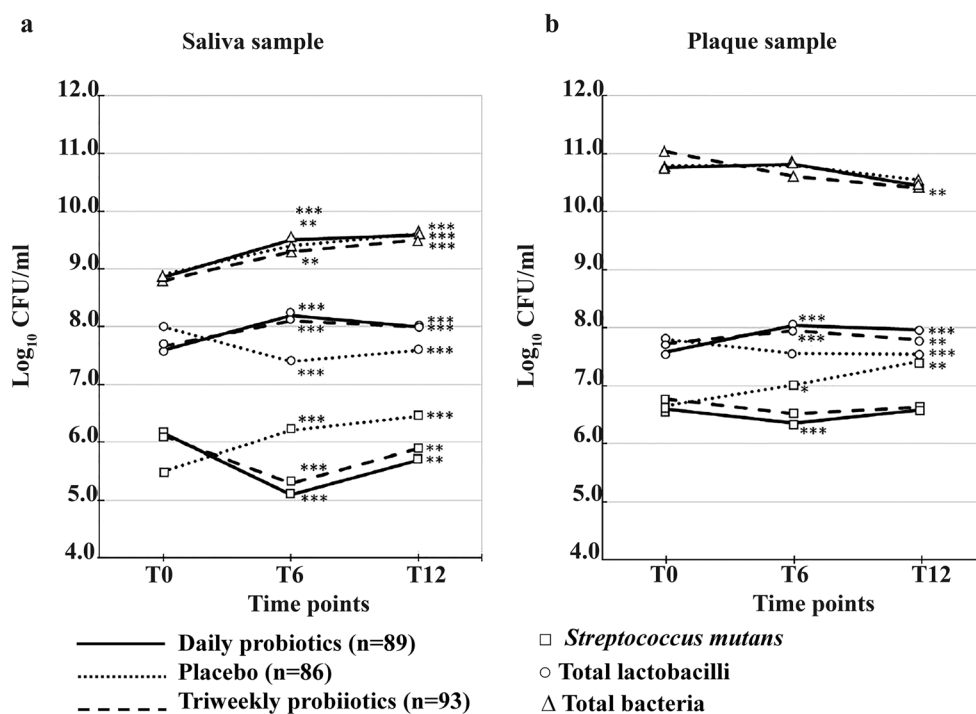
Fig. 3 Linear graphs presenting bacterial quantities as median log₁₀ counts (*y*-axis) of *Streptococcus mutans* (square), total lactobacilli (circle), and total bacteria (triangle) in the **a** saliva and **b** plaque samples. The measurement units for saliva and plaque samples are $\log_{10}$ CFU/ml and $\log_{10}$ CFU/mg, respectively. The dotted, solid, and dashed lines represent the placebo, daily probiotic, and triweekly probiotic groups, respectively. T0, T6, and T12 are the time points at baseline, after 6 months of probiotic intervention and 6 months after probiotic discontinuation, respectively. The significant differences between T6 or T12 and T0 within each group are illustrated. Note that the interquartile ranges are omitted from the linear graphs, but are presented in Table 3. $*p < 0.0167$, $**p < 0.0033$, $***p < 0.00033$

one center for confirmation of results." Furthermore, significant increases in the quantities of total lactobacilli at T6 and T12 compared with T0 imply that *L. paracasei* SD1 administered either daily or triweekly accounts for an increase in the amounts of total lactobacilli in the oral cavity, which can be detected in saliva and constituted in the dental plaque even 6 months after probiotic discontinuation. Accordingly, the beneficial effect on *S. mutans* reduction could be observed at least 6 months after probiotic intervention, possibly as a result of persistent microbial modulation by the probiotic *L. paracasei* SD1, which is consistent with the findings from our previous studies [12, 24]. Such increases in the quantities of total lactobacilli are expected, given that most probiotics are lactobacillus species, and the increases are in line with a previous systematic review and meta-analysis [27]. Due to the possible cariogenicity of lactobacilli, their use for caries prevention may be of concern. However, according to a number of systematic reviews and meta-analyses [25–27] as well as our previous studies [11–14], the use of probiotics is generally considered safe, and neither adverse effects to oral health nor increased caries risks have been reported so far in clinical trials. It is suggested that not all lactobacillus species can induce caries [31], which is in agreement with our finding that only certain lactobacillus species, *Lactobacillus salivarius*, was a strong acid producer [32]. In addition, *L. salivarius* was found to be associated with high caries in children [6].

The ability of *L. paracasei* SD1 to adhere to the tooth surface or to colonize in dental plaque has not yet been tested; however, the ability of *L. paracasei* SD1 to adhere to oral epithelial cells has been previously demonstrated [7]. It is likely that the oral epithelial cells could be a reservoir for *L. paracasei* SD1 to be continuously present in the oral cavity even 6 months after probiotic discontinuation. Moreover, by using an arbitrary primer-PCR method to analyze the bacterial DNA fingerprints, the identical pattern of *L. paracasei* SD1 DNA fingerprints could be found in saliva of volunteers who consumed the probiotic milk [12]. Taken together, early exposure to probiotics, especially during the first 1000 days of life, would have a long-term benefit for prevention of dental caries in young children.

The dosing interval (daily or triweekly) was designed to evaluate the minimal dosage required for the presence and persistence of probiotic benefits over microbial compositions. Our results suggest that the benefits of triweekly consumption are not different from those of daily consumption in terms of the significant reduction of *S. mutans* quantities or the significant increase in total lactobacilli quantities. Both triweekly and daily probiotic groups showed a similar trend for the reduction of *S. mutans* in both the saliva and plaque samples at T6 and T12 compared with T0, although the daily probiotic group showed greater decreases in the quantities of *S. mutans* than did the triweekly group (Fig. 3). Therefore, the inhibitory action of *L. paracasei* SD1 against *S. mutans* was found to be greater and more consistent in the

Table 3 Summary of median quantities together with interquartile ranges of *Streptococcus mutans*, total lactobacilli, and total bacteria in the saliva and plaque samples at baseline (T0), after 6 months of probiotic intervention (T6), and 6 months after probiotic discontinuation (T12)

Bacteria	Median quantities (interquartile range 25th-75th)					
	Saliva samples ($\log_{10}$ CFU/ml)			Plaque samples ($\log_{10}$ CFU/mg)		
	T0	T6	T12	T0	T6	T12
S. mutans						
I (placebo)	5.50 (4.69–6.02)	6.21 (5.78–7.00)***	7.43 (6.81–7.87)**	6.66 (5.97–7.65)	7.02 (6.48–7.76)*	6.45 (5.78–7.05)***
II (daily probiotic)	6.16 (5.57–7.00)	5.10 (4.56–5.69)***	6.59 (6.08–7.32)	6.60 (6.15–7.41)	6.36 (5.60–7.08)**	5.70 (5.33–6.74)**
III (triweekly probiotic)	6.11 (5.55–6.85)	5.30 (4.97–5.74)***	6.63 (5.99–7.28)	6.77 (6.05–7.44)	6.52 (5.72–7.22)	5.90 (5.40–6.56)**
Total lactobacilli						
I (placebo)	8.00 (7.55–8.32)	7.40 (6.91–7.80)***	7.55 (5.82–8.06)**	7.81 (7.39–8.12)	7.56 (7.11–7.97)	7.60 (6.78–8.05)***
II (daily probiotic)	7.60 (7.25–7.99)	8.20 (7.87–8.66)***	7.96 (7.60–8.29)***	7.58 (7.15–8.09)	8.04 (7.71–8.55)***	8.00 (7.60–8.48)***
III (triweekly probiotic)	7.67 (7.08–7.90)	8.10 (7.72–8.50)***	7.79 (7.34–8.17)*	7.73 (7.20–8.01)	7.95 (7.54–8.38)***	8.00 (7.55–8.56)*
Total bacteria						
I (placebo)	8.90 (8.40–9.80)	9.40 (8.80–10.30)**	10.55 (9.69–11.23)	10.80 (9.60–11.69)	10.80 (9.88–11.46)	9.61 (9.00–10.30)**
II (daily probiotic)	8.85 (8.31–9.48)	9.50 (8.69–10.91)***	10.44 (9.55–11.39)	10.76 (9.63–11.77)	10.82 (9.87–11.41)	9.58 (8.69–10.55)***
III (triweekly probiotic)	8.80 (8.36–9.60)	9.30 (8.71–10.12)*	10.40 (9.24–11.34)**	11.04 (9.82–11.57)	10.61 (9.70–11.56)	9.50 (8.80–10.30)*

The significant differences at T6 or T12 compared with T0 were determined using the Wilcoxon signed rank test with Bonferroni adjustment. *$p < 0.0167$, **$p < 0.0033$, ***$p < 0.00033$

daily probiotic than the triweekly probiotic group, suggesting that when promising and stable inhibition against cariogenic bacteria from probiotics is expected, the daily dosage is preferable, yet the triweekly dosage is still acceptable in some circumstances.

Even by stratified randomization, the placebo group in our study began with a significantly smaller median quantity of *S. mutans* (Fig. 2a), and a significantly greater median quantity of total lactobacilli (Fig. 2b), than those of the two probiotic groups at T0 in the saliva samples. These microbial differences among the three intervention groups may have occurred by chance. However, when children in the placebo group were 6 months and one year older, the median quantities of *S. mutans* and of total lactobacilli were, instead, significantly greater and smaller, respectively, than in the other two probiotics groups in both the saliva and plaque samples (Fig. 2a, b). This suggests that without the beneficial effects from consumption of *L. paracasei* SD1, the quantities of *S. mutans* in the placebo group tended to continually increase with age in both the saliva and plaque samples, whereas the quantities of total lactobacilli in this group tended to decrease. Besides the aforementioned changes in the quantities of *S. mutans* and total lactobacilli, total bacteria in the saliva samples of the placebo group tend to increase with age (Fig. 3a). All of these microbial changes in the placebo group are consistent with the results of Damle et al., 2016 [33], which demonstrated that children tend to have high levels of oral bacteria, especially mutans streptococci, when they are older.

When data on the quantities of *S. mutans* (Fig. 4a) and those of total lactobacilli (Fig. 4b) in the three intervention groups at the three periods were pooled, weakly, albeit significantly, positive correlations, were found between the saliva and plaque samples. To the best of our knowledge, there has not yet been a correlation study comparing the microbial quantities between the two oral samples upon probiotic administration. The weak correlations can be explained by the fact that microorganisms live in the plaque biofilm as a somewhat static and stable community compared with much more dynamic changes and fluctuations in both types and quantities of microorganisms in the saliva [34]. Moreover, all tooth surfaces are constantly bathed in the saliva so that it may better reflect changes in the microbial compositions than would the plaque samples [33]. This is confirmed by more drastic alterations in the amounts of both *S. mutans* and total lactobacilli found in the saliva samples than in the plaque samples upon probiotic administration (Fig. 3). However, saliva collection is not easy in young children due to their difficulty in spitting and uncooperative behaviors. This is why only about three quarters of all saliva samples collected from eligible children (Fig. 1) had an adequate volume, i.e., at least 500 µl, required for DNA extraction [35].

The reason why *L. fermentum* was used to establish a standard curve for total lactobacilli is due to its predominance (>80%) among other lactobacilli strains found in the oral cavity of Thai preschool children [6], so the quantities of *L. fermentum*
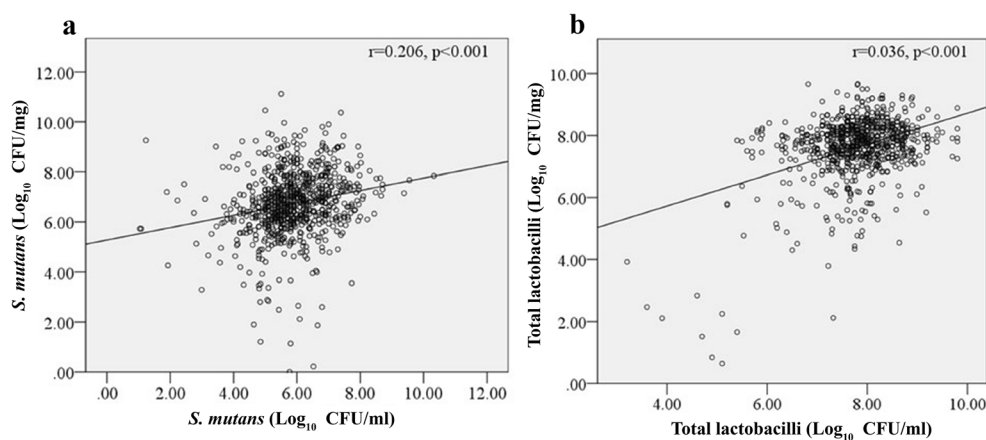
Fig. 4 Significantly, but weakly, positive correlations of **a** *Streptococcus mutans (S. mutans)* quantities and **b** total lactobacilli quantities from pooled data from the three intervention groups (placebo, daily probiotics, and triweekly probiotics) at all three periods (at baseline, after 6 months of probiotic intervention and 6 months after probiotic discontinuation) between the plaque (*y*-axis) and saliva (*x*-axis) samples. Regression lines shows positive correlations of *S. mutans* (**a**) and total lactobacilli (**b**) quantities between the plaque and the saliva samples

could well represent those of total lactobacilli in the saliva and plaque samples. Furthermore, we chose to amplify DNA of total lactobacilli after consumption of milk supplemented with the probiotic *L. paracasei* SD1 was due to the limitation to design a primer pair specific only for the *L. paracasei* SD1 because of the almost identical sequences between the *paracasei* and the *casei* species [24]. Moreover, our previous study had shown a positive correlation between the quantities of total lactobacilli and those of *L. paracasei/casei*, as being quantified by qPCR [24]. A significant increase in the amounts of total lactobacilli after consumption of the probiotic *L. paracasei* SD1 was also demonstrated by a cultivation method [11]. Consumption of the *L. paracasei* SD1 would, therefore, mainly contribute to an increase in the DNA amounts of total lactobacilli observed in the saliva and plaque samples of both probiotic groups (Fig. 3a, b, respectively), indicating that total lactobacilli can be used as a surrogate for monitoring changes in the quantities of the probiotic *L. paracasei* SD1. Regarding future studies, it is of our interest to determine the beneficial effects on both *S. mutans* and caries reduction by a combination of *L. paracasei* SD1 with the other probiotic strain in a prospective study, which lasts longer than 6 months after probiotic discontinuation. In addition, the effects of consumption of the probiotic *L. paracasei* SD1 on salivary flow and buffering capacity are needed to be further examined, although we have previously shown that there was no difference in salivary pH in the probiotic group compared with that in the placebo group [11, 12].

Conclusions

In summary, a 6-month course of daily and triweekly consumption of the probiotic, *L. paracasei* SD1, significantly reduces the quantities of the cariogenic bacteria, *S. mutans*, in both saliva and plaque, and the decreasing effect persists for at least 6 months after discontinuation. Although the daily consumption yields a better benefit in terms of *S. mutans* reduction than the triweekly consumption, the triweekly dosage is still acceptable and is a more practical method of implementation to reduce the cost of probiotic milk in some developing countries. Nevertheless, in children with high caries risk, the daily consumption of probiotics is highly recommended to better control the quantity of *S. mutans* at the initial phase.

Compliance with ethical standards

Conflict of interest The authors declare that they have no conflict of interest.

Ethical approval All procedures involving human participants in this trial were in accordance with the ethical standards of the Ethics Committee, Faculty of Dentistry, Prince of Songkla University (#EC5912-50-L-HR) and the Human Experimentation Committee, Faculty of Dentistry, Chiang Mai University (#10/2018), and with the Declaration of Helsinki (1964) and its later amendments.

Informed consent Informed consent was obtained from all individual participants included in the study.

References

1. Twetman S, Jørgensen MR, Keller MK (2017) Fifteen years of probiotic therapy in the dental context: what has been achieved? J Calif Dent Assoc 45(10):539–545

2. Kassebaum NJ, Bernabe E, Dahiya M, Bhandari B, Murray CJ, Marcenes W (2015) Global burden of untreated caries: a systematic review and metaregression. J Dent Res 94(5):650–658. https://doi.org/10.1177/0022034515573272

3. Hoare A, Marsh PD, Diaz PI (2017) Ecological therapeutic opportunities for oral diseases. Microbiol Spectr 5(4). https://doi.org/10.1128/microbiolspec.BAD-0006-2016

4. Nora AD, Rodrigues CS, Rocha RO, Soares FZM, Braga MM, Lenzi TL (2018) Is caries associated with negative impact on oral health-related quality of life of pre-school children? A systematic review and meta-analysis. Pediatr Dent 40(7):403–411

5. Coqueiro AY, Bonvini A, Raizel R, Tirapegui J, Rogero MM (2018) Probiotic supplementation in dental caries: is it possible to replace conventional treatment? Nutrire 43(1):6–9. https://doi.org/10.1186/s41110-018-0064-3

6. Piwat S, Teanpaisan R, Thitasomakul S, Thearmontree A, Dahlen G (2010) Lactobacillus species and genotypes associated with dental caries in Thai preschool children. Mol Oral Microbiol 25(2):157–164. https://doi.org/10.1111/j.2041-1014.2009.00556.x

7. Teanpaisan R, Piwat S, Dahlen G (2011) Inhibitory effect of oral Lactobacillus against oral pathogens. Lett Appl Microbiol 53(4):452–459. https://doi.org/10.1111/j.1472-765X.2011.03132.x

8. Wannun P, Piwat S, Teanpaisan R (2014) Purification and characterization of bacteriocin produced by oral *Lactobacillus paracasei* SD1. Anaerobe 27:17–21. https://doi.org/10.1016/j.anaerobe.2014.03.001

9. Chooruk A, Piwat S, Teanpaisan R (2017) Antioxidant activity of various oral Lactobacillus strains. J Appl Microbiol 1:271–279. https://doi.org/10.1111/jam.13482

10. Wattanarat O, Makeudom A, Sastraruji T, Piwat S, Tianviwat S, Teanpaisan R, Krisanaprakornkit S (2015) Enhancement of salivary human neutrophil peptide 1-3 levels by probiotic supplementation. BMC Oral Health 15:19. https://doi.org/10.1186/s12903-015-0003-0

11. Teanpaisan R, Piwat S (2014) *Lactobacillus paracasei* SD1, a novel probiotic, reduces mutans streptococci in human volunteers: a randomized placebo-controlled trial. Clin Oral Investig 18(3):857–862. https://doi.org/10.1007/s00784-013-1057-5

12. Teanpaisan R, Piwat S, Tianviwat S, Sophatha B, Kampoo T (2015) Effect of long-term consumption of *lactobacillus paracasei* SD1 on reducing mutans streptococci and caries risk: a randomized placebo-controlled trial. Dent J (Basel) 3(2):43–54. https://doi.org/10.3390/dj3020043

13. Ritthagol W, Saetang C, Teanpaisan R (2014) Effect of probiotics containing *Lactobacillus paracasei* SD1 on salivary mutans streptococci and lactobacilli in orthodontic cleft patients: a double-blinded, randomized, placebo-controlled study. Cleft Palate Craniofac J 51(3):257–263. https://doi.org/10.1597/12-243

14. Pahumunto N, Piwat S, Chankanka O, Akkarachaneeyakorn N, Rangsitsathian K, Teanpaisan R (2018) Reducing mutans streptococci and caries development by *Lactobacillus paracasei* SD1 in preschool children: a randomized placebo-controlled trial. Acta Odontol Scand 76(5):331–337. https://doi.org/10.1080/00016357.2018.1453083

15. Wilson W, Taubert KA, Gewitz M et al (2007) Prevention of infective endocarditis: guidelines from the American Heart Association: a guideline from the American Heart Association Rheumatic Fever, Endocarditis and Kawasaki Disease Committee, Council on Cardiovascular Disease in the Young, and the Council on Clinical Cardiology, Council on Cardiovascular Surgery and Anesthesia, and the Quality of Care and Outcomes Research Interdisciplinary Working Group. J Am Dent Assoc 138(6):739–745 747-760

16. Teanpaisan R, Chooruk A, Wannun A, Wichienchot S, Piwat S (2012) Survival rates of human-derived probiotic Lactobacillus paracasei SD1 in milk powder using spray drying. Songklanakarin J Sci Technol 34:241–245

17. Santos APPD, Soviero VM (2006) Comparison between two visible biofilm indices in the primary dentition. J Clin Pediatr Dent 30(4):292–295. https://doi.org/10.17796/jcpd.30.4.9n1852u276583r3v

18. Santos AP, Sellos MC, Ramos ME, Soviero VM (2007) Oral hygiene frequency and presence of visible biofilm in the primary dentition. Braz Oral Res 21(1):64–69. https://doi.org/10.1590/S1806-83242007000100011

19. Nyvad B, Machiulskiene V, Baelum V (1999) Reliability of a new caries diagnostic system differentiating between active and inactive caries lesions. Caries Res 33(4):252–260. https://doi.org/10.1159/000016526

20. Sellos MC, Soviero VM (2011) Reliability of the Nyvad criteria for caries assessment in primary teeth. Eur J Oral Sci 119(3):225–231. https://doi.org/10.1111/j.1600-0722.2011.00827.x

21. Nyvad B, Baelum V (2018) Nyvad criteria for caries lesion activity and severity assessment: a validated approach for clinical management and research. Caries Res 52(5):397–405. https://doi.org/10.1159/000480522

22. Oho T, Yamashita Y, Shimazaki Y, Kushiyama M, Koga T (2000) Simple and rapid detection of Streptococcus mutans and Streptococcus sobrinus in human saliva by polymerase chain reaction. Oral Microbiol Immunol 15(4):258–262

23. Nadkarni MA, Martin FE, Jacques NA, Hunter N (2002) Determination of bacterial load by real-time PCR using a broad-range (universal) probe and primers set. Microbiology 148(Pt 1):257–266. https://doi.org/10.1099/00221287-148-1-257

24. Pahumunto N, Sophatha B, Piwat S, Teanpaisan R (2019) Increasing salivary IgA and reducing Streptococcus mutans by probiotic *Lactobacillus paracasei* SD1: A double-blind, randomized, controlled study. J Dent Sci. https://doi.org/10.1016/j.jds.2019.01.008

25. Twetman S (2012) Are we ready for caries prevention through bacteriotherapy? Braz Oral Res 26(Suppl 1):64–70. https://doi.org/10.1590/S1806-83242012000700010

26. Twetman S, Stecksén-Blicks C (2008) Probiotics and oral health effects in children. Int J Paediatr Dent 18(1):3–10. https://doi.org/10.1111/j.1365-263X.2007.00885.x

27. Gruner D, Paris S, Schwendicke F (2016) Probiotics for managing caries and periodontitis: Systematic review and meta-analysis. J Dent 48(5):16–25. https://doi.org/10.1016/j.jdent.2016.03.002

28. Zaura E, Twetman S (2019) Critical Appraisal of Oral Pre- and Probiotics for Caries Prevention and Care. Caries Res 53(5):514–526. https://doi.org/10.1159/000499037

29. Lang C, Bottner M, Holz C, Veen M, Ryser M, Reindl A, Pompejus M, Tanzer JM (2010) Specific Lactobacillus/Mutans Streptococcus co-aggregation. J Dent Res 89(2):175–179. https://doi.org/10.1177/0022034509356246

30. Joint Food and Agriculture Organization of the United States/World Health Organization (FAO/WHO) Working Group (2002) Report on Drafting Guidelines for the Evaluation of Probiotics in Food. London Ontario, Canada. http://www.fao.org/3/a-a0512e.pdf. Accessed 27 May 2019

31. Caufield PW, Li Y, Dasanayake A, Saxena D (2007) Diversity of lactobacilli in the oral cavities of young women with dental caries. Caries Res 41(1):2–8. https://doi.org/10.1159/000096099

32. Piwat S, Teanpaisan R, Dahlén G, Thitasomakul S, Douglas CW (2012) Acid production and growth by oral *Lactobacillus* species in vitro. J Investig Clin Dent 3(1):56–61. https://doi.org/10.1111/j.2041-1626.2011.00098.x

33. Damle SG, Loomba A, Dhindsa A, Loomba A, Beniwal V (2016) Correlation between dental caries experience and mutans streptococci counts by microbial and molecular (polymerase chain reaction) assay using saliva as microbial risk indicator. Dent Res J (Isfahan) 13(6):552–559. https://doi.org/10.4103/1735-3327.197035

34. Kilian M, Chapple ILC, Hannig M, Marsh PD, Meuric V, Pedersen AML, Tonetti MS, Wade WG, Zaura E (2016) The oral microbiome – an update for oral healthcare professionals. Br Dent J 221(10):657–666. https://doi.org/10.1038/sj.bdj.2016.865

35. Koni AC, Scott RA, Wang G, Bailey ME, Peplies J, Bammann K, Pitsiladis YP (2011) DNA yield and quality of saliva samples and suitability for large-scale epidemiological studies in children. Int J Obes 35(Suppl 1):S113–S118. https://doi.org/10.1038/ijo.2011.43

Enhancement of human periodontal ligament by preapplication of orthodontic loading

Kittitat Nakdilok,[a] Sarawut Langsa-ard,[b] Suttichai Krisanaprakornkit,[b] Eduardo Yugo Suzuki,[a] and Boonsiva Suzuki[a]
Bangkok and Chiang Mai, Thailand

Introduction: The quantity of remaining periodontal ligament (PDL) on the root surface of donor teeth is essential for the success of tooth autotransplantation. Preapplication of orthodontic loading increases this quantity on rat tooth root surfaces. However, little is known about the effects of preloading on human PDL or the ease of tooth extraction. This study aimed to determine the optimal duration of preloading for enhanced PDL on the root surface of extracted human premolars and for facilitating extraction. **Methods:** Sixty patients received orthodontic preloading with a bracket connected to an archwire on one of their maxillary first premolars for 2, 4, 6, or 8 weeks, whereas the contralateral premolar was not loaded as a control. Premolar extractions were performed with a record of the duration and difficulty of extraction. The extracted premolars were fixed and stained with toluidine blue. Digitized images were recorded under a stereomicroscope, and the percentage of stained PDL was analyzed. **Results:** Orthodontic preloading for 4, 6, and 8 weeks significantly increased the percentage of stained PDL on the root surface compared with the control (P <0.05). The duration and difficulty of extraction were significantly less in preloaded than that of unloaded teeth after 4, 6, and 8 weeks (P <0.05). **Conclusions:** A 4-week duration of orthodontic preloading is suggested as the shortest duration to adequately enhance PDL and ease tooth extraction; both outcomes may be beneficial for tooth autotransplantation. (Am J Orthod Dentofacial Orthop 2020;157:186-93)

The use of premolars extracted because of orthodontic treatment in tooth autotransplantation to replace missing or hopeless teeth has been previously reported in the literature.[1] Compared with osseointegrated dental implants, autotransplantation of a natural tooth has several advantages, including better functional adaptation,[1] alveolar ridge preservation,[2] and esthetics,[3] because the transplanted tooth can maintain periodontal ligament (PDL) homeostasis and normal functional proprioception.[4] Thus, tooth autotransplantation is an ideal choice compared with dental implants if combined therapies between orthodontic tooth movement and tooth autotransplantation are designed for the transplanted tooth.[5,6] However, some complications after tooth autotransplantation can still occur, such as root resorption, dentoalveolar ankylosis, tooth mobility, and periodontal pocket formation.[7] In monkeys, ankylosis of the donor tooth is often due to PDL injury during extraction.[8] Therefore, the quality and quantity of remaining PDL on the root surface of the extracted donor tooth, as well as the ease of extraction (to avoid possible PDL injury) are important factors for the success of tooth autotransplantation.[8]

PDL is a highly vascular and cellular connective tissue situated between the tooth and alveolar bone that provides supportive, attachment, and sensory functions.[9] Because a principal function of the PDL is to anchor the tooth root to the jaw bone and to distribute multidirectional mechanical stresses, such as masticatory forces, it is, perhaps, not surprising that the PDL exhibits features of a shock-absorbing system.[9] Indeed, some of the most interesting features of the PDL are its adaptability to rapidly applied force levels and its remarkable

[a]Department of Orthodontics, Faculty of Dentistry, Bangkokthonburi University, Bangkok, Thailand.
[b]Center of Excellence in Oral and Maxillofacial Biology, Faculty of Dentistry, Chiang Mai University, Chiang Mai, Thailand.
Address correspondence to: Boonsiva Suzuki, Department of Orthodontics, Faculty of Dentistry, Bangkokthonburi University, 16/10 M.2, Taweewattana Rd, Taweewattana District, Taweewattana, Bangkok 10170, Thailand; e-mail, boonsiva.suz@bkkthon.ac.th.

capacity for repair and regeneration.[9] The PDL that remains attached to the root surface is capable of regenerating new PDL after replantation.[10] Moreover, PDL of the transplanted tooth appears to be able to induce bone production, because PDL cells can be genetically differentiated into 3 distinct types of cells,[11] particularly osteoblasts that generate bone around the transplanted tooth.[4]

A few previous studies in an animal model have suggested preapplication of orthodontic force to increase the width of PDL in order to ease tooth extraction, which may decrease damage to PDL during the extraction.[12,13] A previous case report has demonstrated increased mobility of 2 human donor teeth upon orthodontic preloading, as assessed by the Periotest.[14] The increased mobility was shown, immediately, to ease tooth extraction without PDL injury and, after a 1-year follow-up, to have aided in successful tooth autotransplantation. Therefore, it is reasonable to hypothesize that preapplication of orthodontic force to the donor tooth would be useful to increase PDL tissue on the root surface of the preloaded tooth with complete root formation and to reduce PDL injury owing to easier tooth extraction. The objective of this study was to determine an optimal duration for the stimulation of the proliferative activity of PDL tissue on the root surface and the facilitation of extraction after preapplication of orthodontic force for different periods.

MATERIAL AND METHODS

Sixty healthy patients (aged 16-37 years; 21 years, 6 months ± 4 years, 8 months [mean ± standard deviation]; 23 male and 37 female) free from any underlying medical conditions, as revealed by their medical history, were recruited from the Postgraduate Clinic, Faculty of Dentistry, Bangkokthonburi University, Thailand with written informed consent. The study protocol was approved by the human ethics committee of Bangkokthonburi University (approval number: 5/2561). The patients were planned for extractions of their maxillary first premolars as part of orthodontic treatment. The inclusion criteria were that patients had a sound first premolar in each quadrant without caries or restorations, were not taking any steroidal or nonsteroidal anti-inflammatory drugs during force application because of their inhibitory effects on PDL and bone remodeling,[15] and had good oral hygiene and healthy periodontium with pocket depths ≤3 mm. The exclusion criteria were an asymmetrical arch form or any root malformations on either side, such as root dilaceration, which might result in a complicated extraction of the maxillary

first premolars, as evidenced by intraoral and extraoral radiographs.

By drawing sealed randomization envelopes prepared by a person not involved in this study, 60 patients were randomly assigned to the 4 groups (15 each), which comprised orthodontic preloading on either side of their maxillary first premolars for 2, 4, 6, or 8 weeks, respectively, whereas the contralateral premolar was not loaded as a control. The reason for choosing only maxillary premolars in this study was that local anesthesia of mandibular premolars by inferior alveolar nerve block is considered technically more challenging and less predictable than that of local infiltration[16] for the upper premolars. Hence, the duration and difficulty of extraction between different cases and quadrants could not be controlled. The preloading force was obtained from a 0.016-inch improved superelastic nickel-titanium alloy wire (Sentalloy, Tomy International, Tokyo, Japan) inserted into a slot (Roth prescription; 0.018 × 0.025-inch), attached to a preadjusted edgewise bracket (Tomy International), bonded on the maxillary first premolar using compomer (Grengloo, Ormco, Orange, Calif; Fig 1, *A*) whereas the contralateral premolar was not connected to the wire (Fig 1, *B*). The inserted wire was tied with the bracket using an elastomeric ring (DynaFlex, Emergo Group, the Hague, the Netherlands; Fig 1, *A*). According to the manufacturer's instructions (Tomy International), the wire has the shape memory effect that uses body temperature to generate continuous light force (100 g) with a deflection of 0.5-1.8 mm.

After orthodontic preloading for the indicated times, the wire was removed, followed by removal of the bracket on the preloaded tooth, using a bracket remover (Tomy International). The tooth surface was cleaned and polished with white stone (Shofu, Kyoto, Japan). Infiltration with 4% articaine with epinephrine 1:100,000 (Septanest SP, Septodont, Saint-Maur-des-Fossés, France) was conducted through the buccal vestibule on both sides. Premolar extractions were performed by the same surgeon, who was blinded to the tooth condition, with a record for the duration of the extraction procedure that began when the forceps (F150, Hu-Friedy, Chicago, Ill) was clamped on the tooth and ended when the tooth was removed out of its socket. After tooth removal, the surgeon was asked to score on a modified 4-point Likert scale (1 = very easy; 2 = easy; 3 = difficult; 4 = very difficult) based on the surgeon's perception.[17] After extraction, 500 mg of acetaminophen (paracetamol GPO, Government Pharmaceutical Organization, Bangkok, Thailand) was prescribed for the patients every 6 hours as needed for pain.
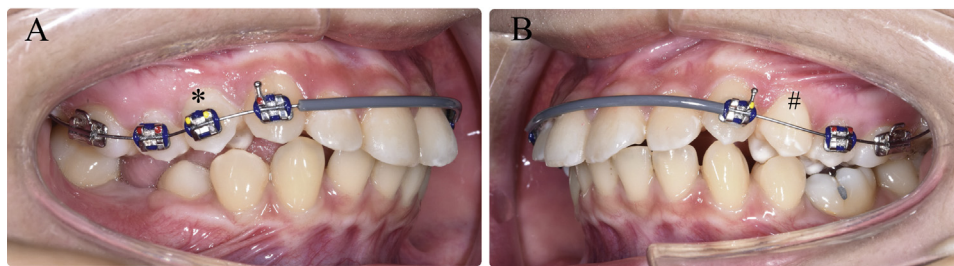
Fig 1. Intraoral photographs. **A,** Preloaded, upper right first premolar (*). **B,** Unloaded control, upper left first premolar (#).

Staining with toluidine blue was performed to determine the amount of PDL tissue with proliferative cells on the root surface using a protocol modified from Iwata et al.[18] Yee[19] reported that the number of mitotic cells representing PDL cell proliferation was increased after orthodontic loading of rats' teeth for 24 hours. In addition, cells with increased mitotic activity are usually detected by toluidine blue staining.[20] In brief, the extracted teeth were washed gently in phosphate-buffered saline (PBS), pH 7.2, and fixed within 30 minutes after extraction with 10% buffered formalin solution in 50-ml tubes (Corning, Inc., Corning, NY) for 24 hours. The teeth were then immersed in PBS for 2 days, stained with 0.04% (w/v) toluidine blue (Sigma-Aldrich, St Louis, Mo) for 10 minutes, and destained with 4 ml of PBS, which was changed daily for 14 days. After destaining, the teeth were left to air dry.

The buccal, palatal, mesial, and distal surfaces of the stained roots were observed under a stereomicroscope (Olympus SZX7; Olympus, Tokyo, Japan), and a digitized image of each root surface was recorded perpendicular to the tooth axis using a charge-coupled device (Olympus E-330; Olympus) attached to the stereomicroscope. By using ImageJ software version 1.51r (National Institute of Health, Bethesda, Md), which is commonly used in previous studies to quantify stained images,[18,21,22] the area of stained PDL in each digital image, represented by blue pixels regardless of their staining intensities, was analyzed and expressed as the percentage of the stained area against the total area, which is a combination of both blue and white pixels, representing the unstained area. The mean percentage of stained PDL in each tooth was derived from an average value of the percentages of stained PDL from all 4 surfaces of that tooth.

Statistical analysis

Differences in the percentage of stained PDL on the root surface, in the duration and ease of tooth extraction between control and preloaded teeth for the various durations of preloading, were analyzed using the paired *t*-test. Two-way analysis of variance (ANOVA) was used for the analysis of the interactions between preloading or control and the 4 periods of orthodontic preloading. Comparisons between 2 different time points within the same group were analyzed using one-way ANOVA (Duncan's multiple comparison test). Correlations between these different parameters were analyzed using either the Spearman or the Pearson correlation test. The statistical analyses were conducted using SPSS version 17.0 (IBM Corporation, Armonk, NY). *P* values of <0.05 were considered statistically significant.

RESULTS

Because of relocation of 2 patients in the 2-week preloading group, as well as root tip fracture of the unloaded control teeth during extraction in 5 patients in the preloading groups for 2 (3 patients) and for 8 (2 patients) weeks, both preloaded and unloaded control teeth of these 7 patients were excluded from analyses of the duration of extraction and PDL staining. Therefore, the number of remaining patients in the preloading groups for 2 and 8 weeks was 10 and 13, respectively. However, from the sample size calculation determined by G*Power software (version 3.1.9.2; Franz Faul, Universität Kiel, Kiel, Germany) with the effect size = 0.59 derived from the preliminary data, $\alpha = 0.05$ and $1-\beta = 0.95$, the calculated number of patients in each period of preloading should be ≥10. In addition, no difference in average ages was found among the 4 preloading groups, including 2, 4, 6, and 8 weeks (data not shown).

It was demonstrated that the duration of average extraction time in preloaded teeth determined from all 4 periods of orthodontic preloading (20.78 ± 1.94 seconds) was reduced to nearly 50% compared with that in unloaded control teeth (40.11 ± 5.29 seconds). The mean duration of
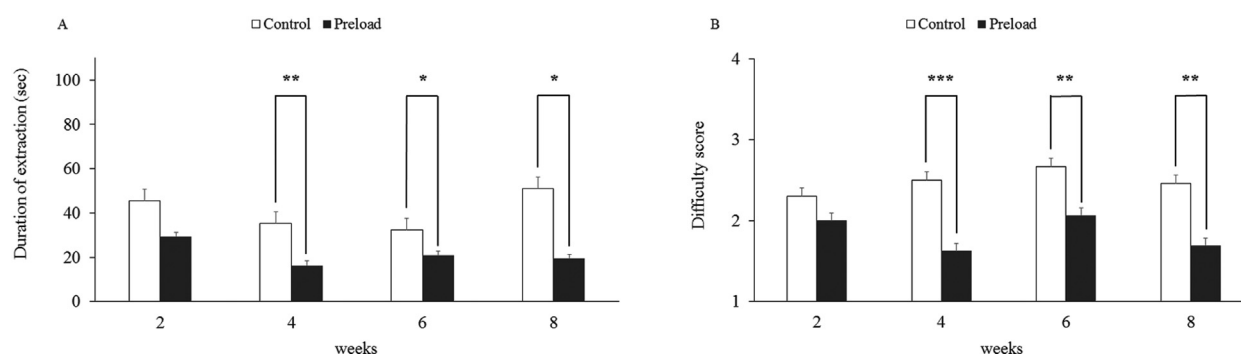
Fig 2. Facilitated tooth extraction by orthodontic preloading force. **A,** The bar graph shows a significant reduction in the duration of extraction in seconds (sec) upon preloading for 4, 6, and 8 weeks. **B,** The bar graph shows a significant decrease in the difficulty score upon preloading at 4, 6, and 8 weeks. The following indicate statistical significance: $*P < 0.05$, $**P < 0.01$, and $***P < 0.001$. Error bars represent standard errors.

extraction in preloaded teeth was significantly less than that of unloaded control teeth at 4, 6, and 8 weeks, but not at 2 weeks, of orthodontic preloading ($P < 0.05$; Fig 2, A). Similarly, the mean scores for the difficulty of extraction were significantly lower in preloaded than those of unloaded control teeth at 4, 6, and 8 weeks ($P < 0.01$; Fig 2, B).

Representative images of stained PDL tissue on the root surface of a preloaded tooth and an unloaded control are illustrated in Figure 3. The areas of stained PDL, irrespective of staining intensity, on all 4 root surfaces in preloaded teeth, were more significant than that of unloaded control teeth. When the average percentages of stained PDL on the 4 root surfaces from 4 different periods of orthodontic preloading were determined and compared between preloaded, and unloaded control groups, it was shown that the average percentage of stained PDL in preloaded teeth (75.67 ± 2.06) was increased by approximately 13% compared with the unloaded control teeth (63.13 ± 2.64). When the percentages of stained PDL on the combined 4 root surfaces in each period of orthodontic preloading were determined and compared, the percentages of stained PDL were significantly increased after orthodontic preloading for 4, 6, and 8 weeks, but not for 2 weeks, compared with the control ($P < 0.05$; Fig 4). When the percentages of stained PDL on each of the 4 root surfaces in each period of orthodontic preloading were compared between preloaded and unloaded groups, the percentages of stained PDL were significantly increased in at least 3 of the 4 root surfaces at 4, 6, and 8 weeks ($P < 0.05$; data not shown).

Furthermore, using a 2-way ANOVA, no interactions between either preloading or control and the 4 periods

of orthodontic preloading were found ($P = 0.379$). In the preloading group, significant increases in the percentages of stained PDL were found at 4 and 8 weeks compared with that at 2 weeks ($P < 0.01$; Fig 4). However, in the control group, no differences in the percentages of stained PDL were found among the 4 periods (Fig 4), indicating that similar amounts of stained PDL remaining on the root surfaces after premolar extraction in the control group are about the same despite different individuals recruited for each period.

When correlations between each pair of the 3 parameters were determined, it was demonstrated that a significant and positive correlation was found between the duration and the difficulty of extraction ($r = 0.689$; $P < 0.001$; Fig 5, A), whereas a significant but negative correlation was found between the duration and the percentage of stained PDL ($r = -0.306$; $P < 0.05$; Fig 5, B). The correlation between the difficulty score and the percentage of stained PDL was not found to be statistically significant (Fig 5, C).

DISCUSSION

In this study, the preapplication of orthodontic loading facilitated tooth extraction by significantly lowering both the duration and the difficulty score of extraction at 4, 6, and 8 weeks, but not at 2 weeks (Fig 2). Consistent, significant increases in the percentages of stained PDL in preloaded premolars compared with unloaded premolars were found at 4, 6, and 8 weeks, but not at 2 weeks (Fig 4). Moreover, orthodontic preloading for 4 weeks yielded significantly higher percentages of stained PDL than that for 2 weeks (Fig 4). Consequently, a 4-week duration of orthodontic preloading is suggested by this study to be the shortest
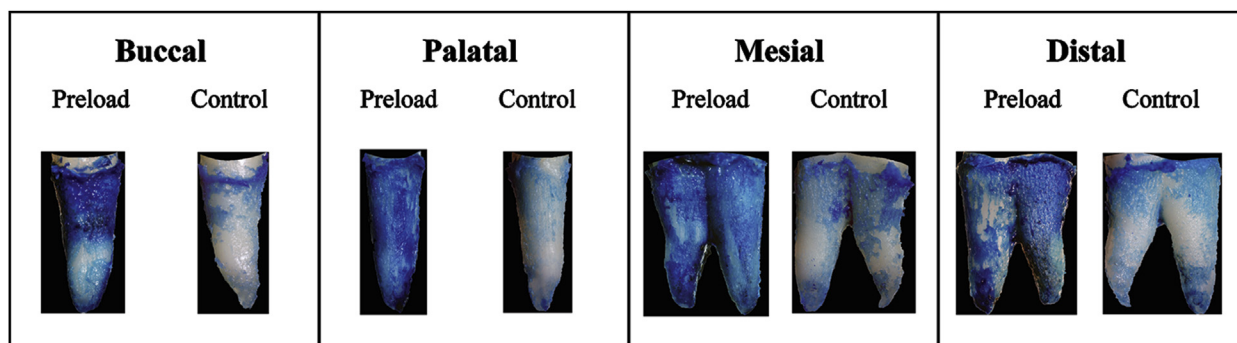
Fig 3. Representative images of PDL stained with toluidine blue on the 4 root surfaces, buccal, palatal, distal and mesial, from a preloaded tooth for 4 weeks and the unloaded control tooth.
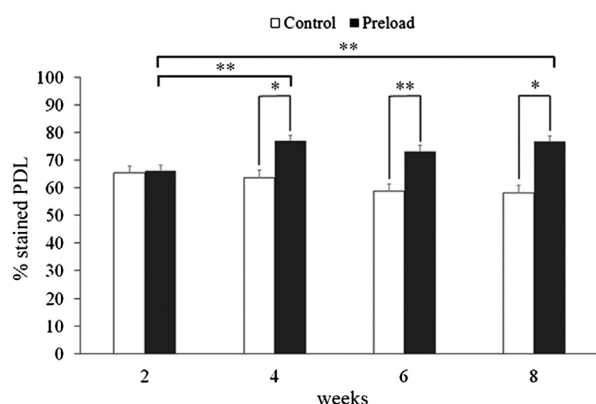

Fig 4. Significant enhancement of PDL upon orthodontic preloading force for at least 4 weeks. Note significant increases in the percentages of stained PDL on the root surfaces of preloaded teeth for 4 and 8 weeks compared with that for 2 weeks. *, ** indicate a statistically significant difference at $P < 0.05$ and $P < 0.01$, respectively. Error bars represent standard errors.

duration for both ease of tooth extraction and enhancement of PDL, both of which outcomes may increase the success rate of tooth autotransplantation. Choi et al[23] have previously reported a significant enhancement in the survival rate of intentional tooth replantation from 91.2% to 98.1% by applying extrusive force before extraction. We speculate that this increase in the survival rate, resulting from preapplication of extrusive force, is due to increased amounts of PDL, as shown in our study; however, it is not possible to replant a tooth stained with toluidine blue back into the alveolar socket.

Tooth autotransplantation is considered an accepted treatment with a 5-year survival rate of around 90% in transplanted premolars with incomplete root formation.[24,25] However, the 5-year survival rate of the transplanted premolars with complete root formation drops

to 60%[24] to 84%[26] because of decreased PDL healing and increased root resorption. Moreover, PDL tissue can be damaged by conventional extraction, which results in several undesirable complications, such as root resorption and dentoalveolar ankylosis. Up to the present, a few methods for enhancing PDL tissue in extracted teeth with complete root formation have been introduced to reduce complications from damaged PDL or denuded root surface, methods such as PDL regeneration by cell culture[18] and preapplication of orthodontic force.[13,23] However, in this study a preloading force for different periods was chosen for an investigation of the remaining PDL tissue because PDL regeneration by cell culture[18] is not clinically practical because there is an increased risk of possible contamination of the cells during the transfer from the mouth to the culture plate.

In the present study, orthodontic preloading for 4, 6, and 8 weeks significantly reduced the duration of extraction. This finding differs from that shown by Choi et al,[23] in which they found no significant difference in the duration of extraction by using an atraumatic forceps technique between preloaded teeth with 50-g orthodontic extrusive force for 2-3 weeks and unloaded control teeth. This discrepancy may be explained by different periods (4-8 vs 2-3 weeks), magnitudes (100 vs 50 g) and types (leveling vs extrusion) of orthodontic preloading used in our study and theirs, respectively. However, in terms of the difficulty of extraction, our finding is consistent with that of Rai and Yadav,[17] who found a significant reduction in the difficulty of extraction in preloaded premolars with leveling orthodontic force. In another study,[13] preapplication of orthodontic force led to the widening of PDL spaces and alveolar sockets. Such widening of PDL spaces and alveolar sockets may be the reason why preapplication of orthodontic force results in facilitated extraction.
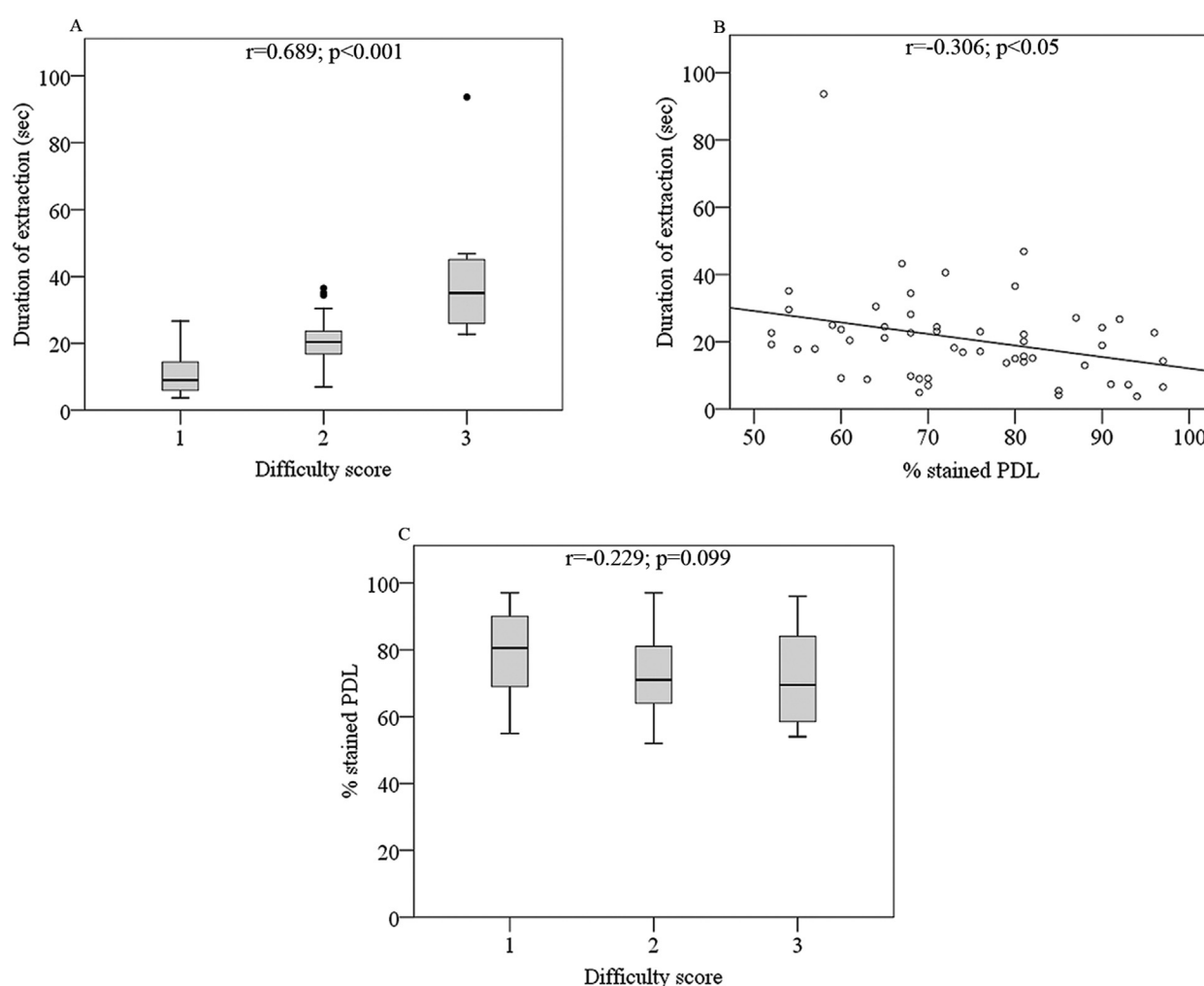
Fig 5. A, Significant and positive correlation between the duration in seconds and the difficulty score of extraction. **B,** Significant but inverse correlation between the duration of extraction and the percentage of stained PDL. **C,** No significant correlation between the difficulty score of extraction and the percentage of stained PDL. Small *black circles* in A represent outliers; *horizontal lines* in **A** and **C** within the boxes represent medians; a *regression line* is shown in **B**.

Staining with toluidine blue is usually recommended to detect cell proliferation.[20] Consequently, stained PDL tissue on the root surface may imply PDL cell proliferation, whereas unstained areas may represent PDL tissue without cell proliferation. In terms of the amounts of proliferative PDL tissue on the root surface, our study demonstrated significant enhancement of human proliferative PDL tissue by orthodontic preloading for at least 4 weeks. This finding corresponds with that demonstrated by Suzaki et al,[13] in which attached PDL was abundant on the root surface after force application in a rat model. Choi et al[23] suggested that PDL volume is increased on the root surface of preloaded teeth; however, there was no quantitative assessment reported in

their study. Because leveling of orthodontic force was used in this study, it is appropriate to determine the overall percentages of stained PDL from the 4 root surfaces rather than to evaluate the percentage in each root surface. In addition, assessment of the combined percentage from the 4 root surfaces (Fig 4) yielded a 3-dimensional perspective of stained PDL as a whole.

When correlations between each pairing of the 3 parameters were analyzed, a significant and positive correlation was found between the duration and the difficulty of extraction. This correlation is logical because a surgeon who spends less time on the extraction of preloaded premolars would perceive the extraction as being easy. Furthermore, the inverse correlation between

the duration and the percentage of stained PDL was found to be significant. However, there was only a trend for the inverse correlation between the difficulty score and the percentage of stained PDL (Fig 5, *C*). These negative relationships imply that the facilitated tooth extraction could avoid PDL injury and then preserve more PDL tissue on the root surface.

In this study, both enhanced PDL on the root surface of extracted human premolars and facilitated tooth extraction after preloading have been demonstrated, which are clinically crucial for cases that tooth autotransplantation has been planned. It is essential to avoid any damage of the PDL on the root surface of the donor tooth that is used for autotransplantation. Moreover, fracture of root tips often complicates extraction of maxillary biradicular premolars, as evidenced in the unloaded control teeth of our preloading groups at 2 and 8 weeks, and their removal could lead to increased alveolar bone destruction, especially for thin buccal plate that would lead to a buccal bone defect and compromise the treatment outcome. Therefore, orthodontic preloading to facilitate tooth extraction would be useful for preventing PDL damage of the donor tooth and preserving the alveolar bone.

In the present study, only conventional 0.018-inch pre-adjustable edgewise brackets combined with 0.016-inch improved superelastic nickel-titanium alloy archwires were used in order to standardize the preloading procedures. The use of other different bracket systems, such as the self-ligating brackets in combination with different archwire sizes, may yield different results in terms of PDL enhancement because of the difference in friction between the bracket types. Additional studies are required to clarify the possibility of different findings. Furthermore, the findings gained from this study, based on both clinical and laboratory findings, could be fundamental for conducting future clinical research that would help determine the benefits of orthodontic preloading for an increase in the survival rate of tooth autotransplantation.

CONCLUSIONS

Orthodontic preloading force for 4 weeks is proposed to be an appropriate duration for facilitated tooth extraction and PDL tissue enhancement.

REFERENCES

1. Slagsvold O, Bjercke B. Indications for autotransplantation in cases of missing premolars. Am J Orthod 1978;74:241-57.
2. Czochrowska EM, Stenvik A, Album B, Zachrisson BU. Autotransplantation of premolars to replace maxillary incisors: a comparison with natural incisors. Am J Orthod Dentofacial Orthop 2000;118:592-600.
3. Zachrisson BU, Stenvik A, Haanaes HR. Management of missing maxillary anterior teeth with emphasis on autotransplantation. Am J Orthod Dentofacial Orthop 2004;126:284-8.
4. Tsukiboshi M. Autotransplantation of teeth: requirements for predictable success. Dent Traumatol 2002;18:157-80.
5. Choi YJ, Han S, Park JW, Lee DW, Kim KH, Chung CJ. Autotransplantation combined with orthodontic treatment to restore an adult's posttraumatic dentition. Am J Orthod Dentofacial Orthop 2013;144:268-77.
6. Fujita K, Kanno Z, Otsubo K, Soma K. Autotransplantation combined with orthodontic treatment in adult patients. Orthod Waves 2008;67:128-34.
7. Kokai S, Kanno Z, Koike S, Uesugi S, Takahashi Y, Ono T, et al. Retrospective study of 100 autotransplanted teeth with complete root formation and subsequent orthodontic treatment. Am J Orthod Dentofacial Orthop 2015;148:982-9.
8. Andreasen JO, Kristerson L. The effect of limited drying or removal of the periodontal ligament. Periodontal healing after replantation of mature permanent incisors in monkeys. Acta Odontol Scand 1981;39:1-13.
9. Lekic P, McCulloch CA. Periodontal ligament cell population: the central role of fibroblasts in creating a unique tissue. Anat Rec 1996;245:327-41.
10. Andreasen JO. Periodontal healing after replantation and autotransplantation of incisors in monkeys. Int J Oral Surg 1981;10:54-61.
11. Yamamura T, Shimono M, Koike H, Terao M, Tanaka Y, Sakai Y, et al. Differentiation and induction of undifferentiated mesenchymal cells in tooth and periodontal tissue during wound healing and regeneration. Bull Tokyo Dent Coll 1980;21:181-221.
12. Qu H, Saito S, Morohashi T, Ohmae M, Seki K, Yamada S, et al. Effects of pre-transplantable jiggling force on root resorption of the experimental autotransplanted of teeth in vivo. Orthod Waves 2001;60:213-25.
13. Suzaki Y, Matsumoto Y, Kanno Z, Soma K. Preapplication of orthodontic forces to the donor teeth affects periodontal healing of transplanted teeth. Angle Orthod 2008;78:495-501.
14. Cho JH, Hwang HS, Chang HS, Hwang YC. Application of orthodontic forces prior to autotransplantation—case reports. Int Endod J 2013;46:187-94.
15. Bartzela T, Türp JC, Motschall E, Maltha JC. Medication effects on the rate of orthodontic tooth movement: a systematic literature review. Am J Orthod Dentofacial Orthop 2009;135:16-26.
16. Hargreaves KM, Keiser K. Local anesthetic failure in endodontics: mechanisms and management. Endod Top 2002;1:26-39.
17. Rai AK, Yadav BK. Facilitating orthodontic teeth extraction–a technique suggestion. Saudi J Dent Res 2016;7:96-100.

18. Iwata T, Mino C, Kawata T. In vitro proliferation of periodontal ligament-like tissue on extracted teeth. Arch Oral Biol 2017;75: 31-6.

19. Yee JA. Response of periodontal ligament cells to orthodontic force: ultrastructural identification of proliferating fibroblasts. Anat Rec 1979;194:603-14.

20. Chieco P, Pagnoni M, Romagnoli E, Melchiorri C. A rapid and simple staining method, using toluidine blue, for analysing mitotic figures in tissue sections. Histochem J 1993;25:569-77.

21. Jensen EC. Quantitative analysis of histological staining and fluorescence using ImageJ. Anat Rec 2013;296:378-81.

22. Grove C, Jerram DA. jPOR: an ImageJ macro to quantify total optical porosity from blue-stained thin sections. Comput Geosci 2011;37:1850-9.

23. Choi YH, Bae JH, Kim YK, Kim HY, Kim SK, Cho BH. Clinical outcome of intentional replantation with preoperative orthodontic extrusion: a retrospective study. Int Endod J 2014;47: 1168-76.

24. Andreasen JO, Paulsen HU, Yu Z, Schwartz O. A long-term study of 370 autotransplanted premolars. Part III. Periodontal healing subsequent to transplantation. Eur J Orthod 1990;12:25-37.

25. Schwartz O, Bergmann P, Klausen B. Resorption of autotransplanted human teeth: a retrospective study of 291 transplantations over a period of 25 years. Int Endod J 1985;18:119-31.

26. Sugai T, Yoshizawa M, Kobayashi T, Ono K, Takagi R, Kitamura N, et al. Clinical study on prognostic factors for autotransplantation of teeth with complete root formation. Int J Oral Maxillofac Surg 2010;39:1193-203.

Reduced ADAM8 levels upon non-surgical periodontal therapy in patients with chronic periodontitis

Tanawat Nimcharoen[a], Win Pa Pa Aung[b], Anupong Makeudom[b], Thanapat Sastraruji[b],
Sakornrat Khongkhunthian[a,b], Benyapha Sirinirund[a], Suttichai Krisanaprakornkit[b,c],
Pattanin Montreekachon[a,b,*]

[a] Department of Restorative Dentistry and Periodontology, Faculty of Dentistry, Chiang Mai University, Chiang Mai, 50200, Thailand
[b] Center of Excellence in Oral and Maxillofacial Biology, Faculty of Dentistry, Chiang Mai University, Chiang Mai, 50200, Thailand
[c] Department of Oral Biology and Diagnostic Sciences, Faculty of Dentistry, Chiang Mai University, Chiang Mai, 50200, Thailand

ABSTRACT

Objective: To determine effect of non-surgical periodontal treatment on a disintegrin and metalloproteinase 8 (ADAM8) levels in gingival crevicular fluid (GCF) of patients with chronic periodontitis (CP) in comparison with those of patients with gingivitis and to find correlations between ADAM8 levels and clinical parameters.
Design: Twenty-two and eleven patients with CP and gingivitis, respectively, were examined for four clinical parameters, probing depth, clinical attachment level, gingival and plaque indices. GCF from the selected gingivitis or periodontitis sites with distinct severities was sampled by Periopaper strips. The non-surgical treatments, including scaling and/or root planing and oral hygiene instruction, were provided for all patients. Clinical measurements and GCF sampling were repeated at three months after the treatments. ADAM8 concentrations were analyzed by ELISA and normalized by GCF volumes or total protein amounts.
Results: All patients exhibited significant improvement of almost every clinical parameter after treatment, whereas the median ADAM8 concentrations were significantly decreased at the moderate and severe periodontitis sites of patients with CP ($p < 0.05$). Moreover, the significantly positive correlations between ADAM8 concentrations and four clinical parameters were found in both moderate and severe groups ($p < 0.05$).
Conclusion: ADAM8 concentrations were decreased by non-surgical periodontal therapy in patients with chronic periodontitis at the moderate and severe sites and were correlated with four clinical parameters, implying that GCF ADAM8 levels reflect inflammatory and bone-resorbing activities in the periodontal pocket.

1. Introduction

The pathogenesis of chronic periodontitis (CP) is caused by overwhelming host immune responses to persistent infections from periodontopathogenic microorganisms within the dental plaque (Cekici, Kantarci, Hasturk, & Van Dyke, 2014). Advanced progression of this disease can lead to damage of tooth supporting structures and eventual tooth loss. Several clinical manifestations and parameters as well as dental radiography are commonly used as a gold standard to define the stages of CP depending on the amounts of alveolar bone destruction and attachment loss. Moreover, a number of inflammatory molecules detected in gingival crevicular fluid (GCF), such as interleukin (IL)-1, IL-6, IL-8, tumor necrosis factor (TNF)-α along with other inflammation-related molecules, like matrix metalloproteinase (MMP)-3, MMP-8 and

receptor activator of nuclear factor kappaB ligand, are proposed to be useful biomarkers to indicate an active state of CP (Hernández et al., 2011; Ohlrich, Cullinan, & Seymour, 2009; Toyman et al., 2015). Besides MMP-3 and MMP-8, our previous study and the others have demonstrated a significant elevation of the other two members of the metzincin superfamily of Zn^{2+}-dependent proteases, including a disintegrin and metalloproteinase (ADAM) 8 and ADAM17 or tumor necrosis factor-α (TACE), in GCF from periodontitis lesions (Bostanci et al., 2008; Elavarasu et al., 2015; Khongkhunthian et al., 2013). Expression of ADAM8 is also enhanced in the synovial membrane and pannus tissues of patients with rheumatoid arthritis (Ainola et al., 2009), indicating a significant role of ADAM8 in inflammation-induced bone loss in rheumatoid arthritis.

ADAM8 is a type I transmembrane glycoprotein that is mostly

expressed on the cell membrane of hematopoietic cells, including neutrophils, monocytes, eosinophils, dendritic cells and B lymphocytes (Richens et al., 2007; Yoshiyama, Higuchi, Kataoka, Matsuura, & Yamamoto, 1997). However, some other non-immune cells, including bronchial and vascular smooth muscle cells, bronchial epithelial cells and human osteoarthritic chondrocytes, have been previously shown to express ADAM8 (Chiba et al., 2009; King et al., 2004; Zack et al., 2009). Particularly relevant to this study, expression of ADAM8 is localized in the epithelium of gingival biopsies from patients with CP and is up-regulated in cultured gingival epithelial cells upon challenges with *Fusobacterium nucleatum* (Aung et al., 2017). ADAM8 mainly functions to cleave various membrane proteins relating to host immune system, including L-selectin, P-selectin glycoprotein ligand-1, CD23, neural ectodomain of close homologue of L1 and TNF-α receptor 1 (Bartsch et al., 2010; Fourie, Coles, Moreno, & Karlsson, 2003; Gómez-Gaviro et al., 2007; Naus et al., 2004; Nishimura et al., 2015). ADAM8 also plays a role in osteoclastogenesis, especially at the late stage of osteoclast differentiation in cultured mouse bone marrow cells (Choi, Han, & Roodman, 2001). Furthermore, an *in vivo* study has shown decreased bone volume while increased trabecular space in transgenic mice with ADAM8 overexpression (Ishizuka et al., 2011). Taken together, all of these studies have pointed towards a pivotal role of ADAM8 in both host immunity and osteoclastogenesis.

Since CP, a bone destructive disease driven by excessive host immune responses, results from enhanced bone resorption by increased osteoclast number and activity (Cekici et al., 2014), it was, therefore, logical to hypothesize that raised ADAM8 levels in GCF of patients with CP would be decreased after periodontal treatment and the ADAM8 levels would be positively correlated with four clinical parameters, including probing depth (PD), clinical attachment level (CAL), gingival index (GI) and plaque index (PI), as a gold standard. The aims of this study were to determine effect of non-surgical periodontal therapy on GCF ADAM8 levels of patients with CP in comparison with those of patients with gingivitis and to find correlations between ADAM8 levels and the four clinical parameters.

2. Methods

2.1. Patient selection

Eleven patients with gingivitis and twenty-two patients with CP were recruited from the Periodontology Clinic, Faculty of Dentistry, Chiang Mai University. The patients with gingivitis exhibited gingival inflammation and bleeding on probing without alveolar bone destruction confirmed by full-mouth radiography, while those with CP were diagnosed according to the classification of the International Workshop for a Classification of Periodontal Diseases and Conditions, 1999 (Armitage, 1999). All patients were enrolled into the study with informed consent. The exclusion criteria were 1) patients with febrile illnesses or underlying chronic diseases, including rheumatoid arthritis, osteoarthritis and diabetes mellitus; 2) former or present smokers; 3) patients with ongoing periodontal or orthodontic treatment; 4) those under antibiotics or antibiotic prophylaxis, steroids, non-steroidal anti-inflammatory or immunosuppressive drugs within 3 months prior to the study enrollment; and 5) pregnant or breast-feeding patients. The protocol of this study was approved by the Human Experimentation Committee, Faculty of Dentistry, Chiang Mai University (52/2016).

2.2. Measurement of clinical parameters and site selection

The following clinical parameters, PD, CAL, PI and GI, were recorded at baseline before treatment and three months after treatment by one periodontist (T.N.; Fig. 1). All teeth except third molars were examined for PD and CAL at six sites of each tooth to the nearest millimeter using the UNC-15 periodontal probe (Hu-Friedy Mfg. Co., Chicago, IL, USA). The cemento-enamel junction was used as a reference

point for CAL. The intra-examiner calibration was performed with kappa values equal to 0.85 and 0.83 for PD and CAL, respectively. The PI was scored by visual examination as follows; 0 = no plaque, 1 = plaque detected by running instrument, 2 = plaque observed by eyes, and 3 = abundant plaque readily seen (Silness & Loe, 1964), while the GI was evaluated upon bleeding on probing (BOP) as 0 = no inflammation, 1 = slight inflammation with no BOP, 2 = inflammation with BOP, and 3 = obvious inflammation with spontaneous bleeding (Löe & Silness, 1963). In this study, non-molar teeth (incisors, canines and premolars) were selected for convenience of GCF collection.

For each patient with gingivitis, two sites that were separated by at least one tooth unit from the other were randomly selected to avoid GCF contamination. For each patient with CP, two sites were chosen according to two different severities as follows; 1) moderate periodontitis (PD = 3–4 mm; CAL = 3–4 mm) and 2) severe periodontitis (PD ≥ 5 mm; CAL ≥ 5 mm; Armitage, 1999). Again, the selected sites in each patient with CP were separated by at least one tooth unit. The sample size calculation was determined by G*Power 3.1 program (Faul, Erdfelder, Lang, & Buchner, 2007) using the previously reported levels of GCF ADAM8 (Khongkhunthian et al., 2013) with the effect size = 1.8 and power = 0.95, which showed a minimum of 10 samples in each group.

2.3. GCF collection

To avoid blood contamination, GCF collection was conducted one week after clinical examination for both before and after non-surgical periodontal treatment (Fig. 1). Supragingival plaque was first removed with sterile cotton pellets, and GCF was sampled as previously described (Khongkhunthian et al., 2013). Briefly, the site was isolated and air dried; a Periopaper™ strip (Oraflow Inc., Plainview, NY, USA) was gently inserted into the gingival crevice until light resistance was felt and left for 30 s. The GCF volume expressed as μl in the strip was measured by Periotron 8000™ (Oraflow Inc.). The strips were kept separately in each individual 1.5-ml Eppendorf tube at −80 °C. GCF was recovered from the strip by vigorously shaking in 225 μl of reagent diluent buffer, containing 50 mM Tris, pH 7.45, 10 mM CaCl$_2$, 0.15 M NaCl and 0.05% Brij35, for ADAM8 ELISA and total protein measurement. The percentage of recovery was separately determined by dotting five known concentrations (125, 250, 500, 1000 and 2000 pg/ml) of human recombinant ADAM8 (R&D Systems, Inc., Minneapolis, MN, USA) onto paper strips. This experiment was done in duplicate with an average percentage ± SD equal to 70 ± 16.

2.4. Non-surgical periodontal therapy

Subsequent to GCF collection, non-surgical periodontal treatments, including full mouth scaling for patients with gingivitis and with CP, using an ultrasonic scaler together with P-10 tips (Thai Dental Products, Bangkok, Thailand) and root planing with periodontal curettes (Hu-Friedy Mfg. Co.) for patients with CP, were provided under local anesthetic injections as needed with less than 1.7 ml of 4% articaine with 1:100,000 epinephrine (Ubistesin™ forte, 3 M ESPE, St. Paul, MN, USA) or of 3% mepivacaine without vasoconstrictors (Mepivastesin™, 3 M ESPE) for patients with hypertension in each visit. The treatments for all patients were given once a week and finished within 1 month with regular recall visits to repeatedly motivate oral hygiene instruction for good home care by every patient.

2.5. ADAM8 ELISA

The analysis of human ADAM8 levels from GCF was performed according to the manufacturer's instruction (DuoSet ELISA Development System for human ADAM8, catalog number DY1031, R&D Systems, Inc.) as previously described (Khongkhunthian et al., 2013). In brief, the ELISA plates were coated overnight with 100 μl per well of the
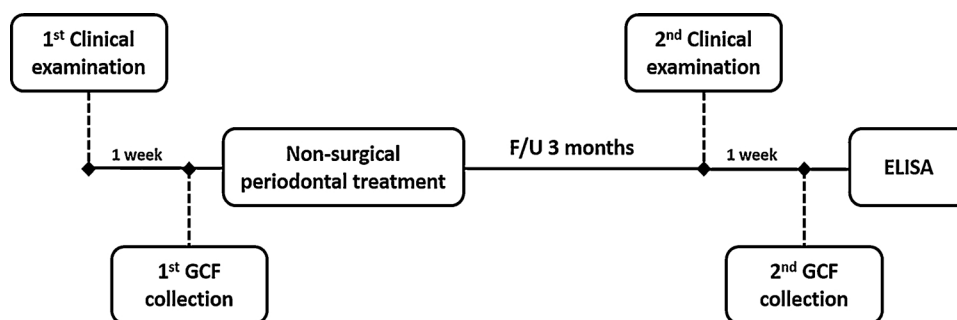
Fig. 1. The flow chart of study design. Non-surgical periodontal treatment included full-mouth scaling and root planing together with oral hygiene instruction. ELISA = enzyme-linked immunosorbent assay, F/U = follow-up, GCF = gingival crevicular fluid.

mouse anti-human ADAM8 antibody diluted in phosphate-buffered saline (PBS) at room temperature. The excess antibody was aspirated, and the plates were washed with buffer, containing 0.05% Tween-20 in PBS, pH 7.4, and blocked with 300 μl per well of blocking buffer, containing 1% bovine serum albumin in PBS with 0.05% NaN_3, for 1 h. Then, a 100-μl aliquot of GCF samples or of standard human ADAM8 (R &D Systems, Inc.) was added in each well for 2 h in duplicate. Thereafter, the plates were washed and 100 μl of the biotinylated goat anti-human ADAM8 detection antibody was added and incubated for 2 h. Subsequently, the streptavidin-horseradish peroxidase was added for 20 min in the dark. The substrate solution (Catalog number DY999, R& D Systems, Inc.) was added for 20 min, followed by the addition of 2 N H_2SO_4 to stop the reaction. The microplate reader (Sunrise™, Tecan group Ltd., Männedorf, Switzerland) was set to 450 nm for readings of the optical density which were subtracted by the readings at 540 nm for wavelength correction. The average ADAM8 concentration in each GCF sample derived from duplicated samples in the unit of pg/ml was determined from a standard curve that was plotted by the mean value of optical density on the *y*-axis against the known concentration on the *x*-axis. The detection limits for ADAM8 concentrations were 15.62-4000 pg/ml. To avoid variations between different ELISA runs, the GCF samples from the same selected sites both before and after treatment were analyzed together in the same plate.

2.6. Total protein measurement

The remaining GCF samples after ADAM8 analysis by ELISA were used for determination of total protein concentrations. Two μl of GCF samples was pipetted into the NanoDrop2000™ spectrophotometer (Thermo Fisher Scientific, Waltham, MA, USA), and the absorbance values measured at the 280-nm wavelength were converted into the concentrations expressed in the unit of μg/ml. The reagent diluent buffer was used as a blank control.

2.7. Statistical analysis

All data were first tested for normal distribution. The age comparison between gingivitis and periodontitis groups was analyzed by the independent t-test, while the comparisons of four clinical parameters between before and after treatment were determined by the paired t-test. These data are reported as mean ± SD. The chi-square test was used to compare the proportion of gender between gingivitis and periodontitis groups. For the non-normally distributed data, the ADAM8 levels per 30 s, normalized by total protein concentrations and by GCF volume, reported as a unit of pg/ml, pg/μg and pg/μl, respectively, were compared between before and after treatment using the Wilcoxon Signed Ranks test. The correlations between ADAM8 levels and clinical parameters were analyzed by the Spearman rank order correlation test. All non-parametric data are illustrated as medians and interquartile ranges in the box plot graphs. All statistical tests were carried out using Statistical Package for Social Sciences software version 17.0 for

Windows (IBM, Chicago, IL, USA) and were considered statistically significant if *p*-values were less than 0.05.

3. Results

3.1. Reduction in four clinical parameters after non-surgical periodontal treatment in CP

The demographic data showed a significantly higher mean age of patients with CP than that with gingivitis ($p < 0.001$; Table 1). The ratio of male to female in the gingivitis group (5:6) did not differ from that in the periodontitis group (9:13; $p = 0.803$). In general, the depth of PD (mm), the distance of CAL (mm) and the GI and PI scores at baseline reported as means ± SD of the severe periodontitis group were higher than those of the moderate periodontitis group (Table 2). Three months after non-surgical periodontal therapy, the mean PD and CAL in the moderate and severe periodontitis groups were significantly reduced ($p < 0.001$; Table 2), and the mean GI and PI scores in these two groups were significantly decreased ($p < 0.001$; Table 2), indicating an improvement of clinical manifestations as a result of treatment and repeated oral hygiene control. Note that the mean PD or CAL after treatment in the gingivitis group was not much altered in comparison with marked changes in the moderate and severe periodontitis groups, whereas the mean GI and PI scores in the gingivitis group were significantly decreased after treatment ($p < 0.001$; Table 2).

3.2. Significantly reduced ADAM8 levels after non-surgical periodontal therapy in the moderate and severe periodontitis groups

The baseline median amounts of ADAM8 per 30 s for the gingivitis, the moderate and the severe periodontitis groups were 13.66, 86.32 and 97.21 pg/ml, respectively (Fig. 2A). The ADAM8 amounts expressed in pg per ml were derived from a standard curve of known ADAM8 concentrations. The median concentrations of ADAM8 in the moderate and the severe periodontitis groups, normalized by total protein concentrations (Fig. 2B) and by GCF volume (Fig. 2C), were higher than those in the gingivitis group. Three months after treatment, the median ADAM8 levels in the moderate and severe periodontitis groups were decreased. Accordingly, the median ADAM8 amounts per 30 s (Fig. 2A) and the median ADAM8 concentrations, normalized by total protein concentrations (Fig. 2B) or GCF volume (Fig. 2C), in the

Table 1
Demographic data of the participants.

Group	N (male/female)	Age Range (years)	Age (mean ± SD)
Gingivitis	11 (5/6)	18-45	28.27 ± 7.75
Periodontitis	22 (9/13)	38-69	52.05 ± 9.42[***]

*** $p < 0.001$.

Table 2
Comparisons of four clinical parameters before and after non-surgical periodontal treatment.

Group	PD (mm; mean ± SD)		CAL (mm; mean ± SD)		GI (mean ± SD)		PI (mean ± SD)	
	before	after	before	after	before	after	before	after
Gingivitis	2.27 ± 0.46	2.04 ± 0.33	0.00	0.18 ± 0.40	1.95 ± 0.49	0.00***	1.32 ± 0.48	0.27 ± 0.46***
Moderate	3.68 ± 0.48	2.55 ± 0.67***	3.73 ± 0.46	2.91 ± 0.53***	1.91 ± 0.30	0.73 ± 0.70***	1.73 ± 0.63	0.41 ± 0.50***
Severe	6.55 ± 1.22	4.41 ± 1.22***	6.91 ± 1.72	5.55 ± 1.56***	2.41 ± 0.50	1.64 ± 0.68***	2.14 ± 0.56	0.36 ± 0.50***

PD = probing depth, CAL = clinical attachment level, GI = gingival index, PI = plaque index and mm = millimeter. *** = statistically significant reduction at $p < 0.001$ between before and after treatment.

moderate and severe periodontitis groups were significantly reduced compared to their corresponding baseline levels, whereas those in the gingivitis group were not found to be different between before and after treatment (Fig. 2).

3.3. Positive correlations between ADAM8 levels and clinical parameters in the moderate and severe periodontitis groups

The correlations were determined between ADAM8 concentrations, normalized by their total protein concentrations, and four clinical parameters, including PD, CAL, GI and PI, in the gingivitis, moderate and severe periodontitis groups. In both moderate and severe periodontitis groups, the significantly positive correlations were found between the ADAM8 concentrations and all four clinical parameters ($p < 0.05$; Figs. 3 and 4, respectively). However, no significant correlations between the ADAM8 concentrations and any of the four clinical parameters were found in the gingivitis group (data not presented).

4. Discussion

This study provided clinical evidence that demonstrated significant reductions in all four clinical parameters and significant decreases in GCF ADAM8 levels after non-surgical periodontal treatment in patients with CP at the moderate and severe periodontitis sites. However, the significantly decreased ADAM8 levels were not found in the gingivitis group after treatment. This may be because ADAM8 plays an important role not only in mouse osteoclastogenesis but also in human joint diseases, such as rheumatoid arthritis (Ainola et al., 2009; Choi et al., 2001; Ishizuka et al., 2011). Therefore, it is likely to observe a marked reduction of ADAM8 levels only in the moderate and severe periodontitis groups after periodontal treatment. Note that the clinical improvement of periodontal diseases after non-surgical treatment in this

study, reflected by decreased PD, CAL, GI and PI (Table 2), is in agreement with several previous clinical studies, as reviewed in Adriaens & Adriaens, 2004; Claffey, Polyzois, & Ziaka, 2004; Mailoa et al., 2015.

In addition to the significant reduction of ADAM8 levels in the moderate and severe periodontitis groups after treatment, the normalized ADAM8 levels were significantly and positively correlated with all four clinical parameters, suggesting that ADAM8 is not only involved with inflammation due to its expression in several types of inflammatory cells but also in osteoclast formation, as aforementioned. Nevertheless, the significant correlations were not found in the gingivitis group, possibly because of no significant reduction in ADAM8 levels after treatment in this group. In the present study, GCF collection among different samples was controlled by the same collection time; furthermore, total protein concentrations and GCF volumes were used to normalize ADAM8 levels, verifying true reduction of ADAM8 levels upon non-surgical treatment (Fig. 2) and positive correlations between ADAM8 levels and four clinical parameters in the moderate and severe periodontitis groups (Figs. 3 and 4).

The limitation of this study is a lack of age match between patients with gingivitis and those with CP owing to the slowly progressive nature of chronic periodontitis, in which the prevalence is commonly found in middle- to old-aged patients, whilst the onset of gingivitis can be as early as childhood (Burt, 2005). Nonetheless, the lack of age match would not affect our findings because comparisons were made only between baseline and after treatment data within the same group. Furthermore, the follow-up period after treatment in this study was three months; it is, therefore, interesting to further determine ADAM8 levels as well as to find correlations between ADAM8 levels and the clinical parameters in a longer follow-up period.

A number of previous studies have revealed a significant increase in several pro-inflammatory markers in GCF collected from CP sites, such as IL-1α, IL-1β, IL-6, TNF-α, C-reactive protein, alkaline phosphatase,
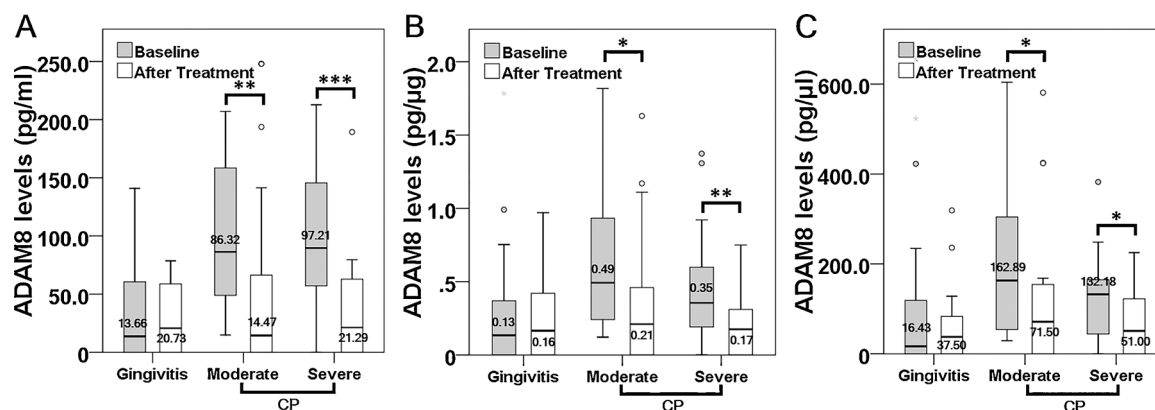
Fig. 2. Significantly decreased ADAM8 levels after non-surgical periodontal therapy in the moderate and severe periodontitis groups. The box plot diagram illustrates ADAM8 levels per 30 s (pg/ml; A), normalized by total protein concentrations (pg/μg; B), and by gingival crevicular fluid (GCF) volumes (pg/μl; C) at baseline (gray boxes) and after treatment (empty boxes), which were measured from GCF of patients with gingivitis and with chronic periodontitis (CP) according to two different severities, including moderate and severe. The numbers shown in the box plot graphs are medians. *, **, *** = statistically significant differences at $p < 0.05$, $p < 0.01$, and $p < 0.001$ respectively. The horizontal lines within each box show the median value and interquartile range, while small circles represent outliers.
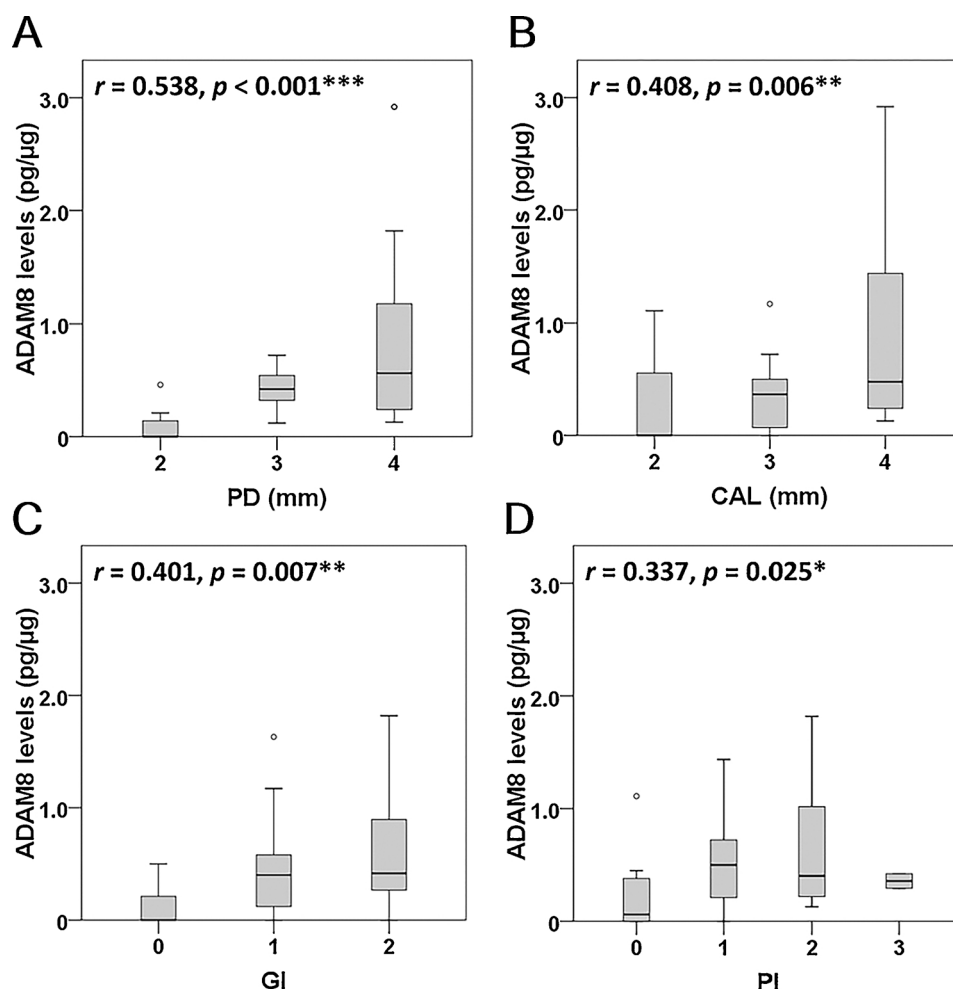
Fig. 3. Significantly positive correlations between ADAM8 levels and four clinical parameters in the moderate periodontitis group. The box plot diagrams illustrate ADAM8 levels (pg/μg), as normalized by the total protein concentrations in gingival crevicular fluid, which were plotted on the *y*-axis, while probing depth (PD) in millimeter (mm; A), clinical attachment level (CAL) in mm (B), gingival index (GI; C) and plaque index (PI; D) were plotted on the *x*-axis. The horizontal lines within each box show the median value and interquartile range, while small circles represent outliers. *, **, *** = statistically significant differences at $p < 0.05$, $p < 0.01$ and $p < 0.001$, respectively.

tissue type plasminogen activator and MMP-3 (Thunell et al., 2010; Toyman et al., 2015; Zhang, Chen, Zhu, & Yan, 2016). However, the design of these studies was cross-sectional. To the best of our knowledge, only four studies with some incongruous data have so far been designed as longitudinal with a follow-up period up to four months. In particular, the GCF levels of IL-1α, IL-1β and TNF-α in patients with CP were significantly decreased after non-surgical periodontal therapy in association with the values of PD and CAL (Reis et al., 2014; Türer, Durmuş, Balli, & Güven, 2017), whereas the significantly reduced IL-1β levels were not correlated with PD or CAL in patients with CP (Gamonal, Acevedo, Bascones, Jorge, & Silva, 2000; Konopka, Pietrzak, & Brzezińska-Błaszczyk, 2012). The reason behind this discrepancy is not known, but our data have indeed indicated that the significantly diminished ADAM8 levels after treatment were correlated with not only PD and CAL but also GI and PI, proposing that ADAM8 may be used to simultaneously monitor the degrees of periodontal tissue inflammation, alveolar bone destruction and clinical attachment loss, since most GCF biomarkers are related to the inflammatory state of periodontal diseases.

It is likely that raised GCF ADAM8 levels in CP are a result of infiltrated inflammatory cells, such as neutrophils and macrophages (Richens et al., 2007), as well as from inflamed epithelial cells within gingival tissues of CP (Aung et al., 2017). In addition, ADAM8 expression in cultured gingival epithelial cells is up-regulated upon challenges with *Fusobacterium nucleatum*, similar to ADAM17 (TACE) induction by *Porphyromonas gingivalis* in T lymphocytes (Bostanci, Reddi, Rangarajan, Curtis, & Belibasakis, 2009). As with the elevated GCF ADAM8 levels in CP, the GCF levels of ADAM17 (TACE) are increased with periodontal disease severity in relation to raised GCF

levels of receptor activator of nuclear factor kappaB ligand (RANKL), suggesting that ADAM17 (TACE) may act as a "sheddase" to cleave membrane-bound RANKL to the soluble form of RANKL, which would activate more osteoclastogenesis (Lee, Choi, Heo, Lee, & Cho, 2011). However, to the best of our knowledge, the association between GCF ADAM8 and RANKL levels has not yet been explored. Therefore, it is interesting to further determine the relationship of these two biomolecules after non-surgical periodontal therapy because the GCF ADAM8 levels were decreased by non-surgical treatment (Fig. 2), whereas the GCF RANKL levels are not affected (Bostanci, Saygan, Emingil, Atilla, & Belibasakis, 2011). Furthermore, TNF-α, which directly activates osteoclastogenesis (Kitaura et al., 2013), can induce ADAM8 expression in neuronal glia cells (Schlomann, Rathke-Hartlieb, Yamamoto, Jockusch, & Bartsch, 2000). Consequently, it is probable that elevated GCF ADAM8 levels result from increased TNF-α levels in GCF as a result of raised ADAM17 (TACE) levels at the CP site (Teles et al., 2010; Zhang et al., 2016).

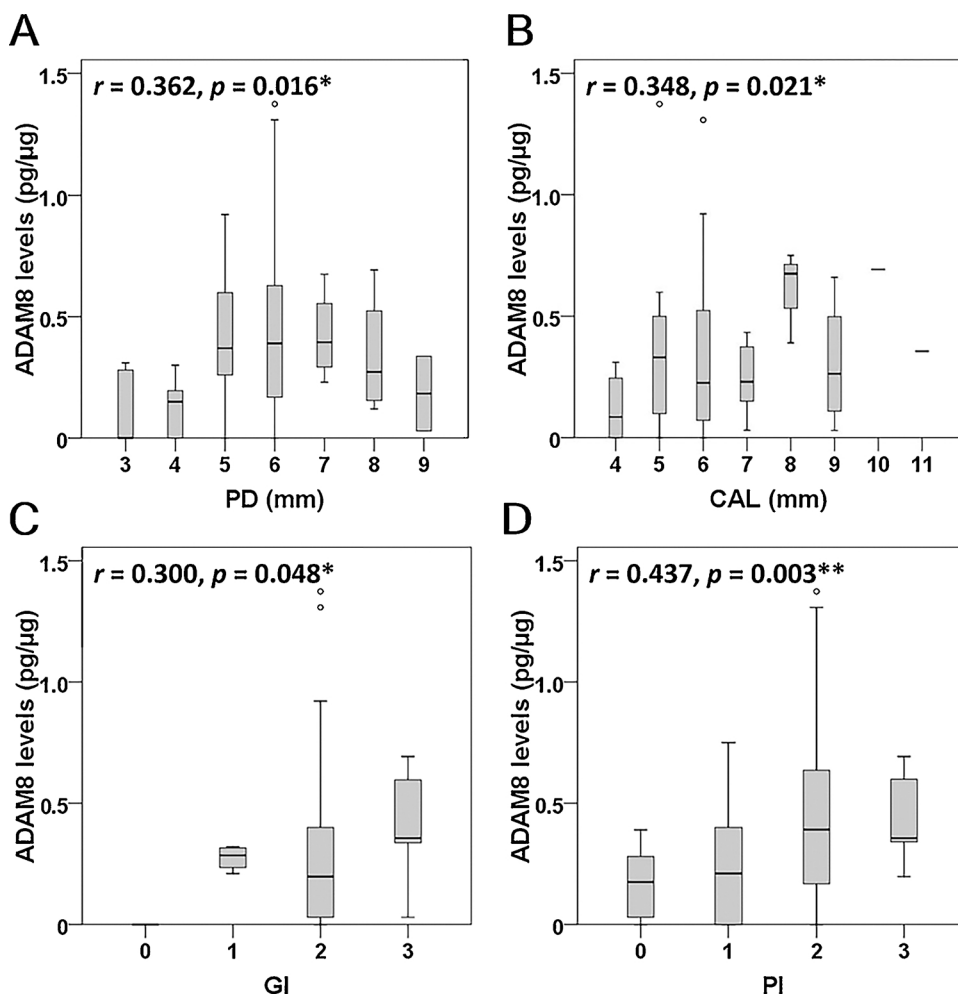## Conflict of interest

Acknowledgements

Fig. 4. Significantly positive correlations between ADAM8 levels and four clinical parameters in the severe periodontitis group. The box plot diagrams illustrate ADAM8 levels (pg/µg), as normalized by the total protein concentrations in gingival crevicular fluid, which were plotted on the y-axis, while probing depth (PD) in millimeter (mm; A), clinical attachment level (CAL) in mm (B), gingival index (GI; C) and plaque index (PI; D) were plotted on the x-axis. The horizontal lines within each box show the median value and interquartile range, while small circles represent outliers. *, ** = statistically significant differences at $p < 0.05$ and $p < 0.01$, respectively.

References

Adriaens, P. A., & Adriaens, L. M. (2004). Effects of nonsurgical periodontal therapy on hard and soft tissues. *Periodontology 2000, 36*, 121–145.

Ainola, M., Li, T. F., Mandelin, J., Hukkanen, M., Choi, S. J., Salo, J., et al. (2009). Involvement of a disintegrin and a metalloproteinase 8 (ADAM8) in osteoclastogenesis and pathological bone destruction. *Annals of the Rheumatic Diseases, 68*(3), 427–434.

Armitage, G. C. (1999). Development of a classification system for periodontal diseases and conditions. *Annals of Periodontology, 4*(1), 1–6.

Aung, W. P. P., Chotjumlong, P., Pata, S., Montreekachon, P., Supanchart, C., Khongkhunthian, S., et al. (2017). Inducible expression of a disintegrin and metalloproteinase 8 in chronic periodontitis and gingival epithelial cells. *Journal of Periodontal Research, 52*(3), 582–593.

Bartsch, J. W., Wildeboer, D., Koller, G., Naus, S., Rittger, A., Moss, M. L., et al. (2010). Tumor necrosis factor-alpha (TNF-alpha) regulates shedding of TNF-alpha receptor 1 by the metalloprotease-disintegrin ADAM8: Evidence for a protease-regulated feedback loop in neuroprotection. *Journal of Neuroscience, 30*(36), 12210–12218.

Bostanci, N., Emingil, G., Afacan, B., Han, B., Ilgenli, T., Atilla, G., et al. (2008). Tumor necrosis factor-α-converting enzyme (TACE) levels in periodontal diseases. *Journal of Dental Research, 87*(3), 273–277.

Bostanci, N., Reddi, D., Rangarajan, M., Curtis, M. A., & Belibasakis, G. N. (2009). *Porphyromonas gingivalis* stimulates TACE production by T cells. *Oral Microbiology and Immunology, 24*(2), 146–151.

Bostanci, N., Saygan, B., Emingil, G., Atilla, G., & Belibasakis, G. N. (2011). Effect of periodontal treatment on receptor activator of NF-κB ligand and osteoprotegerin levels and relative ratio in gingival crevicular fluid. *Journal of Clinical Periodontology, 38*(5), 428–433.

Burt, B., Research, Science and Therapy Committee of the American Academy of Periodontology. (2005). Position paper: epidemiology of periodontal diseases. Journal of Periodontology, 76(8), 1406-1419.

Cekici, A., Kantarci, A., Hasturk, H., & Van Dyke, T. E. (2014). Inflammatory and immune pathways in the pathogenesis of periodontal disease. *Periodontology 2000, 64*(1), 57–80.

Chiba, Y., Onoda, S., Hattori, Y., Maitani, Y., Sakai, H., & Misawa, M. (2009). Upregulation of ADAM8 in the airways of mice with allergic bronchial asthma. *Lung, 187*(3), 179–185.

Choi, S. J., Han, J. H., & Roodman, G. D. (2001). ADAM8: A novel osteoclast stimulating factor. *Journal of Bone and Mineral Research, 16*(5), 814–822.

Claffey, N., Polyzois, I., & Ziaka, P. (2004). An overview of nonsurgical and surgical therapy. *Periodontology 2000, 36*, 35–44.

Elavarasu, S., Suthanthiran, T., Thangavelu, A., Saravanan, J., Selvaraj, S., & Mohandas, L. (2015). Comparative analysis of gingival crevicular fluid a disintegrin and metalloproteinase 8 levels in health and periodontal disease: A clinic-biochemical study. *Journal of Pharmacy & Bioallied Sciences, 7*(Suppl. 2), S470–473.

Faul, F., Erdfelder, E., Lang, A. G., & Buchner, A. (2007). G*power 3: A flexible statistical power analysis program for the social, behavioral, and biomedical sciences. *Behavior Research Methods, 39*(2), 175–191.

Fourie, A. M., Coles, F., Moreno, V., & Karlsson, L. (2003). Catalytic activity of ADAM8, ADAM15, and MDC-L (ADAM28) on synthetic peptide substrates and in ectodomain cleavage of CD23. *The Journal of Biological Chemistry, 278*(33), 30469–30477.

Gamonal, J., Acevedo, A., Bascones, A., Jorge, O., & Silva, A. (2000). Levels of interleukin-1 beta, -8, and -10 and RANTES in gingival crevicular fluid and cell populations in adult periodontitis patients and the effect of periodontal treatment. *Journal of Periodontology, 71*(10), 1535–1545.

Gómez-Gaviro, M., Domínguez-Luis, M., Canchado, J., Calafat, J., Janssen, H., Lara-Pezzi, E., et al. (2007). Expression and regulation of the metalloproteinase ADAM-8 during human neutrophil pathophysiological activation and its catalytic activity on L-selectin shedding. *The Journal of Immunology, 178*(12), 8053–8063.

Hernández, M., Dutzan, N., García-Sesnich, J., Abusleme, L., Dezerega, A., Silva, N., et al. (2011). Host-pathogen interactions in progressive chronic periodontitis. *Journal of Dental Research, 90*(10), 1164–1170.

Ishizuka, H., García-Palacios, V., Lu, G., Subler, M. A., Zhang, H., Boykin, C. S., et al. (2011). ADAM8 enhances osteoclast precursor fusion and osteoclast formation *in vitro* and *in vivo*. *Journal of Bone and Mineral Research, 26*(1), 169–181.

Khongkhunthian, S., Techasatian, P., Supanchart, C., Bandhaya, P., Montreekachon, P., Thawanaphong, S., et al. (2013). Elevated levels of a disintegrin and metalloproteinase 8 in gingival crevicular fluid of patients with periodontal diseases. *Journal of*

Periodontology, 84(4), 520–528.

King, N. E., Zimmermann, N., Pope, S. M., Fulkerson, P. C., Nikolaidis, N. M., Mishra, A., et al. (2004). Expression and regulation of a disintegrin and metalloproteinase (ADAM) 8 in experimental asthma. *American Journal of Respiratory Cell and Molecular Biology, 31*(3), 257–265.

Kitaura, H., Kimura, K., Ishida, M., Kohara, H., Yoshimatsu, M., & Takano-Yamamoto, T. (2013). Immunological reaction in TNF-alpha-mediated osteoclast formation and bone resorption *in vitro* and *in vivo*. *Clinical & Developmental Immunology*(2013) 181849.

Konopka, Ł., Pietrzak, A., & Brzezińska-Błaszczyk, E. (2012). Effect of scaling and root planing on interleukin-1beta, interleukin-8 and MMP-8 levels in gingival crevicular fluid from chronic periodontitis patients. *Journal of Periodontal Research, 47*(6), 681–688.

Lee, J. H., Choi, Y. J., Heo, S. H., Lee, J. M., & Cho, J. Y. (2011). Tumor necrosis factor-α converting enzyme (TACE) increases RANKL expression in osteoblasts and serves as a potential biomarker of periodontitis. *Biochemistry & Molecular Biology Reports, 44*(7), 473–477.

Löe, H., & Silness, J. (1963). Periodontal disease in pregnancy. I. Prevalence and severity. *Acta Odontologica Scandinavica, 21*, 533–551.

Mailoa, J., Lin, G. H., Khoshkam, V., MacEachern, M., Chan, H. L., & Wang, H. L. (2015). Long-term effect of four surgical periodontal therapies and one non-surgical therapy: A systematic review and meta-analysis. *Journal of Periodontology, 86*(10), 1150–1158.

Naus, S., Richter, M., Wildeboer, D., Moss, M., Schachner, M., & Bartsch, J. W. (2004). Ectodomain shedding of the neural recognition molecule CHL1 by the metalloprotease-disintegrin ADAM8 promotes neurite outgrowth and suppresses neuronal cell death. *The Journal of Biological Chemistry, 279*(16), 16083–16090.

Nishimura, D., Sakai, H., Sato, T., Sato, F., Nishimura, S., Toyama-Sorimachi, N., et al. (2015). Roles of ADAM8 in elimination of injured muscle fibers prior to skeletal muscle regeneration. *Mechanisms of Development, 135*, 58–67.

Ohlrich, E. J., Cullinan, M. P., & Seymour, G. J. (2009). The immunopathogenesis of periodontal disease. *Australian Dental Journal, 54*(Suppl. 1), S2–10.

Reis, C., Da Costa, A. V., Guimarães, J. T., Tuna, D., Braga, A. C., Pacheco, J. J., et al. (2014). Clinical improvement following therapy for periodontitis: Association with a decrease in IL-1 and IL-6. *Experimental and Therapeutic Medicine, 8*(1), 323–327.

Richens, J., Fairclough, L., Ghaemmaghami, A. M., Mahdavi, J., Shakib, F., & Sewell, H. F. (2007). The detection of ADAM8 protein on cells of the human immune system and the demonstration of its expression on peripheral blood B cells, dendritic cells and monocyte subsets. *Immunobiology, 212*(1), 29–38.

Schlomann, U., Rathke-Hartlieb, S., Yamamoto, S., Jockusch, H., & Bartsch, J. W. (2000). Tumor necrosis factor alpha induces a metalloprotease-disintegrin, ADAM8 (CD 156): Implications for neuron-glia interactions during neurodegeneration. *Journal of Neuroscience, 20*(21), 7964–7971.

Silness, J., & Loe, H. (1964). Periodontal disease in pregnancy. II. Correlation between oral hygiene and periodontal condition. *Acta Odontologica Scandinavica, 22*, 121–135.

Teles, R., Sakellari, D., Teles, F., Konstantinidis, A., Kent, R., Socransky, S., et al. (2010). Relationships among gingival crevicular fluid biomarkers, clinical parameters of periodontal disease, and the subgingival microbiota. *Journal of Periodontology, 81*(1), 89–98.

Thunell, D. H., Tymkiw, K. D., Johnson, G. K., Joly, S., Burnell, K. K., Cavanaugh, J. E., et al. (2010). A multiplex immunoassay demonstrates reductions in gingival crevicular fluid cytokines following initial periodontal therapy. *Journal of Periodontal Research, 45*(1), 148–152.

Toyman, U., Tüter, G., Kurtiş, B., Kivrak, E., Bozkurt, Ş., Yücel, A. A., et al. (2015). Evaluation of gingival crevicular fluid levels of tissue plasminogen activator, plasminogen activator inhibitor 2, matrix metalloproteinase-3 and interleukin 1-beta in patients with different periodontal diseases. *Journal of Periodontal Research, 50*(1), 44–51.

Türer, Ç. C., Durmuş, D., Balli, U., & Güven, B. (2017). Effect of non-surgical periodontal treatment on gingival crevicular fluid and serum endocan, vascular endothelial growth factor-A, and tumor necrosis factor-alpha levels. *Journal of Periodontology, 88*(5), 493–501.

Yoshiyama, K., Higuchi, Y., Kataoka, M., Matsuura, K., & Yamamoto, S. (1997). CD156 (human ADAM8): Expression, primary amino acid sequence, and gene location. *Genomics, 41*(1), 56–62.

Zack, M. D., Malfait, A. M., Skepner, A. P., Yates, M. P., Griggs, D. W., Hall, T., et al. (2009). ADAM-8 isolated from human osteoarthritic chondrocytes cleaves fibronectin at Ala(271). *Arthritis & Rheumatology, 60*(9), 2704–2713.

Zhang, Q., Chen, B., Zhu, D., & Yan, F. (2016). Biomarker levels in gingival crevicular fluid of subjects with different periodontal conditions: A cross-sectional study. *Archives of Oral Biology, 72*, 92–98.
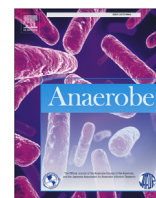
Anaerobes in human infections (dental/oral infections)

Pro-inflammatory cytokine responses in human gingival epithelial cells after stimulation with cell wall extract of *Aggregatibacter actinomycetemcomitans* subtypes

Nuntiya Pahumunto [a], Pareena Chotjumlong [b], Anupong Makeudom [b], Suttichai Krisanaprakornkit [b], Gunnar Dahlen [c], Rawee Teanpaisan [a, *]

[a] *Common Oral Diseases and Epidemiology Research Center, Department of Stomatology, Faculty of Dentistry, Prince of Songkla University, Songkhla 90112, Thailand*
[b] *Center of Excellence in Oral and Maxillofacial Biology, Department of Oral Biology and Diagnostic Sciences, Faculty of Dentistry, Chiang Mai University, Chiang Mai 50200, Thailand*
[c] *Department of Oral Microbiology and Immunology, Institute of Odontology, Sahlgrenska Academy, University of Gothenburg, Gothenburg, Sweden*

ARTICLE INFO

ABSTRACT

Varying cytokine responses of human gingival epithelial cells (HGECs) by *Aggregatibacter actinomycetemcomitans* subtypes have been found. Most studies have used reference strains, whereas a few has evaluated the cytokine expression in response to clinical subtypes of this bacterial species. This study aimed to examine whether there was any difference in cytokine responses of HGECs stimulated with cell wall extract (CWE) from *A. actinomycetemcomitans* subtypes included clinical strains from Thai adult periodontitis, various serotypes and non-serotypeable strains, strains from deep or shallow pockets, and reference serotype strains. Totally 50 clinical strains and 7 reference strains of *A. actinomycetemcomitans* were analyzed for the expression of IL-1β, IL-6, IL-8, and TNF-α mRNAs in HGECs by real time-PCR, and the IL-8 concentrations in cell-free supernatant measured using ELISA. An *in vitro* effect of released IL-8 on neutrophil migration was examined using transwell chambers. Result showed that among four cytokines studied, IL-8 mRNA was highly up-regulated by both clinical and reference strains. Serotype f revealed the highest expression compared to other serotypes. The JP2-like leukotoxin promoter gene and non-serotypeable (NS1 and NS2) demonstrated lower IL-8 responses compared to serotypeable strains, and IL-8 responses upon stimulation with clinical strains from deep pockets were also significantly lower than those isolated from shallow pockets ($P < 0.01$). Our findings suggest that the clinical isolates of *A. actinomycetemcomitans* associating with deep pockets, JP2-like leukotoxin promoter gene, NS1, and NS2 may interfere neutrophil function via minimal and immunosuppressing IL-8 responses, which may enhance their survival and virulence.

© 2017 Elsevier Ltd. All rights reserved.

1. Introduction

Aggregatibacter actinomycetemcomitans is strongly associated with the pathogenesis of aggressive periodontitis [1]. It can be classified into at least seven serotypes from a to g, based on differences in the carbohydrate moieties of cell surface lipopolysaccharide (LPS) and other genetically-dependent components [1,2]. In general, the three serotypes, a, b and c, are more frequently detected among clinical strains than the others [1,2]. Our previous study in a southern Thai adult population with periodontitis demonstrated a higher frequency of *A. actinomycetemcomitans* serotypes a and c compared to serotypes e and f. Serotype b and d were not detected in that study [3], however, serotype b and d could be found low frequency (2 and 8% using antiserum as well as 7 and 0% respectively using PCR for serotype determination) in southern Thai population [4,5]. In addition, a high frequency (54.4%) of non-serotypeable (NS) strains was found in this population and was significantly associated with deep pockets in comparison with shallow pockets [3]. The classical JP2 clone of *A. actinomycetemcomitans*, which possesses highly leukotoxic activity associating with a 530-bp deletion of the *ltx* promoter, was originally classified as serotype b [1,6]. The JP2 clone is endemically present in Northwest Africa and particularly associated with

Northwest African populations [1,6]. However, our recent study has instead shown two novel JP2-like leukotoxin promoter gene strains with serotype c in the Thai patients having the same 530-bp deletion of the *ltx* promoter [3]. These two strains also revealed a higher toxicity than other serotype c indicating that the deletion in the promoter region has an impact on the toxicity similar with JP2 clone reference [6]. Such strains have been confirmed as serotype c, based on repeated serotyping using two different methods, by PCR with specific primers for serotype c and denaturing gradient gel electrophoresis (DGGE) [3].

A. actinomycetemcomitans was shown to possess several virulence factors associated with periodontal disease severity, including leukotoxin expression and activity, internalization into fibroblasts, apoptosis of fibroblasts, and immunomodulation [6–8]. Our previous study demonstrated that clinical isolates of *A. actinomycetemcomitans*, particularly strains from deep pockets expressed a higher virulence, such as leukotoxin activity, internalization into fibroblasts and apoptosis of fibroblasts, than those strains isolated from shallow pockets [8]. Few studies were carried out the regulatory effect of various subtypes of *A. actinomycetemcomitans* on the immune response in host cells. Eberhard et al. showed that the specific immune responses in gingival epithelial cells depended on individual strain and subject, it was demonstrated by stimulating with two wild types and one reference strain [9]. This strain dependency should, therefore, be further analyzed using more than three strains of *A. actinomycetemcomitans*.

Innate immunity is rapidly activated as a first line of defense, when host cells, especially human gingival epithelial cells (HGECs) that act as a physical barrier, initially encounter invading microorganisms [10,11]. Bacterial challenges can result in activation of epithelial cells, leading to production of essential pro-inflammatory cytokine such as interleukin (IL)-1β, IL-6, tumor necrosis factor (TNF)-α, and IL-8 [10,11]. In addition, *A. actinomycetemcomitans* leukotoxin can induce neutrophil movement [12], which may alert and amplify host immune responses. The cytotoxicity of the leukotoxin has also been shown to affect to other cells types besides leukocytes [13,14]. Nevertheless, the knowledge on the immune-regulatory effect of host cells stimulated by various subtypes of *A. actinomycetemcomitans*, especially non-serotypeable clinical isolates is sparse. Therefore, the objective of this study was to compare the ability to modulate host innate immune responses of various reference and clinical strains of *A. actinomycetemcomitans* subtypes included serotype a-f and non-serotypeable strains isolated from deep and shallow pockets on the expression of pro-inflammatory cytokines (IL-1β, IL-6, TNF-α, and IL-8) in HGECs. And to compare the effect of those strains on the migration of neutrophils an *in vitro* study.

2. Materials and methods

2.1. Bacterial strains

Fifty clinical strains of *A. actinomycetemcomitans* subtypes isolated from deep and shallow pockets from 50 Thai adults with periodontitis, and whose clinical characteristics were described previously [3]. All strains were retrieved from the culture collections at the Department of Stomatology, Faculty of Dentistry, Prince of Songkla University, Thailand. Additionally, seven reference strains, serotype a to f, and one JP2 strain were included, all strains and their origin are listed in Table 1. Strains were cultured on the brain heart infusion (BHI) agar (Bacto™, Le Pont de Claix, France) under an anaerobic atmosphere, consisting of 80% N_2, 10% H_2 and 10% CO_2, at 37 °C for 3–5 days before preparation of the cell wall extract, which all strains showed smooth colony morphology on the BHI agar.

2.2. Cell wall extract (CWE) preparation

The cell wall fraction of all strains was prepared by differential centrifugation, as previously described [15]. Briefly, bacterial cell pellets were collected and resuspended in 10 ml of PBS, pH 7.0, at a density of 10^9 CFU/ml. The cells were disrupted by sonication (Sonic and Material, Inc., Newtown, CT, USA) in the presence of a protease inhibitor cocktail (Roche Molecular Biochemicals, Mannheim, Germany). Unbroken cells were removed by low-speed centrifugation at 2,200 g for 10 min at 4 °C, whereas the cell wall fraction was collected from the supernatant by high-speed centrifugation at 30,000 g for 20 min at 4 °C. The cell wall pellet was resuspended in 500 μl of PBS with pH 7.0, and its total protein concentration was determined by the Pierce® BCA Protein Assay kit (Thermo Scientific™, Rockford, IL, USA).

2.3. Human gingival epithelial cell culture and treatment

Non-inflamed gingival tissues overlying bony impaction of third molars were collected from five different donors after providing informed consent, which the research protocol was approved by the Ethics Committee of the Faculty of Dentistry at Prince of Songkla University, Thailand (EC 5811-33-L-HR). Primary HGECs were isolated from the tissues and cultured according to our previous protocol [15,16]. After washing the gingival explant (approximately 2 × 2 mm) in cold HEPES buffer containing antibiotics and antifungal drugs, it was cut into smaller pieces and was incubated with HEPES buffer containing 0.5 mg/ml of thermolysin (Sigma-Aldrich, St. Louis, MO, USA) and 1.125 mM $CaCl_2$ in a 60-mm culture dish (Nunc™, Roskilde, Denmark) for 90 min. Thereafter, the epithelial sheet was separated from the connective tissue. Then, HGECs were isolated from the epithelial sheet by trypsinization with trypsin-EDTA (Invitrogen™, Carlsbad, CA, USA) and cultured in serum-free keratinocyte growth medium (KGM; Lonza, Walkersville, MD, USA), containing bovine pituitary extract, epidermal growth factor, insulin, gentamicin sulfate amphotericin-B, and hydrocortisone. At 80% cell confluence, HGECs were washed twice, trypsinized and then transferred to a new culture flask to expand their cell number. HGECs from the second to the fourth passages were used throughout this study.

To determine cell viability and cytokine expression, HGECs were treated for 24 h with indicated doses of CWEs of tested strains or left untreated as a negative control. Cell viability was determined by an MTT assay (3-(4,5-dimethylthiazol-2-yl)-2,5-diphenyltetrazolium bromide) [15], cytokine mRNA expressions was performed using real time-PCR. Cell-free culture media were also collected for analysis of IL-8 protein levels by ELISA and its function on neutrophil migration *in vitro*, respectively.

2.4. Total RNA isolation and real time-PCR

Total RNA was isolated using the Illustra RNA spin Mini kit (GE Healthcare, Buckinghamshire, UK) following the manufacturer's instruction. cDNA was synthesized by the Superscript™ first-strand cDNA system kit (Thermo Fisher Scientific, Inc., Waltham, MA, USA). A quantitative real time-PCR method was performed using 5% of cDNA (v/v) and the Sensi-fast™SYBR No-ROX reagent (Bioline reagent Ltd., London, UK) with the Roche Lightcycler® 480 instrument (Roche Molecular Biochemicals). Primers for real time-PCR were as follows: IL-1β (5′-CACGCTCCGGGACTCACAGC-3′ and 5′-CTGGCCGCCTTTGGTCCCTC-3′), IL-6 (5′-CGCCCCACACAGACAGCCAC-3′ and 5′-AGCTTCGTCAGCAGGCTGGC-3′), IL-8 (5′-TTTCTGATGGAGAGAGCTCTGTCTGG-3′ and 5′-AGTGGAACAAGACTTGTGGATCCTGG-3′), TNF-α (5′-TTCTGCCTGCTGCACTTTGGA-3′ and 5′-TTGATGGCAGAGAGGAGGTTG-3′), and glyceraldehyde 3-

Table 1
Aggregatibacter actinomycetemcomitans strains used in the present study.

Subtypes	Reference strains[a] N	Clinical strains[b]	
		Deep pockets N = 36	Shallow pockets N = 14
a	1 (CCUG 37004)	8	3
b	1 (CCUG 37002)	ND	ND
c	1 (ATCC 33384)	7	4
d	1 (CCUG 38565)	ND	ND
e	1 (CCUG 37399)	4	3
f	1 (OMGS 3816)	5	2
JP2/JP2-like leukotoxin promoter gene	1 (OMGS 3952)[c]	2[d]	ND
NS1	N/A	5	1
NS2	N/A	5	1

N/A: not applicable, ND: not detected, NS = non-serotypeable.

[a] CCUG = Culture Collection University of Gothenburg, OMGS= Oral Microbiology Gothenburg Sweden, ATCC = American Type Culture Collection.

[b] Deep pockets were defined as having clinical attachment loss (CAL) ≥ 4 mm, a probing pocket depth (PPD) ≥ 5 mm, and bleeding on probing (BOP), while shallow pockets were defined as sites without CAL and BOP, and PPD ≤ 3 mm [3]. All of clinical strains were isolated from different individuals.

[c] Strain OMGS 3952 was formerly designated as P48:2 [3].

[d] Two JP2-like leukotoxin promoter gene strains designated JP2-like1 and JP2-like2.

phosphate dehydrogenase (GAPDH; 5′-ACCA-CAGTCCATGCCATCACTGC-3′ and 5′-TCCACCACCCTGTTGCTGTAGC-3′) [16]. PCR amplification was performed for 45 cycles for all cytokines with the denaturing temperature at 95 °C for 20 s, different annealing temperatures including 65.5, 65.5, 66.5, 59.8 and 60.0 °C for IL-1β, IL-6, IL-8, TNF-α and GAPDH, respectively for 20 s, and the polymerizing temperature at 72 °C for 25 s. The relative induction of cytokine mRNA expression was normalized by expression of GAPDH, which is the most stably expressed gene and one of the most commonly used as housekeeping genes for comparing gene expression and showing the least amount of variability [17]. The induction of cytokine mRNA expressions in the *A. actionmycetemcomitans* CWE treated samples was determined by comparing with the mRNA expression of each respective cytokine of the untreated sample, set to 1.0. All experiments were repeated using HGECs from five different donors and the average induction of each cytokine was expressed from these separate experiment.

2.5. IL-8 ELISA

The concentrations of IL-8 in cell-free conditioned media of HGECs, stimulated with an increasing dose (1, 10, and 100 μg/ml) of the CWEs from *A. actinomycetemcomitans* serotype c strains were measured using a commercially available ELISA kit according to the manufacturer's protocol (Thermo Fisher Scientific Inc.). The serotype c strains of *A. actinomycetemcomitans* used in this experiment included two JP2-like leukotoxin promoter gene (JP2-like1 and JP2-like2), 4 strains with a normal leukotoxin promoter gene, and a reference strain (ATCC33384). All experiments were independently repeated five times, and the median of IL-8 level was determined from these separate experiments.

2.6. Neutrophil migration assay

Neutrophils were prepared from 10 ml of citrate-dextrose blood from three different donors diluted with sterile Dulbecco's PBS at 1:1 (v/v), and then separated using Ficoll-Hypaque (GE Healthcare) density-gradient centrifugation. The red blood cells and granulocytes in the bottom layer were collected and resuspended in sterile PBS. An equal volume of 6% dextran (molecular weight > 200,000; Sigma-Aldrich) in PBS was added and left at room temperature for 45 min. Then, the upper layer was aspirated and saved as neutrophil rich solution, in which contaminated red blood cells were removed by lysis buffer. The number of neutrophils

was counted by the hemacytometer and adjusted to a density of 3 × 10^6 cells/ml by Minimum Essential Medium Eagle-Alpha Modification (alpha-MEM; Lonza).

Migration of neutrophils in response to cell-free culture supernatants was assessed using a 24-well transwell plate with 3-μm polycarbonate membrane (Corning, NY, USA), as previously described [18]. In brief, 600 μl of each tested supernatant or KGM alone was added to the lower chamber. A 200-μl quantity of alpha-MEM containing neutrophils (3 × 10^6 cells/ml) was added to the upper chamber. The migration assay was performed for 2 h at 37 °C in a humidified chamber with 5% CO_2, followed by incubation with 60 μl of 0.5 M EDTA for 15 min at 4 °C. The filters were removed from the transwell plate and the number of cells in the bottom chamber was counted by the hemacytometer. The percentage of chemotaxis was calculated by the number of migrated neutrophils divided by the number of neutrophils seeded in the upper chamber and multiplied by 100.

2.7. Statistical analysis

IL-8 mRNA expressions, IL-8 concentrations, the percentages of chemotaxis, and cell survival among different samples treated with different *A. actinomycetemcomitans* subtypes were analyzed by the Kruskal-Wallis test. Multiple comparisons were analyzed by the Mann-Whitney *U* test. Differences were regarded as significance when P < 0.05.

3. Results

3.1. Cytokine mRNA expressions in HGECs upon stimulation with various subtypes of A. actinomycetemcomitans

The toxicity on HGECs upon stimulation with the CWEs of various *A. actinomycetemcomitans* subtypes was first determined by an MTT assay. The percentages of cell survival after treatment with the CWEs of all reference and clinical strains ranged from 71.5 ± 5.1 to 90.0 ± 6.5; however, there was no significant difference in the percentages of cell survival among different samples (P > 0.05). In general, the clinical strains displayed an ability to induce mRNA expressions of pro-inflammatory cytokines in HGECs similar to that of the reference strains (Table 2). The mRNA expressions of IL-1β, IL-6, and TNF-α were slightly up-regulated by both clinical and reference strains of *A. actinomycetemcomitans* (~1–6 folds of induction), whereas that of IL-8 was strongly induced by all

Table 2
Cytokine mRNA expressions in human gingival epithelial cells (HGECs; N = 5), stimulated with 100 μg/ml of the cell wall extract of the reference and all clinical strains of *Aggregatibacter actinomycetemcomitans*.

Subtypes	Cytokine mRNA expressions/GAPDH expression (folds of induction ± SD)[a]							
	IL-1β		IL-6		IL-8		TNF-α	
	Reference	Clinical	Reference	Clinical	Reference	Clinical	Reference	Clinical
a	3.8 ± 1.1	3.1 ± 0.8	1.4 ± 1.1	1.5 ± 1.0	50.5 ± 1.2**	40.0 ± 5.3	2.5 ± 0.7	2.5 ± 0.7
b	3.5 ± 0.6	N/A	2.3 ± 2.3	N/A	81.4 ± 1.4*	N/A	2.1 ± 0.9	N/A
c	5.5 ± 2.4	4.1 ± 0.7	2.4 ± 1.2	2.0 ± 0.6	56.9 ± 1.8**	40.9 ± 8.4	2.8 ± 1.1	2.8 ± 1.7
d	2.7 ± 0.3	N/A	1.3 ± 0.9	N/A	38.6 ± 1.4	N/A	1.8 ± 0.6	N/A
e	4.4 ± 0.5	2.3 ± 0.3	1.7 ± 0.3	1.1 ± 0.7	40.1 ± 1.9	45.2 ± 11.1	1.0 ± 0.4	1.8 ± 0.6
f	6.5 ± 4.1	3.0 ± 0.1	2.1 ± 1.2	1.0 ± 0.4	156.9 ± 2.1*,**	100.6 ± 32.5*	1.0 ± 0.7	1.6 ± 0.2
JP2/JP2-like leukotoxin promoter gene	5.2 ± 0.7	4.6 ± 1.3	2.3 ± 0.2	0.6 ± 0.2	30.2 ± 3.4	11.7 ± 2.6*,***	2.6 ± 1.0	1.6 ± 0.2
NS1	N/A	5.1 ± 3.1	N/A	0.6 ± 0.1	N/A	30.6 ± 11.3	N/A	0.9 ± 0.3
NS2	N/A	2.7 ± 2.5	N/A	1.7 ± 2.1	N/A	27.7 ± 11.4	N/A	1.3 ± 0.1

N/A: not applicable; * significant difference of IL-8 mRNA expression at P < 0.05 when compared within the same column; ** significantly higher IL-8 mRNA expression in the reference strains than in the clinical strains at P < 0.01; *** significant lower IL-8 mRNA expression in the JP2-like leukotoxin promoter gene strains than in the JP2 at P < 0.01.
  [a] Fold of induction as compared with cytokine mRNA expressions in unstimulated HGECs.

A. actinomycetemcomitans strains (~12–157 folds of induction; Table 2). Therefore, IL-8 responses to stimulation with the CWEs of *A. actinomycetemcomitans* were chosen as an outcome variable in the subsequent experiments.

With respect to IL-8 mRNA induction in HGECs stimulated with the CWEs of reference strains, serotype f revealed the highest induction (156.9 ± 2.1 folds), followed by serotype b, c, a, e, d, and the JP2 genotype (Table 2). Similarly, the CWEs of *A. actinomycetemcomitans* clinical strains, subtype f, induced the greatest IL-8 mRNA expression (100.6 ± 32.5 folds), followed by subtypes e, c, a, NS1, NS2, and the two JP2-like leukotoxin promoter gene strains (Table 2). Note that the clinical strains with subtypes b and d are not available in our collections. Interestingly, the two JP2-like leukotoxin promoter gene strains with serotype c exhibited the least ability to induce IL-8 mRNA expression compared to all other clinical and reference strains (Table 2). Specifically, they induced significantly lower IL-8 mRNA expression than did the JP2 reference strain (P < 0.01; Table 2).

3.2. Dose-dependent effect on IL-8 responses in the HGECs by *A. actinomycetemcomitans* serotype c strains

The dose-dependent inducible effect on IL-8 mRNA expression and protein secretion in HGECs by the CWEs of 7 selected serotype c strains was investigated by treating HGECs with three doses of the CWEs, comprising 1, 10 and 100 μg/ml. The CWEs of the two JP2-like leukotoxin promoter gene strains at the highest dose (100 μg/ml) induced significantly lower IL-8 mRNA expression than those of the other selected serotype c strains (P < 0.05; Fig. 1A), whereas no significant differences were found for the two lower doses (Fig. 1A). Consistently, IL-8 protein concentrations in cell-free conditioned media collected from HGECs treated with the highest dose of the two JP2-like leukotoxin promoter gene strains were significantly lower than those of the other selected serotype c strains (P < 0.05; Fig. 1B), whereas no significant differences in terms of IL-8 levels were found for the two lower doses (Fig. 1B). Therefore, the concentration of CWEs at 100 μg/ml was used to stimulate HGECs in the subsequent experiments.

3.3. IL-8 responses in HGECs after stimulation with strains of *A. actinomycetemcomitans* isolated from deep and shallow pockets

IL-8 responses to the CWEs of eight selected strains isolated from deep pockets, including one strain of each subtype, consisting of a, c, e, f, NS1, NS2, and the two JP2-like leukotoxin promoter gene strains (Table 1), were compared with those to the CWEs of six

selected corresponding subtypes isolated from shallow pockets as no JP2-like leukotoxin promoter gene strain was found in shallow pockets (Table 1). It was demonstrated that all deep pocket strains exhibited significantly lower IL-8 mRNA induction than those originated from the shallow pockets (P < 0.01, Fig. 2A). This lower IL-8 mRNA induction by the deep pocket strains was confirmed in the neutrophil migration assay, in which the deep pocket strains consistently showed significantly lower percentages of chemotaxis than the shallow pocket strains (P < 0.001, Fig. 2B). As two negative controls, incubation with KGM alone caused a slight neutrophil migration possibly from gravitation, whereas cell-free conditioned media collected from untreated HGECs slightly increased the percentages of neutrophil migration due to basal levels of IL-8 mRNA expression (Fig. 2B).

When HGECs from five donors were stimulated with CWEs from *A. actinomycetemcomitans* subtypes isolated from deep and shallow periodontal pockets, the IL-8 mRNA induction was significantly lower for each subtype from deep pockets compared to the corresponding subtypes isolated from the shallow pockets (P < 0.05, Fig. 3A). The NS1 and NS2 strains exhibited a low IL-8 mRNA expression compared to other strains with the mean of expression as 12.1 ± 4.6 and 14.6 ± 3.3 folds of induction and was statistically significant compared to the strains isolated from shallow pockets (P < 0.001, Fig. 3A). Significant differences in terms of percentages of chemotaxis were also found between the deep and the shallow pocket strains serotype c, f, NS1, and NS2 strains (P < 0.05; Fig. 3B) with corresponding mean of function as 20.2 ± 2.4, 22.2 ± 4.9, 17.6 ± 4.5, and 16.1 ± 5.9%, respectively.

4. Discussion

This study compared the pro-inflammatory cytokine responses of HGECs from five donors after exposure to CWEs prepared from various clinical subtypes of *A. actinomycetemcomitans* isolated from both deep and shallow pockets of Thai adults with periodontitis and from reference strains. IL-8 mRNA expression was the predominant cytokine produced from both clinical and reference strains of *A. actinomycetemcomitans*. The main two findings were that certain subtypes of *A. actinomycetemcomitans*, NS1 and NS2, and the JP2-like leukotoxin promoter gene strains induced significantly lower IL-8 responses in HGECs than other subtypes, and all strains from deep periodontal pockets also gave lower IL-8 responses than strains from shallow pockets.

Among the virulence factors of *A. actinomycetemcomitans*, leukotoxin has been reviewed a great deal of attentions by which it can activate and kill leukocytes resulting in degranulation and IL-1β
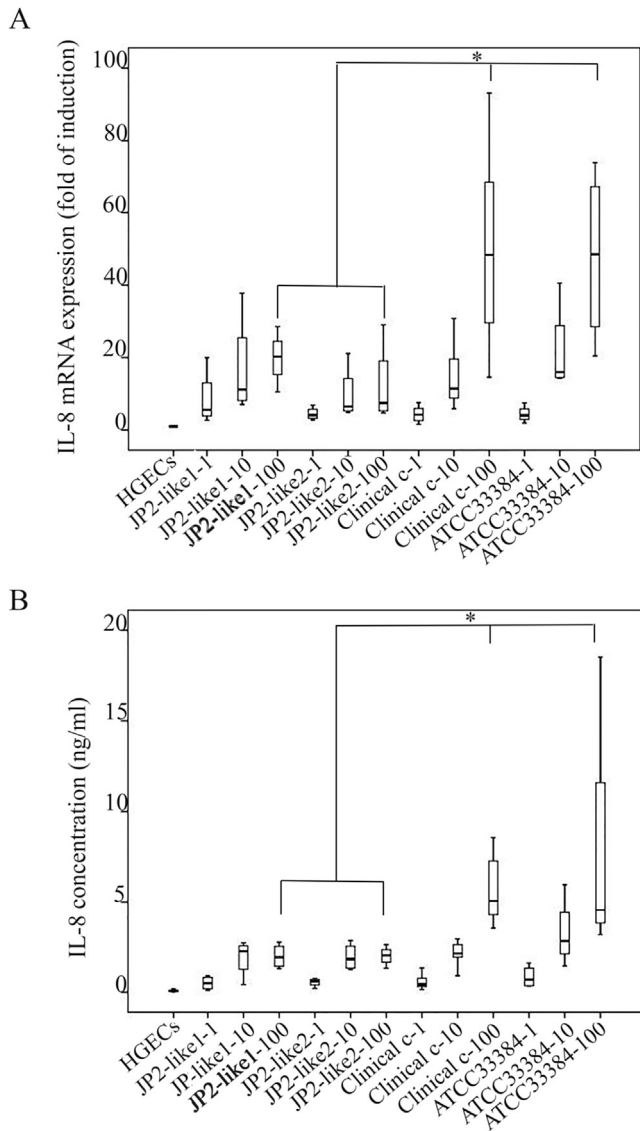
A

B

A

B

Fig. 2. A biphasic secretion pattern of IL-8 mRNA expressions (A) and IL-8 functions in neutrophil migration (B) in response to CWEs from *A. actinomycetemcomitans* isolated from deep (N = 8) and shallow pockets (N = 6). Untreated HGECs in (A) and (B) and KGM alone in (B) were used as negative control. (A) The cell lysate of HGECs, treated with 100 μg/ml of the CWEs of strains from deep and shallow pockets, was harvested to determine IL-8 mRNA expression by real time-PCR. * indicates statistically significant difference compared with the other groups (P < 0.01). (B) Migration of neutrophils was measured by transwell system. Cell-free culture supernatants added to the lower chamber and neutrophils migrated to the lower chamber were counted by the hemacytometer. * indicates statistically significant difference compared with the other groups (P < 0.001).

Fig. 1. Dose-dependent IL-8 mRNA induction (A) and IL-8 protein secretion (B) in HGECs from different donors by CWEs from various serotype c strains of *A. actinomycetemcomitans* included two JP2-like leukotoxin promoter gene strains including JP2-like1 and JP2-like2, four clinical serotype c strains, and a reference serotype c strain (ATCC 33384). Untreated HGECs was used as negative control. (A) The expressions of IL-8 mRNA as measured by real time-PCR. *indicates statistically significant difference between 100 μg/ml of the CWEs of two JP2-like leukotoxin promoter gene strains and of the CWEs of other clinical and reference strains (P < 0.05). (B) IL-8 concentrations as measured by enzyme-linked immunosorbent assay (ELISA). *indicates statistically significant difference between 100 μg/ml of the CWEs of two JP2-like leukotoxin promoter gene strains and of the CWEs of other clinical and reference strains (P < 0.05).

release, that is the important cytokine associating with progressive periodontitis especially to stimulate bone resorption [1,12,19]. However, host-microbial interaction with the HGECs is thought to be an important primary step in the host-defense reaction of periodontal disease. HGECs are among the first innate immune cell types [10,11] that respond to the recognition of periodontal pathogens by producing of several cytokines that can initiate inflammation within the periodontal tissues to subsequently activate other host immune systems by releasing a cascade of pro-inflammatory mediators to protect the sub-epithelial tissues from bacterial invasion [19]. Several studies have reported that IL-8 was
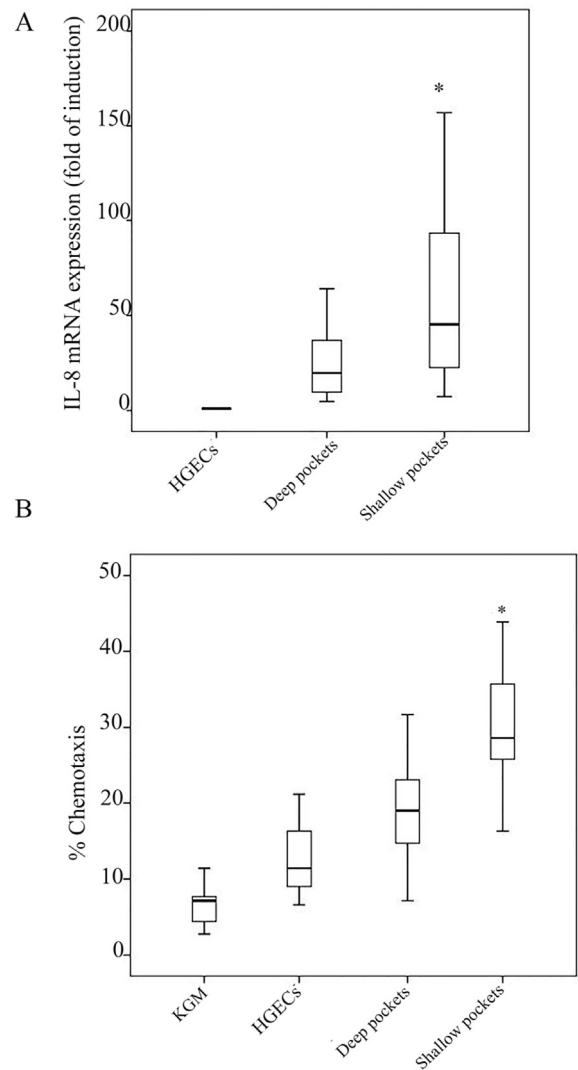
the predominant cytokine in comparison to IL-1β, IL-6 and TNF-α expressed by HGECs after exposure to bacteria or bacterial products [10,11,19,20], which is confirmed in the present study to be valid also for various subtypes of *A. actinomycetemcomitans*. IL-8 is a potent chemokine necessary for enhancement of neutrophil migration into the infectious site to eliminate invading pathogens [19,21]. The present study also showed that various subtypes of *A. actinomycetemcomitans*, induced IL-8 mRNA expression of different magnitudes (~12—157 folds). This may have a significant impact on the virulence of different subtypes of *A. actinomycetemcomitans*.

Previous studies have reported a variable IL-8 stimulation of *A. actinomycetemcomitans* related to serotypes. Serotype b was found to exhibit the strongest IL-8 stimulation compared to
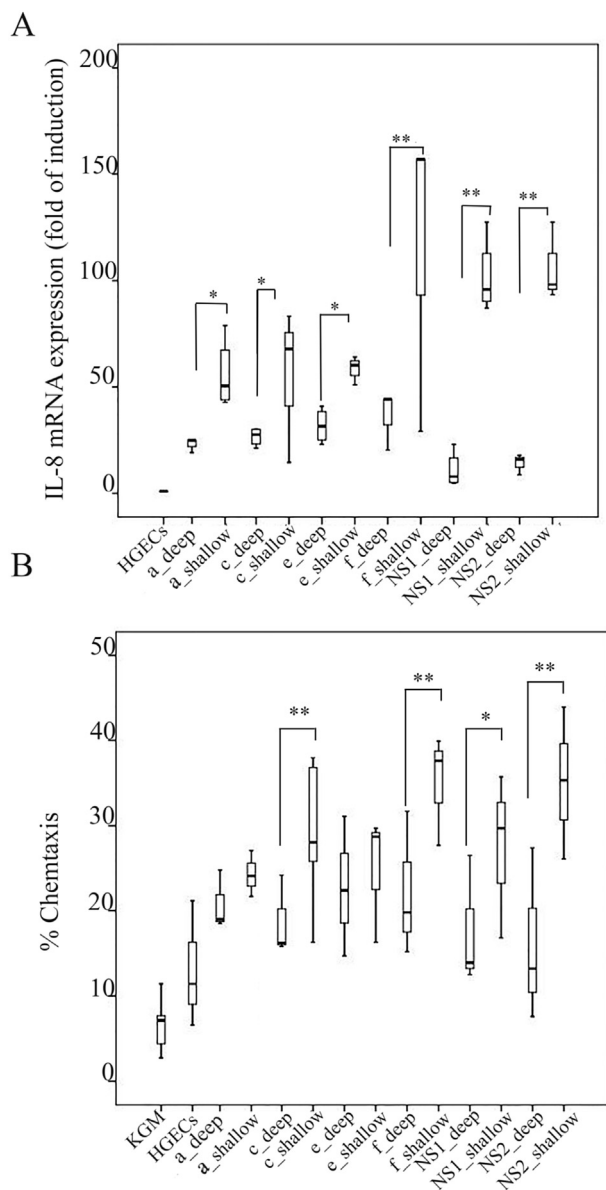
A

B

Fig. 3. HGECs were stimulated with 100 μg/ml of the CWEs of various *A. actinomycetemcomitans* subtypes isolated from deep and shallow pockets. NS: non-serotypeable. Untreated HGECs in (A) and (B) and KGM alone in (B) were used as negative controls. (A) IL-8 mRNA expression by real time-PCR. * indicates statistically significant difference compared with control at $P < 0.05$; ** indicates statistically significant difference compared with control at $P < 0.001$. (B) Neutrophil migration presented as the percentages of chemotaxis by transwell system. * indicates statistically significant difference compared with control at $P < 0.05$; ** indicates statistically significant difference compared with control at $P < 0.01$.

serotype a, c, and e [11,22,23]. In this study, it was found that serotype f showed significantly stronger response than other reference and clinical subtypes and that the two clinical JP2-like leukotoxin promoter gene strains (serotype c) showed significantly IL-8 weaker response than other subtypes.

The two non-serotypeable subgroups NS1 and NS2 showed a significantly lower IL-8 response indicating that an immunosuppression may take place and which is not entirely dependent on the antigenic structure of the bacterial cell wall. The subtyping of *A. actinomycetemcomitans* strains into serotypes and non-serotypeable strains is based on the carbohydrate moieties of cell surface LPS. Therefore, the difference in HGECs IL-8 expression of

A. actinomycetemcomitans serotypes may be dependent on the genetically based o-polysaccharide antigen component of the LPS structures present in the CWEs from the serotypeable strains. The cell wall characteristics and the reason for stains being non-serotypeable are not known but it might be the antigenic structure is either lacking or being hidden by other structures such as proteins. Such antigenic structures might also stimulate differently in the neutrophil recruitment during the innate immune response, which may have important pathophysiological consequences. In this study, we observed that CWEs of *A. actinomycetemcomitans* contained different components in CWEs including some proteins, which may have an effect on the cytokine response. Heat treatment of the CWEs may be one way to exclude the effects of proteins from LPS. This will be a matter for further studies.

The findings JP2-like leukotoxin promoter gene strains showed only minimal IL-8 mRNA expression in HGECs, even exposure to the highest dose of 100 μg/ml of CWEs indicated that these strains exhibited a significant immunosuppressive characteristic compared to other strains. The low IL-8 responses by the high dose (100 μg/ml) of the two JP2-like leukotoxin promoter gene strains were not due to the toxicity of their CWEs, because no significant differences of cell viability were found among treated CWEs samples of other strains. Immunosuppression recognized as a diminished IL-8 expression and secretion by certain subtypes of *A. actinomycetemcomitans* may function as a significant virulence factor, which may hamper the local immunity and migration of neutrophils to the infection site and protect the bacteria from being eliminated by the host. The two JP2-like leukotoxin promoter gene strains exhibited high internalization to fibroblast cells of these strains, which may be due to a similar immunosuppression [8]. Diminishing IL-8 expression and secretion of HGECs stimulated with the two JP2-like leukotoxin promoter gene strains made them more virulent than other strains. However, IL-8 responses showed the different mechanism with leukotoxin which is an important virulent factor of *A. actinomycetemcomitans*. The effect of IL-8 is chemotactic cytokine to accumulate white blood cells especially neutrophil [18] while leukotoxin is toxin used to kill neutrophil, macrophage, etc [1,3,6,12]. This was supported by another study that also demonstrated that the JP2 strain could prevent production of inflammatory cytokines by mononuclear cells (MNCs) [21]. They explained it by saying that 'LtxA-mediated killing or induction of a state of anergy in MNCs … ' may render the bacteria ' … immunologically silent' [24].

Strains from deep pockets showed significantly lower IL-8 expression as well as function on neutrophil migration *in vitro* compared to strains from shallow pockets, and the same results were also found for serotype c and f, and the non-serotypeable (NS1 and NS2). Moreover, *A. actinomycetemcomitans* isolated from deep pockets in particular NS1 and NS2, showed an inverse correlation between IL-8 responses and leukotoxin expression (p = 0.003, r = −0.335), indicating that the highly leukotoxin-producing strains elicit low IL-8 responses in HGECs. The NS1 and NS2 strains also showed a lower IL-8 response in comparison with the serotypeable strains (serotype a-f, serotype b and d were lacking). This pattern of IL-8 expression and function may be due to an ecologically driven adaptation in the deep periodontal pocket exhibiting a more alkaline environment and a lower redox potential compared to shallow pockets [25]. It is, therefore, suggested that certain subtypes of *A. actinomycetemcomitans* by such adaptation increase their survival rate and virulence in the deep periodontal pockets as also has been previously suggested [3,8]. This increased virulence may be facilitated through mechanisms that involve immunosuppression of the IL-8 release from HGECs. The mechanism of IL-8 stimulation by *A. actinomycetemcomitans* and its products is unclear in detail, and it is a matter for further studies.

A substantial variation was noticed between the five donors of HGECs used in this study, which also needs to be considered in relation to the magnitude of the gingival inflammatory reactions and the susceptibility of periodontal disease. It was also revealed that significantly different up-regulation in IL-8 responses was found among individuals where HGECs originated from different hosts [9]. However, any factors influence the expression of various cytokines in hosts by the subgingival biofilm *in vivo* in view of the presence of a complex polymicrobial microbiota can only be speculated about. This will need for further investigations including more donors and with different degrees of periodontitis.

5. Conclusion

Our study demonstrated that the *A. actinomycetemcomitans* stimulated HGECs to produce various pro-inflammatory cytokines mRNA expression and IL-8 mRNA in particular. JP2-like leukotoxin promoter gene subtypes exhibited the lowest IL-8 mRNA expression and concentration and showed no response even at 100 μg/ml of their CWEs and showed significant immunosuppression on the HGECs. Similarly, *A. actinomycetemcomitans* subtypes isolated from deep pockets, especially NS1 and NS2 subtypes, could evade host immune activation by minimal production of IL-8, consistent with its inability to promote neutrophil migration *in vitro*. The cytokine up-regulation of *A. actinomycetemcomitans* subtypes in HGECs is likely to be directed genetically by the structure of the cell wall o-polysaccharide component and by the phenotypic expression of bacterial immune modulating factors driven by environmental conditions.

Conflict of interest statement

All authors report no competing interest related to this study.

Acknowledgements

References

[1] C.H. Aberg, P. Kelk, A. Johansson, *Aggregatibacter actinomycetemcomitans*: virulence of its leukotoxin and association with aggressive periodontitis, Virulence 6 (2015) 188−195.

[2] O. Tsuzukibashi, M. Saito, T. Kobayashi, U. Koji, N. Fumio, F. Nagahama, T. Hiroi, M. Hirasawa, K. Takada, A gene cluster for the synthesis of serotype g-specific polysaccharide antigen in *Aggregatibacter actinomycetemcomitans*, Arch. Microbiol. 196 (2014) 261−265.

[3] N. Pahumunto, P. Ruangsri, M. Wongsuwanlert, S. Piwat, G. Dahlen, R. Teanpaisan, *Aggregatibacter actinomycetemcomitans* serotypes and DGGE subtypes in Thai adult chronic periodontitis, Arch. Oral Biol. 60 (2015) 1789−1796.

[4] G. Dahlen, F. Widar, R. Teanpaisan, P.N. Papapanou, V. Baelum, O. Fejerskov, *Actinobacillus actinomycetemcomitans* in a rural adult population in southern Thailand, Oral Microbiol. Immun. 17 (2002) 137−142.

[5] P. Bandhaya, P. Saraithong, K. Likittanasombat, B. Hengprasith, K. Torrungruang, *Aggregatibacter actinomycetemcomitans* serotypes, the JP2 clone and cytolethal distending toxin genes in a Thai population, J. Clin. Periodontol. 39 (2012) 519−525.

[6] D. Haubek, A. Johansson, Pathogenicity of the highly leukotoxic JP2 clone of *Aggregatibacter actinomycetemcomitans* and its geographic dissemination and role in aggressive periodontitis, J. Oral Microbiol. 6 (2014) 1−22.

[7] B. Henderson, J. Ward, D. Ready, *Aggregatibacter (Actinobacillus) actinomycetemcomitans*: a triple A* periodontopathogen? Periodontology 2000 (54) (2010) 78−105.

[8] N. Pahumunto, P. Ruangsri, M. Wongsuwanlert, S. Piwat, G. Dahlen, R. Teanpaisan, Virulence of *Aggregatibacter actinomycetemcomitans* serotypes and DGGE subtypes isolated from chronic adult periodontitis in Thailand, Anareobe 36 (2015) 60−64.

[9] J. Eberhard, T. Banasch, S. Jepsen, H. Dommisch, Differential epithelial cell response upon stimulation with the *Aggregatibacter actinomycetemcomitans* strains VT 1169, VT 1560 DAM- and ATCC 4318, Epigenetics 5 (2010) 710−715.

[10] P.G. Stathopoulou, M.R. Benakanakere, J.C. Galicia, D.F. Kinane, Epithelial cell pro-inflammatory cytokine response differs across dental plaque bacterial species, J. Clin. Periodontol. 37 (2010) 24−29.

[11] Y. Uchida, H. Shiba, H. Komatsuzawa, T. Takemoto, M. Sakata, T. Fujita, H. Kawaguchi, M. Sugai, H. Kuriharal, Expression of IL-1 beta and IL-8 by human gingival epithelial cells in response to *Actinobacillus actinomycetemcomitans*, Cytokine 14 (2001) 152−161.

[12] J. Hirschfeld, H.M. Roberts, I.L.C. Chapple, M. Parcina, S. Jepsen, A. Johansson, R. Claesson, Effects of *Aggregatibacter actinomycetemcomitans* leukotoxin on neutrophil migration and extracellular trap formation, J. Oral Microbiol. 8 (2016) 1−8.

[13] A. Dietmann, A. Millonig, V. Combes, P.O. Couraud, S.C. Kachlany, G.E. Graua, Effects of *Aggregatibacter actinomycetemcomitans* leukotoxin on endothelial cells, Microb. Pathog. 61−62 (2013) 43−50.

[14] S.C. Kachlany, A.B. Schwartz, N.V. Balashova, C.E. Hioe, M. Tuen, A. Le, Anti-leukemia activity of a bacterial toxin with natural specificity for LFA-1 on white blood cells, Leuk. Res. 34 (2010) 777−785.

[15] S. Krisanaprakornkit, A. Weinberg, P.N. Perez, B.A. Dale, Expression of the peptide antibiotic human β-Defensin 1 in cultured gingival epithelial cells and gingival tissue, Infect. Immun. 66 (1998) 4222−4228.

[16] S. Krisanaprakornkit, J.R. Kimball, A. Weinberg, R.P. Darveau, B.W. Bainbridge, B.A. Dale, Inducible expression of human β-Defensin 2 by *Fusobacterium nucleatum* in oral epithelial cells: multiple signaling pathways and role of commensal bacteria in innate immunity and the epithelial barrier, Infect. Immun. 682 (2000) 2907−2915.

[17] R.D. Barber, D.W. Harmer, R.A. Coleman, B.J. Clark, GAPDH as a housekeeping gene: analysis of GAPDH mRNA expression in a panel of 72 human tissues, Physiol. Genomics 21 (2005) 389−395.

[18] P.A. Nuzzi, M.A. Lokuta, A. Huttenlocher, Analysis of neutrophil chemotaxis, Methods Mol. Biol. 370 (2007) 23−36.

[19] N. Silva, L. Abusleme, D. Bravo, N. Dutzan, J. Garcia-Sensnich, R. Vernal, M. Hernandez, J. Gamona, Host response mechanisms in periodontal diseases, J. Appl. Oral Sci. 23 (2015) 329−355.

[20] K. Ohta, H. Shigeishi, M. Taki, H. Nishi, K. Higashikawa, M. Takechi, N. Kamata, Different regulation of CXCL9, CXCL10, and CXCL11 expression induced by IFN-γ, TNF-α and IL-4 in human oral keratinocytes and fibroblasts, J. Dent. Res. 87 (2008) 1161−1165.

[21] R.M. Chung, J.T. Grbic, I.B. Lamster, IL-8 and β-Glucoronidase in gingival crevicular fluid, J. Clin. Periodontol. 24 (1997) 146−152.

[22] T. Chino, D.M. Santer, D. Giordano, C. Chen, C. Li, C.H. Chen, R.P. Darveau, E.A. Clark, Effects of oral commensal and pathogenic bacteria on human dendritic cells, Oral Microbiol. Immunol. 24 (2009) 96−103.

[23] T. Shimada, N. Sugano, R. Nishihara, K. Suzuki, H. Tanaka, K. Ito, Differential effects of five *Aggregatibacter actinomycetemcomitans* strains on gingival epithelial cells, Oral Microbiol. Immunol. 23 (2008) 455−458.

[24] C. Damgaard, J. Reinholdt, Y. Palarasah, C. Enevold, C. Nielsen, M.K. Brimnes, P. Holmstrup, C.H. Nielsen, In vitro complement activation, adherence to red blood cells and induction of mononuclear cell cytokine production by four strains of *Aggregatibacter actinomycetemcomitans* with different fimbriation and expression of leukotoxin, J. Periodontal Res. (2016) 1−12.

[25] M. Kilian, I.L.C. Chapple, M. Hanning, P.D. Marsh, V. Meuric, A.M. Pedersen, M.S. Tonetti, W.G. Wade, E. Zaura, The oral microbiome-an update for oral healthcare professionals, Br. Dent. J. 221 (2016) 657−666.

Effects of low-dose irradiation on human osteoblasts and periodontal ligament cells

Jarinya Pathomburi[a], Sakarat Nalampang[b], Anupong Makeudom[c], Jeerawan Klangjorhor[d], Chayarop Supanchart[a,c], Suttichai Krisanaprakornkit[b,c,*]

[a] *Department of Oral and Maxillofacial Surgery, Faculty of Dentistry, Chiang Mai University, Chiang Mai, Thailand*
[b] *Department of Oral Biology and Diagnostic Sciences, Faculty of Dentistry, Chiang Mai University, Chiang Mai, Thailand*
[c] *Center of Excellence in Oral and Maxillofacial Biology, Faculty of Dentistry, Chiang Mai University, Chiang Mai, Thailand*
[d] *Musculoskeletal Science and Translational Research Center, Department of Orthopedics, Faculty of Medicine, Chiang Mai University, Chiang Mai, Thailand*

A B S T R A C T

Objective: To investigate the effects of dental x-ray on proliferation and mineralization in human primary osteoblasts as well as on proliferation and apoptotic potential in human periodontal ligament (PDL) cells.
Design: Primary osteoblasts and PDL cells were irradiated with various doses of periapical radiography by repeated exposures and further incubated for 1, 3 or 7 days. Cell proliferation was assayed by BrdU incorporation. The effect of dental x-ray on mineralization in osteoblasts either before or after x-ray exposures was determined by Alizarin red staining. Both mRNA and protein expressions of *BCL-2*, an anti-apoptotic gene, and *BAX*, a pro-apoptotic gene, in PDL cells were analyzed by RT-qPCR and immunoblotting analysis, respectively.
Results: Neither the proliferative nor the mineralization ability of irradiated osteoblasts was different from that of non-irradiated osteoblasts at any doses or time points. By contrast, there was a significant decrease in the proliferation of PDL cells on day 3 after repeated exposures to dental x-ray for 20 times ($P < 0.05$), whereas the ratio of *BCL-2* to *BAX* mRNA and protein expressions in these irradiated PDL cells was significantly increased ($P < 0.05$).
Conclusions: Upon multiple exposures to dental x-ray used in intraoral radiography up to 20 times, there is no effect on the proliferation or the mineralization of osteoblasts, whereas the proliferative and apoptotic potentials of PDL cells are transiently decreased.

1. Introduction

In dentistry, x-ray is used to detect and localize pathologic lesions and foreign bodies in jaw bones, to assess human growth and development, and to explore hard tissue structures in a 3D image. It is classified as an ionizing radiation similar to others that are used in radiotherapy of cancers (Xu et al., 2012). While x-ray travels through living cells, it can induce the formation of free radicals, regardless of the amounts of radiation (Iannucci & Howerton, 2016). So, although the dental x-ray is regarded as low-dose irradiation (< 1 Gy; Marcu, 2017), it may cause adverse effects directly and indirectly on oral cells, especially from scattering radiation (White & Pharoah, 2014) and from a bystander effect, an indirect effect through cell to cell communications (Ojima, Eto, Ban, & Kai, 2011).

There have been several studies into the effects of both intraoral and

extraoral radiographies on various cell types. For example, the full-mouth intraoral radiography, the panoramic/lateral cephalometric radiography, and the cone-beam computed tomography altered a nuclear morphology, closely relating to cytotoxicity and cell death in exfoliated epithelial cells from buccal mucosa of children and adults (Angelieri, de Oliveira, Sannomiya, & Ribeiro, 2007; Cerqueira et al., 2004; Kesidi, Maloth, Reddy, & Geetha, 2017; Lorenzoni, Fracalossi, Carlin, Ribeiro, & Sant'Anna, 2012; Ribeiro & Angelieri, 2008; Ribeiro, De Oliveira, De Castro, & Angelieri, 2008). In addition, the stochastic effect on DNA damage that could increase the probability of carcinogenesis by the dental cone-beam computed tomography in radio-sensitive cells of chldren has been recently shown (De Felice, Di Carlo, Saccucci, Tombolini, & Polimeni, 2019). Certain doses of intraoral x-ray increased the number of rat macrophages and lymphocytes (Asymal, Astuti, & Devijanti, 2018), but decreased expression of cyclin D1 in a

mouse osteoblastic cell line, MC3T3-E1, indicating altered cell proliferation (Pramojanee, Pratchayasakul, Chattipakorn, & Chattipakorn, 2012). On the contrary, another study showed a significant increase in alkaline phosphatase activity, implying an increase in differentiated osteoblasts, in a human fetal osteoblastic cell line exposed to the intraoral radiography using digital x-ray (Kurt, Oztas, & Atalay, 2016). Therefore, the effects of dental x-ray on proliferation and differentiation of different cell types are still inconclusive.

Both osteoblasts and periodontal ligament (PDL) cells differentiate from mesenchymal stem cells in PDL (Ivanovski, Gronthos, Shi, & Bartold, 2006). Osteoblasts function in bone remodeling by synthesizing bone matrix to maintain bone homeostasis, while PDL cells are involved in soft tissue remodeling to maintain the periodontal ligament width (Garant, 2003). Because of their adjacent location within the periodontium upon exposure to dental irradiation, it was logical to hypothesize that they would be similarly affected by dental x-ray. However, to the best of our knowledge, no study has so far determined the effects of dental x-ray on primary human osteoblasts and PDL cells. Moreover, because of considerable variations in cellular compositions and specific gene expressions in response to radiation from one species to another (Czekanska, Stoddart, Richards, & Hayes, 2012), the results of a previous study (Pramojanee et al., 2012) using the mouse osteoblastic cell line are still questionable for clinical applications in humans. In addition, although cell lines are phenotypically stable and proliferate continuously without a need for cell isolation, they cannot reflect the whole range of primary osteoblast phenotypes (Czekanska et al., 2012). Consequently, the objective of this study was to examine the effects of repeated exposures of intraoral x-ray on the proliferation of primary human osteoblasts and PDL cells, on the mineralization of osteoblasts, and on the expressions of the apoptotic-related genes in PDL cells.

2. Materials and methods

2.1. Culture of primary human osteoblasts

Human osteoblasts were obtained from the Orthopedics Laboratory and Research Network, Faculty of Medicine, Chiang Mai University, Chiang Mai, Thailand, under the approved research project, #ORT-2557-02717. The present study was also approved by the Human Experimentation Committee, Faculty of Dentistry, Chiang Mai University (#17/2018). The osteoblasts were harvested during surgical treatment of a traumatically injured long bone of four donors (8–12 years old, 2 females and 2 males) with written informed consent according to a previous protocol of Pruksakorn et al. (2016). The osteoblasts were derived from these children with a high osteogenic capacity during the first two decades of life (Czekanska et al., 2012; Evans, Galasko, & Ward, 1990; Fedarko, Vetter, Weinstein, & Robey, 1992). All donors had no history of taking drugs related to bone metabolism, and the bone specimens were diagnosed without any orthopedic diseases or bone cancer. In brief, the bone specimen was flushed several times with phosphate-buffered saline, pH 7.2, to remove mesenchymal stem cells and blood cells and sequentially digested using collagenase type I-trypsin (Gibco, Grand Island, NY, USA) at 37 °C for 18 h to isolate primary osteoblasts from the bone specimen. The cells were cultured in alpha modifications of Eagle's Minimum Essential Medium (Gibco), supplemented with 10% fetal bovine serum (FBS; Gibco), 2 mM L-glutamine (Gibco) and 1% penicillin/streptomycin (Gibco) at 37 °C in a humidified chamber with 5% CO_2. When the number of cells reached 80% confluence, they were detached using 0.25% EDTA trypsin (Gibco) and grown in appropriate culture plates at the cell density of 1×10^5 cells per ml to expand the number of cells. To confirm the osteoblastic phenotypes of cultured primary cells, some cells from the second passage were used for assessment of the doubling time, for expressions of the osteogenic markers, including collagen type I, osteonectin, and bone sialoprotein, for alkaline phosphatase activity assay, and for mineralization assay by Alizarin red staining, as previously described

(Pruksakorn et al., 2016). The remaining cells were cultured for 24 h before irradiation.

2.2. Culture of primary human periodontal ligament cells

PDL cells were isolated from third molars extracted for medical reasons that did not have extensive caries, severe periodontal infection or periapical lesions of four patients (18–25 years old, 2 females and 2 males) with written informed consent as previously described and characterized (Truntipakorn et al., 2017). The morphology of PDL cells was typically like that of fibroblasts. Briefly, the PDL tissues were gently scraped from the middle third of the roots to avoid contamination from gingival fibroblasts and cut into small pieces. Tissue explants were immersed in Dulbecco's Modified Eagle Medium (DMEM; Gibco), supplemented with 10% FBS, 2 mM L-glutamine, 5 μg/ml amphotericin B (Gibco) and 1% penicillin/streptomycin at 37 °C in a humidified chamber with 5% CO_2. After having grown out from the explants, PDL cells were trypsinized using 0.25% EDTA trypsin and sub-cultured at a ratio of 1:3 for further expansions. At 80% confluence, PDL cells were detached and seeded in appropriate culture plates at the same cell density as primary osteoblasts. The cells were cultured for 24 h before irradiation.

2.3. Irradiation protocol

Both osteoblasts and PDL cells, seeded in nine wells at the center of 96-well plates (Corning, NY, USA), in four wells at the center of 24-well plates (Corning), or 35-mm culture dishes (Corning) for proliferation assay, mineralization assay, or gene expressions, respectively, were repeatedly exposed to the same dose (60 kVp and 0.25 s for an exposure time) of the intraoral radiography for 5, 10 and 20 times (5x, 10x, and 20x, respectively) using a dental x-ray machine generator, commercially available in clinical dentistry (Heliodent Plus HF, Sirona, Germany), within an 8-inch distance between radiation source and cells. In this study, three repeated exposure times in the irradiation protocol (5x, 10x and 20x) were chosen from a design of the previous study (Pramojanee et al., 2012) and the fact that the total number of full-mouth intraoral radiography in routine dental practice is no more than 20 films. The amount of irradiation for a single dose was 2.1 mGy, as measured at the tip of the x-ray tube in the absence of cells and growth medium by an x-ray test device (TNT 12000D®, Fluke Biomedical, Cleveland, OH, USA). This dose falls in the range of one typical conventional periapical exposure. Cultured osteoblasts and PDL cells without irradiation were a negative control, while the cells treated with phorbol-13-myristate 12-acetate (PMA; Sigma-Aldrich, St. Louis, MO, USA) at 10 ng per ml for 24 h were a positive control for cell proliferation. However, from our pilot study, treatment of osteoblasts with 10 ng per ml of PMA in the presence of ascorbic acid, dexamethasone and β-glycerophosphate, whose concentrations are mentioned in 2.7, showed no further enhancement of mineralization (data not shown). Therefore, the positive control was not included in the mineralization assay.

2.4. Cell proliferation assay

After irradiation, both cell types were further incubated for 1, 3, or 7 days with medium replacement every other day, and the BrdU colorimetric immunoassay (Roche, Basel, Switzerland) was performed. Three periods after dental x-ray exposure (1, 3 and 7 days) were selected because there is usually no repeated full-mouth radiography within 7 days. In brief, BrdU was added to the medium and incubated for 4 h at 37 °C. After medium removal, the cells were fixed and their DNA was denatured for 30 min at room temperature. Then, anti-BrdU antibody was added and incubated at room temperature for 90 min. After that, the cells were rinsed to remove an excess of the antibody, and the immune complexes were detected by reacting with the

substrate at room temperature for 30 min, which was stopped by addition of H_2SO_4. The absorbance value of each sample was measured using the microplate reader (Tecan Sunrise™, Männedorf, Switzerland) at the 450-nm wavelength with the reference wavelength at 690 nm and compared with that of the non-irradiated cells as a negative control, set to 100%. This experiment was separately conducted for four times using primary osteoblasts and PDL cells from four different donors.

2.5. RNA extraction and RT-qPCR

After irradiation, PDL cells were further incubated for 1, 3, or 7 days with medium replacement every other day, and total RNA was harvested using the RNAspin Mini isolation kit (GE Healthcare, Little Chalfont, Buckinghamshire, UK) according to the manufacturer's instructions. The quality of isolated total RNA was confirmed by the integrity of 18 s and 28 s ribosomal RNA on agarose gel stained with ethidium bromide (Bio-Rad Laboratories, Inc., Hercules, CA, USA; data not shown), and its quantity was measured by the Nanodrop™ 2000 spectrophotometer (Thermo Fisher Scientific, Rochester, NY, USA) at 260-nm and 280-nm wavelengths. The ratio of absorbance value at 260 nm relative to that at 280 nm in each sample was more than 1.8. A two-μg quantity of total RNA from each sample was converted to complementary DNA (cDNA) using the RevertAid cDNA Synthesis kit (Thermo Fisher Scientific, Waltham, MA, USA). Quantitative PCR was performed using the SYBR No-ROX kit (SensiFAST™, Bioline, London, UK), containing *Taq* polymerase and the SYBR green I dye, by the LightCycler 480 instrument II (Roche, Rotkreuz, Switzerland) with specific primer pairs for B-cell lymphoma 2 (*BCL-2*), BCL-2-associated X protein (*BAX*), and glyceraldehyde-3-phosphate dehydrogenase (*GAPDH*). The intron-spanning primer sequences of *BCL-2* and *BAX* were derived from our previous study (Pramojanee, Pavasant, & Panmekiate, 2008), whereas those of *GAPDH* were from Truntipakorn et al. (2017)). Selection of *GAPDH* as a reference gene was based on our previous study to determine expressions of *NANOG* and *OCT4* mRNA in the same cell type, *i.e.*, human PDL cells (Truntipakorn et al., 2017). Moreover, from the melting curve analysis of *BCL-2*, *BAX* and *GAPDH* mRNA expressions, a sharp peak was demonstrated for each gene at the expected temperature, indicating that qPCR products were homogeneous without primer dimers, and the chosen primers specifically amplified the *BCL-2*, *BAX* and *GAPDH* cDNAs. However, agarose gel electrophoresis of RT-qPCR products to verify a single band at its predicted size was not performed. Furthermore, western blot hybridization using antibodies specific for BCL-2 and BAX was performed as described in the Section 2.6 to verify the findings of *BCL-2* and *BAX* mRNA expressions in irradiated human PDL cells. All primer sequences are summarized in Table 1. The PCR conditions were pre-incubation at 95 °C for 10 min for one cycle, followed by denaturation at 95 °C for 20 s, annealing at 55 °C for 20 s, and elongation at 72 °C for 25 s, for 45 cycles. The expressions of *BCL-2* and *BAX* in each sample were normalized to that of *GAPDH* with aid of calculation algorithm of LightCycler 480 software version 1.5 (Roche) to obtain ΔC_t. Then, the ratio of *BCL-2* to *BAX* expression in each sample was computed from the ΔC_t value of *BCL-2* divided by that of *BAX*, and this ratio was adjusted to

percentage of the *BCL-2* to *BAX* expression in comparison to that of the non-irradiated PDL cells, set to 100%, to obtain the $\Delta\Delta C_t$ value of each sample. However, the RT-qPCR efficiency for each individual gene by the corrected calculation method using serially diluted samples as shown by Rao, Huang, Zhou, & Lin, 2013 was not determined. This experiment was independently conducted four times using primary PDL cells from four different donors, and the average percentage was determined from the four PDL cell lines.

2.6. Protein extraction and western blot analysis

After irradiation, PDL cells were further incubated for 1, 3, or 7 days with medium replacement every other day, and total proteins were extracted from the cells using RIPA buffer, containing 5 mM HEPES, 1% NP-40, 5 mg per ml sodium deoxycholate, 150 mM sodium chloride, 50 mM sodium fluoride, 10 μg per ml aprotinin, 5 mM benzamidine, 2 mM PMSF and 1 mM sodium orthovanadate (Supanchart et al., 2012), supplemented with the cOmplete™ tablet, Mini, EDTA-free, EASYpack Protease Inhibitor Cocktail (Roche Biochemicals, Indianapolis, IN, USA). Protein concentrations were determined using the bicinchoninic acid (BCA) protein assay kit (Pierce, Rockford, IL, USA). A 20-μg quantity of total protein from each sample was resolved by 12% SDS-PAGE and transferred to nitrocellulose membranes. The membranes were incubated in 5% nonfat dried milk in 0.1% tween-TBS for 1 h at room temperature, followed by incubation with primary antibody against BCL-2 (1:1000; ABCAM, Cambridge, MA, USA), BAX (1:500; Santa Cruz Biotechnology, Santa Cruz, CA, USA) or β-actin (1:1000; Santa Cruz) overnight at 4 °C. After washing four times with 0.1% tween-TBS, the blot of BCL-2 was incubated with HRP-conjugated swine anti-rabbit immunoglobulins (1:2000), while the blots of BAX and β-actin were incubated with HRP-conjugated rabbit anti-mouse immunoglobulins (1:2000) for 1 h at room temperature. The membranes were then reacted with the LumiGLO Reserve™ Chemiluminescent substrate (KPL, Gaithersburg, MD, USA). The protein bands were detected by the ChemiDoc™ XRS instrument (Bio-Rad Laboratories, Inc.). The band intensities were quantified by ImageJ program. The expressions of BCL-2 and BAX in each sample were normalized by that of β-actin. Then, percentage of the ratio of normalized BCL-2 to BAX expression in each sample was calculated and compared with that in the non-irradiated cells as a control, set to 100%. This experiment was independently conducted four times using primary PDL cells from four different donors.

2.7. Mineralization assay

To simulate heterogeneous populations of osteoblasts in bone upon irradiation, the cultures of primary osteoblasts, seeded in 24-well plates, were divided into two groups, comprising group I: exposure to x-ray before induction of mineralization (X-Min) and group II: exposure to x-ray after induction of mineralization by osteogenic medium, containing 50 μg/ml ascorbic acid (Sigma-Aldrich), 100 nM dexamethasone (Sigma-Aldrich) and 10 mM β-glycerophosphate (Sigma-Aldrich), for 7 days (Min-X). In each group, the cells were repeatedly exposed to x-ray for different times as aforementioned. After irradiation, the cells in group I were further incubated in the osteogenic medium as mentioned above for 14 days, whereas those in group II were further incubated in the osteogenic medium for another 7 days. Subsequently, the cells were fixed with 10% neutral buffered formalin for 30 min and stained with 0.5 ml of 40 mM Alizarin red S (AMRESCO, Solon, OH, USA), pH 4.2–4.5, at room temperature for 15 min. The cells were excessively washed with cold deionized water until the washing solution was clear. Digitized images of Alizarin red staining were recorded by a charge-coupled device attached to the stereomicroscope (Olympus E-330; Olympus, Inc., Tokyo, Japan) prior to addition of a 0.5-ml volume of 10% acetic acid for 30 min with shaking, followed by addition of a 0.2-ml volume of 10% ammonium hydroxide. For

Table 1
Oligonucleotide primer sequences used in RT-qPCR.

Gene	Forward (5'-3') Reverse (5'-3')	NCBI-BLAST accession
BCL-2	AGG AAG TGA ACA TTT CGG TGA C GCT CAG TTC CAG GAC CAG GC	NM_000633.2
BAX	TGC TTC AGG GTT TCA TCC AG GGC GGC AAT CAT CCT CTG	NM_138761.4
GAPDH	TGA AGG TCG GAG TCA ACG GAT TCA CAC CCA TGA CGA ACA TGG	NM_002046.7

quantitative analysis, a 150-µl aliquot of the supernatant in each sample was transferred to a 96-well plate with opaque wall and clear bottom (Corning) and measured for its absorbance value at the 405-nm wavelength by the microplate reader (Tecan Sunrise™). The absorbance value of each sample was compared with that of the non-irradiated cell sample, set to 100%. This experiment was separately conducted four times using primary osteoblasts from four different donors. The negative control for the mineralization assay was a culture without osteogenic reagents that showed no calcified nodules (data not shown), while the control in Fig. 3 was non-irradiated osteoblasts cultured in osteogenic medium.

2.8. Statistical analysis

All data were found to be normally distributed by the Shapiro-Wilk test and were presented as means ± standard deviations. The comparisons among different doses of x-ray in each time point were determined using one way analysis of variance (ANOVA), followed by the Tukey test for multiple comparisons if any significant differences were found. *P*-values less than 0.05 were considered to be statistically different. The statistical analyses were performed using SPSS software version 17.0 for Windows (IBM, Armonk, NY, USA).

3. Results

3.1. Differential effects of dental x-ray on human osteoblast and PDL cell proliferation

Using the BrdU assay, it was shown that the proliferation rate of primary human osteoblasts was not affected by dental x-ray at any doses or any time points after irradiation (Fig. 1). Although there were no differences in the mean percentages of cell proliferation in primary human osteoblasts, there was a trend for decreased cell proliferation upon repeated exposures to dental x-ray on day 7 after irradiation. However, it was not possible to extend the BrdU assay performed in cell cultures beyond day 7 due to cell confluence over 100%. As a positive control, treatment with PMA at 10 ng/ml slightly increased the mean percentages of human osteoblast proliferation on days 1 and 7 after treatment, but a significant increase in the mean percentage of cell proliferation was found on day 3 after PMA treatment ($P < 0.05$;
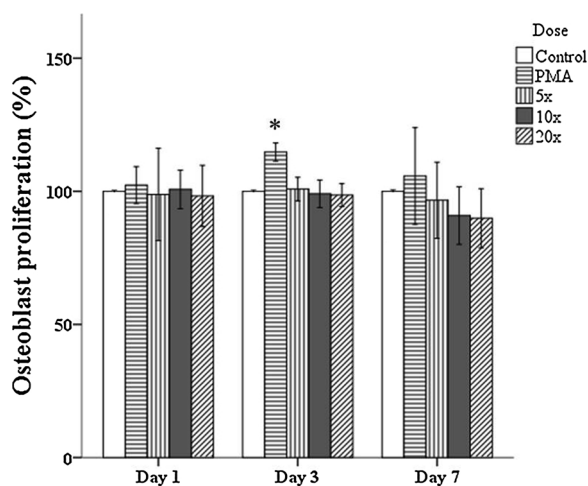

Fig. 1. Percentage of cell proliferation in primary human osteoblasts upon repeated exposures to conventional dental x-ray for various doses (5x, 10x or 20x) at different time points (1, 3 or 7 days after irradiation). PMA = treatment with 10 ng per ml of phorbol-13-myristate 12-acetate for 24 h. The proliferation rate was analyzed by a BrdU assay. Error bars represent standard deviations of four independent experiments using osteoblasts from four different donors. * = $P < 0.05$.
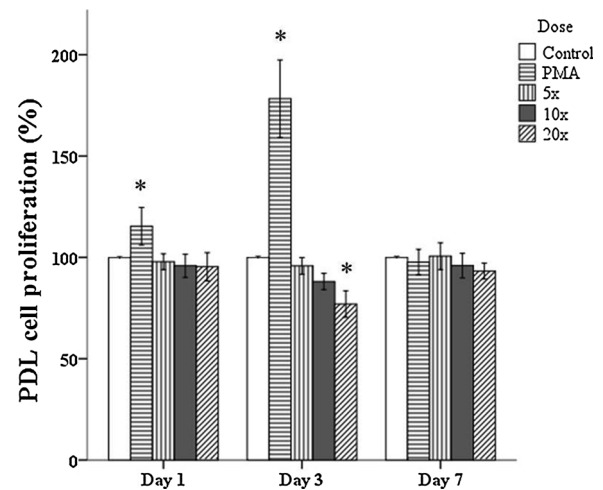

Fig. 2. Percentage of cell proliferation in primary human periodontal ligament (PDL) cells upon repeated exposures to conventional dental x-ray for various doses (5x, 10x or 20x) at different time points (1, 3 or 7 days after irradiation). PMA = treatment with 10 ng per ml of phorbol-13-myristate 12-acetate for 24 h. The proliferation rate was analyzed by a BrdU assay. Error bars represent standard deviations of four separate experiments using PDL cells from four different donors. * = $P < 0.05$.

Fig. 1). In contrast to no effect of dental x-ray on the proliferation of human osteoblasts, there was a significant decrease in the mean percentage of human PDL cell proliferation upon repeated exposures for 20 times, or 42 mGy, to periapical radiography on day 3 after irradiation ($P < 0.05$; Fig. 2). As a positive control, there were significant increases in the mean percentages of human PDL cell proliferation on days 1 and 3 after PMA treatment ($P < 0.05$; Fig. 2).

3.2. No effect of dental x-ray on human osteoblast mineralization

The representative digitized images from four separate experiments of the two groups, group I (X-Min) and group II (Min-X), irradiated at any of the three doses (5x, 10x or 20x) illustrated no obvious difference in color intensity after Alizarin red staining as compared to the control, *i.e.*, non-irradiated osteoblasts (Fig. 3A). The quantitative analysis of staining intensities also confirmed no differences in the mean percentages of staining in the two irradiated groups at any doses compared to that in the control (Fig. 3B).

3.3. Transient decrease in apoptosis of irradiated PDL cells with dental x-ray

Due to the transiently decreasing effect of dental x-ray at 42 mGy on the proliferation of PDL cells (Fig. 2), we then further explored the effect of dental x-ray on cell apoptosis by determining mRNA and protein expressions of an anti-apoptotic gene, *BCL-2*, and a pro-apoptotic gene, *BAX*. Interestingly, instead of promotion of cell apoptosis by high-dose irradiation (> 1 Gy), reported in different types of fibroblasts (Ding et al., 2005), low-dose irradiation by repeated exposures to dental x-ray for 20 times, or 42 mGy, significantly increased the mean percentage of the ratio of *BCL-2* to *BAX* mRNA expression on day 3 after irradiation compared to that in the negative control, *i.e.*, non-irradiated PDL cells ($P < 0.05$; Fig. 4). In comparison to BAX protein expression in non-irradiated control PDL cells, that in irradiated PDL cells on days 1 and 3 after irradiation was down-regulated in a dose-dependent manner (Fig. 5A). However, BCL-2 protein expression was approximately equivalent among different radiation doses and time points (Fig. 5A). Expression of β-actin was approximately equal among different samples (Fig. 5A). By densitometry of the BCL-2 and BAX protein bands, consistent with the aforementioned mRNA finding, a significant
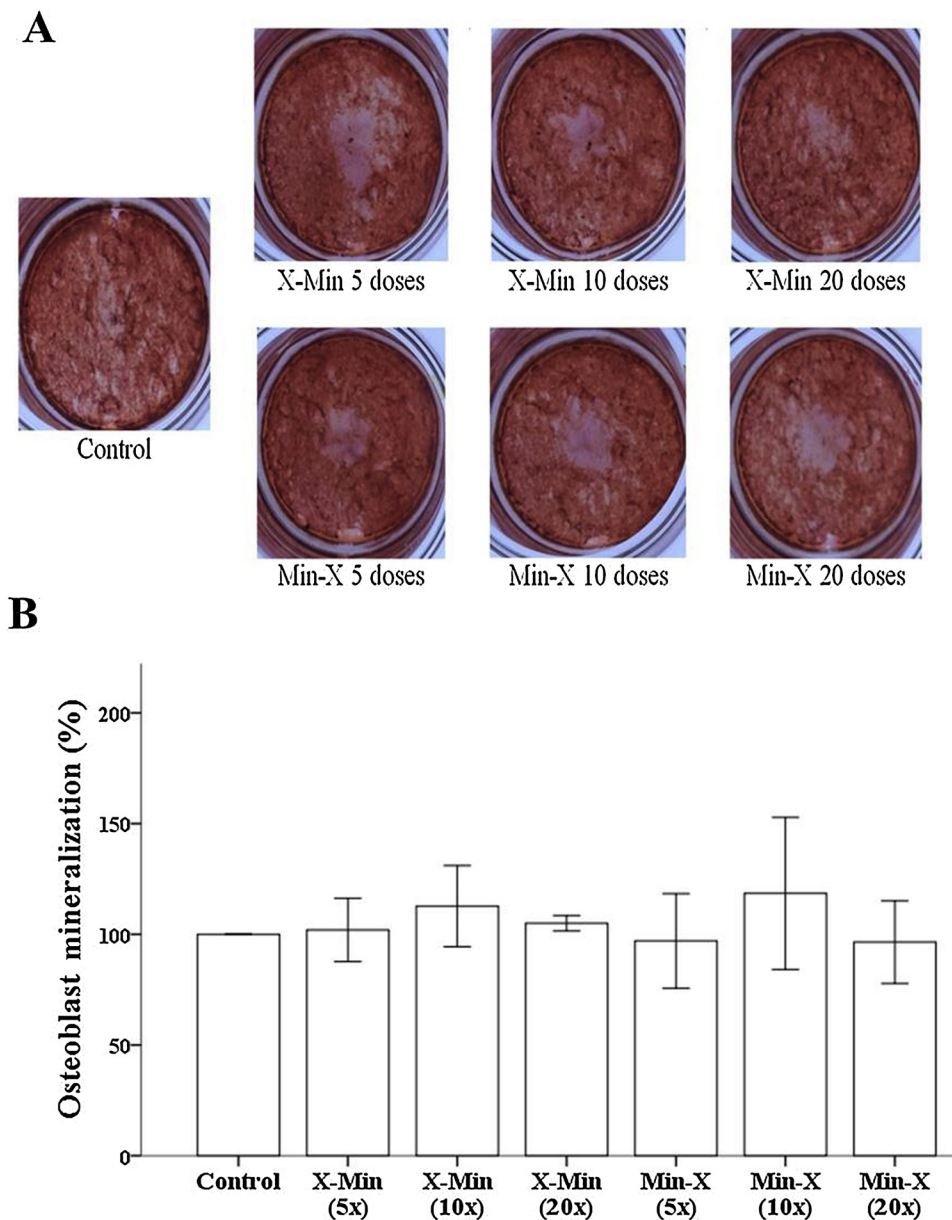
A

B

increase in the mean percentage of the ratio of BCL-2 to BAX protein expression was found on day 3 after repeated exposures to dental x-ray for 20 times (Fig. 5B), although there were trends for a dose-dependent increase in these ratios in PDL cells on days 1, 3 and 7 after irradiation (Fig. 5B).

4. Discussion

Although the effects of dental radiation have been shown on certain cell types of the oral cavity, there is little or no evidence for the effect of dental x-ray on primary human osteoblasts or PDL cells. In this study, the proliferation of primary human osteoblasts as assayed by BrdU incorporation was not affected by repeated exposures to dental x-ray even at the maximal dose (20 times or 42 mGy), consistent with no significant effect of dental x-ray at 40 mGy or at 9.1 mGy on the proliferation of primary rat osteoblasts from calvarias (Dare et al., 1997) or of human fetal osteoblasts (Kurt et al., 2016), respectively. However, a previous study has instead revealed that the expression of cyclin D1, a marker of cell proliferation, was significantly down-regulated in the mouse osteoblastic cell line, MC3T3-E1, upon exposure to dental x-ray

at 15 mGy (Pramojanee et al., 2012). The reason behind this discrepancy may be due to distinct cellular responses to dental x-ray between primary osteoblasts used in this study and the others (Dare et al., 1997) and the osteoblastic cell line.

In contrast to no effect of dental x-ray on osteoblast proliferation, the proliferation of human PDL cells was significantly, but temporarily, decreased on day 3 after dental irradiation at the maximal dose (42 mGy), which corresponds with the finding from a recent study (Truong et al., 2018) that showed a higher percentage of irradiated NIH3T3 mouse fibroblasts in the G0/G1 phase of the cell cycle than control non-irradiated fibroblasts on days 1 and 3 after being irradiated with low-dose x-ray. This suggests an initial pause in cell proliferation that could be a protective mechanism of the cells to minimize DNA damage caused by irradiation (Landsverk, Lyng, & Stokke, 2004). Moreover, the distinct responses to dental x-ray between osteoblasts and PDL cells reflect different radiosensitivity between two neighboring mesenchymal cell types within the same field of irradiation and indicate higher sensitivity to radiation of proliferative cells, such as PDL cells due to their high turnover rate (Garant, 2003), than more differentiated cells like osteoblasts. The inhibitory effect on PDL cell proliferation as
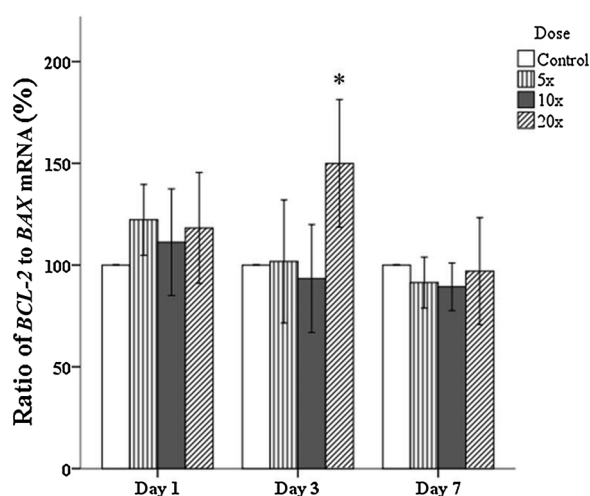
Fig. 4. Percentage of the ratios of *BCL-2* to *BAX* mRNA expressions in primary human periodontal ligament (PDL) cells upon repeated exposures to conventional dental x-ray for various doses (5x, 10x or 20x) at different time points (1, 3 or 7 days after irradiation). The ratio of *BCL-2* to *BAX* mRNA expression was computed in each sample in comparison to that of non-irradiated control cells, set to 100%. Error bars represent standard deviations of four separate experiments using PDL cells from four different donors. * = P < 0.05.

shown by the BrdU assay also verifies the true absence of suppressive effect on the osteoblast proliferation. Interestingly, the transiently decreased proliferation of PDL cells on day 3 after exposure to the maximal dose of dental x-ray returned to the normal level on day 7 as compared to that of the non-irradiated PDL cells, indicating reversible damage of low-dose dental x-ray and the ability of PDL cells to recover and resume their normal proliferation rate as shown in Fig. 2.

As a positive control for cell proliferation, PMA treatment distinctly enhanced proliferation of human osteoblasts and PDL cells on day 3 and

on days 1 and 3, respectively. The reason behind the differences in the proliferative induction of PMA in two different cell types is due to distinct rates of cell proliferation between human osteoblasts and PDL cells (approximately 60 h *versus* 20 h, respectively; Basdra & Komposch, 1997; Kasperk et al., 1995). In addition, typical cultured cells with active growth reach their 100% confluence after 7 days in culture; therefore, the proliferative effect of PMA would not be evident on day 7 possibly due to inhibition of cell proliferation by cell-to-cell contacts (Xu et al., 2012). The BrdU assay, which directly measures increased amounts of cellular DNA, is more suitable and sensitive to detect any changes in terms of cellular proliferation than other colorimetric assays that use various dyes to analyze the activity of mitochondrial enzymes, which is instead enhanced by linear energy transfer from ionizing radiation (Spitz, Azzam, Li, & Gius, 2004; Yamamori et al., 2012) that may cause false findings. Nevertheless, due to the influences of cell numbers, an extent of S-phase fraction, and an S-phase checkpoint activity over BrdU incorporation into newly synthesized DNA strands, the time course of two dimensional FACS analysis for DNA contents and BrdU incorporation would provide more accurate information for cell proliferation. Additional experiments, such as the annexin FACS analysis, the TUNEL assay, are needed to further verify the diminished apoptotic potential of irradiated human PDL cells for 20 times observed on day 3.

Similar to no effect of dental x-ray on osteoblast proliferation, the ability of primary human osteoblasts to deposit calcified nodules as shown by Alizarin red staining was also unaffected by dental x-ray at any of the three doses (10.5, 21 or 42 mGy), which is in agreement with a previous finding that showed no significant effect of x-ray at 40 mGy on mineralization as determined by alkaline phosphatase activity or von Kossa staining in the MC3T3-E1 cell line and rat osteoblasts (Dare et al., 1997). Therefore, it is reasonable to assume that the low-dose dental x-ray has no inhibitory effect on mineralization determined by various techniques in the osteoblastic cell lines or primary osteoblasts from different species. It is interesting to note that irradiation with
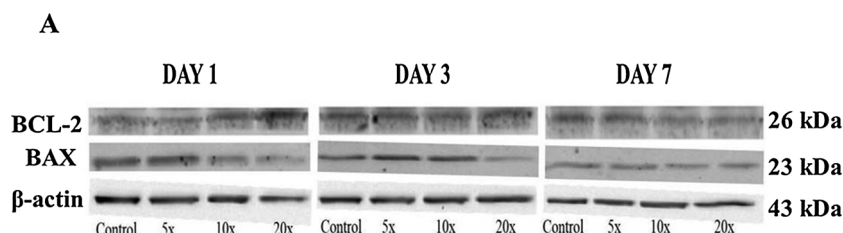
Fig. 5. Representative blots (A) of BCL-2, BAX and β-actin expressions in primary human periodontal ligament (PDL) cells from one donor after repeated exposures to conventional dental x-ray for various doses (5x, 10x or 20x) at different time points (1, 3 or 7 days after irradiation). Percentage (B) of the ratios of BCL-2 to BAX expressions normalized by β-actin expression in primary human PDL cells. The ratio of BCL-2 to BAX protein expression in each sample was computed in comparison to that of non-irradiated control cells, set to 100%. Error bars represent standard deviations of four separate experiments using PDL cells from four different donors. * = P < 0.05.
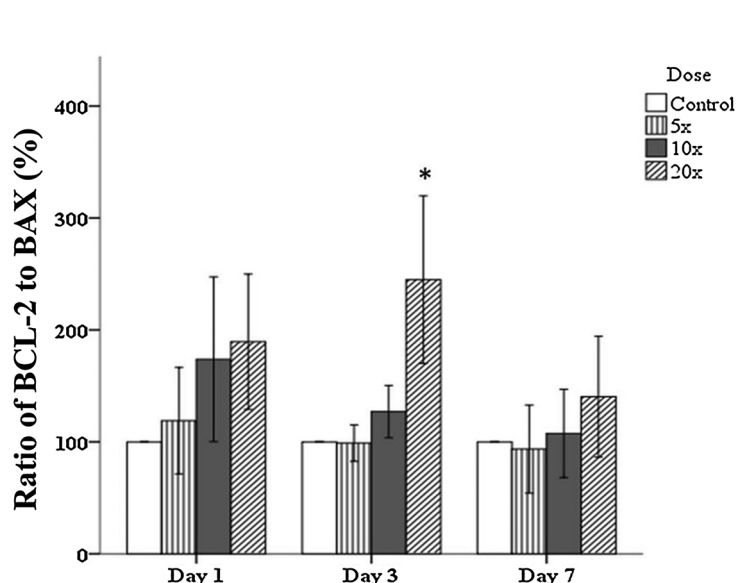
digital x-ray at a very low dose (0.781 mGy) enhanced the alkaline phosphatase activity in human fetal osteoblasts (Kurt et al., 2016). However, the doses of conventional x-ray, also used in diagnosis similar to digital x-ray, are higher than those of the digital x-ray; it is, therefore, not possible for us to determine the promoting effect on mineralization of such a very low dose from using the conventional x-ray in this study. In addition to no effect of various x-ray doses on mineralization, the mineralization ability of primary human osteoblasts was unaffected by two different conditions designed to mimic heterogeneous populations of osteoblasts in human alveolar bone, including exposure to x-ray before induction of mineralization (X-Min) and exposure to x-ray after induction of mineralization (Min-X).

It is worthwhile to note the significant, but transient, increases in the mean ratios of *BCL-2* to *BAX* expressions at both mRNA and protein levels on day 3 after exposure to dental x-ray at 42 mGy in human PDL cells (Figs. 4 and 5, respectively), implying that low-dose irradiation temporarily diminishes apoptosis of PDL cells. These significant increases coincide with the significantly transient decrease in PDL cell proliferation (Fig. 2). These findings may imply a cellular phenomenon, known as a radioadaptive response, an acquirement of cellular resistance to the genotoxic effects of radiation. To survive oxidative stress and deleterious effects from radiation, cells usually activate the programmed defense system through various mechanisms depending on organisms and cell types (Barcellos-Hoff, 1998), such as transcriptional activation of early response genes together with the reduction of apoptotic cell death (Sasaki et al., 2002). BCL-2, which is an anti-apoptotic protein, antagonizes the activity of BAX, a pro-apoptotic protein, by forming the BCL-2/BAX heterodimer. An alteration in the ratio of BCL-2 to BAX protein expression relates to changing in the mitochondrial membrane potential ($\Delta\psi$) (Zhang, Yu, Park, Kinzler, & Vogelstein, 2000). When the ratio is low, it induces loss of $\Delta\psi$ and releases cytochrome c into the cytoplasm, which activates caspase-3 function leading to cellular apoptosis (Schmidt-Ullrich, Dent, Grant, Mikkelsen, & Valerie, 2000). In contrast, if the ratio is increased as shown in this study (Figs. 4 and 5), it may represent the radioadaptive protection of irradiated human PDL cells after being exposed to low-dose ionizing radiation (< 100 mGy) in mammalian cells, as suggested by Sasaki (1995) and Shadley (1994). Accordingly, low-dose irradiation (75 mGy) has been recently shown to relieve cardiotoxicity from treatment with doxorubicin by inhibition of cardiomyocyte apoptosis (Jiang et al., 2018), which is in line with a tendency of higher *BCL-2/BAX* mRNA and protein ratios observed in irradiated PDL cells on day 1 than those in the non-irradiated cells (Figs. 4 and 5). Consistent with a finding from the previous study (Pramojanee et al., 2012), which showed that the maximal dose at 15 mGy had no effect on protein expressions of BCL-2 or BAX in the MC3T3-E1 cell line, our result also demonstrated that there were no differences in the ratios of *BCL-2* to *BAX* mRNA or protein expressions in irradiated PDL cells at 10.5 mGy (5 repeated exposures) compared to those of non-irradiated PDL cells at any time points (Figs. 4 and 5).

During irradiation, monolayers of both osteoblasts and periodontal cells were cultured *in vitro* without other tissue structures that may help absorb dental x-ray and reduce its actual dosage on these cells as it passes through the tissue. Therefore, the generalizability of our *in vitro* findings for clinical scenarios should be carefully interpreted as the cells would probably react to the x-ray differently in the tissue context. Moreover, three limitations are noted from this study. The first is the use of primary human osteoblasts harvested from the long bone rather than the alveolar bone due to a considerable number of osteoblasts from each donor required to complete the proliferation and mineralization assays for various doses of dental x-ray at different time points after irradiation designed in this study. It is not possible for us to isolate such large numbers of osteoblasts from the alveolar bone. However, it is noteworthy that the doubling time and the expressions of alkaline phosphatase and osteocalcin between osteoblasts from different origins are different (Kasperk et al., 1995), especially from intramembranous

alveolar bones *versus* endochondral long bones, and these discrepancies require a further study to address the differential effects of dental x-ray on different types of osteoblasts. The second is the use of heterogeneous populations of periodontal cells that were only characterized by visual assessment, not by analyses of marker gene expressions, which were conducted to fully characterize osteoblasts mentioned in the Section 2.1. The third is the selection of *GAPDH* gene as a reference gene in this study. Although this gene was used previously in another study (Truntipakorn et al., 2017), it does not imply that the expression of *GAPDH* is stable during multiple x-ray exposures, and, therefore, may not be optimal for target gene normalization. Furthermore, the findings from melting curve analysis and western blot hybridization only showed the specificity, but not the stability of *GAPDH* detection. To address this issue, a separate analysis, as performed by Kirschneck et al., 2017, based on several candidate reference genes, is required for irradiated PDL cells, since it has been previously demonstrated that the expression of *GAPDH* is not as stably expressed as desirable for normalization purposes (Kirschneck et al., 2017).

5. Conclusion

Multiple exposures to conventional dental x-ray in the full-mouth intraoral radiography had no effect on the proliferation or the mineralization of primary human osteoblasts. However, multiple exposures to dental x-ray for 20 times (42 mGy) temporarily decreased the proliferation of primary human PDL cells on day 3 after irradiation, which coincided with a transient reduction in the apoptotic potential, as evidenced by a significant increase in the ratios of *BCL-2* to *BAX* mRNA and protein expressions. The transiently reduced proliferation of PDL cells returned to the normal level on day 7. Therefore, dental x-ray is relatively safe in terms of the clinical deterministic effect for patients even with the full-mouth intraoral radiography, but precaution and care should be taken if the radiography has to be repeated within one week. In addition, the risk of carcinogenesis from the stochastic effect of dental x-ray, which is not determined in this study, is still concerned.

Author contribution

Jarinya Pathomburi: Culture of PDL cells, BrdU assay, Alizarin red staining, RT-qPCR, data collection and analysis

Sakarat Nalampang: Experimental design and irradiation protocol

Anupong Makeudom: BrdU assay, Alizarin red staining and RT-qPCR

Jeerawan Klangjorhor: Characterization and culture of human osteoblasts

Chayarop Supanchart: Experimental design and manuscript preparation

Suttichai Krisanaprakornkit: Experimental design and manuscript preparation

Declaration of Competing Interest

All authors declare no conflict of interest relating to this study.

References

Angelieri, F., de Oliveira, G. R., Sannomiya, E. K., & Ribeiro, D. A. (2007). DNA damage and cellular death in oral mucosa cells of children who have undergone panoramic dental radiography. *Pediatric Radiology, 37*(6), 561–565. https://doi.org/10.1007/s00247-007-0478-1.

Asymal, A., Astuti, E. R., & Devijanti, R. (2018). Changes in the number of macrophage and lymphocyte cells in chronic periodontitis due to dental x-ray exposure. *Dental Journal (Majalah Kedokteran Gigi), 51*(2), 99–103. https://doi.org/10.20473/j.djmkg.v51.i2.p99-103.

Barcellos-Hoff, M. H. (1998). How do tissues respond to damage at the cellular level? The role of cytokines in irradiated tissues. *Radiation Research, 150*(5), 109–120. https://doi.org/10.2307/3579813.

Basdra, E. K., & Komposch, G. (1997). Osteoblast-like properties of human periodontal ligament cells: An in vitro analysis. *European Journal of Orthodontics, 19*(6), 615–621. https://doi.org/10.1093/ejo/19.6.615.

Cerqueira, E., Gomes-Filho, I., Trindade, S., Lopes, M., Passos, J., & Machado-Santelli, G. (2004). Genetic damage in exfoliated cells from oral mucosa of individuals exposed to X-rays during panoramic dental radiographies. *Mutation Research/Genetic Toxicology and Environmental Mutagenesis, 562*(1), 111–117. https://doi.org/10.1016/j.mrgentox.2004.05.008.

Czekanska, E., Stoddart, M., Richards, R., & Hayes, J. (2012). In search of an osteoblast cell model for *in vitro* research. *European Cells & Materials, 24*(4), 1–17. https://doi.org/10.22203/eCM.v024a01.

Dare, A., Hachisu, R., Yamaguchi, A., Yokose, S., Yoshiki, S., & Okano, T. (1997). Effects of ionizing radiation on proliferation and differentiation of osteoblast-like cells. *Journal of Dental Research, 76*(2), 658–664. https://doi.org/10.1177/00220345970760020601.

De Felice, F., Di Carlo, G., Saccucci, M., Tombolini, V., & Polimeni, A. (2019). Dental cone beam computed tomography in children: Clinical effectiveness and cancer risk due to radiation exposure. *Oncology, 96*(4), 1–6. https://doi.org/10.1159/000497059.

Ding, L.-H., Shingyoji, M., Chen, F., Hwang, J.-J., Burma, S., Lee, C., et al. (2005). Gene expression profiles of normal human fibroblasts after exposure to ionizing radiation: A comparative study of low and high doses. *Radiation Research, 164*(1), 17–26. https://doi.org/10.1667/RR3354.

Evans, C. E., Galasko, C. S., & Ward, C. (1990). Effect of donor age on the growth *in vitro* of cells obtained from human trabecular bone. *Journal of Orthopaedic Research, 8*(2), 234–237. https://doi.org/10.1002/jor.1100080212.

Fedarko, N., Vetter, U., Weinstein, S., & Robey, P. G. (1992). Age-related changes in hyaluronan, proteoglycan, collagen, and osteonectin synthesis by human bone cells. *Journal of Cellular Physiology, 151*(2), 215–227. https://doi.org/10.1002/jcp.1041510202.

Garant, P. R. (2003). Periodontal ligament. In P. R. Garant (Ed.). *Oral cells and tissues* (pp. 153–178). Carol Stream, Illinois: Quintessence Publishing Company.

Iannucci, J., & Howerton, L. J. (2016). Radiation biology. In J. Iannucci, & L. J. Howerton (Eds.). *Dental radiography: Principles and techniques* (pp. 31–41). (5th ed.). St. Louis, Missouri: Elsevier Health Sciences.

Ivanovski, S., Gronthos, S., Shi, S., & Bartold, P. (2006). Stem cells in the periodontal ligament. *Oral Diseases, 12*(4), 358–363. https://doi.org/10.1111/j.1601-0825.2006.01253.x.

Jiang, X., Hong, Y., Zhao, D., Meng, X., Zhao, L., Du, Y., et al. (2018). Low dose radiation prevents doxorubicin-induced cardiotoxicity. *Oncotarget, 9*(1), 332. https://doi.org/10.18632/oncotarget.23013.

Kasperk, C., Wergedal, J., Strong, D., Farley, J., Wangerin, K., Gropp, H., et al. (1995). Human bone cell phenotypes differ depending on their skeletal site of origin. *The Journal of Clinical Endocrinology and Metabolism, 80*(8), 2511–2517. https://doi.org/10.1210/jcem.80.8.7629252.

Kesidi, S., Maloth, K. N., Reddy, K. V. K., & Geetha, P. (2017). Genotoxic and cytotoxic biomonitoring in patients exposed to full mouth radiographs–A radiological and cytological study. *Journal of Oral and Maxillofacial Radiology, 5*(1), 1–6. https://doi.org/10.4103/jomr.jomr_47_16.

Kirschneck, C., Batschkus, S., Proff, P., Köstler, J., Spanier, G., & Schröder, A. (2017). Valid gene expression normalization by RT-qPCR in studies on hPDL fibroblasts with focus on orthodontic tooth movement and periodontitis. *Scientific Reports, 7*(1), 14751. https://doi.org/10.1038/s41598-017-15281-0.

Kurt, M. H., Oztas, B., & Atalay, A. (2016). Effects of radiation doses from different dental imaging modalities on cell-implant interaction: A comparison with cell culture study. *Journal of Oral and Maxillofacial Radiology, 4*(1), 6–13. https://doi.org/10.4103/2321-3841.177053.

Landsverk, K. S., Lyng, H., & Stokke, T. (2004). The response of malignant B lymphocytes to ionizing radiation: Cell cycle arrest, apoptosis and protection against the cytotoxic effects of the mitotic inhibitor nocodazole. *Radiation Research, 162*(4), 405–415. https://doi.org/10.1667/RR3235.

Lorenzoni, D. C., Fracalossi, A. C. C., Carlin, V., Ribeiro, D. A., & Sant'Anna, E. F. (2012).

Mutagenicity and cytotoxicity in patients submitted to ionizing radiation: A comparison between cone beam computed tomography and radiographs for orthodontic treatment. *The Angle Orthodontist, 83*(1), 104–109. https://doi.org/10.2319/013112-88.1.

Marcu, L. G. (2017). Photons–radiobiological issues related to the risk of second malignancies. *Physica Medica, 42*, 213–220. https://doi.org/10.1016/j.ejmp.2017.02.013.

Ojima, M., Eto, H., Ban, N., & Kai, M. (2011). Radiation-induced bystander effects induce radioadaptive response by low-dose radiation. *Radiation Protection Dosimetry, 146*(1–3), 276–279. https://doi.org/10.1093/rpd/ncr169.

Pramojanee, S. N., Pratchayasakul, W., Chattipakorn, N., & Chattipakorn, S. C. (2012). Low-dose dental irradiation decreases oxidative stress in osteoblastic MC3T3-E1 cells without any changes in cell viability, cellular proliferation and cellular apoptosis. *Archives of Oral Biology, 57*(3), 252–256. https://doi.org/10.1016/j.archoralbio.2011.09.004.

Pramojanee, S. N., Pavasant, P., & Panmekiate, S. (2008). Effects of dental radiation on the expression of apoptotic-related genes in primary human bone cells. *Chulalongkorn Dental Journal, 31*, 415–425. http://cuir.car.chula.ac.th/handle/123456789/53376.

Pruksakorn, D., Teeyakasem, P., Klangjorhor, J., Chaiyawat, P., Settakorn, J., Diskul-Na-Ayudthaya, P., et al. (2016). Overexpression of KH-type splicing regulatory protein regulates proliferation, migration, and implantation ability of osteosarcoma. *International Journal of Oncology, 49*(3), 903–912. https://doi.org/10.3892/ijo.2016.3601.

Rao, X., Huang, X., Zhou, Z., & Lin, X. (2013). An improvement of the 2ˆ(–delta delta CT) method for quantitative real-time polymerase chain reaction data analysis. *Biostatistics, Bioinformatics and Biomathematics, 3*(3), 71–85.

Ribeiro, D., & Angelieri, F. (2008). Cytogenetic biomonitoring of oral mucosa cells from adults exposed to dental X-rays. *Radiation Medicine, 26*(6), 325–330. https://doi.org/10.1007/s11604-008-0232-0.

Ribeiro, D., De Oliveira, G., De Castro, G., & Angelieri, F. (2008). Cytogenetic biomonitoring in patients exposed to dental X-rays: Comparison between adults and children. *Dentomaxillofacial Radiology, 37*(7), 404–407. https://doi.org/10.1259/dmfr/58548698.

Sasaki, M. (1995). On the reaction kinetics of the radioadaptive response in cultured mouse cells. *International Journal of Radiation Biology, 68*(3), 281–291. https://doi.org/10.1080/09553009514551211.

Sasaki, M. S., Ejima, Y., Tachibana, A., Yamada, T., Ishizaki, K., Shimizu, T., et al. (2002). DNA damage response pathway in radioadaptive response. *Mutation Research/Fundamental and Molecular Mechanisms of Mutagenesis, 504*(1), 101–118. https://doi.org/10.1016/S0027-5107(02)00084-2.

Schmidt-Ullrich, R. K., Dent, P., Grant, S., Mikkelsen, R. B., & Valerie, K. (2000). Signal transduction and cellular radiation responses. *Radiation Research, 153*(3), 245–257. https://doi.org/10.1667/0033-7587(2000)153[0245:STACRR]2.0.CO;2.

Shadley, J. D. (1994). Chromosomal adaptive response in human lymphocytes. *Radiation Research, 138*(1), 9–12. https://doi.org/10.2307/3578750.

Spitz, D. R., Azzam, E. I., Li, J. J., & Gius, D. (2004). Metabolic oxidation/reduction reactions and cellular responses to ionizing radiation: A unifying concept in stress response biology. *Cancer Metastasis Reviews, 23*(3–4), 311–322. https://doi.org/10.1023/B:CANC.0000031769.14728.bc.

Supanchart, C., Thawanaphong, S., Makeudom, A., Bolscher, J. G., Nazmi, K., Kornak, U., et al. (2012). The antimicrobial peptide, LL-37, inhibits *in vitro* osteoclastogenesis. *Journal of Dental Research, 91*(11), 1071–1077. https://doi.org/10.1177/0022034512460402.

Truntipakorn, A., Makeudom, A., Sastraruji, T., Pavasant, P., Pattamapun, K., & Krisanaprakornkit, S. (2017). Effects of prostaglandin E2 on clonogenicity, proliferation and expression of pluripotent markers in human periodontal ligament cells. *Archives of Oral Biology, 83*, 130–135. https://doi.org/10.1016/j.archoralbio.2017.07.017.

Truong, K., Bradley, S., Baginski, B., Wilson, J. R., Medlin, D., Zheng, L., et al. (2018). The effect of well-characterized, very low-dose x-ray radiation on fibroblasts. *PloS One, 13*(1), e0190330. https://doi.org/10.1371/journal.pone.0190330.

White, S. C., & Pharoah, M. J. (2014). Radiobiology. In S. C. White, & M. J. Pharoah (Eds.). *Oral radiology: Principles and interpretation* (pp. 16–28). (7th ed.). St. Louis, Missouri: Elsevier Health Sciences.

Xu, W., Xu, L., Chen, M., Mao, Y. T., Xie, Z. G., Wu, S. L., et al. (2012). The effects of low dose x-irradiation on osteoblastic MC3T3-E1 cells *in vitro*. *BMC Musculoskeletal Disorders, 13*(1), 94–102. https://doi.org/10.1186/1471-2474-13-94.

Yamamori, T., Yasui, H., Yamazumi, M., Wada, Y., Nakamura, Y., Nakamura, H., et al. (2012). Ionizing radiation induces mitochondrial reactive oxygen species production accompanied by upregulation of mitochondrial electron transport chain function and mitochondrial content under control of the cell cycle checkpoint. *Free Radical Biology & Medicine, 53*(2), 260–270. https://doi.org/10.1016/j.freeradbiomed.2012.04.033.

Zhang, L., Yu, J., Park, B. H., Kinzler, K. W., & Vogelstein, B. (2000). Role of BAX in the apoptotic response to anticancer agents. *Science, 290*(5493), 989–992. https://doi.org/10.1126/science.290.5493.989.

CrossMark

Decreased levels of matrix metalloproteinase-2 in root-canal exudates during root canal treatment

Kassara Pattamapun[a], Sira Handagoon[a], Thanapat Sastraruji[b], James L. Gutmann[c], Prasit Pavasant[d], Suttichai Krisanaprakornkit[b,*]

[a] Department of Restorative Dentistry and Periodontology, Faculty of Dentistry, Chiang Mai University, Thailand
[b] Center of Excellence in Oral and Maxillofacial Biology, Department of Oral Biology and Diagnostic Sciences, Faculty of Dentistry, Chiang Mai University, Thailand
[c] Department of Endodontics, Texas A & M University College of Dentistry, Dallas, TX 75225, USA
[d] Department of Anatomy, Faculty of Dentistry, Chulalongkorn University, Bangkok 10330, Thailand

ARTICLE INFO

ABSTRACT

Objective: To determine the matrix metalloproteinase-2 (MMP-2) levels in root-canal exudates from teeth undergoing root-canal treatment.

Material and methods: The root-canal exudates from six teeth with normal pulp and periradicular tissues that required intentional root canal treatment for prosthodontic reasons and from twelve teeth with pulp necrosis and asymptomatic apical periodontitis (AAP) were sampled with paper points for bacterial culture and aspirated for the detection of proMMP-2 and active MMP-2 by gelatin zymography and the quantification of MMP-2 levels by ELISA.

Results: By gelatin zymography, both proMMP-2 and active MMP-2 were detected in the first collection of root-canal exudates from teeth with pulp necrosis and AAP, but not from teeth with normal pulp, and their levels gradually decreased and disappeared at the last collection. Consistently, ELISA demonstrated a significant decrease in MMP-2 levels in the root-canal exudates of teeth with pulp necrosis and AAP following root canal procedures ($p < 0.05$). Furthermore, the MMP-2 levels were significantly lower in the negative bacterial culture than those in the positive bacterial culture ($p < 0.001$).

Conclusions: The levels of MMP-2 in root-canal exudates from teeth with pulp necrosis and AAP were gradually reduced during root canal procedures. Future studies are required to determine if MMP-2 levels may be used as a biomolecule for the healing of apical lesions, similar to the clinical application of MMP-8 as a biomarker.

1. Introduction

Pulpal infection and periradicular lesions are caused by oral microorganisms (Kakehashi, Stanley, & Fitzgerald, 1965; M & ller, Fabricius, Dahlén, Ohman, & Heyden, 1981). In the process, invading microbes activate human immune responses, including both protective and destructive reactions that lead to pulpitis and eventually total pulp necrosis. If untreated, destruction of the bone surrounding the root apex of the affected tooth ensues (Nair, 1997). In order to prevent or manage the periradicular lesions, root-canal treatment is indicated. A major aim of this treatment is to eliminate bacteria and their byproducts from the root-canal system through mechanical cleansing and chemical irrigation (Bystrom, Happonen, Sjogren, & Sundqvist, 1987; Nair, 2004).

A bacterial culture from the root-canal exudate has been regarded in the past by some clinicians and researchers to predict the successful

outcome of treatment. However, bacterial culture is a time-consuming process and is costly if anaerobic culture is required to grow fastidious bacteria (Sathorn, Parashos, & Messer, 2007). Therefore, host-derived biomolecules from apical tissues and root-canal exudates would be an alternative for prediction of treatment outcomes.

In the pathogenesis and the healing processes of periradicular lesions, a number of biomolecules are involved, such as the family members of Zn^{2+}-dependent matrix metalloproteinases (MMPs) (Marton & Kiss, 2000; Nair, 2004). MMPs are capable of degrading extracellular matrix and basement membrane constituents (Birkedal-Hansen et al., 1993; Visse & Nagase, 2003). MMPs play an important role in several physiological phenomena, as well as in pathological conditions, such as atherosclerosis, rheumatoid arthritis, recurrent aphthous ulcers, periodontitis and apical periodontitis (Hannas, Pereira, Granjeiro, & Tjaderhane, 2007; Makela, Salo, Uitto, & Larjava,

---

1994; Malemud, 2006; Mantyla et al., 2003; Sorsa, Tjaderhane, & Salo, 2004; Sousa et al., 2014). In particular, MMP-2, or gelatinase A, is a 72-kDa enzyme known to degrade type IV collagen, a major component found in the basement membrane. This enzyme plays a predominant role in the regulation of angiogenesis and inflammation. MMP-2 is expressed in inflamed pulp tissue and periradicular pathosis, and thus plays an important role in inflammation (Corotti et al., 2009; Letra et al., 2013; Shin, Lee, Baek, & Lim, 2002).

In addition to MMP-2, MMP-8, a 75-kDa neutrophil collagenase, is found in inflamed connective tissue. MMP-8 is activated by autolytic cleavage and its function is to degrade collagen types I, II and III. MMP-8 up-regulation is demonstrated in inflamed pulp and periradicular lesions, and its levels are raised in root-canal exudates (Wahlgren et al., 2002). Therefore, it is suggested that elevated MMP-8 levels could be used to indicate ongoing inflammation in the apical tissue, reflecting the success of root-canal treatment. However, there is a paucity of information regarding the levels of human MMP-2 in root-canal exudates and little is known about the changes in MMP-2 and MMP-8 levels in the root-canal exudates of human teeth undergoing root canal procedures. Therefore, the objective of this study was to detect the presence of MMP-2 in root-canal exudates of human teeth, diagnosed with normal pulp and periradicular tissues or with pulp necrosis and asymptomatic apical periodontitis (AAP). Furthermore, the alterations in MMP-2 and MMP-8 levels were investigated during each treatment visit and compared with bacterial culture results.

2. Materials and methods

2.1. Patients

Eleven patients (age range: 17–69 years old) scheduled for root canal treatment at the Department of Restorative Dentistry and Periodontology, Faculty of Dentistry, Chiang Mai University, were included in this study. A total of twelve teeth, having only one root canal, which were diagnosed with pulp necrosis and AAP from nine patients and six teeth, having only one root canal, which were diagnosed with normal pulp and periradicular tissues that required root-canal therapy for prosthodontic reasons from two patients were selected. Patients with underlying systemic diseases were excluded from this study. Clinical and radiographic examinations were conducted, and the diagnosis was based on clinical symptoms, vitality testing and radiographic interpretation, according to the guidelines of the American Association of Endodontists (Glickman, 2009). Teeth with pulp necrosis and AAP responded negatively to pulp testing, and their radiographic findings showed a radiolucent lesion or loss of lamina dura; patients had no pain on percussion. Teeth with normal pulp responded positively to pulp testing and radiographs showed an intact lamina dura without thickening of periodontal ligament space. All root-canal exudates were collected at baseline and during each treatment visit; all procedures were performed with the approval of the Human Experimentation Committee, Faculty of Dentistry, Chiang Mai University. Informed consent was obtained from all patients prior to sample collection.

2.2. Sample collection

Access to the pulp was achieved using sterile dental burs under dental dam isolation. Radiographic images and an electrical apex locator were used to determine the root-canal length. All root canals were instrumented with a step back technique using master apical files to at least size 40. During instrumentation, the canals were disinfected with 5.25% sodium hypochlorite (NaOCl), and the smear layer was removed by 17% EDTA, using passive ultrasonic irrigation for one minute and a final rinse with 5.25% NaOCl. Root canals were dried with sterile paper points, and a sterile dry cotton pellet dampened with camphorated monochlorophenol (CMP) was placed in the pulp chamber. The access cavity was sealed with Cavit-G (3M ESPE, St. Paul, MN, USA). All

patients were recalled within a few days, and the temporary filling and the medicated cotton pellet were removed using an aseptic technique. A 10-μl quantity of sterile buffer, containing 50 mM Tris-HCl pH 7.5, 0.15 M NaCl and 1 mM $CaCl_2$, was added into the root canal for two minutes, and the same volume was aspirated from each root-canal exudate and transferred to an eppendorf tube, containing 40 μl of the same buffer to dilute the exudate fivefold. This dilution was chosen from data obtained in a pilot study that showed two clear and discrete gelatinolytic bands between proMMP-2 and active MMP-2. A sterile paper point was inserted into the canal, left for 30 s, and then put in the tube, containing thioglycollate medium that was further incubated at 37 °C for a standard protocol of bacterial culture. The canal was rinsed with NaOCl and dried. For the teeth with normal pulp, the root canals were filled in this visit, but for those with pulp necrosis and AAP, calcium hydroxide paste, pH 12.5 (Biocalc, Orion, Helsinki, Finland) was placed into the canal and the cavity was sealed. After two weeks, the paste in the root canal was removed and replaced with a sterile dry cotton ball dampened with CMP. A few days later, the procedure for collection of root-canal exudates was repeated and the collections were continued until the bacterial culture was negative. The root canals were filled with gutta-percha and zinc oxide-eugenol sealer (Tubliseal EWT, Kerr Co., Romulus, MI, USA) using cold lateral compaction in the next appointment. All collected root-canal exudates were stored at −80 °C for further analysis.

2.3. Gelatin zymography

Total protein concentrations of all root-canal exudates were determined by the Bio-Rad Protein assay kit (Bio-Rad Laboratories, Hercules, CA, USA), based on the method of Bradford (Bradford, 1976), and expressed in units of mg/ml. An equal amount of total protein from each root-canal exudate was loaded in each lane for detection of MMP-2 activity by gelatin zymography as described previously (Pattamapun, Tiranathanagul, Yongchaitrakul, Kuwatanasuchat, & Pavasant, 2003). Briefly, the root-canal exudates and the conditioned medium collected from primary human periodontal ligament cells, treated with 10 ng/ml of Concanavalin A (Sigma-Aldrich, St. Louis, MO, USA) for 24 h as a positive control for the presence of proMMP-2 and active MMP-2 (Kawagoe, Tsuruga, Oka, Sawa, & Ishikawa, 2013; Overall et al., 2000), were mixed with non-reducing sample buffer, containing 0.5 M Tris-HCl pH 6.8, glycerol, 10% sodium dodecyl sulfate (SDS) without β-mercaptoethanol, and loaded onto 0.1% gelatin-containing SDS-polyacrylamide gel electrophoresis along with the molecular weight markers (Bio-Rad Laboratories) at 100 V for two h. Following electrophoresis, the gels were gently washed with buffer, containing 2.5% Triton-X100 (Sigma-Aldrich) at room temperature three times for 30 min each to remove SDS, and then incubated in activating buffer, containing 0.15 M NaCl, 10 mM $CaCl_2$, 50 mM Tris-HCl pH 7.5, 0.1% Brij-35, at 37 °C for 20 h. The gels were stained with 2.5% Coomassie Brilliant Blue R-250 (Sigma-Aldrich) in 30% methanol and 10% acetic acid, and then de-stained for 30 min in 5% methanol and 7.5% acetic acid. The digitized images of the gelatin zymograms were captured using a LaserJet M1522 MFP Series PCL scanner (Hewlett-Packard, Palo Alto, CA, USA), and the intensities of proMMP-2 and active MMP-2 bands were measured by Scion Image software version beta 4.0.3 (Scion Corporation, Rockville, MA, USA). The ratios of active MMP-2 to proMMP-2 were determined for all root-canal exudate samples.

2.4. Sandwich ELISA for MMP-2 and MMP-8 measurements

The levels of total MMP-2, including proMMP-2 and active MMP-2, and of MMP-8 in the root-canal exudates were determined by the human MMP-2 Immunoassay kit (Quantikine, R & D Systems, Inc., Minneapolis, MN, USA) and by the human total MMP-8 kit (Quantikine, R & D Systems, Inc.), respectively, according to the manufacturer's instructions. Briefly, the root-canal exudates were first diluted with the

Calibrator Diluent RD5-10 buffer at 1:10 for MMP-2 measurement, and further diluted with the same buffer at 1:2 for MMP-8 measurement. A 50-μl quantity of each root-canal sample and of the standards was assayed in duplicate in 96-well plates, coated with a captured antibody against either MMP-2 or MMP-8. Then, a 150-μl quantity of the Assay Diluent RD1-52 buffer was added into each well and incubated for two h at room temperature on an orbital shaker. Thereafter, the wells were washed four times and 200 μl of horseradish peroxidase-conjugated detection antibody against either MMP-2 or MMP-8 was added into each well and incubated for two h at room temperature on the shaker. Subsequently, the wells were washed four times and left to air-dry. A 200-μl quantity of the substrate solution was added to each well and incubated for 30 min at room temperature under light protection, followed by the addition of 50 μl stop solution. The absorbance value of each sample was measured within 30 min at 450 nm with the correction wavelength at 540 nm using a microplate reader (Sunrise™ TECAN Group Ltd., Mannedorf, Switzerland), and the concentrations of total MMP-2 and MMP-8 in ng/ml were determined from their standard curve. The concentration of total MMP-2 and that of MMP-8 were normalized by the total protein concentration in each sample and expressed as ng/mg.

2.5. Statistical analysis

The Friedman test and the Wilcoxon Signed Ranks test were used to determine the differences in the ratio between the intensities of active MMP-2 and those of proMMP-2 and in the levels of total MMP-2 and MMP-8 in the root-canal exudates between different appointments. The Mann Whitney U test was used to compare the MMP-2 and MMP-8 levels between the negative and the positive bacterial culture results. The analyses were performed using the Statistical Package for Social Sciences (SPSS) version 17.0 for Windows (IBM, Inc., Chicago, IL, USA), and p-values less than 0.05 were considered statistically significant.

3. Results

3.1. Bacterial culture findings

For the first collection of root-canal exudates, no evidence of microbial growth was found in any exudate samples from six teeth with normal pulp and periradicular tissues, whereas eight out of the twelve exudate samples ($8/12 = 67\%$) from teeth with pulp necrosis and AAP were positive for microbial growth. However, all root-canal exudate samples from teeth with pulp necrosis and AAP were negative for microbial growth in the last collection before root-canal obturation.

3.2. Decreased expression of proMMP-2 and active MMP-2 upon endodontic treatment

Using gelatin zymography, two clear gelatinolytic bands of proMMP-2 and active MMP-2 at the predicted molecular weights, 72 and 62 kDa, respectively, were detected in the first collection of root-canal exudates from all teeth with pulp necrosis and AAP, whereas no clear band was detectable in those from any teeth with normal pulp and periradicular tissues (Fig. 1), although total protein concentrations were equivalent among the different root-canal exudate samples. In addition, the sizes of these two gelatinolytic bands were comparable to those of the two clear bands detected in the conditioned medium of cultured periodontal ligament cells treated with Concanavalin A (Fig. 1; Kawagoe et al., 2013; Overall et al., 2000). The intensities of proMMP-2 and active MMP-2 bands in the root-canal exudates were gradually decreased in the subsequent collections, and these bands were virtually absent in the last collection before root-canal obturation (Fig. 1). Using densitometry, the median ratios of the intensities between active MMP-2 and proMMP-2 gradually decreased from the first to the last collection (Fig. 2), and significant reductions in these ratios were found between
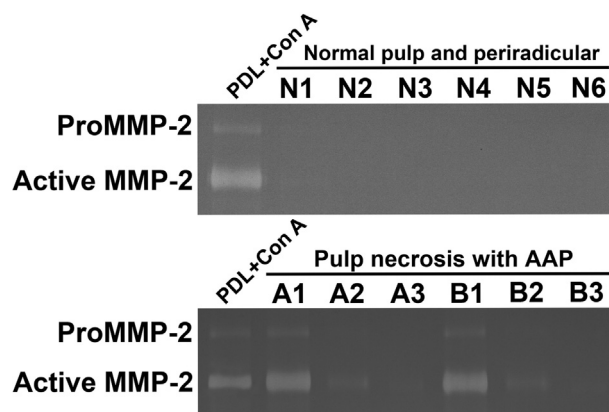
Fig. 1. Detection of proMMP-2 and active MMP-2 by gelatin zymography. The root-canal exudates from six teeth with normal pulp and periradicular tissues (N1-N6; upper panel) and the representative root-canal exudates from two teeth (A and B; lower panel), diagnosed with pulp necrosis and asymptomatic apical periodontitis (AAP) from three collections (1–3), along with the conditioned medium collected from human periodontal ligament cells, treated with 10 ng/ml of Concanavalin A (PDL + Con A) for 24 h as a positive control, were resolved by 0.1% gelatin-containing non-reducing gel electrophoresis as described in Materials and Methods. Note the absence of two clear gelatinolytic bands for proMMP-2 and active MMP-2 in the root-canal exudates from normal pulp and periradicular tissues, whereas these bands, detected in the root-canal exudates from the first collection, were gradually decreased upon treatment.
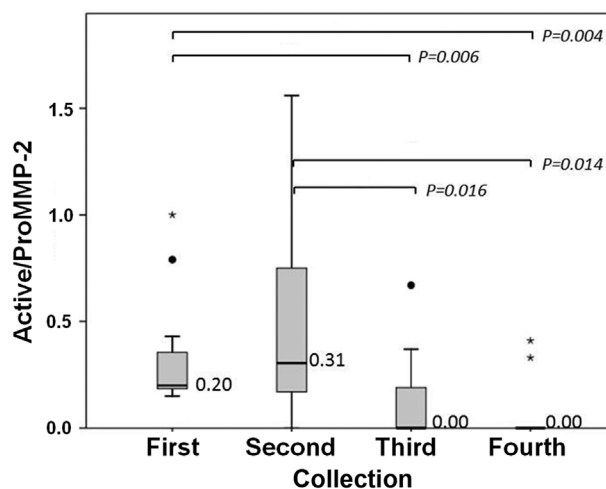
Fig. 2. Significant reduction in the ratios between active MMP-2 and proMMP-2 upon root-canal treatment. The intensities of the two clear gelatinolytic bands for proMMP-2 and active MMP-2 in Fig. 1 were measured from the root-canal exudates of twelve teeth with pulp necrosis and asymptomatic apical periodontitis from the first to the fourth collection in two teeth or from the first to the third collection for the remaining ten teeth depending on the bacterial culture result. Then, the ratios between active MMP-2 and proMMP-2 (Active/ProMMP-2) were calculated in each exudate sample and plotted on the y-axis of the box plot graph. The median ratio for each collection is indicated in the graph. The black circles and the small asterisks are outlier and extreme values, respectively.

the first and the third or the fourth collections ($p < 0.01$) and between the second and the third or the fourth collections ($p < 0.05$).

3.3. Significant reduction of total MMP-2 and MMP-8 levels upon root-canal therapy

To further verify the zymogram results in Figs. 1 and 2, an ELISA was conducted to quantitatively measure the levels of total MMP-2 in the root-canal exudates collected from teeth diagnosed with pulp necrosis and AAP because no gelatinolytic bands were detected for either proMMP-2 or active MMP-2 in the root-canal exudates of teeth with normal pulp and periradicular tissues (Fig. 1). The ELISA result demonstrated a gradual and significant decrease in the median levels of
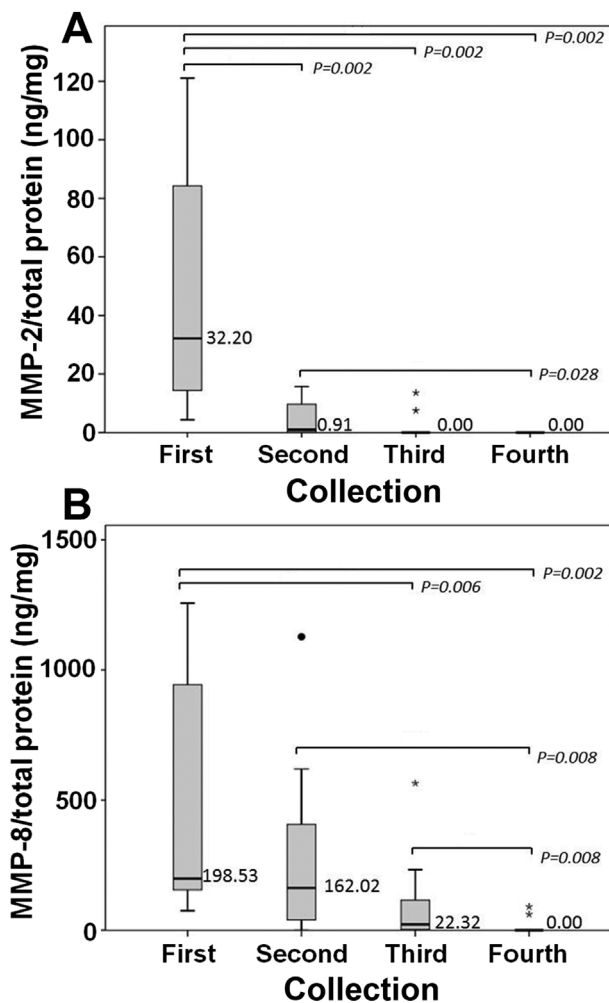
Fig. 3. Significant decrease in total MMP-2 and MMP-8 levels in the root-canal exudates upon root-canal treatment. The levels of total MMP-2 (A) and MMP-8 (B) in units of ng/mg on the *y*-axis were determined by ELISA in the root-canal exudate samples from twelve teeth with pulp necrosis and asymptomatic apical periodontitis and normalized by their total protein concentration in each sample. The median levels of total MMP-2 (A) and MMP-8 (B) for each collection from the first to the fourth collection are indicated in the graphs. The black circle and the small asterisks are outlier and extreme values, respectively.

total MMP-2 ($p < 0.05$) in the root-canal exudates upon endodontic treatment (Fig. 3A). In addition, the total MMP-2 level was not detectable at all in the last collection prior to root-canal filling (Fig. 3A). Similarly to the gradual and significant reduction of total MMP-2 levels upon root-canal treatment, the median levels of total MMP-8 in the root-canal exudates of teeth with pulp necrosis and AAP were also gradually and diminished significantly by root-canal treatment ($p < 0.01$), and very low levels of total MMP-8 were detected in the last collection (Fig. 3B). Interestingly, the levels of total MMP-8 were approximately tenfold higher than those of total MMP-2.

3.4. Low levels of total MMP-2 and MMP-8 in agreement with the negative bacterial culture

Since the root-canal exudates were also sampled for bacterial culture as one of the indicators before root-canal obturation, the differences in both total MMP-2 and MMP-8 levels between the negative and the positive bacterial culture results were determined. The median level of total MMP-2 (Fig. 4A) and that of MMP-8 (Fig. 4B) were significantly lower in the negative bacterial culture than in the positive culture ($p < 0.001$), suggesting that both decreased levels of MMP-2 and MMP-8 and the negative bacterial culture reflect a possible decrease in
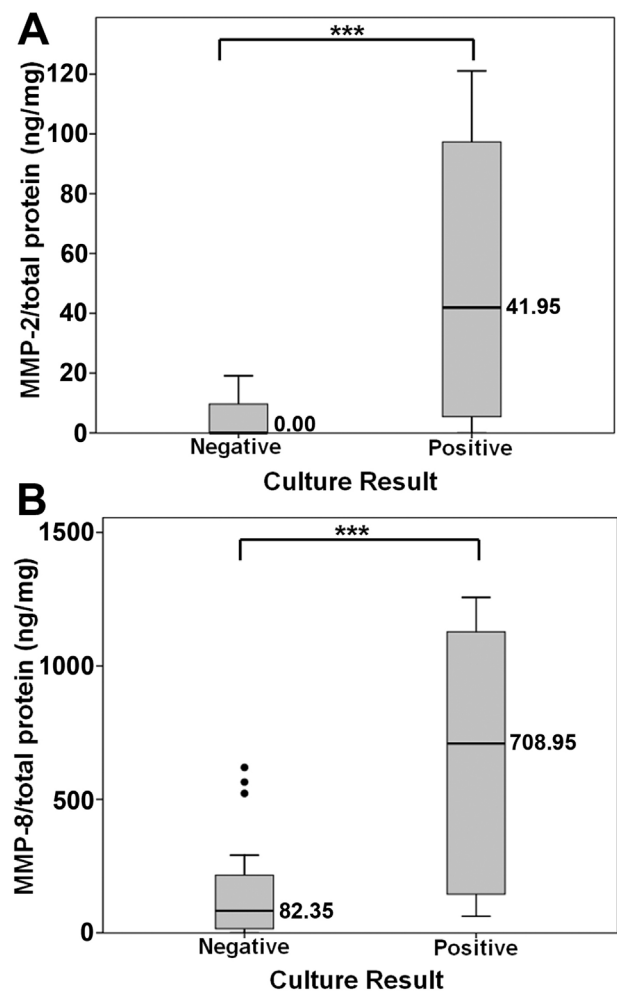
Fig. 4. Significantly lower MMP-2 and MMP-8 levels in the negative bacterial culture than those in the positive bacterial culture. The levels of total MMP-2 (A) and MMP-8 (B) in the root-canal exudate samples from twelve teeth with pulp necrosis and asymptomatic apical periodontitis were normalized by their total protein concentration in units of ng/mg and plotted on the *y*-axis of the box plot graphs. All exudate samples were categorized into two groups, the negative bacterial culture group and the positive bacterial culture group on the *x*-axis, irrespective of the different periods of collection. The median levels of total MMP-2 (A) and MMP-8 (B) for the negative and the positive bacterial culture are indicated in the graphs. The black circles are outlier values. *** $p < 0.001$.

inflammation in the periradicular tissues after elimination of microbial infection within the root-canal system, which may then result in healing.

4. Discussion

In this study, an investigation for the MMP-2 levels in the root-canal exudates collected at various times during root-canal therapy from teeth diagnosed with pulp necrosis and AAP was performed by both gelatin zymography and ELISA. The results from both assays showed a similar trend for gradual and significant reduction in the ratios between active MMP-2 and proMMP-2 and in the total MMP-2 levels in the root-canal exudates. Interestingly, both MMP-2 ratios and levels were not measurable at the last exudate collection prior to root-canal obturation, corresponding with the negative bacterial culture. Therefore, in addition to the negative bacterial culture, the absence of MMP-2 in the root-canal exudates may be considered a possible indicator for when to fill the root canal. As a negative control, both active MMP-2 and proMMP-2 bands at their expected sizes were not detectable in the root-canal exudates collected from teeth with normal pulp and periradicular tissues, although total protein concentrations in these exudate samples

were measurable, confirming a true negative finding. The reason for collecting the exudates from teeth with normal pulp and periradicular tissues only one time is that it would be inappropriate to delay the root-canal obturation for intentional root-canal therapy. Moreover, the reason to evaluate MMP levels in exudates collected from patients with pulp necrosis rather than with irreversible pulpitis (Wahlgren et al., 2002) was to determine the effect of instrumentation and chemical debridement on the removal of residual microorganisms, which are more likely to be present in dentinal tubules of teeth diagnosed with pulp necrosis rather than those with irreversible pulpitis, following the reduction of both MMP-2 and MMP-8 levels.

The levels of total MMP-2 in the negative bacterial culture were much lower than those in the positive bacterial culture, suggesting that the MMP-2 levels in the root-canal exudates may reflect the degrees of inflammation in the apical tissues that are induced by the presence of microbial infection in the root-canal system. In other words, if the bacteria in the root-canal system are effectively eliminated, the inflammation should subside, resulting in lower levels of inflammation-related molecules, like MMP-2, and eventual healing. One of the main purposes for root-canal treatment in teeth with pulp necrosis is to effectively eliminate the bacteria and their byproducts within the root-canal system (Bystrom et al., 1987), and disinfected root canals can then no longer stimulate the inflammation in the periradicular tissues leading to a decrease in MMP-2 synthesis and activation in the root-canal exudates.

Similar to the significant reduction of MMP-2 in the root-canal exudates upon root-canal therapy, the MMP-8 levels in the root-canal exudates were also significantly decreased, consistent with the findings from some previous studies conducted in both animals and humans (Ding et al., 1997; Paula-Silva, da Silva, & Kapila, 2010; Sorsa et al., 1999; Wahlgren et al., 2002). These studies have proposed MMP-8 as a biomarker for the healing of apical tissue. Therefore, it may be possible to introduce MMP-2 as another biomolecule that could potentially be applied in the clinical setting as a biomarker for the healing of the periradicular tissue. However, the cell types that produce and secrete MMP-2 and MMP-8 are different. In particular, MMP-8 is predominantly released from neutrophils that migrate into the periradicular tissue during inflammation (Sousa et al., 2014), whereas MMP-2 is mainly synthesized by a mesenchymal cell lineage, such as periodontal ligament cells (Birkedal-Hansen et al., 1993; Birkedal-Hansen, 1993; Hipps et al., 1991). Moreover, proMMP-2 entrapped in the dentin matrix (Mazzoni et al., 2007, 2009) can be possibly detached and present in root-canal exudates upon mechanical instrumentation and chemical debridement. ProMMP-2, irrespective of its sources (dentin matrix or periodontal ligament cells), can be converted into an active form by bacterial enzymes and acidic byproducts during the state of inflammation at the periapical tissues. Therefore, it is not critical to determine the source of MMP-2, but it would rather be interesting to examine levels of active MMP-2 in root-canal exudates as shown by gelatin zymography in this study. It is possible that reduced levels of active MMP-2 would be clinically useful for an appropriate time of root-canal obturation.

MMP-2 has been demonstrated to be expressed in dog periodontal ligament cells by immunohistochemistry and its expression is reduced upon root-canal treatment as well (Corotti et al., 2009). Furthermore, human periodontal ligament cells can produce and secrete proMMP-2 *in vitro*, which is later converted into active MMP-2 by proteases secreted from *Porphyromonas gingivalis* (Grayson, Douglas, Heath, Rawlinson, & Evans, 2003) and the culture supernatants of *Porphyromonas gingivalis* via induction of membrane type 1-matrix metalloproteinase (Pattamapun et al., 2003) and *Aggregatibacter actinomycetemcomitans* through reduction of the secretion of tissue inhibitor of metalloproteinase-2 (Tiranathanagul, Pattamapun, Yongchaitrakul, & Pavasant, 2004). Therefore, it is interesting to further examine the relationship between diminished levels of active MMP-2 and those of bacterially-derived proteases in root-canal exudates upon endodontic

treatment.

The reason we did not investigate MMP-9 in root-canal exudates although it is mainly produced by inflammatory cells was because the gelatinolytic bands at the expected size of MMP-9 were faint and inconsistently detected in the root-canal exudates by gelatin zymography (data not shown). As a result, MMP-8 was selected as a known biomolecule for the state of apical inflammation in the root-canal exudates (Wahlgren et al., 2002). In addition to the analyses of MMP-8 levels in the root-canal exudates examined in previous studies (Shin et al., 2002; Wahlgren et al., 2002), the present investigation into the MMP-2 levels in the root-canal exudates is well justified because these two MMPs are synthesized by different cell types and the measurement of MMP-2 levels in parallel with that of MMP-8 levels could be sufficiently sensitive to detect any low grade, residual inflammation that still remains in the periradicular tissue. Consequently, it is possible that the development of a chair-side diagnostic tool to simultaneously measure the levels of both MMP-2 and MMP-8 in the root-canal exudates could be clinically helpful to reflect the degree of inflammation at the apical tissue. This may be beneficial for clinicians to determine the appropriate time for root-canal obturation. It is worthwhile to note that some exudate samples from teeth with pulp necrosis and AAP were not positive for microbial growth in the first collection. This may be because the aerobic culture performed in this study was not able to grow uncultivable anaerobes in the root-canal exudates, and our culture technique can be considered one of the limitations. Therefore, the proposed diagnostic tool could replace the time-consuming bacterial culture with more reliability and effectiveness in clinical practice.

In summary, MMP-2 and MMP-8 were detected in the root-canal exudates from teeth with periradicular lesions and their levels were gradually reduced upon root-canal treatment. The reduction of both MMP-2 and MMP-8 levels may imply that both biomolecules have a potential to be developed as biomarkers for the healing of periradicular lesions and may possibly lead to the development of a chair-side diagnostic tool similar to the ones developed for gingival crevicular fluid in periodontitis (Mantyla et al., 2003; Sorsa et al., 1999) and for peri-implant sulcular fluid in peri-implantitis (Sorsa et al., 1999).

Competing financial interests

References

Birkedal-Hansen, H., Moore, W. G., Bodden, M. K., Windsor, L. J., Birkedal-Hansen, B., DeCarlo, A., & Engler, J. A. (1993). Matrix metalloproteinases: A review. *Critical Reviews in Oral Biology and Medicine, 4*(2), 197–250.

Birkedal-Hansen, H. (1993). Role of cytokines and inflammatory mediators in tissue destruction. *Journal of Periodontal Research, 28*(6 Pt. 2), 500–510.

Bradford, M. M. (1976). A rapid and sensitive method for the quantitation of microgram quantities of protein utilizing the principle of protein-dye binding. *Analytical Biochemistry, 72*, 248–254.

Bystrom, A., Happonen, R. P., Sjogren, U., & Sundqvist, G. (1987). Healing of periapical lesions of pulpless teeth after endodontic treatment with controlled asepsis. *Endodontics and Dental Traumatology, 3*(2), 58–63.

Corotti, M. V., Zambuzzi, W. F., Paiva, K. B., Menezes, R., Pinto, L. C., Lara, V. S., & Granjeiro, J. M. (2009). Immunolocalization of matrix metalloproteinases-2 and -9 during apical periodontitis development. *Archives of Oral Biology, 54*(8), 764–771.

Ding, Y., Haapasalo, M., Kerosuo, E., Lounatmaa, K., Kotiranta, A., & Sorsa, T. (1997). Release and activation of human neutrophil matrix metallo- and serine proteinases

during phagocytosis of *Fusobacterium nucleatum, Porphyromonas gingivalis* and *Treponema denticola. Journal of Clinical Periodontology, 24*(4), 237–248.

Glickman, G. N. (2009). AAE consensus conference on diagnostic terminology: Background and perspectives. *Journal of Endodontics, 35*(12), 1619–1620.

Grayson, R., Douglas, C. W. I., Heath, J., Rawlinson, A., & Evans, G. S. (2003). Activation of human matrix metalloproteinase 2 by gingival crevicular fluid and *Porphyromonas gingivalis. Journal of Clinical Periodontology, 30*(6), 542–550.

Hannas, A. R., Pereira, J. C., Granjeiro, J. M., & Tjaderhane, L. (2007). The role of matrix metalloproteinases in the oral environment. *Acta Odontologica Scandinavica, 65*(1), 1–13.

Hipps, D. S., Hembry, R. M., Docherty, A. J., Reynolds, J. J., & Murphy, G. (1991). Purification and characterization of human 72-kDa gelatinase (type IV collagenase). Use of immunolocalisation to demonstrate the non-coordinate regulation of the 72-kDa and 95-kDa gelatinases by human fibroblasts. *Biological Chemistry Hoppe-Seyler, 372*(4), 287–296.

Kakehashi, S., Stanley, H. R., & Fitzgerald, R. J. (1965). The effects of surgical exposures of dental pulps in germ-free and conventional laboratory rats. *Oral Surgery, Oral Medicine, Oral Pathology, 20*, 340–349.

Kawagoe, M., Tsuruga, E., Oka, K., Sawa, Y., & Ishikawa, H. (2013). Matrix metalloproteinase-2 degrades fibrillin-1 and fibrillin-2 of oxytalan fibers in the human eye and periodontal ligaments in vitro. *Acta Histochemica et Cytochemica, 46*(5), 153–159.

Letra, A., Ghaneh, G., Zhao, M., Ray, H., Jr., Francisconi, C. F., Garlet, G. P., & Silva, R. M. (2013). MMP-7 and TIMP-1, new targets in predicting poor wound healing in apical periodontitis. *Journal of Endodontics, 39*(9), 1141–1146.

Möller, A. J., Fabricius, L., Dahlén, G., Ohman, A. E., & Heyden, G. (1981). Influence on periapical tissues of indigenous oral bacteria and necrotic pulp tissue in monkeys. *Scandinavian Journal of Dental Research, 89*(6), 475–484.

Makela, M., Salo, T., Uitto, V. J., & Larjava, H. (1994). Matrix metalloproteinases (MMP-2 and MMP-9) of the oral cavity: Cellular origin and relationship to periodontal status. *Journal of Dental Research, 73*(8), 1397–1406.

Malemud, C. J. (2006). Matrix metalloproteinases (MMPs) in health and disease: An overview. *Frontiers in Bioscience, 11*, 1696–1701.

Mantyla, P., Stenman, M., Kinane, D. F., Tikanoja, S., Luoto, H., Salo, T., & Sorsa, T. (2003). Gingival crevicular fluid collagenase-2 (MMP-8) test stick for chair-side monitoring of periodontitis. *Journal of Periodontal Research, 38*(4), 436–439.

Marton, I. J., & Kiss, C. (2000). Protective and destructive immune reactions in apical periodontitis. *Oral Microbiology and Immunology, 15*(3), 139–150.

Mazzoni, A., Mannello, F., Tay, F. R., Tonti, G. A. M., Papa, S., Mazzotti, G., ... Breschi, L. (2007). Zymographic analysis and characterization of MMP-2 and -9 forms in human sound dentin. *Journal of Dental Research, 86*(5), 436–440.

Mazzoni, A., Pashley, D. H., Tay, F. R., Gobbi, P., Orsini, G., Ruggeri, A., Jr., & Breschi, L. (2009). Immunohistochemical identification of MMP-2 and MMP-9 in human dentin: Correlative FEI-SEM/TEM analysis. *Journal of Biomedical Materials Research, 88A*, 697–703.

Nair, P. N. (1997). Apical periodontitis: A dynamic encounter between root canal infection and host response. *Periodontology 2000, 13*, 121–148.

Nair, P. N. (2004). Pathogenesis of apical periodontitis and the causes of endodontic failures. *Critical Reviews in Oral Biology and Medicine, 15*(6), 348–381.

Overall, C. M., Tam, E., McQuibban, G. A., Morrison, C., Wallon, U. M., Bigg, H. F., ... Roberts, C. R. (2000). Domain interactions in the gelatinase A. TIMP-2. MT1-MMP activation complex. The ectodomain of the 44-kDa form of membrane type-1 matrix metalloproteinase does not modulate gelatinase A activation. *Journal of Biological Chemistry, 275*(50), 39497–39506.

Pattamapun, K., Tiranathanagul, S., Yongchaitrakul, T., Kuwatanasuchat, J., & Pavasant, P. (2003). Activation of MMP-2 by Porphyromonas gingivalis in human periodontal ligament cells. *Journal of Periodontal Research, 38*(2), 115–121.

Paula-Silva, F. W., da Silva, L. A., & Kapila, Y. L. (2010). Matrix metalloproteinase expression in teeth with apical periodontitis is differentially modulated by the modality of root canal treatment. *Journal of Endodontics, 36*(2), 231–237.

Sathorn, C., Parashos, P., & Messer, H. H. (2007). How useful is root canal culturing in predicting treatment outcome? *Journal of Endodontics, 33*(3), 220–225.

Shin, S. J., Lee, J. I., Baek, S. H., & Lim, S. S. (2002). Tissue levels of matrix metalloproteinases in pulps and periapical lesions. *Journal of Endodontics, 28*(4), 313–315.

Sorsa, T., Mantyla, P., Ronka, H., Kallio, P., Kallis, G. B., Lundqvist, C., ... Tikanoja, S. (1999). Scientific basis of a matrix metalloproteinase-8 specific chair-side test for monitoring periodontal and peri-implant health and disease. *Annals of the New York Academy of Sciences, 878*, 130–140.

Sorsa, T., Tjaderhane, L., & Salo, T. (2004). Matrix metalloproteinases (MMPs) in oral diseases. *Oral Diseases, 10*(6), 311–318.

Sousa, N. G., Cardoso, C. R., Silva, J. S., Kuga, M. C., Tanomaru-Filho, M., & Faria, G. (2014). Association of matrix metalloproteinase inducer (EMMPRIN) with the expression of matrix metalloproteinases-1, -2 and -9 during periapical lesion development. *Archives of Oral Biology, 59*(9), 944–953.

Tiranathanagul, S., Pattamapun, K., Yongchaitrakul, T., & Pavasant, P. (2004). MMP-2 activation by *Actinobacillus actinomycetemcomitans* supernatant in human PDL cells was corresponded with reduction of TIMP-2. *Oral Diseases, 10*(6), 383–388.

Visse, R., & Nagase, H. (2003). Matrix metalloproteinases and tissue inhibitors of metalloproteinases: Structure, function, and biochemistry. *Circulation Research, 92*(8), 827–839.

Wahlgren, J., Salo, T., Teronen, O., Luoto, H., Sorsa, T., & Tjaderhane, L. (2002). Matrix metalloproteinase-8 (MMP-8) in pulpal and periapical inflammation and periapical root-canal exudates. *International Endodontic Journal, 35*(11), 897–904.

The Korean Journal of Orthodontics – Manuscript Submission

Manuscript Draft

Title: Periodontal Ligament Proliferation and Expressions of Bone Biomolecules upon Orthodontic Preloading: Clinical Implications for Tooth Autotransplantation

Article Type: Original Article

Abstract: Objectives: Preservation of periodontal ligament (PDL) is vital to the success of tooth autotransplantation (TAT). Increased human PDL amounts and facilitated tooth extraction have been observed upon orthodontic preloading. However, it is unclear whether there would be any changes in expressions of bone biomolecules in the increased PDL volumes. This study aimed to determine the expressions of Runt-related transcription factor 2 (RUNX2), alkaline phosphatase (ALP), receptor activator of nuclear factor kappa-B ligand (RANKL) and osteoprotegerin (OPG) in human PDL upon preloading.
Materials and Methods: Seventy-two premolars from 18 participants were randomly assigned to experimental groups that received a leveling force for one, two or four weeks or to a control unloaded group. Following extraction, PDL volumes from 32 premolars of eight participants (21.0 ± 3.8 years) were evaluated using toluidine blue staining. The expressions of the biomolecules in PDL from 40 premolars of ten participants (21.4 ± 4.0 years) were analyzed by immunoblotting.
Results: The median percentage of stained PDL was significantly increased at two and four weeks compared to the unloaded ($p<0.05$). The median RUNX2 and ALP expressions were significantly higher in the loaded PDL at two and four weeks than those in the unloaded ($p<0.05$), whereas the median RANKL to OPG ratios were significantly increased upon preloading at one and four weeks ($p<0.05$).
Conclusions: Orthodontic preloading for four weeks enhances the amounts of PDL tissue together with the RUNX2 and ALP expressions and the RANKL/OPG ratio in the PDL, suggesting that this loading period is suitable for successful TAT.

Keywords: Transplantation, Bone biology, Cell / Molecular biology, Periodontics, Periodontal ligament, Preloading

Periodontal Ligament Proliferation and Expressions of Bone Biomolecules upon Orthodontic Preloading: Clinical Implications for Tooth Autotransplantation

Objectives: Preservation of periodontal ligament (PDL) is vital to the success of tooth autotransplantation (TAT). Increased human PDL amounts and facilitated tooth extraction have been observed upon orthodontic preloading. However, it is unclear whether there would be any changes in expressions of bone biomolecules in the increased PDL volumes. This study aimed to determine the expressions of Runt-related transcription factor 2 (RUNX2), alkaline phosphatase (ALP), receptor activator of nuclear factor kappa-B ligand (RANKL) and osteoprotegerin (OPG) in human PDL upon preloading.

Materials and Methods: Seventy-two premolars from 18 participants were randomly assigned to experimental groups that received a leveling force for one, two or four weeks or to a control unloaded group. Following extraction, PDL volumes from 32 premolars of eight participants (21.0±3.8 years) were evaluated using toluidine blue staining. The expressions of the biomolecules in PDL from 40 premolars of ten participants (21.4±4.0 years) were analyzed by immunoblotting.

Results: The median percentage of stained PDL was significantly increased at two and four weeks compared to the unloaded ($p<0.05$). The median RUNX2 and ALP expressions were significantly higher in the loaded PDL at two and four weeks than those in the unloaded ($p<0.05$), whereas the median RANKL to OPG ratios were significantly increased upon preloading at one and four weeks ($p<0.05$).

Conclusions: Orthodontic preloading for four weeks enhances the amounts of PDL tissue together with the RUNX2 and ALP expressions and the RANKL/OPG ratio in the PDL, suggesting that this loading period is suitable for successful TAT.

Introduction

Preservation of vital periodontal ligament (PDL) on a donor tooth is a key factor for successful tooth autotransplantation (TAT).[1] The PDL attached to the root surface contains several cell types essential for prevention of root resorption.[2] PDL injuries often occur during extraction of the donor teeth, leading to root resorption and ankylosis, which result in unsuccessful TAT.[3] Two main tissues involved in TAT healing comprise PDL and alveolar bone. For the healing of PDL after TAT, proliferative fibroblasts are the most prevalent cell type within the PDL responsible for production and alignment of collagen fiber bundles, whereas the bone remodeling process that begins with bone resorption by osteoclasts coupled with bone formation by osteoblasts is essential for the healing of alveolar bone.[2] In addition to the synthesis and organization of collagen fibers, the proliferative PDL fibroblasts secrete various bone mediators that control osteoblast and osteoclast differentiation in response to mechanical stresses.[4]

Several bone mediators have been studied during orthodontic tooth movement and their levels are changed in the PDL of animals and humans.[5-8] Among these mediators, Runt-related transcription factor 2 (RUNX2)[5, 9] and alkaline phosphatase (ALP)[9-11] are commonly used to monitor osteoblast differentiation under mechanical stresses. RUNX2 is a specific transcription factor that activates mesenchymal cells of the bone marrow leading to their differentiation into osteoblasts. Additionally, this transcription factor can regulate osteoblast maturation.[6] ALP is commonly used to assess osteoblasts' phenotypic development,[12] whose expression reflects an early stage of osteoblastic differentiation.[11] Osteoblasts also directly regulate osteoclast activity during bone remodeling.[10] Osteoblastic lineage cells express receptor activator of nuclear factor kappa-B ligand (RANKL),[13] one of the key factors mediating osteoclastogenesis that is regarded as an osteoclastic biomarker.[10] RANKL triggers osteoclast formation and activity once it binds to its specific receptor, called RANK, on the

osteoclast precursor cell membrane. To exert further control, osteoblasts also produce a potent inhibitor of RANKL, osteoprotegerin (OPG),[14] which is a member of the tumor necrosis factor receptor family. OPG functions by binding to RANKL and interrupting the RANKL-RANK interaction, resulting in inhibition of osteoclastogenesis.[13]

In a few previous studies, orthodontic force application before TAT resulted in increased PDL tissue volume.[15] Consequently, such force application is recommended to enhance the success rate of transplantation.[16] However, the expressions of bone biomolecules within the PDL at different loading durations and the optimal preloading duration to obtain the greatest PDL volume remain unclear. Therefore, the aims of this study were to evaluate the optimal orthodontic preloading duration to increase PDL volume and to determine the expressions of bone biomolecules, RUNX2, ALP, RANKL, and OPG in human PDL tissue upon loading with a leveling force at different time points.

Materials and Methods

Patient Selection

Healthy, non-smoking patients requiring extraction of first premolars for orthodontic treatment, were recruited from the Postgraduate Clinic, Faculty of Dentistry, OOO University, Thailand, with written informed consent. The study protocol (#9/2018) was approved by the OOO University Human Ethics Committee. The inclusion criteria were patients who had sound first premolars with complete root formation in their four quadrants without caries or restorations and had good oral hygiene and healthy periodontium. The exclusion criteria were patients with systemic infections or diseases, who required medications, such as nonsteroidal inflammatory drugs, or with severe crowding at the extraction sites.

Eighteen orthodontic patients were randomly divided into two groups for measurement of the PDL volume and determination of protein expression. For the measurement of the PDL volume, 32 first premolars from eight orthodontic patients (mean age 21.0±3.8 years; six females and two males) were selected. The calculation for the sample size of at least eight teeth for each period of loading was determined using G*Power software version 3.1.9.2 (Franz Faul, University of Kiel, Kiel, Schleswig-Holstein, Germany), with the effect size = 1.45 derived from the preliminary data, $\alpha = 0.05$ and $1-\beta = 0.95$. To determine the protein expression, 40 first premolars from ten remaining patients (mean age 21.4±4.0 years; eight females and two males) were selected. The sample size of at least nine teeth for each period of loading was determined with the effect size = 1.33 derived from the preliminary data, $\alpha = 0.05$ and $1-\beta = 0.95$.

Orthodontic preloading and tooth extraction

The orthodontic leveling force was obtained from a **continuous archwire**, 0.016-inch, improved superelastic nickel‑titanium alloy wire (**Sentalloy blue,** Sentalloy®, Tomy International, Inc., Tokyo, Japan), inserted into a pre‑adjusted edgewise bracket (Roth prescription; 0.018 x 0.025 inch, Tomy International, Inc.) that was bonded on the first premolar **and all remaining teeth. The bracket position was performed using indirect bonding technique in order to allow precise bracket positioning.[17] For the first premolars, brackets were passively placed to avoid either intrusive or extrusive movements. The wire possesses a shape-memory effect, enabling the generation of light continuous force at 30-70 g in oral cavity.[18]** The control unloaded premolars were extracted at the first visit of each patient, whereas the experimental loaded premolars were

extracted after orthodontic loading for one, two or four weeks. Simple exodontia was carried out by one oral surgeon under local anesthesia with 4% articaine and 1:100,000 epinephrine (Septanest SP®, Septodont, Co., Paris, France) by an infiltration technique (1.0 ml for the maxillary premolars) or an inferior alveolar nerve block together with lingual and long buccal nerve blocks (1.7 ml for the mandibular premolars) using a conventional aspirating dental syringe and a disposable 30-gauge and 21-mm-short needle (Septoject XL®, Septodont, Co., Paris, France) for the infiltration or a disposable 27-gauge and 30-mm-long needle (Septoject XL®) for the nerve blocks. Both experimental and control premolars were atraumatically extracted by gentle separation of gingiva using a no. EL3S straight elevator no. EL3S (Hu-Friedy Mfg. Co., LLC, Chicago, IL, USA), followed by a no. 151 forceps (Hu-Friedy Presidential®, Hu-Friedy Mfg. Co., LLC) to avoid injury to the PDL tissue. The extracted premolars were then washed with normal saline to remove blood and tissue debris.

Assessment of periodontal ligament tissue

Toluidine blue staining and determination of remaining PDL tissue on the root surface were performed using the protocol of Nakdilok et al.[19] Briefly, the extracted teeth were stained with 0.04% (w/v) toluidine blue (Sigma-Aldrich, St. Louis, MO, USA), and de-stained with PBS for 14 days. A stereomicroscope (Olympus SZX7; Olympus, Inc., Tokyo, Japan) was used to observe all surfaces of the stained roots. A digitized image in a plane perpendicular to the tooth axis was then recorded using a charge-coupled device (Olympus E-330; Olympus, Inc.) attached to the stereomicroscope. The ImageJ2 (National Institute of Health, Bethesda, MD, USA) software program was used to quantify the stained images, and the stained area in each image was determined as a percentage of the total area. This percentage of stained PDL was achieved, using the ImageJ2 program, by differentiating between the white and blue pixels, which represent the unstained and stained areas, respectively. The percentage of the stained PDL of each tooth was then calculated.

Expressions of bone biomolecules in periodontal ligament tissue

The PDL tissue of the extracted premolars was scraped off from 3 mm below the cemento-enamel junction to the root apex. Total protein was isolated by grinding the PDL tissue in a glass homogenizer using 350 µl of lysis buffer from a NucleoSpin® RNA/Protein isolation kit (MACHEREY-NAGEL GmbH & Co. KG, Düren, Germany) and 1% (v/v) β-mercaptoethanol (Bio-Rad Laboratories, Inc., Hercules, CA, USA). The lysate was transferred to a 1.5-ml Eppendorf® tube and stored at -80 ºC until simultaneous Western blot analysis of every sample from the ten patients. The frozen lysates were thawed and their total protein was extracted using the NucleoSpin® RNA/Protein isolation kit (MACHEREY-NAGEL GmbH & Co. KG) following the manufacturer's instruction. In brief, the lysates were first centrifuged at 1,100 g for one minute to remove tissue debris using filter tubes, and the filtrated lysates were mixed with 70% ethanol at an equal volume. The mixtures were centrifuged using the NucleoSpin® columns to collect their protein fraction from the flow-through solution. Protein in the solution was precipitated and dissolved in protein solving buffer, containing a reducing agent, Tris (2-carboxyethyl) phosphine hydrochloride. The quantity of total protein in each sample was determined using UV absorbance at 280 nm in a NanoDrop™ 2000 spectrophotometer (Thermo Scientific™, Rockford, IL, USA). A 20-µg quantity of total protein was resolved by 10% sodium dodecyl sulfate polyacrylamide gel electrophoresis under electrical current at 100V/300W for 135 minutes and transferred to nitrocellulose membranes under electrical current at 100mA/300W for 12 hours. To block non-specific binding, the membranes were incubated for one hour in 5% (w/v) non-fat dry milk (Santa Cruz Biotechnology, Inc., Santa Cruz, CA, USA) in 0.1% (v/v) Tween-20/Tris-buffered saline. Subsequently, the membranes were incubated overnight at 4°C with the primary antibodies. On the following day, the membranes were washed and incubated with the secondary antibodies for one hour. The primary and secondary antibodies used in this

study are summarized in Table 1. After washing, the membranes were reacted with LumiGLO Reserve™ Chemiluminescent reagent (KPL, Gaithersburg, MD, USA). Chemiluminescent signals were captured using the ChemiDoc XRS gel documentation system (Bio-Rad Laboratories, Inc.). The intensities of RUNX2, ALP, RANKL and OPG bands at their predicted size were measured using the ImageJ2 software and normalized by that of the beta actin band in each sample. Then, the normalized intensities of the aforementioned proteins were compared between the experimental and the control groups. In addition, the relative ratios of normalized RANKL to OPG were determined and compared between the experimental and the control groups.

Statistical Analysis

Data were analyzed using SPSS 19.0 software for Windows® (SPSS Inc., Chicago, IL, USA). Comparisons between the percentages of overall stained PDL tissue at different time points, the significant differences between protein expressions and the ratios of RANKL to OPG in different orthodontic loading durations were tested using the Friedman Test, followed by the Wilcoxon Signed Ranks Test. The differences were considered statistically significant if *p*-values were less than 0.05. Spearman's method was used to analyze correlations between the percentages of stained PDL, protein expressions or the RANKL/OPG ratio and increased loading durations.

Results

Enhancement of periodontal ligament tissue upon orthodontic preloading

Larger areas of stained PDL were observed on the root surface of the loaded teeth, particularly those loaded for two and four weeks, compared to those in the control unloaded teeth (Figure 1). The median percentages of stained PDL were significantly greater in the

teeth loaded for two and four weeks than those in the control unloaded teeth and in the teeth loaded for one week ($p<0.05$; Figure 2). In addition, a strong positive correlation was found between the percentage of stained PDL and increased preloading durations (r=0.608, $p<0.001$).

Significant increases in RUNX2, ALP and the RANKL/OPG ratio upon orthodontic preloading

The expressions of RUNX2 and ALP were found to be enhanced in premolars loaded for one, two and four weeks as compared to the control unloaded teeth, whereas those of RANKL and OPG varied among the unloaded and the loaded teeth for different preloading durations (Figure 3). The expression of beta actin was approximately equal among different samples within each individual. By densitometry, the normalized median RUNX2 and ALP expressions were significantly greater in the premolars loaded for two and four weeks than those in the control unloaded premolars (Figure 4A and B). Moreover, moderately positive correlations were found between the normalized RUNX2 or the normalized ALP expression and increased preloading durations (r=0.384, $p=0.015$ and r=0.403, $p=0.010$, respectively). By contrast, there was no difference in the normalized median RANKL or OPG expression between the loaded and the unloaded premolars (data not shown). However, the median ratios of RANKL relative to OPG expression were significantly higher in the premolars loaded for one and four weeks than that in the unloaded premolars ($p<0.05$; Figure 4C). Furthermore, the RANKL/OPG ratio was positively correlated with increased preloading durations (r=0.329, $p=0.038$).

Discussion

PDL is a fiber-reinforced tissue, containing various types of cells that play an important role in response to mechanical stresses, maintaining the periodontium and

promoting periodontal regeneration.[9] The results of this study demonstrated that orthodontic preloading led to macroscopic and molecular alterations in the PDL tissue. During the early stage of this process, *i.e.*, after application of the leveling force for one week, no significant changes were observed in the percentages of stained PDL, whereas significant increases in RUNX2 expression and the RANKL/OPG ratio were noted. Two weeks after orthodontic preloading, the amounts of PDL tissue and the ALP expression were found to be significantly increased, whereas the degree of RUNX2 expression still remained high. At the end of the observation, *i.e.*, after four weeks of preloading with the leveling force, the amounts of PDL tissue and the expressions of RUNX2 and ALP along with the RANKL/OPG ratio were approximately at their maximal levels and greater than for the unloaded teeth. Taken together, the preloading duration appears to be a crucial factor that induces the amounts of proliferative PDL, as shown by an increase in the percentage of stained PDL, the expressions of RUNX2 and ALP as well as the RANKL/OPG ratio within the PDL.

Pre-application of orthodontic loading with various loading durations has been previously performed in several studies. In an animal study, the preloading of light continuous orthodontic force for seven days resulted in rich PDL tissue attached to the extracted teeth.[15] A study performed in humans also demonstrated that preoperative extrusion force for two to three weeks helped prevent extraction failure and increased the success rate of tooth replantation.[16] Moreover, our previous study has shown a significant increase in the amounts of PDL and facilitated tooth extraction upon orthodontic preloading for four weeks.[19] However, the time-course study of orthodontic preloading that may help promote the success rate of TAT has not been discussed.

Our study suggests that increased proliferative PDL and the expression profiles of the four bone biomolecules derived from the proliferative PDL are associated with various clinical phases of orthodontic tooth movement. In the initial phase, PDL becomes

disorganized; the collagen fiber orientation in the PDL is considerably changed by the function of PDL fibroblasts.[20] These cells play crucial roles in synthesizing new collagen fibers and ground substances while simultaneously breaking down old connective tissue in the PDL.[21] Therefore, no significant changes in the net PDL tissue amounts were observed at the first week, which correspond to no change in the median percentage of stained PDL (Figure 2). However, at the molecular level, the mechanosensitive PDL cells can convert mechanical stimuli from orthodontic preloading force into biological signals, which regulate osteoblastogenesis[22] and osteoclastogenesis.[23] These are consistent with significant increases in the RUNX2 expression and the RANKL/OPG ratio, respectively, at the first week. The upregulated RUNX2 expression indicates an induction of mesenchymal cells into differentiated osteoblasts.[5] On the contrary, an increase in the RANKL/OPG ratio, either from enhanced RANKL expression due to inflammation within PDL caused by orthodontic preloading,[8, 13] from decreased OPG expression in PDL,[8, 13] or both, probably accounts for the significantly increased RANKL/OPG ratio by orthodontic preloading observed at the first week that would lead to enhanced osteoclastogenesis and then alveolar bone resorption during the initial phase.[24]

Subsequently, the lag and the post-lag phases involve reorganization of the fibrous attachment apparatus by augmented production of new periodontal fibrils, which takes place throughout the PDL.[20] Consequently, enhanced synthesis of PDL fibers would be in line with significant increases in the percentage of stained PDL observed at two and four weeks after orthodontic preloading. In addition, significant increases in the RUNX2 and ALP expressions in the PDL observed at two and four weeks after orthodontic preloading would help recruit and activate new osteoblast progenitors and quiescent bone lining cells to commence the production of new bone matrix.[25] After four weeks of orthodontic force application, continuous PDL cell division, resulting in continual collagen synthesis,[26] and high capacities

of PDL and alveolar bone remodeling[27] are substantiated by significant and continuing enhancement of PDL volume and expressions of RUNX2 and ALP as well as the RANKL/OPG ratio.

The kinetic profiles of induced RUNX2 and ALP protein expressions and the increased RANKL/OPG ratio in human PDL tissue upon receiving the leveling force observed in this study are in agreement with the findings from previous *in vivo* studies that have shown upregulated RUNX2 expression,[28] raised ALP levels,[29] elevated GCF and salivary RANKL levels, and decreased GCF and salivary OPG levels[8, 30] upon orthodontic preloading in a time-dependent manner. However, it is noteworthy that there was no difference in the expression of RANKL or that of OPG found between different loading durations (data not shown). This may be attributable to the first observation period at one week that is too late to be able to detect any initial changes in the levels of RANKL or OPG, which have been previously reported to be significantly elevated or declined, respectively, upon orthodontic loading for 24 hours in human GCF.[8]

This study reveals that orthodontic preloading induces alterations at the macroscopic level, as evidenced by the significant increase in the proliferative PDL tissue, which may help prevent the occurrence of denuded root surfaces due to tooth extraction, possibly leading to a reduction in ankylosis and root resorption after TAT. In addition, orthodontic preloading aids in facilitated tooth extraction,[19] which would decrease the possibility of root fracture of the donor tooth. Moreover, at the molecular level, orthodontic preloading results in significant increases in the expressions of RUNX2 and ALP that are essential for osteoblast differentiation and new bone formation and in the RANKL/OPG ratio that induces bone resorption. All of these molecular changes that affect bone formation and resorption would facilitate adaptation of the donor tooth to the alveolar bone at the recipient site and promote bone remodeling during the healing of transplanted teeth. **<u>Therefore, application of</u>**

orthodontic preloading results in both PDL proliferation and increased expressions of bone-related molecules. Increased PDL volume ensures easy and atraumatic extraction and provides thick PDL coverage around the radicular portion, which is beneficial for reducing ankylosis risks. Furthermore, increased expressions of bone-related molecules, which are involved in bone remodeling, would modulate the bone healing response. These combined beneficial effects would provide clinical implications of orthodontic preloading for good PDL and bone healing, which lead to increased TAT success rate. However, further clinical studies are necessary to investigate the overall benefits of orthodontic preloading on TAT.

Although there were no differences in the PDL volumes and bone biomolecules expressions between two and four weeks, the optimal orthodontic preloading duration to gain benefits both in PDL and bone tissue responses is suggested at four weeks in this study, when all parameters tested were found to be significantly increased as compared to the controls. (Table 2) Additionally, this study is the first to show not only the enhancement of PDL tissues but also the time-course changes in expressions of important bone biomolecules within human PDL tissues upon orthodontic preloading using the leveling force. Moreover, our investigations for protein expressions were performed in the human PDL tissues rather than in GCF or saliva as previously reported.[8,30]

In this study, continuous leveling force was used to determine the effect of orthodontic preloading on the amounts of PDL tissue as well as the expressions of bone biomolecules within the PDL. **Despite the leveling force used to generate jiggling movement for the first premolars, it is likely that the expressions of bone biomolecules vary between the pressure and the tension sides. This issue was not, however, addressed in this study due to the collection of total proteins from PDL tissue of the whole root**

surface. Consequently, our results should be cautiously interpreted as the total effect of PDL responses upon orthodontic preloading, not the specific effect at the pressure or the tension side. Other factors, such as the magnitudes and the types of force, may differently influence the biological responses of PDL tissue. Therefore, it would be interesting to further investigate the effect of these factors on the PDL. Moreover, future long-term clinical research is essential to confirm the success rate of TAT by an application of orthodontic preloading force on the donor tooth for four weeks.

Conclusions

The findings from this study demonstrated that orthodontic preloading for four weeks significantly increased proliferative PDL tissue, expressions of RUNX2 and ALP, and the RANKL/OPG ratio, which may be beneficial for improving the success rate of TAT.

Conflict of interest

None declared.

Funding

Acknowledgements

References

1. Andreasen JO. Periodontal healing after replantation and autotransplantation of incisors in monkeys. Int J Oral Surg 1981;10:54-61.

2. Tsukiboshi M, Andreasen JO. Autotransplantation of teeth: Quintessence Pub. Co.; 2001.

3. Sugai T, Yoshizawa M, Kobayashi T, Ono K, Takagi R, Kitamura N, et al. Clinical study on prognostic factors for autotransplantation of teeth with complete root formation. Int J Oral Maxillofac Surg 2010;39:1193-203.

4. Li M, Zhang C, Yang Y. Effects of mechanical forces on osteogenesis and osteoclastogenesis in human periodontal ligament fibroblasts: A systematic review of in vitro studies. Bone Joint Res 2019;8:19-31.

5. Brooks PJ, Nilforoushan D, Manolson MF, Simmons CA, Gong SG. Molecular markers of early orthodontic tooth movement. Angle Orthod 2009;79:1108-13.

6. Li B, Zhang YH, Wang LX, Li X, Zhang XD. Expression of OPG, RANKL, and RUNX2 in rabbit periodontium under orthodontic force. Genet Molecular Res 2015;14:19382-8.

7. Garlet TP, Coelho U, Silva JS, Garlet GP. Cytokine expression pattern in compression and tension sides of the periodontal ligament during orthodontic tooth movement in humans. Eur J Oral Sci 2007;115:355-62.

8. Nishijima Y, Yamaguchi M, Kojima T, Aihara N, Nakajima R, Kasai K. Levels of RANKL and OPG in gingival crevicular fluid during orthodontic tooth movement and effect of compression force on releases from periodontal ligament cells in vitro. Orthod Craniofac Res 2006;9:63-70.

9. Zhang L, Liu W, Zhao J, Ma X, Shen L, Zhang Y, et al. Mechanical stress regulates osteogenic differentiation and RANKL/OPG ratio in periodontal ligament stem cells by the Wnt/beta-catenin pathway. Biochim Biophys Acta 2016;1860:2211-9.

10. Tripuwabhrut P, Mustafa M, Gjerde CG, Brudvik P, Mustafa K. Effect of compressive force on human osteoblast-like cells and bone remodelling: an in vitro study. Arch Oral Biol 2013;58:826-36.

11. Pavlin D, Dove SB, Zadro R, Gluhak-Heinrich J. Mechanical loading stimulates differentiation of periodontal osteoblasts in a mouse osteoinduction model: effect on type I collagen and alkaline phosphatase genes. Calcif Tissue Int 2000;67:163-72.

12. Banerjee C, McCabe LR, Choi JY, Hiebert SW, Stein JL, Stein GS, et al. Runt homology domain proteins in osteoblast differentiation: AML3/CBFA1 is a major component of a bone-specific complex. J Cell Biochem 1997;66:1-8.

13. Yamaguchi M. RANK/RANKL/OPG during orthodontic tooth movement. Orthod Craniofac Res 2009;12:113-9.

14. Kapasa ER, Giannoudis PV, Jia X, Hatton PV, Yang XB. The Effect of RANKL/OPG Balance on Reducing Implant Complications. J Funct Biomater 2017;8:42.

15. Suzaki Y, Matsumoto Y, Kanno Z, Soma K. Preapplication of orthodontic forces to the donor teeth affects periodontal healing of transplanted teeth. Angle Orthod 2008;78:495-501.

16. Choi YH, Bae JH, Kim YK, Kim HY, Kim SK, Cho BH. Clinical outcome of intentional replantation with preoperative orthodontic extrusion: a retrospective study. Int Endod J 2014;47:1168-76.

17. **Yugo Suzuki E, Suzuki B. Guiding Template for Direct Bracket Placement: A Hybrid Technique. Austin J Dent. 2019; 6: 1127.**

18. **Miura F, Mogi M, Ohura Y, Hamanaka H. The super-elastic property of the Japanese NiTi alloy wire for use in orthodontics. Am J Orthod Dentofacial Orthop 1986;90:1-10.**

19. Nakdilok K, Langsa-ard S, Krisanaprakornkit S, Suzuki EY, Suzuki B. Enhancement of human periodontal ligament by pre-application of orthodontic loading. Am J Orthod Dentofacial Orthop **2020;157:186-193.**

20. Thilander B. Tissue Reactions in Orthodontics. In: Graber LW, Vanarsdall RL, Vig KWL. Orthodontics: current principles and techniques. 5th ed. Philadelphia: Elsevier/Mosby; 2011. p. 247-86

21. Ten Cate AR, Deporter DA, Freeman E. The role of fibroblasts in the remodeling of periodontal ligament during physiologic tooth movement. Am J Orthod 1976;69:155-68.

22. Shen T, Qiu L, Chang H, Yang Y, Jian C, Xiong J, et al. Cyclic tension promotes osteogenic differentiation in human periodontal ligament stem cells. Int J Clin Exp Pathol 2014;7:7872-80.

23. Kanzaki H, Chiba M, Shimizu Y, Mitani H. Periodontal ligament cells under mechanical stress induce osteoclastogenesis by receptor activator of nuclear factor kappaB ligand up-regulation via prostaglandin E2 synthesis. J Bone Miner Res 2002;17:210-20.

24. Dunn MD, Park CH, Kostenuik PJ, Kapila S, Giannobile WV. Local delivery of osteoprotegerin inhibits mechanically mediated bone modeling in orthodontic tooth movement. Bone. 2007;41:446-55.

25. Krishnan V, Davidovitch Z. Cellular, molecular, and tissue-level reactions to orthodontic force. Am J Orthod Dentofacial Orthop 2006;129:469.e1-32.

26. Bumann A, Carvalho RS, Schwarzer CL, Yen EH. Collagen synthesis from human PDL cells following orthodontic tooth movement. Eur J Orthod 1997;19:29-37.

27. Pilon JJ, Kuijpers-Jagtman AM, Maltha JC. Magnitude of orthodontic forces and rate of bodily tooth movement. An experimental study. Am J Orthod Dentofacial Orthop 1996;110:16-23.

28. Han J, Xu X, Zhang B, Chen B, Hang W. Expression of ATF4 and RUNX2 in periodontal tissue of pressure side during orthodontic tooth movement in rat. Int J Clin Exp Med 2015;8:934-8.

29. Insoft M, King GJ, Keeling SD. The measurement of acid and alkaline phosphatase in gingival crevicular fluid during orthodontic tooth movement. Am J Orthod Dentofacial Orthop 1996;109:287-96.

30. Florez-Moreno GA, Isaza-Guzman DM, Tobon-Arroyave SI. Time-related changes in salivary levels of the osteotropic factors sRANKL and OPG through orthodontic tooth movement. Am J Orthod Dentofacial Orthop 2013;143:92-100.

Legends for Illustrations

Figure 1 Representative image illustrating stained PDL for unloaded tooth (control) and after orthodontic loading for one (1), two (2) or four (4) weeks

Figure 2 Percentage of stained PDL in unloaded teeth compared to loaded teeth for different loading durations. *$p<0.05$

Figure 3 Representative immunoblotting results of Runt-related transcription factor 2 (RUNX2), alkaline phosphatase (ALP), receptor activator of nuclear factor kappa-B ligand (RANKL), osteoprotegerin (OPG), and beta actin expressions in human periodontal ligament tissues after orthodontic loading for one (1), two (2), four (4) weeks or unloaded as a control.

Figure 4 Box plot diagrams showing significantly enhanced RUNX2 (A) and ALP (B) expressions normalized by beta actin expressions as well as RANKL/OPG ratio (C) at different loading durations (gray boxes) compared to those of control unloaded (empty boxes). Moderately positive correlations were found between RUNX2 (A), ALP (B) or RANKL/OPG and loading durations from one to four weeks. The horizontal line within each box represents the median. *$p<0.05$; **$p<0.01$

Table1 List of antibodies

Antibody	Donor	Dilution	Supplier
Primary antibody			
Polyclonal IgG anti-human Runx2/CBFA1	Goat	1:2000	R&D systems, Minneapolis, MN, USA
Monoclonal IgG$_1$ anti-human ALPL	Mouse	1:2000	R&D systems
Monoclonal IgG$_1$ anti-human RANKL	Mouse	1:500	Santa Cruz Biotechnology, Santa Cruz, CA, USA
Monoclonal IgG$_1$ anti-human OPG	Mouse	1:500	Santa Cruz Biotechnology
Monoclonal IgG$_1$ anti-human beta-actin	Mouse	1:1000	Santa Cruz Biotechnology
Secondary antibody			
Anti-rabbit immunoglobulins	Horseradish peroxidase (HRP)-conjugated swine	1:2000	Dako, Glostrup, Denmark
Anti-mouse immunoglobulins	HRP-conjugated Rabbit	1:2000	R&D systems
Anti-goat IgG (H+L)	HRP-Mouse	1:2000	Thermoscientific, Rockford, IL, USA

Table 2 Outcomes of orthodontic preloading compare to unloading

Outcome	Loading duration (week)		
	1	2	4
Enhancement of PDL tissue	NS	*	*
RUNX2	**	*	*
ALP	NS	*	**
RANKL/OPG ratio	*	NS	**

NS: No significant, *p<0.05, **p<0.01
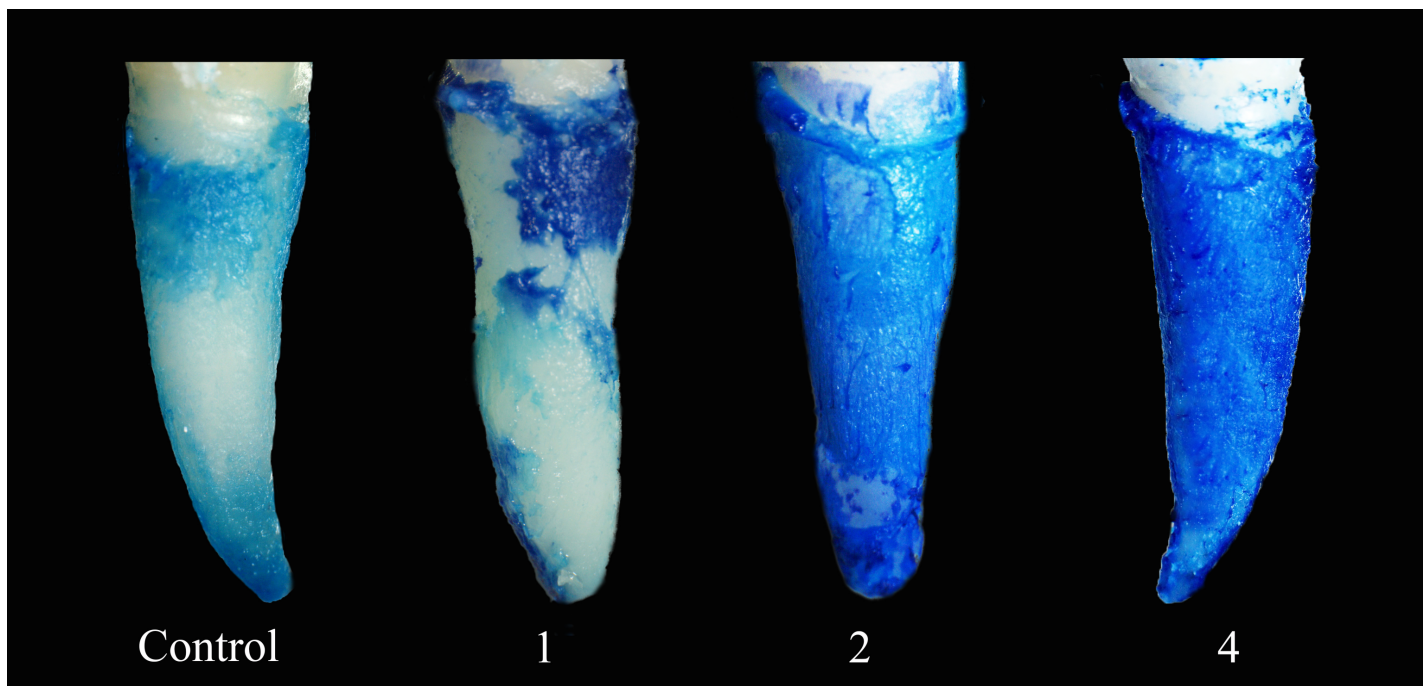
Fig. 1. Figure 1 Representative image illustrating stained PDL for unloaded tooth (control) and after orthodontic loading for one (1), two (2) or four (4) weeks
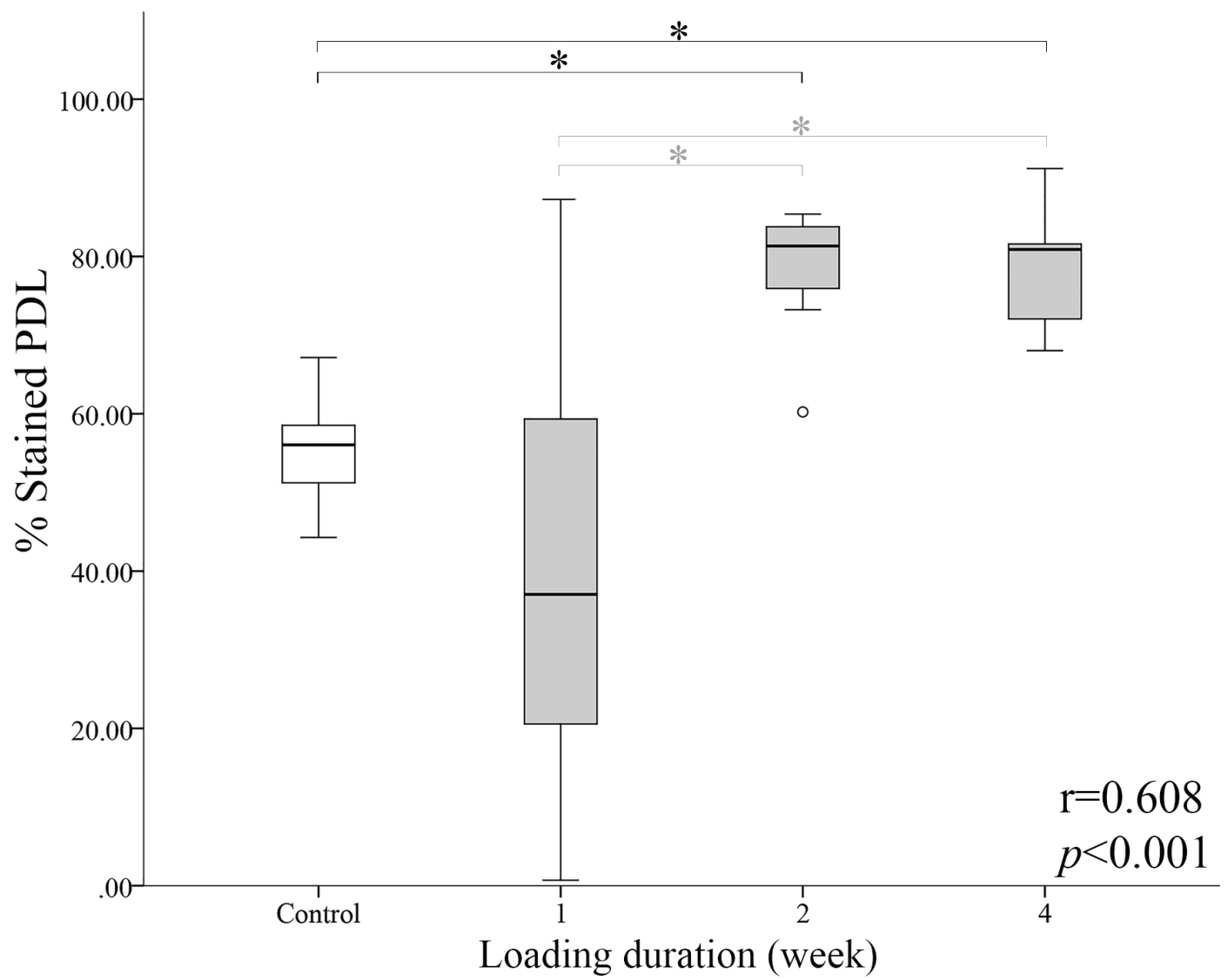
Fig. 2. Figure 2 Percentage of stained PDL in unloaded teeth compared to loaded teeth for different loading durations. *p<0.05
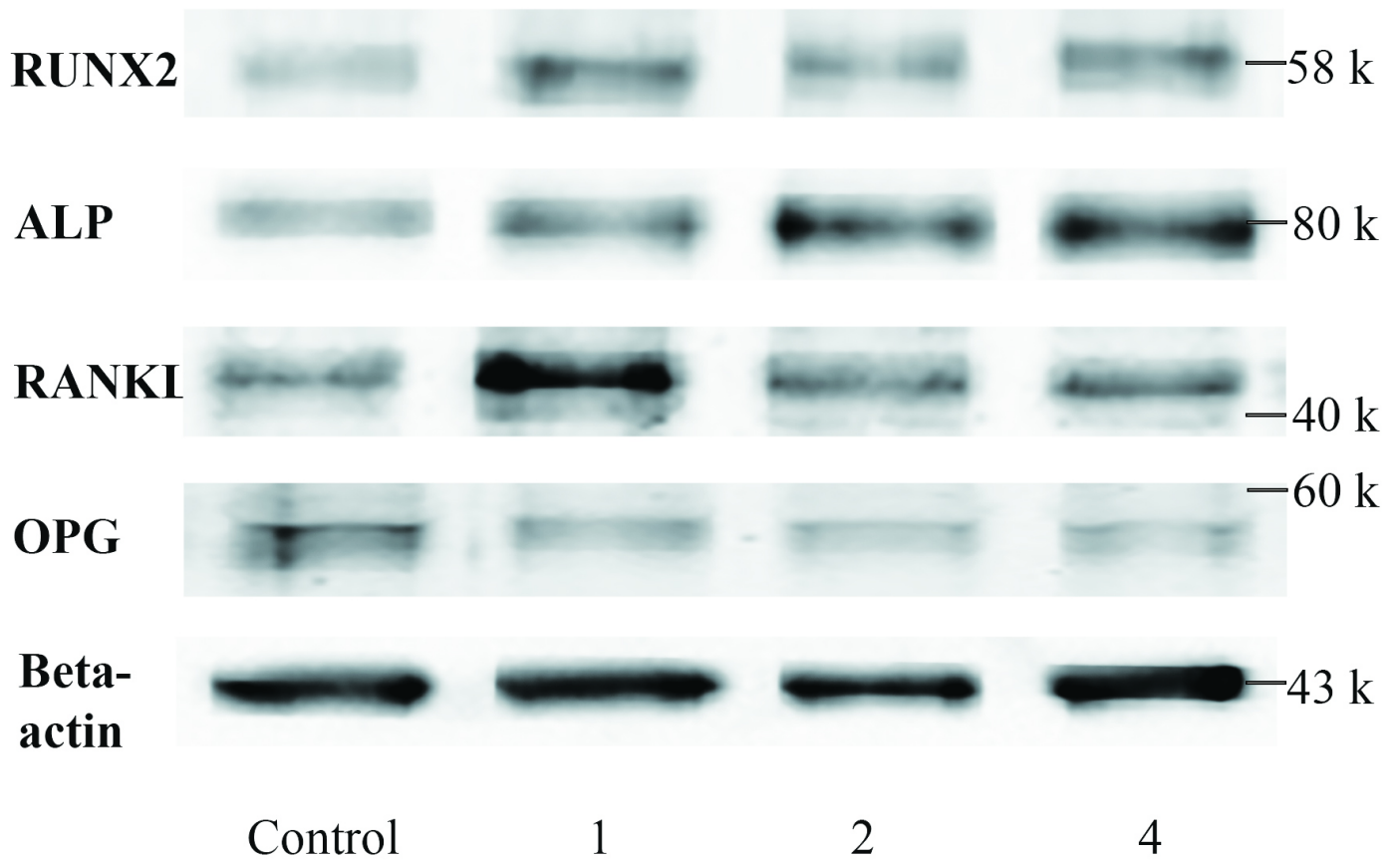
Fig. 3. Figure 3 Representative immunoblotting results of Runt-related transcription factor 2 (RUNX2), alkaline phosphatase (ALP), receptor activator of nuclear factor kappa- ligand (RANKL), osteoprotegerin (OPG), and beta actin expressions in human periodontal ligament tissues after orthodontic loading for one (1), two (2), four (4) weeks or unloaded as a control.
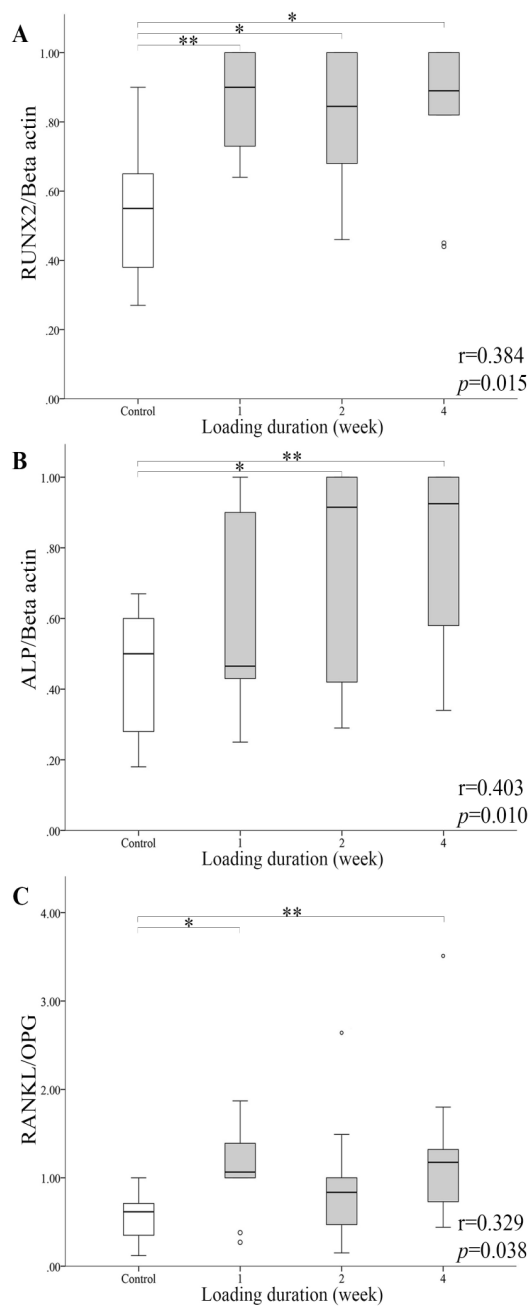
Fig. 4. Figure 4 Box plot diagrams showing significantly enhanced RUNX2 (A) and ALP (B) expressions normalized by beta actin expressions as well as RANKL/OPG ratio (C) at different loading durations (gray boxes) compared to those of control unloaded (empty boxes). Moderately positive correlations were found between RUNX2 (A), ALP (B) or RANKL/OPG and loading durations from one to four weeks. The horizontal line within each box represents the median. *p<0.05; **p<0.01

American Journal of Orthodontics & Dentofacial Orthopedics

Periodontal ligament enhancement in mesio-angulated impaction of third molars following orthodontic tooth movement: A prospective cohort study
--Manuscript Draft--

Manuscript Number:	AJODO-D-19-00339R2
Article Type:	Original Article
Corresponding Author:	Eduardo Yugo Suzuki, DDS, PhD Faculty of Dentistry, Bangkok Thonburi University Bangkok, Bangkok THAILAND
First Author:	Pattarin Promchaiwattana, DDS
Order of Authors:	Pattarin Promchaiwattana, DDS
	Boonsiva Suzuki, DDS, Ph.D
	Suttichai Krisanaprakornkit, DDS, Ph.D
	Eduardo Yugo Suzuki, DDS, PhD

Abstract:	Introduction: Mesio-angulated impaction of mandibular third molars makes them unsuitable as donor teeth for tooth autotransplantation (TAT). However, the uprighted molars may be applicable for TAT. This study aimed to determine the amount of periodontal ligament (PDL) on the root surfaces of extracted third molars after an application of uprighting force and examine the amount of PDL at the tension and compression sites. Methods: In this prospective cohort study, fifteen mesio-angulated mandibular third molars (iM8s) from 15 patients, planned for orthodontic extraction, were uprighted using springs connected to miniscrews, while 15 non-opposing and fully erupted mandibular third molars from the other 15 patients served as controls. Altered angulation was monitored and assessed from panoramic radiographs. All 30 molars, removed by simple extraction, were stained with 0.04% (w/v) toluidine blue to analyze the percentages of stained PDL on the root surfaces. Results: An average period of 3.4 months was necessary to upright the iM8s at a mean rate of 8.3 degrees/month. The mean percentage of stained PDL on the loaded iM8s was significantly greater than that on the unloaded molars (p<0.05). The mean percentages of stained PDL were significantly increased at the cervical and middle thirds, and the buccal, mesial and distal surfaces of the loaded iM8s compared to those of the unloaded molars (p<0.05), whereas the apical third and the lingual surface, corresponding to the compression sites, showed no significant increase. Conclusions: Orthodontic uprighting leads to significantly increased proliferative PDL on certain radicular portions and surfaces of iM8s, which might be useful for TAT.

Our responses

Thank you for your patience while I considered your revised manuscript. I appreciate the work you have put in on this paper, and I believe that with a few minor, additional changes, it can be accepted for publication. Please refer to the comments appended below.

Thank you for your kindness. We made additional changes as suggested.

Please make the changes in your text in a colored typeface to help us easily identify them. When you submit the revised copy, please include blinded Revision Notes describing the changes you have made. The title page of your article should include complete author information, including each author's contribution to the research.

The changes in our text are in red characters to be easily identified. This Revision Notes describe the changes done to our manuscript. The title page has already contained the complete author information, including each author's contribution to the research.

Comments from the Reviewers:

Associate Editor:

The authors revised the manuscript to address the points of information requested by the reviewers, according to my assessment and that of Reviewer #2. Reviewer #1 did not respond to requests to review the revised manuscript.

I have a minor request to improve the flow of the manuscript. Figures 6 was added to demonstrate the activation of the uprighting/distalizing spring and the figure appears to be out of place currently. Figure 6 should either become part of Figure 1 or become Figure 2 as it relates closely to concepts demonstrated in Figure 1. The change, if Figure 6 becomes Figure 2, would entail a renumbering the subsequent figures and making adjustment to content sequencing and Figure number references in the text.

Thank you for your suggestion. The Figure 6 becomes Figure 2 as suggested. Other figures are now renumbered as shown in red characters.

Efforts to date to revise the manuscript have been appreciated.

We are grateful for your advice on developing our manuscript.

Reviewer #2: The authors addressed the reviewers' comments satisfactorily.

Thank you.

Periodontal ligament enhancement in mesio-angulated impaction of third molars following orthodontic tooth movement: A prospective cohort study

Pattarin Promchaiwattana,[a] Boonsiva Suzuki,[b] Suttichai Krisanaprakornkit,[c] and Eduardo Yugo Suzuki[d]

[a]Master candidate, Department of Orthodontics, Faculty of Dentistry, Bangkokthonburi University, Bangkok, Thailand; Email, super_ped@icloud.com

[b]Associate professor, Department of Orthodontics, Faculty of Dentistry, Bangkokthonburi University, Bangkok, Thailand; Email, boonsiva.suz@bkkthon.ac.th

[c]Professor, Department of Oral Biology and Diagnostic Sciences, Center of Excellence in Oral and Maxillofacial Biology, Faculty of Dentistry, Chiang Mai University, Chiang Mai, Thailand; Email, suttichai.k@cmu.ac.th

[d]Lecturer, Department of Orthodontics, Faculty of Dentistry, Bangkokthonburi University, Bangkok, Thailand; Email, eduardo.suz@bkkthon.ac.th

Authors' contributions

Pattarin Promchaiwattana: Experimental design, data acquisition, collection and analysis, drafting and final approval of the manuscript

Boonsiva Suzuki: Experimental conception, revising and final approval of the manuscript

Suttichai Krisanaprakornkit: Experimental conception, drafting and final approval of the manuscript

Eduardo Yugo Suzuki: Experimental design, data acquisition, collection and analysis, drafting and final approval of the manuscript, correspondence

Running title: PDL increase by uprighting force

Abstract count: 249

Number of figures: 6

Number of tables: 1

Corresponding Author:

Dr. Eduardo Yugo Suzuki

Department of Orthodontics, Faculty of Dentistry, Bangkokthonburi University

16/10 Leabklongtaweewatana Rd., Taweewatana District, Bangkok 10170

Thailand, Phone: +66-53-274420, E-mail: eduardo.suz@bkkthon.ac.th

Highlights

- The average period of uprighting mesio-angulated lower 3rd molars was 3.4 months.

- The mean rate of reduced angulation was 8.3 degrees per month.

- The reduced angulation was correlated with an increased period of uprighting.

- The mean percentage of stained PDL on uprighted molars was significantly increased.

- Significant PDL enhancement was observed at the tension sites.

Abstract

Introduction: Mesio-angulated impaction of mandibular third molars makes them unsuitable as donor teeth for tooth autotransplantation (TAT). However, the uprighted molars may be applicable for TAT. This study aimed to determine the amount of periodontal ligament (PDL) on the root surfaces of extracted third molars after an application of uprighting force and examine the amount of PDL at the tension and compression sites.

Methods: In this prospective cohort study, fifteen mesio-angulated mandibular third molars (iM8s) from 15 patients, planned for orthodontic extraction, were uprighted using springs connected to miniscrews, while 15 non-opposing and fully erupted mandibular third molars from the other 15 patients served as controls. Altered angulation was monitored and assessed from panoramic radiographs. All 30 molars, removed by simple extraction, were stained with 0.04% (w/v) toluidine blue to analyze the percentages of stained PDL on the root surfaces.

Results: An average period of 3.4 months was necessary to upright the iM8s at a mean rate of 8.3 degrees/month. The mean percentage of stained PDL on the loaded iM8s was significantly greater than that on the unloaded molars ($p<0.05$). The mean percentages of stained PDL were significantly increased at the cervical and middle thirds, and the buccal, mesial and distal surfaces of the loaded iM8s compared to those of the unloaded molars ($p<0.05$), whereas the apical third and the lingual surface, corresponding to the compression sites, showed no significant increase.

Conclusions: Orthodontic uprighting leads to significantly increased proliferative PDL on certain radicular portions and surfaces of iM8s, which might be useful for TAT.

Keywords: Mesio-angulation, orthodontic loading, periodontal ligament, third molars, tooth autotransplantation

Introduction

Maintaining cell viability within human periodontal ligament (PDL) and good tissue adaptation of PDL are among the most important considerations for successful tooth autotransplantation (TAT).[1] However, PDL can be damaged mechanically during extraction.[2] Complete PDL healing after tooth replantation can be expected if damage to the PDL of the donor tooth during extraction is reduced or limited,[3] whereas development of root resorption is regarded as the beginning of failure, resulting from trauma to the PDL at the time of replantation.[4] PDL cells possess an ability to produce and secrete a wide range of regulatory molecules, which are crucial components of PDL tissue remodeling and homeostasis.[5] The multi-lineage differentiation potential of PDL stem cells essentially partakes in PDL homeostasis by giving rise to various types of progenitor cells.[6] Despite cellular, genetic, biochemical and mechanical factors working together to maintain this homeostasis, much of the research investigating PDL homeostasis has dealt extensively with mechanical stress from applied physical force and its consequent biochemical signaling molecules, leading to changes in the metabolism and organization of the soft connective tissue within PDL.[7]

Both animal and clinical studies have shown that applying orthodontic force to the donor tooth is beneficial for TAT in terms of facilitating extraction and of stimulating PDL proliferation, consequently resulting in reduced rates of root resorption.[8-10] An animal study by Suzaki et al[8] reported that preloading of light orthodontic force for seven days before extraction significantly increased the PDL space as well as the width of the alveolar socket, as observed histologically, resulting in rich PDL tissues attached to the root surface of the extracted teeth. Moreover, the length of active root resorption lacunae was less than that in the contralateral control unloaded teeth, thus suggesting that the increased width of PDL space and alveolar socket may prevent crushing of the PDL during extraction. Cho et al[9] applied preloading orthodontic forces to third molars in two cases to increase tooth mobility before TAT, using uprighting springs and removable appliances. The teeth were easily extracted, and then successfully transplanted. The authors concluded that the pre-application of orthodontic force reduces the risks of PDL damage, and, therefore, lessens the risk of ankylosis. Choi et al,[10] in a retrospective study, observed the effects of intentional PDL stimulation through the application of orthodontic extrusive forces applied to the donor teeth before autotransplantation. A higher success rate was observed in the teeth with preoperative orthodontic extrusion than in the teeth without orthodontic extrusion. Collectively, these studies support the use of orthodontic force application before transplantation; such force application contributes significantly to successful TAT. However, direct assessment of enhanced PDL on the root surfaces and evaluation of PDL amounts at the tension and compression sites have not yet been performed.

Although mandibular third molars have been reported to be the most frequently-used donor teeth for TAT,[3,11,12] they are often present as impacted teeth, especially at the mesio-angulated position, thus making them unsuitable candidates for TAT. In this study, the orthodontic extraction approach for atraumatic extraction of mesio-angulated third molars (iM8s) was used to evaluate the effects of controlled orthodontic preloading force on human PDL. It was hypothesized that use of springs to upright iM8s, providing controlled orthodontic preloading forces, would make possible the clinical application of iM8s as suitable donor teeth for TAT. Therefore, the purposes of this study were 1) to determine the amounts of PDL on the root surfaces of extracted third molars after an application of uprighting force, and 2) to examine the amounts of PDL at the tension and the compression sites after tooth displacement.

Materials and Methods

Participants

In this prospective cohort study, thirty patients, at the Graduate Clinic, Department of Orthodontics, Faculty of Dentistry, ███████ University, consisting of 22 females and 8 males, who were referred for the removal of their mandibular third molars as part of their orthodontic treatment plan, were recruited from January to September, 2018, during the period of orthodontic treatment plan. The 30 patients were categorized into two groups; the experimental group including 15 patients (11 females and 4 males; age 20-36 years) who had at least one mesio-angulated mandibular third molar in their mouth, and the control group consisting of 15 patients (11 females and 4 males; age 20-34 years) who had at least one non-opposing and fully-erupted mandibular third molar. The sample size calculation (n≥10 for each group) was determined by G*Power software (Franz Faul, University of Kiel, Kiel, Schleswig-Holstein, Germany) version 3.1.9.2 with the effect size (Glass's Δ) = 1.8 derived from the preliminary data, α = 0.05 and 1-β = 0.95. The inclusion criteria were: 1) patients with good general health; 2) no radiographic sign of periodontal bone loss as shown by full-mouth periapical radiographs; 3) non-carious mandibular third molars with complete root formation; 4) partial eruption of mesio-angulated third molars with depth A or B according to the Pell & Gregory classification[13] and the Winter classification,[14] respectively, for the experimental group; 5) similar root form and shape between the experimental and the control groups, as evidenced by the full-mouth periapical radiographs; and 6) all 30 selected roots were free from dilacerations or other malformations that might have hindered the extraction. Exclusion criteria were: 1) patients with systemic diseases; 2) patients requiring any medications; 3) patients with a smoking habit; 4) presence of periodontal disease or periapical lesions; 5) teeth with extensive caries or restorations; 6) teeth with incomplete root formation; 7) teeth with abnormal root form and shape. Approval for the use of dental tissues for research activities was received from the human ethics committee of the ███████ University (approval number: ████). Written informed consent was obtained from all patients before initiation of the study.

Orthodontic loading condition and tooth extraction

Smart Spring

Two hundred grams of force was applied to 15 mandibular third molars in the experimental group that met the inclusion criteria, using a custom-made uprighting device so-called Smart Spring that was developed by E.Y.S. and was adjusted for each individual patient (Fig. 1). The Smart Spring contained a closed stainless-steel (SS) coil spring (an asterisk in Fig. 1A; Dynaflex®, St. Ann, MO, USA) and 150 gram-open nickel-titanium (NiTi)

coil spring (an arrowhead in Fig. 1A; Sentalloy®, Tomy Orthodontics; Tokyo, Japan), wrapping around a 0.017 x 0.025-inch SS rectangular wire (an arrow in Fig. 1A; Highland Metals Inc., Franklin, IN, USA), which was bended to form a hook and a helical loop at the mesial and the distal ends, respectively. The wire connected to a single 1.6 x 8.0 mm miniscrew anchorage (Jeil Medical®, Seoul, Korea) using an elastomeric ligature to prevent the wire from being rotated around the buccal miniscrew. The purposes of the hook at the mesial end of the Smart Spring were 1) to allow the application of additional force, if necessary, using an elastomeric chain or ligature tie connecting the hook to the head of miniscrew; 2) to limit the maximal amount of distal movement for the iM8s in order to prevent their excessive distal movement as a "fail-safe" mechanism, albeit the relatively heavy distalizing force (150g) used in this study; 3) to protect soft tissues in the oral cavity from being injured in order to maximize comfort for each patient; and 4) to hold the spring. In addition to the adjustable hook, the Smart Spring could be bended and contoured to adapt to the intraoral anatomy of each patient. On the distal end of the wire, the helical loop provided increased flexibility and served as a stopper of the main wire. The helical loop was adjusted to deliver controlled tip back force (50 gram-force; gf) to upright the iM8s. The distal portion of the Smart Spring was inserted into a 0.022-inch Roth prescription buccal tube (Tomy Orthodontics; Fig. 1A) that was bonded at the buccal surface of each iM8 with Super-Bond C&B cement (Sun Medical, Shiga, Japan). When the Smart Spring is inserted into the buccal tube, a stable connection is obtained, thus avoiding any undesirable rotation of the wire. The orthodontic miniscrew was precisely placed inter-radicularly in the premolar area (Fig. 1A), using a 3-D surgical guide, following Suzuki's protocol[15] for safe placement. The changes in position and angulation (light grey in Fig. 1B versus dark grey in Fig. 1C) of the iM8s were assessed using pre- and post-operative panoramic radiographs (Fig. 1D-F). Careful positioning of the patients was verified to reduce positioning errors in panoramic radiography, as previously described.[16] Loading duration was recorded from the beginning of orthodontic force application until each tooth was uprighted to an angulation, at which the iM8s could be removed by simple and atraumatic exodontia, based on clinical judgement of an experienced oral surgeon. Smart springs were re-activated monthly by adjusting the closed coil spring (an asterisk in Fig. 1A) to ensure adequate tooth movement. Passive and activated stages of the Smart Spring device are illustrated in Figure 2.

Tooth extraction

The control 15 mandibular third molars received no force application. Prior to tooth extraction, a total of 1.7 ml for inferior alveolar nerve, lingual nerve, and long buccal nerve blocks using 4% articaine with epinephrine 1:100,000 (Septanest SP®, Septodont, Co., Paris, France) was administered by S.L. using a conventional aspirated dental syringe and a disposable 27-gauge and 30-mm-long needle (Terumo®, Terumo, Co., Tokyo, Japan). Both

experimental and control teeth were removed by gentle separation of gingiva using a straight elevator no. EL3S (Hu-Friedy Mfg. Co., LLC, Chicago, IL, USA), followed by the tooth forceps no. 151 (Hu-Friedy Presidential®, Hu-Friedy Mfg. Co., LLC) to avoid injury to the PDL tissue. After that, the extracted teeth were first checked for the complete integrity of their root without any root tip fracture before being immersed in normal saline to remove blood, fixed and assessed for remaining PDL. After extraction of third molars in both loaded and unloaded groups, all 30 patients showed up for a 1-week follow-up to check their extraction wounds.

Assessment of remaining PDL on the roots of extracted third molars

The extracted molars, consisting of 15 loaded and 15 unloaded teeth, were used for assessment of remaining PDL on the root surfaces, following the protocol of Nakdilok et al.[17] Briefly, the extracted molars were soaked in 10% neutral buffered formalin solution for 24 hours to fix periodontal tissue. Then, the teeth were rinsed gently with phosphate buffered saline (PBS; pH 7.2) for 30 seconds to remove residual formalin solution. The remaining PDL on the root surfaces of the extracted teeth was stained using 0.04% (w/v) toluidine blue (Sigma-Aldrich, St. Louis, MO, USA), freshly prepared for each tooth, for 10 minutes. Then, the teeth were de-stained in 20 ml of PBS (pH 7.2) with daily replacement of PBS for 14 days. The buccal, lingual, mesial, and distal radicular surfaces were observed by an Olympus SZX7 stereomicroscope (Olympus America Inc., Center Valley, PA, USA), with each surface digitally photographed perpendicular to the tooth axis. The stained PDL area against the total area of each radicular surface on each root surface was analyzed using ImageJ2 software[18] (National Institute of Mental Health, Bethesda, MD, USA) with fixed values of hue, saturation, and brightness for every digitized image. The percentage of stained PDL area in each tooth was derived from an average of the percentage of stained PDL area from the four radicular surfaces. For further image analysis of the radicular portion, the roots were divided equally, according to its length, into three portions, including apical third, middle third and cervical third (Fig. 3). The percentage of stained PDL area in each portion of the root was calculated from an average of the percentage of stained PDL area from the four radicular surfaces. The intra-examiner reliability of the measurements was 0.968 as determined by the intraclass correlation coefficient.

Statistical analysis

Comparisons of mean age and the proportion of gender between the experimental and control groups were analyzed using the Independent *t*-test and the Chi-square test, respectively. The data of all variables studied, including loading condition, different tooth surfaces, and different tooth portions, were first tested for normality

by the Shapiro-Wilk test and their distributions were found to be normal. The percentages of overall stained PDL tissue in each tooth, of stained PDL tissue on each surface, and of stained PDL tissue on each portion of the root between the experimental and control teeth were analyzed and compared using the Independent t-test. The percentages of stained PDL tissue on the four surfaces, on the three portions, and on the four surfaces and the three portions were compared using one-way ANOVA followed by multiple comparisons using the Dunnett T3 test due to unequal variances of all tested groups. The Pearson method was used for analyzing a correlation between reduced angulation and increased loading duration. Data were analyzed using SPSS 19.0 software (SPSS Inc., Chicago, IL, USA). The results were considered statistically significant if p-values were less than 0.05.

Results

The mean age in the experimental loaded group (23.6 ± 1.1 years; 95% confidence interval=21.33-25.87; Table 1) was not different from that in the control unloaded group (24.5 ± 1.0 years; 95% confidence interval=22.41-26.66; *p*=0.525). The proportion of gender in both groups was also not different (11 females versus 4 males; *p*=1.0).

Decrease in the angulation of mesio-angulated mandibular third molars upon orthodontic loading

Demographic data, angulations of the iM8s before and after orthodontic preloading, differences in the degrees and percentages of angulation changes, loading durations, and rates of tooth movement are shown in Table 1. The mean percentage of uprighted angulation was reduced to approximately half of the initial angulation (54.0 ± 4.3). The mean duration of tooth movement was 3.4 ± 0.5 months and the mean rate of tooth movement was 8.3 ± 1.2 degrees per month. Using the Pearson correlation, the reduction of angulation was significantly and strongly correlated with an increase in the duration of orthodontic loading (r=0.63; *p*=0.011).

Significant enhancement of PDL tissue at the tension sites following orthodontic loading

Successfully uprighted iM8s were removed by simple extraction without flap opening. After being stained with toluidine blue, the stained PDL area on the loaded teeth was generally large than that on the unloaded teeth in all four surfaces (Fig. 4). Following the analysis of the stained radicular area, the mean percentage of stained PDL tissue on the loaded teeth (62.4 ± 4.4) was significantly greater than that on the unloaded teeth (42.7 ± 5.7; *p*<0.05; Fig. 5A). Regarding each radicular surface, the mean percentages of stained PDL area were significantly increased on the buccal, mesial and distal surfaces of loaded teeth compared to those of unloaded teeth (*p*<0.05; Fig. 5B). Although the mean percentage of stained PDL on the lingual surface was higher in loaded teeth than in unloaded teeth, the difference was not significant (Fig. 5B). Using ANOVA, there was no difference among the four surfaces in either the loaded or the unloaded group (Fig. 5B). When considering each portion of the root (Fig. 5C), the mean percentages of stained PDL at the cervical third and the middle third of all four surfaces of loaded teeth were significantly greater than those of unloaded teeth (*p*<0.05; Fig. 5C), but there was no difference in the apical third. The most profound difference in the mean percentage between the loaded and the unloaded teeth was observed in the middle third of the root (20.6), followed by the cervical third (20.4) and the apical third (18.6), respectively. Using ANOVA, there was no difference among the three portions of the root in either the loaded or the unloaded group (Fig. 5C). Although the results in Fig. 5D showed that the mean

percentages of stained PDL on the loaded teeth were generally greater than those on the unloaded teeth on all surfaces, the significant differences ($p<0.05$) between the loaded and the unloaded teeth were observed only at the buccal surface of the middle third, proposed to be the tension site of tooth movement as shown in Fig. 6B, and the distal surface of the cervical third, consistent with a previous finding from the finite element analysis that showed the tensile stress at the lower area of the distal surface of uprighted lower second molars.[19] Note that the mean percentage of stained PDL area on the loaded teeth was two times more than that on the unloaded teeth at the buccal surface of the middle third (Fig. 5D).

Discussion

This study assessed the amounts of remaining PDL tissue on the root surfaces of iM8s after orthodontic loading. The amounts of PDL tissue on the loaded iM8s were generally greater than those on the unloaded control third molars on all radicular surfaces and portions with the significant increases in the amounts of PDL tissue observed at the tension sites of tooth displacement. Toluidine blue staining is a method for identification of proliferative cells.[20] Therefore, it was used to detect proliferative PDL cells in this study. The stained area on the root surface refers to remaining proliferative PDL cells after the extraction. The results demonstrated that there was greater proliferative PDL cells on the root surfaces of the loaded teeth than on those of the unloaded teeth. This is consistent with the finding of Suzaki et al,[8] in which rich attached PDL on the root surfaces of the extracted rat teeth upon loading was reported. Also, the effect of orthodontic force on PDL tissue enhancement in humans has previously been described.[2,9,10,17] The direct assessment of the remaining PDL in this study allowed the precise description of the sites of proliferative PDL. Our results showed that the significantly increased proliferative PDL tissue was related to the application of orthodontic loading from the uprighting spring at the proposed tension sites, including the lower area of the distal surface and the buccal surface (lined areas in Fig. 6). When the uprighting spring was activated, tensile (lined areas) and compressive (dark grey areas) stress were consecutively produced on different surfaces of the iM8s as illustrated in Fig. 6 before the teeth were finally uprighted.

A mechanical analysis of simulated tooth movement in molar uprighting was investigated in the finite element study performed by Kojima et al.[19] In their study, compressive stress was produced in the upper area of the distal surface, while tensile stress was produced in the lower area. The patterns of the stress on the mesial surface were opposite to those on the distal surface. The alteration of blood flow in the PDL in accordance with the pressure-tension theory of tooth movement has been previously investigated.[21] Such an alteration results in decreased oxygen levels on the pressure side due to compression of the PDL, whereas increased oxygen levels are observed on the tension side. Low oxygen levels lead to reduced adenosine triphosphate (ATP) activity, which finally results in decreased cell replication and fiber production.[22] Nevertheless, in this study, increased proliferative PDL, but not significantly, was instead observed on the compression sites of the root. This discrepancy may be due to the late stage of tooth movement in this study compared to the early stage in those studies.[21,22] In the initial stage after orthodontic force application, the aforementioned cell replication and proliferative activities are reduced on the pressure or compression side. However, in the late stage, extracellular matrix fiber production is upregulated by proliferating and active fibroblasts at the compression site.[23-25] The compressed PDL is finally disassembled and restored in the late stage of tooth movement that might explain

enhancement, but did not reach the significance level, of PDL tissue observed at the compression sites, including the whole lingual surface and the apical third (Fig. 5B and C, respectively). On the contrary, increased oxygen levels on the tension side, leading to increased cellular activities and PDL fiber production, would result in enhancement of the remodeling process of PDL,[26] which corresponds to the significant enhancement of stained PDL area observed at the tension sites. The type of tooth movement performed in this study was basically tipping, not bodily, movement in order to upright the iM8s. This tipping movement may generate particular sites of compression and tension (Fig. 6), reflecting a non-uniform pattern of proliferative PDL on the radicular surfaces found in this study. The classical zones of compression and tension sites in tipping movement are, therefore, not the same as those in bodily movement, in which uniform tension and compression sites on each radicular surface are observed.[27]

In this study, the percentage of angulation changes and the rate of tooth movement (degrees per month) indicate that there was tooth displacement in an upright direction using the aforementioned Smart Spring device. The orthodontic force was applied to iM8s until the iM8s could be removed by simple and atraumatic extraction with the mean duration of orthodontic loading for approximately three months and the mean reduction of angulation more than 50 percent. However, the duration required to upright the iM8s varied between patients, regardless of differences in the initial angulations of the iM8s, gender or age (Table 1). This may imply that variable periods of time required for third molar uprighting are dependent on distinct bone remodeling and turnover rate between different individuals. Nevertheless, the duration still tended to be proportional to the amount of correction required, as shown by a strong correlation between a decrease in the angulation of mesio-angulated mandibular third molars and increase in the duration of orthodontic loading. The loading duration for several months, which plays an important role in PDL remodeling, allowed complete regeneration of the PDL on all surfaces, both compression and tension sites. The regeneration of new tissue begins as soon as the adjacent bone and degenerated membranous PDL tissue have been removed. The periodontal ligament space is wider than that before the force application, reflecting that more PDL tissue under repair is rich in cells.[28]

TAT is a viable treatment option for replacing missing teeth because of a considerable number of advantages.[12] The alveolar bone of a transplanted tooth can be maintained due to physiological stimulation of the PDL.[29] In addition, successful TAT enhances esthetics, arch form and integrity, dentofacial development, mastication, and speech.[30] Mandibular third molars are important donor teeth for TAT.[3,11,12] However, the mandibular third molar is the most frequently impacted tooth, with an incidence of 18-32%.[31] Thus, uprighting iM8s is an approach which raises the possibility of using any iM8 for autotransplantation. Furthermore, the quality

and quantity of proliferative PDL ensure safe recovery of PDL healing after autotransplantation and, consequently, reduce risks of failure, such as ankylosis and root resorption. Remaining PDL attached to the extracted tooth is a key factor for periodontal healing after replantation or transplantation. The extent of root resorption coincides with the disruption of the PDL attached to the root after extraction.[8] The larger the exposed root surface, the more extensive the root resorption that might occur. Several studies have reported that loss of the PDL from the root surface causes root resorption or dentoalveolar ankylosis.[32-35] In the present study, several sites of poor PDL attachment were clearly observed in the control teeth. Such sites potentially contribute to ankylosis and external root resorption. Following the application of orthodontic force, these sites were covered by a rich layer of PDL on almost all radicular surfaces, possibly providing protection against ankylosis and external root resorption. The effects of pre-application of orthodontic force before extraction on PDL have been investigated in animal and clinical studies.[8-10] However, to the best of our knowledge, this is the first study that demonstrates quantitatively the effects of pre-application of orthodontic force on human PDL tissue of the iM8s.

In this study, orthodontic tooth movement results in the PDL enhancement on all radicular surfaces, while there was no difference in terms of the percentage of stained PDL found for the four tooth surfaces or the three tooth portions in the loaded or the unloaded group. Moreover, application of orthodontic force also enlarges PDL space and increases the width of alveolar sockets. These facilitate tooth extraction and then prevent destruction of PDL during extraction that, consequently, leads to greater area of PDL on the loaded teeth.[8] Therefore, the results of this study highlight the effect of orthodontic tooth movement on PDL enhancement. However, due to various durations for the device activation to upright the iM8s among different subjects, which were based on clinical judgement for simple exodontia by the oral surgeon, an optimal period of proliferative PDL tissue that can be applicable for TAT is not investigated in this study. The application of orthodontic tooth movement for PDL enhancement before TAT still requires further clinical investigations.

Conclusions

The application of orthodontic force leads to tooth movement, which, consequently, increases the amounts of PDL tissue on impacted third molars. This application of orthodontic force before tooth extraction may be beneficial for facilitating removal of impacted third molar in order to reduce a risk of surgical complications and increasing the success rates of tooth autotransplantation, while reducing the risk of ankylosis. Further clinical studies are necessary to evaluate the effects of orthodontic loading on the success rate of tooth autotransplantation. Moreover, the application of orthodontic loading in this study may be used to upright tilted molars and protract them to close an edentulous space.

References

1. Andreasen JO. Interrelation between alveolar bone and periodontal ligament repair after replantation of mature permanent incisors in monkeys. J Periodontal Res. 1981;16:228-235.

2. Iwata T, Mino C, Kawata T. In vitro proliferation of periodontal ligament-like tissue on extracted teeth. Arch Oral Biol. 2017;75:31-36.

3. Tsukiboshi M. Autotransplantation of teeth: requirements for predictable success. Dent Traumatol. 2002;18:157-180.

4. Andreasen JO, Paulsen HU, Yu Z, et al. A long-term study of 370 autotransplanted premolars. Part II. Tooth survival and pulp healing subsequent to transplantation. Eur J Orthod. 1990;12:14-24.

5. Beertsen W, McCulloch CA, Sodek J. The periodontal ligament: a unique, multifunctional connective tissue. Periodontol 2000. 1997;13:20-40.

6. Ivanovski S, Gronthos S, Shi S, Bartold PM. Stem cells in the periodontal ligament. Oral Dis. 2006;12:358-363.

7. McCulloch CA, Lekic P, McKee MD. Role of physical forces in regulating the form and function of the periodontal ligament. Periodontol 2000. 2000;24:56-72.

8. Suzaki Y, Matsumoto Y, Kanno Z, Soma K. Preapplication of orthodontic forces to the donor teeth affects periodontal healing of transplanted teeth. Angle Orthod. 2008;78:495-501.

9. Cho JH, Hwang HS, Chang HS, Hwang YC. Application of orthodontic forces prior to autotransplantation - case reports. Int Endod J. 2013;46:187-194.

10. Choi YH, Bae JH, Kim YK, et al. Clinical outcome of intentional replantation with preoperative orthodontic extrusion: a retrospective study. Int Endod J. 2014;47:1168-1176.

11. Aoyama S, Yoshizawa M, Niimi K, et al. Prognostic factors for autotransplantation of teeth with complete root formation. Oral Surg Oral Med Oral Pathol Oral Radiol. 2012;114(5 Suppl):S216-228.

12. Kokai S, Kanno Z, Koike S, et al. Retrospective study of 100 autotransplanted teeth with complete root formation and subsequent orthodontic treatment. Am J Orthod Dentofacial Orthop. 2015;148:982-989.

13. Pell GJ GB. Impacted mandibular third molars: classification and modified techniques for removal. Dent Dig. 1933;39:330–338.

14. GB W. Impacted mandibular third molars. St Louis, MO: American Medical Book Co.; 1926.

15. Suzuki EY, Suzuki B. Accuracy of miniscrew implant placement with a 3-dimensional surgical guide. J Oral Maxillofac Surg. 2008;66:1245-1252.

16. Kaviani F, Johari M, Esmaeili F. Evaluation of common errors of panoramic radiographs in tabriz faculty of dentistry. J Dent Res Dent Clin Dent Prospects. 2008;2:99-101.

17. Nakdilok K, Langsa-ard S, Krisanaprakornkit S, Suzuki EY, Suzuki B. Enhancement of human periodontal ligament by pre-application of orthodontic loading. Am J Orthod Dentofacial Orthop. In press.

18. Rueden CT, Schindelin J, Hiner MC, et al. ImageJ2: ImageJ for the next generation of scientific image data. BMC Bioinformatics. 2017;18:529.

19. Kojima Y, Mizuno T, Fukui H. A numerical simulation of tooth movement produced by molar uprighting spring. Am J Orthod Dentofacial Orthop. 2007;132:630-638.

20. Chieco P, Pagnoni M, Romagnoli E, Melchiorri C. A rapid and simple staining method, using toluidine blue, for analysing mitotic figures in tissue sections. Histochem J. 1993;25:569-577.

21. Schwarz AM. Tissue changes incidental to orthodontic tooth movement. Int J Orthod. 1932;18:331-352.

22. Tuncay OC, ed. The invisalign system. London, UK: Quintessence Publishing Company, Ltd.; 2006.

23. Wise GE, King GJ. Mechanisms of Tooth Eruption and Orthodontic Tooth Movement. J Dent Res. 2008;87:414-434.

24. Huang H, Williams RC, Kyrkanides S. Accelerated orthodontic tooth movement: Molecular mechanisms. Am J Orthod Dentofacial Orthop. 2014;146:620-632.

25. Howard PS, Kucich U, Taliwal R, Korostoff JM. Mechanical forces alter extracellular matrix synthesis by human periodontal ligament fibroblasts. J Periodontal Res. 1998;33:500-508.

26. Li Y, Jacox LA, Little SH, Ko CC. Orthodontic tooth movement: The biology and clinical implications. Kaohsiung J Med Sci. 2018;34:207-214.

27. Gomez JP, Pena FM, Martinez V, et al. Initial force systems during bodily tooth movement with plastic aligners and composite attachments: A three-dimensional finite element analysis. Angle Orthod. 2015;85:454-460.

28. Reitan K. Tissue behavior during orthodontic tooth movement. Am J Orthod. 1960;46:881-900.

29. Marques-Ferreira M, Rabaca-Botelho MF, Carvalho L, et al. Autogenous tooth transplantation: evaluation of pulp tissue regeneration. Med Oral Patol Oral Cir Bucal. 2011;16:e984-989.

30. Mendes RA, Rocha G. Mandibular third molar autotransplantation--literature review with clinical cases. J Can Dent Assoc. 2004;70:761-766.

31. Svendsen H MJ. Etiology of third molar impaction. In: Andreasen JO PJ, Laskin DM, eds, ed. Textbook and Color Atlas of Tooth Impactions. Copenhagen: Munskgaard; 1997.

32. Andreasen JO, Kristerson L. The effect of limited drying or removal of the periodontal ligament. Periodontal healing after replantation of mature permanent incisors in monkeys. Acta Odontol Scand. 1981;39:1-13.

33. Cvek M, Hollender L, Nord CE. Treatment of non-vital permanent incisors with calcium hydroxide. VI. A clinical, microbiological and radiological evaluation of treatment in one sitting of teeth with mature or immature root. Odontol Revy. 1976;27:93-108.

34. Lindskog S, Blomlof L, Hammarstrom L. Repair of periodontal tissues in vivo and in vitro. J Clin Periodontol. 1983;10:188-205.

35. Andreasen JO. A time-related study of periodontal healing and root resorption activity after replantation of mature permanent incisors in monkeys. Swed Dent J. 1980;4:101-110.

Figure legends

Fig. 1 (A) Components of the Smart Spring device applied to the experimental tooth, comprising a closed coil spring (asterisk), an open coil spring (arrowhead) and a stainless-steel wire (arrow). (B and C) Diagrams of tooth displacement: the measurement of angulation (degrees) between the second molar (M7) and the mesio-angular impacted third molar (iM8) before and after activation, respectively. Note the angulation was reduced from light grey to dark grey. Panoramic radiographs for initial (D), one month after activation (E), and after complete activation for the uprighted tooth (F).

Fig. 2 A diagram for the passive and activated stages of the Smart Spring device. During the activation, the open NiTi coil spring delivered 150 gram-force (gf) and the helical loop delivered controlled tip back force at 50 gf. MI = miniscrew, SS = stainless-steel rectangular wire.

Fig. 3 The radicular portion was divided equally according to its length into three parts: apical third (1/3), middle third and cervical third.

Fig. 4 Representative images demonstrating all four surfaces, including buccal, lingual, mesial and distal, of unloaded (upper row) and loaded (lower row) teeth.

Fig. 5 Enhancement of stained PDL area on the radicular surfaces of loaded teeth. (A) Percentage of stained PDL comparing between unloaded (N=15) and loaded teeth (N=15). (B) Percentage of stained PDL on each surface of the root comparing between unloaded and loaded teeth. (C) Percentage of stained PDL on each portion of the root comparing between unloaded and loaded teeth. (D) Percentage of stained PDL on each portion of the root, which is further divided into each of the four surfaces, comparing between unloaded and loaded teeth. Error bars represent standard errors of the means. * $p<0.05$.

Fig. 6 Diagrams of compression and tension sites during activation of the device. (A) the buccal and (B) the occlusal views. Dark grey areas on the mesio-angular impacted third molar (iM8) indicate compression sites. Lined areas on the iM8 indicate tension sites. Dotted lines indicate the initial position of iM8. The straight and curved arrows indicate the directions of tooth movement. Dotted lines in the premolar region in (A) and (B) illustrate the initital position of the mesial hook from the buccal and the occlusal views, respectively.

Figure 1   Click here to access/download;Figure;FIG1.TIF ±

Figure 2

Smart Spring

Figure 3

1/3   cervical

1/3   middle

1/3   apical

Figure 4
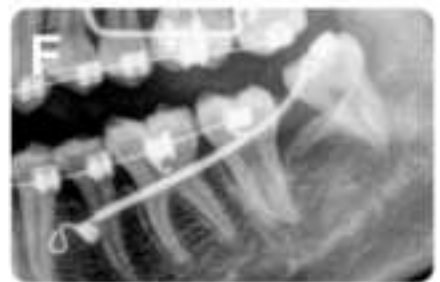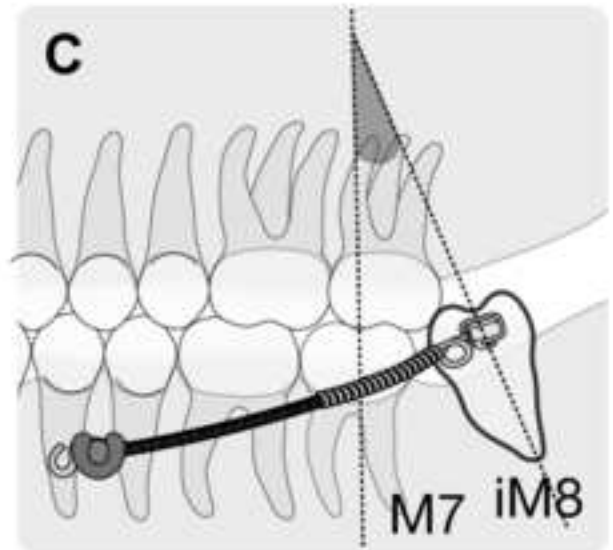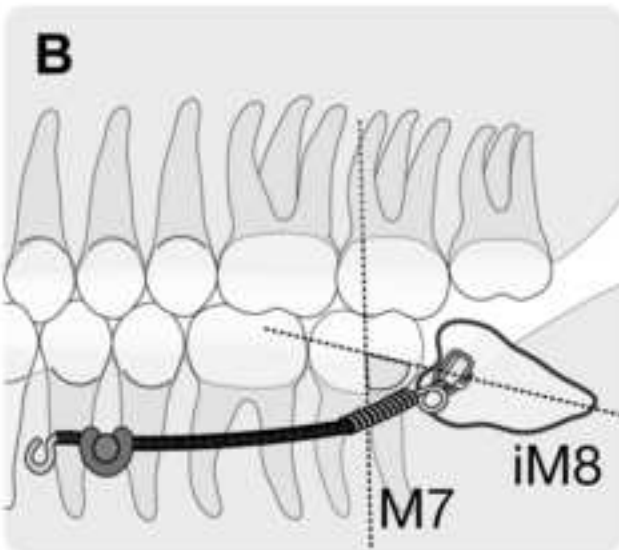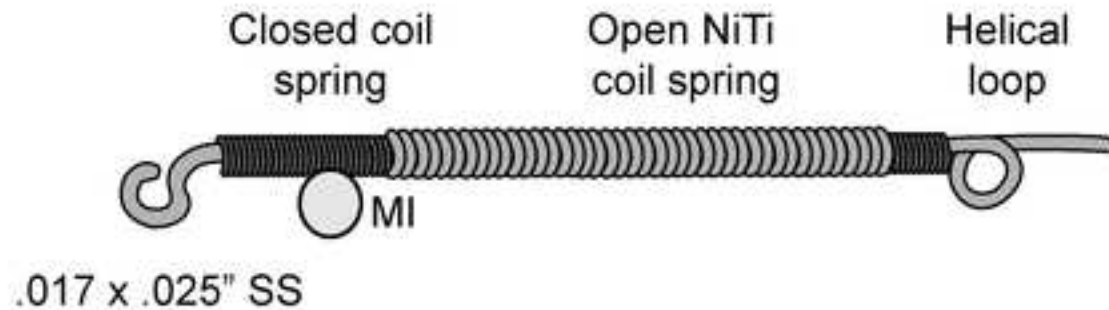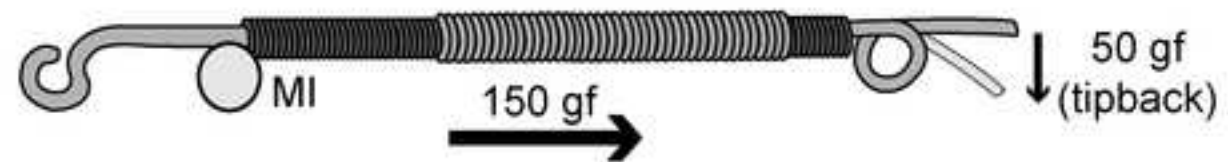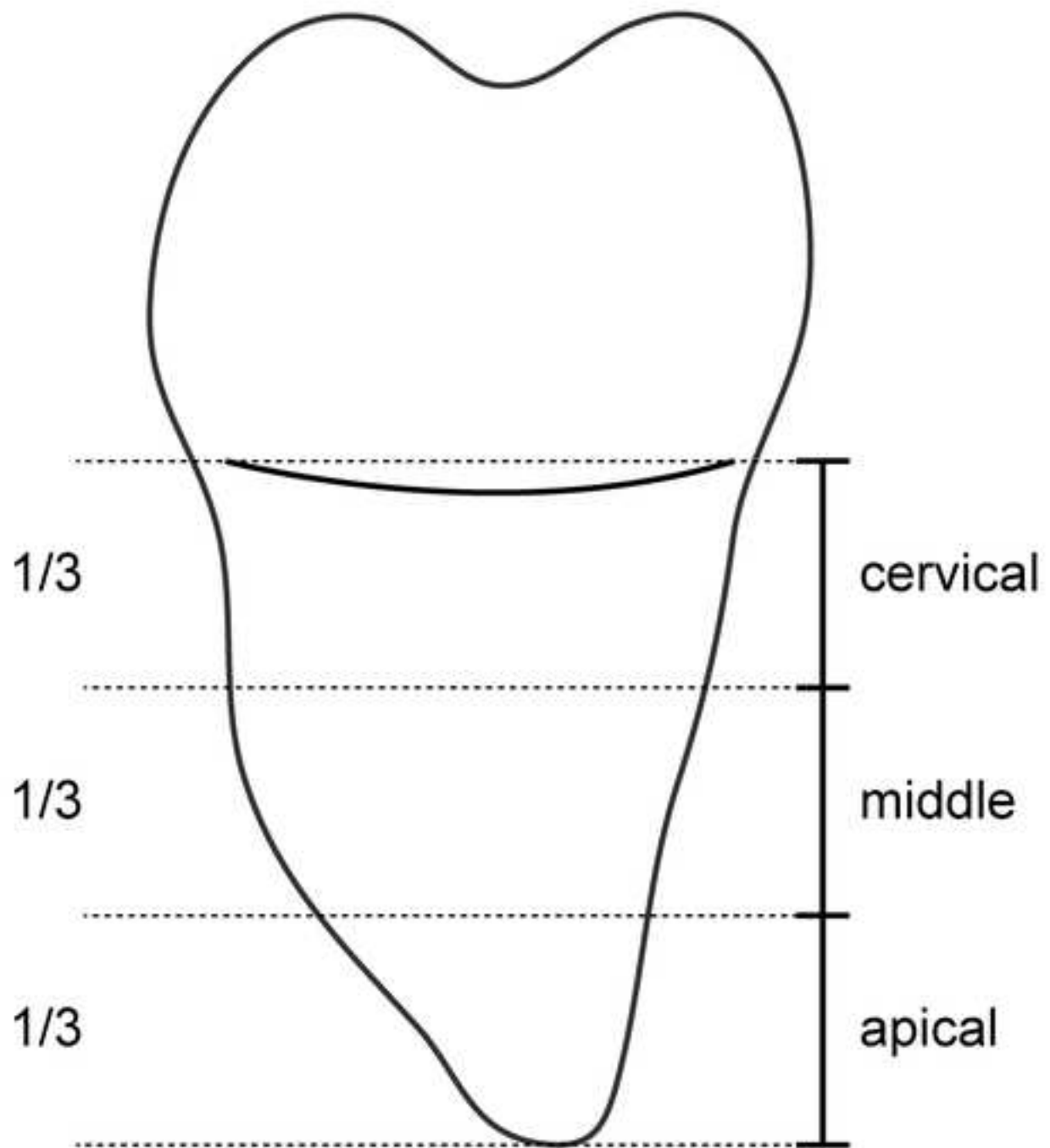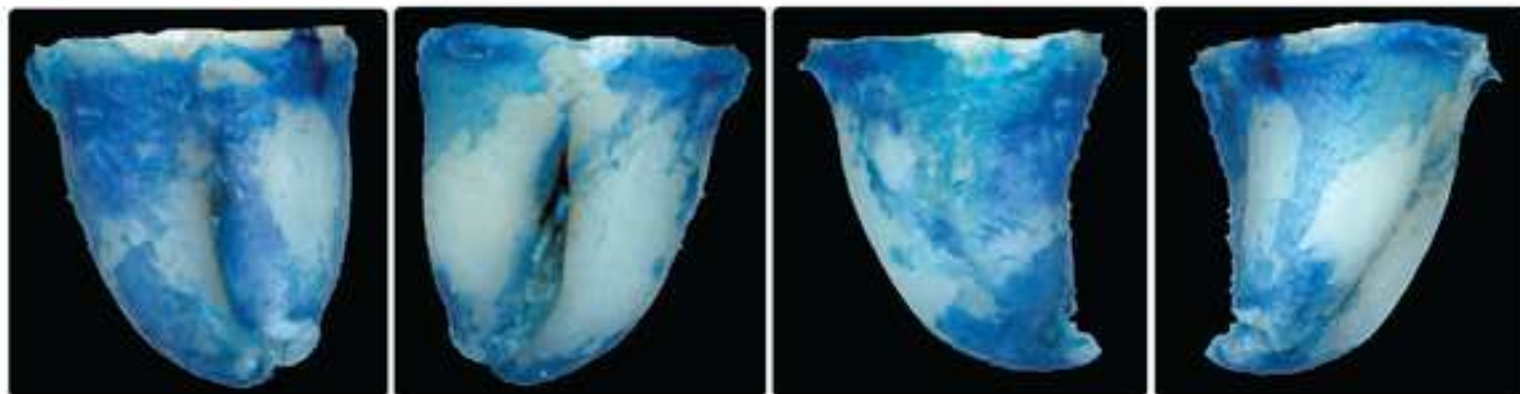
	Buccal	Lingual	Mesial	Distal
Unloaded				
Loaded				

Figure 5   Click here to access/download;Figure;FIG5.tiff

Figure 5

Figure 6
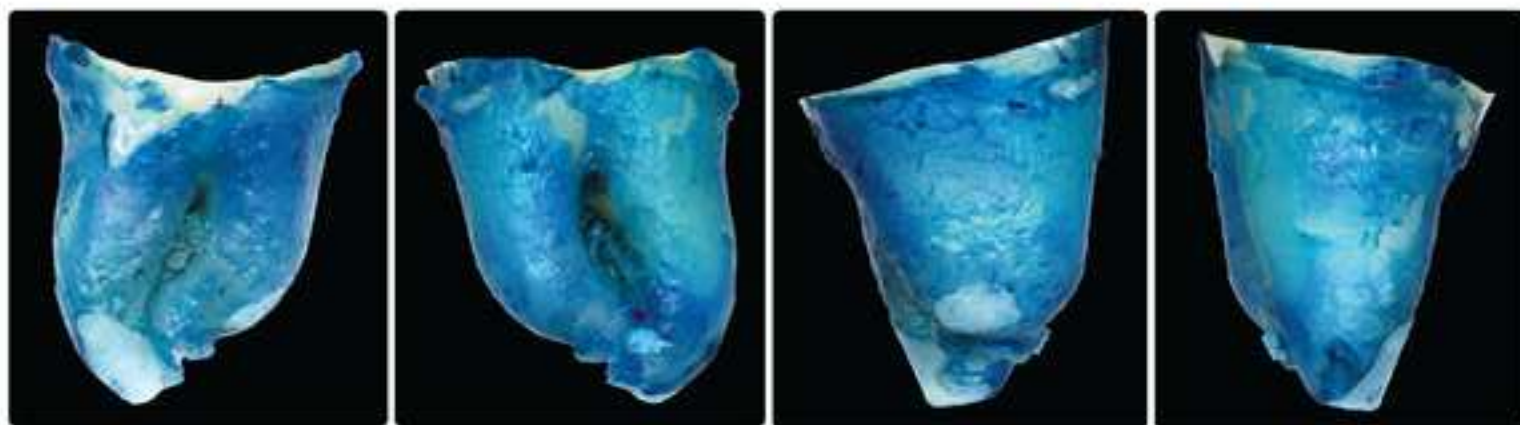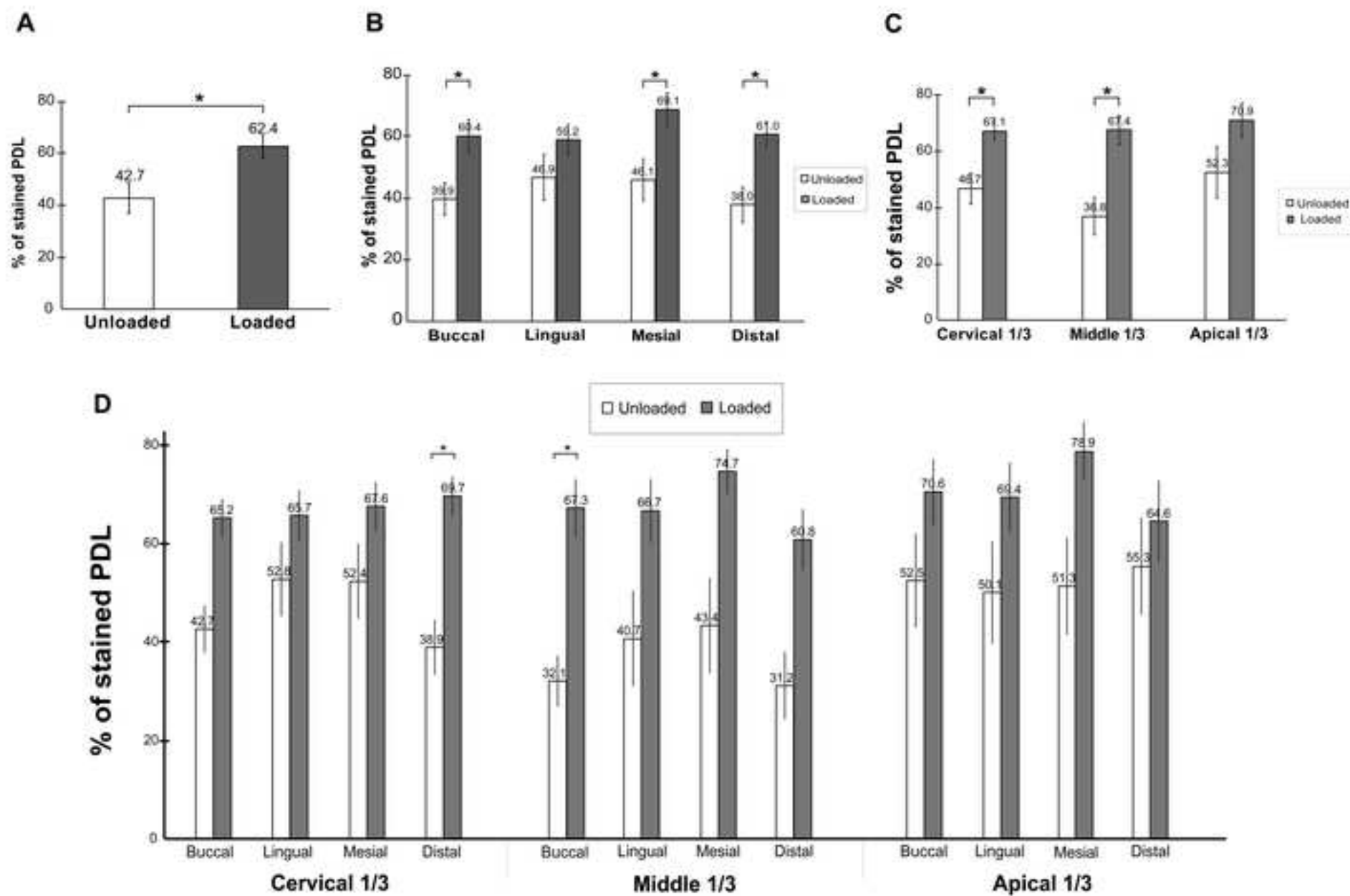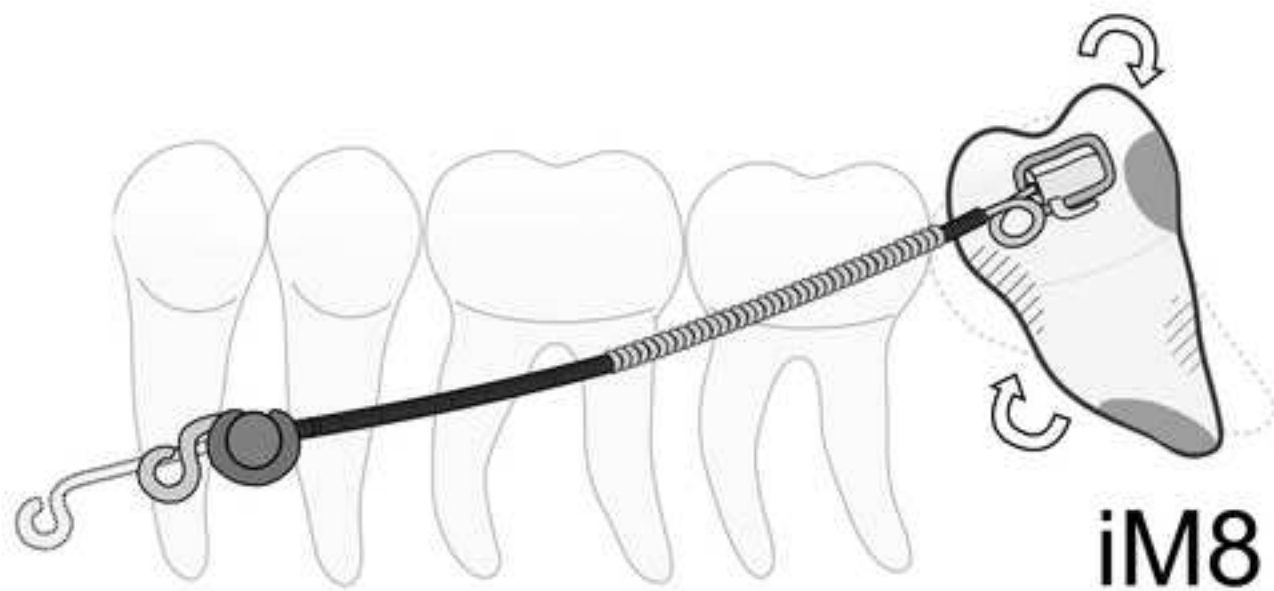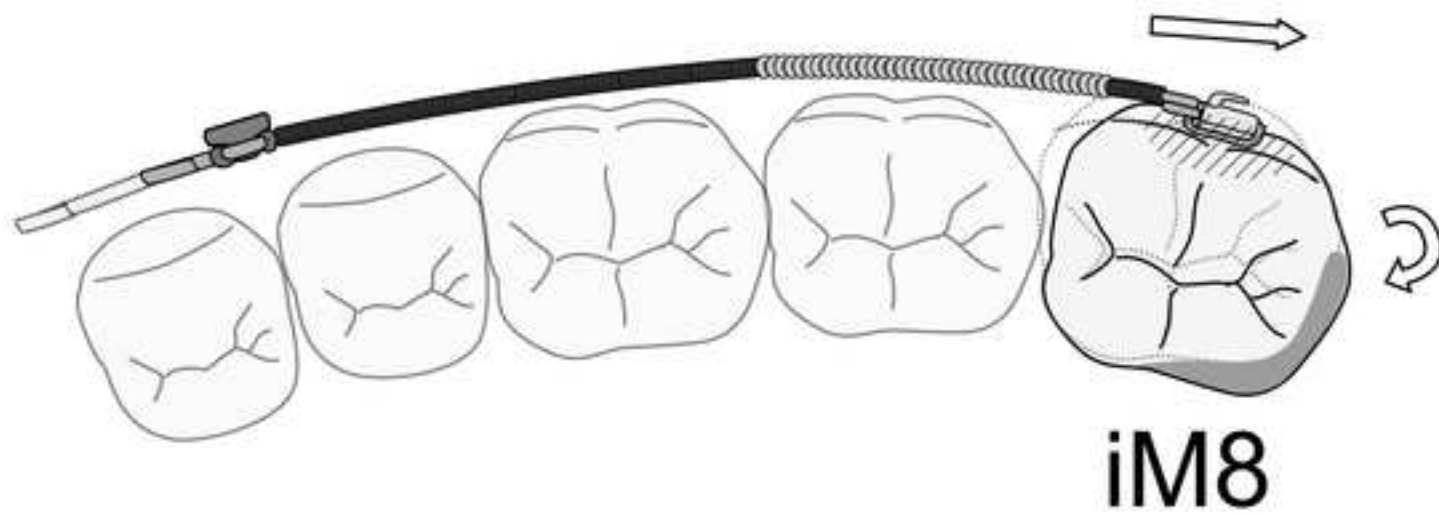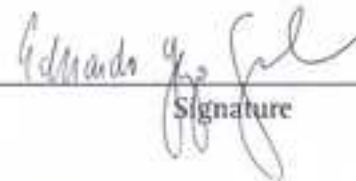
Table 1

Table 1 A summary of the degrees, durations, and rate of tooth movement for uprighting 15 mesio-angulated mandibular molars.

Case No.	Age	Sex	Mesio-angulated Third Molar		Difference (Degrees)	Difference (%)	Duration (Months)	Rate (Degrees/month)
			Before (Degrees)	After (Degrees)				
1	20	F	70.3	19.3	51.0	72.6	6.0	8.5
2	21	F	42.0	18.5	23.5	56.0	2.3	10.2
3	23	F	4.5	1.6	2.8	63.5	1.2	2.5
4	28	F	62.0	34.1	27.9	44.9	5.8	4.8
5	21	F	56.4	44.2	12.2	21.6	5.8	2.1
6	23	F	38.9	23.2	15.7	40.3	1.6	9.7
7	21	F	91.2	37.6	53.6	58.8	5.5	9.7
8	26	F	56.9	32.4	24.5	43.1	2.8	8.9
9	36	F	46.8	9.2	37.6	80.3	3.2	11.7
10	24	M	16.1	9.0	7.1	44.1	2.5	2.8
11	22	M	23.8	11.1	12.7	53.2	0.7	18.3
12	24	M	47.6	7.2	40.4	84.8	4.1	9.7
13	21	M	71.4	39.9	31.5	44.1	2.3	13.7
14	20	F	70.0	28.0	42.0	60.0	4.8	8.7
15	24	F	26.0	15.0	11.0	42.3	3.0	3.7
Mean	23.6		48.3	22.0	26.2	54.0	3.4	8.3
SE	1.1		6.1	3.5	4.2	4.3	0.5	1.2

American Journal of Orthodontics and Dentofacial Orthopedics

COPYRIGHT STATEMENT

Must be signed by ALL authors

The corresponding author must be named Eduardo Yugo Suzuki
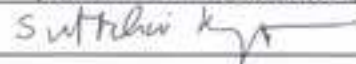
(Type name)   Signature

Each author's name must be typed underneath the signature.

(Pattarin Promchaiwattana)   (Boonsiva Suzuki)

(Suttichai Krisanaprakornkit)

Date: 29/03/2019

*ICMJE Statement on Conflict of Interest for each author

Click here to access/download
ICMJE Statement on Conflict of Interest for each author
coi_disclosure_Boonsiva Suzuki.pdf

*ICMJE Statement on Conflict of Interest for each author

Click here to access/download
ICMJE Statement on Conflict of Interest for each author
coi_disclosure_Eduardo Yugo Suzuki.pdf

*ICMJE Statement on Conflict of Interest for each author

*ICMJE Statement on Conflict of Interest for each author

Click here to access/download
ICMJE Statement on Conflict of Interest for each author
coi_disclosure_Pattarin Promchaiwattana.pdf
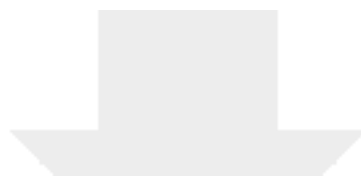
*ICMJE Statement on Conflict of Interest for each author

Click here to access/download
ICMJE Statement on Conflict of Interest for each author
coi_disclosure_Suttichai Krisanaprakornkit.pdf
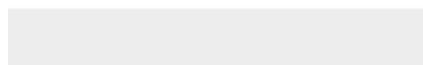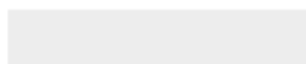
Associations between Expression Levels of O-GlcNAc Transferase (OGT) and Chemo-Response in Osteosarcoma

Rattanakuntee S, DDS[1], Chaiyawat P, PhD[2], Pruksakorn D, MD, PhD[2,3], Kritsanaprakornkit S, DDS, PhD[4,5], Makeudom A, PhD[4], Supanchart C, DDS, PhD[1]

[1] Department of Oral and Maxillofacial Surgery, Faculty of Dentistry, Chiang Mai University, Chiang Mai, Thailand

[2] Musculoskeletal Science and Translation Research Center, Faculty of Medicine, Chiangmai University, Chiang Mai, Thailand

[3] Department of Orthopedics, Faculty of Medicine, Chiangmai University, Chiang Mai, Thailand

[4] Center of Excellence in Oral and Maxillofacial Biology, Faculty of Dentistry, Chiang Mai University, Chiang Mai, Thailand

[5] Department of Oral Biology and Diagnostic Sciences, Faculty of Dentistry, Chiang Mai University, Chiang Mai, Thailand

Objective: The present study aimed to investigate global levels of O-GlcNAcylation (O-GlcNAc), expressions of O-GlcNAc transferase (OGT) and O-GlcNAcase (OGA) in osteosarcoma and to explore a prognostic marker.

Materials and Methods: The authors studied in three independent experiments. Western blot analysis was performed to detect the expressions of O-GlcNAcylated proteins, OGT, and OGA in cell lines derived from seven patients with osteosarcoma stage IIB. The band intensities were analyzed using Scion Image software. The correlations between clinicopathologic characters of osteosarcoma cases and expression levels of O-GlcNAcylated proteins, OGT, and OGA were analyzed by using Student's t-test.

Results: The results demonstrated a tendency of higher OGT expression in primary osteosarcoma cells. Furthermore, the level of OGT was elevated in patients who poorly responded to chemotherapy and had shorter survival time ($p < 0.05$). The present study revealed a promising use of OGT as a prognostic marker in osteosarcoma.

Conclusion: The present study showed significant higher levels of OGT in osteosarcoma patients who poorly responded to chemotherapy. Furthermore, levels of OGT relate to survival time of osteosarcoma. These findings suggest a role for OGT in chemo-response of osteosarcoma cells. The present study was performed in a limited number of cases, thereby the finding requires further validation in a larger cohort.

Keywords: Osteosarcoma, O-GlcNAcylation, O-GlcNAc transferase (OGT), O-GlcNAcase (OGA)

Osteosarcoma is the primary malignant bone tumor that commonly affects children, adolescents, and young adults. Osteosarcoma usually occurs in the metaphysis of long bones, and most commonly occurs in the distal femur, proximal tibia, or humerus[1]. The incidence has been reported at 1.6 to 2.8 per million of children under 15 years and are more common in male than female at a ratio of 1.6:1[2].

Due to the complexity of the genomic background and heterogeneity, the causes of osteosarcoma remain unclear. The current treatment strategy for osteosarcoma includes neoadjuvant chemotherapy, followed by surgical removal of the primary tumor along with all clinically evident metastatic disease, plus the addition of adjuvant chemotherapy.

O-GlcNAcylation (O-GlcNAc) is one of post-translation modifications (PTM) of protein. This PTM play important roles in regulating various functions of proteins through an addition of N-acetylglucosamine (GlcNAc) to hydroxyl group of serine or threonine residues of target proteins. O-GlcNAc is regulated by a pair of enzymes, O-GlcNAc transferase (OGT) and O-GlcNAcase (OGA), which add and remove a

Correspondence to:

Supanchart C.

Department of Oral and Maxillofacial Surgery, Faculty of Dentistry, Chiang Mai University, Chiang Mai 50200, Thailand.

Phone: +66-89-1916049, **Fax:** +66-53-222844

Email: supanchart_c@yahoo.com

"Preprint manuscript version"

Table 1. Clinicopathologic characteristics of osteosarcoma cases

Case	Age at diagnosis (years)	Sex	Enneking stage	Chemotherapy	Tumor necrosis (%)	Status	Metastasis (lung)
OS1	9	Female	IIb	Carbo/Doxo	90.0	Alive	No
OS2	15	Female	IIb	Adria/Cis	90.0	Alive	No
OS3	17	Female	IIb	Cis/Adria	80.0	Alive	No
OS4	14	Male	IIb	Carbo/Doxo	90.0	Alive	No
OS5	21	Male	IIb	Cis/Adria	15.0	Death	Yes
OS6	61	Female	IIb	Cis/Adria	35.5	Death	Yes
OS7	5	Female	IIb	Carbo/Adria Cis/Doxo HD-MTX	10.0	Death	Yes

OS=osteosarcoma primary cells; Carbo=carboplatin; Doxo=doxorubicin; Adria=adriamycin; Cis=cisplatin; HD-MTX=high-dose methotrexate

O-GlcNAc molecule from the proteins, respectively. Uridine diphosphate N-acetylglucosamine (UDP-GlcNAc) is a substrate of O-GlcNAc process and an end-product of hexosamine biosynthesis pathway (HBP). HBP pathway is one of the glucose metabolic pathways in which about 2% to 5% of glucose enters the HBP[3,4]. Glucose is imported into the cell via a glucose transporter, then phosphorylated by hexokinase to be glucose-6-phosphate (Glc-6-P) and then converted into fructose-6-phosphate (Fruc-6-P) by Glc-6-P isomerase. Glutamine donates the amino group to form glucosamine-6-phosphate (GlcN-6-P), using glucosamine:fructose-6-phosphate aminotransferase (GFAT). Acetyl-CoA is added to GlcN-6-P by glucosamine-6-phosphate N-acetylglucosamine transferase to generate N-acetylglucosamine-6-phosphate (GlcNAc-6-P) and converted to N-acetylglucosamine-1-phosphate (GlcNAc-1-P) by phosphoacetylglucosamine mutase. Finally, uridine-5'-triphosphate (UTP) is phosphorylased by UDP-GlcNAc pyrophosphorylyse (UAP) to create UDP-GlcNAc. The rate limiting enzyme of HBP is GFAT1. This is due to feedback inhibition by the products including both GlcN-6-P and the final product: UDP-GlcNAc[5].

O-GlcNAc governs diverse intracellular processes such as translation, transcription, cell cycle regulation, and epigenetic control of gene expression in response to nutrient and cellular stress[6,7]. Balance of the enzymes regulating O-GlcNAc is required to maintain normal cellular function. High level of O-GlcNAc has been found in many diseases such as diabetes, Alzheimer disease, and cancers.

In various types of cancers, increased level of O-GlcNAc seem to be involved with tumor invasion and distant metastasis. Several lines of research suggested that decreasing levels of O-GlcNAc by OGT inhibition or OGT knockdown could reduce migration and invasion of cancer cells in vitro and decrease distant metastasis in vivo in breast, prostate, and colorectal cancer. Champattanachai et al[8] showed an increase of OGT protein and O-GlcNAc levels relating to the histological grade of breast tumors. Furthermore, Slawson et al[9] showed an association of increased OGA activity and breast cancer tumor grade.

Until now, there is a lack of information about O-GlcNAc-modified proteins and their roles in osteosarcoma. In the present study, the authors studied the level of O-GlcNAc, expression of OGT and OGA in patient-derived osteosarcoma cells using immunoblotting analysis. The authors also explored an association of O-GlcNAc profile and its regulating enzymes with clinical outcomes of the patients.

Materials and Methods
Patients characteristics

Primary osteosarcoma cells were derived from seven selected osteosarcoma patients diagnosed as stage IIB osteosarcoma and treated at Maharaj Nakorn Chiang Mai Hospital, Thailand. Patients had been treated with a standard neoadjuvant regimen or underwent surgery at Maharaj Nakorn Chiang Mai Hospital. Exclusion criteria were patient who died from other systemic disease or accidental trauma and patient who had been diagnosed with serious systemic diseases that restricted tumor surgery.

The Research Ethics Committee of the Faculty of Medicine, Chiang Mai University, approved the present study. Clinicopathologic characteristics, including age, gender, Enneking staging, chemotherapy, percentage of tumor necrosis, and metastasis status is shown in Table 1. The response of treatment, defined by the tumor necrosis in the previous study, showed
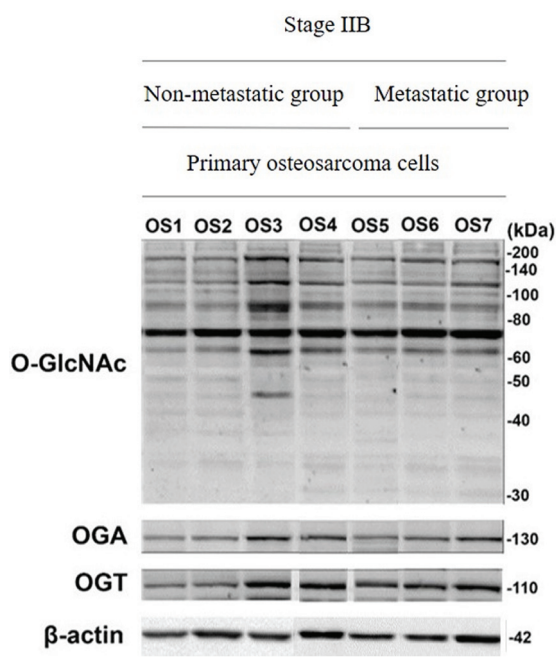
Figure 1. Immunoblots of O-GlcNAcylation, OGT, and OGA.

OS=osteosarcoma primary cells

a significant greater result of 90% tumor necrosis[10]. Metastasis is indicated if the cancer was identified in distant organ by computed tomography.

Primary cells and culture condition

All primary osteosarcoma cells were derived from musculoskeletal, sciences, and Translational Research Biobank. Primary osteosarcoma cells were isolated from chemo-naïve tissues of the seven patients[11] at Maharaj Nakorn Chiang Mai Hospital. All cells were cultured and maintained in Dulbecco's modified Eagle's medium (DMEM) supplemented with 10% fetal calf serum (Invitrogen™) and 1% penicillin and streptomycin (Invitrogen™). All primary cells were incubated at 37°C in a humidified chamber with 5% CO_2. Culture medium was refreshed every two days until 80% confluence.

Protein extraction and western blotting analysis

Whole cell lysates were extracted using radio-immunoprecipitation assay (RIPA) buffer supplemented with protease inhibitor and Thimet-G. Total protein concentration in the whole cell lysates was first determined by Bradford assay according to the manufacturer's protocol. The absorbance is then measured by using microplate reader (Sunrise™, Tecan). Each whole cell lysate sample was denatured by heating at 100°C for five minutes in a sampling buffer. Ten µg of protein of whole cell lysates reduced for titrate error were separated on sodium dodecyl sulfate polyacrylamide gels (SDS-PAGE) and transferred to polyvinylidene difluoride (PVDF) membranes. After transferring, the membranes were blocked with 1% casein in phosphate buffered saline (PBS), buffer at room temperature for one hour with gentle agitation. Then, the membranes were incubated with primary antibody against β-Actin (Santa Cruz Biotechnology, Inc.), O-GlcNAc (RL2, Santa Cruz Biotechnology, Inc.), OGT (F-12, RL2, Santa Cruz Biotechnology, Inc.) or OGA (ab124807, Abcam) at 4°C for 16 to 18 hours. The membranes were washed three times with PBS buffer for 15 minutes each time. Secondary antibodies in 1% casein PBS, including horseradish peroxidase (HRP)-conjugated antibodies against mouse immunoglobulins or rabbit immunoglobulins, where then added into the membranes at dilution 1:5,000 for one hour at room temperature. After washing with PBS buffer, reserve chemiluminescent reagent (KPL, Gaithersburg, MD, USA) was used as a substrate. The signal was later captured by a CCD camera attached to the ChemiDoc XRS gel documentation system (Bio-Rad Laboratories). This protocol was repeated three times.

Image analysis

Scion Image software was used to quantify the intensities of all O-GlcNAcylated protein, OGT, and OGA bands in the same level by using line and measured the area under the graph. Level of O-GlcNAcylated proteins, OGT, and OGA of each sample was normalized by β-Actin expression.

Statistical analysis

Statistical analysis was performed using GraphPad Prism, version 8.0.1 (GraphPad Software, Inc., San Diego, CA, USA). The different levels of O-GlcNAc, OGT, and OGA among osteosarcoma cells and association to clinicopathological characteristic of patients were tested using Student's t-test.

Results
Level of O-GlcNAc, OGT, and OGA expression levels in osteosarcoma cells

Levels of O-GlcNAc, OGT, and OGA were examined in seven cases of primary osteosarcoma cells using immunoblotting technique as shown in Figure 1. The results revealed variable levels of O-GlcNAc in the osteosarcoma cells. The results showed a tendency of higher OGT expression in the

Table 2. Level of O-GlcNAc and expression of OGT and OGA in primary osteosarcoma cells

Factor	Total patients	Expression levels; mean±SD					
		O-GlcNAcylated proteins	p-value	OGT	p-value	OGA	p-value
Distant invasion			0.20		0.17		0.52
Non-metastasis	4	5.32±1.57		0.51±0.26		0.58±0.26	
Metastasis	3	6.96±1.25		0.76±0.10		0.69±0.06	
Chemoresistance			0.06		0.02*		0.04*
Good responders (tumor necrosis ≥90%)	3	4.77±1.37		0.41±0.21		0.47±0.15	
Poor responders (tumor necrosis <90%)	4	6.97±1.25		0.77±0.08		0.75±0.13	
Status			0.20		0.17		0.52
Alive	4	5.32±1.57		0.51±0.26		0.58±0.26	
Died	3	6.96±1.25		0.76±0.10		0.69±0.06	

OGT=O-GlcNAc transferase; OGA=O-GlcNAcase

* $p<0.05$ is considered significant

metastasis primary osteosarcoma cells compared with the non-metastasis primary osteosarcoma.

Correlation of levels of O-GlcNAc, OGT, OGA, and clinicopathological factors

O-GlcNAc and OGT levels were elevated in metastasis, poor responders, and dead group (Table 2). Furthermore, the osteosarcoma patients who poorly responded to chemotherapy (tumor necrosis of less than 90%) expressed higher levels of OGT compared with the good responders (tumor necrosis of 90% or more) (p=0.04) as shown in Table 2.

Discussion

From the current knowledge, the present study is the first study that investigated levels of O-GlcNAcylated proteins, OGT, and OGA in osteosarcoma. Levels of O-GlcNAc as well as expression of OGT and OGA were observed in primary osteosarcoma cells derived from chemo-naïve tissues of osteosarcoma patients.

To minimize the inconsistence of treatment decision and clinical outcome, the study focused to observe protein expression in osteosarcoma with clinical stage IIB, which is the most commonly detected.

Accumulating evidences revealed increasing levels of O-GlcNAc and OGT in various diseases including cancers. The study of pancreatic tumors indicated higher O-GlcNAc and OGT levels, together with down-regulated expression of OGA in cancerous tissues in comparison to normal tissues[12]. Lynch et al showed that O-GlcNAc and OGT levels were higher in prostate cancer cells compared with normal

cells lines[13]. Furthermore, Itkonen et al suggested that OGT inhibitor could be used as a target therapy for prostate cancer, in that OGT was upregulated in prostate cancer and inhibition of OGT reduced c-MYC protein stability[14]. Besides from prostate cancer, it is reported that O-GlcNAc levels and an expression of OGT was upregulated in breast cancer cells[8,15]. Moreover, Gu et al also found that level of O-GlcNAc was upregulated in breast cancer tissues and metastatic lymph node[16]. Interestingly, Champattanachai et al found that upregulated OGT was related with degree of cell differentiation and OGT knockdown of breast cancer cell lines resulting in decrease colony formation, but not affecting cell viability or cell proliferation[8].

The present study revealed that OGT level was significantly associated with chemo-response in stage IIB osteosarcoma patients, in which expression of OGT was higher in patients who poorly responded to chemotherapy compared to good responders. Roles of OGT on an aggressiveness of cancers have been widely studied. Krzeslak et al measured O-GlcNAc cycling enzymes messenger RNA (mRNA) levels in 76 endometrial cancer patients using real-time reverse transcription polymerase chain reaction (RT-PCR) analysis. Both OGT and OGA mRNA expression were significantly higher in high grade tumors compared with low grade groups. They also showed an association between OGT and OGA expression and myometrial invasion[17], indicating that OGT was related to aggressiveness and prognosis of cancer cells. Furthermore, a significant decrease of in vitro cell migration and invasion upon OGT knockdown was observed in three different breast cell lines[16].

From the study of Caldwell, inhibition of OGT for treatment in MCF-10A-ErbB2 and MDA-MB-231 breast tumor cells by using Transwell assays shows a decrease of cell migration[15]. OGT knockdown in the PC3-ML prostate tumor cell line also reduced their ability to migrate compared with control cells[13]. Another study in prostate tumor cells demonstrated that OGT knockdown decreased invasiveness of LNCaP cells[18].

Correlation of levels of O-GlcNAc, OGT as well as OGA and status of patient after diagnosis were investigated in the present study. The results showed a relationship between OGT and O-GlcNAc level with status after diagnosis of stage IIB-osteosarcoma patients but not OGA. Higher level of OGT and O-GlcNAc were associated with dead patients. Elevated O-GlcNAc and altered expression of its cycling enzymes were previously observed in nearly all cancer types. OGT overexpression was associated with prostate cancer progression and recurrence, and high O-GlcNAc immunohistochemistry (IHC) staining was an independent prognostic factor for poor survival[18]. Lin et al showed that the high-OGT group of patients with lung adenocarcinoma had shorter recurrence free survival and overall survival in comparison with the low-OGT[19]. Pham et al also showed that patients with high OGT expression in diffuse large B-cell lymphoma had the worst progression free survival compared with patients with low or intermediate OGT mRNA expression[20]. Recent study from Xu et al that the 3-year overall survival rate in patient with high OGT expression was lower than that with low expression[21].

The present study was performed in limited number of cases, thereby the finding required further validation in a larger cohort.

Conclusion

From a previous study, increased OGT levels were used as prognostic factors in various type of cancer but there are still lack of information about OGT levels and their roles in osteosarcoma. The present study showed significant higher levels of OGT in osteosarcoma cells line isolated from patients who poorly responded to chemotherapy. Furthermore, level of OGT relates to aggressiveness of osteosarcoma. These findings suggest that the intensive study of O-GlcNAc in specific protein might reveal the pathogenesis of osteosarcoma.

What is already known on this topic?

Several studies reported the O-GlcNAc protein and the increased OGT levels were used as prognostic factors in various type of cancer.

What this study adds?

This study showed significant higher levels of OGT in osteosarcoma patients that poorly responded to chemotherapy.

Ethics approval and consent to participate

Ethical approval and clearance was obtained from the Research Ethics Committee of Faculty of Medicine, Chiang Mai University (Research ID: 2717, Study code: ORT-2557-02717).

Conflicts of interest

The authors declare no conflict of interest.

References

1. Isakoff MS, Bielack SS, Meltzer P, Gorlick R. Osteosarcoma: Current treatment and a collaborative pathway to success. J Clin Oncol 2015;33:3029-35.
2. Craft AW. Osteosarcoma and chondrosarcoma. In: Voûte PA, Barrett A, Lemerle J, editors. Cancer in children. Berlin, Heidelberg: Springer; 1992. p. 282-94.
3. Marshall S, Bacote V, Traxinger RR. Discovery of a metabolic pathway mediating glucose-induced desensitization of the glucose transport system. Role of hexosamine biosynthesis in the induction of insulin resistance. J Biol Chem 1991;266:4706-12.
4. Bouché C, Serdy S, Kahn CR, Goldfine AB. The cellular fate of glucose and its relevance in type 2 diabetes. Endocr Rev 2004;25:807-30.
5. Broschat KO, Gorka C, Page JD, Martin-Berger CL, Davies MS, Huang Hc HC, et al. Kinetic characterization of human glutamine-fructose-6-

phosphate amidotransferase I: potent feedback inhibition by glucosamine 6-phosphate. J Biol Chem 2002;277:14764-70.

6. Hart GW, Slawson C, Ramirez-Correa G, Lagerlof O. Cross talk between O-GlcNAcylation and phosphorylation: roles in signaling, transcription, and chronic disease. Annu Rev Biochem 2011;80:825-58.

7. Ma Z, Vosseller K. O-GlcNAc in cancer biology. Amino Acids 2013;45:719-33.

8. Champattanachai V, Netsirisawan P, Chaiyawat P, Phueaouan T, Charoenwattanasatien R, Chokchaichamnankit D, et al. Proteomic analysis and abrogated expression of O-GlcNAcylated proteins associated with primary breast cancer. Proteomics 2013;13:2088-99.

9. Slawson C, Pidala J, Potter R. Increased N-acetyl-beta-glucosaminidase activity in primary breast carcinomas corresponds to a decrease in N-acetylglucosamine containing proteins. Biochim Biophys Acta 2001; 1537:147-57.

10. Raymond AK, Chawla SP, Carrasco CH, Ayala AG, Fanning CV, Grice B, et al. Osteosarcoma chemotherapy effect: a prognostic factor. Semin Diagn Pathol 1987;4:212-36.

11. Pruksakorn D, Teeyakasem P, Klangjorhor J, Chaiyawat P, Settakorn J, Diskul-Na-Ayudthaya P, et al. Overexpression of KH-type splicing regulatory protein regulates proliferation, migration, and implantation ability of osteosarcoma. Int J Oncol 2016;49:903-12.

12. Ma Z, Vocadlo DJ, Vosseller K. Hyper-O-GlcNAcylation is anti-apoptotic and maintains constitutive NF-kappaB activity in pancreatic cancer cells. J Biol Chem 2013;288:15121-30.

13. Lynch TP, Ferrer CM, Jackson SR, Shahriari KS, Vosseller K, Reginato MJ. Critical role of O-Linked beta-N-acetylglucosamine transferase in prostate cancer invasion, angiogenesis, and metastasis. J Biol Chem 2012;287:11070-81.

14. Itkonen HM, Minner S, Guldvik IJ, Sandmann MJ, Tsourlakis MC, Berge V, et al. O-GlcNAc transferase integrates metabolic pathways to regulate the stability of c-MYC in human prostate cancer cells. Cancer Res 2013;73:5277-87.

15. Caldwell SA, Jackson SR, Shahriari KS, Lynch TP, Sethi G, Walker S, et al. Nutrient sensor O-GlcNAc transferase regulates breast cancer tumorigenesis through targeting of the oncogenic transcription factor FoxM1. Oncogene 2010;29:2831-42.

16. Gu Y, Mi W, Ge Y, Liu H, Fan Q, Han C, et al. GlcNAcylation plays an essential role in breast cancer metastasis. Cancer Res 2010;70:6344-51.

17. Krześlak A, Wójcik-Krowiranda K, Forma E, Bieńkiewicz A, Bryś M. Expression of genes encoding for enzymes associated with O-GlcNAcylation in endometrial carcinomas: clinicopathologic correlations. Ginekol Pol 2012;83:22-6.

18. Kamigaito T, Okaneya T, Kawakubo M, Shimojo H, Nishizawa O, Nakayama J. Overexpression of O-GlcNAc by prostate cancer cells is significantly associated with poor prognosis of patients. Prostate Cancer Prostatic Dis 2014;17:18-22.

19. Lin YC, Lin CH, Yeh YC, Ho HL, Wu YC, Chen MY, et al. High O-linked N-acetylglucosamine transferase expression predicts poor survival in patients with early stage lung adenocarcinoma. Oncotarget 2018;9:31032-44.

20. Pham LV, Bryant JL, Mendez R, Chen J, Tamayo AT, Xu-Monette ZY, et al. Targeting the hexosamine biosynthetic pathway and O-linked N-acetylglucosamine cycling for therapeutic and imaging capabilities in diffuse large B-cell lymphoma. Oncotarget 2016;7:80599-611.

21. Xu D, Wang W, Bian T, Yang W, Shao M, Yang H. Increased expression of O-GlcNAc transferase (OGT) is a biomarker for poor prognosis and allows tumorigenesis and invasion in colon cancer. Int J Clin Exp Pathol 2019;12:1305-14.

ความสัมพันธ์ของระดับการแสดงออกเอนไซม์ O-GlcNAc transferase ต่อการตอบสนองการรักษาด้วยเคมีบำบัดในผู้ป่วยมะเร็งกระดูกออสทีโอซาร์โคมา

ศิวกร รัตนกุณฑี, ภรัณยา ชัยวัฒน์, ดำเนินสันต์ พฤกษากร, สุทธิชัย กฤษณะประกรกิจ, อนุพงศ์ เมฆอุดม, ชยารพ สุพรรณชาติ

วัตถุประสงค์: เพื่อศึกษาระดับของ O-GlcNAcylation การแสดงออกของเอนไซม์ O-GlcNAc transferase และ O-GlcNAcase ในมะเร็งกระดูกออสทีโอซาร์โคมา และหาตัวชี้วัดการพยากรณ์โรค

วัสดุและวิธีการ: การวิเคราะห์การแสดงออกของโปรตีนใช้กระบวนการแยกโปรตีนในเจล ใช้เพื่อวัดระดับของ O-GlcNAcylation การแสดงออกของเอนไซม์ O-GlcNAc transferase และ O-GlcNAcase ในการเพาะเลี้ยงเนื้อเยื่อซึ่งได้มาจากผู้ป่วยมะเร็งกระดูกออสทีโอซาร์โคมาจำนวนเจ็ดราย โดยวัดความเข้มข้นของแถบโปรตีนด้วยโปรแกรม Scion Image และหาความสัมพันธ์กับลักษณะการแสดงออกทางคลินิกของผู้ป่วยโดยใช้การทดสอบที (Student's t-test) โดยทำการศึกษาทั้งหมดสามครั้ง และเป็นการศึกษาที่เป็นอิสระต่อกันทั้งสามการทดลอง

ผลการศึกษา: ผลการศึกษาพบว่ามีแนวโน้มของการเพิ่มขึ้นของการแสดงออกของเอนไซม์ O-GlcNAc transferase ในมะเร็งกระดูกออสทีโอซาร์โคมา โดยพบระดับที่เพิ่มขึ้นอย่างมีนัยสำคัญในกลุ่มที่มีการตอบสนองต่อการรักษาด้วยยาเคมีบำบัดต่ำ ($p<0.05$) ซึ่งการศึกษานี้พบว่าอาจจะสามารถใช้เอนไซม์ O-GlcNAc transferase ในการพยากรณ์โรคของมะเร็งกระดูกออสทีโอซาร์โคมาได้

สรุป: การศึกษานี้พบการแสดงออกที่เพิ่มขึ้นอย่างมีนัยสำคัญของการแสดงออกของเอนไซม์ O-GlcNAc transferase ในมะเร็งกระดูกออสทีโอซาร์โคมา ที่มีการตอบสนองต่อการรักษาด้วยยาเคมีบำบัดต่ำ และเกี่ยวเนื่องกับการรอดชีวิตของผู้ป่วย การศึกษานี้มีข้อจำกัดในเรื่องของจำนวนผู้ป่วย ควรทำการศึกษาในกลุ่มประชากรที่ใหญ่ขึ้นหากมีการศึกษาต่อเนื่องในอนาคต

Overexpression of ADAM9 in oral squamous cell carcinoma

PATTARAMON TANASUBSINN[1], WIN PA PA AUNG[1], SUPANSA PATA[2,3],
WITIDA LAOPAJON[3], ANUPONG MAKEUDOM[1], THANAPAT SASTRARUJI[1],
WATCHARA KASINRERK[2,3] and SUTTICHAI KRISANAPRAKORNKIT[1]

[1]Center of Excellence in Oral and Maxillofacial Biology, Department of Oral Biology and
Diagnostic Sciences, Faculty of Dentistry; [2]Division of Clinical Immunology, Department of Medical Technology,
Faculty of Associated Medical Sciences; [3]Biomedical Technology Research Center, National Center for
Genetic Engineering and Biotechnology, National Sciences and Technology Development Agency at
The Faculty of Associated Medical Sciences, Chiang Mai University, Chiang Mai 50200, Thailand

Abstract. Overexpression of a disintegrin and metalloproteinase 9 (ADAM9) has been shown in various types of cancer. Some studies have reported inconclusive findings regarding chromosomal aberrations in the *ADAM9*-containing region and ADAM9 expression in oral cancer. Therefore, in this study, ADAM9 protein expression was determined and compared between oral squamous cell carcinoma (OSCC) and normal oral tissues, and between oral cancer cell lines and human oral keratinocytes (HOKs). In total, 34 OSCC and 10 healthy paraffin-embedded tissue sections were probed with an anti-ADAM9 antibody, and the immunohistochemical score was determined by multiplying the percentage of positively stained cells with the intensity score. Four different oral cancer and eight independent HOK cell lines were cultured, and the expression of membrane ADAM9 and active ADAM9 at 84 kDa in these cell lines was assayed by flow cytometry and western blot hybridization, respectively. The results showed that the median immunohistochemical score of ADAM9 expression in OSCC tissues was significantly greater than that in normal tissues (P<0.001). Furthermore, among OSCC cases, intense staining of ADAM9 expression was detected in well-differentiated and in moderately-differentiated OSCC; ADAM9 expression was also correlated with an increased degree of cell differentiation (*r*=0.557; P=0.001). Expression of membrane ADAM9 was present in 3/4 cancer cell lines. Expression of active ADAM9 varied among all the tested cell lines, but significantly higher ADAM9 expression was present in certain cancer cell lines than those in HOKs (P<0.05). In summary, ADAM9 expression is enhanced in OSCC and oral cancer cell lines, suggesting its role in the pathogenesis of oral cancer. Similar to the overexpression of ADAM9 in well-differentiated prostate cancer, high degrees of ADAM9 expression have also been observed in well-differentiated OSCC.

Introduction

Approximately 300,000 new cases of oral cancer, or ~2.1% of all cancer cases, were reported worldwide in 2012, with a greater prevalence in males than in females at a ratio of 2:1 (1). Generally, oral squamous cell carcinoma (OSCC) accounts for ~94% of all oral cancer cases reported (2). OSCC is a devastating disease with 145,000 mortalities (~1.8% of the total cancer-associated mortalities) reported in 2012 (1). In Thailand, oral cancer is the sixth most common type of cancer, and there were 3,689 new cases diagnosed in 2012 (1). The conventional treatment for oral cancer includes surgical and radiation therapy, with or without adjuvant chemotherapy (3,4), but the five-year survival rate for patients with OSCC remains low, depending on the Tumor-Node-Metastasis (TNM) staging (5). Consequently, a 'targeted therapy' has been introduced as a possible and adjuvant treatment for patients with cancer (6). An example of a possible target molecule relevant to the present study has been reported in a previous study, which demonstrated that the inhibition of a disintegrin and metalloproteinase 9 (ADAM9) expression in prostate cancer cells *in vitro* results in enhanced cancer cell death and increased sensitivity to radiotherapy and chemotherapy (7).

ADAM9, otherwise known as metalloproteinase disintegrin cysteine-rich protein 9 or meltrin γ, was first discovered in 1995 (8). The *ADAM9* gene is in the chromosomal region 8p11.23-11.22 (9). ADAM9 is first synthesized as an intracellular pro-form protein with the molecular weight of 110 kDa, and is later cleaved to create a mature 84-kDa type I membrane-anchored protein (10). ADAM9 contains several domains, including a propeptide domain, a metalloproteinase

Correspondence to: Dr Suttichai Krisanaprakornkit, Center of Excellence in Oral and Maxillofacial Biology, Department of Oral Biology and Diagnostic Sciences, Faculty of Dentistry, Chiang Mai University, 110 Suthep Road, Chiang Mai 50200, Thailand
E-mail: suttichai.k@cmu.ac.th

domain, a disintegrin domain, a cysteine-rich domain, an epidermal growth factor-like domain, a transmembrane domain and a cytoplasmic tail (11). ADAM9 is widely expressed in human tissues (11), especially in the suprabasal layers of the skin, indicating the association between ADAM9 expression and cell differentiation (12). ADAM9 possesses shedding and adhesive properties due to its metalloproteinase and disintegrin domains, respectively (13). Several specific substrates for ADAM9 have been reported, including heparin-binding epidermal growth factor (HB-EGF), β-amyloid precursor protein, fibronectin, β-casein, gelatin, tumor necrosis factor (TNF)-α, fibroblast growth factor, p75 TNF receptor, and c-kit ligand-1 (14,15). Therefore, ADAM9 can function in both physiological and pathological conditions.

Regarding its involvement in pathologic conditions, ADAM9 overexpression has been identified in a variety of cancer types, including breast cancer (16), renal cancer (17), prostate cancer (18), skin melanoma (19), uterine cervical cancer (20,21), hepatocellular carcinoma (22), non-small cell lung cancer (23), colon cancer (24), gastric cancer (15), esophageal cancer (25) and head and neck squamous cell carcinoma (HNSCC) (26). In the oral cavity, conflicting results of chromosomal aberrations in the *ADAM9*-containing region have been identified by the array comparative genomic hybridization technique (9,27). Furthermore, no significant difference in ADAM9 mRNA expression has been observed between OSCC and normal tissues, or between oral cancer cell lines and normal oral keratinocytes (9,28). Conversely, a significant difference in ADAM9 mRNA expression has been reported between HNSCC and normal tissues (26). Therefore, these inconclusive data prompted the determination of the ADAM9 protein expression profile in OSCC tissues and oral cancer cell lines. The objectives of the present study were: (1) To compare ADAM9 protein expression between OSCC and normal oral tissue specimens; (2) to determine membrane ADAM9 expression in oral cancer cell lines; (3) to compare ADAM9 protein expression between oral cancer cell lines and normal human oral keratinocytes (HOKs).

Materials and methods

Antibodies. The goat polyclonal anti-ADAM9 antibody (cat no. sc-23290) and the mouse monoclonal anti-β-actin antibody (cat no. sc-47778) used in immunohistochemistry and western blot hybridization were from Santa Cruz Biotechnology, Inc. (Dallas, TX, USA). The rabbit anti-ADAM9 antibody (cat no. LS-C100638) used in flow cytometry was from LifeSpan BioSciences, Inc. (Seattle, WA, USA). The phycoerythrin (PE)-conjugated goat F (ab')$_2$ anti-rabbit antibody (cat no. P2771MP) was obtained from Invitrogen (Thermo Fisher Scientific, Inc., Waltham, MA, USA).

Immunohistochemistry. A total of 34 formalin-fixed and paraffin-embedded OSCC tissue specimens, including all four clinical stages according to Sobin *et al* (29), and ten tissue specimens of healthy oral mucosa were retrieved from the tissue archive of the Dental Hospital, Faculty of Dentistry, Chiang Mai University, (Chiang Mai, Thailand). Of 34 OSCC cases, 17 were female and 17 were male, with a mean age of 66.94 years (43-85 years). Other clinicopathological

characteristics of the 34 OSCC cases are summarized in Table I. The histological grading of the OSCC specimens was examined by an oral pathologist (Department of Oral Biology and Diagnostic Sciences, Faculty of Dentistry, Chiang Mai University). The research protocol (no. 54/2014) was approved by the Human Experimentation Committee, Faculty of Dentistry, Chiang Mai University. The specimens were sectioned at 5-μm thickness and placed on silanized glass slides (Dako; Agilent Technologies, Inc., Santa Clara, CA, USA). The immunohistochemical protocol used in the present study was modified from that of Iamaroon and Krisanaprakornkit, 2009 (30). Briefly, the tissue sections were deparaffinized in xylene, rehydrated through graded alcohol and distilled water, and incubated with 3% hydrogen peroxide at room temperature for 10 min. Antigen unmasking was performed in 0.01 M sodium citrate buffer pH 6.0, prepared from sodium citrate monobasic (cat no. 71497; Sigma-Aldrich; Merck KGaA, Darmstadt, Germany), at 100˚C for 15 min, and the sections were cooled down at room temperature for 20 min. The sections were blocked with 1.5% normal blocking serum (cat no. sc-2023; ImmunoCruz ABC Staining Systems; Santa Cruz Biotechnology, Inc.) in Tris-buffered saline (TBS) for 20 min at room temperature, and then incubated overnight in 100 μl goat polyclonal anti-ADAM9 antibody diluted in TBS (1:100) at 4˚C. For the negative control, the sections were incubated in normal blocking serum without the addition of primary antibody. The sections were subsequently reacted with the secondary anti-goat antibody (cat no. sc-2023; ImmunoCruz ABC Staining Systems; Santa Cruz Biotechnology, Inc.) diluted in PBS (1:100), and then with avidin-biotinylated horseradish peroxidase (ImmunoCruz ABC Staining Systems; Santa Cruz Biotechnology, Inc.) for 20 min at room temperature. The sections were washed and developed in 3,3'-diaminobenzidine (Vector Laboratories, Inc., Burlingame, CA, USA). The reaction was stopped in water when brown staining was observed without background staining, monitored using light microscopy (CHK-H model; Olympus Corporation, Tokyo, Japan). Subsequently the sections were counterstained with hematoxylin and mounted. Digitized images of the tissue sections were captured by a charge-coupled device (CCD) camera (DP71; Olympus Corporation), attached to a bright-field microscope (BX41; Olympus Corporation) and a desktop computer system.

Determination of immunohistochemical (IHC) score. The sections were scored by two independent observers, with kappa values equal to 0.908 and 0.848 for the intra-examiner and the inter-examiner calibrations, respectively. The observers were blinded to the clinicopathological data for each specimen. ImageJ software (version 1.48; National Institutes of Health, Bethesda, MA, USA) was used to score the number of positively stained cells, regardless of their staining intensity, under x400 magnification. Prior to scoring, each section was observed under x100 magnification to determine the orientation of the epithelium and connective tissue. In normal tissues, scoring was performed only in the epithelial layer; in oral cancer tissues, scoring was performed in the epithelial cell nest in the connective tissue layer. Each section was first screened and then selected for three representative fields of vision. The staining intensities were scored as follows: 0=none, 1=weak,

Table I. Clinicopathologic characteristics of OSCC cases.

Variables	Number of cases
Clinical diagnostic staging[a]	
I	6
II	6
III	5
IV	17
Histological grading	
Well-differentiated	14
Moderately-differentiated	12
Poorly-differentiated	8
Location	
Buccal mucosa	10
Lateral tongue	5
Gingiva/alveolar mucosa	13
Labial mucosa	1
Retromolar pad	1
Lip vermillion	2
Mandible	2

[a]Criteria described in (29) as follows: I, tumor size ≤2 cm without regional lymph node spreading; II, tumor size >2-4 cm without regional lymph node spreading; III, tumor size >4 cm or of any size with spread to a single ipsilateral lymph node (≤3 cm); IV, tumor of any size with spread to ≥1 ipsilateral lymph node (>3 cm) or with spread to ≥1 contralateral lymph node, or tumor invasion to adjacent organs or spreading to other parts of the body regardless of lymph node involvement.

2=moderate, and 3=intense staining (31). The percentage of positive cells was calculated by dividing against the total number of cells in each field of view. Then, the average percentage of positive cells in each section was determined. Finally, the average percentage of positive cells was multiplied by the staining intensity score, and the IHC score (0-3) was obtained for each section (25).

Cell culture. Four oral cancer cell lines, including HN5, HN6, HN15 and HN008, have been previously studied for the over-expression and activation of Akt2 (30). Primary HOKs were isolated from non-inflamed oral tissues overlying the impacted third molars of eight healthy and non-smoking donors (n=8), with their informed consent, as previously described (30). As a positive control cell line for expression of both pro-form and active form of ADAM9 (32), the hepatoblastoma cell line, HepG2, was obtained from Professor Prachya Kongtawelert, Thailand Excellence Center for Tissue Engineering and Stem Cells, Department of Biochemistry, Faculty of Medicine, Chiang Mai University. HOKs were cultured in serum-free keratinocyte growth medium (Lonza, Walkersville, MA, USA), while the four oral cancer cell lines and HepG2 cells were cultured in Dulbecco's modified Eagle's medium (Invitrogen; Thermo Fisher Scientific, Inc.), supplemented with 10% fetal bovine serum and 1% penicillin/streptomycin (Invitrogen; Thermo Fisher Scientific, Inc.). All cells were maintained at 37°C in a humidified chamber with 5% CO_2. Culture medium was changed every two days, until the cells reached 80% confluency, prior to flow cytometry and western blot hybridization.

Flow cytometry. To determine the expression of membrane ADAM9 in four cancer cell lines and HepG2 cells, flow cytometry was performed. In brief, the tested cells ($2x10^6$ cells) were washed with PBS twice, removed from 100-mm culture dishes by scraping in 0.5 mM EDTA pH 7.3, centrifuged at 400 x g at room temperature for 5 min, and again washed twice with PBS pH 7.2. To block nonspecific Fc-receptor-mediated antibody binding, cells were pre-incubated with 10% AB serum from a healthy donor with blood group AB (from whom written informed consent was obtained), at 4°C for 1 h. The blocked cells were then incubated for 30 min at 4°C with the anti-ADAM9 antibody (1:20) or the rabbit immunoglobulins (1:20; final concentration, 20 µg/ml); normal rabbit serum, which was purified using a protein G column, was used as the control. The cells that were not incubated with primary antibodies or purified rabbit immunoglobulins served as a negative conjugate control. The cells were washed twice with FACS buffer, PBS containing 1% bovine serum albumin (code A7906; Sigma-Aldrich) and 0.02% sodium azide (code 0639; Amresco LLC, Solon, OH, USA), and then incubated with the PE-conjugated goat anti-rabbit immunoglobulin antibody (dilution, 1:1,000) at 4°C for 30 min. The fluorescent signals were analyzed by a FACSCalibur flow cytometer (BD Biosciences, San Jose, CA, USA).

Western blot hybridization. Whole cell lysates from all cell lines were extracted using radio-immunoprecipitation assay (RIPA) buffer (33). The total protein was quantified using a BCA Protein Assay kit (Pierce; Thermo Fisher Scientific, Inc.) according to the manufacturer's protocol. The whole cell lysates (20 µg) were denatured by heating at 100°C for 5 min, then resolved via 7.5% SDS-PAGE prior to transfer to a nitro-cellulose membrane (Bio-Rad Laboratories, Inc., Hercules, CA, USA). Unoccupied binding sites on the membranes were blocked with 5% non-fat dry milk (Santa Cruz Biotechnology, Inc.) at room temperature for 1 h. Then, the membranes were incubated overnight with the anti-ADAM9 antibody (dilution, 1:500) or the mouse monoclonal anti-β-actin antibody (dilution, 1:1,000) at 4°C. The membranes were subsequently incubated for 1 h at room temperature with either HRP-conjugated mouse anti-goat immunoglobulins (cat no. 31400; Thermo Fisher Scientific, Inc.) or HRP-conjugated rabbit anti-mouse immunoglobulins (cat no. P0260; Dako; Agilent Technologies) at 1:2,000 dilutions. The LumiGLO Reserve® chemiluminescent reagent (KPL, Gaithersburg, MA, USA) was used as a substrate, and the signals were captured using a CCD camera attached to the ChemiDoc™ XRS gel documentation system (Bio-Rad Laboratories, Inc.). To quantify the expression of active ADAM9 in each cell line, the intensities of the bands at 84 kDa were measured using the Scion Image program (Scion Corporation, Frederick, MA, USA), and the intensity of ADAM9 expression was normalized to that of β-actin expression in each sample. Then, the ratios of ADAM9 to β-actin expression were adjusted for the percentages of ADAM9 expression by comparing the ratio of ADAM9 to β-actin

Table II. A semi-quantitative analysis of the intensity score for ADAM9 expression in OSCC, according to different levels of histological grading.

Intensity score[a]	Well-differentiated N (%)	Moderately-differentiated N (%)	Poorly-differentiated N (%)
0	0 (0)	0 (0)	0 (0)
1	2 (14.3)	1 (8.3)	3 (37.5)
2	3 (21.4)	8 (66.7)	5 (62.5)
3	9 (64.3)	3 (25)	0 (0)
Total	14 (100)	12 (100)	8 (100)

[a]0, no staining; 1, weak (light brown staining, visible only with high magnification); 2, moderate (between 1 and 3); 3, intense (dark brown staining, visible with low magnification) (31). ADAM9, a disintegrin and metalloproteinase 9; OSCC, oral squamous cell carcinoma.

expression in each cell line with the highest ratio of ADAM9 to β-actin expression observed in HN008 cells, set to 100%.

Statistical analysis. The Mann-Whitney U test was used to compare the IHC scores, representing ADAM9 expression, between the OSCC and normal oral tissues. The Spearman's correlation coefficient was used to determine the correlations between the IHC scores and the histological grading or clinical staging. The independent sample t-test was used to compare the percentages of ADAM9 expression between oral cancer cell lines and normal HOKs. The data from the Mann-Whitney U test are presented as medians and interquartile ranges; the data from the independent sample t-test are presented as means and standard deviations. All statistical analyses were carried out with SPSS software version 17 (SPSS, Inc., Chicago, IL, USA). P<0.05 was considered to indicate a statistically significant difference.

Results

Overexpression of ADAM9 in OSCC. Using immunohistochemistry, intense ADAM9 staining was observed in both the cytoplasm and the membrane of the majority of cancer cell nests, which were localized in the connective tissue layer of OSCC specimens (arrowheads in Fig. 1A); comparatively, weak and diffuse ADAM9 staining was observed in the cytoplasm of normal epithelial cells, particularly in the suprabasal cell layers (Fig. 1A). The intensity of ADAM9 staining in the overlying epithelium of the OSCC tissues was also weak (bracket in Fig. 1A). No staining in the OSCC sections was observed in the absence of the anti-ADAM9 antibody (data not presented). The median IHC score in the OSCC group was significantly higher than that in the normal group (P<0.001; Fig. 1B).

Positive correlation between ADAM9 expression and cell differentiation in OSCC. All 34 OSCC cases were grouped into four clinical diagnostic stages (Table I) according to tumor size and nodal status (29), based on the histopathological reports. Using the Spearman's correlation test, the IHC scores, representing ADAM9 expression, were not determined to correlate with these four clinical diagnostic stages (r=-0.082, P=0.661), indicating that ADAM9 protein expression in OSCC has no significant association with OSCC severity and aggressiveness.
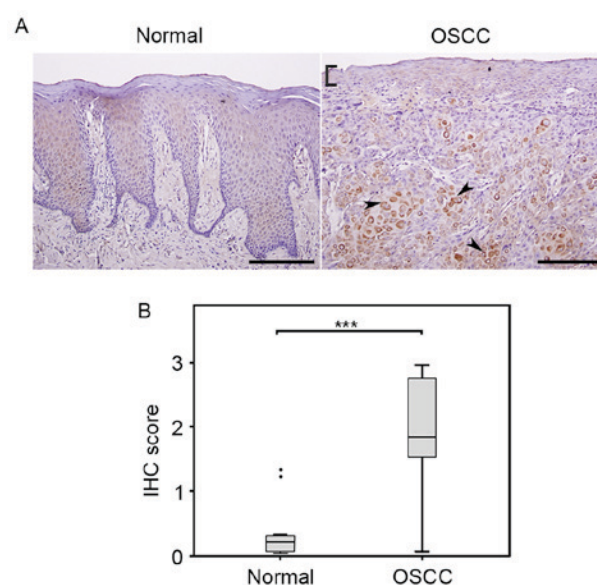
Figure 1. ADAM9 overexpression in OSCC. (A) A representative image of ADAM9 expression in normal and OSCC tissues. Weak ADAM9 staining is present in the suprabasal layers of normal epithelium and in the overlying epithelium of OSCC (bracket); intense cytoplasmic staining of ADAM9 is in tumor cell nests within the connective tissue layer of OSCC (arrowheads). Bar=200 micron. (B) A box plot diagram demonstrating significantly higher IHC scores (0-3) for ADAM9 expression in the OSCC group than in the normal group. ***P<0.001. Two small black circles represent outliers in the normal group. ADAM9, a disintegrin and metalloproteinase 9; OSCC, oral squamous cell carcinoma; IHC, immunohistochemical.

However, when all OSCC cases were stratified according to their histological grade, including 14 well-differentiated, 12 moderately-differentiated and 8 poorly-differentiated cases (Table I), it was revealed that the intensity of ADAM9 staining was greatest in the well-differentiated OSCC tissues, followed by in the moderately and the poorly-differentiated OSCC tissues, respectively (Fig. 2A). A semi-quantitative analysis of the staining intensity in all OSCC specimens is summarized in Table II. In general, the intense score (=3) was applicable in >60% of the well-differentiated OSCC cases, whereas it was assigned in only 25 and 0% of the moderately and the poorly-differentiated OSCC cases, respectively (Table II). By contrast, >60% of the moderately and the poorly-differentiated OSCC cases were scored as moderate staining (=2). Similar to the staining intensity scores, the average percentage of
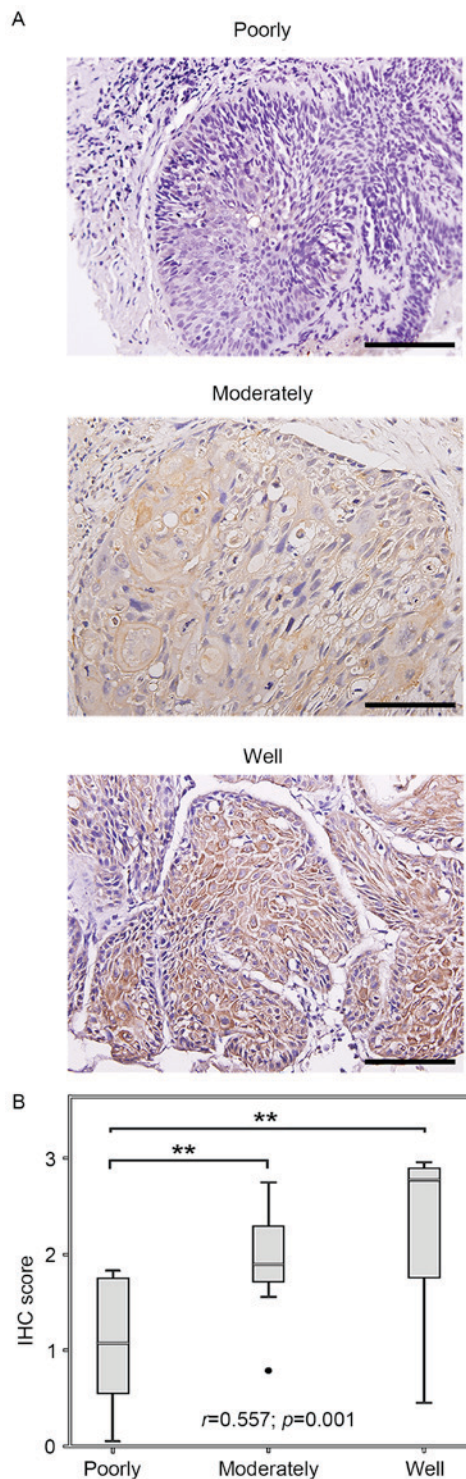
Figure 2. A positive correlation between ADAM9 expression and cell differentiation in OSCC. (A) A representative image of ADAM9 expression in each histological grading. Note the strongest intensity of ADAM9 staining in the well-differentiated OSCC, followed by the moderately-differentiated and the poorly-differentiated OSCC. Bar = 100 micron. (B) A box plot diagram showing the positive correlation between increased IHC scores (0-3) for ADAM9 expression and enhanced levels of cell differentiation. **P<0.01. A small black circle represents an outlier in the moderately-differentiated OSCC. ADAM9, a disintegrin and metalloproteinase 9; OSCC, oral squamous cell carcinoma; IHC, immunohistochemical.

positively-stained cells, irrespective of staining intensity, was greater in the well and in the moderately-differentiated OSCC tissues than in the poorly-differentiated OSCC (data

not presented). Using the Spearman's correlation test, the IHC scores were positively correlated with an increased degree of cell differentiation (r=0.557, P=0.001; Fig. 2B). Therefore, the median IHC scores for the moderately and well-differentiated OSCC tissues were significantly higher than that of the poorly-differentiated OSCC (P<0.01; Fig. 2B). However, there was no significant difference in the median IHC score between the well and moderately-differentiated OSCC (Fig. 2B), suggesting that ADAM9 expression may not be used as a diagnostic marker to distinguish well-differentiated OSCC from moderately-differentiated OSCC.

Significantly increased expression of active ADAM9 in oral cancer cell lines. We first determined the expression of membrane ADAM9 in four different oral cancer cell lines, HN5, HN6, HN15 and HN008, by flow cytometry. It was found that membrane ADAM9 was expressed in 3/4 tested oral cancer cell lines, HN6, HN15 and HN008, whereas membrane ADAM9 was not expressed in HN5 cells (Fig. 3). As expected, membrane ADAM9 was expressed in HepG2 cells. No expression signals were detected in any of the tested cell lines, either those incubated with the purified rabbit immunoglobulins control or without the anti-ADAM9 antibody (Fig. 3). Varying degrees of ADAM9 expression for the pro-form, previously reported as 110 or 120 kDa (10,34), and for the active form (84 kDa) were detected in the whole cell lysates of HN5, HN6, HN15, HN008 and 8 independent HOK cell lines (Fig. 4A). In general, the expression of active ADAM9 in HN6, HN15 and HN008 cells was greater than that in HOKs, whereas the expression of the active form of ADAM9 in HN5 cells was less than that in the HOKs (Fig. 4A), which is consistent with the absence of a fluorescent signal for membrane ADAM9 in HN5 cells (Fig. 3). Expression of β-actin was equivalent among the various samples (Fig. 4A). Using densitometry, the average percentage expression of the active form of ADAM9 in HN6 and HN008 cells was significantly higher than that in the 8 independent HOKs (P<0.05 and P<0.001, respectively); however, there was no significant increase in the expression of the active form of ADAM9 in HN15 cells (Fig. 4B). By contrast, the mean percentage expression of the active form of ADAM9 in HN5 cells was significantly lower than that in HOKs (P<0.001; Fig. 4B).

Discussion

In this study, a significant increase in ADAM9 protein expression in OSCC tissues, compared with in normal oral tissues, was demonstrated by immunohistochemistry, a finding that agrees with the results of other prior studies, which demonstrated ADAM9 protein overexpression in various types of cancer (9,15,17,18,20-23,25,26). Though particularly in squamous cell carcinoma, ADAM9 protein overexpression is also present in cancer of the cervix, the esophagus, the pharynx, the larynx, and the skin around the head and neck region (9,21,25,26). However, few previous studies have demonstrated no significant difference in ADAM9 mRNA expression between OSCC and normal tissues, or between oral cancer cell lines and normal oral keratinocytes (9,28), a finding that differs from our results on ADAM9 protein overexpression. This discrepancy may suggest a possible post-transcriptional or epigenetic modification of
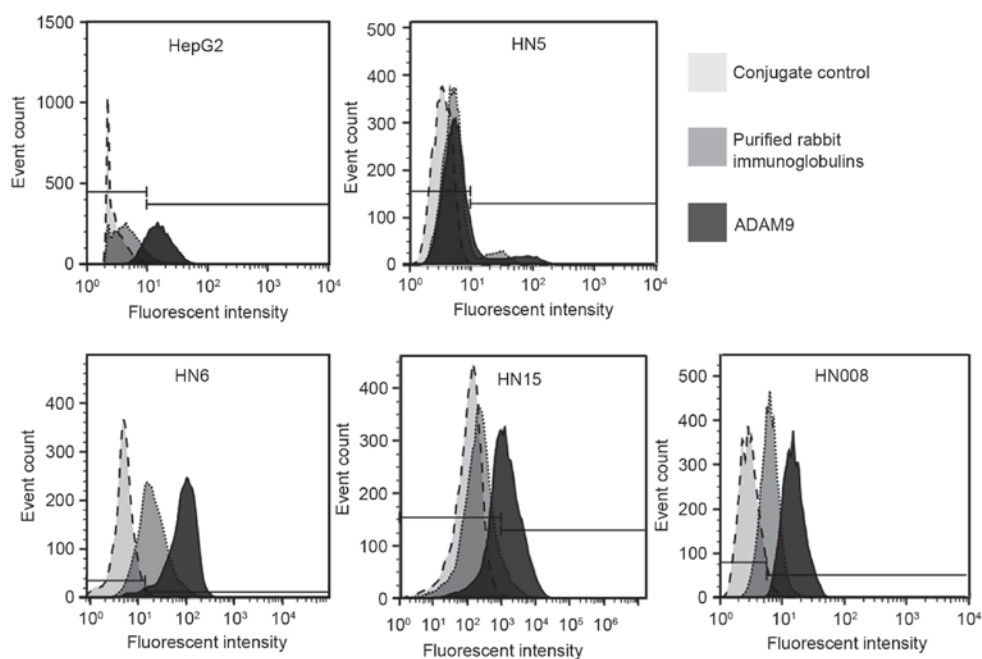
Figure 3. Expression of membrane ADAM9 in oral cancer cell lines. A representative histogram for expression of membrane ADAM9 in the four oral cancer cell lines, HN5, HN6, HN15 and HN008, from three separate experiments is presented. Note the expression of membrane ADAM9 (black area) in HN6, HN15 and HN008 cells, whereas membrane ADAM9 expression was not detected in HN5 cells. Membrane ADAM9 was expressed in HepG2 cells, which were used as the positive control, while there was no membrane ADAM9 expression in all four oral cancer cell lines and HepG2 cells stained with only the PE-conjugated goat anti-rabbit immunoglobulin antibody as the conjugate control (light gray area) or with purified rabbit immunoglobulins (dark gray area), used as the two negative controls. ADAM9, a disintegrin and metalloproteinase 9.
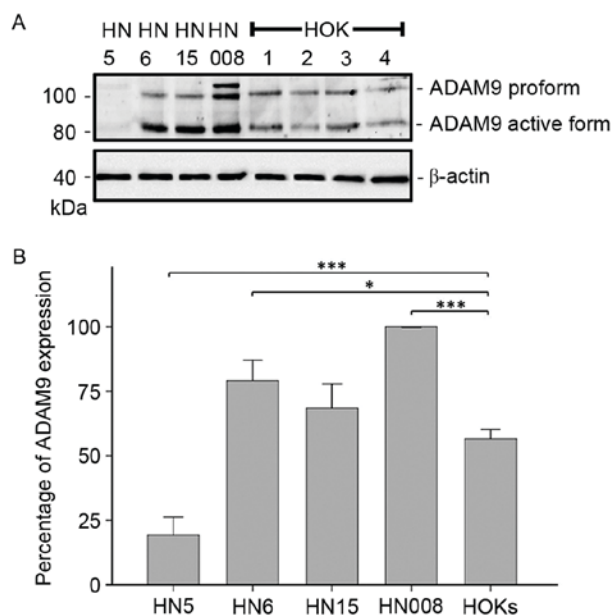
Figure 4. A significant increase in the expression of active ADAM9 in certain oral cancer cell lines. (A) A representative blot demonstrating varying expression of the ADAM9 pro-form (110 and 120 kDa) and of its active form (84 kDa) in the four oral cancer cell lines, HN5, HN6, HN15 and HN008, and in four normal human oral keratinocytes (HOK 1-4). Expression of β-actin was equal among all the samples. (B) A bar graph demonstrating a significant increase in the average percentage of active ADAM9 expression in HN6 and HN008 cells, and a significant decrease in the average percentage in HN5 cells, determined from five separate experiments (n=5) and compared with the average percentage of ADAM9 expression in eight independent HOK cell lines (n=8). The percentage of ADAM9 expression in each oral cancer and HOK cell line was determined by comparison with the percentage in HN008 cells, set to 100%. Error bars=standard deviations; *P<0.05; ***P<0.001. ADAM9, a disintegrin and metalloproteinase 9; HOK, human oral keratinocytes.

ADAM9 expression, as demonstrated in esophageal squamous cell carcinoma (25).

A significant and positive correlation was demonstrated between ADAM9 expression and an increased degree of oral cancer cell differentiation. This finding is similar to the results shown in mouse prostate and breast cancer, wherein higher ADAM9 mRNA expression is present in well-differentiated lesions, compared with in poorly-differentiated lesions (35). Moreover, the significantly greater ADAM9 protein expression in well and moderately-differentiated OSCC, compared with in poorly-differentiated OSCC, may suggest a possible role for ADAM9 during the transition from well-differentiated to poorly-differentiated carcinomas, as proposed by Peduto *et al* (35). Poorly-differentiated OSCC is generally associated with cancer aggressiveness due to its high recurrence rate and poor disease-free survival rate, compared with well and moderately-differentiated OSCC (36). As a result, it is speculated that decreased ADAM9 expression in OSCC may regulate a change from low-grade to high-grade cancer that then results in increased cancer aggressiveness and severity.

The significantly increased ADAM9 protein expression in well and in moderately-differentiated OSCC also corresponds with ADAM9 expression in the suprabasal layers of normal epidermis and in differentiated skin keratinocyte cell lines (12), indicating the association between ADAM9 expression and epithelial cell differentiation in both OSCC and normal tissues. However, the present study determined that ADAM9 expression in OSCC was not correlated with tumor size or nodal status, suggesting that the degree of ADAM9 expression is not involved with the clinical features or anatomical extent of oral cancer. A lack of this involvement is consistent with higher ADAM9 expression in well-differentiated OSCC compared

with in poorly-differentiated OSCC (Fig. 2), as well as with no association observed between ADAM9 expression and the TNM staging of prostate and lung cancer (18,23). Nonetheless, the correlation results were based on the histopathological reports of 34 OSCC cases. A notable limitation of the present study was the lack of treatment and follow-up data for the 34 patients with OSCC; it would, therefore, be useful to further determine whether distinct degrees of ADAM9 expression are associated with OSCC aggressiveness, particularly the recurrence and the five-year survival rates.

Consistent with ADAM9 protein expression on the surface of cancer cells in OSCC tissues, expression of membrane ADAM9 was detected in 3/4 tested oral cancer cell lines using flow cytometry (Fig. 3). Furthermore, using western blot hybridization, the expression of membrane ADAM9 (active form) at 84 kDa was significantly enhanced in 2/3 oral cancer cell lines (Fig. 4B), which were positive for membrane ADAM9 expression. These results are similar to those of Uehara et al (28), who demonstrated increased ADAM9 mRNA expression in certain oral cancer cell lines, and also add up their results (28) by demonstrating the presence of membrane ADAM9 in oral cancer cell lines and a significant increase in membrane ADAM9 expression, suggesting that ADAM9 can possibly function as a shedding enzyme for HB-EGF (14,25). In addition, varying degrees of active ADAM9 expression among oral cancer and HOK cell lines are similar to the different degrees of ADAM9 mRNA expression in other oral cancer and normal epithelial cell lines (28).

ADAM9 overexpression has been demonstrated to serve an essential role in the pathogenesis of numerous cancer types, particularly through enhanced cancer cell survival due to an anti-apoptotic activity mediated by the epidermal growth factor receptor (EGFR)/Akt pathway in squamous cell carcinoma of the skin and the esophagus (19,25). The active ADAM9 overexpression in oral cancer cell lines is concordant with the results of our previous study (30), which recorded the overexpression and activation of Akt2 in the same oral cancer cell lines. Thus, the possible function of active ADAM9 as a sheddase that activates EGFR and Akt via phosphorylation in these oral cancer cell lines warrants further investigation. It is also necessary to examine the behavior and aggressiveness of the HN6 and HN008 cells, in which ADAM9 expression was significantly enhanced compared with HN5 cells that minimally expressed ADAM9. Further investigations into the effect of ADAM9 inhibition in both normal oral cells and highly expressing ADAM9 oral cancer cell lines are also required.

As ADAM9 does not appear to be essential to development, fertility or adult homeostasis, inhibition of ADAM9 expression in tumors may only affect cancer cells, and not normal cells, resulting in fewer complications than conventional therapies, including surgical, chemo and radiation therapies (37). Recently, studies have proposed the usage of ADAM9 as a prognostic or a therapeutic marker in various types of cancer. One example is a study conducted using high and low ADAM9-expressing gastric cancer cell lines (15). It was observed that monoclonal antibodies, or small interfering RNA, specifically targeted against ADAM9 could reduce cell proliferation and invasion in high ADAM9-expressing cell lines but not in low ADAM9-expressing cell lines (15). Therefore, it is reasonable to assume that silencing ADAM9

expression could prove useful in decreasing aggressive behavior in high ADAM9-expressing oral cancer cell lines, which warrants further investigation.

In summary, the present study is the first, to the best of our knowledge, to demonstrate that ADAM9 protein is overexpressed in OSCC tissues and in oral cancer cell lines. Its expression is positively correlated with cancer cell differentiation, consistent with other cancer types and with increased ADAM9 expression in the suprabasal layers of the skin. Nevertheless, ADAM9 overexpression in OSCC is not correlated with tumor size or nodal status, which corresponds with low levels of ADAM9 expression in poorly-differentiated OSCC tissues. Certain oral cancer cell lines that highly express active ADAM9 on their cell surface also strongly express Akt2 and phosphorylated-Akt (30), suggesting a possible connection between active ADAM9 and the activation of EGFR and Akt2 via phosphorylation in these oral cancer cell lines. Additional studies are still required to explore the functional role of ADAM9 in the pathogenesis and aggressiveness of OSCC.

Acknowledgements

References

1. Ferlay J, Soerjomataram I, Dikshit R, Eser S, Mathers C, Rebelo M, Parkin DM, Forman D and Bray F: Cancer incidence and mortality worldwide: Sources, methods and major patterns in GLOBOCAN 2012. Int J Cancer 136: E359-E386, 2015.
2. Neville B, Damm DD, Allen C and Bouquot J: Oral and Maxillofacial Pathology 4th edition. Elsevier Health Sciences, Canada, pp409-421, 2009.
3. Deng H, Sambrook PJ and Logan RM: The treatment of oral cancer: An overview for dental professionals. Aust Dent J 56: 244-252, 2011.
4. Rosebush MS, Rao SK, Samant S, Gu W, Handorf CR, Pfeffer LM and Nosrat CA: Oral cancer: Enduring characteristics and emerging trends. J Mich Dent Assoc 94: 64-68, 2012.
5. Warnakulasuriya S: Global epidemiology of oral and oropharyngeal cancer. Oral Oncol 45: 309-316, 2009.
6. Howard JD, Lu B and Chung CH: Therapeutic targets in head and neck squamous cell carcinoma: Identification, evaluation, and clinical translation. Oral Oncol 48: 10-17, 2012.
7. Josson S, Anderson CS, Sung SY, Johnstone PA, Kubo H, Hsieh CL, Arnold R, Gururajan M, Yates C and Chung LW: Inhibition of ADAM9 expression induces epithelial phenotypic alterations and sensitizes human prostate cancer cells to radiation and chemotherapy. Prostate 71: 232-240, 2011.
8. Barrett A, Woessner J and Rawlings N (eds): Handbook of Proteolytic Enzymes 2nd edition. Elsevier Inc, Europe, pp715, 2013.
9. Vincent-Chong VK, Anwar A, Karen-Ng LP, Cheong SC, Yang YH, Pradeep PJ, Rahman ZA, Ismail SM, Zaini ZM, Prepageran N, et al: Genome wide analysis of chromosomal alterations in oral squamous cell carcinomas revealed over expression of MGAM and ADAM9. PLoS One 8: e54705, 2013.

10. Roychaudhuri R, Hergrueter AH, Polverino F, Laucho-Contreras ME, Gupta K, Borregaard N and Owen CA: ADAM9 is a novel product of polymorphonuclear neutrophils: Regulation of expression and contributions to extracellular matrix protein degradation during acute lung injury. J Immunol 193: 2469-2482, 2014.
11. Hooper NM and Lendeckel U (eds): The ADAM family of protease. Springer, The Netherlands, pp75-81, 2005.
12. Zigrino P, Steiger J, Fox JW, Löffek S, Schild A, Nischt R and Mauch C: Role of ADAM-9 disintegrin-cysteine-rich domains in human keratinocyte migration. J Biol Chem 282: 30785-30793, 2007.
13. Sung SY: ADAM9 (ADAM metallopeptidase domain 9 (meltrin gamma)). Atlas Genet Cytogenet Oncol Haematol 14: 270-274, 2010.
14. Klein T and Bischoff R: Active metalloproteases of the A Disintegrin and Metalloprotease (ADAM) family: Biological function and structure. J Proteome Res 10: 17-33, 2011.
15. Kim JM, Jeung HC, Rha SY, Yu EJ, Kim TS, Shin YK, Zhang X, Park KH, Park SW, Chung HC and Powis G: The effect of disintegrin-metalloproteinase ADAM9 in gastric cancer progression. Mol Cancer Ther 13: 3074-3085, 2014.
16. Fry JL and Toker A: Secreted and membrane-bound isoforms of protease ADAM9 have opposing effects on breast cancer cell migration. Cancer Res 70: 8187-8198, 2010.
17. Fritzsche FR, Wassermann K, Jung M, Tölle A, Kristiansen I, Lein M, Johannsen M, Dietel M, Jung K and Kristiansen G: ADAM9 is highly expressed in renal cell cancer and is associated with tumour progression. BMC Cancer 8: 179, 2008.
18. Fritzsche FR, Jung M, Tölle A, Wild P, Hartmann A, Wassermann K, Rabien A, Lein M, Dietel M, Pilarsky C, *et al*: ADAM9 expression is a significant and independent prognostic marker of PSA relapse in prostate cancer. Eur Urol 54: 1097-1106, 2008.
19. Singh B, Schneider M, Knyazev P and Ullrich A: UV-induced EGFR signal transactivation is dependent on proligand shedding by activated metalloproteases in skin cancer cell lines. Int J Cancer 124: 531-539, 2009.
20. Zubel A, Flechtenmacher C, Edler L and Alonso A: Expression of ADAM9 in CIN3 lesions and squamous cell carcinomas of the cervix. Gynecol Oncol 114: 332-336, 2009.
21. Shaker M, Yokoyama Y, Mori S, Tsujimoto M, Kawaguchi N, Kiyono T, Nakano T and Matsuura N: Aberrant expression of disintegrin-metalloprotease proteins in the formation and progression of uterine cervical cancer. Pathobiology 78: 149-161, 2011.
22. Tao K, Qian N, Tang Y, Ti Z, Song W, Cao D and Dou K: Increased expression of a disintegrin and metalloprotease-9 in hepatocellular carcinoma: Implications for tumor progression and prognosis. Jpn J Clin Oncol 40: 645-651, 2010.
23. Zhang J, Qi J, Chen N, Fu W, Zhou B and He A: High expression of a disintegrin and metalloproteinase-9 predicts a shortened survival time in completely resected stage I non-small cell lung cancer. Oncol Lett 5: 1461-1466, 2013.
24. Li J, Ji Z, Qiao C, Qi Y and Shi W: Overexpression of ADAM9 promotes colon cancer cells invasion. J Invest Surg 26: 127-133, 2013.
25. Liu R, Gu J, Jiang P, Zheng Y, Liu X, Jiang X, Huang E, Xiong S, Xu F, Liu G, *et al*: DNMT1-microRNA126 epigenetic circuit contributes to esophageal squamous cell carcinoma growth via ADAM9-EGFR-AKT signaling. Clin Cancer Res 21: 854-863, 2015.
26. Stokes A, Joutsa J, Ala-Aho R, Pitchers M, Pennington CJ, Martin C, Premachandra DJ, Okada Y, Peltonen J, Grénman R, *et al*: Expression profiles and clinical correlations of degradome components in the tumor microenvironment of head and neck squamous cell carcinoma. Clin Cancer Res 16: 2022-2035, 2010.
27. Ambatipudi S, Gerstung M, Gowda R, Pai P, Borges AM, Schäffer AA, Beerenwinkel N and Mahimkar MB: Genomic profiling of advanced-stage oral cancers reveals chromosome 11q alterations as markers of poor clinical outcome. PLoS One 6: e17250, 2011.
28. Uehara E, Shiiba M, Shinozuka K, Saito K, Kouzu Y, Koike H, Kasamatsu A, Sakamoto Y, Ogawara K, Uzawa K and Tanzawa H: Upregulated expression of ADAM12 is associated with progression of oral squamous cell carcinoma. Int J Oncol 40: 1414-1422, 2012.
29. Sobin LH, Gospodarowicz MK and Wittekind C: TNM classification of malignant tumours. Blackwell Publishing Ltd, United Kingdom, pp5-29, 2009.
30. Iamaroon A and Krisanaprakornkit S: Overexpression and activation of Akt2 protein in oral squamous cell carcinoma. Oral Oncol 45: e175-e179, 2009.
31. Pirker R, Pereira JR, von Pawel J, Krzakowski M, Ramlau R, Park K, de Marinis F, Eberhardt WE, Paz-Ares L, Störkel S, *et al*: EGFR expression as a predictor of survival for first-line chemotherapy plus cetuximab in patients with advanced non-small-cell lung cancer: Analysis of data from the phase 3 FLEX study. Lancet Oncol 13: 33-42, 2012.
32. Kohga K, Takehara T, Tatsumi T, Ishida H, Miyagi T, Hosui A and Hayashi N: Sorafenib inhibits the shedding of major histocompatibility complex class I-related chain A on hepatocellular carcinoma cells by down-regulating a disintegrin and metalloproteinase 9. Hepatology 51: 1264-1273, 2010.
33. Chotjumlong P, Bolscher JG, Nazmi K, Reutrakul V, Supanchart C, Buranaphatthana W and Krisanaprakornkit S: Involvement of the P2X7 purinergic receptor and c-Jun N-terminal and extracellular signal-regulated kinases in cyclooxygenase-2 and prostaglandin E2 induction by LL-37. J Innate Immun 5: 72-83, 2013.
34. Izumi Y, Hirata M, Hasuwa H, Iwamoto R, Umata T, Miyado K, Tamai Y, Kurisaki T, Sehara-Fujisawa A, Ohno S and Mekada E: A metalloprotease-disintegrin, MDC9/meltrin-gamma/ADAM9 and PKCdelta are involved in TPA-induced ectodomain shedding of membrane-anchored heparin-binding EGF-like growth factor. EMBO J 17: 7260-7272, 1998.
35. Peduto L, Reuter VE, Shaffer DR, Scher HI and Blobel CP: Critical function for ADAM9 in mouse prostate cancer. Cancer Res 65: 9312-9319, 2005.
36. Lindenblatt Rde C, Martinez GL, Silva LE, Faria PS, Camisasca DR and Lourenço Sde Q: Oral squamous cell carcinoma grading systems-analysis of the best survival predictor. J Oral Pathol Med 41: 34-39, 2012.
37. Peduto L: ADAM9 as a potential target molecule in cancer. Curr Pharm Des 15: 2282-2287, 2009.

Effects of prostaglandin E₂ on clonogenicity, proliferation and expression of pluripotent markers in human periodontal ligament cells

Avirut Truntipakorn[a], Anupong Makeudom[b], Thanapat Sastraruji[b], Prasit Pavasant[c], Kassara Pattamapun[a], Suttichai Krisanaprakornkit[b],*

[a] Department of Restorative Dentistry and Periodontology, Faculty of Dentistry, Chiang Mai University, Chiang Mai 50200, Thailand
[b] Center of Excellence in Oral and Maxillofacial Biology, Department of Oral Biology and Diagnostic Sciences, Faculty of Dentistry, Chiang Mai University, Chiang Mai 50200, Thailand
[c] Mineralized Tissue Research Unit, Faculty of Dentistry, Chulalongkorn University, Bangkok 10330, Thailand

ARTICLE INFO

ABSTRACT

Background and objective: Based on our earlier work on the response of periodontal ligament (PDL) cells to mechanical stress by induction of cyclooxygenase expression and production of prostaglandin PGE₂ that could regulate mineralization of PDL cells, it was hypothesized that PGE₂ had potential effects on PDL stemness. In this study, we aimed to investigate clonogenicity, proliferation and expression of certain pluripotent markers, considered to be characteristics of PDL stemness, in response to treatment with exogenously-added PGE₂.
Material and methods: Human PDL cells were cultured and treated with various doses of PGE₂, and the aforementioned characteristics of PDL stemness were analyzed.
Results: The clonogenicity and proliferation were significantly enhanced by PGE₂ at low concentrations (0.01, 0.1 and 1 ng/ml; $P < 0.05$), but only the proliferation was significantly diminished by PGE₂ at a high concentration (100 ng/ml; $P < 0.05$). Expression of NANOG and OCT4 mRNA and protein was increased by PGE₂ treatment at 0.1 and 1 ng/ml. Consistently, expression of stage-specific embryonic antigen 4, a putative stem cell marker, was significantly augmented by PGE₂ treatment at 1 ng/ml ($P < 0.05$).
Conclusion: Our findings suggest that although a high dose of PGE₂ (100 ng/ml) inhibits proliferation of PDL cells, PGE₂ at low doses appears to play a role in the maintenance of PDL stemness.

1. Introduction

Periodontal ligament (PDL) tissue possesses a high regenerative capacity and a rapid turnover rate. Its principal cell types consist of fibroblasts, endothelial cells, epithelial cell rests of Malassez and undifferentiated mesenchymal cells. Fibroblasts function as a major producer of extracellular matrix and other substances, which in turn play a role in maintaining periodontal homeostasis (Hinz, 2013) and result in the maintenance of periodontal ligament width over lifetime (Lim et al., 2014). Periodontal homeostasis is suggested to rely very much on multipotency of undifferentiated mesenchymal cells in PDL (Kawanabe et al., 2010) which allows a rise of various progenitor cells, including precementoblasts, prefibroblasts and preosteoblasts (Ivanovski, Gronthos, Shi, & Bartold, 2006). Although cellular, genetic, biochemical and mechanical factors are believed to work in concert to maintain this homeostasis, much of research investigating periodontal homeostasis has dealt extensively with mechanical stress and its subsequent

biochemical signaling mechanisms, in which prostaglandin (PG) E₂ was shown to act a mediator to control the mineralization of human PDL cells. This regulation seems to be an important aspect of periodontal homeostasis (Manokawinchoke, Pimkhaokhum, Everts, & Pavasant, 2014).

Prostaglandins (PGs), produced from arachidonic acid by the action of cyclooxygenases (COX), are lipid autacoids responsible for sustaining homeostasis and mediating pathological changes in tissue. There are four types of PGs generated *in vivo*, including PGE₂, prostacyclin, prostaglandin D₂ and prostaglandin F₂α. PGE₂ works in an autocrine and/or a paracrine manner *via* E prostanoid receptors in human PDL fibroblasts (Luckprom, Wongkhantee, Yongchaitrakul, & Pavasant, 2010). PGE₂ at low levels is proposed to help maintain the homeostasis of periodontal tissue (Manokawinchoke, Pimkhaokhum, Everts, & Pavasant, 2014), whereas surges in amount of PGE₂ are commonly reported in the acute state of inflammation in different tissue types (Ricciotti & Fitzgerald, 2011). Our previous works have

demonstrated that PDL cells respond to mechanical stress by increasing the rate of ATP efflux (Wongkhantee, Yongchaitrakul, & Pavasant, 2008). Subsequently, an increase in extracellular ATP can directly regulate RANKL expression in PDL cells through the P2Y1/PKA/NFκB-mediated induction of cyclooxygenase and PGE_2 release (Luckprom, Wongkhantee, Yongchaitrakul, & Pavasant, 2010). Based on these two findings, it was proposed in this study that increased amounts of PGE_2 from mechanical stress during normal mastication might benefit stemness maintenance of PDL cells. Besides, PGE_2 down-regulated mRNA expression of *RUNX2*, an osteoblastic differentiation marker, in a dose-dependent manner in human PDL cells that were cultured in regular growth medium (unpublished data), implying that PDL stemness is likely to be maintained by PGE_2 treatment.

Consistently, PGE_2 has formerly been shown to enhance stemness of cancer cell lines, *e.g.* colorectal carcinoma, hepatocellular carcinoma and rat bladder carcinoma (Chu et al., 2014; Liu et al., 2016; Moon et al., 2014). PGE_2 at low concentrations also up-regulates expression of certain pluripotency-related markers in human tendon stem cells (Zhang & Wang, 2014) and inhibits mineral deposition in cultured human PDL cells (Manokawinchoke, Pimkhaokhum, Everts, & Pavasant, 2014). All of these studies thus suggested that the stemness of PDL cells is probably retained by PGE_2 at low doses. However, to the best of our knowledge, it is still unknown as to whether PGE_2 can influence the clonogenicity, proliferation and expression of pluripotent markers, which are some characteristics of PDL stemness. Accordingly, we aimed to study effects of PGE_2 on these three parameters.

2. Materials and methods

2.1. Cell culture

The protocol to retrieve human PDL cells was approved by the Human Experimentation Committee, Faculty of Dentistry, Chiang Mai University (#40/2016). Third molars without extensive caries, severe periodontal infection and periapical lesions were collected from three donors (aged 18–25 years) with informed consent to avoid potential PDL cell stimulation with high doses of PGE_2 from already-existing inflammation in PDL tissues and contamination in cultures of PDL cells from teeth with pulp, periapical or periodontal infection. The tissues were gently removed from the middle third of the roots and dissected into small pieces. Tissue explants were grown in Dulbecco's Modified Eagle Medium (DMEM; Gibco, Grand Island, NY, USA) supplemented with 10% fetal bovine serum (FBS; Gibco), 2 mM glutamine (Gibco), 100 U/ml penicillin, 100 µg/ml, streptomycin and 5 µg/ml amphotericin B (Gibco) under 100% humidified atmosphere at 37 °C and 5% CO_2. Cell culture medium was replenished every 48 h. After having grown out from the explants and having reached confluence, PDL cells were sub-cultured at a ratio of 1:3 for further expansions. Cells isolated from each of the three donors in the third to fifth passages were kept separately and used in all subsequent assays.

2.2. AlamarBlue® cytotoxicity and proliferation assay

PDL cells (1×10^4 cells per well) were seeded in 24-well plates with 500 µl of complete DMEM and incubated overnight at 37 °C under 100% humidified atmosphere containing 5% CO_2. The cells in the wells were treated with PGE_2 (Tocris Biosciences, Bristol, UK) in 500 µl complete DMEM at the following concentrations, including 0.01, 0.1, 1, 10 and 100 ng/ml. Because dimethyl sulfoxide (DMSO; Sigma-Aldrich, St. Louis, MO, USA) was used as a solvent for PGE_2, the concentration of DMSO in every condition was finally equated to 0.1% v/v. Cells maintained in cultures in the presence of 0.1% DMSO (v/v) without PGE_2 treatment were used as a negative control. Culture medium in all conditions was replenished every 72 h.

To determine effects of PGE_2 on both cytotoxicity and proliferative potential, AlamarBlue® (Thermo Scientific™, Rockford, IL, USA) assay

was performed on days 1, 3 and 7. A quantity of 50 µl of AlamarBlue® (10X) solution was added into each well. After 4 h of incubation at 37 °C, a 100-µl quantity of the supernatant from each well was transferred to a 96-well microplate for absorbance readings at 540-nm and 595-nm wavelength with a microplate spectrophotometer (Sunrise, Tecan, Grödlg, Austria). Percentage of reduction was calculated against a positive control well where AlamarBlue® (1X) in complete DMEM was autoclaved for 15 min in order to obtain full reduction. A standard curve plotting the percentages of reduction against the number of cells in each PDL cell line was constructed. Population doubling times (PDTs), expressed in h, between days 3 and 7 were calculated by using the following formula, $PDT = T \ln 2 / \ln(X_e / X_b)$ where T stands for incubation time, X_b for cell number at the beginning of incubation, and X_e for cell number at the end of incubation.

2.3. Clonogenic assay

Five hundred PDL cells per well were seeded in 6-well culture plates and maintained in complete DMEM as described in the previous section. After incubation with PGE_2 at the concentrations mentioned above for 14 d, the cells were fixed with 10% v/v paraformaldehyde for 10 min, washed with phosphate-buffered saline (PBS) twice and stained with crystal violet (Sigma-Aldrich). The colony forming units, consisting of more than 50 cells, were counted under stereomicroscope (Olympus, Tokyo, Japan).

2.4. BrdU cell proliferation assay

PDL cells (3×10^3 cells per well) were seeded in 96-well tissue culture plates with 100 µl of complete DMEM in each well. The cells were treated with PGE_2 at the concentrations described above. A culture condition without PGE_2 was used as a negative control, whereas the cells treated with 100 ng/ml of phorbol 12-myristate 13-acetate (PMA; Sigma-Aldrich) served as a positive control for PDL cell proliferation. Proliferation was determined at the end of the treatment period for 48 h by using the cell proliferation ELISA BrdU kit (Roche Diagnostics Ltd., Mannheim, Germany). After attachment to the bottom of the plates, the cells were grown in complete DMEM containing 10 µM BrdU for another 4 h at 37 °C. The medium was then discarded and the cells were fixed with FixDenat solution at room temperature for 30 min and further incubated with 100 µl of the anti-BrdU-POD working solution for 90 min at room temperature. The wells were then washed with PBS and the substrate solution was added and incubated at room temperature for 30 min. Finally, the reaction was stopped by 1 M H_2SO_4. The absorbance was read at 450 nm against that of the reference wavelength at 595 nm with a microplate reader (Sunrise). The absorbance values at 595 nm were, therefore, subtracted from those at 450 nm. All absorbance values were subtracted again by the absorbance value of the blank wells where no cells were seeded.

2.5. RNA extraction and real-time RT-PCR

PDL cells (1.2×10^5 per well) were seeded in 6-well plates and cultured in complete DMEM. Then, the cells were treated with PGE_2 at according concentrations for 72 h or left untreated as a negative control. Total RNA was extracted with the RNA Minispin kit (GE Healthcare, Little Chalfont, Buckinghamshire, UK) according to manufacturer's instructions. One µg of each RNA sample was converted to cDNA with the Tetro cDNA Synthesis kit (SensiFAST™, Taunton, MA, USA) for 1.5 h at 45 °C at a total volume of 20 µl. Subsequently, all cDNA products were diluted 1:5 (v/v) with nuclease-free water. Real-time PCR was performed by using LightCycler® 480 instrument II (Roche, Rotkreuz, Switzerland) with specific primer pairs for *NANOG, OCT4* and glyceraldehyde-3-phosphate dehydrogenase (*GAPDH*), a housekeeping gene (Table 1). All primer sequences were taken from our previous work (Osathanon, Subbalekha, Sastravaha, & Pavasant, 2012).

Table 1
Oligonucleotide sequences of forward and reverse primers used in real-time PCR.

Gene	Forward (5′-3′)	Reverse (5′-3′)
NANOG	GGAAGAGTAGAGGCTGGGGT	TCTCTCCTCTTCCTTCTCCA
OCT4	AGACCCAGCAGCCTCAAAATC	GCAACCTGGAGAATTTGTTCCT
GAPDH	TGAAGGTCGGAGTCAACGGAT	TCACACCCATGACGAACATGG

PCR was performed with the SYBR No-ROX kit (SensiFAST™), containing *Taq* polymerase and SYBR green I, up to 45 cycles. The reaction mixture consisted of 16 pmol of each primer and 5 µl of a diluted cDNA product, making a total volume of 20 µl. The PCR working conditions were set as follows: pre-incubation at 95 °C for 10 min, denaturation at 95 °C for 20 s, annealing at 65 °C for 20 s and elongation at 72 °C for 25 s. The levels of *NANOG* and *OCT4* expression in each cDNA sample were normalized with that of *GAPDH* expression with the aid of a calculation algorithm, LightCycler® 480 Software version 1.5 (Roche). Relative quantifications of *NANOG* and *OCT4* expression were determined by making a comparison between PGE_2-treated and PGE_2-untreated samples.

2.6. Nuclear protein extraction and Western blot hybridization

PDL cells (1×10^8 cells) were cultured in complete DMEM in 15-cm culture dishes and treated with PGE_2 at varying concentrations as described above for 72 h or left untreated as a negative control. The cells were harvested with 0.5% trypsin in EDTA (Gibco) and then nuclear protein was extracted with the NE-PER™ Nuclear and Cytoplasmic Extraction reagent (Thermo Scientific™). Total protein content of each sample was quantified by the BCA reaction (BCA Protein Assay Kit; Pierce®, Rockford, IL, USA). A 3-µg quantity of nuclear extract in Laemmli sample buffer (2X), consisting of 125 mM Tris-HCl at pH 6.8, 20% (v/v) glycerol, 4% (w/v) sodium dodecyl sulfate and 0.004% (w/v) bromophenol blue and 5% (v/v) β-mercaptoethanol, was heated for 5 min, resolved by 10% sodium dodecyl sulfate polyacrylamide gel electrophoresis under electrical current at 100 V/300 W for 2 h and 15 min and transferred to nitrocellulose membranes (Bio-Rad Laboratories, Hercules, CA, USA) under electrical current at 100 mA/300W for 12 h. The membranes were blocked for 1 h in 5% (w/v) non-fat dry milk (Santa Cruz Biotechnology, Santa Cruz, CA, USA) in 0.1% (v/v) Tween-20/Tris-buffered saline. Subsequently, the membranes were incubated with rabbit polyclonal anti-human NANOG (1:1000; EMD Millipore Corporation, Temecula, CA, USA), rabbit polyclonal anti-human OCT4 (1:500; EMD Millipore Corporation) and rabbit polyclonal anti-human histone deacetylase 1 (HDAC1; 1:1000; EMD Millipore Corporation) antibodies overnight at 4 °C. On the following day, the membranes were incubated with horseradish peroxidase-conjugated mouse anti-rabbit antibody (1:2000; Dako, Glostrup, Denmark) for 1 h and reacted with LumiGLO Reserve Chemiluminescent reagent (KPL, Gaithersburg, MD, USA). Chemiluminescent signals were captured with ChemiDoc XRS gel documentation system (Bio-Rad Laboratories).

2.7. Immunofluorescence

PDL cells (1×10^4 cells) were seeded in chamber slides (Nunc™ Lab-Tek™ II Chamber Slide™ System; Thermo Scientific™) with complete DMEM overnight. The cells were then treated with PGE_2 at varying concentrations (see above) for 72 h or left untreated as a negative control. After treatment, the cells were fixed with 4% paraformaldehyde in PBS for 10 min, permeabilized with Triton X-100 for 5 min, and incubated with phycoerythrin-conjugated mouse monoclonal anti-human stage-specific embryonic antigen 4 (SSEA4) antibody (Thermo Scientific™) for 90 min. The cells were washed with PBS twice, reacted with DAPI (Sigma-Aldrich) for 5 min and mounted in

fluorescence mounting medium. Immunofluorescence images were captured with a fluorescence microscope (AxioImager II, Zeiss, Göttingen, Germany). Percentages of SSEA4-positive cells were reported against the total number of cells in four different fields of counting using Zen 2 software (blue edition 2011, Carl Zeiss Microscopy GmbH, Zeiss) to measure the fluorescent intensity where the positive cells had a higher mean fluorescent intensity than that of the background signal.

2.8. Statistical analysis

Since data derived from all assays performed in this study were normally distributed by the test of normality with the Shapiro-Wilk, analysis of variance (ANOVA) with Tukey's multiple comparisons was used to compare the numbers of clones, PDTs, newly-synthesized DNA amount, relative mRNA expression of *NANOG* and *OCT4*, and percentages of SSEA4-positive cells of the test groups with those of the control groups. Statistical analysis was calculated with Statistical Package for Social Sciences version 17 (SPSS; Chicago, IL, USA).

3. Results

3.1. Effect of PGE_2 on the number of clones

Clonogenic assays were first conducted with 500 cultured PDL cells for 14 d. The representative images of PDL clones stained with crystal violet in response to PGE_2 treatments are illustrated in Fig. 1A. Densely formed colonies were observed in PGE_2-treated groups at low doses (0.01, 0.1 and 1 ng/ml) compared with those of the untreated group (Fig. 1A). Quantitatively, the number of colonies was significantly increased by treatment with PGE_2 at concentrations from 0.01 to 10 ng/ml ($P < 0.001$), whereas the number of colonies upon PGE_2 treatment at 100 ng/ml did not significantly differ from that of the untreated group ($P = 0.051$; Fig. 1B). Note that several tiny colonies were situated in close proximity such that enhanced staining intensity of the colonies was demonstrated. However, an increase in the number of colonies could be clearly observed under higher magnification powers.

3.2. Effect of PGE_2 on the proliferation of PDL cells

The proliferative potential was first determined by AlamarBlue® assay at three different time points (1, 3 and 7 days). Because metabolic activity of PGE_2-treated PDL cells increased dramatically from day 3 to 7 (data not shown), PDTs were thus calculated from the numbers of cells between days 3 and 7. PDTs tended to decline by PGE_2 treatment at 0.1 ng/ml; however, the decrease did not statistically reach significance (Fig. 2A). Therefore, BrdU assay with a higher sensitivity to evaluate cell proliferation was conducted. The absorbance values, representing the amounts of DNA-bound BrdU, of the samples treated with PGE_2 at low doses (0.01, 0.1 and 1 ng/ml) and with 100 ng/ml of PMA significantly increased compared with those of the control ($P < 0.05$; Fig. 2B). However, there was no significant difference between these PGE_2-treated groups and the PMA group. On the contrary, a treatment with 100 ng/ml of PGE_2 significantly reduced the absorbance value compared with that of the control ($P < 0.05$; Fig. 2B), suggesting that a high dose of PGE_2 adversely affects PDL cell proliferation.

3.3. Effect of PGE_2 on expression of pluripotency-related markers

Next, the PDL stemness was further explored at the gene expression level. The mRNA expression of *NANOG* and *OCT4* was measured by real-time PCR. Treatment with PGE_2 at 0.1 and 1 ng/ml significantly enhanced *NANOG* ($P < 0.001$) and *OCT4* ($P < 0.05$), whereas treatment with PGE_2 at 0.01, 10 and 100 ng/ml did not significantly induce *NANOG* and *OCT4* expression (Fig. 3A). It is noteworthy that the
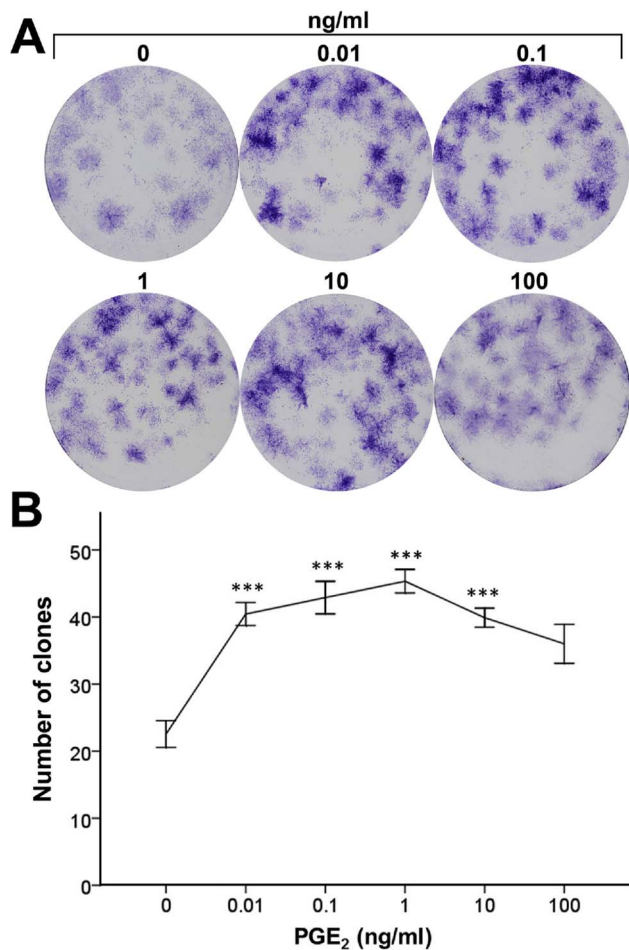
Fig. 1. Treatment with prostaglandin (PG) E$_2$ at low doses significantly induces the number of clones. Five hundred periodontal ligament (PDL) cells were seeded in 6-well culture plates and treated with PGE$_2$ at varying concentrations for 14 d. Cells were fixed and stained with crystal violet. Representative images of colony forming units upon PGE$_2$ treatment at indicated doses are shown in A. The number of clones consisting of more than 50 cells was counted under stereomicroscope and plotted in a linear graph (B). Error bars = standard deviation; $n = 3$. $^{***} = P < 0.001$.

induction of *NANOG* was greater than that of *OCT4*. Consistent with the induction of *NANOG* and *OCT4* mRNA expression, expression of the nuclear protein counterparts was up-regulated by treatment with PGE$_2$ at 0.1 and 1 ng/ml (Fig. 3B). Expression of HDAC1, a housekeeping gene control for nuclear protein fraction (Galbán et al., 2003), was approximately equal among the different samples.

3.4. Induction of SSEA4 expression by PGE$_2$ treatment

SSEA4, a human embryonic stem cell marker, was apparently expressed in human PDL cells treated with PGE$_2$ at according concentrations as observed by more intense fluorescent signals than those of the untreated cells (Fig. 4A). Correspondingly, treatments with PGE$_2$ at any concentrations from 0.01 to 100 ng/ml tended to cause the percentages of SSEA4-positive cells to increase; however, the percentage of SSEA4-positive cells was significantly increased only by treatment with PGE$_2$ at 1 ng/ml ($P < 0.05$; Fig. 4B).

4. Discussion

Although PGE$_2$ has previously been shown to cause an alteration in PDL mineralization where PDL stemness is expected to change (Manokawinchoke, Pimkhaokhum, Everts, & Pavasant, 2014), the effect of direct PGE$_2$ treatment in cultured PDL cells where characteristics of
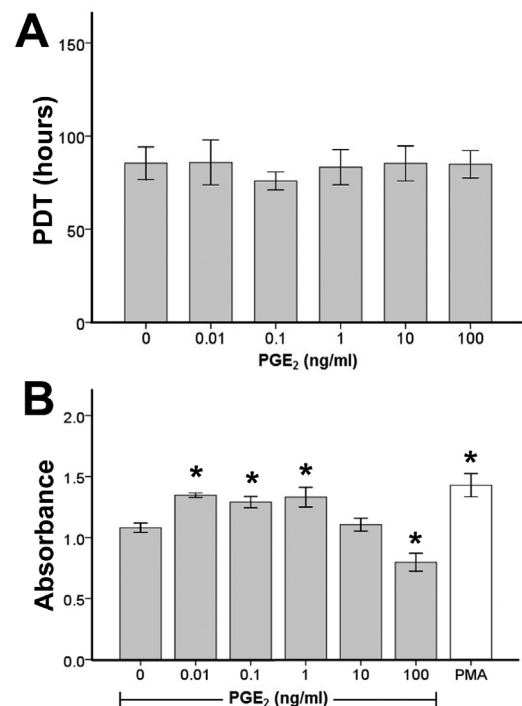
Fig. 2. PGE$_2$ at low doses significantly increases PDL cell proliferation. (A) A bar graph demonstrates population doubling times (PDTs) upon treatment with PGE$_2$ at varying concentrations, calculated from the number of cells as determined by an AlamarBlue® assay between days 3 and 7. Note PDTs tended to decline by treatment with PGE$_2$ at 0.1 ng/ml. (B) A bar graph shows a significant increase in absorbance values reflecting increased amounts of BrdU incorporation as determined by a BrdU assay in PDL cells treated with PGE$_2$ at low doses (0.01, 0.1 and 1 ng/ml) and with 100 ng/ml of phorbol 12-myristate 13-acetate (PMA, empty bar) compared with that of the untreated control group. Note treatment with PGE$_2$ at 100 ng/ml decreased the absorbance value compared with that of the control. Error bars = standard deviation; $n = 3$. $^{*} = P < 0.05$.

cellular stemness are examined has yet to be reported in scientific literature. Therefore, in the present work some aspects of stemness were studied in primary human PDL cells isolated from PDL tissues, cultured and exposed to PGE$_2$ at varying nontoxic concentrations. Firstly, proliferative potential and clonogenicity had been examined. Secondly, expression of pluripotency-related markers, including NANOG and OCT4, in response to treatment with PGE$_2$ at varying concentrations was determined at both transcriptional and translational levels. Finally, expression of SSEA4, a human embryonic stem cell marker, was investigated. The results revealed that treatment of PDL cells with PGE$_2$ at low concentrations (0.01, 0.1 and 1 ng/ml) significantly increased cell proliferation and the number of clones. Furthermore, PGE$_2$ at low doses (0.1 and 1 ng/ml) might help maintain PDL stemness, as evidenced by significantly up-regulated expression of NANOG and OCT4 at both mRNA and protein levels. Nevertheless, significantly increased expression of SSEA4 in terms of the number of SSEA4-positive cells was only observed in cells treated with PGE$_2$ at 1 ng/ml.

Even though this study is limited to *in vitro* findings that cannot yet reflect the physiological status or are not ready to be translated into clinical applications, it is rather clear that PDL cells have a threshold where expression of important embryonic stem cells is enhanced. It is speculative that in the physiological condition, PDL cells would similarly exhibit this feature which indicates a status where stemness is retained or even enhanced. Additional animal or clinical studies are, therefore, required to address a possible translation of the *in vitro* findings to physiological and clinical significances and to prove whether or not PGE$_2$ has any differential effects comparable to the *in vitro* results.

PDL cells originate from ectomesenchymal cells in the dental follicle surrounding the developing tooth bud. Although most of the
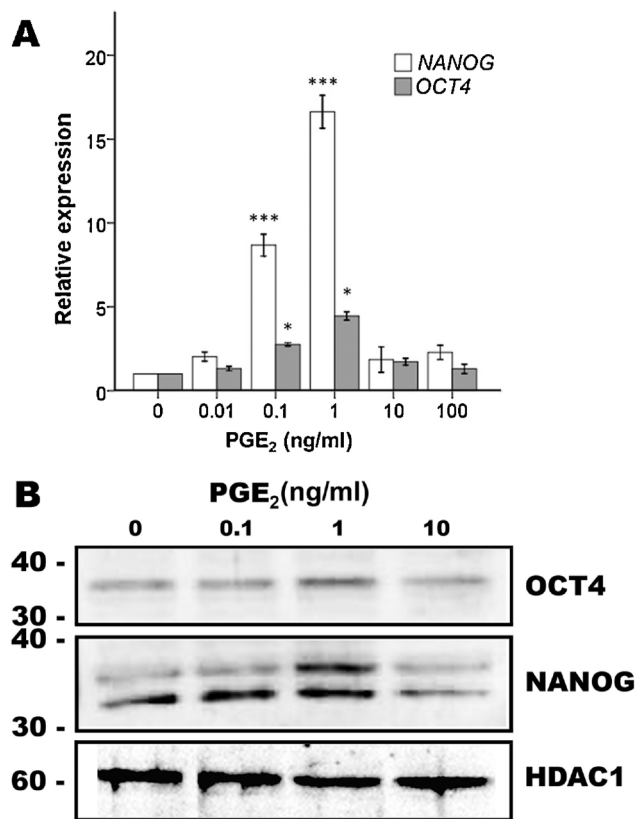
Fig. 3. Treatment with PGE$_2$ at low doses for 72 h up-regulates mRNA and protein expression of NANOG and OCT4. (A) Significant induction of *NANOG* (empty bars) and *OCT4* (gray bars) mRNA expression upon treatment with PGE$_2$ at 0.1 and 1 ng/ml. Error bars = standard deviation; $n = 3$. *** $= P < 0.001$; * $= P < 0.05$. (B) Up-regulation of NANOG and OCT4 protein expression in nuclear extract of PDL cells treated with PGE$_2$ at 1 ng/ml. Expression of human histone deacetylase 1 (HDAC1) was equal among the different samples. Note the molecular weights of OCT4 and HDAC1 are as predicted, whereas there are two bands above 30 kDa for NANOG protein expression in the nuclear extract similar to a previous result shown in mouse embryonic stem cells (Hatano et al., 2005). These blots are representative of three independent experiments using three different PDL cell lines.

Fig. 4. Expression of stage-specific embryonic antigen 4 (SSEA4) is induced by PGE$_2$ treatment. (A) Representative immunofluorescence images demonstrate punctate distribution of SSEA4 expression in PDL cells, especially more intense fluorescent signals observed in cells treated with PGE$_2$ for 72 h than those of the untreated cells. (B) A bar graph shows a significant increase in percentage of SSEA4-positive cells upon treatment of PDL cells with PGE$_2$ at 1 ng/ml. Error bars = standard deviation; $n = 3$. * $= P < 0.05$.

ectomesenchymal cells have undergone cellular differentiations into several specific cell types, including osteoblasts, cementoblasts, fibroblasts, the remaining cells retain themselves in an undifferentiated state where multipotency is still maintained. Multipotency of PDL cells has been demonstrated in a few studies in which mesenchymal cells could differentiate into specialized cells belonging to three embryonic germ layers, including ectodermal (neurons), mesodermal (adipocytes, osteoblasts and chondrocytes) and endodermal (hepatocytes) lineages (Gay, Chen, & MacDougall, 2007; Kawanabe et al., 2010). In physiological conditions, it has been proposed that continual masticatory force is important for PDL functions in maintaining homeostasis of periodontium (Pavasant & Yongchaitrakul, 2011) partly because mechanical stress from masticatory force appears to involve the maintenance of multipotency in PDL by stimulating an extracellular release of ATP and a subsequent induction of COX/PGE$_2$ synthesis and PGE$_2$ secretion by PDL cells (Luckprom, Wongkhantee, Yongchaitrakul, & Pavasant, 2010; Wongkhantee, Yongchaitrakul, & Pavasant, 2008). It is well known that PGE$_2$ has a broad spectrum of cellular activities because not only are there at least four major types of prostaglandin E receptors distributed unevenly elsewhere in different tissue types, but also differential affinity of PGE$_2$ for various EP receptors leads to different cellular responses. Therefore, the concentration of PGE$_2$ should be considered carefully in any experimental studies because different concentrations render distinct biological effects.

PGE$_2$ at low doses was reported to promote proliferation of several

different cell types. For example, endogenous PGE$_2$ exerted positive influence on proliferation of human mesenchymal stem cells derived from umbilical cord blood and adipose tissue (Lee et al., 2016). Inhibition of either COX or its downstream molecule, *i.e.* microsomal PGE synthase-1 (mPGES-1), led to G$_1$ cell cycle arrest that inhibited cell division according to the fluorescence-activated cell sorter analysis (Lee et al., 2016). Inhibition of the COX/PGE$_2$ axis in ankylosing spondylitic fibroblasts with inhibitors significantly decreased cell proliferation as per EdU (5-ethynyl-2′-deoxyuridine) incorporation assay (Zou, Yang, Yuan, Zhang, & Li, 2016). Consistent with the findings from these aforementioned studies, the result from this study showed a significant increase in proliferation of PDL cells with PGE$_2$ treatment at 0.01, 0.1 and 1 ng/ml. Similarly, the number of clones was significantly increased and the clones were densely populated by PGE$_2$ treatment at these low doses.

In agreement with increased cell proliferation and enhanced number of clones, expression of pluripotency-related markers, NANOG and OCT4, was up-regulated at both transcriptional and translational levels with PGE$_2$ treatment at low doses (0.1 and 1 ng/ml). Although concentrations of PGE$_2$ used to enhance expression of pluripotent markers vary among cell types due to cell-type-specific responses, our results appear to be consistent with those of many studies, previously demonstrating the importance of PGE$_2$ on stemness maintenance in different cell types. For instance, at low levels (0.01 and 0.1 ng/ml) did PGE$_2$ increase expression of *NANOG* and *OCT4* in human tendon stem cells, implying stemness retention, but at a high level did it increase expression of *RUNX2*, inferring cellular differentiation (Zhang & Wang, 2014). Moreover, silencing the expression of mPGES-1 with siRNA transfection in prostate cancer cells resulted in a decrease in expression of *NANOG* and *OCT4* as well as vimentin, a protein involved in a process of epithelial-mesenchymal transition (Finetti et al., 2015).

In addition to expression of NANOG and OCT4, SSEA4 was used as a screening marker for stemness of PDL cells treated with PGE_2 basically because SSEA4 is rarely expressed in differentiating cells (Draper, Pigott, Thomson, & Andrews, 2002). SSEA4-positive cells were reported to locate in different tissues of mesenchymal origin, for example, limbal stromal cells, patellar tendon cells and PDL cells (Kawanabe et al., 2010; Lim et al., 2012; Zhang & Wang, 2014). Besides, these SSEA4-positive cells possess multipotency with which the cells could differentiate into several cell lineages (Kawanabe et al., 2010; Lim et al., 2012; Zhang & Wang, 2013). The finding from this study showed that PGE_2 treatment at low doses (0.01, 0.1 and 1 ng/ml) increased the number of SSEA4-positive cells; however, only at 1 ng/ml could PGE_2 yield a statistically significant increase in SSEA4 expression. This finding corresponds with expression of surface markers found in tendon stem cells where both STRO-1 and SSEA4 were enhanced in terms of increased positive cell numbers with PGE_2 treatment at a low dose (0.01 ng/ml), albeit a difference in optimal concentrations (Zhang & Wang, 2014). Moreover, enhancement of SSEA4 in this study coincides with induction of NANOG and OCT4 expression, collectively suggesting that stemness might have been enhanced to a certain extent. However, it is noteworthy that expression of SSEA-4 in mesenchymal stem cells may be an artificial induction in the culture as fetal calf serum contains globoseries glycosphingolipids, which can be recognized by an SSEA-4 antibody, and *in vitro* exposure to fetal calf serum may also induce SSEA-4 expression (Suila et al., 2011).

The results from this study may provide clinical translation of PGE_2 thresholds in stemness maintenance of PDL cells where high proliferative rate, clone-formation ability and multipotency are held, and thus the determination of PGE_2 concentration in gingival crevicular fluid is herein speculated to be used for an estimation of optimal PGE_2 levels that support a niche to PDL stemness. Unfortunately, clinical investigations into the baseline PGE_2 levels in gingival crevicular fluid collected from gingival sulci surrounding non-inflamed periodontium of healthy volunteers have yet to be established. These levels may prove useful for orthodontic tooth movement where the ability of PDL cells to maintain their stemness is possibly critical for a stem cell reservoir in PDL tissues during periodontal tissue remodeling after an application of orthodontic force. In summary, some aspects of stemness maintenance, including proliferative potential, clone-formation ability, and induction of pluripotency-related markers, by PGE_2 treatment at low doses have been demonstrated in cultured human PDL cells. However, it is still necessary to perform cell differentiation assays to assure that PDL stemness is truly maintained in a future study. Moreover, involvement of signaling pathways that mediate the effects of PGE_2 at low doses on stemness maintenance in PDL cells warrants further investigations.

Competing financial interest

All authors deny any competing financial interests.

Ethical approval

The protocol to retrieve human PDL cells was approved by the Human Exprierimentation committe, Faculty of Dentistry, Chiang Mai University (# 40/2016).

Acknowledgements

References

Chu, T. H., Chan, H. H., Kuo, H. M., Liu, L. F., Hu, T. H., Sun, C. K., ... Tai, M. H. (2014). Celecoxib suppresses hepatoma stemness and progression by up-regulating PTEN. *Oncotarget, 5*(6), 1475–1490.

Draper, J. S., Pigott, C., Thomson, J. A., & Andrews, P. W. (2002). Surface antigens of human embryonic stem cells: Changes upon differentiation in culture. *Journal of Anatomy, 200*(Pt 3), 249–258.

Finetti, F., Terzuoli, E., Giachetti, A., Santi, R., Villari, D., Hanaka, H., & Donnini, S. (2015). mPGES-1 in prostate cancer controls stemness and amplifies epidermal growth factor receptor-driven oncogenicity. *Endocrine-Related Cancer, 22*(4), 665–678.

Galbán, S., Martindale, J. L., Mazan-Mamczarz, K., López de Silanes, I., Fan, J., Wang, W., ... Gorospe, M. (2003). Influence of the RNA-binding protein HuR in pVHL-regulated p53 expression in renal carcinoma cells. *Molecular and Cellular Biology, 23*(20), 7083–7095.

Gay, I. C., Chen, S., & MacDougall, M. (2007). Isolation and characterization of multipotent human periodontal ligament stem cells. *Orthodontics and Craniofacial Research, 10*(3), 149–160.

Hatano, S. Y., Tada, M., Kimura, H., Yamaguchi, S., Kono, T., Nakano, T., ... Tada, T. (2005). Pluripotential competence of cells associated with Nanog activity. *Mechanisms of Development, 122*(1), 67–79.

Hinz, B. (2013). Matrix mechanics and regulation of the fibroblast phenotype. *Periodontology 2000, 63*(1), 14–28.

Ivanovski, S., Gronthos, S., Shi, S., & Bartold, P. M. (2006). Stem cells in the periodontal ligament. *Oral Diseases, 12*(4), 358–363.

Kawanabe, N., Murata, S., Murakami, K., Ishihara, Y., Hayano, S., Kurosaka, H., & Yamashiro, T. (2010). Isolation of multipotent stem cells in human periodontal ligament using stage-specific embryonic antigen-4. *Differentiation, 79*(2), 74–83.

Lee, B. C., Kim, H. S., Shin, T. H., Kang, I., Lee, J. Y., Kim, J. J., ... Kang, K. S. (2016). PGE2 maintains self-renewal of human adult stem cells via EP2-mediated autocrine signaling and its production is regulated by cell-to-cell contact. *Scientific Reports, 6*, 26298.

Lim, M. N., Hussin, N. H., Othman, A., Umapathy, T., Baharuddin, P., Jamal, R., & Zakaria, Z. (2012). Ex vivo expanded SSEA-4+ human limbal stromal cells are multipotent and do not express other embryonic stem cell markers. *Molecular Vision, 18*, 1289–1300.

Lim, W. H., Liu, B., Cheng, D., Williams, B. O., Mah, S. J., & Helms, J. A. (2014). Wnt signaling regulates homeostasis of the periodontal ligament. *Journal of Periodontal Research, 49*(6), 751–759.

Liu, Q., Yuan, W., Tong, D., Liu, G., Lan, W., Zhang, D., ... Jiang, J. (2016). Metformin represses bladder cancer progression by inhibiting stem cell repopulation via COX2/PGE2/STAT3 axis. *Oncotarget, 7*(19), 28235–28246.

Luckprom, P., Wongkhantee, S., Yongchaitrakul, T., & Pavasant, P. (2010). Adenosine triphosphate stimulates RANKL expression through P2Y1 receptor-cyclo-oxygenase-dependent pathway in human periodontal ligament cells. *Journal of Periodontal Research, 45*(3), 404–411.

Manokawinchoke, J., Pimkhaokhum, A., Everts, V., & Pavasant, P. (2014). Prostaglandin E2 inhibits in-vitro mineral deposition by human periodontal ligament cells via modulating the expression of TWIST1 and RUNX2. *Journal of Periodontal Research, 49*(6), 777–784.

Moon, C. M., Kwon, J. H., Kim, J. S., Oh, S. H., Lee, J. K., Park, J. J., ... Kim, W. H. (2014). Nonsteroidal anti-inflammatory drugs suppress cancer stem cells via inhibiting PTGS2 (cyclooxygenase 2) and NOTCH/HES1 and activating PPARG in colorectal cancer. *International Journal of Cancer, 134*(3), 519–529.

Osathanon, T., Subbalekha, K., Sastravaha, P., & Pavasant, P. (2012). Notch signalling inhibits the adipogenic differentiation of single-cell-derived mesenchymal stem cell clones isolated from human adipose tissue. *Cell Biology International, 36*(12), 1161–1170.

Pavasant, P., & Yongchaitrakul, T. (2011). Role of mechanical stress on the function of periodontal ligament cells. *Periodontology 2000, 56*(1), 154–165.

Ricciotti, E., & Fitzgerald, G. A. (2011). Prostaglandins and inflammation. *Arteriosclerosis, Thrombosis, and Vascular Biology, 31*(5), 986–1000.

Suila, H., Pitkänen, V., Hirvonen, T., Heiskanen, A., Anderson, H., Laitinen, A., ... Valmu, L. (2011). Are globoseries glycosphingolipids SSEA-3 and −4 markers for stem cells derived from human umbilical cord blood? *Journal of Molecular Cell Biology, 3*(2), 99–107.

Wongkhantee, S., Yongchaitrakul, T., & Pavasant, P. (2008). Mechanical stress induces osteopontin via ATP/P2Y1 in periodontal cells. *Journal of Dental Research, 87*(6), 564–568.

Zhang, J., & Wang, J. H. (2013). Human tendon stem cells better maintain their stemness in hypoxic culture conditions. *PloS One, 8*(4), e61424.

Zhang, J., & Wang, J. H. (2014). Prostaglandin E2 (PGE2) exerts biphasic effects on human tendon stem cells. *PloS One, 9*(2), e87706.

Zou, Y. C., Yang, X. W., Yuan, S. G., Zhang, P., & Li, Y. K. (2016). Celastrol inhibits prostaglandin E2-induced proliferation and osteogenic differentiation of fibroblasts isolated from ankylosing spondylitis hip tissues in vitro. *Drug Design Development and Therapy, 10*, 933–948.

ORIGINAL RESEARCH

Supplementary techniques for pain control during root canal treatment of lower posterior teeth with irreversible pulpitis: A systematic review and meta-analysis

Pinpana Tupyota, DDS, MSc[1]; Pattama Chailertvanitkul, DDS, PhD[1],* (iD); Malinee Laopaiboon, PhD[2]; Chetta Ngamjarus, PhD[2]; Paul V. Abbott, BDSc, MDS, FRACDS(Endo), FPFA, FADI, FICD, FACD[3] (iD); and Suttichai Krisanaprakornkit, DDS, MSD, PhD[4]

1 Department of Restorative Dentistry, Faculty of Dentistry, Khon Kaen University, Khon Kaen, Thailand
2 Department of Biostatistics and Demography, Faculty of Public Health, Khon Kaen University, Khon Kaen, Thailand
3 School of Dentistry, University of Western Australia, Nedlands, Western Australia, Australia
4 Department of Oral Biology and Diagnostic Sciences, Faculty of Dentistry Center of Excellence in Oral and Maxillofacial Biology, Chiang Mai University, Chiang Mai, Thailand

Abstract

The purpose of this systematic review and meta-analysis was to evaluate utilisation of supplementary techniques for pain control during root canal treatment of lower molars with irreversible pulpitis. The literature was searched using electronic databases up to year 2012. Seventeen studies with 1504 participants were included and each study compared experimental interventions with a standard treatment, i.e. the inferior alveolar nerve block. Changing the injection techniques or supplemental injection had no significant effect on pulp anaesthesia compared to the standard treatment ($P = 1.00$ or $P = 0.14$), whereas changing anaesthetic features and increasing anaesthetic volumes resulted in significantly higher rates of anaesthesia than those of the standard treatment ($P = 0.03$ and $P = 0.007$, respectively). Premedication with non-steroidal anti-inflammatory drugs (NSAIDs) also significantly increased the success rate of anaesthesia ($P = 0.001$). Taken together, increased anaesthetic volumes and premedication with NSAIDs provide predictable anaesthesia and more pain control during endodontic treatment of lower molars with irreversible pulpitis.

Introduction

The inferior alveolar nerve block (IANB) is the most commonly used local anaesthetic technique for root canal treatment of mandibular teeth. In healthy teeth, the failure rate of IANB is 15%, whereas this rate increases dramatically to be as high as 44–81% in teeth with acute irreversible pulpitis (1). Numerous studies have evaluated the efficacy of different pain management strategies as well as the influences of various supplemental anaesthetic techniques and pre-operative medications with distinct methods and results. The purpose of this systematic review was, therefore, to assess the effectiveness of various interventions for pain relief during root canal treatment in lower molars with irreversible pulpitis.

Materials and Methods

Inclusion criteria for eligible studies

Type of studies

Randomised control trials (RCTs) that compared various interventions with a standard intervention (IANB) for pain relief during root canal treatment in lower molars with irreversible pulpitis.

Type of participants

Adults aged 18 years and above who were experiencing pain in mandibular molars as a result of irreversible pulpitis. Radiographs showed no periapical radiolucency other than a widened periodontal ligament space. The

participants were able to understand and use a visual pain scale. The participants were in good health and not taking any medications that would alter their pain perception, and females were neither pregnant nor breastfeeding.

Type of interventions

Any supplementary interventions, such as changing the injection techniques, supplemental injection, changing the characteristics of local anaesthetic agents, or using pre-operative medications with analgesic drugs, were considered. The standard intervention was defined as use of local anaesthetic injection by IANB.

Type of outcome measures

The primary outcome was clinical success of pulp anaesthesia such that the participants felt only mild or no pain during root canal treatment.

Search methods for identification of studies and data collection

The following databases were searched for relevant trials from the inception of each electronic database to April 2013: Cochrane Central Register of Controlled Trials (CENTRAL) http://www.thecochranelibrary.com/view/0/index.htmll, MEDLINE (Pubmed) http://www.ncbi.nlm.nih.gov/pubmed?holding=ithkkumlib, SCOPUS http://www.scopus.com/home.url, and MEDLINE (Ovid) http://ovidsp.tx.ovid.com/sp3.8.0a/ovidweb.cgi. The following keywords were used: 'inferior alveolar nerve block', 'irreversible pulpitis', and 'randomised or randomised control trials'.

Hand searching was performed in relevant journals from 2003 to 2012 plus Journal of the Endodontic Society of Thailand, Khon Kaen University Dental Journal, Mahidol Dental Journal, Chiang Mai Dental Journal, Journal of the Dental Association of Thailand, Srinakharinwirot University Dental Journal, Chulalongkorn University Dental Journal, North-Eastern Thai Journal of Neuroscience, Thai Journal of Oral and Maxillofacial Surgery, Journal of Orofacial Pain and Songklanagarind Medical Journal.

Two reviewers (PT and PC) independently screened abstracts of the potential articles obtained from all the electronic and hand searching to decide whether the studies met the inclusion criteria. Any disagreements were resolved by discussion. A third reviewer (ML) was consulted if there was any unresolved disagreement. Full texts of the eligible articles were then separately reviewed by the first two reviewers.

Assessment for the methodological quality of included studies

The risk of bias for all included studies was assessed using seven domains as described in the Cochrane Handbook for Systematic Reviews of Interventions (2), including sequence generation, allocation concealment, blinding of participants, personnel and outcome assessors, incomplete outcome data, selective outcome reporting and other potential sources of bias. The judgment for each item was 'Yes' indicating low risk of bias, 'No' indicating high risk of bias, or 'Questionable' indicating the lack of information. If the sequence generation and allocation concealment of each study were judged to have a low risk of bias, its quality was assumed to have a low risk of bias.

Data analysis

Data analysis was carried out using Revman 5.2 software (Cochrane Collaboration, Oxford, UK) (2). The rate of successful pulp anaesthesia was expressed as relative risk (RR) with 95% confidence interval (CI). The RR and 95% CI for pain relief improvement of individual studies were presented using forest plots. The heterogeneity of results from included studies was investigated by I square (I^2). The statistical heterogeneity was presented as significant when I^2 was over 50% or $P < 0.10$. Sub-group analysis was conducted to investigate whether there was a statistically significant difference between interventions. The random effect meta-analysis was used to combine success rates of anaesthesia. A funnel plot of successful pulp anaesthesia was conducted to identify a publication bias.

Results

A total of 113 articles were retrieved from PubMed ($n = 34$), CENTRAL ($n = 17$), SCOPUS ($n = 33$) and Ovid ($n = 29$), while there was no additional article found through other sources by hand searching (Fig. 1). All articles were evaluated by reading their titles and abstracts. Seventy-seven articles were rejected as being from the same journals and fourteen articles were rejected because they did not meet the inclusion criteria. Twenty-two full texts were evaluated independently by two reviewers (PT and PC), from which five studies were rejected as not meeting the inclusion criteria. Thus, 17 studies were assessed for quality and their data were analysed (Fig. 1).

There were 1504 participants involved in these 17 studies (Table 1), and each study compared the experimental (supplemental) techniques with the standard intervention of IANB. The 17 studies were divided into

```
┌─────────────────────────────┐
│  113 records identified     │        ┌──────────────────────────┐
│  through searching          │        │  No additional record    │
│  electronic databases       │        │  identified by hand      │
│  [PubMed (34), CENTRAL      │        │  searching (n = 0)       │
│  (17), SCOPUS (33) and      │        └──────────────────────────┘
│  Ovid (29)]                 │
└─────────────────────────────┘
```

Figure 1 — PRISMA flow diagram:

- 113 records identified through searching electronic databases [PubMed (34), CENTRAL (17), SCOPUS (33) and Ovid (29)]
- No additional record identified by hand searching (n = 0)
- 77 records removed due to duplication
- 36 records screened from their abstracts
- 14 records excluded
- 22 full-text articles assessed for eligibility
- 5 full-text articles excluded (did not meet criteria)
- 17 studies included in qualitative synthesis
- 16 studies included in quantitative synthesis (meta-analysis)

Figure 1 PRISMA flow diagram of the meta-analysis.

five categories for comparison, and some studies were used for more than one comparison. Of the 17 studies, 15 studies showed comparable baseline characteristics of the participants, such as gender, age, initial pain and distribution of teeth. The quality of included articles was good since most of them had low risk (Fig. 2). As summarised in Table 1, the indicators used to determine clinically successful IANB in 17 studies varied as ten studies used lip numbness, while five studies used lip numbness plus a cold pulp test and two studies used electric pulp testing. Thirteen studies used the Heft-Parker visual analogue scale, two studies used a verbal analogue scale, one study used a visual analogue scale and one study used verbal description of pain whilst having root canal treatment. A funnel plot of primary outcome from eight included studies relating to changing the features of local anaesthetic is shown in Figure 3, and the symmetry of eight plots, which means no publication bias, was demonstrated.

Effects of interventions

1. Changing the techniques of local anaesthetic injection versus standard intervention. Buccal infiltration with 4% articaine and 1:100 000 epinephrine was compared in

Table 1 Characteristics of 17 included studies

Study	Methods	Participants	Interventions	Outcome
Poorni *et al.* (3)	156 volunteers	Healthy, aged 18–30 years with active pain of at least 54 mm. HP-VAS in mandibular molars, prolonged response to cold testing with ice stick and EPT, absence of any periapical radiolucency on radiograph except widening PDL space, vital coronal pulp on access opening	Group I: IANB with 4% articaine with 1:100 000 adrenaline (*n* = 52) Group II: Buccal infiltration with 4% articaine with 1:100 000 adrenaline (*n* = 52) Group III (control): IANB using 2% lidocaine with 1:100 000 adrenaline (*n* = 52)	Success was the ability to access and instrument the tooth without pain (VAS score 0) or mild pain (VAS ≤ 54)
Aggarwal *et al.* (4)	87 patients with actively experiencing pain	Good health, not taking any medication that would alter pain perception, actively experiencing pain in a mandibular molar, prolonged response to cold testing with an ice stick and EPT, absence of any periapical radiolucency on radiographs, except for a widened PDL and vital coronal pulp on access opening	Group I: Supplemental with buccal and lingual infiltration with 2% articaine with 1:200 000 epinephrine two min after IANB with 1.8 mL of 2% lidocaine with 1:200 000 epinephrine (*n* = 31) Group II: Supplemental with buccal and lingual infiltration with 2% lidocaine with 1:200 000 epinephrine two min after IANB with 1.8 mL of 2% lidocaine with 1:200 000 epinephrine (*n* = 31) Group III (control): IANB with 1.8 mL of 2% lidocaine with 1:200 000 epinephrine (*n* = 25)	Success rate to pulpal anaesthesia: no pain or weak/ mild pain during access preparation and instrumentation
Parirokh *et al.* (5)	84 patients	Older than 18 years, healthy, having a first mandibular molar with irreversible pulpitis and normal periapical radiographic appearance (clinical diagnosis of irreversible pulpitis was confirmed by a positive response to an EPT and a prolonged response with moderate to severe pain to a cold test using Roeko Endo-Frost)	Group I (control): IANB using 1.8 mL 2% lidocaine with 1:80 000 epinephrine (*n* = 28) Group II: IANB using 3.6 mL 2% lidocaine with 1:80 000 epinephrine (*n* = 28) Group III: IANB using 1.8 mL 2% lidocaine with 1:80 000 epinephrine plus buccal infiltration using 1.8 mL 2% lidocaine with 1:80 000 epinephrine (*n* = 28)	Success was no pain or weak/mild pain during endodontic access preparation and instrumentation
Aggarwal *et al.* (6)	55 volunteers selected from dental emergency department	Good health, none were taking any medication that would alter pain perception, as determined by oral questioning and written questionnaire, actively experiencing pain in a mandibular molar (>54 mm on Heft-Parker visual analogue scale: HP-VAS), prolonged response to cold testing with an ice stick and EPT, absence of any periapical radiolucency on radiographs, except for a widened PDL and vital coronal pulp on access opening, American Society of Anesthesiologists class I or II medical history and ability to understand the use of pain scale	Group I (control): IANB using 1.8 mL of 2% lidocaine with 1:200 000 epinephrine (*n* = 27) Group II: IANB using 3.6 mL of 2% lidocaine with 1:200,000 epinephrine (*n* = 28)	Success was no pain or weak/mild pain during endodontic access preparation and instrumentation

(continued)

Table 1 (continued)

Study	Methods	Participants	Interventions	Outcome
Bigby *et al.* (7)	50 patients diagnosed with irreversible pulpitis of a mandibular posterior tooth	A vital mandibular posterior tooth (molar or premolar), actively experiencing pain, had a prolonged response to cold testing with Endo-ice	Group I (control): IANB using 1.8 mL of 36 mg of lidocaine with 18 µg of epinephrine (n = 24) Group II: IANB using 3.6 mL of 36 mg of lidocaine with 18 µg of epinephrine plus 36 mg of meperidine with 18 µg of epinephrine (n = 26)	Success was the ability to access and instrument the tooth without pain (VAS score 0) or mild pain (VAS ≤ 54)
Kreimer *et al.* (8)	106 patients participated in the studies: 55 patients enrolled in study I and 51 patients enrolled in study II. Study II was excluded from data analysis due to an inability to compare with standard treatment (IANB 2% lidocaine)	Adults with a vital mandibular posterior tooth (molar or premolar, actively experiencing pain and had a prolonged response to cold testing with Endo-ice	Group I (control): IANB using 3.18 mL formulation containing 63.6 mg of lidocaine with 31.8 µg epinephrine (n = 27) Group II: IANB using 5 mL formulation containing 63.6 mg of lidocaine with 31.8 µg epinephrine (3.18 mL) plus 1.82 mL of 0.5 mol L^{-1} mannitol (n = 28)	Success was the ability to access and instrument the tooth without pain (VAS score 0) or mild pain (VAS ≤ 54)
Claffey *et al.* (9)	72 patients diagnosed with irreversible pulpitis of a mandibular posterior tooth	Good health, had a vital mandibular posterior tooth (molar or premolar), actively experiencing pain and had a prolonged response to cold testing with Endo-ice	Group I: IANB using 2.2 mL of 4% articaine with 1:100 000 epinephrine (n = 37) Group II (control): IANB using 2.2 mL of 2% lidocaine with 1:100 000 epinephrine (n = 35)	Success was the ability to access and instrument the tooth without pain (VAS score 0) or mild pain (VAS ≤ 54)
Sampaio *et al.* (10)	70 patients	18–50 years old, good health according to a health history questionnaire, had at least one molar adjacent to a molar presenting irreversible pulpitis and a healthy contralateral canine with no deep carious lesions, extensive restoration, advanced periodontal disease, a history of trauma, or sensitivity, had a moderate to severe spontaneous pain, positive response to the electric pulp test and a prolonged response to cold testing with Endo-Frost	Group I (control): IANB using 3.6 mL of 2% lidocaine with 1:100 000 epinephrine (n = 35) Group II: IANB using 3.6 mL of 0.5% bupivacaine with 1:200 000 epinephrine (n = 35)	Success was defined as no pain (pain score 0 or 1) during endodontic access preparation and root canal instrumentation
Tortamano *et al.* (11)	40 patients with actively experiencing pain	18–50 years old, good health as determined by a health history questionnaire. Moderate severe spontaneous pain and exhibited a positive response to EPT and a prolonged response to cold testing with Endo-Frost. Had at least one adjacent tooth plus a healthy contralateral canine or a contralateral canine without deep carious lesions, extensive restoration, advanced periodontal disease, history of trauma or sensitivity	Group I (control): IANB using 3.6 mL of 2% lidocaine with 1:100 000 epinephrine (n = 20) Group II: IANB using 3.6 mL of 4% articaine with 1:100 000 epinephrine (n = 20)	Success was no pain (pain score 0 or 1) during access preparation and root canal instrumentation

(continued)

Table 1 (continued)

Study	Methods	Participants	Interventions	Outcome
Aggarwal et al. (12)	72 patients actively experiencing pain	Good health, not taking any medication that would alter pain perception, actively experiencing pain in a mandibular molar, a prolonged response to cold testing with an ice stick and EPT, absence of any periapical radiolucency on radiographs, except for widened PDL and vital coronal pulp on access opening and ability to understand the use of pain scale	Group I: Premedication with ibuprofen 600 mg one h before IANB with 2% lidocaine with 1:200 000 epinephrine (n = 24) Group II: Premedication with ketorolac 20 mg one h before IANB with 2% lidocaine with 1:200 000 epinephrine (n = 24) Group III (control): Premedication with starch (placebo) one h before IANB with 2% lidocaine with 1:200 000 epinephrine (n = 24)	Success was no pain or weak/mild pain during endodontic access preparation and instrumentation
Oleson et al. (13)	100 patients diagnosed with irreversible pulpitis of a mandibular posterior tooth	Not taken any analgesics for at least eight hours before enrolment, a vital mandibular posterior tooth, actively experiencing pain, a prolonged response to cold test, had no periradicular pathosis (other than widened PDL), vital coronal pulp tissue on access	Group I: Premedication with ibuprofen 800 mg 45 min before IANB with 2% lidocaine with 1:100 000 epinephrine (n = 49) Group II (control): Premedication with placebo 45 min before IANB with 2% lidocaine with 1:100 000 epinephrine (n = 51)	Success was the ability to access and instrument the tooth without pain (VAS score 0), or mild pain (VAS ≤ 54)
Parirokh et al. (14)	150 patients with irreversible pulpitis	Over 18 years of age, healthy, having a first or second mandibular molar with irreversible pulpitis and normal periapical radiographic appearance (clinical diagnosis of irreversible pulpitis was confirmed by a response to an electric pulp test and a prolonged and exaggerated response with moderate to severe pain to cold test using Roeko Endo-Frost)	Group I: Premedication with 600 mg ibuprofen one h before IANB with 2% lidocaine with 1:80 000 epinephrine (n = 50) Group II: Premedication with 75 mg indomethacin one h before IANB with 2% lidocaine with 1:80 000 epinephrine (n = 50) Group III (control): Premedication with placebo one h before IANB with 2% lidocaine with 1:80 000 epinephrine (n = 50)	Success was no pain or weak/mild pain during endodontic access preparation and instrumentation
Prasanna et al. (15)	114 patients with irreversible pulpitis of a mandibular posterior tooth	Age range of 21–40 years who reported to the dental emergency department, healthy (ASA I or II), experiencing pain in a mandibular molar with a prolonged response to cold testing (lingering pain more than 45 s) and EPT, vital pulp, absence of periapical radiolucency on radiograph except for widened PDL space, ability to understand the use of pain scales	Group I: Premedication with 8 mg lornoxicam one h before IANB with 1.8 mL 2% lidocaine containing 1:200 000 epinephrine (n = 38) Group II: Premedication with 50 mg diclofenac potassium 1 h before IANB with 1.8 mL 2% lidocaine containing 1:200 000 epinephrine (n = 38) Group III (control): Premedication with placebo 1 h before IANB with 1.8 mL 2% lidocaine containing 1:200 000 epinephrine (n = 38)	Success was no pain during endodontic access preparation and root canal instrumentation

(continued)

Table 1 (continued)

Study	Methods	Participants	Interventions	Outcome
Shahi et al. (16)	165 patients	Adults had not taken any analgesics for at least 12 hours before enrolment in the study and had a first or second mandibular molar with asymptomatic irreversible pulpitis and a normal periapical radiographic appearance. The clinical diagnosis of irreversible pulpitis was verified by a prolonged response to cold testing with Green Endo-Ice	Group I (control): Premedication with placebo + IANB using 1.8 mL 2% lidocaine with 1:80 000 epinephrine (n = 55) Group II: Premedication with 0.5 dexamethasone + IANB using 1.8 mL 2% lidocaine with 1:80 000 epinephrine (n = 55) Group III: Premedication with 400 mg ibuprofen + IANB using 1.8 mL 2% lidocaine with 1:80 000 epinephrine (n = 55)	Success was no pain or mild pain (VAS < 20) during endodontic access preparation and instrumentation
Ianiro et al. (17)	40 patients diagnosed with irreversible pulpitis of a posterior mandibular tooth	Nine years or older, diagnosis of irreversible pulpitis in a posterior mandibular tooth, good health, had no contra-indication to taking acetaminophen, ibuprofen or sugar placebo	Group I: (n = 14): Premedication with 1000 mg acetaminophen + IANB with 3.6 mL of 2% lidocaine with 1:100 000 epinephrine Group II (n = 13): Premedication with 1000 mg acetaminophen + 600 mg ibuprofen + IANB with 3.6 mL of 2% lidocaine with 1:100 000 epinephrine Group III (control; n = 13): Premedication with placebo + IANB with 3.6 mL of 2% lidocaine with 1:100 000 epinephrine	If access and subsequent treatment were rendered without pain, the IANB was recorded as a success
Simpson et al. (18)	100 patients with a clinical diagnosis of symptomatic irreversible pulpitis	Adult patients had not taken any analgesics for at least eight hours before enrolment in the study, had a vital mandibular posterior tooth (molar or premolar), actively experiencing moderate to severe pain and had a prolonged response to cold testing with Green Endo-Ice	Group I: Premedication with a combination of 800 mg ibuprofen USP powder and 1000 mg acetaminophen USP powder + IANB using 1.8 mL 2% lidocaine with 1:100 000 epinephrine (n = 50) Group II: Premedication with placebo + IANB using 1.8 mL 2% lidocaine with 1:100 000 epinephrine (n = 50)	Success was the ability to access, clean, and shape the tooth without pain (VAS score 0) or mild pain (VAS ≤ 54)
Aggarwal et al. (19)	98 volunteers selected from dental emergency department	Actively experiencing pain, good health, not taking any medication that would alter pain perception, as determined by oral questioning and written questionnaire, actively experiencing pain in a mandibular molar (>54 mm on Heft-Parker visual analogue scale: HP-VAS), a prolonged response to cold testing with an ice stick and EPT, absence of any periapical radiolucency on radiographs, except for widened PDL and vital coronal pulp on access opening, American Society of Anesthesiologists class I or II medical history and ability to understand the use of pain scale	Group I: IANB using 1.8 mL of 2% lidocaine with 1:200 000 epinephrine + buccal infiltration of 4% articaine with 1:100 000 epinephrine (n = 24) Group II: IANB using 1.8 mL of 2% lidocaine with 1:200 000 epinephrine + buccal infiltration of 30 mg mL^{-1} of ketorolac tromethamine (n = 26) Group III: IANB using 1.8 mL of 2% lidocaine with 1:200 000 epinephrine + buccal infiltration of 4 mg mL^{-1} of dexamethasone (n = 24) Group IV (control): IANB using 1.8 mL of 2% lidocaine with 1:200 000 epinephrine + did not receive buccal infiltration (n = 24)	Success was no pain or weak/mild pain during endodontic access preparation and instrumentation

Figure 2 Quality of 17 included studies: (+) indicates adequate quality; (?) indicates questionable quality.

one study ($n = 104$) with a standard intervention, i.e. IANB with 2% lidocaine (3). There was no statistically significant difference in terms of pulp anaesthesia between these two techniques (RR = 1.00; 95% CI = 0.76–1.32; Fig. 4).

2. Supplemental injection plus standard intervention versus standard intervention. Two studies ($n = 107$) reported a comparison of different methods of supplemental injection. The standard intervention, i.e. IANB using 2% lidocaine, was followed by the buccal and lingual infiltration as the supplemental injection in one study (4), whereas only the buccal infiltration was performed for the supplemental injection in the other study (5). Although there was a statistically significant

difference in pulp anaesthesia ($P = 0.002$; RR = 4.41; 95% CI = 1.71–11.37), favouring IANB plus supplemental buccal infiltration (5), there was no statistically significant difference in pulp anaesthesia between IANB and IANB plus supplemental injection for pooled data from these two studies ($P = 0.14$; pooled RR = 2.37; 95% CI = 0.75–7.46; Fig. 5).

3. Changing the features of local anaesthetic versus standard intervention. A meta-analysis of eight studies (3, 5–11), including a total of 492 participants, is reported in Figure 6. The overall success rate of pulp anaesthesia with supplemental interventions was statistically significantly higher than that of the standard intervention ($P = 0.03$; pooled RR = 1.26; 95% CI = 1.02–1.56). However, the results among these eight studies were low in consistency with overlapped CIs and $I^2 = 20$%. Thus, the source of heterogeneity was conducted by sub-group analysis: (i) increasing volumes of local anaesthetic (ii) increasing volumes and changing components of local anaesthetic and (iii) changing types of local anaesthetic. Among the three sub-groups, a statistically significant higher success rate of pulp anaesthesia was found only in the sub-group where there was an increase in anaesthetic volumes ($P = 0.007$; RR = 2.25; 95% CI = 1.25–4.05; Fig. 6).

4. Premedication with non-steroidal anti-inflammatory drugs (NSAIDs), acetaminophen, or a combination of acetaminophen and ibuprofen versus standard intervention. Seven studies ($n = 696$; 12–18) were included for this comparison. The supplemental interventions were divided into three sub-groups: (I) premedication with NSAIDs (II) premedication with acetaminophen and (III) premedication with a combination of acetaminophen and ibuprofen. The results derived from these seven studies could not be pooled due to two comparisons being reported in one study (17). However, five studies (12–16) using premedication with NSAIDs as the supplemental intervention showed a statistically significantly higher rate of successful pulp anaesthesia than that of the standard intervention ($P = 0.001$; random pooled RR = 1.75, 95% CI = 1.24–2.48; Fig. 7).

5. Supplemental infiltration with other local anaesthetic agents, including 2% articaine with 1:200 000 epinephrine, 4% articaine with 1:100 000 epinephrine, 30 mg mL^{-1} of ketorolac tromethamine, and 4 mg mL^{-1} of dexamethasone, versus standard intervention. Two studies ($n = 194$) (4, 19) provided four comparisons of the supplemental infiltration with different local anaesthetic agents versus the standard intervention, i.e. IANB using 2% lidocaine with 1:200 000 epinephrine. Of four different interventions, only supplemental buccal and lingual infiltration with 2% articaine and 1:200 000 epinephrine yielded a statistically significant higher rate
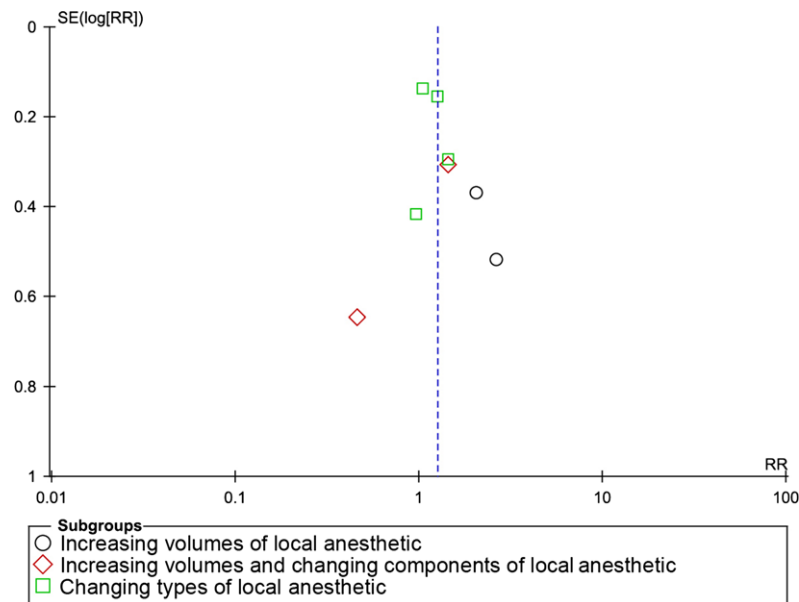
Figure 3 Funnel plot of primary outcome from eight included studies. RR, relative risk; SE, standard error.
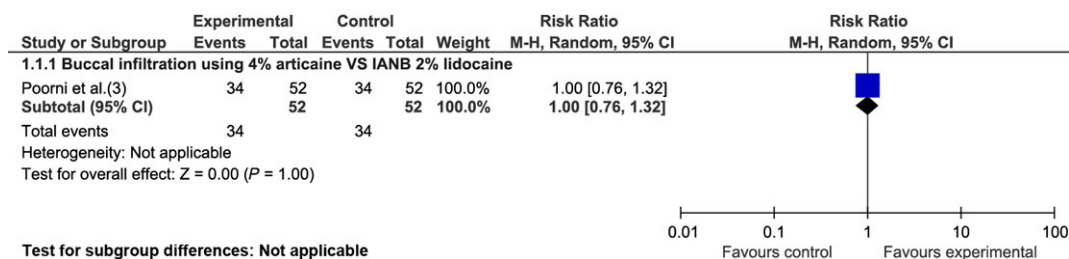
Figure 4 Changing the techniques of local anaesthetic injection versus standard intervention. CI, confidence interval; IANB, inferior alveolar nerve block.
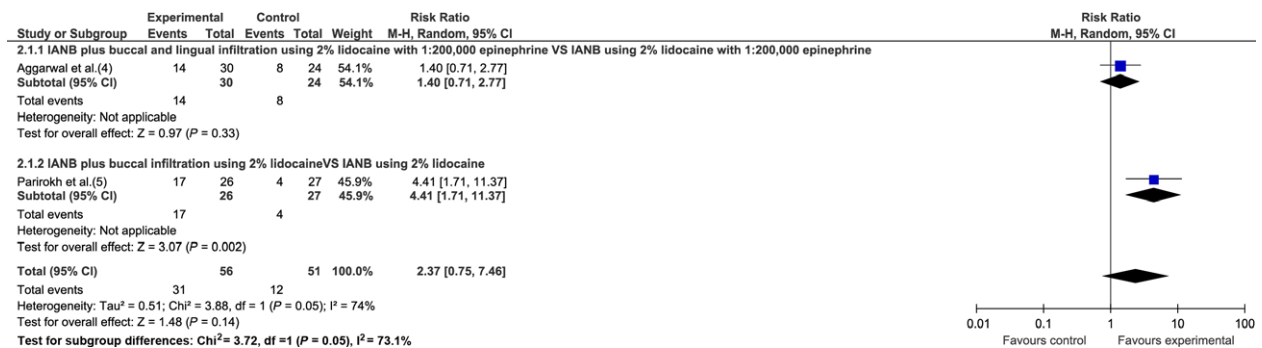
Figure 5 Supplemental injection plus standard intervention versus standard intervention. CI, confidence interval; IANB, inferior alveolar nerve block.

of pulp anaesthesia than the standard intervention ($P = 0.03$; RR = 2.00, 95% CI = 1.08–3.72; Fig. 8), whereas the differences between supplemental infiltration and the standard intervention for the remaining three comparisons did not reach the significance level (Fig. 8).

Discussion

The current review included 17 studies with a total of 1504 participants. The results demonstrate that more effective local anaesthesia and pain control occurs when supplemental interventions are used in addition

Study or Subgroup	Experimental Events	Total	Control Events	Total	Weight	Risk Ratio M-H, Random, 95% CI	Risk Ratio M-H, Random, 95% CI
3.1.1 Increasing volumes of local anesthetic							
Aggarwal et al.(6)	15	28	7	27	7.4%	2.07 [1.00, 4.27]	
Parirokh et al.(5)	11	28	4	27	4.0%	2.65 [0.96, 7.32]	
Subtotal (95% CI)		56		54	11.4%	2.25 [1.25, 4.05]	
Total events	26		11				
Heterogeneity: Tau² = 0.00; Chi² = 0.16, df = 1 (P = 0.69); I² = 0%							
Test for overall effect: Z = 2.69 (P = 0.007)							
3.1.2 Increasing volumes and changing components of local anesthetic							
Bigby et al.(7)	3	25	6	23	2.6%	0.46 [0.13, 1.63]	
Kreimer et al.(8)	15	28	10	27	10.3%	1.45 [0.79, 2.64]	
Subtotal (95% CI)		53		50	12.9%	0.93 [0.31, 2.84]	
Total events	18		16				
Heterogeneity: Tau² = 0.43; Chi² = 2.68, df = 1 (P = 0.10); I² = 63%							
Test for overall effect: Z = 0.12 (P = 0.90)							
3.1.3 Changing types of local anesthetic							
Claffey et al.(9)	9	35	8	30	6.0%	0.96 [0.43, 2.19]	
Poorni et al.(3)	36	52	34	52	31.4%	1.06 [0.81, 1.38]	
Sampaio et al.(10)	28	35	22	35	27.4%	1.27 [0.94, 1.72]	
Tortamano et al.(11)	13	20	9	20	10.8%	1.44 [0.81, 2.58]	
Subtotal (95% CI)		142		137	75.6%	1.16 [0.97, 1.40]	
Total events	86		73				
Heterogeneity: Tau² = 0.00; Chi² = 1.55, df = 3 (P = 0.67); I² = 0%							
Test for overall effect: Z = 1.61 (P = 0.11)							
Total (95% CI)		251		241	100.0%	1.26 [1.02, 1.56]	
Total events	130		100				
Heterogeneity: Tau² = 0.02; Chi² = 8.79, df = 7 (P = 0.27); I² = 20%							
Test for overall effect: Z = 2.17 (P = 0.03)							
Test for subgroup differences: Chi² = 4.59, df = 2 (P = 0.10), I² = 56.4%							

Figure 6 Changing the features of local anaesthetic versus standard intervention. CI, confidence interval.

Study or Subgroup	Experimental Events	Total	Control Events	Total	Weight	Risk Ratio M-H, Random, 95% CI	Risk Ratio M-H, Random, 95% CI
4.1.1 Premedication with NSAIDs before IANB VS premedication with placebo before IANB							
Aggarwal et al.(12)	15	45	7	24	8.2%	1.14 [0.54, 2.41]	
Oleson et al.(13)	20	49	18	51	16.9%	1.16 [0.70, 1.91]	
Parirokh et al.(14)	70	100	16	50	22.3%	2.19 [1.43, 3.34]	
Prasanna et al.(15)	52	76	10	38	14.2%	2.60 [1.49, 4.52]	
Shahi et al.(16)	14	55	7	55	6.8%	2.00 [0.87, 4.57]	
Subtotal (95% CI)		325		218	68.5%	1.75 [1.24, 2.48]	
Total events	171		58				
Heterogeneity: Tau² = 0.07; Chi² = 7.03, df = 4 (P = 0.13); I² = 43%							
Test for overall effect: Z = 3.20 (P = 0.001)							
4.1.2 Premedication with Acetaminophen before IANB VS premedication with placebo before IANB							
Ianiro et al.(17)	10	14	6	13	10.0%	1.55 [0.79, 3.04]	
Subtotal (95% CI)		14		13	10.0%	1.55 [0.79, 3.04]	
Total events	10		6				
Heterogeneity: Not applicable							
Test for overall effect: Z = 1.27 (P = 0.20)							
4.1.3 Premedication with a combination of Acetaminophen and Ibuprofen before IANB VS premedication with placebo before IANB							
Ianiro et al.(17)	10	13	6	13	10.4%	1.67 [0.86, 3.22]	
Simpson et al.(18)	16	50	12	50	11.1%	1.33 [0.70, 2.52]	
Subtotal (95% CI)		63		63	21.5%	1.49 [0.94, 2.35]	
Total events	26		18				
Heterogeneity: Tau² = 0.00; Chi² = 0.24, df = 1 (P = 0.62); I² = 0%							
Test for overall effect: Z = 1.69 (P = 0.09)							
Total (95% CI)		402		294	100.0%	1.69 [1.35, 2.11]	
Total events	207		82				
Heterogeneity: Tau² = 0.01; Chi² = 7.83, df = 7 (P = 0.35); I² = 11%							
Test for overall effect: Z = 4.60 (P < 0.00001)							
Test for subgroup differences: Chi² = 0.36, df = 2 (P = 0.84), I² = 0%							

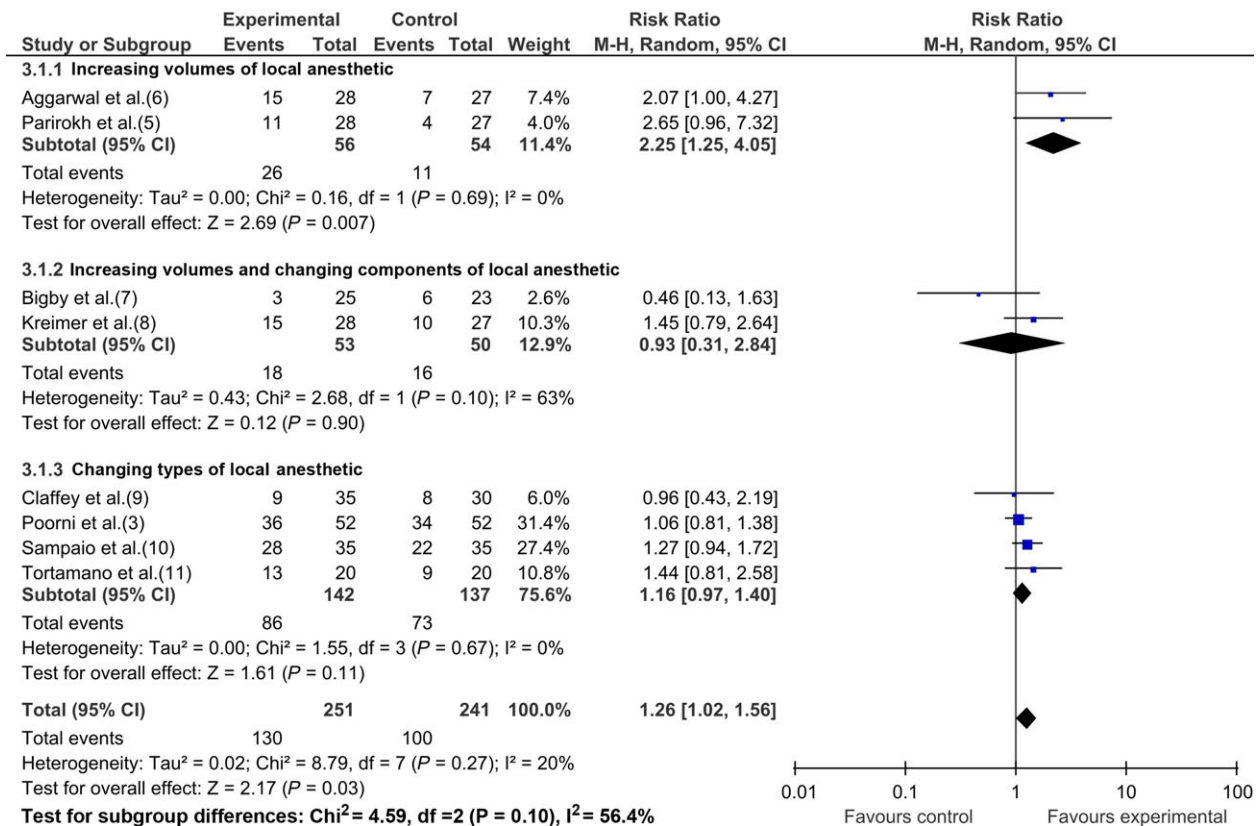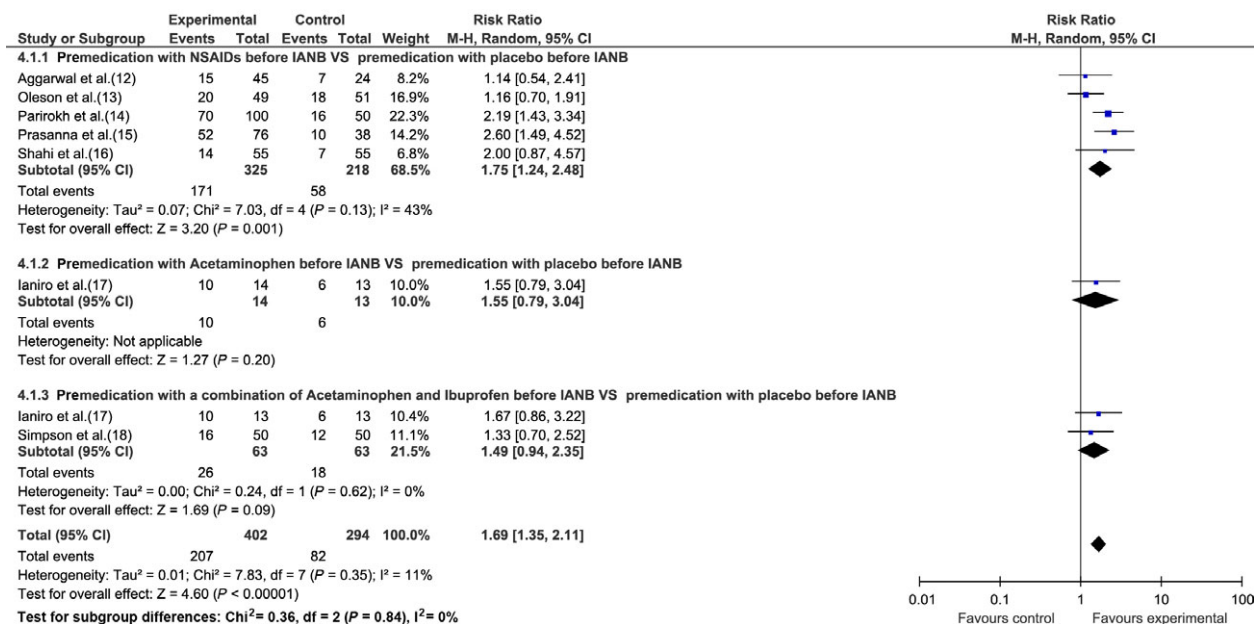**Figure 7** Premedication with non-steroidal anti-inflammatory drugs (NSAIDs), acetaminophen, or a combination of acetaminophen and ibuprofen versus standard intervention. CI, confidence interval; IANB, inferior alveolar nerve block.
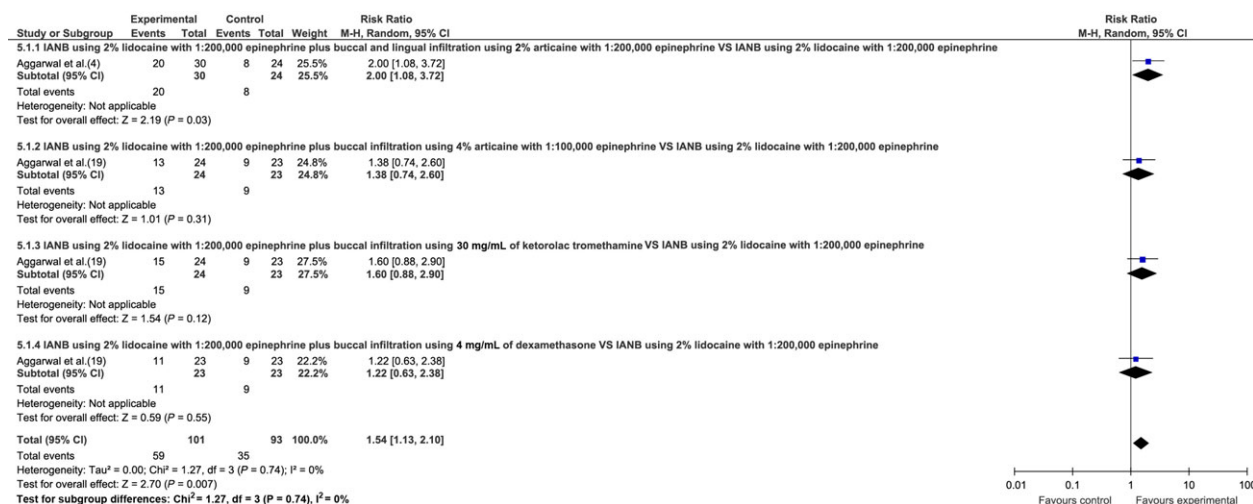
Figure 8 Supplemental infiltration with other local anaesthetic agents, including 2% articaine with 1:200 000 epinephrine, 4% articaine with 1:100 000 epinephrine, 30 mg mL^{-1} of ketorolac tromethamine, and 4 mg mL^{-1} of dexamethasone, versus standard intervention. CI, confidence interval; IANB, inferior alveolar nerve block.

to the standard inferior alveolar nerve block whilst performing root canal treatment on lower molars with irreversible pulpitis. These supplemental interventions that improved the success of pulp anaesthesia were increasing the anaesthetic volumes and premedication with NSAIDs. This result is similar to a study by Li *et al.* in 2012 (20) who used similar criteria and a similar methodology.

The review process of the current study was done independently by two reviewers for the selection of eligible studies, for assessment of the quality of each study, and for data extraction. Discussion with the third reviewer was only required when disagreement occurred. Eleven of the 17 included studies (65%) were judged to have a low risk of bias and none of the 17 included studies was judged as having a high risk of bias in any domains of methodological quality (Fig. 2). Baseline characteristics were balanced between the intervention groups. Hence, this review provides evidence that should be reliable and of benefit to clinical practice.

Most studies reviewed have used lip numbness as the criteria for successful anaesthesia but some used this along with a cold pulp test or electric pulp testing. Most studies used the Heft-Parker visual analogue scale, although some used a verbal analogue scale or verbal description of pain during root canal treatment.

The risk ratio was used in this review because prospective studies were selected. The random effect model was used due to heterogeneity of the selected studies in which a very low possibility of no difference among those studies was expected. Even though no heterogeneity was

observed, the results of random and fix models are still the same.

Although some results of this study were statistically significant, the 1.75–2.25 times of difference may not be considered by some as being of clinical significance. However, clinical significance is very subjective and it can be affected by many individual patient and operator factors. The most important consideration when treating patients is to try and minimise the pain they feel and ideally this should be done in a proactive or anticipatory manner. That is, it is better for the patient not to experience any pain at all than to experience pain and then have to have further anaesthetic administered. This can result in the patient losing confidence in the procedure and/or the operator in addition to possibly increasing the amount of post-operative pain experienced. Hence, this systematic review provides readers with beneficial information that can be adapted for the clinical situation to minimise pain for the patient. For example, operators should consider using pre-operative medications with NSAIDs where appropriate and supplemental injection to increase the volume of anaesthetic solution used prior to commencing root canal treatment.

Conclusions

Increasing the volume of anaesthetic and premedication with NSAIDs provided more predictable pulp anaesthesia and pain control during root canal treatment of lower molars with irreversible pulpitis.

Acknowledgements

Conflict of Interests

None declared. All authors have read, edited and approved this manuscript.

References

1. Minea LRD, Safaei M, Khan M, Dent M, Tjandra S. What is the best approach to achieve anesthesia of a hot tooth? An evidence based support. Community Dentistry, Faculty of Dentistry, University of Toronto, Canada. 2009. Available from URL: http://www.dentistry.utoronto.ca/system/files/w1eblreport-2009.pdf

2. Higgins JPT, Green S. Cochrane Handbook for Systematic Reviews of Interventions Version 5.1.0. The Cochrane Collaboration 2011. [March 2011.] Available from URL: www.cochrane-handbook.org

3. Poorni S, Veniashok B, Senthilkumar AD, Indira R, Ramachandran S. Anesthetic efficacy of four percent articaine for pulpal anesthesia by using inferior alveolar nerve block and buccal infiltration techniques in patients with irreversible pulpitis: a prospective randomized double-blind clinical trial. J Endod 2011; 37: 1603–7.

4. Aggarwal V, Jain A, Kabi D. Anesthetic efficacy of supplemental buccal and lingual infiltrations of articaine and lidocaine after an inferior alveolar nerve block in patients with irreversible pulpitis. J Endod 2009; 35: 925–9.

5. Parirokh M, Satvati SA, Sharifi R *et al.* Efficacy of combining a buccal infiltration with an inferior alveolar nerve block for mandibular molars with irreversible pulpitis. Oral Surg Oral Med Oral Pathol Oral Radiol Endod 2010; 109: 468–73.

6. Aggarwal V, Singla M, Miglani S, Kohli S, Singh S. Comparative evaluation of 1.8 mL and 3.6 mL of 2% lidocaine with 1:200,000 epinephrine for inferior alveolar nerve block in patients with irreversible pulpitis: a prospective, randomized single-blind study. J Endod 2012; 38: 753–6.

7. Bigby J, Reader A, Nusstein J, Beck M. Anesthetic efficacy of lidocaine/meperidine for inferior alveolar nerve blocks in patients with irreversible pulpitis. J Endod 2007; 33: 7–10.

8. Kreimer T, Kiser R 2nd, Reader A, Nusstein J, Drum M, Beck M. Anesthetic efficacy of combinations of 0.5 mol/L mannitol and lidocaine with epinephrine for inferior alveolar nerve blocks in patients with symptomatic irreversible pulpitis. J Endod 2012; 38: 598–603.

9. Claffey E, Reader A, Nusstein J, Beck M, Weaver J. Anesthetic efficacy of articaine for inferior alveolar nerve blocks in patients with irreversible pulpitis. J Endod 2004; 30: 568–71.

10. Sampaio RM, Carnaval TG, Lanfredi CB, Horliana AC, Rocha RG, Tortamano IP. Comparison of the anesthetic efficacy between bupivacaine and lidocaine in patients with irreversible pulpitis of mandibular molar. J Endod 2012; 38: 594–7.

11. Tortamano IP, Siviero M, Costa CG, Buscariolo IA, Armonia PL. A comparison of the anesthetic efficacy of articaine and lidocaine in patients with irreversible pulpitis. J Endod 2009; 35: 165–8.

12. Aggarwal V, Singla M, Kabi D. Comparative evaluation of effect of preoperative oral medication of ibuprofen and ketorolac on anesthetic efficacy of inferior alveolar nerve block with lidocaine in patients with irreversible pulpitis: a prospective, double-blind, randomized clinical trial. J Endod 2010; 36: 375–8.

13. Oleson M, Drum M, Reader A, Nusstein J, Beck M. Effect of preoperative ibuprofen on the success of the inferior alveolar nerve block in patients with irreversible pulpitis. J Endod 2010; 36: 379–82.

14. Parirokh M, Ashouri R, Rekabi AR *et al.* The effect of premedication with ibuprofen and indomethacin on the success of inferior alveolar nerve block for teeth with irreversible pulpitis. J Endod 2010; 36: 1450–4.

15. Prasanna N, Subbarao CV, Gutmann JL. The efficacy of pre-operative oral medication of lornoxicam and diclofenac potassium on the success of inferior alveolar nerve block in patients with irreversible pulpitis: a double-blind, randomised controlled clinical trial. Int Endod J 2011; 44: 330–6.

16. Shahi S, Mokhtari H, Rahimi S *et al.* Effect of premedication with ibuprofen and dexamethasone on success rate of inferior alveolar nerve block for teeth with asymptomatic irreversible pulpitis: a randomized clinical trial. J Endod 2013; 39: 160–2.

17. Ianiro SR, Jeansonne BG, McNeal SF, Eleazer PD. The effect of preoperative acetaminophen or a combination of acetaminophen and Ibuprofen on the success of inferior alveolar nerve block for teeth with irreversible pulpitis. J Endod 2007; 33: 11–14.

18. Simpson M, Drum M, Nusstein J, Reader A, Beck M. Effect of combination of preoperative ibuprofen/acetaminophen on the success of the inferior alveolar nerve block in patients with symptomatic irreversible pulpitis. J Endod 2011; 37: 593–7.

19. Aggarwal V, Singla M, Rizvi A, Miglani S. Comparative evaluation of local infiltration of articaine, articaine plus ketorolac, and dexamethasone on anesthetic efficacy of inferior alveolar nerve block with lidocaine in patients with irreversible pulpitis. J Endod 2011; 37: 445–9.

20. Li C, Yang X, Ma X, Li L, Shi Z. Preoperative oral nonsteroidal anti-inflammatory drugs for the success of the inferior alveolar nerve block in irreversible pulpitis treatment: a systematic review and meta-analysis based on randomized controlled trials. Quintessence Int 2012; 43: 209–19.

ORIGINAL ARTICLE

WILEY | Dental Traumatology

Inhibitory effect of Thai propolis on human osteoclastogenesis

Nattaporn Wimolsantirungsri[1] | Anupong Makeudom[2] | Phumisak Louwakul[1] |
Thanapat Sastraruji[2] | Pattama Chailertvanitkul[3] | Chayarop Supanchart[2,4] | Suttichai Krisanaprakornkit[2,5] iD

[1]Department of Restorative Dentistry and Periodontology, Faculty of Dentistry, Chiang Mai University, Chiang Mai, Thailand

[2]Center of Excellence in Oral and Maxillofacial Biology, Faculty of Dentistry, Chiang Mai University, Chiang Mai, Thailand

[3]Department of Restorative Dentistry, Faculty of Dentistry, Khon Kaen University, Khon Kaen, Thailand

[4]Department of Oral and Maxillofacial Surgery, Faculty of Dentistry, Chiang Mai University, Chiang Mai, Thailand

[5]Department of Oral Biology and Diagnostic Sciences, Faculty of Dentistry, Chiang Mai University, Chiang Mai, Thailand

Correspondence
Suttichai Krisanaprakornkit, Center of Excellence in Oral and Maxillofacial Biology, Faculty of Dentistry, Chiang Mai University, Muang District, Chiang Mai, Thailand.
Email: suttichai.k@cmu.ac.th

Abstract

Background/Aim: Avulsed teeth should be immediately replanted into the socket or otherwise kept in a physiologic storage medium to maintain periodontal ligament cell viability. A previous study has demonstrated that Thai propolis extract can maintain viability of human periodontal ligament cells. However, root resorption by osteoclasts often occurs when the avulsed teeth are replanted. The aim of this study was to determine the inhibitory effect of Thai propolis extract on human osteoclastogenesis in vitro.

Materials and methods: Human peripheral blood mononuclear cells were isolated for osteoclast precursors and cultured in the presence or absence of various non-toxic concentrations of propolis extract, as determined by the alamarBlue® assay, during in vitro induction of osteoclastogenesis. Osteoclast formation was examined by tartrate-resistant acid phosphatase staining, actin ring formation, and real-time polymerase chain reaction. The resorption pit assay was performed to determine osteoclast function.

Results: Non-toxic concentrations of propolis extract suppressed osteoclast formation by significantly decreasing the percentages of tartrate-resistant acid phosphatase-positive multinuclear cells and the ratios of cells with F-actin ring formation ($P < .01$) in a dose-dependent fashion. Expression of several osteoclast-specific genes was significantly downregulated by propolis in a dose-dependent manner ($P < .05$). The percentages of resorption areas on dentin slices were significantly decreased by propolis ($P < .05$).

Conclusions: Thai propolis can inhibit human osteoclast formation and function, which may be beneficial for prevention of root resorption following replantation of avulsed teeth.

KEYWORDS
osteoclastogenesis, propolis, root resorption, tartrate-resistant acid phosphatase, tooth avulsion

1 | INTRODUCTION

Avulsion is defined as total displacement of a tooth out of the socket. It is the most severe type of dental injury and it damages multiple tissues, including the periodontal ligament (PDL), alveolar bone, cementum, gingiva, and dental pulp. The damages include severance of PDL, fracture of alveolar bone, tear of cementum, disruption of gingival and dental pulp tissues.[1] The incidence of tooth avulsion ranges from 1% to 16% of all traumatic injuries to the permanent dentition.[2] It is recommended by the International Association for

Dental Traumatology that avulsed teeth be immediately replanted in the socket because long-term success without any complications depends on the extra-oral period.[3] Extended extra-oral dry time is associated with decreased PDL viability[4] and increased root resorption.[5] If immediate replantation is not possible, avulsed teeth should be stored in a physiologic storage medium such as Hank's Balanced Salt Solution (HBSS) to maintain PDL cell viability until the teeth are replanted. Besides HBSS, the preservative effect of Thai propolis extract on viability of PDL cells from extracted human premolars for up to 3 hours has been investigated.[6]

Some previous studies have reported that root resorption after tooth replantation is common, ranging from 60% to 85% of replanted teeth,[7–9] and it is considered to be a major cause of loss of the teeth. Osteoclasts, multinucleated giant cells with F-actin rings, are differentiated from hematopoietic cells of the monocyte/macrophage lineage and they play a major role in root resorption.[10] Therefore, it is probable that any constituents within the storage medium that can help reduce osteoclast formation and function may enhance the long-term success rate of replanted teeth.

Propolis or bee glue is a natural non-toxic resinous substance collected from several types of plants by honeybees. Its chemical composition and biological properties vary with different geographical locations and climate characteristics. Khurshid and co-workers[11] have reviewed various biological properties of propolis in therapeutic medicine, ranging from antimicrobial, anticancer, antioxidant, anti-inflammatory activities to wound-healing promotion. In dentistry, some studies have demonstrated the preventive effect of propolis against dental caries[12] as well as its therapeutic benefits for oral mucositis,[13] plaque inhibition,[14] and pulp capping.[15] Moreover, Pileggi et al[16] have previously demonstrated that Brazilian propolis from the southern region of Brazil in the vicinity of Sao Paulo inhibits osteoclast maturation. Therefore, it was hypothesized in this study that Thai propolis could also prevent osteoclastogenesis similar to the inhibitory effect of the Brazilian propolis. Hence, the aim of this study was to determine the inhibitory effect of Thai propolis extract on human osteoclastogenesis in vitro.

2 | MATERIALS AND METHODS

As previously described,[6] propolis was collected and extracted in a single batch used for all experiments in this study. Briefly, propolis obtained from beehives in Nong Khai province, Thailand, was ground and dissolved in 95% ethanol (1 g per 5 mL). After that, the mixture was stirred in an orbital shaker at 200 rpm for 5 days and filtered with Whatman No. 1 filter paper several times. Then, the ethanol in the extract was evaporated and lyophilized in a freeze-dryer (CHRIST, ALPHA 2-4 LD plus, Martin Christ, Germany). The semisolid and brownish propolis extract at 1.185 g per mL was kept in the bottle, wrapped with aluminum foil, and stored at 4°C until further uses.

The research protocol (no. 6/2017) was approved by the Human Experimentation Committee of Faculty of Dentistry, Chiang Mai University. Peripheral blood mononuclear cells (PBMCs), as osteoclast progenitor cells, were separated from heparinized whole blood, drawn from twelve healthy volunteers (20-35 years old) with informed consent, by density gradient centrifugation using Ficoll-Paque™ (GE Healthcare Bio-Sciences, Uppsala, Sweden) as previously described.[17] In brief, heparinized venous blood was diluted with sterile phosphate-buffered saline (PBS) at the ratio 1:1, and the diluted blood was gently overlaid onto the Ficoll-Paque solution at the ratio 3:1. After centrifugation at 400 g for 30 minutes at 25°C, PBMCs were collected from the buffy coat, washed two times with 20 mL of PBS, and cultured in complete medium, containing minimum essential medium alpha Eagle's (αMEM; Lonza, Walkersville, MD, USA), supplemented with 10% fetal bovine serum (FBS; Invitrogen, Thermo Fisher Scientific, Inc., Waltham, MA, USA), 2 mmol L^{-1} L-glutamine (Lonza), 1% penicillin/streptomycin (Invitrogen), and 15 ng mL^{-1} of recombinant human macrophage-colony-stimulating factor (M-CSF; R&D Systems, Inc., Minneapolis, MN, USA), at the density of 5×10^5 cells per cm^2 in appropriate culture vessels for subsequent experiments.

Peripheral blood mononuclear cells were seeded in black and clear bottom 96-well culture plates (Nunc A/S, Roskilde, Denmark) and cultured in complete medium at 37°C in 5% CO$_2$ and 95% humidity. After 48 hours, the complete medium was replenished, and cells were treated with various concentrations (0.025-10 mg mL^{-1}) of the propolis extract, diluted in absolute ethanol at the final concentration of 1% (v/v), or with 1% (v/v) of absolute ethanol as a solvent control for 24 hours or 7 days. After that, a 100-μL quantity of 10% FBS-containing αMEM together with 4 μL of the alamarBlue® reagent (AbD Serotec®, Bio-Rad Laboratories, Raleigh, NC, USA) was added and incubated at 37°C for 4 hours. The fluorescent intensity was measured by a multimode microplate reader (Synergy4, BioTek, Winooski, VT, USA) at 540 nm for an excitation wavelength and at 590 nm for an emission wavelength. The fluorescent intensities of treated samples were adjusted for the ratios of cell viability by comparing to those of the untreated control, set to 1.0.

Peripheral blood mononuclear cells were seeded into 96-well culture plates (Nunc A/S) and cultured in complete medium with or without 30 ng mL^{-1} of recombinant human receptor activator of nuclear factor kappaB ligand (RANKL; R&D Systems, Inc.) in the presence or absence of non-toxic doses of propolis extract that were chosen from the cytotoxicity assay. As a solvent control, cells were treated with absolute ethanol at the final concentration of 1% (v/v) instead of the propolis extract. The medium replacement and treatment were performed every other day. After 7 days, cells were fixed with 4% paraformaldehyde (Sigma-Aldrich; Merck KGaA, Darmstadt, Germany) in PBS at 4°C for 10 minutes and stained with tartrate-resistant acid phosphatase (TRAP) reagent, comprising 0.2 mmol L^{-1} Naphthol AS-MX phosphate disodium salt (Sigma-Aldrich) and 1.5 mmol L^{-1} Fast red violet (Sigma-Aldrich) in 40 mmol L^{-1} sodium acetate (Sigma-Aldrich) and 10 mmol L^{-1} sodium tartrate (Sigma-Aldrich), for 2 hours, as previously described.[18] Three images that covered around 80% of each well of the 96-well plate were captured by a digital camera (EOS 600D, Canon, Inc., Tokyo, Japan) attached

to an inverted phase contrast microscope (Olympus Corporation, Tokyo, Japan), and the number of TRAP-positive multinuclear cells, containing at least three nuclei, in each image was manually counted and combined. The percentage of TRAP-positive multinuclear cells was determined in the propolis-treated or the absolute ethanol-treated sample compared to that in the M-CSF- and RANKL-treated sample, set to 100.

Peripheral blood mononuclear cells were seeded in Lab-Tek™ chamber slides (Thermo Fisher Scientific, Inc.) and cultured in complete medium with or without 30 ng mL^{-1} of RANKL in the presence or absence of non-toxic concentrations of propolis extract or 1% (v/v) absolute ethanol. The medium replacement and treatment were performed every other day. After 7 days, cells were fixed with 4% paraformaldehyde in PBS at 4°C for 10 minutes and then permeabilized with 0.1% Triton X-100 (Amresco, Solon, OH, USA) and 3% bovine serum albumin (Sigma-Aldrich) in PBS. Subsequently, cells were stained with 0.1% Alexa Fluor®488-conjugated phalloidin (Invitrogen) and 4′,6-diamidino-2-phenylindole (DAPI; Biotium, Inc., Hayward, CA, USA). The presence of actin rings was visualized, and their images were captured by a fluorescence microscope (Axio Imager Z2 m, Carl Zeiss Microscopy GmbH, Göttingen, Germany). The number of cells with F-actin ring formation in propolis-treated or absolute ethanol-treated samples was adjusted for the relative ratio of cells with F-actin rings in comparison with that of the M-CSF- and RANKL-treated sample, set to 1.0.

Peripheral blood mononuclear cells were seeded in 6-well culture plates and cultured in complete medium with or without 30 ng mL^{-1} of RANKL in the presence or absence of non-toxic doses of propolis extract or 1% (v/v) absolute ethanol for 7 days. Total RNA was isolated by the RNAspin Mini RNA isolation kit (GE Healthcare UK limited, Buckinghamshire, UK) according to the manufacturer's protocol. The quantity of RNA was measured by the NanoDrop™ 2000 UV-Vis spectrophotometer (Thermo Fisher Scientific, Inc.). A 400-nanogram quantity of total RNA was used for synthesis of complementary DNA (cDNA) using the RevertAid H Minus First Strand cDNA Synthesis kit (Thermo Fisher Scientific, Inc.).[19] Real-time PCR was performed in a 20-μL total volume of reaction mixture, containing 1 μL of cDNA, 0.4 μmol L^{-1} of each forward and reverse primer for several genes (Table 1), including nuclear factor of activated T cell 2 (NFAT2), cathepsin K (CTSK), receptor activator of nuclear factor kappa B (RANK), chloride channel 7 (CLCN7), calcitonin receptor (CTR), and colony-stimulating factor 1 (CSF1) for M-CSF, and 10 μL of the SensiFAST™ SYBR No-ROX reagent (Bioline, Taunton, MA, USA) in the LightCycler® 480 instrument (Roche Molecular Biochemicals, Mannheim, Germany) for 40 cycles with a profile of 95°C for 20 seconds, 60°C for 20 seconds, and 72°C for 25 seconds. To compare the degrees of gene expression among samples, the relative gene expression (ΔC_t) of each gene was normalized by that of glyceraldehyde 3-phosphate dehydrogenase (GAPDH) as a housekeeping gene control. GAPDH is considered one of the most common genes used for normalization of gene expression.[20] Moreover, a few previous studies have shown that GAPDH expression levels are changed only by treatment with glucose, insulin, or heat shock.[21,22] Consequently,

TABLE 1 Oligonucleotide primer sequences for the real-time reverse transcription polymerase chain reaction

Gene	Sequence (5′-3′)
NFAT2 (forward)	GTACGGCTGGTGTTCCGCGT
NFAT2 (reverse)	AAAAAGCACCCCCACGCGCTCA
CTSK (forward)	CCACTGGGAGCTATGGAAGA
CTSK (reverse)	GCCTCAAGGTTATGGATGGA
RANK (forward)	GGCTGGGTACCACTGGAG
RANK (reverse)	TGCACACTGTGTCCTTGTTG
CLCN7 (forward)	ACTGTCCTTCTGGGTGTTGC
CLCN7 (reverse)	TGAGGAAGCACTTGATCTGG
CTR (forward)	TGGTGCCAACCACTATCCATGC
CTR (reverse)	CACAAGTGCCGCCATGACAG
CSF1 (forward)	CACATGATTGGGAGTGGACA
CSF1 (reverse)	TAATTTGGCACGAGGTCTCC
GAPDH (forward)	TGCACCACCAACTGCTTAGC
GAPDH (reverse)	GGCATGGCTGTGGTCATGAG

NFAT2, nuclear factor of activated T cell 2; CTSK, cathepsin K; RANK, receptor activator of nuclear factor kappaB; CLCN7, chloride channel 7; CTR, calcitonin receptor; CSF1, colony-stimulating factor 1; GAPDH, glyceraldehyde 3-phosphate dehydrogenase.

GAPDH was selected for normalization in this study; furthermore, previous osteoclast differentiation studies[17,18] used GAPDH as a housekeeping gene control without any significant changes in the levels of GAPDH expression among different conditions. The ΔC_t values of samples treated with the propolis extract or with absolute ethanol were compared with that of the untreated sample, set to 1.0, to obtain $\Delta\Delta C_t$.

Dentin slices were immersed in 70% ethanol for 1 hour and stored in complete medium at 37°C in 5% CO_2 and 95% humidity for 24 hours. After that, PBMCs were seeded on the dentin slices that were placed in 96-well culture plates and cultured in complete medium with or without 30 ng mL^{-1} of RANKL in the presence or absence of various non-toxic concentrations of propolis extract or 1% (v/v) absolute ethanol for 7 days. The medium replacement and treatment were conducted every 2 days. Then, the dentin slices were washed with water and stained with Indian ink for 30 seconds, and excessive dye was wiped out. The images of stained dentin slices were examined by a bright field microscope (BX41, Olympus Corporation). To quantify the percentage of resorption areas, four images were taken from each dentin slice by a charge-coupled device camera (DP71, Olympus Corporation) attached to a microscope and then combined. The resorption areas, containing stained pits and grooves, against the total area of each dentin slice were determined as the percentage using ImageJ software version 1.48 (National Institutes of Health, Bethesda, MD, USA), which was then compared with the percentage of resorption area in the M-CSF- and RANKL-treated sample, set to 100.

All experiments were conducted in triplicate using three different cell lines from three different donors. Data were compared by

mean ± standard deviation. Differences in the ratios of cell viability, in the percentages of TRAP-positive cells, in the ratios of cells with F-actin ring formation, in the relative gene expression, and in the percentages of resorption areas between the propolis-treated or the solvent-treated sample and the untreated control sample were analyzed using one-way analysis of variance, and individual sample comparisons were made using the Tukey HSD test. All statistical analyses were carried out with SPSS software version 17.0 (IBM SPSS Statistics, IBM Corp., Armonk, NY, USA). *P*-values <.05 were considered to indicate a statistically significant difference.

3 | RESULTS

Using the alamarBlue® assay, the mean ratios of cell viability in PBMCs treated with propolis extract from 0.025 to 5 mg mL^{-1} for 24 hours (Figure 1A) or from 0.025 to 0.5 mg mL^{-1} for 7 days (Figure 1B) were not different from that of PBMCs treated with 1% (v/v) absolute ethanol as a solvent control. However, the mean ratios of cell viability for treatment with propolis at 10 mg mL^{-1} for 24 hours (Figure 1A) and for treatment with propolis at 1 mg mL^{-1} or greater for 7 days (Figure 1B) were significantly lower than that of the untreated sample (*P* < .05), indicating that the doses of propolis extract at 0.5 mg mL^{-1} or less were not toxic to PBMCs even if they were treated for 7 days and were then chosen for subsequent experiments.

With TRAP staining, the propolis extract at 0.1 mg mL^{-1} or higher inhibited the number of TRAP-positive multinuclear cells compared to that of the M-CSF- and RANKL-treated or of the ethanol-treated sample (black arrowheads in Figure 2A). Accordingly, the percentages of TRAP-positive multinuclear cells were significantly decreased by propolis treatment in a dose-dependent fashion, especially at the concentrations of 0.1, 0.25, and 0.5 mg mL^{-1} (*P* < .001; Figure 2B). By contrast, there was no difference in the percentage of TRAP-positive multinuclear cells between the M-CSF- and RANKL-treated and the ethanol-treated samples. As expected, there was no TRAP-positive multinuclear cell in PBMCs treated with only M-CSF (Figure 2A,B). Similar to the inhibition of TRAP-positive cells, the propolis extract at 0.1 mg mL^{-1} or higher suppressed the formation of actin rings, observed in the M-CSF- and RANKL-treated or the ethanol-treated sample (white arrowheads in Figure 3A). Note that the propolis extract at 0.25 and 0.5 mg mL^{-1} could prevent cell fusion (Figure 3A). Consistent with the significant inhibition of treatment with propolis at 0.1 mg mL^{-1} or higher on the percentages of TRAP-positive cells (Figure 2B), treatment with propolis at 0.1 mg mL^{-1} or greater significantly decreased the ratios of cells with F-actin ring formation compared to that of the sample treated with M-CSF and RANKL (*P* < .01; Figure 3B), whereas no difference was found between the M-CSF- and RANKL-treated sample and the ethanol-treated sample.

At the gene expression level, the propolis extract at 0.1 and 0.5 mg mL^{-1} significantly downregulated expression of certain osteoclast-specific genes, NFAT2, CTSK, RANK, CLCN7, and CTR, in a dose-dependent fashion compared to the M-CSF- and
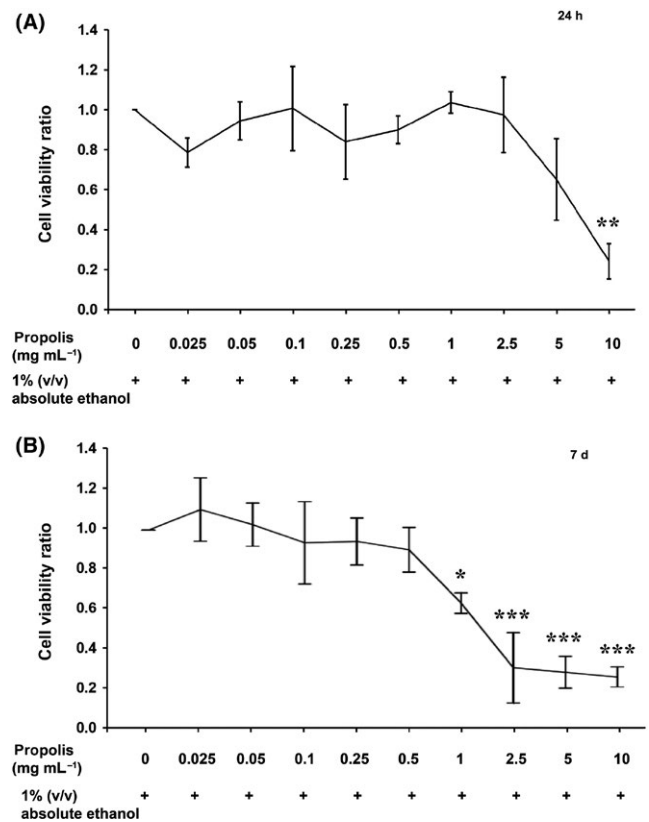

FIGURE 1 The cytotoxicity test of Thai propolis extract by an alamarBlue® assay. Peripheral blood mononuclear cells were treated with indicated doses of propolis for 24 h (A) or 7 d (B). The linear graphs demonstrate the ratios of cell viability in the propolis-treated samples relative to that of the sample treated with M-CSF and 1% (v/v) of absolute ethanol, as a solvent control, set to 1.0. Error bars = SD; * *P* < .05; ** *P* < .01; *** *P* < .001; n = 3. M-CSF, macrophage-colony-stimulating factor

RANKL-treated or the ethanol-treated sample (*P* < .05; Figure 4). However, mRNA expression of the CSF1 gene, which is not inhibited by treatment with the human cathelicidin antimicrobial peptide LL-37 that can block expression of several other osteoclast-specific genes,[18] was not altered by propolis or absolute ethanol treatment (Figure 4), suggesting the specificity of propolis treatment to inhibit only genes related to osteoclast maturation markers.

To investigate whether the Thai propolis extract inhibited osteoclast function, PBMCs were seeded on dentin slices and differentiated into multinuclear osteoclast-like cells in the presence or absence of propolis. The propolis extract at 0.1 mg mL^{-1} or greater decreased the amounts of stained pits and grooves compared to the M-CSF- and RANKL-treated sample (Figure 5A). Correspondingly, the percentages of resorption area were significantly reduced by propolis treatment in a dose-dependent manner (*P* < .05; Figure 5B). Very little stained pit or groove was observed in the sample treated with M-CSF alone that could not drive differentiation into osteoclast-like cells (Figure 5). Due to the significant reduction in cell viability by treatment with the propolis at 1 mg mL^{-1} upon treatment for 7 days (Figure 1B), the percentage of resorption area was

FIGURE 2 Propolis inhibits in vitro osteoclast formation. A, Representative images from three independent experiments showing a decrease in the number of TRAP-positive multinuclear cells by treatment with three non-toxic doses (0.1, 0.25 and 0.5 mg mL^{-1}) of the propolis extract for 7 d. Note the TRAP-positive multinuclear cells (black arrowheads) were generated by M-CSF and RANKL treatment in the presence or absence of absolute ethanol as a solvent control, while no TRAP-positive multinuclear cells were seen in the sample treated with M-CSF alone. Bar = 200 μm. B, The bar graph demonstrates a dose-dependent and significant decline in the percentages of TRAP-positive multinuclear cells in the propolis-treated samples relative to that of the untreated sample, set to 100. Error bars = SD; *** $P < .001$; n = 3. M-CSF, macrophage-colony-stimulating factor; RANKL, receptor activator of nuclear factor kappaB ligand; TRAP, tartrate-resistant acid phosphatase
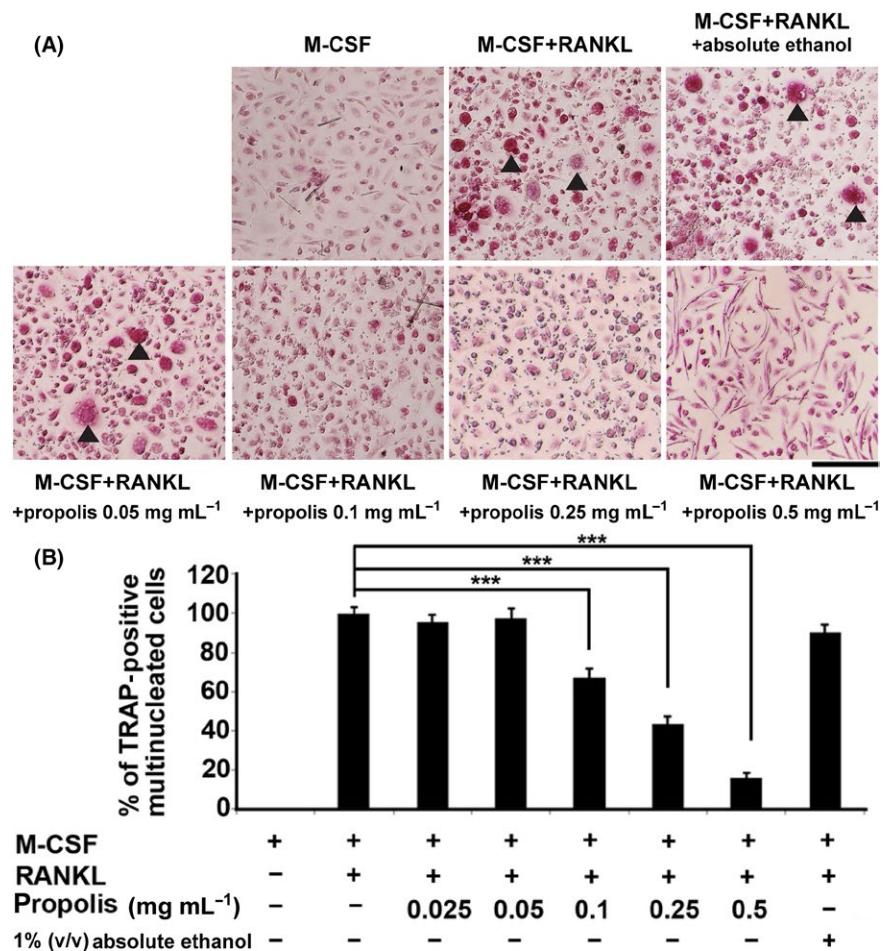
considerably reduced close to that of the sample treated with M-CSF (Figure 5B).

4 | DISCUSSION

In this study, Thai propolis extract was shown to exert anti-osteoclastogenesis induced by RANKL in vitro in human peripheral blood mononuclear cells, which is consistent with the previously demonstrated inhibition of Brazilian propolis extract on maturation of mouse osteoclasts that were derived from bone marrow cells.[16] This result also corresponds with a significant decrease in root resorption after an application of propolis extract on the root surface of extracted rat teeth compared to immersion of the rat teeth in the control physiologic saline.[23] Moreover, a dose-dependent inhibitory effect of Thai propolis on human osteoclast formation and function was demonstrated from 0.1 to 0.5 mg mL^{-1}. These concentrations are comparable to a single effective dose of the Brazilian propolis extract at around 0.334 mg mL^{-1}, previously reported to suppress mouse osteoclast maturation.[16] In addition to the inhibitory effect of Brazilian propolis on a few osteoclast characteristics, including TRAP and F-actin ring staining,[16] this study provided more evidence for the suppressive effect of the Thai propolis extract on osteoclast function and expression of osteoclast-specific genes. In addition,

although Thai propolis extract at these low doses inhibited in vitro osteoclastogenesis as shown in this study, it did not affect the proliferation of human periodontal ligament cells,[6] implying the specificity of Thai propolis extract for a certain cell type. Nonetheless, it is interesting to investigate the effect of Thai propolis on differentiation of PBMCs into macrophages.

The alamarBlue® assay was selected to determine the cytotoxicity of propolis extract at various concentrations in the present study because the brownish extract could interfere with the measurements of cell viability by the colorimetric MTT assay. Furthermore, the fluorescent activity from the alamarBlue® assay, representing the metabolic activity and growth of living cells, can minimize the interference from the color of propolis extract, as shown in a previous study.[6] It is noteworthy that the lowest dose (0.1 mg mL^{-1}) of the Thai propolis extract that significantly decreased the percentage of TRAP-positive cells, the ratio of cells with F-actin rings, the expression of osteoclast-specific genes, and the percentage of resorption area was less than the toxic dose of this extract on PBMCs at 10 mg mL^{-1} for 24 hours (Figure 1A) or at 1 mg mL^{-1} for 7 days (Figure 1B), indicating the safety of the extract for possible use as a storage medium[6] or at least as a component of the storage medium to prevent root resorption of replanted teeth in the future. However, this possibility warrants further investigations in an animal model and a clinical trial. Note that avulsed teeth are usually
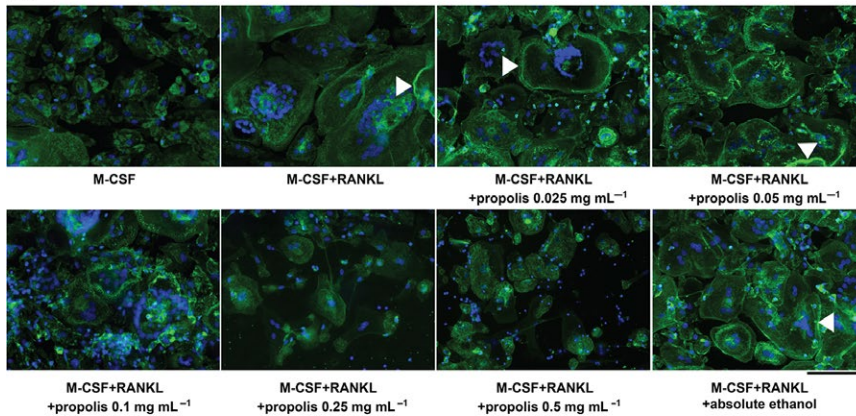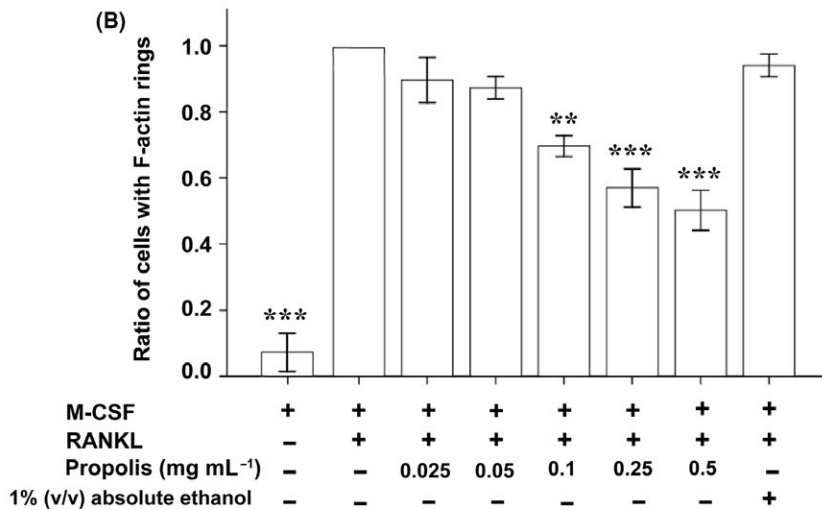
FIGURE 3 Propolis blocks formation of F-actin rings. Peripheral blood mononuclear cells were incubated with M-CSF and RANKL in the presence or absence of non-toxic doses of propolis or absolute ethanol as a solvent control for 7 d. A, The formation of F-actin rings (white arrowheads) was inhibited by treatment with propolis extract at 0.1 mg mL^{-1} or higher. The nuclei were stained with DAPI (blue). These fluorescence images are representative of three separate experiments with similar results. Bar = 100 μm. B, The bar graph demonstrates the ratio of cells with F-actin ring formation in each condition mentioned in A relative to that of the sample treated with M-CSF and RANKL, set to 1.0. Error bars = SD; ** $P < .01$; *** $P < .001$; n = 3. M-CSF, macrophage-colony-stimulating factor; RANKL, receptor activator of nuclear factor kappaB ligand
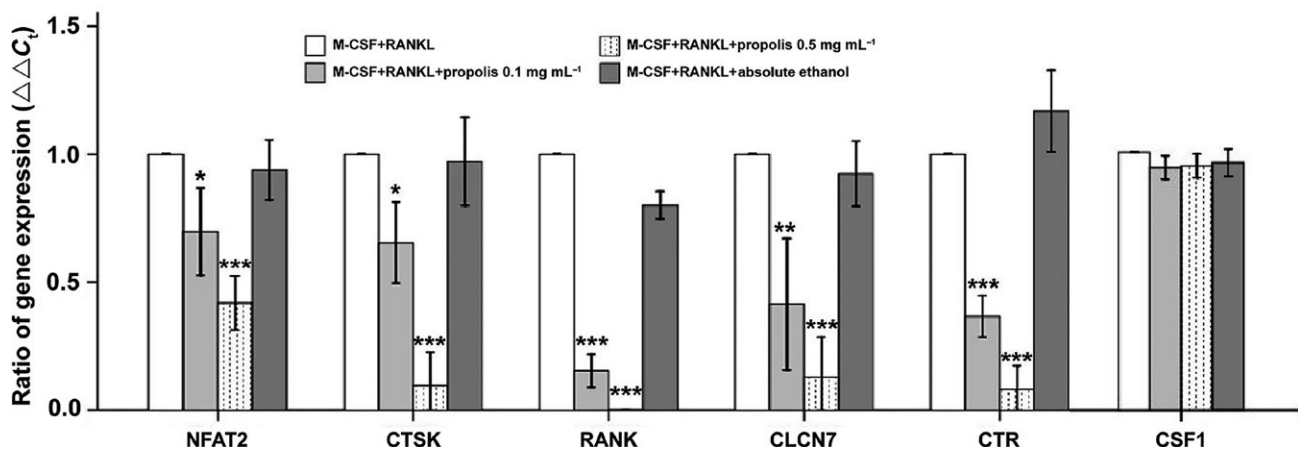

FIGURE 4 Propolis significantly downregulates expression of osteoclast-specific genes. Peripheral blood mononuclear cells were induced by M-CSF and RANKL with or without treatment with 0.1 (light gray bars) or 0.5 (stippled bars) mg mL^{-1} of the propolis extract or absolute ethanol (dark gray bars) as a solvent control for 7 d. The bar graph illustrates the relative ratios ($\Delta\Delta C_t$) of mRNA expressions for nuclear factor of activated T cell 2 (NFAT2), cathepsin K (CTSK), receptor activator of nuclear factor kappaB (RANK), chloride channel 7 (CLCN7), calcitonin receptor (CTR), and colony-stimulating factor 1 (CSF1) in the propolis-treated or absolute ethanol-treated sample to those of the untreated sample (empty bars), set to 1.0. Note that CSF1 mRNA expression was not altered by either dose of propolis or absolute ethanol. Error bars = SD; * $P < .05$; ** $P < .01$; *** $P < .001$; n = 3. M-CSF, macrophage-colony-stimulating factor; mRNA, messenger ribonucleic acid; RANKL, receptor activator of nuclear factor kappaB ligand
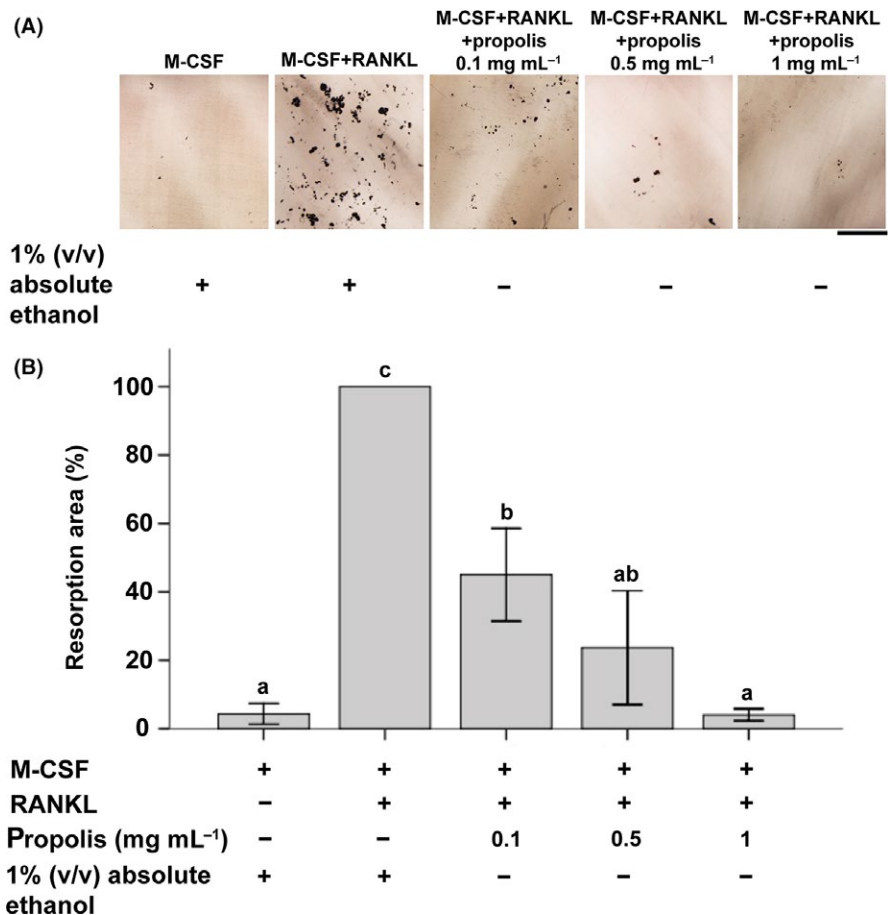
FIGURE 5 Propolis inhibits in vitro dentin resorption. A, Representative images from three independent experiments showing a dose-dependent inhibition of resorption pits, formed by in vitro generation of osteoclast-like cells under M-CSF and RANKL treatment for 7 d, by propolis at 0.1, 0.5 and 1 mg mL^{-1}, diluted in absolute ethanol at 1% (v/v). Note that absolute ethanol at 1% (v/v) was added in cultures treated either with M-CSF or with M-CSF and RANKL, as a solvent control. Bar = 200 μm. B, The bar graph shows the percentages of resorption area in the propolis-treated samples relative to that of the M-CSF- and RANKL-treated sample, set to 100. Error bars = SD; n = 3. Different letters denote statistically significant differences at $P < .05$. M-CSF, macrophage-colony-stimulating factor; RANKL, receptor activator of nuclear factor kappaB ligand

kept in the storage medium for no longer than a few hours before being replanted, so the effective doses of Thai propolis extract at 0.5 mg mL^{-1} or less can still be regarded as a safe storage medium for avulsed teeth.

Root resorption is the most common complication after delayed tooth replantation into the socket.[24] Several different materials have been introduced by a number of studies for application to the root surface to prevent resorption, such as Emdogain,[25] fluoride,[26] doxycycline,[27] alendronate,[28] and dexamethasone.[29] None of them has yet been effective for improving the survival rate of avulsed teeth after delayed replantation. However, Gulinelli et al[23] found that an application of the Brazilian propolis extract on the root surface of extracted rat teeth enhanced the resistance to resorption after delayed replantation. Unlike other materials, the propolis extract may, therefore, hold promise for prevention of root resorption by osteoclasts after delayed tooth replantation. Propolis is generally a complex mixture of various naturally occurring constituents, in which its main active compounds consist of flavonoids and phenolic and aromatic compounds.[30,31] Using the aluminum chloride and 2,4-dinitrophenylhydrazine and the Folin-Ciocalteu colorimetric methods, a previous study has shown that the Thai propolis extract contains around 10% (w/w) of total flavonoids, which are more than total phenolic compounds by four times.[32] Flavonoids are known to possess the anti-inflammatory and antioxidant activities via suppression of the NF-kappaB

pathway.[33] Furthermore, NF-kappaB is an essential transcription factor for osteoclast formation.[34] Consequently, it is speculative that flavonoids within the Thai propolis extract exert their inhibitory effect on human osteoclastogenesis in this study, possibly via blockade of the NF-kappaB activity. This warrants further investigations with the fractionated flavonoids.

In the present study, Thai propolis extract was tested for its inhibitory action against osteoclastogenesis, as it is impractical to use the active compounds of propolis for storage of avulsed teeth or these active chemicals may not be stable due to their short shelf life. In summary, there is a potential to further develop Thai propolis extract as a storage medium or even as a mixture of HBSS and the propolis extract for storage of avulsed teeth to gain clinical benefits from not only maintaining PDL cell viability[6] but also inhibiting osteoclast formation and function as shown in this study. Nevertheless, further animal studies are required before clinical application.

CONFLICT OF INTEREST

The authors confirm that they have no conflict of interest.

ORCID

Suttichai Krisanaprakornkit http://orcid.org/0000-0001-9189-0333

REFERENCES

1. Barrett E, Kenny D. Avulsed permanent teeth: a review of the literature and treatment guidelines. Dent Traumatol. 1997;13:153–63.
2. Flores MT, Andersson L, Andreasen JO, Bakland LK, Malmgren B, Barnett F et al. Guidelines for the management of traumatic dental injuries. II. Avulsion of permanent teeth. Dent Traumatol. 2007;23:130–6.
3. Andreasen J. Effect of extra-alveolar period and storage media upon periodontal and pulpal healing after replantation of mature permanent incisors in monkeys. Int J Oral Surg. 1981;10:43–53.
4. Söder PÖ, Otteskog P, Andreasen J, Modeer T. Effect of drying on viability of periodontal membrane. Eur J Oral Sci. 1977;85:164–8.
5. Van Hassel HJ, Oswald RJ, Harrington GW. Replantation 2. The role of the periodontal ligament. J Endod. 1980;6:506–8.
6. Prueksakorn A, Puasiri S, Ruangsri S, Makeudom A, Sastraruji T, Krisanaprakornkit S et al. The preservative effect of Thai propolis extract on the viability of human periodontal ligament cells. Dent Traumatol. 2016;32:495–501.
7. Andreasen JO, Borum MK, Jacobsen HL, Andreasen FM. Replantation of 400 avulsed permanent incisors. 2. Factors related to pulpal healing. Endod Dent Traumatol. 1995;11:59–68.
8. Soares Ade J, Gomes BP, Zaia AA, Ferraz CC, de Souza-Filho FJ. Relationship between clinical-radiographic evaluation and outcome of teeth replantation. Dent Traumatol. 2008;24:183–8.
9. Petrovic B, Markovic D, Peric T, Blagojevic D. Factors related to treatment and outcomes of avulsed teeth. Dent Traumatol. 2010;26:52–9.
10. Kamat M, Puranik R, Vanaki S, Kamat S. An insight into the regulatory mechanisms of cells involved in resorption of dental hard tissues. J Oral Maxillofac Pathol. 2013;17:228–33.
11. Khurshid Z, Naseem M, Zafar MS, Najeeb S, Zohaib S. Propolis: a natural biomaterial for dental and oral healthcare. J Dent Res Dent Clin Dent Prospects. 2017;11:265–74.
12. Parolia A, Thomas MS, Kundabala M, Mohan M. Propolis and its potential uses in oral health. Int J Med Med Sci. 2010;2:210–5.
13. Abdulrhman M, Samir Elbarbary N, Ahmed Amin D, Saeid Ebrahim R. Honey and a mixture of honey, beeswax, and olive oil–propolis extract in treatment of chemotherapy-induced oral mucositis: a randomized controlled pilot study. Pediatr Hematol Oncol. 2012;29:285–92.
14. Murray MC, Worthington HV, Blinkhorn AS. A study to investigate the effect of a propolis-containing mouthrinse on the inhibition of de novo plaque formation. J Clin Periodontol. 1997;24:796–8.
15. Bretz WA, Chiego D, Marcucci M, Cunha I, Custódio A, Schneider L. Preliminary report on the effects of propolis on wound healing in the dental pulp. Z Naturforsch. 1998;53:1045–8.
16. Pileggi R, Antony K, Johnson K, Zuo J, Shannon Holliday L. Propolis inhibits osteoclast maturation. Dent Traumatol. 2009;25:584–8.
17. Makeudom A, Supanchart C, Montreekachon P, Khongkhunthian S, Sastraruji T, Krisanaprakornkit J et al. The antimicrobial peptide,

18. human beta-defensin-1, potentiates in vitro osteoclastogenesis via activation of the p44/42 mitogen-activated protein kinases. Peptides. 2017;95:33–9.
18. Supanchart C, Thawanaphong S, Makeudom A, Bolscher JG, Nazmi K, Kornak U et al. The antimicrobial peptide, LL-37, inhibits in vitro osteoclastogenesis. J Dent Res. 2012;91:1071–7.
19. Montreekachon P, Chotjumlong P, Bolscher JG, Nazmi K, Reutrakul V, Krisanaprakornkit S. Involvement of P2X(7) purinergic receptor and MEK1/2 in interleukin-8 up-regulation by LL-37 in human gingival fibroblasts. J Periodontal Res. 2011;46:327–37.
20. Arya M, Shergill IS, Williamson M, Gommersall L, Arya N, Patel HR. Basic principles of real-time quantitative PCR. Expert Rev Mol Diagn. 2005;5:209–19.
21. Suzuki T, Higgins P, Crawford D. Control selection for RNA quantitation. Biotechniques. 2000;29:332–7.
22. Bustin SA. Absolute quantification of mRNA using real-time reverse transcription polymerase chain reaction assays. J Mol Endocrinol. 2000;25:169–93.
23. Gulinelli JL, Panzarini SR, Fattah CM, Poi WR, Sonoda CK, Negri MR et al. Effect of root surface treatment with propolis and fluoride in delayed tooth replantation in rats. Dent Traumatol. 2008;24:651–7.
24. Andreasen JO, Borum MK, Jacobsen HL, Andreasen FM. Replantation of 400 avulsed permanent incisors. 1. Diagnosis of healing complications. Endod Dent Traumatol. 1995;11:51–8.
25. Iqbal MK, Bamaas N. Effect of enamel matrix derivative (EMDOGAIN) upon periodontal healing after replantation of permanent incisors in beagle dogs. Dent Traumatol. 2001;17:36–45.
26. Shulman LB, Gedalia I, Feingold RM. Fluoride concentration in root surfaces and alveolar bone of fluoride-immersed monkey incisors three weeks after replantation. J Dent Res. 1973;52:1314–6.
27. Cvek M, Cleaton-Jones P, Austin J, Lownie J, Kling M, Fatti P. Effect of topical application of doxycycline on pulp revascularization and periodontal healing in reimplanted monkey incisors. Endod Dent Traumatol. 1990;6:170–6.
28. Lustosa-Pereira A, Garcia RB, de Moraes IG, Bernardineli N, Bramante CM, Bortoluzzi EA. Evaluation of the topical effect of alendronate on the root surface of extracted and replanted teeth. Microscopic analysis on rats' teeth. Dent Traumatol. 2006;22:30–5.
29. Kum KY, Kwon OT, Spangberg LS, Kim CK, Kim J, Cho MI et al. Effect of dexamethasone on root resorption after delayed replantation of rat tooth. J Endod. 2003;29:810–3.
30. Ahn MR, Kumazawa S, Hamasaka T, Bang KS, Nakayama T. Antioxidant activity and constituents of propolis collected in various areas of Korea. J Agric Food Chem. 2004;52:7286–92.
31. Parolia A, Kundabala M, Rao NN, Acharya SR, Agrawal P, Mohan M et al. A comparative histological analysis of human pulp following direct pulp capping with Propolis, mineral trioxide aggregate and Dycal. Aust Dent J. 2010;55:59–64.
32. Chailertvanitkul P, Namsirikul T, Damrongrungruang T, Peerapatana J. Phenolic and flavonoids contents and antibacterial activity of ethanolic extract of propolis. Isan J Pharm Sci. 2017;13:59–67.
33. Vezza T, Rodríguez-Nogales A, Algieri F, Utrilla MP, Rodriguez-Cabezas ME, Galvez J. Flavonoids in inflammatory bowel disease: a review. Nutrients. 2016;8:211–32.
34. Abu-Amer Y. NF-κB signaling and bone resorption. Osteoporos Int. 2013;24:2377–86.

ORIGINAL ARTICLE

Anesthetic efficacies of intrapapillary injection in comparison to inferior alveolar nerve block for mandibular premolar extraction: a randomized clinical trial

Duangkamon Wongpang[1] · Anupong Makeudom[2] · Thanapat Sastraruji[2] · Sakornrat Khongkhunthian[3] · Suttichai Krisanaprakornkit[2,4] · Chayarop Supanchart[1,2]

Abstract

Objective Intrapapillary injection (IPI) has been suggested to improve pulpal anesthesia of mandibular teeth and to avoid complications from inferior alveolar nerve block (IANB). This study aimed to determine and compare clinical efficacies and prostaglandin E_2 (PGE_2) levels between IPI and IANB.

Materials and methods IANB was randomly selected for mandibular premolar anesthesia on one side of 40 patients, whereas IPI was locally administered to the contralateral premolar. Pulpal anesthesia, pain during injection and extraction, patients' satisfaction, and complications were assessed from 30 patients. Gingival crevicular fluid from ten patients was collected for PGE_2 quantification by ELISA.

Results Of 30 patients, 18 preferred IPI after injection due to significantly faster mean onset of pulpal anesthesia ($p < 0.001$) and lower mean score of injection pain ($p = 0.017$) than IANB, but 21 preferred IANB instead after extraction due to less postoperative pain, consistent with the significantly lower median PGE_2 level on the IANB side than that on the IPI at 30 min ($p = 0.047$). However, there was no difference in the mean satisfaction score between the two techniques. Ulcerated epithelium and sloughing tissues were found at the IPI site in some patients with complete healing within 2 weeks.

Conclusions The anesthetic efficacies of IPI for mandibular premolar extraction are comparable to those of IANB. However, postoperative pain and local complications at the IPI site should be considered.

Clinical relevance IPI may be used for dental procedures that require only a short anesthetic duration to avoid failure of pulpal anesthesia, complications, and discomfort from IANB.

Keywords Complication · Inferior alveolar nerve block · Intrapapillary injection · Local anesthesia · Prostaglandin E_2

✉ Chayarop Supanchart
    chayarop.supanchart@cmu.ac.th

1   Department of Oral and Maxillofacial Surgery, Faculty of Dentistry, Chiang Mai University, Chiang Mai, Thailand

2   Center of Excellence in Oral and Maxillofacial Biology, Faculty of Dentistry, Chiang Mai University, Chiang Mai, Thailand

3   Department of Restorative Dentistry and Periodontology, Faculty of Dentistry, Chiang Mai University, Chiang Mai, Thailand

4   Department of Oral Biology and Diagnostic Sciences, Faculty of Dentistry, Chiang Mai University, Chiang Mai, Thailand

Introduction

Local anesthesia is essential for pain management during dental procedures and considered to be safe and effective compared to general anesthesia. For local anesthetic injection in the mandible, the diffusion of anesthetic agents is impeded by a dense cortical bone, so inferior alveolar nerve block (IANB) into the pterygomandibular space is recommended as a primary technique for mandibular tooth anesthesia [1]. However, IANB is not always successful and its success rate ranges from 60 to 92% [1–3]. Moreover, several studies have previously revealed some complications of IANB compared to other techniques, such as post-injection paresthesia that is most commonly found, transient facial nerve paralysis generally caused by too deep injection into the capsule of the parotid gland, and trismus caused by trauma to the muscles and blood

vessels in the infratemporal space with an increased risk from multiple injections [4–6]. In addition, an incidence rate of toxic overdose reaction was higher by IANB than that by an infiltration technique [7].

To avoid these disadvantages, several alternative injection methods have been introduced to achieve mandibular tooth anesthesia [8–11]. Particularly, intrapapillary injection (IPI) [12] is a technique that administers anesthetic agents coronally to the alveolar bone crest, whose prominent feature is a perforated bone compared to the outer compact bone in the other areas of the mandible. IPI may promote drug diffusion into the marrow space, possibly leading to pulpal anesthesia. Giffin [12] reported an almost 100% success rate of local anesthesia in both maxillary and mandibular teeth by IPI, formerly called crestal anesthesia. However, only a few experimental studies have so far investigated both drug distribution and clinical efficacies of IPI compared to other techniques with contradictory results. Whereas one study showed the diffusion of anesthetic agent into the cancellous bone of the mandible together with a higher success rate (> 90%) of IPI for posterior mandibular tooth anesthesia than that of IANB [13], the other instead reported the drug distribution within only soft tissue, resulting in less profound effect and a shorter duration of anesthesia than periodontal ligament injection (PLI) [14]. Note that while simple exodontia was conducted in the former study, only assessment of pulpal anesthesia was performed in the latter.

In general, dental practitioners do not use IPI as a sole technique for mandibular tooth anesthesia since IPI is only chosen as a supplement after the failure of IANB or to avoid the complications from IANB [15]. Therefore, with the limited information to confirm the anesthetic efficacies of IPI, it is interesting to compare the clinical efficacies of IPI with those of IANB in order to verify its future use as a technique of choice for mandibular tooth anesthesia. Moreover, no study has yet assessed tissue trauma from IPI in addition to that from an extraction wound that may affect postoperative pain perception of the patient. Prostaglandin E_2 (PGE_2) is known to be one of the essential inflammatory and pain mediators involved in pulp and periodontal diseases and in the surgical wound [16–18]. Consequently, measurement of PGE_2 levels would represent the amount of tissue trauma and inflammation, resulting in patients' pain sensation. It was hypothesized in this study that the clinical efficacies—including the success rate of pulpal anesthesia, injection and extraction pain, patients' satisfaction, and complications—or PGE_2 levels of IPI were not different from those of IANB. Thus, the purposes of this study were to determine and compare clinical efficacies and PGE_2 levels in gingival crevicular fluid (GCF) collected from the gingival crevices of the adjacent teeth, mesially and distally to the extracted mandibular premolar, between IPI and IANB.

Materials and methods

Patient selection

Forty patients (18–30 years old), whose physical and health statuses were categorized as class I by the American Society of Anesthesiologists, were recruited from the clinic of Oral and Maxillofacial Surgery, Faculty of Dentistry, Chiang Mai University. This study was approved by the local Human Experimentation Committee of Faculty of Dentistry, Chiang Mai University (No.42/2017), and registered with the Thai Clinical Trials Registry (No. TCTR20181218001). The inclusion criteria of this prospective study with a split-mouth design were healthy patients who required extraction for orthodontic treatment of their bilateral mandibular first or second premolars that were sound teeth without any pathologies, but with similar difficulty for uncomplicated exodontia. Moreover, there were at least two normal adjacent teeth without periodontitis located mesially and distally to the premolar to be extracted still remaining with normal interdental papilla (IDP), as classified by Nordland and Tarnow [19]. The exclusion criteria were patients who had contraindications for articaine and epinephrine use, were pregnant or breastfeeding, were taking any analgesics that could alter pain perception within the last 2 weeks [20–22], or were unable to assess their pain. The crowding premolars and complicated extraction cases as well as abnormal root configurations, as evidenced by the panoramic radiographs, were excluded. The experiment was discontinued as patients requested or life-threatening complications from IPI or IANB occurred.

Of 40 patients, the sample sizes of 30 and 10 patients for assessment of clinical efficacies and for PGE_2 quantification, respectively, were sufficient to detect the mean difference of 22 for injection pain score and of 293 pg/µl for PGE_2 levels between IPI and IANB. The sample size calculation was based on a previous study [13] and our pilot study using G*Power software (version 3.1.9.2) [23] with alpha = 0.05 and beta = 0.20.

Study design

The flowchart of study design for assessment of clinical efficacies in the first 30 patients and quantification of PGE_2 levels in the next ten patients is illustrated in Fig. 1 a and b, respectively. IANB using 4% articaine with epinephrine 1:100,000 (1.7 ml per cartridge; Septanest SP®, Septodont, Co., Paris, France) was first administered on one side of the mouth, randomly chosen using an available program from http://www.randomizer.org. A conventional aspirated dental syringe and a disposable 30-mm-long and 27-gauge needle (Terumo®, Terumo, Co., Tokyo, Japan) were used to slowly block
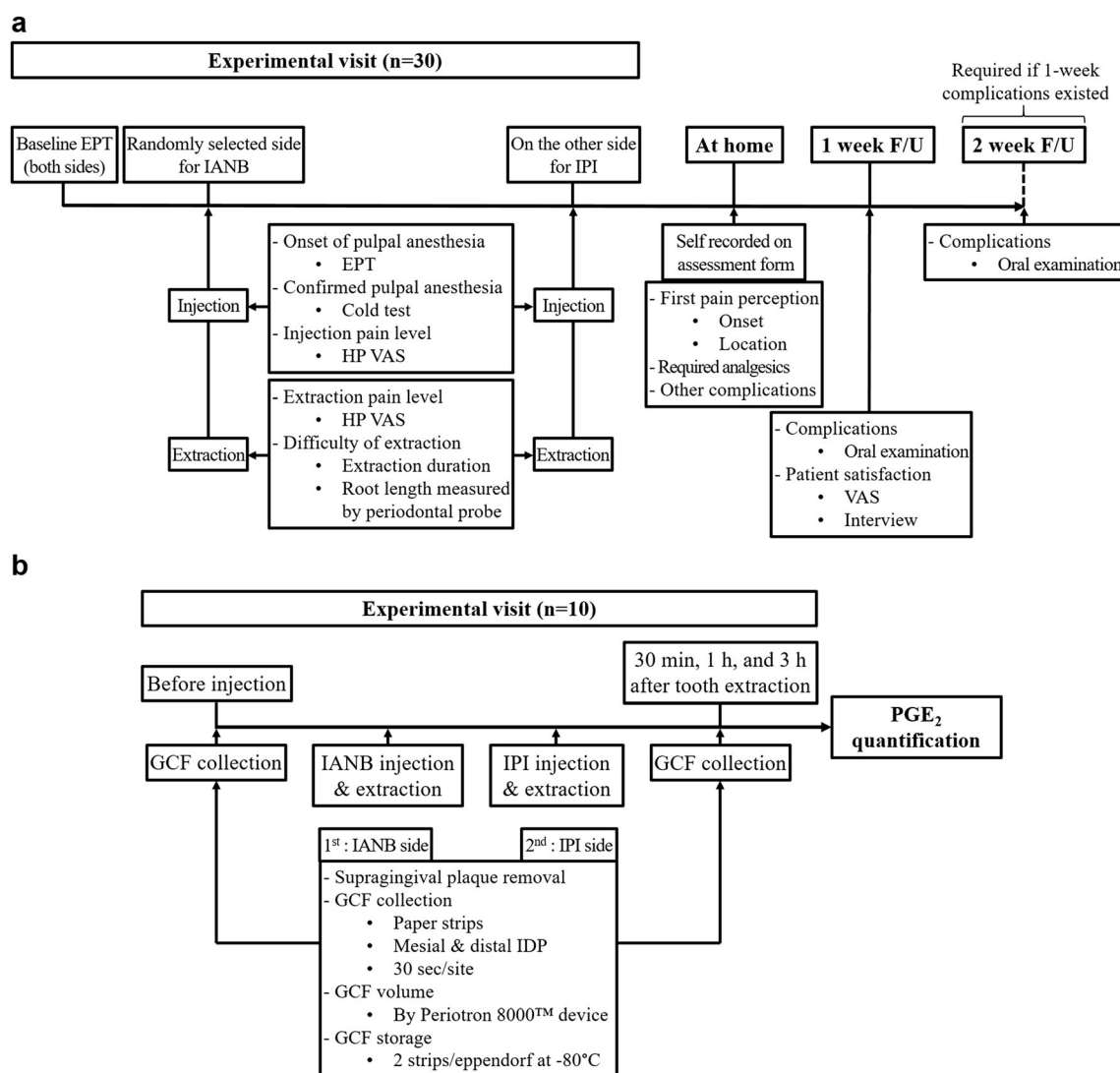
Fig. 1 The flowcharts summarize the study design for **a** an assessment of clinical efficacies and complications with a sample size of 30 patients and **b** PGE$_2$ quantification in GCF with a sample size of ten patients. EPT = electrical pulp testing, F/U = follow-up, GCF = gingival crevicular fluid, HP VAS = Heft-Parker visual analogue scale, IANB = inferior alveolar nerve block, IDP = interdental papilla, IPI = intrapapillary injection, PGE$_2$ = prostaglandin E$_2$

inferior alveolar nerve and lingual nerve with the total volume of anesthetic solution equal to 1.4 ml. To anesthetize buccal mucosa of premolars, long buccal nerve block was performed by administering 0.3 ml of the anesthetic solution. Prior to tooth extraction, pulpal anesthesia was confirmed by electric pulp testing (EPT) and cold test, and soft tissue numbness around the tooth to be extracted was tested by an explorer. If sharp pain was still felt, additional injections by an infiltration technique were provided at the soft tissue surrounding the tooth. The tooth extraction was performed by the experienced oral surgeon (D.W.), who also administered local anesthesia, using an atraumatic technique with a duration of extraction no longer than 5 min (or 300 s). In brief, soft tissue surrounding the tooth to be extracted was gently separated by a straight elevator no. EL3S (Hu-Friedy Mfg. Co., LLC, Chicago, IL,

USA) that also provided a wedge action to loosen the tooth, which was later removed by the tooth forceps no. 151 (Hu-Friedy Presidential®, Hu-Friedy Mfg. Co., LLC).

After tooth extraction on the IANB side, IPI using the aforementioned anesthetic agent was administered on the other side by the same operator at the same appointment so that the orthodontic treatment already planned was not delayed. IPI was done by a high-pressure syringe (Sopira® Citoject®, Kulzer GmbH, Hanau, Germany) to better control the volume and delivery of anesthetic agent [10] with a fixed volume of anesthetic solution at 0.06 ml per each pressing and a disposable 21-mm-long and 27-gauge needle (Septoject XL®, Septodont, Co.) on both mesial and distal IDP of the tooth to be extracted. The needle angle was approximately 45° to the tooth axis [12]. The needle was inserted into the center

of IDP below the IDP tip about 2–3 mm [11] with the depth approximately 2–3 mm for the final position of the needle's bevel facing toward the alveolar crest. If the needle contacted the alveolar bone, it was slightly withdrawn. The injection was performed by pressing a lever of the syringe five times with an interval for 2 s between each time. After the last time of injection, the needle was held in place for 10 s before withdrawal [24]. In total, a 0.3-ml volume of the anesthetic solution was given for each IDP over 20 s [12, 13]. Blanched IDP and surrounding gingiva is a sign of the IPI achievement. The pulpal anesthesia and soft tissue numbness around the tooth to be extracted and the tooth extraction protocol were followed as aforementioned.

Assessment of clinical efficacies

To determine pulpal anesthesia, an electric pulp tester (vitality scanner model 2006, SybronEndo, Co., Orange, CA, USA), with the maximum stimulation of 80 and the setting rate of 7 to reach the maximum within 14 s, was used. After the patient's lip was numb on the IANB side or immediately after finishing IPI on the other side [13], the tooth to be extracted was isolated with gauze rolls, dried with air blow, and tested with EPT every 30 s for IANB and continuously for IPI until the absence of response to two consecutive maximum stimulations that indicated pulpal anesthesia [1, 25]. However, an onset of pulpal anesthesia was reported at the first absence of response to EPT (Fig. 1a). To confirm the result of pulpal anesthesia by EPT, a foam pellet (Roeko Endo-Frost Pellets, Coltene Whaledent, Inc., Langenau, BW, Germany) sprayed with dichlorodifluoromethane (Roeko Endo-Frost) was applied onto the tooth (Fig. 1a) [26]. The successful criterion of pulpal anesthesia was an absence of response to either the maximum stimulation by EPT or cold test within 15 min for IANB [27] or 2 min for IPI from the first injection.

The pain perception was evaluated by using the Heft-Parker visual analogue scale (HP VAS) [28] at two periods, pain during injection (immediately after injection; Fig. 1a), and pain during extraction (immediately after extraction; Fig. 1a). According to the HP VAS, the patients rated their pain on a 170-mm-long line together with eight modified descriptive terms for pain, including none, faint, weak, mild, moderate, strong, intense, and maximum possible [29]. The HP VAS was then rated as none = 0 mm on the line; 0 < mild pain ≤ 54 mm that included faint, weak, and mild; 54 < moderate pain < 114 mm; and 114 ≤ severe pain ≤ 170 mm that included strong, intense, and maximum possible according to Robertson et al. [29]. In addition to rating their pain after injection and extraction, patients were instructed to record their pain onset, location, required analgesic intake, and any other complications after extraction at home (Fig. 1a). Acetaminophen (Beramol, B.M.Pharmacy Co., Ltd.,

Bangkok, Thailand) at 500 mg was prescribed as needed for pain every 4 h.

For postoperative assessment, all patients were weekly recalled up to 2 weeks depending on the complications of injection and extraction (Fig. 1a). Overall patients' satisfaction score for IPI and IANB was rated by a 100-mm line of VAS at 1 week after the extraction. Moreover, each patient was interviewed for his/her preference over the two anesthetic techniques together with his/her reasons.

GCF collection

GCF was collected from the gingival crevices of the two adjoined teeth, mesially and distally to the extracted tooth, on both IPI and IANB sides for four periods: baseline (before injection), 30 min, 1 h, and 3 h after tooth extraction (Fig. 1b), as previously described [30]. Briefly, the supragingival plaque was gently removed by sterile gauze prior to GCF collection. Then, a paper strip (Periopaper™, Oraflow, Inc., Smithtown, NY, USA) was gently inserted into each sulcus of the two teeth until light resistance was felt, and left for 30 s. The GCF volume in each strip was measured by a Periotron 8000™ device (Oraflow, Inc.). The two paper strips from the same extraction site were kept in the same Eppendorf tube at − 80 °C for further PGE_2 analysis. If analgesics were requested by these ten patients during GCF collection, tramadol HCl (Matradol®, Charoon Bhesaj, Co., Ltd., Bangkok, Thailand) at a single oral dose of 50 mg was instead prescribed due to the suppressive effect of acetaminophen on PGE_2 levels [18].

PGE_2 quantification in GCF

To measure the PGE_2 levels in GCF, sequential competitive ELISA was performed using the 96-well plate PGE_2 assay commercial kit (R&D systems, Inc., Minneapolis, MN, USA) following the manufacturer's instruction. The sensitivity of this assay is reported at 16.0–41.4 pg/ml. In brief, GCF was eluted from the paper strips by shaking in phosphate-buffered saline at 10 °C for 30 min. The 96-well plate pre-coated with goat anti-mouse polyclonal antibody was added with the eluted GCF samples or the serial dilutions of PGE_2 standard in duplicate, followed by addition of mouse monoclonal antibody against human PGE_2. The mixture was incubated at room temperature for 1 h on a shaker set at 500 rpm. Thereafter, horseradish peroxidase-labeled PGE_2 was added and incubated at room temperature for 2 h on the shaker. The plate was washed with the prepared washing buffer for four times before being incubated with mixed substrate solution for 30 min at room temperature under light protection. The reaction was terminated by the addition of 2N H_2SO_4. An ELISA plate reader (Tecan Group, Ltd., Männedorf, Zürich, Switzerland) was used to measure an optical density value at

450 nm with the correction wavelength at 540 nm. The average concentration of PGE_2 in each unknown sample was derived from the standard curve of PGE_2, then normalized by GCF volume determined by the Periotron 8000™, and expressed as a unit of pg/μl [31]. To determine the recovery rate of PGE_2 from the paper strip, 100-pg and 200-pg amounts of PGE_2 standard were applied onto the paper strips, left to air dry, and stored at -80 °C until simultaneous analysis with the GCF samples as mentioned above. The average percentage of PGE_2 recovered from the paper strips was equal to 66.77.

Statistical analysis

The mean root length that was measured from the cemento-enamel junction to the root apex, the mean duration of extraction, the mean injection pain score, the mean onset of pulpal anesthesia, and the mean satisfaction score between IPI and IANB groups were tested for significant differences by paired t test. The proportions of anesthetic success and of two extraction pain categories, no and mild pain between the two groups were compared by Fisher's exact test. Moreover, the proportions of two injection pain categories, mild and moderate pain, between the two groups were compared by chi-square test. To assess the differences in PGE_2 levels among four time points within the IPI or IANB group, Friedman test followed by Wilcoxon signed-rank test were used, whereas the differences in PGE_2 levels between the two groups in each time point and the difference in cumulative PGE_2 levels for 3 h after extraction between IPI and IANB groups were analyzed by Wilcoxon signed-rank test. The statistical analyses were analyzed by SPSS version 17.0 for IBM (SPSS, Chicago, IL, USA) with the significance level at $p < 0.05$.

Results

Comparable clinical efficacies between intrapapillary injection and inferior alveolar nerve block

A cohort of the first 30 patients, which comprised ten males and 20 females, whose ages ranged from 18 to 30 years (20.73 ± 2.77), was recruited for the comparisons of clinical efficacies. The characteristics of IPI and IANB groups are summarized in Table 1. There was no difference in the root length or in the duration of extraction that indicated similar difficulty of extraction between the two groups. The clinical efficacies of IPI and IANB groups are summarized in Table 2. A 96.67% success rate of pulpal anesthesia within the first injection was shown for 29 premolars in the IANB group, and an 86.67% success rate of pulpal anesthesia (26 premolars) was demonstrated in the IPI group due to leakage of anesthetic agent in four cases. However, there was no difference in the success rate between the two groups (Table 2).

Regarding the remaining one tooth in the IANB group and four teeth in the IPI group that failed to achieve pulpal anesthesia within the first set of injections, pulpal anesthesia was achieved by the second set of injections. Note that the success rates of pulpal anesthesia in each technique between the left and the right were not different (data not shown).

Of 30 patients, five were excluded from the analysis of the onset of pulpal anesthesia because three premolars in the IANB group and two premolars in the IPI group were still positive to EPT within the durations indicated in the "Materials and Methods" section although these five teeth were considered to achieve pulpal anesthesia due to their negative response to cold test (Table 2). Therefore, only 25 teeth in each group were used for the analysis of the mean onset of pulpal anesthesia. The mean onset in the IPI group (< 1 min) was significantly faster than that in the IANB group (~ 7 min; $p < 0.001$).

Regarding the injection pain on the 170-mm HP VAS, a significant difference was found between IPI and IANB groups, in which the mean injection pain perceived by the patients in the IPI group (35.92) was significantly lower than that in the IANB group (50.65; $p = 0.017$). Consistently, 18 patients (60%) preferred IPI, probably owing to less injection pain and faster onset of pulpal anesthesia. However, when the injection pain was categorized as no, mild, moderate, and severe according to the aforementioned criteria, no difference in the proportions of mild or moderate pain was found between the two groups (Table 2).

With respect to pain during premolar extraction classified as no, mild, moderate, and severe, only one patient perceived mild pain on the IANB side (Table 2) and rated her pain at 22 mm on the 170-mm HP VAS (data not shown). Additional injection was then provided. No difference in the proportions of no or mild extraction pain was found between the two groups (Table 2).

With regard to the anesthetic duration, since three patients did not report any pain on either IPI or IANB side in an evaluation form, they were excluded from the assessment because the anesthetic duration could not be determined if the patients did not feel any pain after local anesthesia wore off. So, the duration of anesthesia started from pulpal anesthesia to the pain onset on the IPI side of the remaining 27 patients because analgesic intake would affect pain perception on the IANB side that happened later. The pain onset of 27 patients varied from 3 to 62 min after pulpal anesthesia, implying that the range of anesthetic duration for IPI was 3–62 min with mean $\pm$ SD equal to 27.11 ± 16.43 min (Table 2).

From an interview at 1-week follow-up, 21 patients (70%) had a more satisfied experience with IANB than with IPI due to less postoperative pain, while the remaining nine patients (30%) preferred IPI because of no prolonged soft tissue numbness, often resulting in patients' discomfort. In addition, while being asked for the next mandibular tooth anesthesia, 16

Table 1 Characteristics of intrapapillary injection (IPI) and inferior alveolar nerve block (IANB) groups ($n = 30$)

Variable		IPI	IANB	P value
Duration of extraction (sec)	Mean ± SD	113.03 ± 57.36	120.60 ± 60.60	0.437[a]
	Min − max	20–250	35–254	
Root length (mm)	Mean ± SD	15.48 ± 1.72	15.30 ± 2.03	0.239[a]
	Min − max	13–20	12–21	

[a] Paired t test

(53.33%) and 14 (46.67%) patients would request IANB and IPI, respectively, consistent with a slightly higher mean satisfaction score in the IANB group than that in the IPI group, but no difference was found (Table 2).

Of 11 patients who exhibited postoperative complications from IPI, six had ulcerated gingival epithelium at the injected IDP (Fig. 2a), four had sloughing tissue over the IDP (Fig. 2b), and one displayed alveolar osteitis (Fig. 3a). These patients recovered from the aforementioned complications to normal wound healing within 2 weeks. Five patients exhibited postoperative complications on the IANB side, including self-inflicted lip and tongue trauma ($n = 2$), transient trismus ($n = 1$), increased heart rate ($n = 1$) [32], and alveolar osteitis ($n = 1$; Fig. 3b) with a complete recovery within 1 week. Of these five patients, one patient who had trismus on the IANB side also had ulcerated gingival epithelium on the IPI side, while the other who had increased heart rate on the IANB side also had sloughing tissue on the IPI side.

A significant increase in PGE$_2$ levels by the intrapapillary injection

GCF samples were collected from a group of the next ten patients, which comprised three males and seven females, whose ages ranged from 18 to 24 years ($21.00 ± 2.11$). PGE$_2$ concentrations in GCF were normalized by GCF volume and reported as a unit of pg/μl (Fig. 4). PGE$_2$ levels in GCF collected from the gingival crevices of the two teeth next to the extracted premolars tended to continuously elevate up to 3 h after tooth extraction with significant increases found in both IPI and IANB groups ($p < 0.05$; Fig. 4a). Interestingly, when PGE$_2$ levels were compared between the two groups at each of the four time points, the median PGE$_2$ level in the IPI group (684.04 pg/μl) was significantly higher than that in the IANB group (430.01 pg/μl) at 30 min after extraction ($p = 0.047$; Fig. 4a). However, there was no difference in the median PGE$_2$ levels at baseline between the two groups (471.54 and 345.59 pg/μl in IPI and IANB groups, respectively; $p = 0.203$; Fig. 4a) or in the cumulative PGE$_2$ levels up to 3 h after extraction between the two groups (2144.01 and 1965.28 pg/μl in IPI and IANB groups, respectively; $p = 0.285$; Fig. 4b), indicating that the degrees of inflammation nearby the extraction wound on the IPI side are

temporarily increased, but do not differ from those on the IANB side throughout the study period.

Discussion

This study demonstrated that the patients preferred IPI after injection because of its faster mean onset of pulpal anesthesia and lower mean score of injection pain than those of IANB. Unlike the 96.67% achievement of pulpal anesthesia by IANB, the success rate of pulpal anesthesia by IPI was slightly lower, but no difference was found. In addition, the overall patients' satisfaction at a 1-week follow-up period between the two groups was not different. In contrast to the patients' preference for IPI after injection, the majority of patients (70%) were more satisfied with IANB than IPI after tooth extraction due to their lower postoperative pain, possibly as a result of a longer anesthetic duration by IANB. However, the real anesthetic duration of IANB could not be determined in this study because the patients had already taken analgesics after local anesthesia wore off on the IPI side. The higher postoperative pain on the IPI side perceived by these patients is also corroborated with the transiently higher median PGE$_2$ level observed in GCF collected from the adjacent teeth on the IPI side than that on the IANB side at 30 min after tooth extraction.

The complications at the injected IDP by IPI, such as ulcerated gingival epithelium and sloughing tissue, were reversible and similar to those found by the PLI and intraseptal injection (ISI) due to anesthetic injection [9, 33, 34]. The probable causes are high pressure during injection and excessive volumes of the anesthetic solution used [9]. Therefore, use of a conventional syringe as an alternative to the high-pressure syringe may help avoid these complications. On the other hand, the complications of IANB, including self-inflicted lip and tongue trauma albeit repeated postoperative care instruction, transient trismus, and increased heart rate, were regarded as distant from the injection site. It is noteworthy that alveolar osteitis was equally found in both IPI and IANB (Fig. 3); therefore, IPI does not increase an incidence of alveolar osteitis, so does PLI as compared to IANB [35]. All complications occurring from IPI and IANB were resolved to normal wound healing within a 2-week follow-up period.

In this study, the rapid onset of pulpal anesthesia by IPI was approximately 1 min after being examined by the first EPT

Table 2 Comparisons of clinical efficacies between intrapapillary injection (IPI) and inferior alveolar nerve block (IANB) in a cohort of 30 patients

Variable		IPI	IANB	P value
Success within the 1st injection	n (%)	26 (86.67)	29 (96.67)	0.353[a]
Onset of anesthesia (sec)	n	25[1]	25[1]	< 0.001[b]
	Mean ± SD	53.36 ± 14.92	441.16 ± 161.58	
	Min − max	32–88	210–858	
Injection pain (max = 170 mm)	Mean ± SD	35.92 ± 31.58	50.65 ± 29.92	0.017[b]
Injection pain categories	No pain, n (%)	1 (3.33)	1 (3.33)	
	Mild pain, n (%)	21 (70.00)	15 (50.00)	0.104[c]
	Moderate pain, n (%)	8 (26.67)	14 (46.67)	
	Severe pain, n (%)	0	0	
Extraction pain (max = 170 mm)				
Extraction pain categories	No pain, n (%)	30 (100)	29 (96.67)	1.000[a]
	Mild pain, n (%)	0	1 (3.33)	
	Moderate pain, n (%)	0	0	
	Severe pain, n (%)	0	0	
Anesthetic duration (min)	n	27[2]	ND	N/A
	Mean ± SD	27.11 ± 16.43		
	Min–max	3–62		
Satisfaction score (max = 100 mm)	Mean ± SD	72.33 ± 18.38	77.56 ± 14.10	0.244[b]
	Min − max	31.00–100.00	55.00–100.00	

ND not determined, *N/A* not applicable

[1] Five patients were excluded before the analysis of mean onset

[2] Three patients were excluded since they did not feel any pain

[a] Fisher's exact test

[b] Paired t test

[c] Chi-square test

(Table 2), which is consistent with the immediate pulpal anesthesia after IPI as previously demonstrated [12, 13], and is sensible due to direct injection into the operation area. In addition, it was necessary to measure EPT immediately and continuously on the IPI side until the first absence of response to maximal stimuli due to the aforementioned rapid onset [12, 13] and a short duration of pulpal anesthesia by IPI. However, owing to a much delayed onset of pulpal anesthesia by IANB (mean onset = 7.4 min) [36], EPT was, therefore, conducted after lip numbness and continued every 30 s to avoid patients' discomfort. The rapid mean onset of pulpal anesthesia by IPI was comparable to that by ISI [11–13, 37], but the needle tip in the ISI technique has to penetrate into the crestal bone in comparison with no direct contact to the alveolar crest in the IPI technique.

Moreover, although not significantly different, 70% of the patients rated mild injection pain on the IPI side, whereas 50% rated mild injection pain and around 47% rated moderate injection pain on the IANB side. This is in line with a previous finding from the survey study of pain during local anesthetic injections in the oral cavity, which has indicated that IANB was the most painful injection technique, followed by PLI, mental nerve block, and local infiltration, respectively [38]. Less injection pain from IPI than from IANB may help reduce patients' dental fear and anxiety. To rate patients' pain, Robertson et al. [29] showed that the HP VAS with a 170-mm scale was easy for patients to assess their pain due to eight distinct pain descriptive and self-explainable terms on the scale. Moreover, the 170-mm length of the HP VAS is unique for this scale that would yield more precise pain evaluation than the 100-mm length of the VAS, which is generally used in questionnaires. The HP VAS together with these terms was, therefore, chosen to assess patients' pain in this study because this scale has been previously used to rate patients' pain in a number of clinical studies and provides high sensitivity for pain perception by patients due to these comprehensible descriptive terms [28].

In this study, the success rate of pulpal anesthesia by IPI was slightly lower than those previously reported by Giffin at 99% for mandibular teeth [12] and by Taheritalesh et al. at 94–
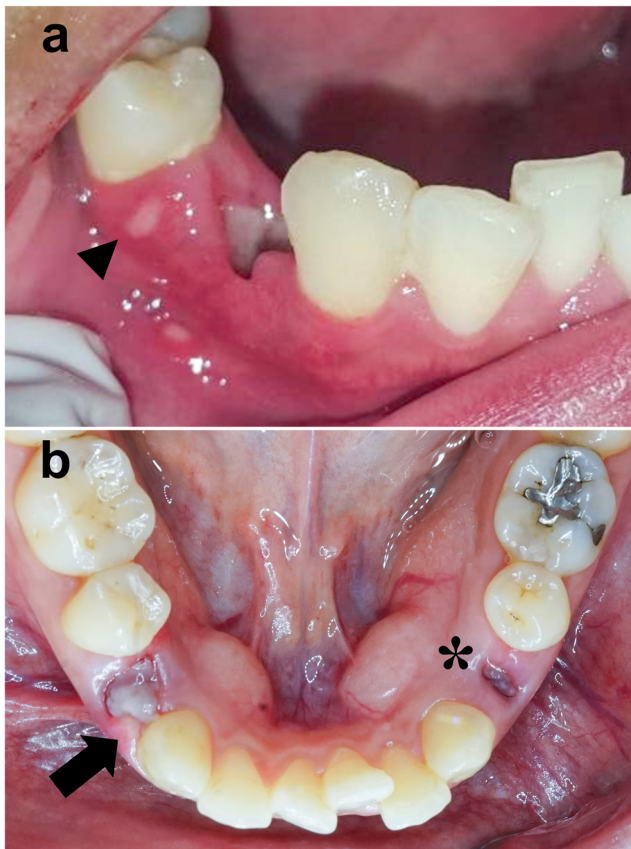
Fig. 2 Postoperative complications at 1-week follow-up after simple extraction under local anesthesia with the intrapapillary injection technique, **a** ulcerated gingival epithelium (an arrowhead) in the middle of interdental papilla (IDP; injection site) distal to extracted 44, **b** sloughing tissue (an arrow) at the injected IDP mesial to extracted 44 compared with an extraction wound of 34 under local anesthesia by the inferior alveolar nerve block technique (an asterisk)

the remaining 26 cases could be predicted by the operator's sensation of initial back pressure and oozing solution that are two signs for a proper position of the needle tip [12, 13]. Note that the almost complete success rate of pulpal anesthesia in mandibular premolars by IANB in this study compared to 81% in the previous study [13] may be due to the absence of any pathology in sound premolars selected in this study. Therefore, it would be interesting to further study and compare the anesthetic efficacies between IPI and IANB in teeth with pulpal diseases with or without periapical lesions. Regarding the patients' satisfaction, 14 patients preferred IPI for their next mandibular tooth anesthesia because of the absence of prolonged lip and tongue numbness, so the patients would resume their routine activities as early as possible similar to the results of two previous studies [12, 13]. On the other hand, 16 patients preferred IANB due to the main reason of less pain sensation after tooth extraction.

Three possible reasons for less postoperative pain on the IANB side may be involved with (1) a complete inhibition of nociceptive inputs from the extraction site that travel along the afferent nerve fibers to sensitize central nervous system, resulting in a longer duration and deeper anesthesia [39, 40]; (2) the preemptive analgesics that was taken to relieve the patients' first pain perception on the IPI side would continuously exert its analgesic effect for several hours after extraction on the IANB side [39]; and (3) more tissue trauma at the injected IDP from IPI, as reflected by a significant increase in PGE_2 levels, representing tissue trauma and pain, on the IPI side compared to the IANB side, which would provoke more pain sensation.

Several previous clinical studies have demonstrated constantly raised PGE_2 levels up to 4 h with its variable levels during the first hour postoperatively in serum from the extraction socket after surgical removal of the mandibular third molars [18, 41–45]. Moreover, another study that extended an observation of PGE_2 levels up to 7 days postoperatively in saliva and urine has demonstrated an increase in PGE_2 concentrations up to 3 days [46]. To the best of our knowledge, our study is the first to determine PGE_2 levels in GCF collected from the gingival crevices of the adjacent teeth in association with tissue trauma from IPI. The continual increment in GCF PGE_2 levels found at both IPI and IANB sides up to 3 h

95% for mandibular premolars [13]. However, Taheritalesh et al. had stated that the anesthetic success rate in the molars was higher than that in premolars because broad alveolar bone crest in the molar region accompanied by large and numerous nutrient canals promotes diffusion of the anesthetic solution [13]. The narrower alveolar bone crest plus thinner IDP in the premolar region, which often causes the leakage of anesthetic solution observed in our four failed cases, may, therefore, be one of the reasons for the failure of pulpal anesthesia by IPI. In addition, the success of pulpal anesthesia by IPI observed in

Fig. 3 Pie charts illustrate the number (percentage) of **a** postoperative complications in 30 patients for the intrapapillary injection and **b** for the inferior alveolar nerve block groups
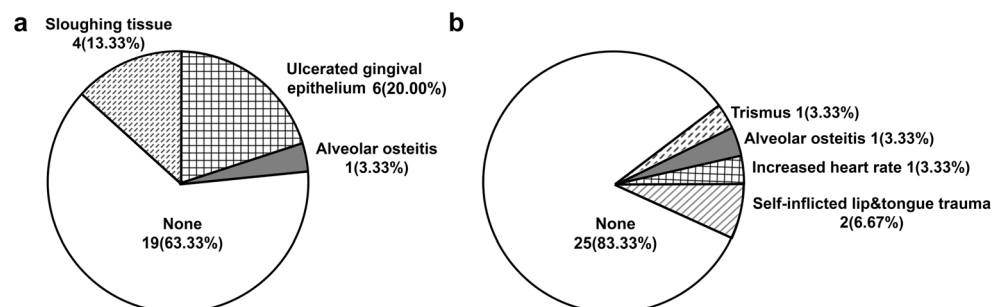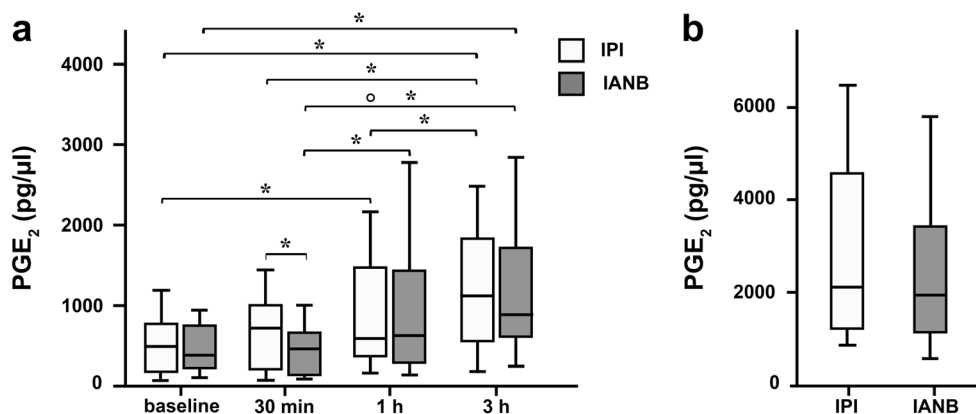
Fig. 4 Box plots show the median, quartiles, and extreme values of prostaglandin E$_2$ (PGE$_2$) levels per volumes of gingival crevicular fluid measured by the Periotron 8000™ device. **a** The PGE$_2$ levels of intrapapillary injection (IPI; empty boxes) and inferior alveolar nerve block (IANB; gray boxes) groups at baseline, 30 min, 1 h, and 3 h after tooth extraction; **b** the cumulative PGE$_2$ levels derived from addition of the PGE$_2$ levels at 30 min, 1 h, and 3 h after premolar extraction in the IPI and IANB groups. An open circle in **a** represents an outlier. The horizontal black line across the box indicates the median. *$p < 0.05$

is consistent with the results of those studies. Furthermore, the significantly higher median PGE$_2$ level in IPI than that in IANB at 30 min after extraction coincided with the mean onset of patients' pain sensation at 27 min (Table 2). Therefore, it is likely that mechanical trauma from IPI at the injected IDP affects PGE$_2$ production during an initial phase. The mean duration of pulpal anesthesia by IPI, or better called periodontal anesthesia since the tooth vitality examined by EPT could not be continually conducted in the extracted premolar, was 27 min, corresponding with 20- to 60-min intervals shown by the two previous studies [12, 13]. The shorter duration of pulpal anesthesia by IPI than by IANB is expected because of more rapid distribution of anesthetic solution into high vascularity within the medullary bone and less anesthetic volumes used in IPI than in IANB. The rationales for choosing GCF collection at 30 min, 1 h, and 3 h were the mean duration of pulpal anesthesia on the IPI side at 27 min, the findings from several previous studies [18, 41–45] that revealed a dramatic increase in PGE$_2$ levels at 1 h after tooth removal and the duration of soft tissue anesthesia for 3 h after injection with articaine [47], respectively.

Conclusion

Since there was no difference in the root length or in the duration of extraction that indicated similar difficulty of extraction between the two injection techniques, the clinical efficacies of IPI comparable to those of IANB suggest that IPI may be used to replace IANB for mandibular premolar anesthesia only for short and simple dental procedures in order to avoid failure of pulpal anesthesia, complications, and discomfort from IANB. Nevertheless, if the simple procedures turn out to be complex, IANB is still required. Moreover, more postoperative pain and the higher rate of complications from

IPI than from IANB (11 versus 5 cases, respectively) must be taken into consideration.

Compliance with ethical standards

Conflict of interest The authors declare that they have no conflict of interest.

Ethical approval All procedures performed in studies involving human participants were in accordance with the ethical standards of the institutional and/or national research committee and with the 1964 Helsinki declaration and its later amendments or comparable ethical standards.

Informed consent Informed consent was obtained from all individual participants included in the study.

References

1. Malamed SF (2012) Techniques of mandibular anesthesia. In: Malamed SF (ed) Handbook of local anesthesia, 6th edn. Elsevier Mosby, St. Louis, pp. 225, 231

2. El-Kholey KE (2017) Anesthetic efficacy of 4% articaine during extraction of the mandibular posterior teeth by using inferior alveolar nerve block and buccal infiltration techniques. J Maxillofac Oral Surg 16:90–95. https://doi.org/10.1007/s12663-015-0877-z

3. Poorni S, Veniashok B, Senthilkumar AD, Indira R, Ramachandran S (2011) Anesthetic efficacy of four percent articaine for pulpal anesthesia by using inferior alveolar nerve block and buccal infiltration techniques in patients with irreversible pulpitis: a prospective randomized double-blind clinical trial. J Endod 37:1603–1607. https://doi.org/10.1016/j.joen.2011.09.009

4. Malamed SF (2012) Local complications. In: Malamed SF (ed) Handbook of local anesthesia, 6th edn. Elsevier Mosby, St. Louis, pp. 291–310

5. Garisto GA, Gaffen AS, Lawrence HP, Tenenbaum HC, Haas DA (2010) Occurrence of paresthesia after dental local anesthetic administration in the United States. J Am Dent Assoc 141:836–844. https://doi.org/10.14219/jada.archive.2010.0281

6. Stone J, Kaban LB (1979) Trismus after injection of local anesthetic. Oral Surg Oral Med Oral Pathol 48:29–32. https://doi.org/10.1016/0030-4220(79)90231-7

7. Bartlett SZ (1972) Clinical observations on the effects of injections of local anesthetic preceded by aspiration. Oral Surg Oral Med Oral Pathol 33:520–526. https://doi.org/10.1016/0030-4220(72)90363-5

8. Meechan JG (2002) Supplementary routes to local anaesthesia. Int Endod J 35:885–896. https://doi.org/10.1046/j.1365-2591.2002.00592.x

9. Malamed SF (2012) Supplemental injection technique. In: Malamed SF (ed) Handbook of local anesthesia, 6th edn. Elsevier Mosby, St. Louis, pp. 253, 255

10. Malamed SF (1982) The periodontal ligament (PDL) injection: an alternative to inferior alveolar nerve block. Oral Surg Oral Med Oral Pathol 53:117–121. https://doi.org/10.1016/0030-4220(82)90273-0

11. Saadoun AP, Malamed S (1985) Intraseptal anesthesia in periodontal surgery. J Am Dent Assoc 111:249–256. https://doi.org/10.14219/jada.archive.1985.0111

12. Giffin KM (1994) Providing intraosseous anesthesia with minimal invasion. J Am Dent Assoc 125:1119–1121. https://doi.org/10.14219/jada.archive.1994.0128

13. Taheritalesh K, Yazdani J, Ghavimi M, Khashabi E (2009) Crestal anesthesia: an efficient, fast and reliable technique in posterior mandibular exodontia; a case-control clinical and CT scan assessment. Res J Biol Sci 4:369–374

14. Kämmerer PW, Palarie V, Schiegnitz E, Ziebart T, Al-Nawas B, Daubländer M (2012) Clinical and histological comparison of pulp anaesthesia and local diffusion after periodontal ligament injection and intrapapillary infiltration anaesthesia. J Pain Relief 1:5. https://doi.org/10.4172/2167-0846.1000108

15. Anderson JAM, Brewer A, Creagh D, Hook S, Mainwaring J, McKernan A, Yee TT, Yeung CA (2013) Guidance on the dental management of patients with haemophilia and congenital bleeding disorders. Br Dent J 215:497–504. https://doi.org/10.1038/sj.bdj.2013.1097

16. Petrini M, Ferrante M, Ciavarelli L, Brunetti L, Vacca M, Spoto G (2012) Prostaglandin E_2 to diagnose between reversible and irreversible pulpitis. Int J Immunopathol Pharmacol 25:157–163. https://doi.org/10.1177/039463201202500118

17. Sanchez GA, Miozza VA, Delgado A, Busch L (2013) Salivary IL-1beta and PGE_2 as biomarkers of periodontal status, before and after periodontal treatment. J Clin Periodontol 40:1112–1117. https://doi.org/10.1111/jcpe.12164

18. Lee YS, Kim H, Brahim JS, Rowan J, Lee G, Dionne RA (2007) Acetaminophen selectively suppresses peripheral prostaglandin E_2 release and increases COX-2 gene expression in a clinical model of acute inflammation. Pain 129:279–286. https://doi.org/10.1016/j.pain.2006.10.020

19. Nordland WP, Tarnow DP (1998) A classification system for loss of papillary height. J Periodontol 69:1124–1126. https://doi.org/10.1902/jop.1998.69.10.1124

20. Younan M, Atkinson TJ, Fudin J (2013) A practical approach to discontinuing NSAID therapy prior to a procedure. Pract Pain Manag 13:45–51

21. Trescot AM, Datta S, Lee M, Hansen H (2008) Opioid pharmacology. Pain Physician 11:133–153

22. Richelson E (2001) Pharmacology of antidepressants. Mayo Clin Proc 76:511–527. https://doi.org/10.4065/76.5.511

23. Faul F, Erdfelder E, Lang AG, Buchner A (2007) G*Power 3: a flexible statistical power analysis program for the social, behavioral, and biomedical sciences. Behav Res Methods 39:175–191. https://doi.org/10.3758/BF03193146

24. Roberts GJ, Rosenbaum NL (1991) A colour atlas of dental analgesia & sedation. Wolfe, London, p 50

25. Lin J, Chandler NP (2008) Electric pulp testing: a review. Int Endod J 41:365–374. https://doi.org/10.1111/j.1365-2591.2008.01375.x

26. Weisleder R, Yamauchi S, Caplan DJ, Trope M, Teixeira FB (2009) The validity of pulp testing: a clinical study. J Am Dent Assoc 140:1013–1017. https://doi.org/10.14219/jada.archive.2009.0312

27. Lai TN, Lin CP, Kok SH, Yang PJ, Kuo YS, Lan WH, Chang HH (2006) Evaluation of mandibular block using a standardized method. Oral Surg Oral Med Oral Pathol Oral Radiol Endod 102:462–468. https://doi.org/10.1016/j.tripleo.2005.12.003

28. Heft MW, Parker SR (1984) An experimental basis for revising the graphic rating scale for pain. Pain 19:153–161. https://doi.org/10.1016/0304-3959(84)90835-2

29. Robertson D, Nusstein J, Reader A, Beck M, McCartney M (2007) The anesthetic efficacy of articaine in buccal infiltration of mandibular posterior teeth. J Am Dent Assoc 138:1104–1112. https://doi.org/10.14219/jada.archive.2007.0324

30. Khongkhunthian S, Techasatian P, Supanchart C, Bandhaya P, Montreekachon P, Thawanaphong S, Krisanaprakornkit S (2013) Elevated levels of a disintegrin and metalloproteinase 8 in gingival crevicular fluid of patients with periodontal diseases. J Periodontol 84:520–528. https://doi.org/10.1902/jop.2012.120262

31. Chotjumlong P, Bolscher JG, Nazmi K, Reutrakul V, Supanchart C, Buranaphatthana W, Krisanaprakornkit S (2013) Involvement of the $P2X_7$ purinergic receptor and c-Jun N-terminal and extracellular signal-regulated kinases in cyclooxygenase-2 and prostaglandin E_2 induction by LL-37. J Innate Immun 5:72–83. https://doi.org/10.1159/000342928

32. Malamed SF (2012) Systemic complications. In: Malamed SF (ed) Handbook of local anesthesia, 6th edn. Elsevier Mosby, St. Louis, pp. 322–323

33. Kaufman E, Galili D, Garfunkel AA (1983) Intraligamentary anesthesia: a clinical study. J Prosthet Dent 49:337–339. https://doi.org/10.1016/0022-3913(83)90273-1

34. Bonar T, Nusstein J, Reader A, Drum M, Fowler S, Beck M (2017) Anesthetic efficacy of articaine and lidocaine in a primary intraseptal injection: a prospective, randomized double-blind study. Anesth Prog 64:203–211. https://doi.org/10.2344/anpr-64-04-10

35. Kammerer PW, Adubae A, Buttchereit I, Thiem DGE, Daublander M, Frerich B (2018) Prospective clinical study comparing intraligamentary anesthesia and inferior alveolar nerve block for extraction of posterior mandibular teeth. Clin Oral Investig 22:1469–1475. https://doi.org/10.1007/s00784-017-2248-2

36. Tortamano IP, Siviero M, Lee S, Sampaio RM, Simone JL, Rocha RG (2013) Onset and duration period of pulpal anesthesia of articaine and lidocaine in inferior alveolar nerve block. Braz Dent J 24:371–374. https://doi.org/10.1590/0103-6440201302072

37. Biocanin V, Brkovic B, Milicic B, Stojic D (2013) Efficacy and safety of intraseptal and periodontal ligament anesthesia achieved by computer-controlled articaine + epinephrine delivery: a dose-finding study. Clin Oral Investig 17:525–533. https://doi.org/10.1007/s00784-012-0724-2

38. Kaufman E, Epstein JB, Naveh E, Gorsky M, Gross A, Cohen G (2005) A survey of pain, pressure, and discomfort induced by commonly used oral local anesthesia injections. Anesth Prog 52:122–127. https://doi.org/10.2344/0003-3006(2005)52[122:ASP]2.0.CO;2

39. Woolf CJ, Chong MS (1993) Preemptive analgesia-treating postoperative pain by preventing the establishment of central sensitization. Anesth Analg 77:362–379. https://doi.org/10.1213/00000539-199377020-00026

40. Hargreaves KM, Khan A (2005) Surgical preparation: anesthesia & hemostasis. Endod Top 11:32–55. https://doi.org/10.1111/j.1601-1546.2005.00160.x

41. Roszkowski MT, Swift JQ, Hargreaves KM (1997) Effect of NSAID administration on tissue levels of immunoreactive prostaglandin E$_2$, leukotriene B$_4$, and (S)-flurbiprofen following extraction of impacted third molars. Pain 73:339–345

42. Fornai M, Colucci R, Graziani F, Cei S, Antonioli L, Tonelli M (2006) Cyclooxygenase-2 induction after oral surgery does not entirely account for analgesia after selective blockade of cyclooxygenase 2 in the preoperative period. Anesthesiology 104:152–157

43. Gordon SM, Brahim JS, Rowan J, Kent A, Dionne RA (2002) Peripheral prostanoid levels and nonsteroidal anti-inflammatory drug analgesia: replicate clinical trials in a tissue injury model. Clin Pharmacol Ther 72:175–183. https://doi.org/10.1067/mcp.2002.126501

44. Khan AA, Brahim JS, Rowan JS, Dionne RA (2002) *In vivo* selectivity of a selective cyclooxygenase 2 inhibitor in the oral surgery model. Clin Pharmacol Ther 72:44–49. https://doi.org/10.1067/mcp.2002.125560

45. Dionne RA, Gordon SM, Rowan J, Kent A, Brahim JS (2003) Dexamethasone suppresses peripheral prostanoid levels without analgesia in a clinical model of acute inflammation. J Oral Maxillofac Surg 61:997–1003. https://doi.org/10.1016/S0278-2391(03)00310-0

46. Mehra P, Reebye U, Nadershah M, Cottrell D (2013) Efficacy of anti-inflammatory drugs in third molar surgery: a randomized clinical trial. Int J Oral Maxillofac Surg 42:835–842. https://doi.org/10.1016/j.ijom.2013.02.017

47. Malamed SF (2012) Clinical action of specific agents. In: Malamed SF (ed) Handbook of local anesthesia, 6th edn. Elsevier Mosby, St. Louis, pp. 66